

PLATE JACKING TEST - HORIZONTAL

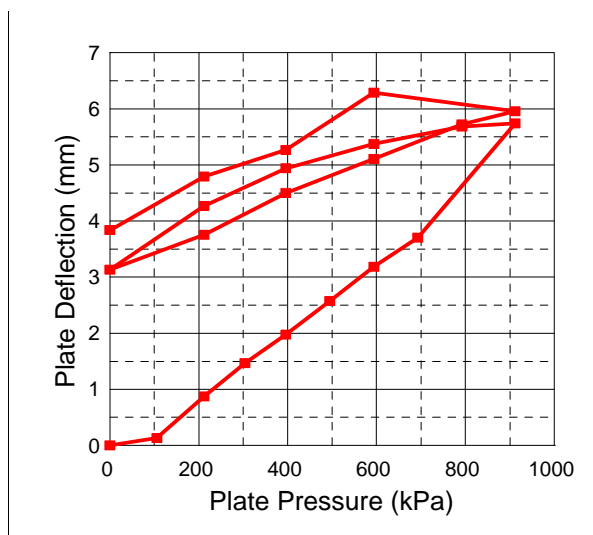
Client	RWBE		
Location	Koekenaaps Site	PLT.WTG 46 (1.3 - 1.8m)	
Date	30th July 2010	Test No	4A
Job No	10174	Checked By	CD

Direction of Test	Horizontal	Plate Diameter (mm)	300.00
Jack Number	C106	Ram Diameter (mm)	42.82
Gauge No:	80MPa	Calibration Cert No.	2177
		Calibration Date	2 sept 2010

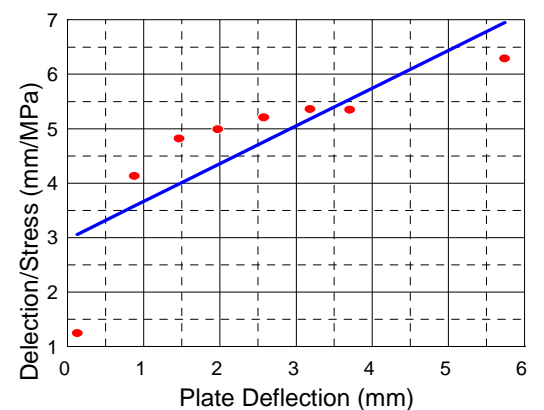
Direct Readings & Analysis

Graphical Representation of Stress/Strain

Gauge Pressure (MPa)	Ram Load (kN)	Plate Stress (kPa)	Plate Defln (mm)	Incremental Value of E (MPa)	Average Value of E (MPa)
0	0.0	0	0.00	0.00	0
5	7.5	106	0.13	176.89	176.89
10	15.0	212	0.88	31.46	53.42
15	21.5	304	1.47	34.43	45.78
20	28.0	396	1.98	39.83	44.25
25	35.0	495	2.58	36.46	42.43
30	42.0	594	3.19	35.86	41.18
35	49.0	693	3.71	41.87	41.27
45	64.5	912	5.74	23.86	35.12
40	56.0	792	5.68		
30	42.0	594	5.38		
20	28.0	396	4.94		
10	15.0	212	4.27		
0	0.0	0	3.14		
10	15.0	212	3.75		
20	28.0	396	4.50		
30	42.0	594	5.11		
40	56.0	792	5.73		
45	64.5	912	5.96		
30	42.0	594	6.29		
20	28.0	396	5.27		
10	15.0	212	4.80		
0	0.0	0	3.84		
	0.0	0			
	0.0	0			
	0.0	0			
	0.0	0			
	0.0	0			
	0.0	0			
	0.0	0			
	0.0	0			
	0.0	0			
	0.0	0			
	0.0	0			
	0.0	0			
	0.0	0			



Hyperbolic Representation



Hyperbolic Transformation value of E (MPa) **47.91**

**APPENDIX H:
TEST PIT PROFILES**

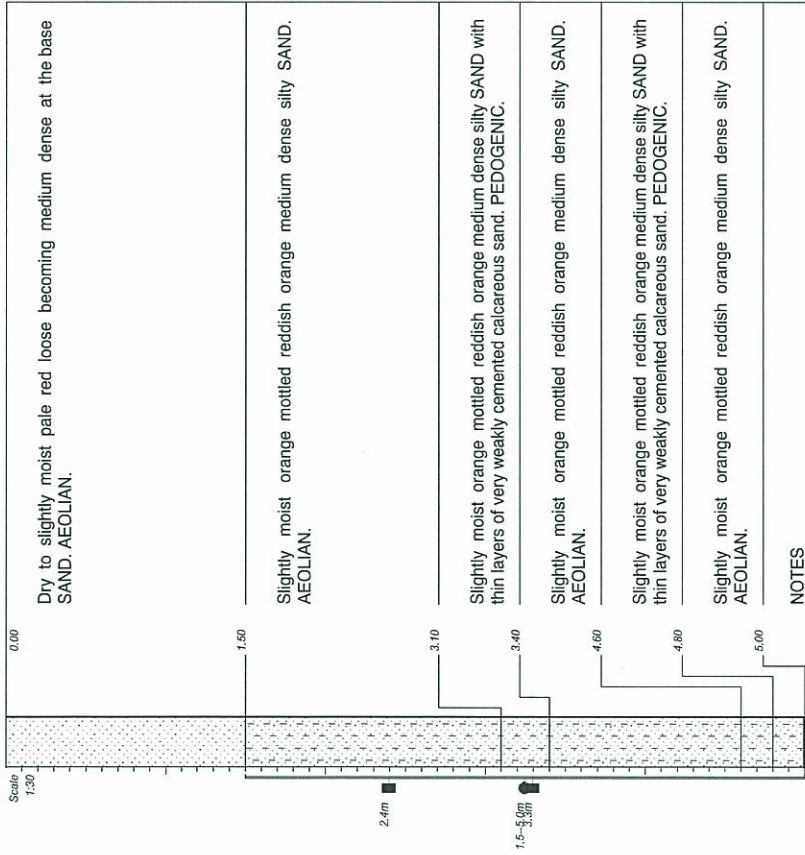
BKS Palace Consortium



ESKOM
SERE WIND ENERGY FACILITY
WIND TURBINE POSITION

HOLE No: T WTG16
Sheet 1 of 1

JOB NUMBER: J01386



NOTES

- 1) No groundwater seepage encountered.
- 2) Sidewalls stable.
- 3) Bulk and foundation indicator samples taken at 1.5--5.0m.
- 4) Undisturbed samples taken at 2.4m and 3.3m.
- 5) Test pit excavated to maximum reach of the machine.
- 6) Excavated next to wind turbine position WTG16.

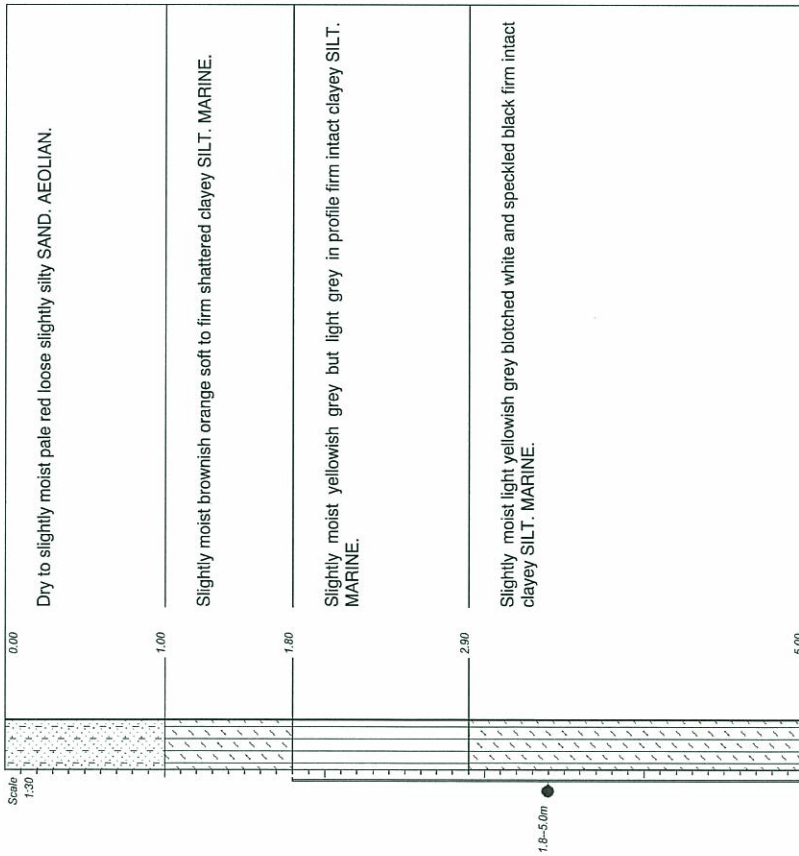
CONTRACTOR: AURET COMPANY
MACHINE: KOMATSU PC 200-6
DRILLED BY: F. JOSEPH
PROFILED BY: VS MUASI
TYPE SET BY: VS MUASI
SETUP FILE: V.SET

INCLINATION:
DIA: TRENCH
DATE: 30/08/2010
DATE: 17/11/10 15:52
TEXT: ...TEXT\PIATEL-1.TXT

ELEVATION:
X-COORD: 34 J 224285
Y-COORD: 6507745

HOLE No: T WTG16





NOTES

- 1) No groundwater seepage encountered.
- 2) Sidewalls stable.
- 3) Bulk and foundation indicator samples taken at 1.8--5.0m.
- 4) Test pit excavated to maximum reach of the machine.
- 5) Excavated next to wind turbine position WTG26.

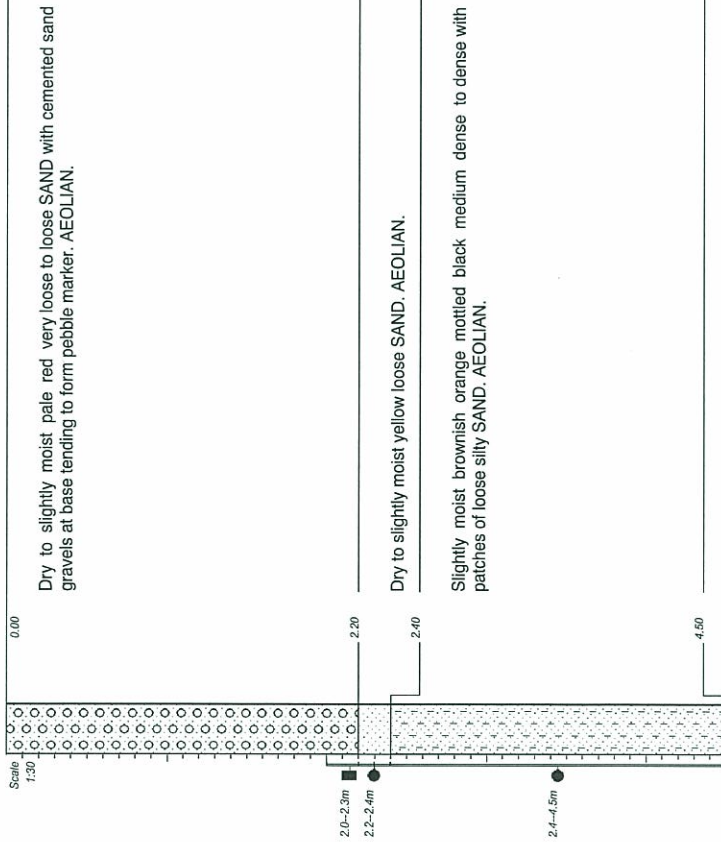
CONTRACTOR: AURET COMPANY
 MACHINE: KOMATSU PC 200-6
 DRILLED BY: F JOSEPH
 PROFILED BY: VS MUASI
 TYPE SET BY: VS MUASI
 SETUP FILE: V.SET

INCLINATION:
 DIAM: TRENCH
 DATE: 02/09/2010
 DATE: 17/11/10 15:52
 TEXT: ..TEXT\PIATEL-1.TXT

ELEVATION:
 X-COORD: 34-J 222799
 Y-COORD: 6510767

HOLE No: T WTG26





Dry to slightly moist pale red very loose to loose SAND with cemented sand gravels at base tending to form pebble marker. AEOLIAN.

Dry to slightly moist yellow loose SAND. AEOLIAN.

Slightly moist brownish orange mottled black medium dense to dense with patches of loose silty SAND. AEOLIAN.

NOTES

- 1) No groundwater seepage encountered.
- 2) Sidewalls unstable in the upper layer.
- 3) Foundation indicator sample taken at 2.2--2.4m and bulk and foundation indicator samples taken at 2.4--4.5m.
- 4) Undisturbed sample taken at 2.0--2.3m.
- 5) Test pit terminated due to sidewalls collapse.
- 6) Logged from the spoil.
- 7) Excavated next to wind turbine position WTG34.

CONTRACTOR: AURET COMPANY
MACHINE: KOMATSU PC 200-6
DRILLED BY: F JOSEPH
TYPE SET BY: VS MUASI
SETUP FILE: V.SET

INCLINATION:
DIA: TRENCH
DATE: 30/08/2010
DATE: 17/11/10 15:52
TEXT: ...TEXT\PIATEL-1.TXT

ELEVATION:
X-COORD: 34-J 225580
Y-COORD: 6509300

HOLE No: T WTG34



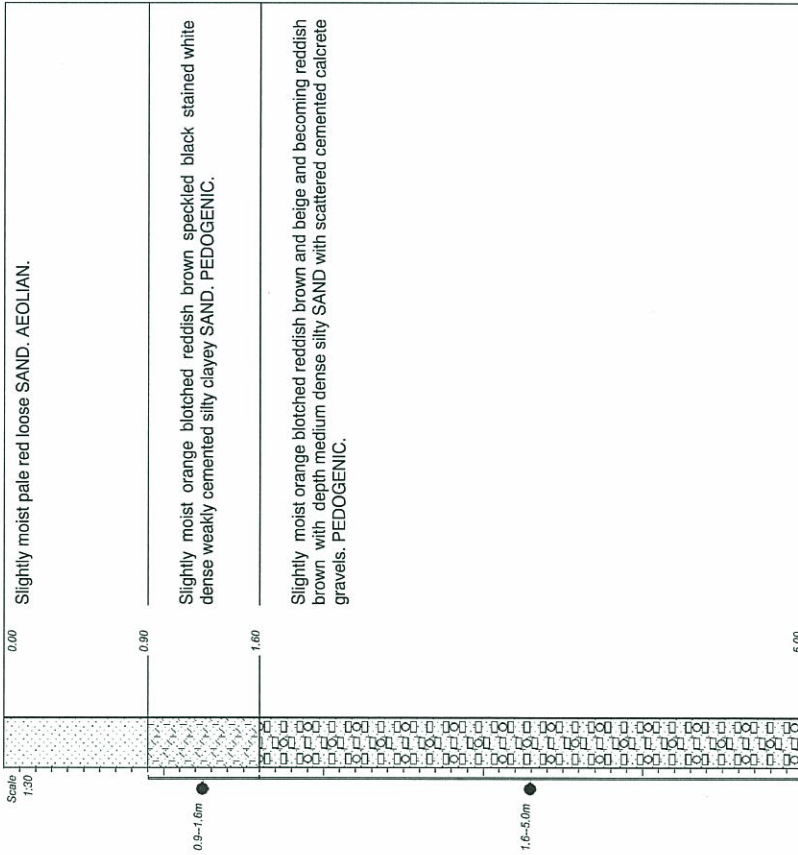
BKS Palace Consortium



ESKOM
SERE WIND ENERGY FACILITY
WIND TURBINE POSITION

HOLE No: T WTG41
Sheet 1 of 1

JOB NUMBER: J01386



NOTES

- 1) No groundwater seepage encountered.
- 2) Sidewalls stable.
- 3) Bulk and foundation indicator samples taken at 0.9--1.6m and 1.6--5.0m.
- 4) Test pit excavated to maximum reach of the machine.
- 5) Excavated next to wind turbine position WTG41.

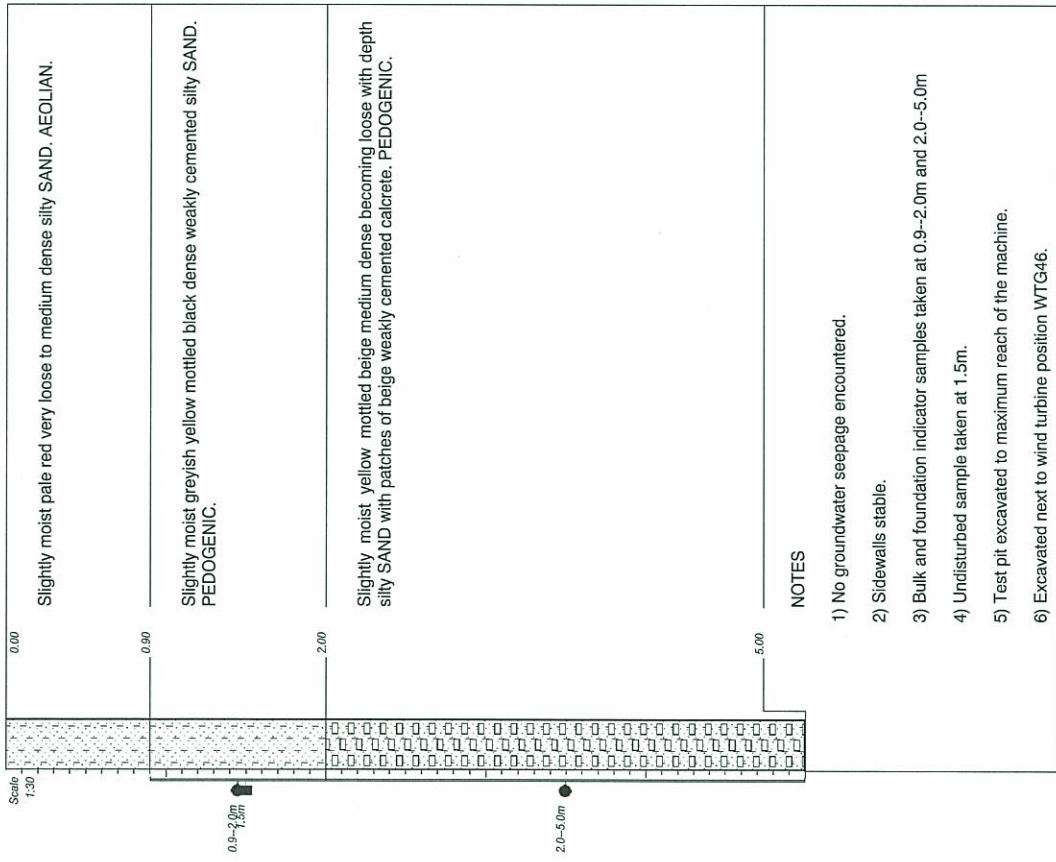
CONTRACTOR: AJURET COMPANY
MACHINE: KOMATSU PC 200-6
DRILLED BY: F JOSEPH
PROFILED BY: VS MUASI
TYPE SET BY: VS MUASI
SETUP FILE: V.SET

INCUMINATION:
DIAM: TRENCH
DATE: 03/09/2010
DATE: 17/11/10 15:52
TEXT: ..\TEXT\PLATE1-1.TXT

ELEVATION:
X-COORD: 34 J 223831
Y-COORD: 6511990

HOLE No: T WTG41





NOTES

- 1) No groundwater seepage encountered.
- 2) Sidewalls stable.
- 3) Bulk and foundation indicator samples taken at 0.9-2.0m and 2.0-5.0m
- 4) Undisturbed sample taken at 1.5m.
- 5) Test pit excavated to maximum reach of the machine.
- 6) Excavated next to wind turbine position WTG46.

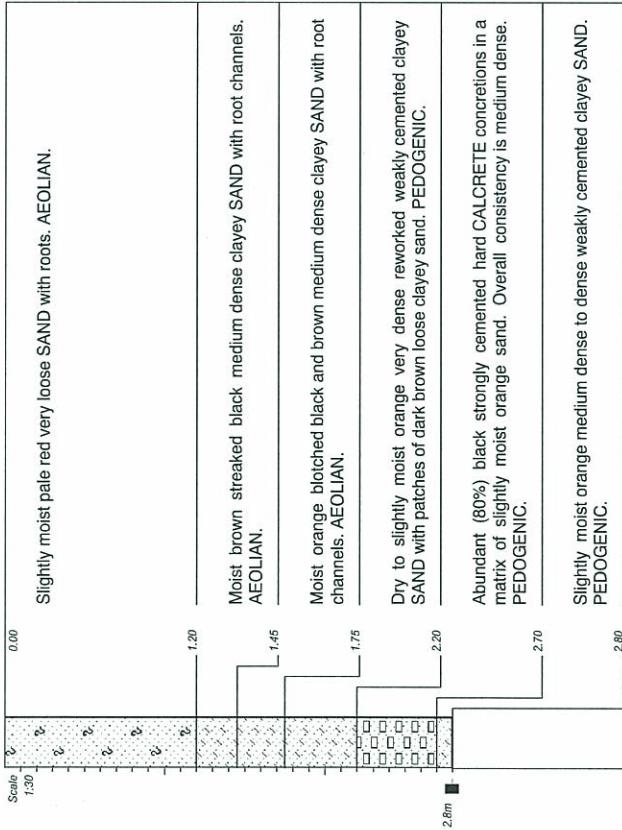
CONTRACTOR: **AURET COMPANY**
 MACHINE: **KOMATSU PC 200-6**
 DRILLED BY: **F JOSEPH**
 PROFILED BY: **VS MUJASI**
 TYPE SET BY: **VS MUJASI**
 SETUP FILE: **V.SET**

INCLINATION:
 DIAM: **TRENCH**
 DATE: **30/08/2010**
 DATE: **17/11/10 15:52**
 TEXT: **..TEXT\PLATEL-1.TXT**

ELEVATION:
 X-COORD: **34 J 225889**
 Y-COORD: **6510743**

HOLE No: **T WTG46**





NOTES

- 1) No groundwater seepage encountered.
- 2) Sidewalls stable.
- 3) Undisturbed samples taken at 2.8m.
- 4) Vertical and horizontal plate load tests done at 2.1m and 2.5m respectively.

CONTRACTOR: AURET COMPANY	INCLINATION:	ELEVATION:
MACHINE: KOMATSU PC 200-6	DIAM: TRENCH	X-COORD: 34 J 226746
DRILLED BY: F. JOSEPH	DATE: 04/08/2010	Y-COORD: 6505119
PROFILED BY: WS van der Merwe	DATE: 09/11/10 08:37	HOLE No: T WTG 4
TYPE SET BY: WS van der Merwe	TEXT: ...TEXT\PLATE1-1.TXT	
SETUP FILE: V.SET		



APPENDIX I:
SEISMIC REFRACTION AND ELECTRICAL RESISTIVITY

MULTI-CHANNEL ANALYSIS OF
SURFACE WAVES, SEISMIC
REFRACTION AND ELECTRICAL
RESISTIVITY IMAGING ON
TURBINE SITES.

SERE WIND ENERGY FACILITY,
LUTZVILLE,
SOUTH AFRICA

Report for

BKS (Pty) Ltd

BKS (Pty) Ltd
Block D, Hatfield Gardens
333 Grosvenor Street, Hatfield
PRETORIA, 0083

BKS Representative: Mr Ron Tluczek

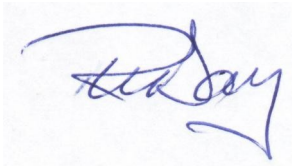
Dear Mr Tluczek,

**RE: MULTI-CHANNEL ANALYSIS OF SHEAR WAVES SURVEY, SEISMIC REFRACTION
AND ELECTRICAL RESISTIVITY IMAGING (TURBINE SITES)
SERE WIND ENERGY FACILITY, WEST COAST, SOUTH AFRICA**

E&EGS are pleased to present this report for the geophysical surveys carried out near Lutzville, on the west coast of South Africa. These surveys were carried out as part of geotechnical investigations of turbine sites for the proposed Sere Wind Energy Facility.

If you have any questions in relation to the report, or if we can be of further assistance, please do not hesitate to contact the undersigned.

Yours sincerely,



RICHARD DAY

Distribution:

Original held by E&EGS CC
1 digital copy BKS Group Pty Ltd

1 SUMMARY

In July 2010, E&EGS CC was contracted by BKS Group (Pty) Ltd (BKS) to conduct Multi-channel Analysis of Shear Waves (MASW), Seismic Refraction, and Electrical Resistivity Imaging (ERI) surveys at the Sere Wind Energy Facility near Lutzville South Africa. Field work commenced on the 31st July and completed by the 2nd October, including the time used to collect data at potential borrow pit sites.

Based on drilling information provided by BKS, site geology comprises variably sand, silty sand, clayey sand, sandstone, quartzite and phyllite, the latter two being regarded as bedrock.

The objective of the geophysical survey was to measure in-situ physical properties, namely P-wave velocity, S-wave velocity and electrical resistivity, at fifty potential turbine sites. Estimates of shear wave velocity were required to a depth of 50m. To achieve this it was necessary to conduct multiple MASW surveys at each site with different source and receiver geometries, and with the application of an additional technique, refraction micro-tremor (ReMI). Seismic refraction data gathered at the same time as the shear wave measurements and ERI data provides images of near surface and deeper changes in rock properties, as well as near-surface resistance measurements for electrical grounding calculations.

The three data-sets (MASW/ReMi, seismic refraction and ERI) usually exhibit a high degree of correlation between each other and to the lithology. Exceptions to this appear in the refraction data; in some instances the pressure wave velocity does not vary in a fashion as would be predicted from the MASW/ReMi data, instead being faster than expected perhaps because of moisture within the overburden matrix.

Whilst a degree of caution should be taken when using p-wave refraction velocities, on the basis of the this high degree of correlation between different geophysical techniques as demonstrated by the data synthesis sections, a high degree of confidence can be assumed when using the derived physical properties for further geotechnical engineering and design.

2 Table of Contents

1Summary.....	3
2Table of Contents.....	4
3Introduction.....	5
4Survey Methodology	8
5Results and Interpretation.....	12
6Results and Interpretation.....	13
7Disclaimer.....	14
8References.....	14
9Appendix A: ERI and Refraction with MASW overlain.....	15
10Appendix B: ERI with drillholes overlain.....	16

3 Introduction

In July 2010, E&EGS CC (E&EGS) was contracted by BKS Group Pty Ltd (BKS) to conduct Multi-channel Analysis of Shear Waves (MASW), Seismic Refraction, and Electrical Resistivity Imaging (ERI) surveys at the Sere Wind Energy Facility near Lutzville South Africa.

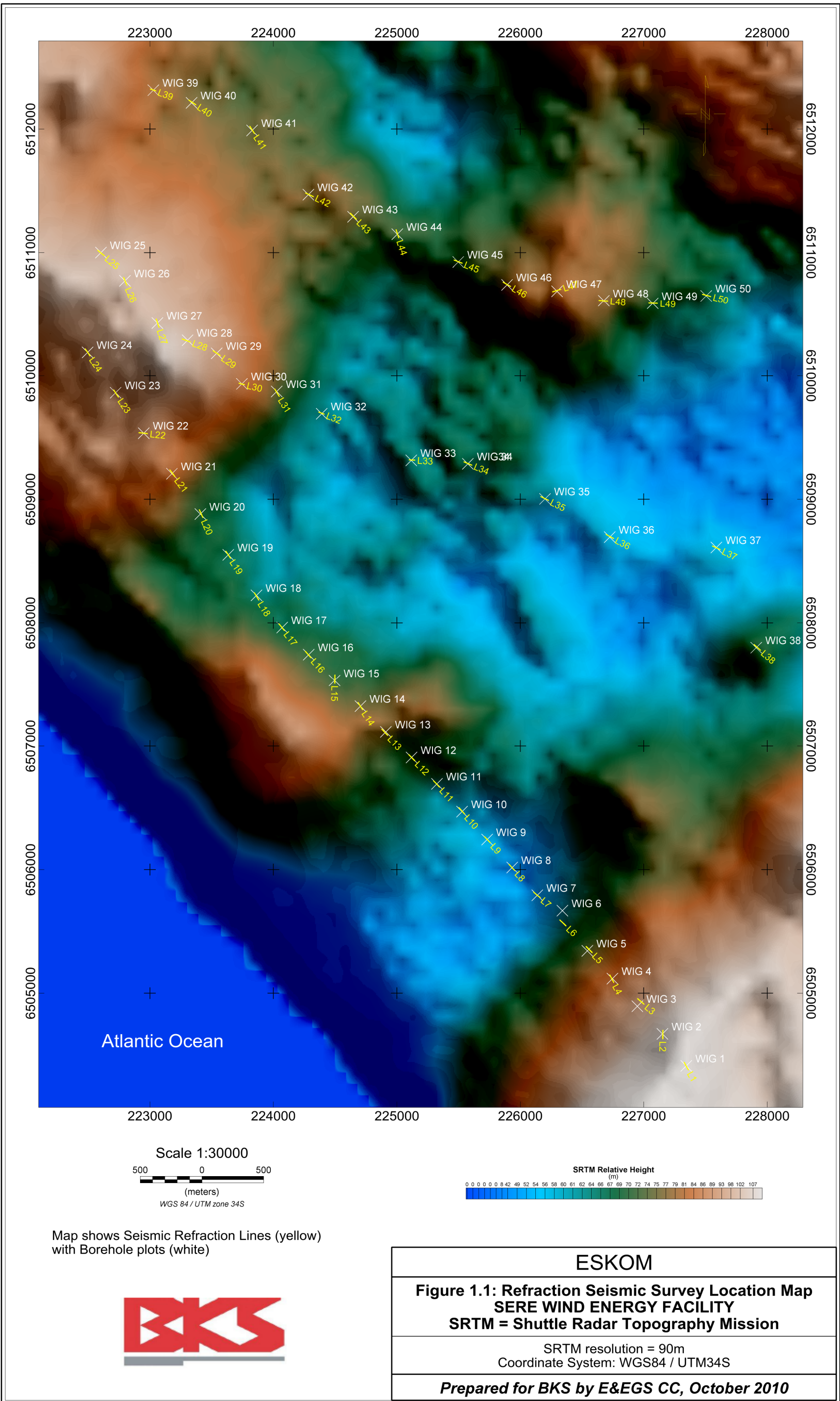
Based on drilling information provided by BKS, site geology consists of sand, silty sand, clayey sand, sandstone, quartzite and phyllite. The latter two are regarded as bedrock whilst the various sands constitute overburden. Bedrock is commonly at great depth; many of the boreholes drilled to a depth of 50m and more failed to intersect either phyllite or quartzite.

The objective of the geophysical survey was to measure in-situ physical properties, namely P-wave velocity, S-wave velocity and electrical resistivity, at fifty potential turbine sites. Estimates of shear wave velocity were required to a depth of 50m. To achieve this it was necessary to conduct multiple MASW surveys at each site with different source and receiver geometries, and with the application of an additional technique, refraction micro-tremor (ReMi). Seismic refraction data gathered at the same time as the shear wave measurements and ERI data provides images of near surface and deeper changes in rock properties, as well as near-surface resistance measurements for electrical grounding calculations.

Data collection commenced at the end of July with the collection of ERI data. Seismic work did not start until the late August due to delays in the shipping of new cables and geophones ordered especially for this work. Data collection was completed at the beginning of October when a break was taken whilst the potential borrow-pit positions were identified. Work on the borrow pits commenced on the 14th and was completed at the end of the month. The field crew demobilised by the 2nd October.

MASW, ReMi, seismic refraction and ERI data were collected at each of the fifty sites. MASW and ReMi spreads were deployed such that the centre of the receiver array coincided with boreholes or as close as could be practically achieved, however, it was found that survey orientations had to be altered sometimes to enable the best compromise in terms of acquiring data of the greatest possible quality so that, for example, full advantage was taken of background energy sources (e.g. ocean swell) suitable for the ReMi survey technique. Resistivity lines were also collected along the three rows of turbine sites.

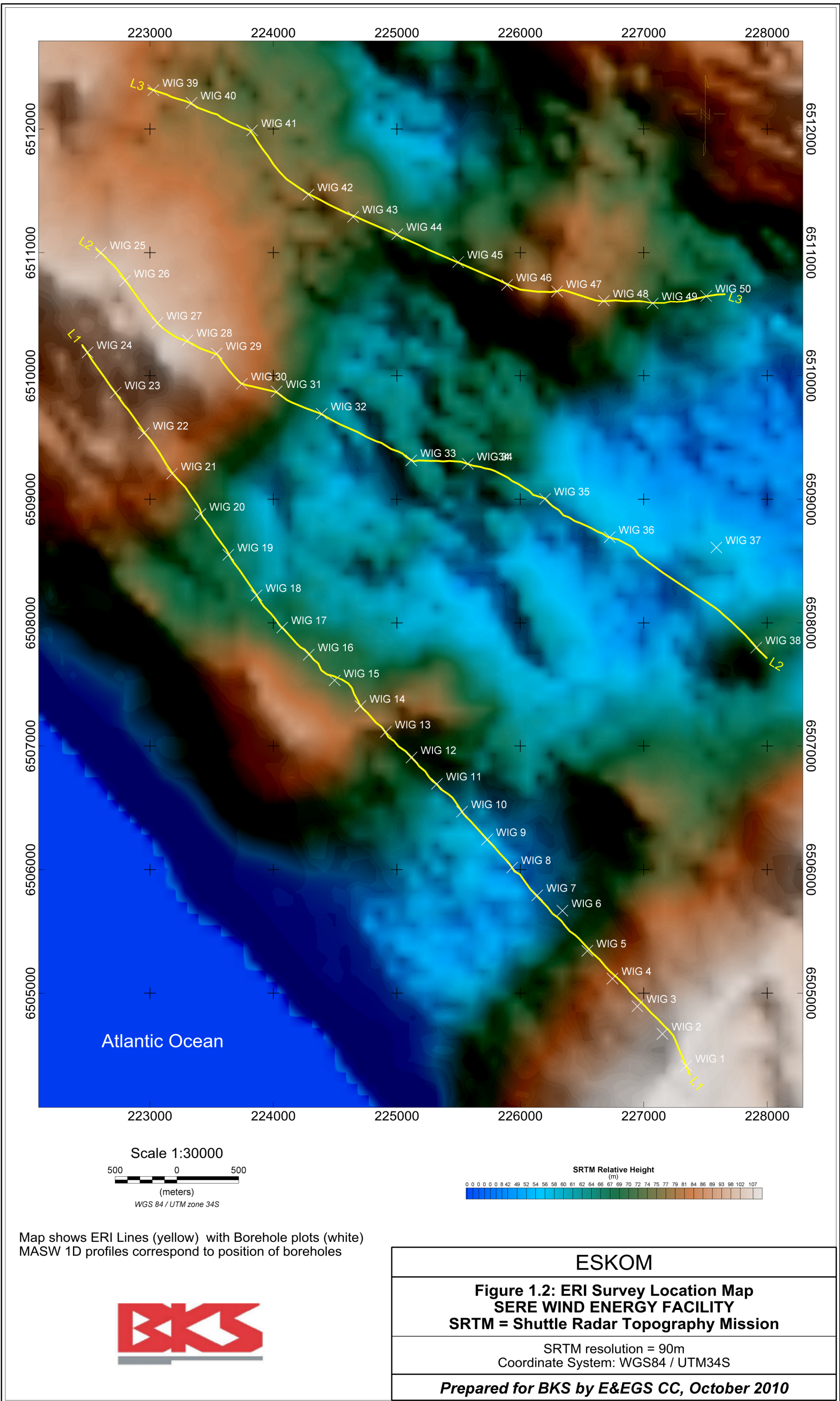
The locations of the survey lines are shown in Figure 1.1 and Figure 1.2.



Map shows Seismic Refraction Lines (yellow) with Borehole plots (white)



ESKOM
Figure 1.1: Refraction Seismic Survey Location Map SERE WIND ENERGY FACILITY SRTM = Shuttle Radar Topography Mission
SRTM resolution = 90m Coordinate System: WGS84 / UTM34S
<i>Prepared for BKS by E&EGS CC, October 2010</i>



4 Survey Methodology

The following sections provide a brief explanation of the techniques used for sub-surface imaging at the Sere Wind Energy Facility sites.

4.1 *Multi-Channel Surface Analysis of Surface Waves*

The MASW technique records surface (Rayleigh) wave energy generated using a nearby acoustic source using a linear array of receivers. A dispersion curve (phase velocity versus frequency), generated from the acquired field data using a phase velocity transform, is then inverted and used to generate a 1-D shear wave velocity profile that is generally assigned to the physical centre of the receiver array.

In order to acquire optimal data over the required depth range for the Sere Wind Energy Facility sites, it was found that two survey geometries needed to be deployed at each site as outlined in Table 1.

Advantages of the method include the following:

- The technique is unaffected by the absence or presence of ground water, due to the inability for shear wave energy to propagate through a liquid. Thus measured velocities using the MASW technique are a true representation of the shear wave velocity structure. This is in contrast to seismic refraction where the presence of groundwater can obscure the true compressional wave velocity of the rock matrix.
- Due to the simultaneous recording of multiple receivers, the technique has statistical redundancy to enable the accurate measurement of shear wave velocity in the presence of high levels of background acoustic noise.
- The technique is capable of resolving complex geological structure, in particular, situations where velocity inversions are encountered .

Limitations of the method include the following:

- The technique assumes lateral heterogeneity over the receiver array and as such interpreted velocities may be anomalous if significant dip is encountered.
- The minimum depth of investigation is controlled by the shortest wavelength which is directly related to the geophone spacing used. Conversely, the maximum depth of investigation is controlled by the longest wavelength (lowest frequency) which can be recorded. Thus the receiver array geometry must be a compromise between these two constraints to trade off shallow high spatial resolution against acquiring reliable velocity estimates to depth.
- The depth of investigation (both shallow and deep) is also dependent on the frequency bandwidth generated by the seismic source (a function of the type of source and local ground conditions) and the frequency bandwidth detected by the receiver array.

Table 1. – **MASW acquisition parameters**

Instrumentation	Geometrics Geode 24 channel seismograph
Survey spread	Either 2m or 3m spacing depending on the background noise
Source type	Variable - hammer (2m) and weight drop (3m)
Station interval	1D profiles – therefore not applicable
Measurement window	2 seconds
Sample interval	250 microseconds
Data positioning	As per BKS collar locations for wind farm site geotechnical drill holes

4.2 Refraction Micro-tremor

The Refraction Micro-tremor (ReMi) method, like MASW, utilises surface (Rayleigh) wave energy generated from background passive acoustic source, which is recorded at predetermined receiver locations, in this case for the Sere Wind Energy Facility, over intervals of 10m. (For 'passive' read sources both natural and artificial sound sources at a distance from the array that, incidentally, are not used to trigger the recording of the data.) A dispersion curve is picked in the phase velocity verses frequency domain which is then inverted and used to generate a 1-D shear wave velocity profile generally “tied” to the physical centre of the receiver array.

ReMi data has a slightly lower spatial resolution than the MASW technique due to the longer wavelengths of surface wave energy being recorded. However, it provides information at the lower end of the frequency spectrum which in turn provides information regarding the velocity structure at greater depths often down to 80-100m. Typical sources suitable for ReMi acquisition include car travelling over speed bumps, haul trucks, earthmoving equipment, large weight drops and ocean swell.

For the purpose of subsurface profiling at the Sere Wind Energy Facility, where sufficient background acoustic energy was present for the ReMi technique to function effectively, MASW and ReMi data were combined and then inverted together to provide 1-D shear wave velocity (V_s) profiles from surface to the target depth of 50m.

For the purpose of subsurface profiling at the Sere Wind Energy Facility ReMi survey parameters used during the survey are listed in Table 2 below.

Table 2. – **Refraction Micro-tremor acquisition parameters**

Instrumentation	Geometrics Geode 24 channel seismograph
Survey spread	24 geophones at 10m spacing
Measurement window	40 seconds
Sample interval	1 millisecond
Data positioning	As per BKS collar locations for wind farm site geotechnical drill holes

4.3 Seismic Refraction

The seismic refraction method is based on the measurement of the travel time of seismic waves refracted at the interfaces between subsurface layers of different velocity. For shallow applications seismic energy is provided by a source which normally comprises a hammer and plate or weight drop located on the surface. Shots are deployed at regular intervals along the length of the receiver array, and at and beyond both ends of the geophone spread in order to acquire refracted energy as first arrivals at each geophone position.

Energy radiates out from the shot point, either travelling directly through the upper layer (direct arrivals), or travelling down to and then laterally along higher velocity layers (refracted arrivals) before returning to the surface. This energy is detected on surface using a linear array (or spread) of geophones spaced at regular intervals.

The data is digitally acquired and computer processed using a seismic refraction tomography approach that allows imaging of subsurface velocity structure including faults, strong lateral velocity variation and other velocity anomalies. The smooth tomographic inversion method applied to the data iteratively modifies velocities in the model on the basis of the misfit between observed and calculated travel times generated in the forward model.

The main limitations in determining these parameters from seismic refraction surveys are:

- Low signal-to-noise ratios owing due to cultural noise, wind noise, rain, or other local sources of vibrations that restrict the depth of investigation of hammer source surveys to approximately 30 metres or less.
- Lateral resolution provided by one spread is governed by the geophone spacing. Vertical resolution of a stratum requires that it have a thickness that is a substantial fraction of the depth to surface.
- Hidden (seismic) layers may exist. The seismic refraction method requires that seismic velocity increases with depth. It is not possible to resolve a low velocity layer beneath a high velocity layer. In addition a thin layer with respect to depth may be overlooked if there is an insufficient velocity contrast between it and the layer beneath it.

For the purpose of subsurface profiling at the Sere Wind Energy Facility refraction survey parameters used during the survey are listed in Table 3 below.

Table 3. – Seismic refraction acquisition parameters

Instrumentation	Geometrics Geode 24 channel seismograph
Survey spread	24 geophones
Shot offset and source	-16m, -1m, 16½m, 34½m, 52½m, 70m and 85m (hammer)
Station interval	3m
Measurement window	0.2 seconds
Sample interval	250 microseconds
Data positioning	As per BKS collar locations for turbines (boreholes)

4.4 Electrical Resistivity Imaging

An ABEM Lund resistivity meter was used to collect the resistivity data. Resistivity measurements are obtained by injecting a current into the ground through two electrodes and measuring the resulting potential between another electrode pair. By systematically increasing the electrode separation in a fashion otherwise known as a vertical electrical sounding, a picture is obtained of resistance variations with depth. A set of adjacent soundings is known as a continuous vertical electrical sounding (CVES) and such a data set provides a resistivity image or cross section of the ground. The ABEM system automates the collection of such data set by accessing multiple electrodes through a multicore cable.

The maximum depth of investigation is determined by the spacing between the electrodes and the number of electrodes in the array. For an 80 electrode array with an electrode spacing of 10m as used on the three long traverses the depth is approximately 100m.

The field (apparent resistivity) data for the long traverses was modelled using RES2DINV, a commercial package that iteratively fits a model to the observed data. The detailed work carried out for the grounding-mat design is summarised into tables. The summaries give average apparent resistivity values (ρ) for each electrode separation and resistance values (R) calculated using the relationship $\rho = 2naR$, where 'a' is the electrode separation.

A summary of the acquisition parameters is displayed in Table 4

Table 4. – ERI acquisition parameters

Instrumentation	ABEM SAS1000 with an ES10-64 switch box
Survey configuration	80 electrodes (stainless steel) @ 10m spacing or ½m for the detailed work at each turbine site.
Array type	2D (Wenner)

5 Results and Interpretation

5.1 Data Quality

Overall, data quality for the seismic techniques (MASW, ReMi and seismic refraction) was good although wind-generated noise resulted in some degradation during the refraction acquisition program. Repeats of some of the survey lines were carried out to improve data quality. After successful completion of the affected site, first arrivals could be confidently picked for all shots.

Data quality for the ERI surveys was reasonable but due to significant heterogeneity both laterally and vertically, the section plots presented in Appendix A and Appendix B appear patchy. Limitations of the inversion package used to process the data may have contributed to some of the artefacts present in the sections, however, in general the sections correlate with the results from the seismic survey, suggesting that most of the complexity observed in the ERI data can be attributed to genuine changes in ground resistivity. Additionally, the Wenner array used for the ERI surveys is optimally suited to resolve vertical variations in resistivity such as horizontal bedding, as was expected on the site, but is less capable in accurately mapping horizontal changes, for example vertical pillar like structures.

5.2 Data Display

All shear wave data sets were mapped to a maximum depth of 50m, the proposed depth of investigation. The maximum depth of statistically significant ray path coverage achieved with individual refraction lines were used to define the maximum depth extent for display of pressure wave data over the length of each geophone array. Shear velocity profiles are provided in ASCII format (Excel Spreadsheets) as well as in colour scale down-hole logs plotted over both the ERI and refraction data as shown in Appendix A. The ERI with lithology (for currently available drill hole information) is given in Appendix B.

For each row of the proposed wind turbine sites, cross-section data is displayed in sections of approximately 1000 m to eliminate the need to apply disproportionate vertical exaggeration to the plots. These figures are presented with line distance along the upper X-axis and WGS84 Zone 34S Easting or Northing coordinates along the lower X-axis. The elevation (relative RL) is annotated on the Y-axis using elevations derived from Shuttle Radar Topography Mission (SRTM).

The data sets are coloured as follows:

- Shear Velocity (V_s) is coloured in such that faster V_s are warmer colours (yellows through reds) and slower V_s are cooler colours.
- P-wave (V_p) velocity is coloured such that faster V_p are warmer colours (yellows through reds) and slower V_p are cooler colours.
- ERI data (resistivity) is coloured such that more resistive layers are warmer colours (yellows through reds) and areas of lower resistivity are cooler colours.

6 Results and Interpretation

6.1 MASW and ReMi

As a general guide, typical shear wave velocities for lithologies known to be present from geotechnical drilling at the Sere Wind Energy Facility are (Barton, 2007):

- 100 – 200 m/s Soft unconsolidated sand / silt
- 200 – 400 m/s Weakly to moderately consolidated gravels and sands
- 400 – 600 m/s Weathered rock
- 600 – 1,000 m/s Slightly weathered to competent rock
- > 1,000 m/s Fresh hard rock

The MASW data indicate that for some sites, slower (less stiff layers) can be expected at depths greater than was able to be imaged with the seismic refraction data. The MASW data also demonstrate that harder lithological units may be present at shallow depths, an observation that is corroborated by high resistivity values in the same areas in the ERI sections. Evidence also exists from the MASW and ReMi data that near surface velocity inversions are likely to be present.

The limitations associated with the use of Rayleigh wave frequency-phase velocity dispersion phenomena techniques should be taken into account when this technique is used. In particular, if the thickness of any particular layer is less than the depth to that layer, it will not be resolved, but rather appear as a smooth layer between the overlying and underlying layers.

6.2 Seismic Refraction

The seismic refraction data has demonstrated that harder, more competent lithologies such as sandstone and quartzite are likely to be present in the near surface (less than 20m). The existence of such units is, at some sites, confirmed by a sharp increase in shear wave velocity as derived from MASW / ReMi data. However, in some circumstances this correlation does not exist. The lack of correlation between the two techniques is attributed to differences in the way in which the techniques interact with the environment (for example saturated vs unsaturated ground and its effect on the correlation between p-wave velocity from refraction and s-wave velocity from MASW/ReMi. In this situation the two techniques may demonstrate a high degree of similarity in the dry situation, but have no apparent correlation if the ground is saturated, particularly if the p-wave velocity of the ground is low.

6.3 Electrical Resistivity Imaging

The dominant feature in the ERI data is a four layer geometry, with a high-conductivity layer approximately 10m thick at surface. (A thin resistor blanketing the area is not resolved in these sections but it is clearly visible in the data collected for the mat design.) This correlates well with a similar thickness surface layer in the refraction profiles that is defined by a low p-wave velocity, and is mapped as sand in available borehole data. In many areas there is also a good correlation between low velocities in the MASW/ReMi profiles and the low resistivity in the ERI sections.

Beneath the surface layer, there is a layer that is highly variable in thickness and resistivity. On average this more resistive layer often coincides with silty sand and clayey silt. The lateral heterogeneity may reflect changes in porosity linked to variations in lithology, leading to changes in water content.

Beneath this layer, most of the sections exhibit a second increase in resistivity associated with sand, clayey sand and silt, according to the borehole logs. Finally at the base of the ERI sections, a highly resistive interface is reached which correlates very well with intersections of phyllite, quartzite and sandstone in the drill holes.

7 Disclaimer

The interpretations contained in this report are based on the training and experience of the author and information passed on during the course of the investigation. As with all geophysical data, multiple interpretations are possible. The client is advised to consider information from all available sources prior to making a decision on how to proceed.

8 References

Barton, N., 2007, Rock quality, seismic velocity, attenuation and anisotropy: Taylor & Francis / Balkema.

APPENDIX I:

SEISMIC REFRACTION AND ELECTRICAL RESISTIVITY

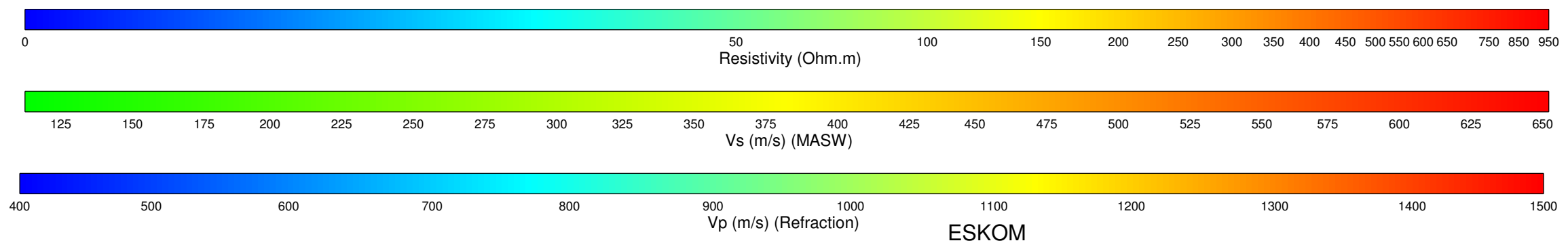
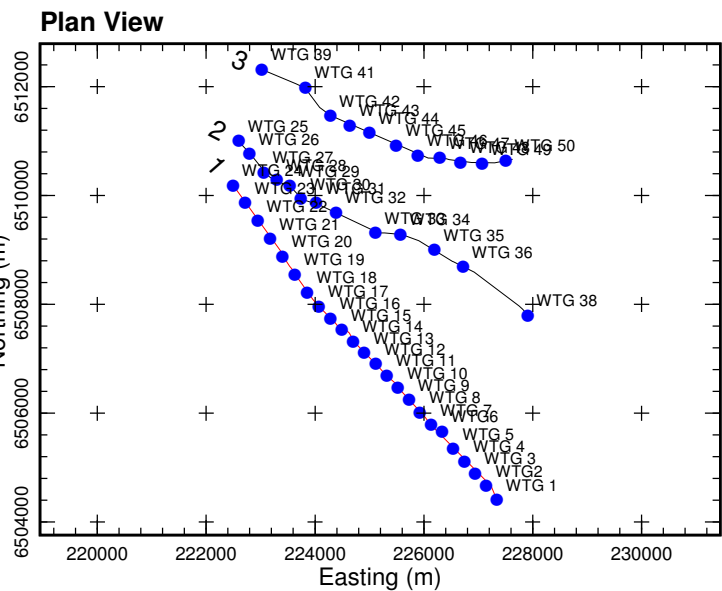
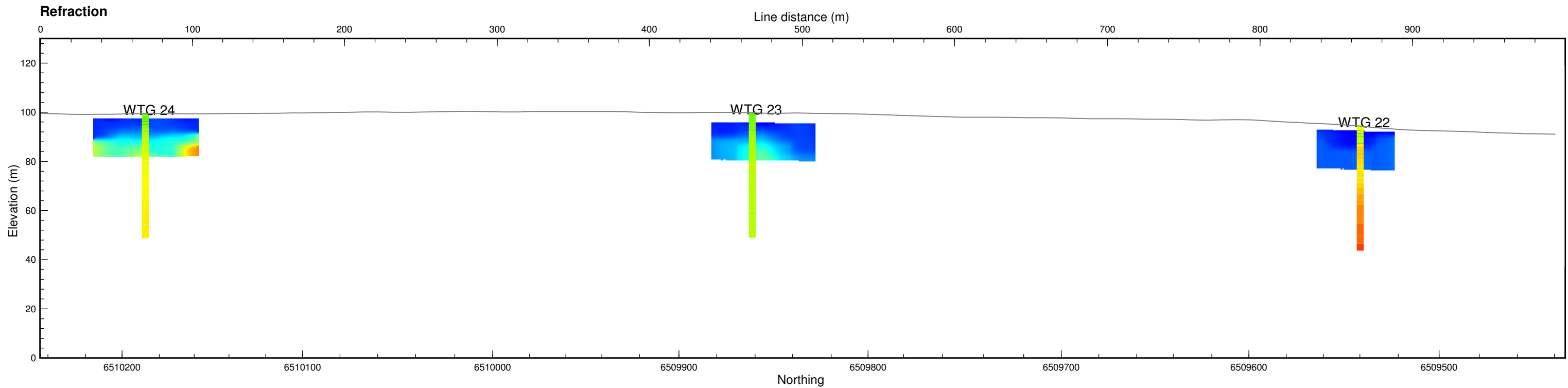
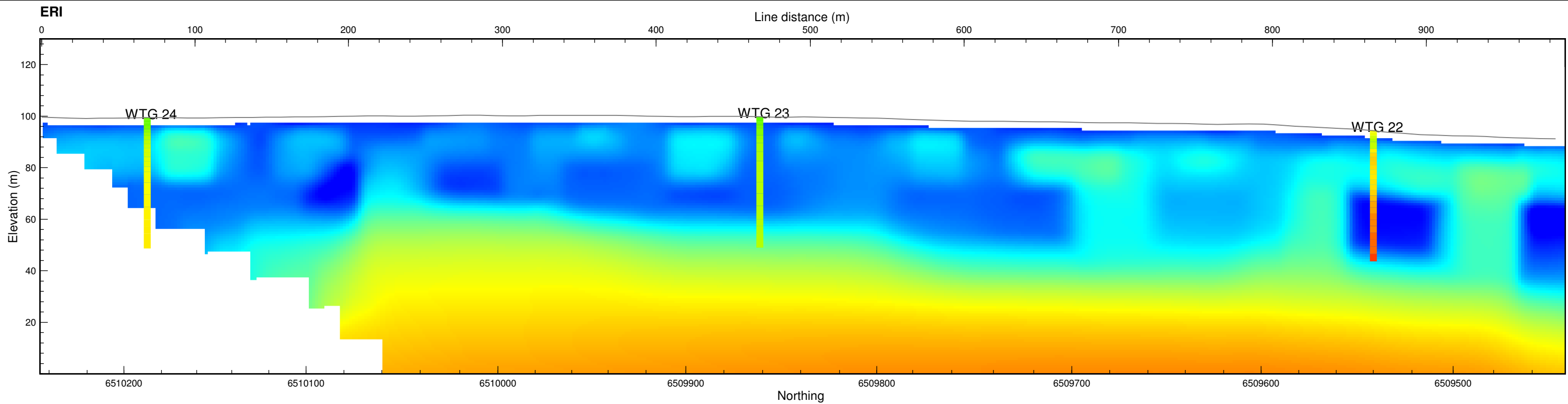
- a) ERI, Refraction with MASW Overlain**
- b) ERI with Boreholes Overlain**

APPENDIX I:

SEISMIC REFRACTION AND ELECTRICAL RESISTIVITY

a (i) ERI, Refraction with MASW Overlain

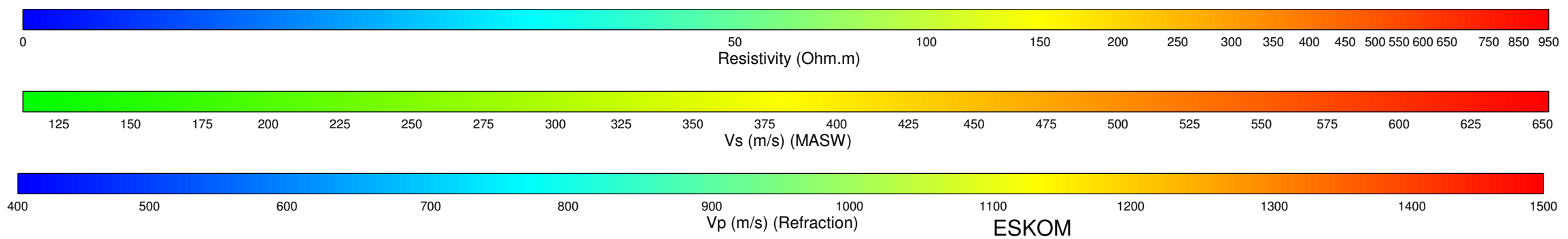
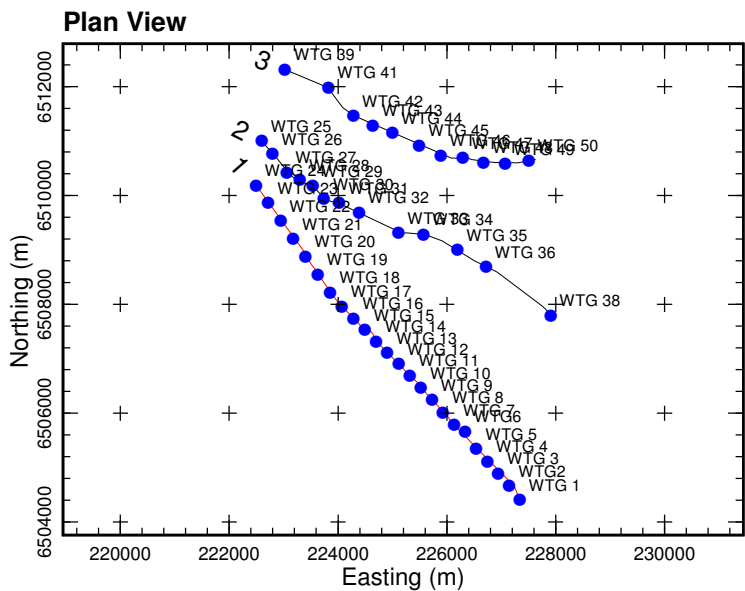
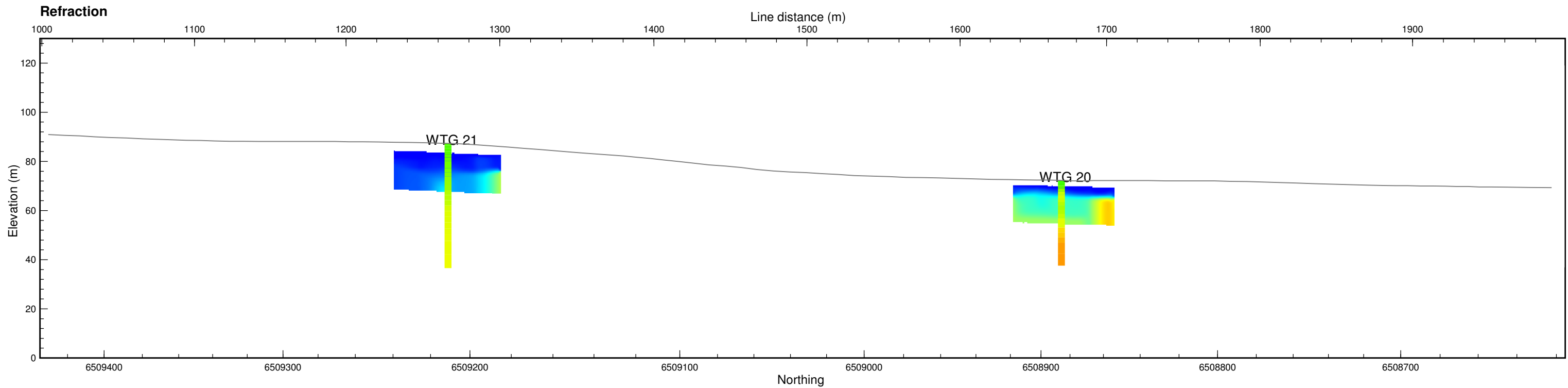
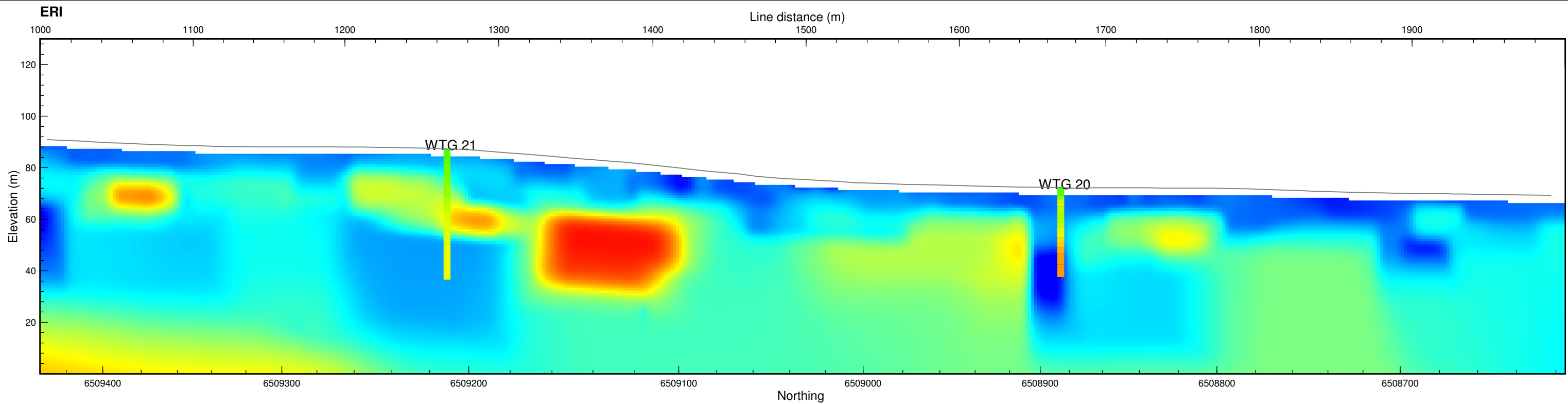
Line 1



Notes:
 Plot 1: ERI pseudosection with MASW data overlain
 Plot 2: Refraction sections with MASW data overlain
 Data displayed in WGS84 zone S34
 Active line displayed in red on plan view

SERE WIND ENERGY FACILITY
 ERI and Refraction with MASW overlain
 Row 1: 0-1000m
 Prepared for BKS by E & EGS

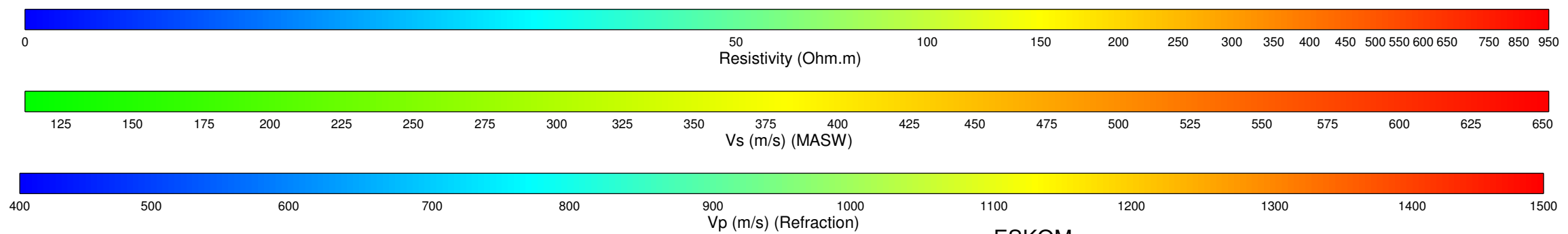
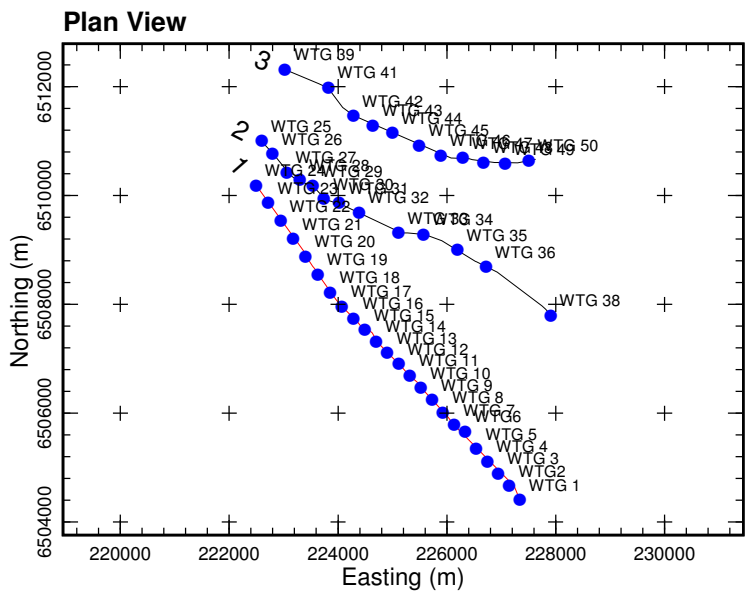
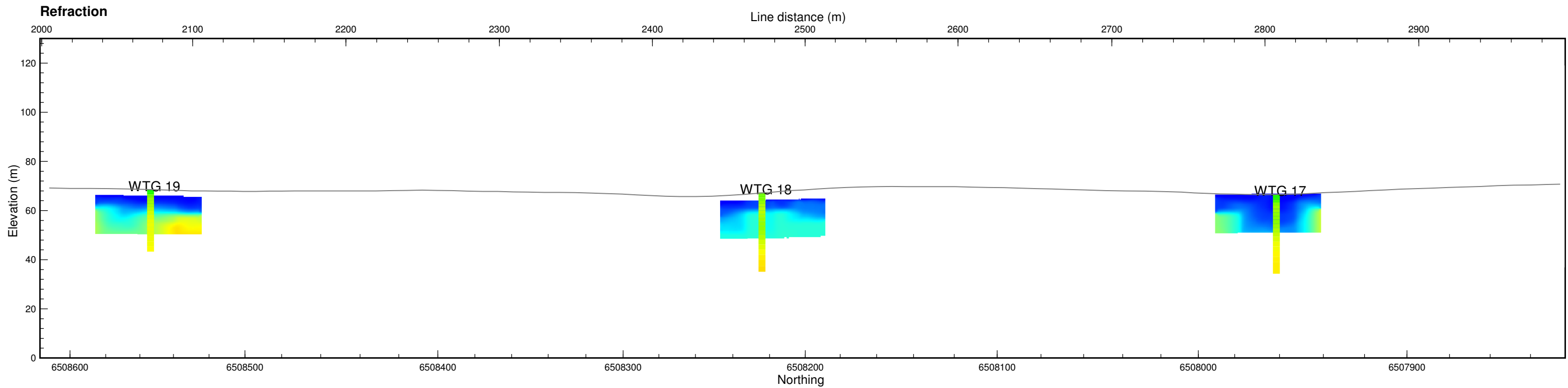
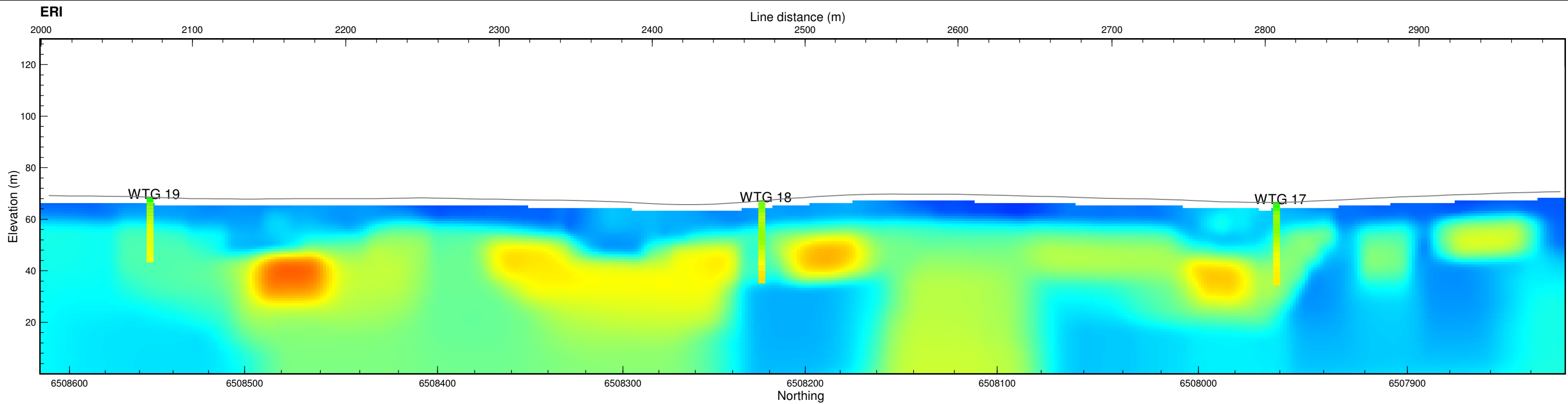




Notes:
 Plot 1: ERI pseudosection with MASW data overlain
 Plot 2: Refraction sections with MASW data overlain
 Data displayed in WGS84 zone S34
 Active line displayed in red on plan view

SERE WIND ENERGY FACILITY
 ERI and Refraction with MASW overlain
 Row 1: 1000-2000m
 Prepared for BKS by E & EGS

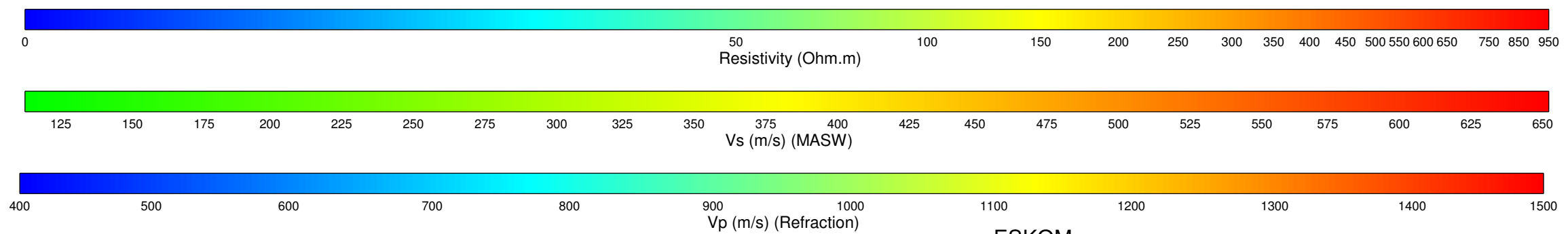
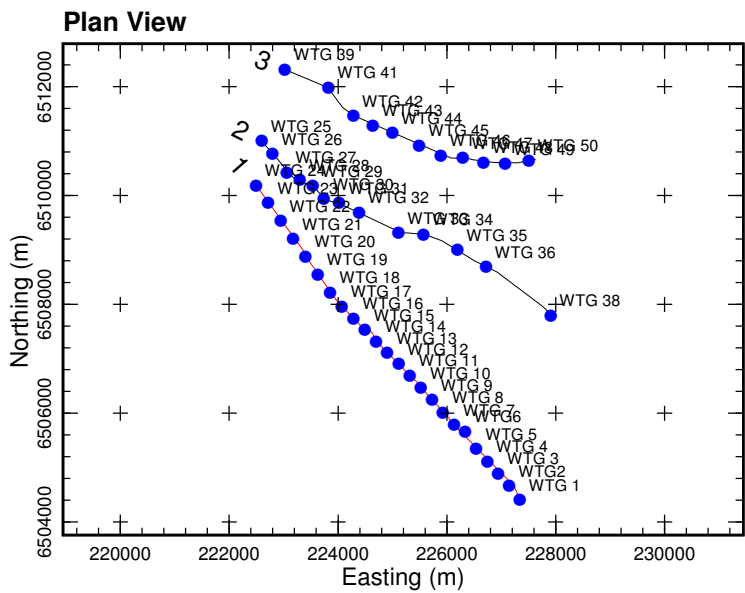
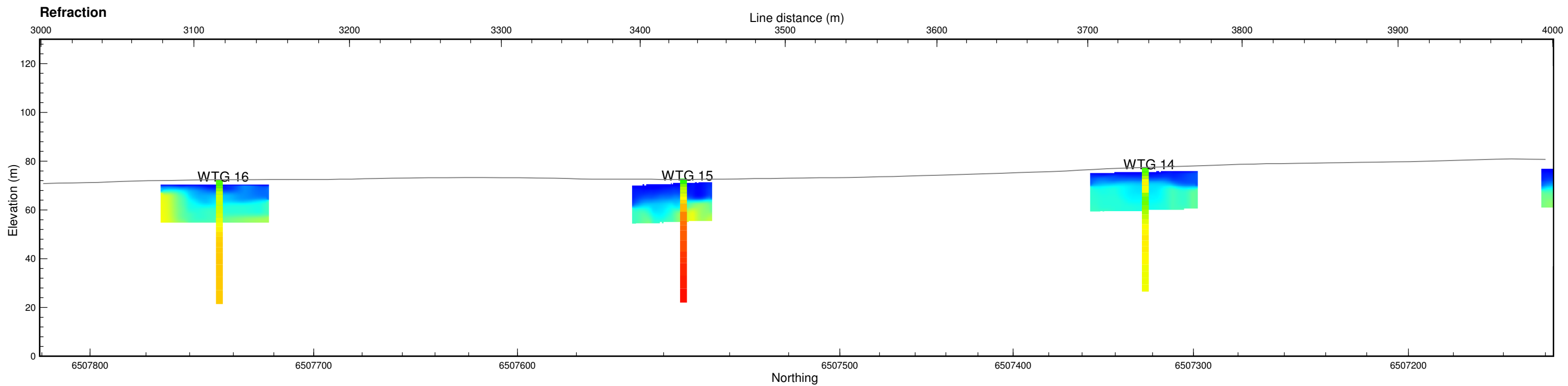
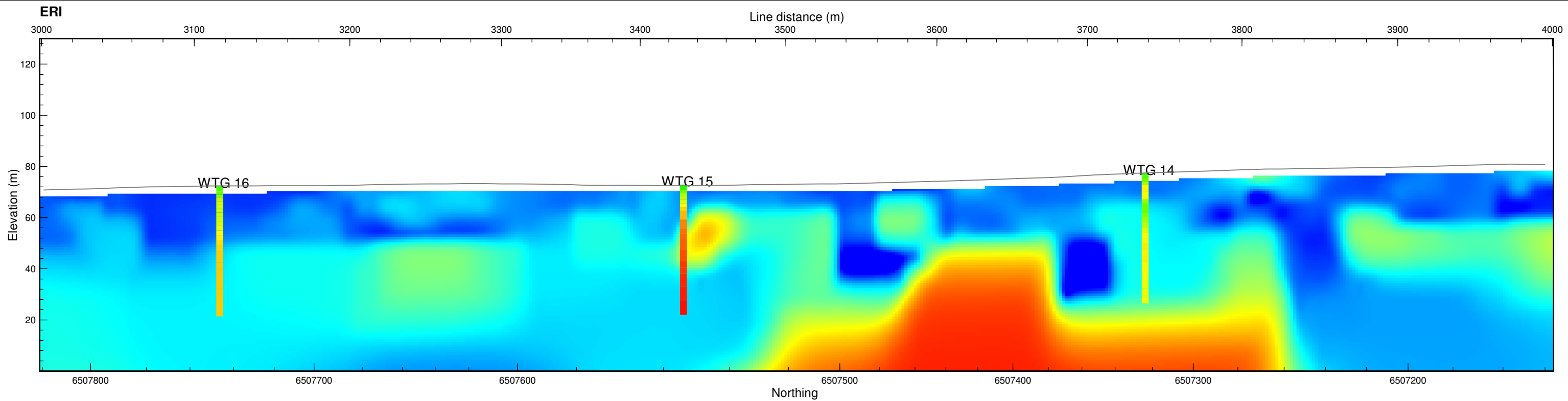




Notes:
 Plot 1: ERI pseudosection with MASW data overlay
 Plot 2: Refraction sections with MASW data overlay
 Data displayed in WGS84 zone S34
 Active line displayed in red on plan view

ESKOM
 SERE WIND ENERGY FACILITY
 ERI and Refraction with MASW overlay
 Row 1: 2000-3000m
 Prepared for BKS by E & EGS

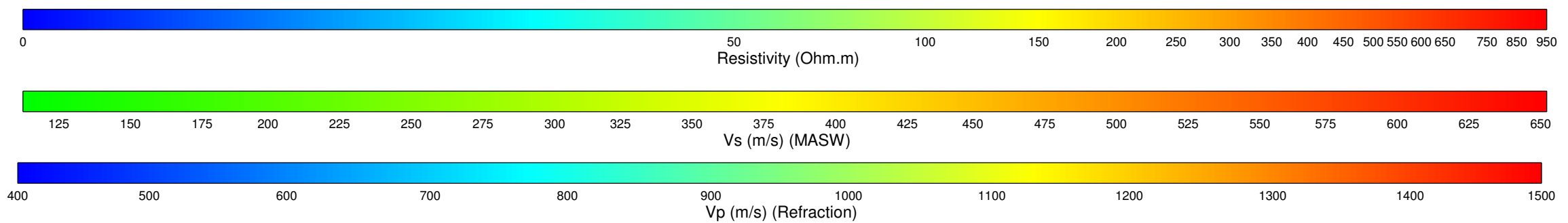
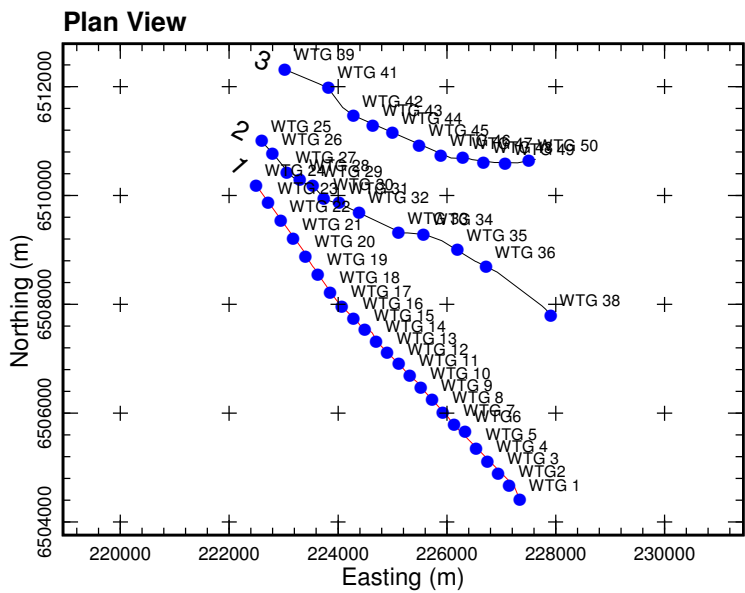
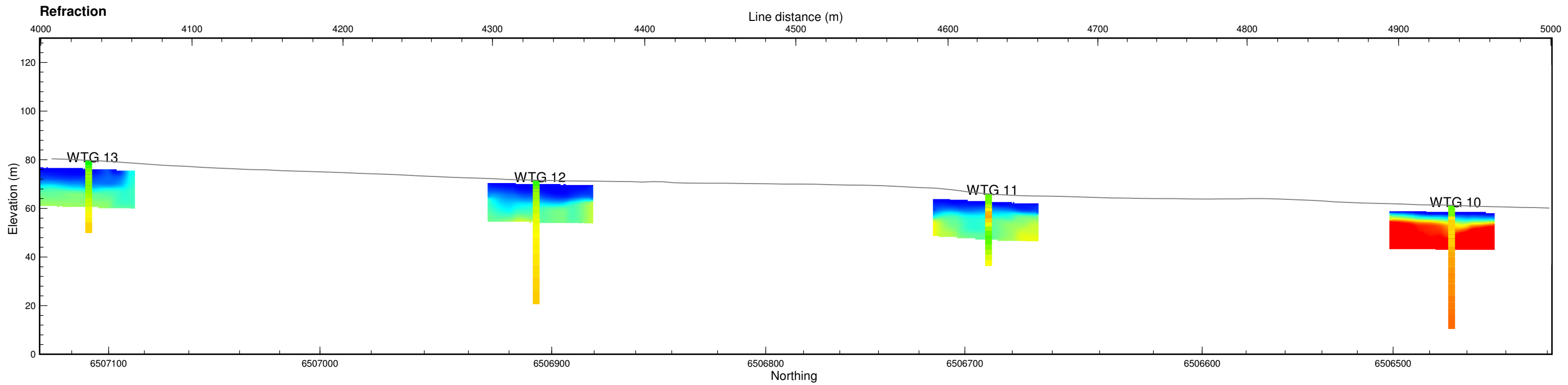
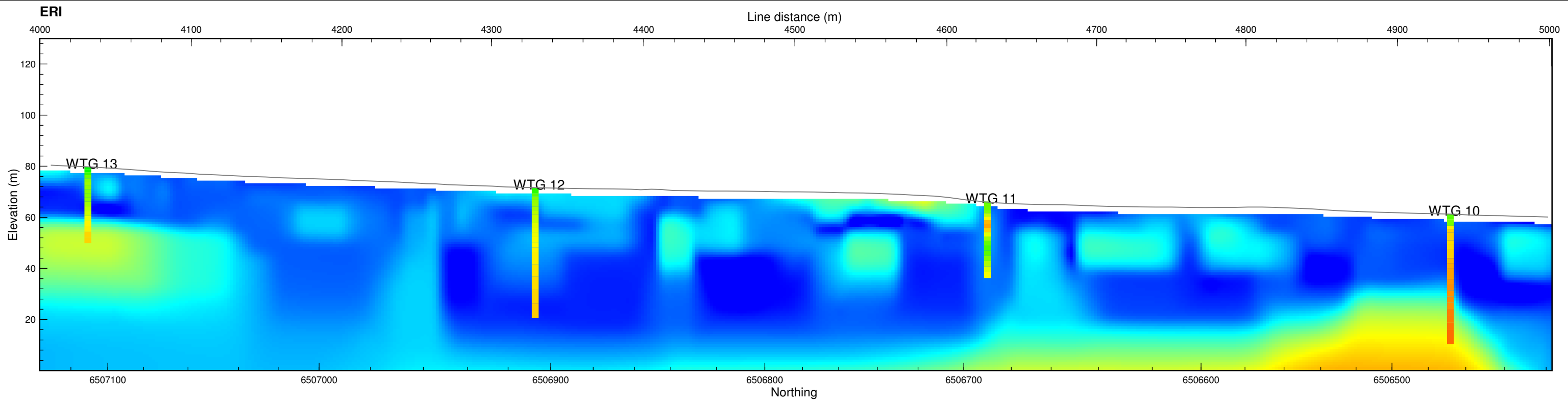




Notes:
Plot 1: ERI pseudosection with MASW data overlay
Plot 2: Refraction sections with MASW data overlay
Data displayed in WGS84 zone S34
Active line displayed in red on plan view

ESKOM
SERE WIND ENERGY FACILITY
ERI and Refraction with MASW overlay
Row 1: 3000-4000m
Prepared for BKS for E & EGS

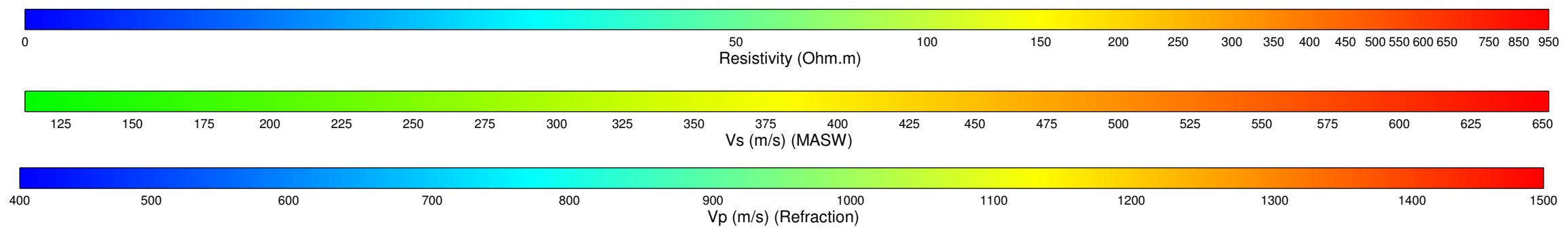
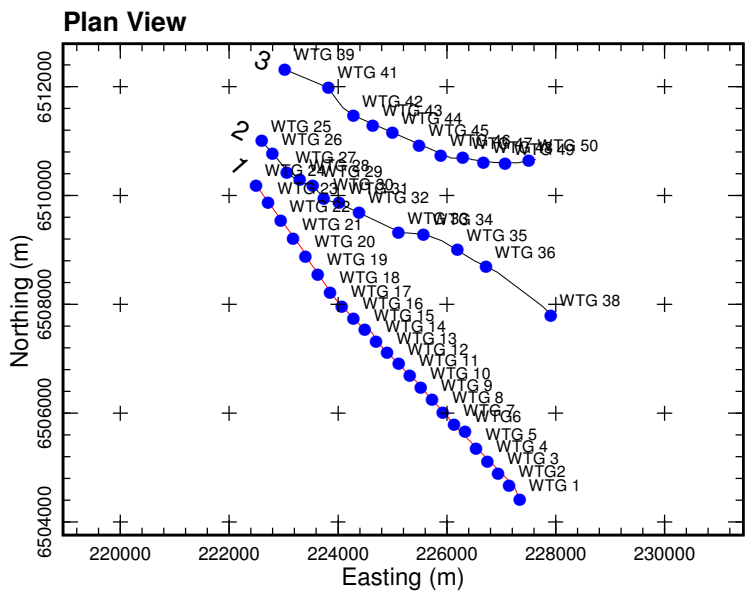
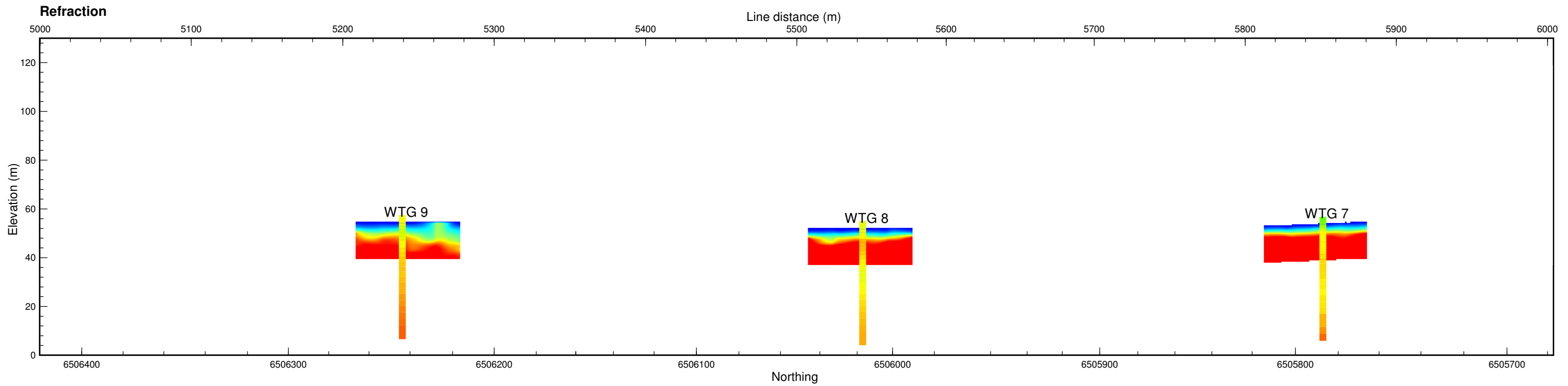
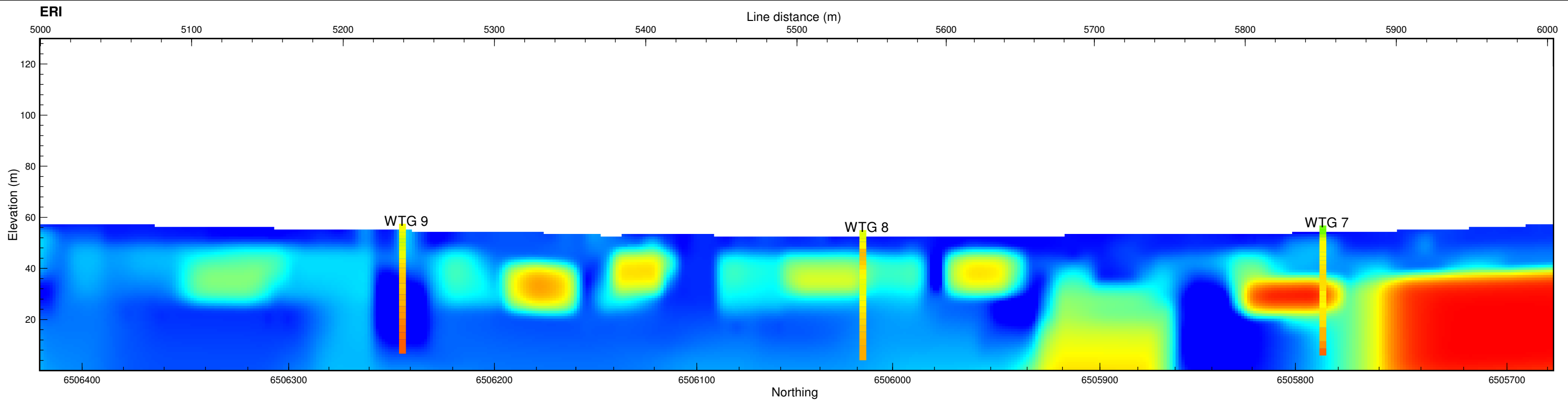




Notes:
 Plot 1: ERI pseudosection with MASW data overlay
 Plot 2: Refraction sections with MASW data overlay
 Data displayed in WGS84 zone S34
 Active line displayed in red on plan view

ESKOM
 SERE WIND ENERGY FACILITY
 ERI and Refraction with MASW overlay
 Row 1: 4000-5000m
 Prepared for BKS by E & EGS

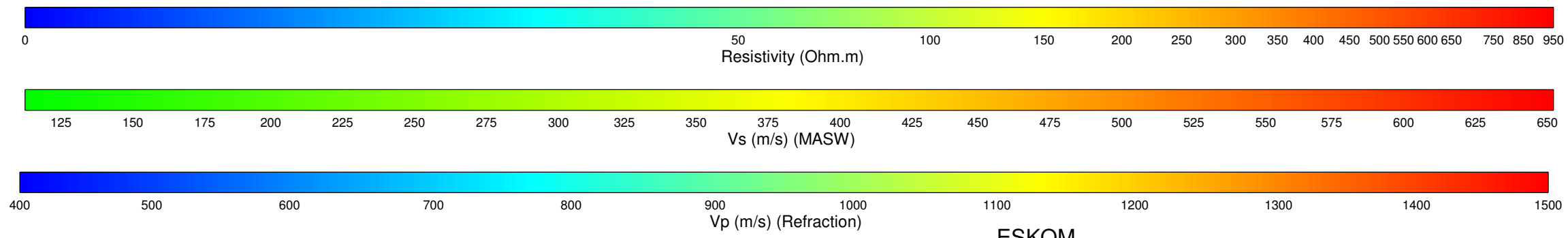
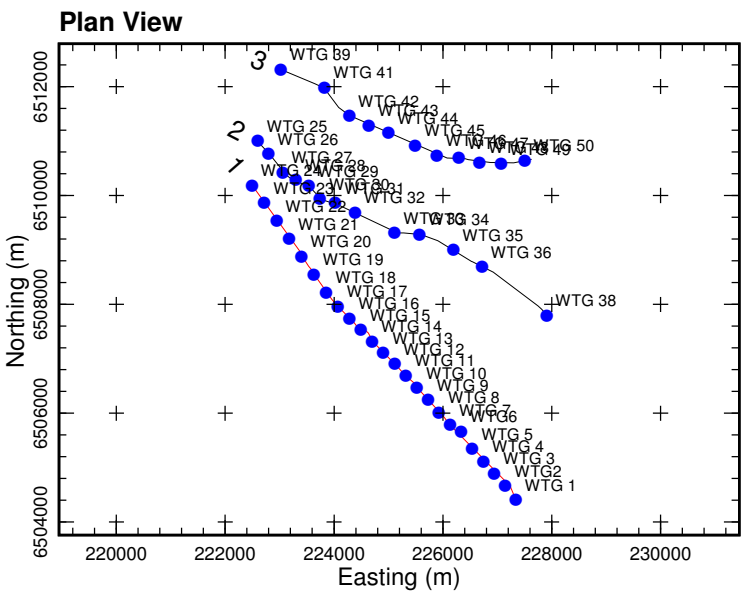
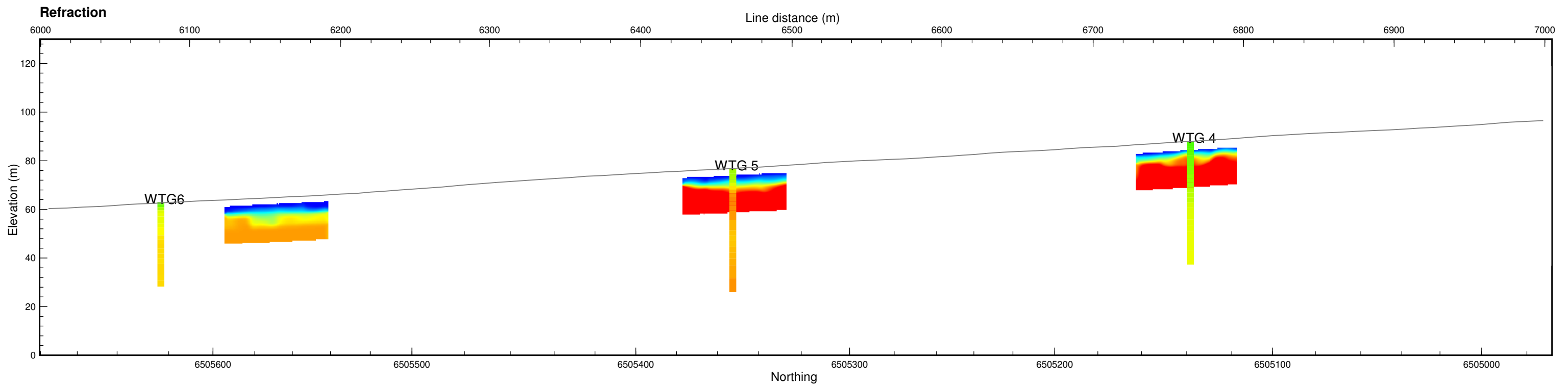
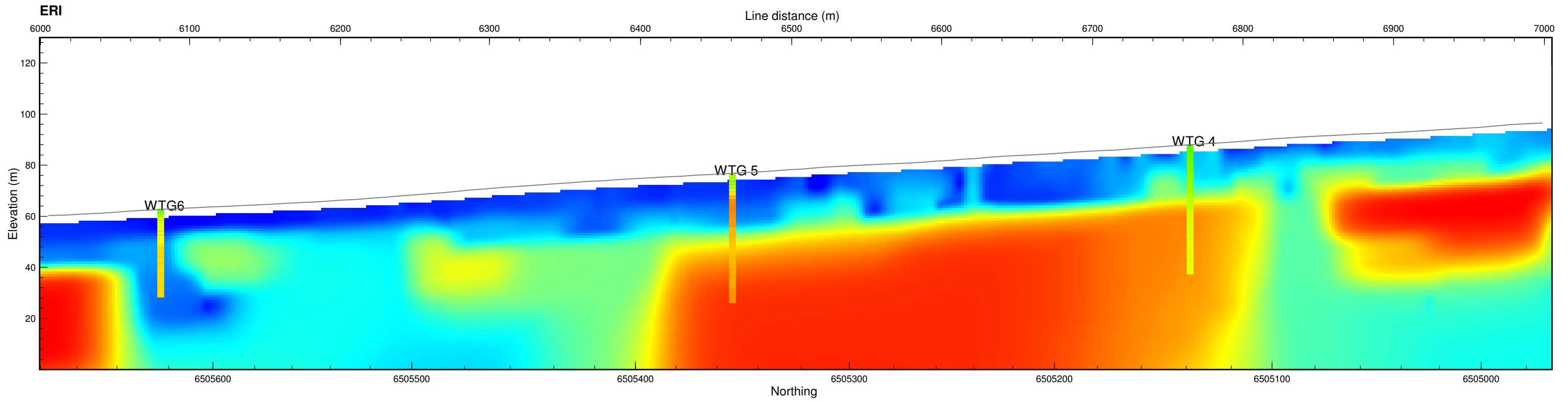




Notes:
 Plot 1: ERI pseudosection with MASW data overlay
 Plot 2: Refraction sections with MASW data overlay
 Data displayed in WGS84 zone S34
 Active line displayed in red on plan view

ESKOM
 SERE WIND ENERGY FACILITY
 ERI and Refraction with MASW overlay
 Line 1: 5000-6000m
 Prepared for BKS by E & EGS

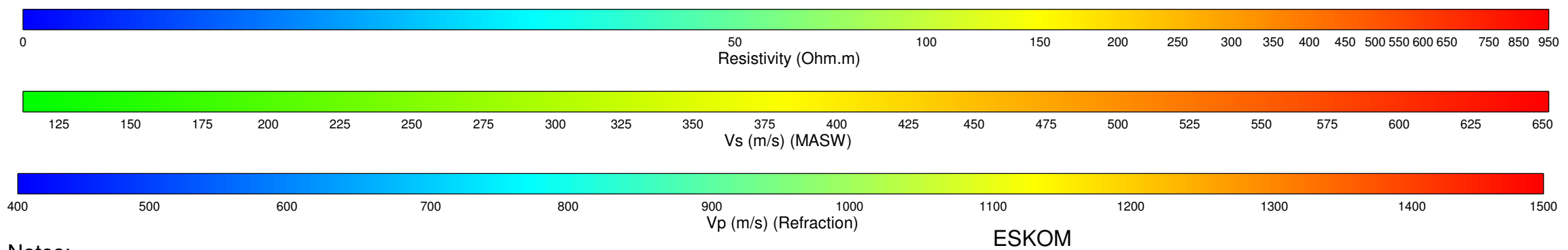
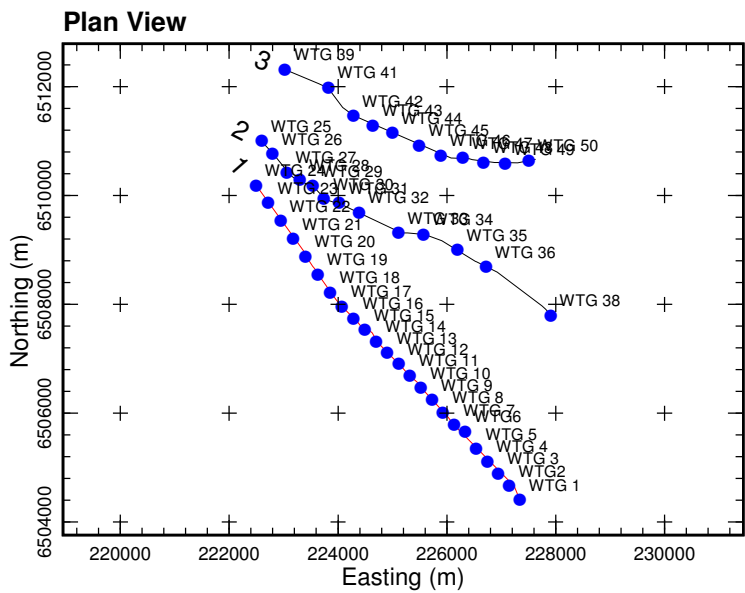
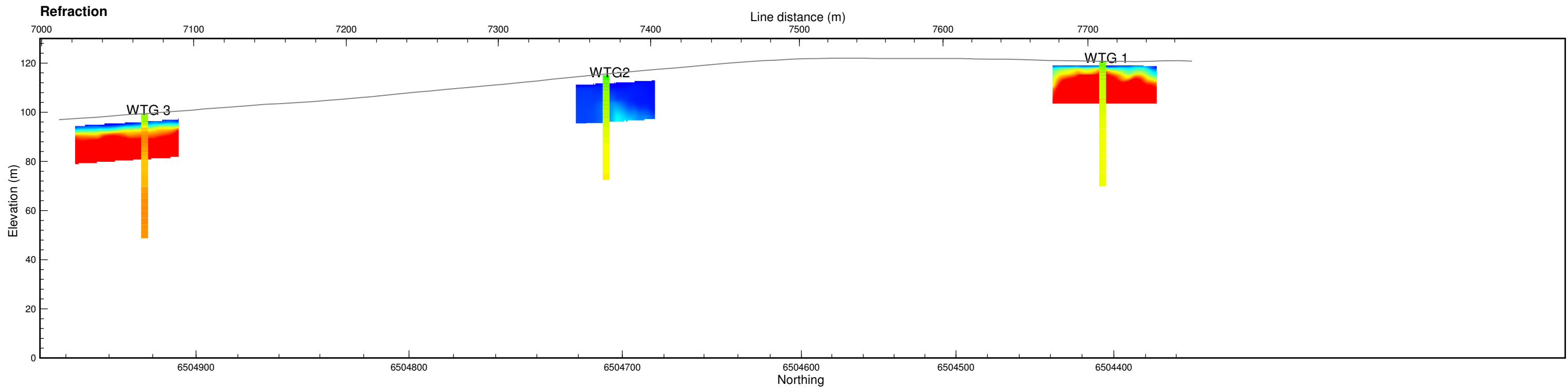
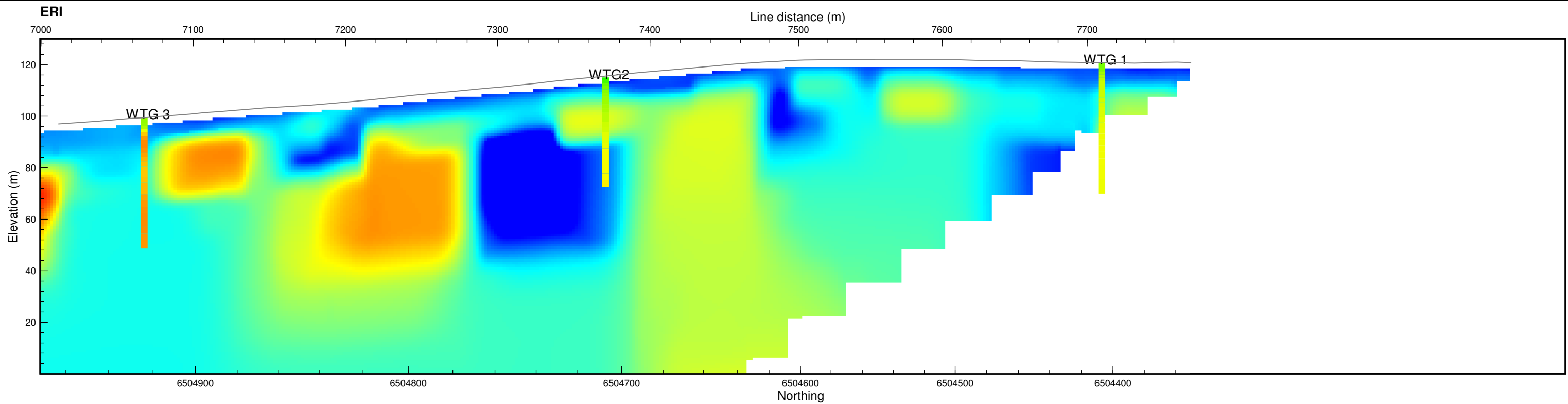




Notes:
 Plot 1: ERI pseudosection with MASW data overlay
 Plot 2: Refraction sections with MASW data overlay
 Data displayed in WGS84 zone S34
 Active line displayed in red on plan view

ESKOM
 SERE WIND ENERGY FACILITY
 ERI and Refraction with MASW overlay
 Row 1: 6000-7000m
 Prepared for BKS by E & EGS





Notes:
 Plot 1: ERI pseudosection with MASW data overlay
 Plot 2: Refraction sections with MASW data overlay
 Data displayed in WGS84 zone S34
 Active line displayed in red on plan view

ESKOM
 SERE WIND ENERGY FACILITY
 ERI and Refraction with MASW overlay
 Row 1: 7000-8000m
 Prepared for BKS by E & EGS

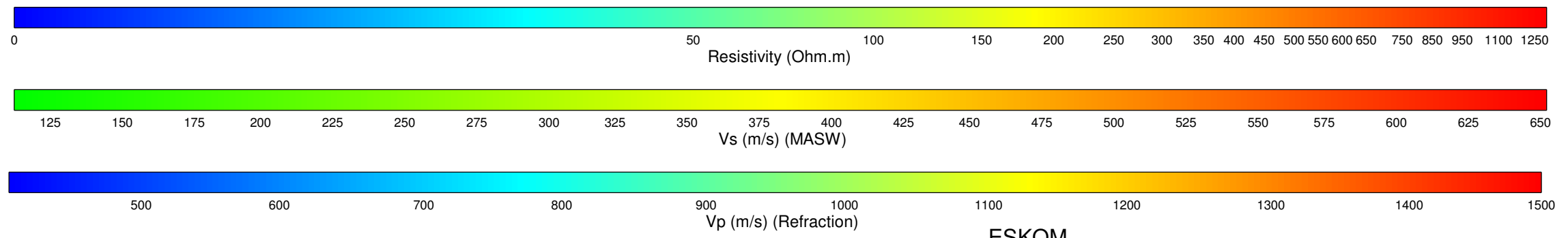
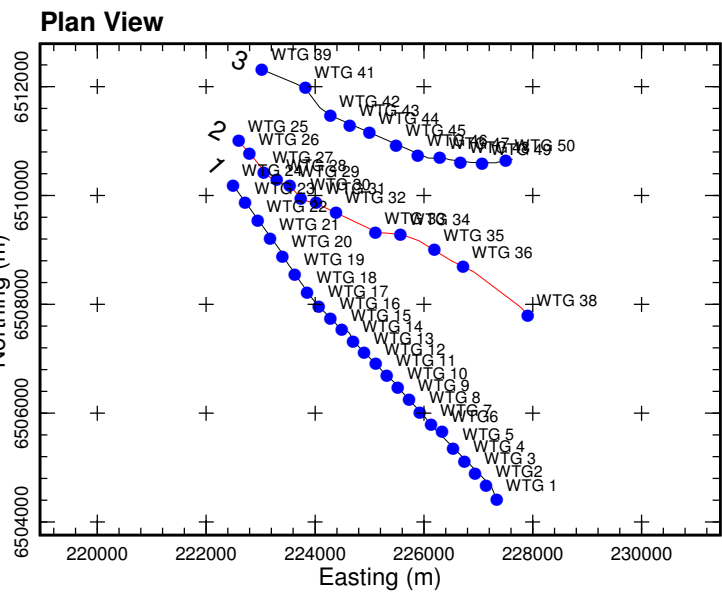
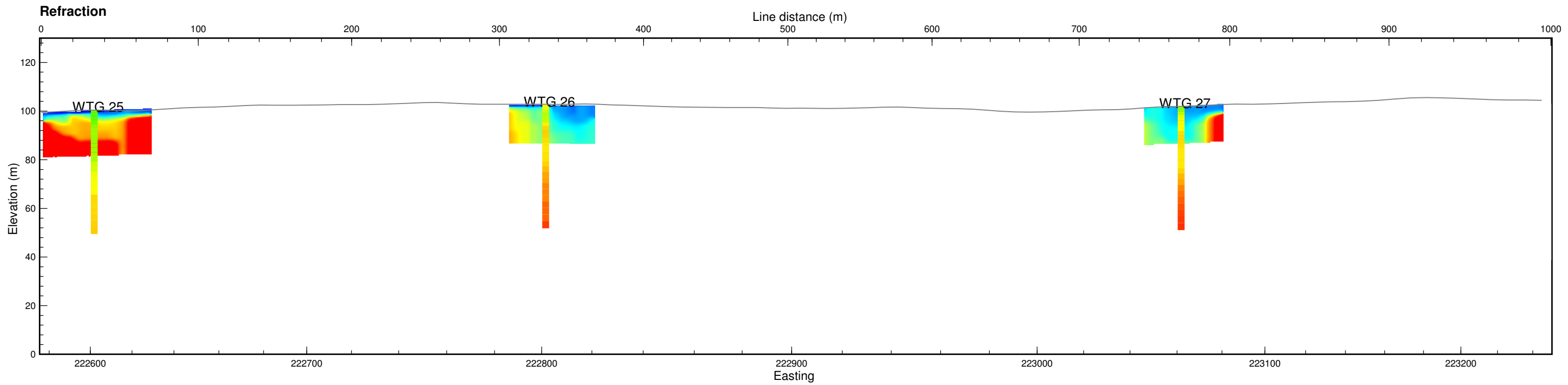
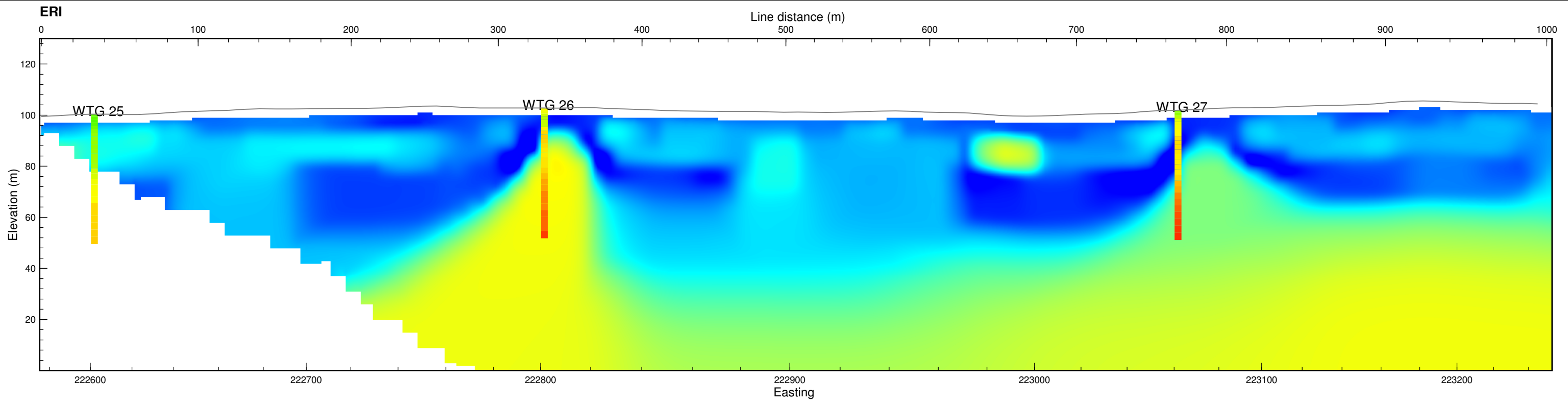


APPENDIX I:

SEISMIC REFRACTION AND ELECTRICAL RESISTIVITY

a (ii) ERI, Refraction with MASW Overlain

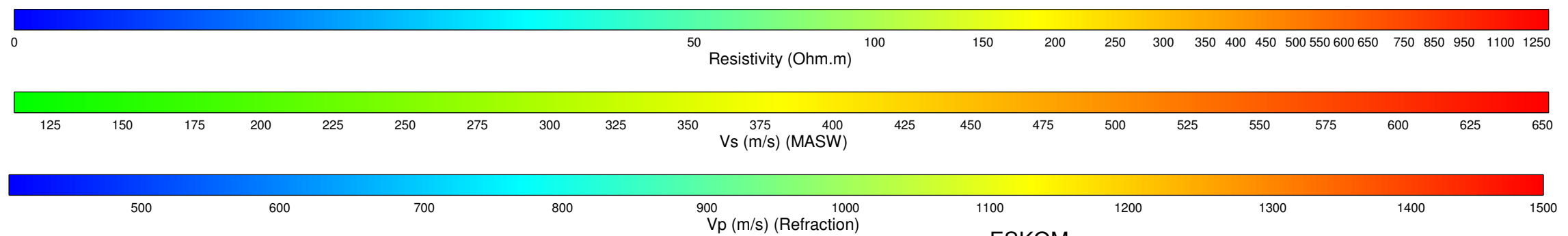
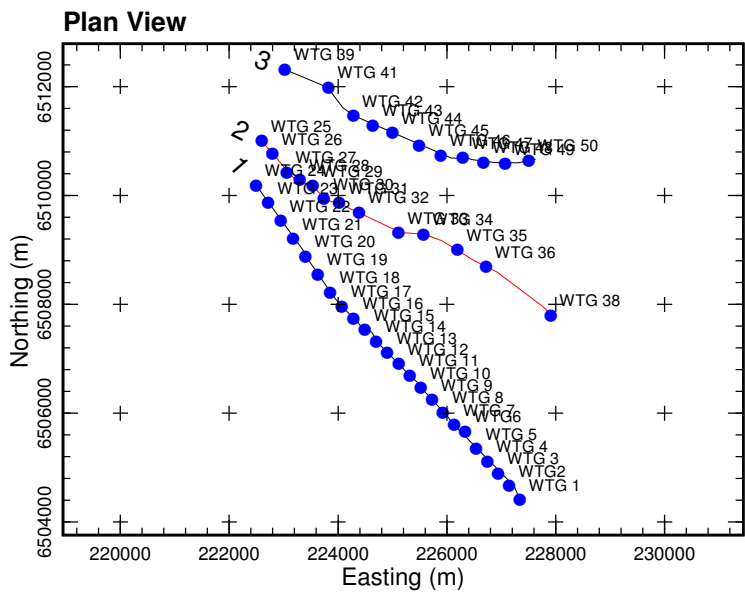
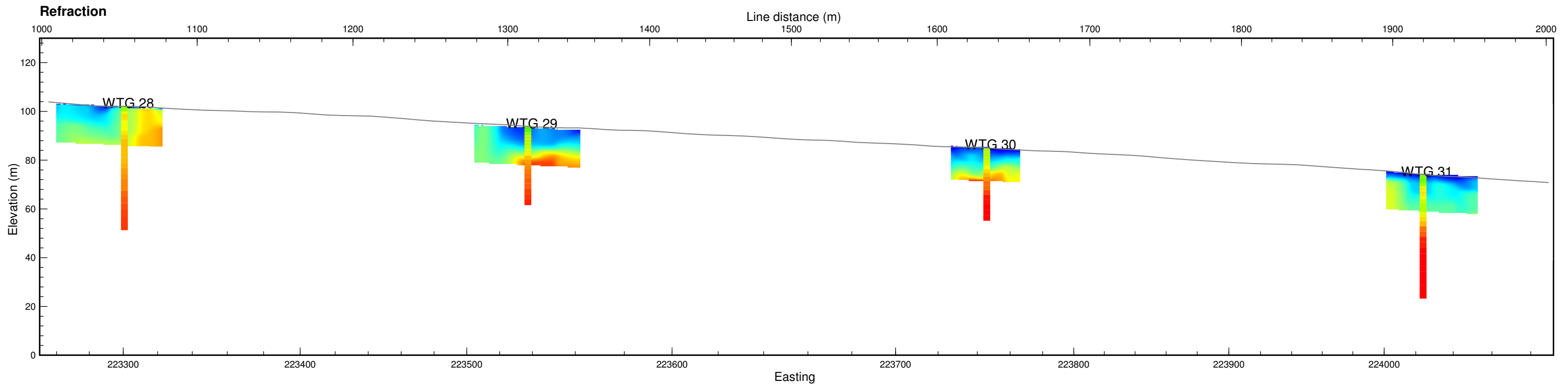
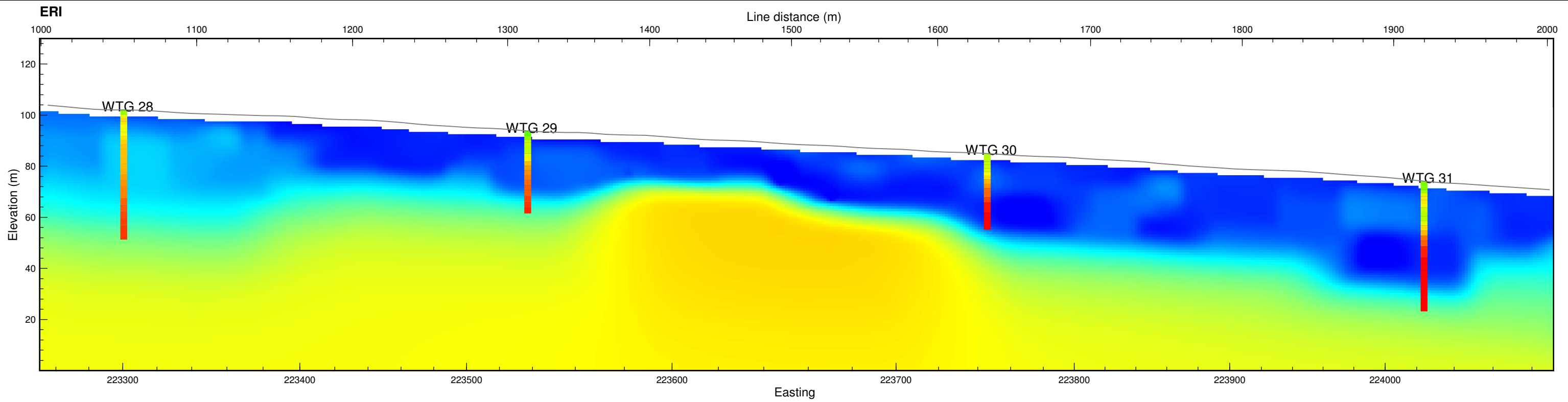
Line 2



Notes:
 Plot 1: ERI pseudosection with MASW data overlain
 Plot 2: Refraction sections with MASW data overlain
 Data displayed in WGS84 zone S34
 Active line displayed in red on plan view

ESKOM
 SERE WIND ENERGY FACILITY
 ERI and Refraction with MASW overlain
 Row 2: 0-1000m
 Prepared for BKS by E & EGS

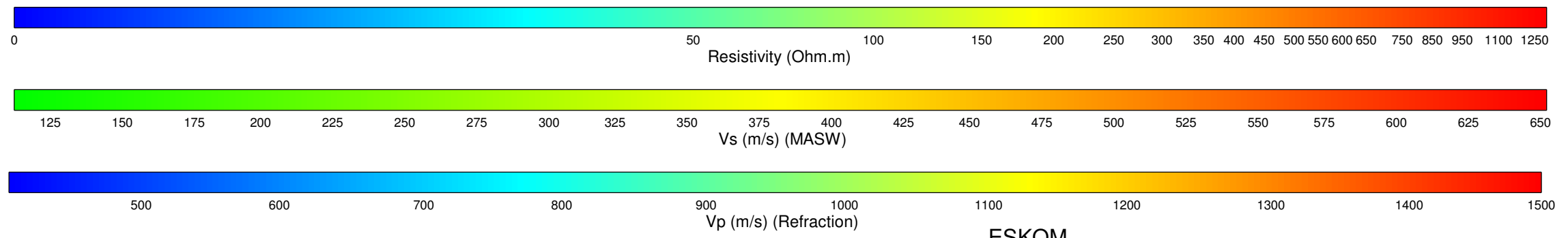
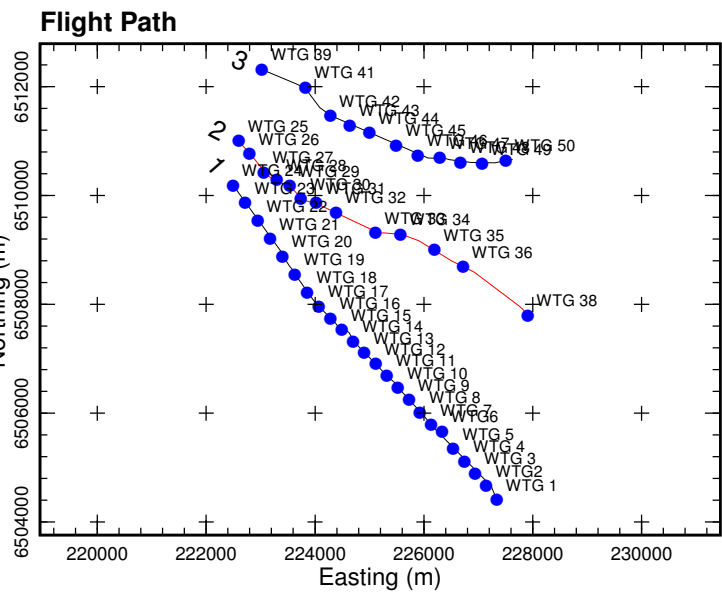
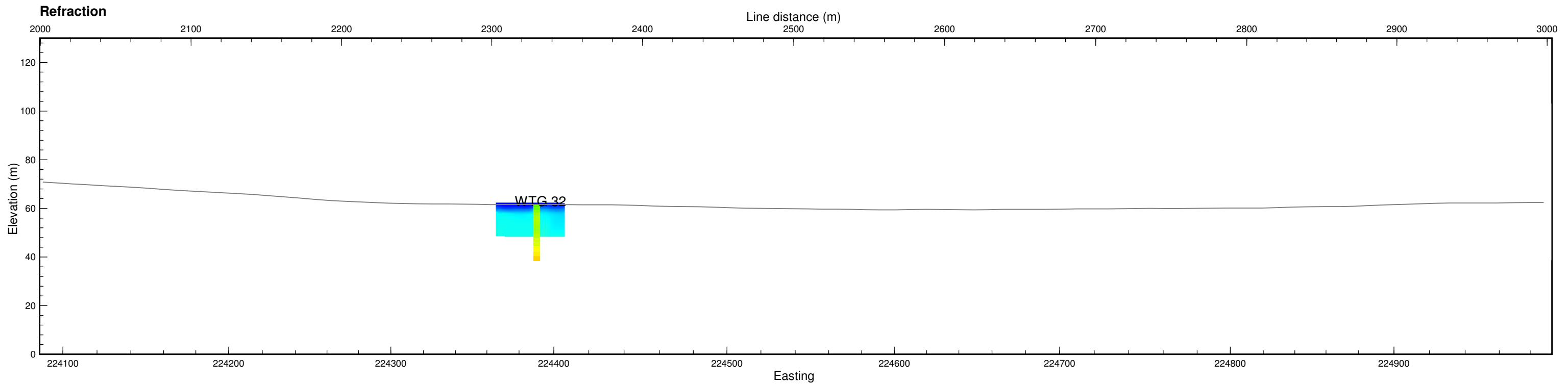
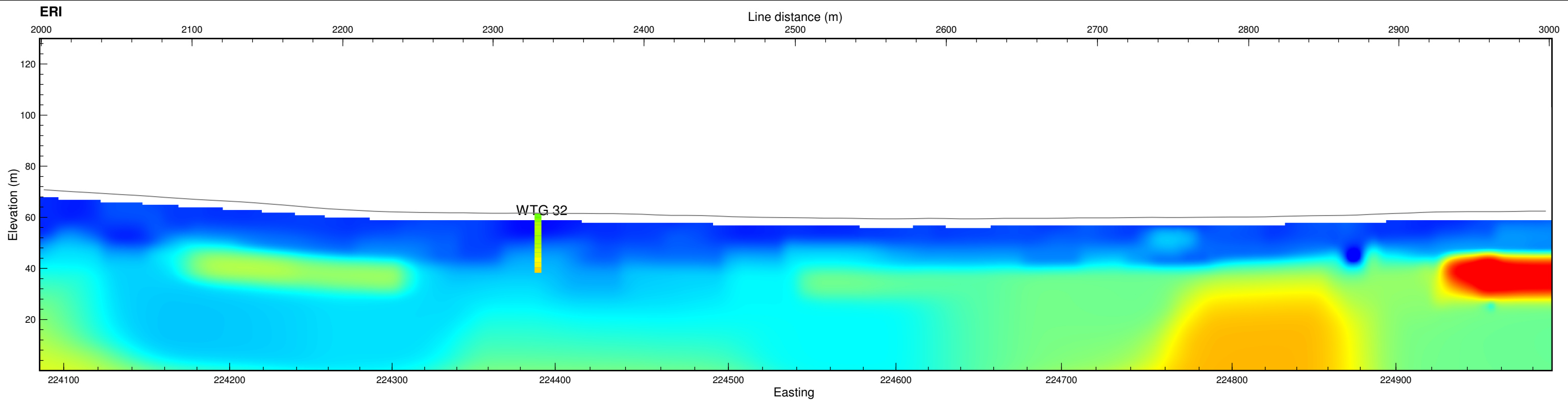




Notes:
 Plot 1: ERI pseudosection with MASW data overlay
 Plot 2: Refraction sections with MASW data overlay
 Data displayed in WGS84 zone S34
 Active line displayed in red on plan view

ESKOM
 SERE WIND ENERGY FACILITY
 ERI and Refraction with MASW overlay
 Row 2: 1000-2000m
 Prepared for BKS by E & EGS

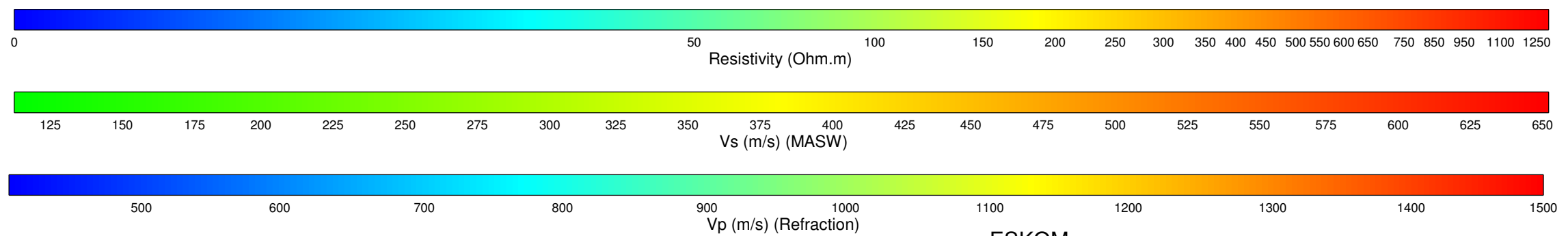
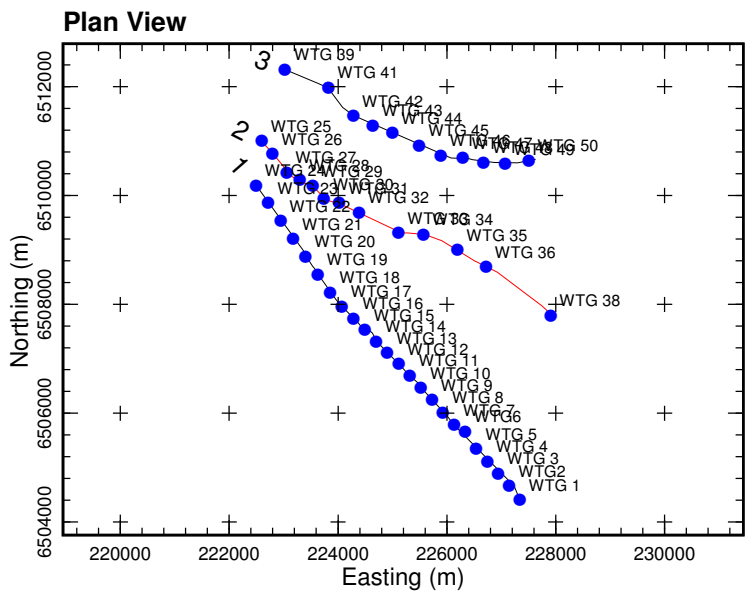
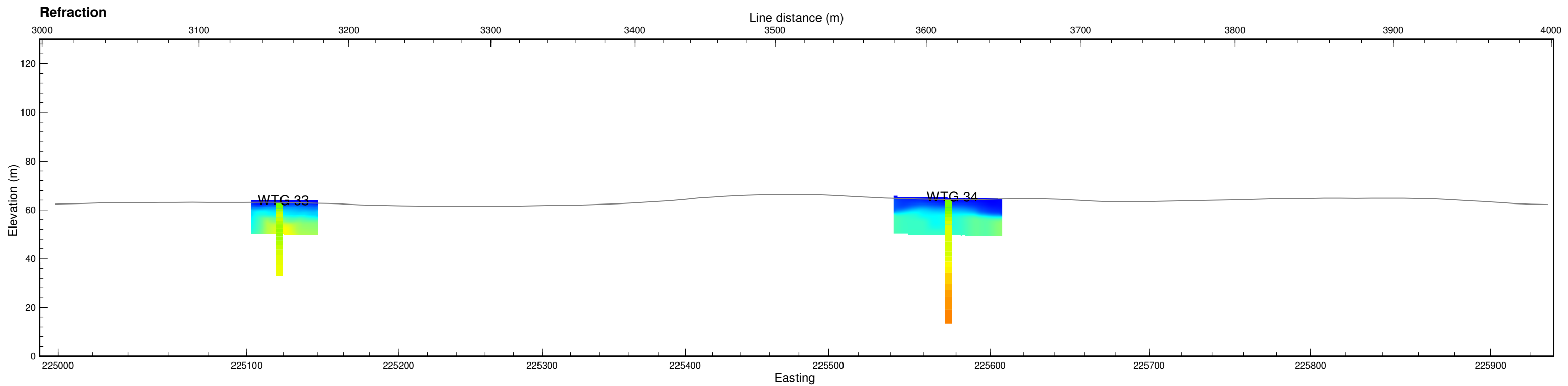
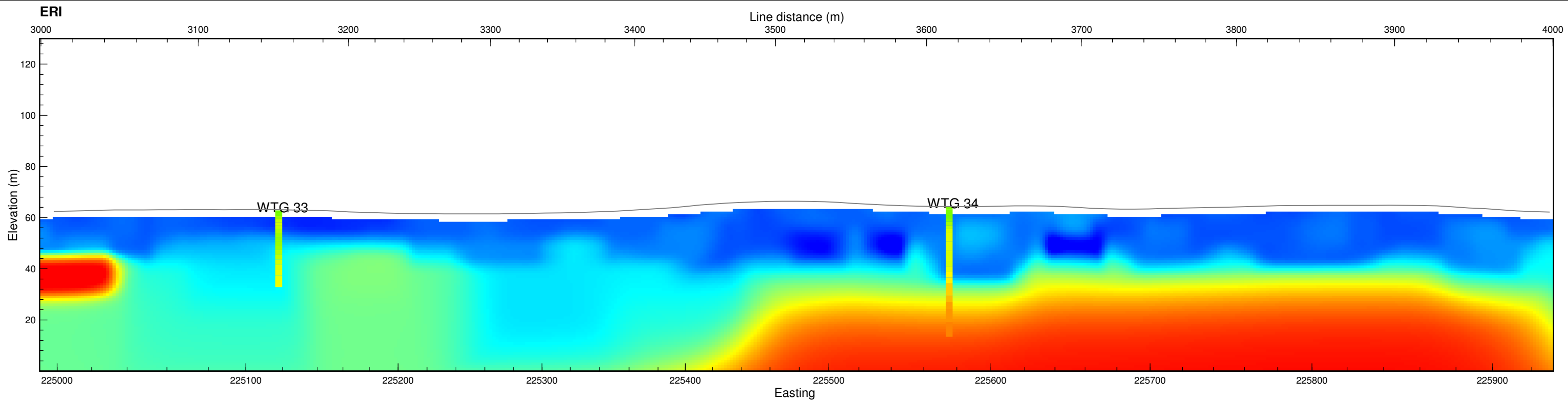




Notes:
 Plot 1: ERI pseudosection with MASW data overlain
 Plot 2: Refraction sections with MASW data overlain
 Data displayed in WGS84 zone S34
 Active line displayed in red on plan view

ESKOM
 SERE WIND ENERGY FACILITY
 ERI and Refraction with MASW overlain
 Row 2: 2000-3000m
 Prepared by BKS by E & EGS

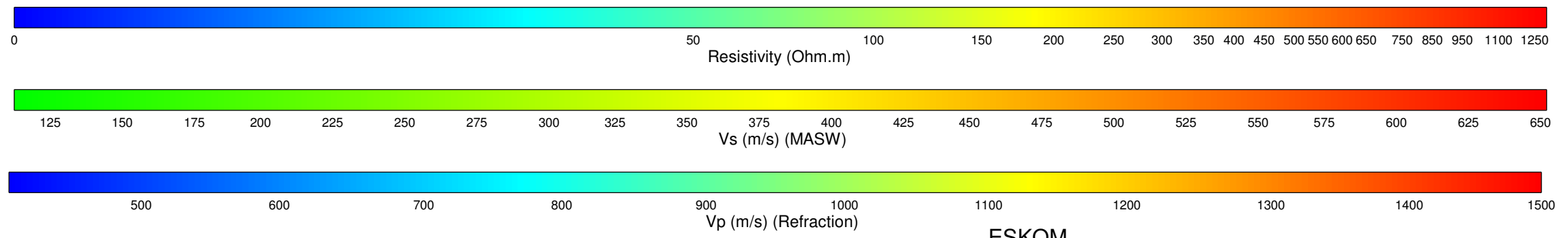
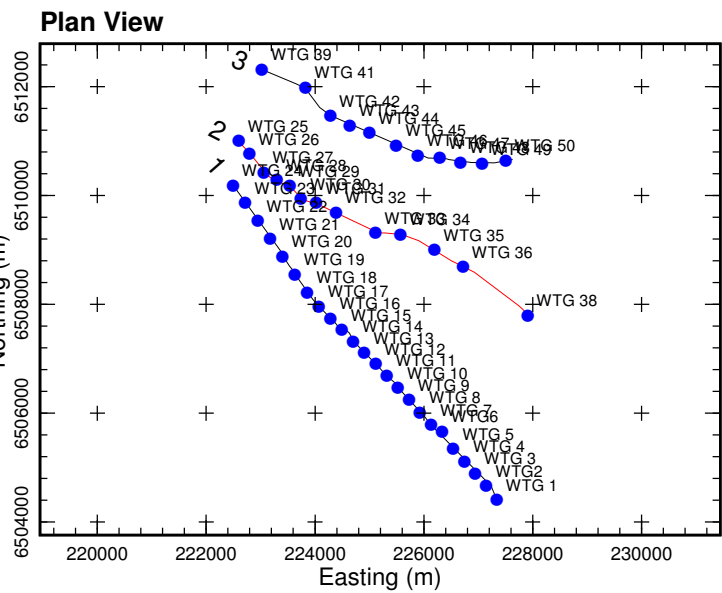
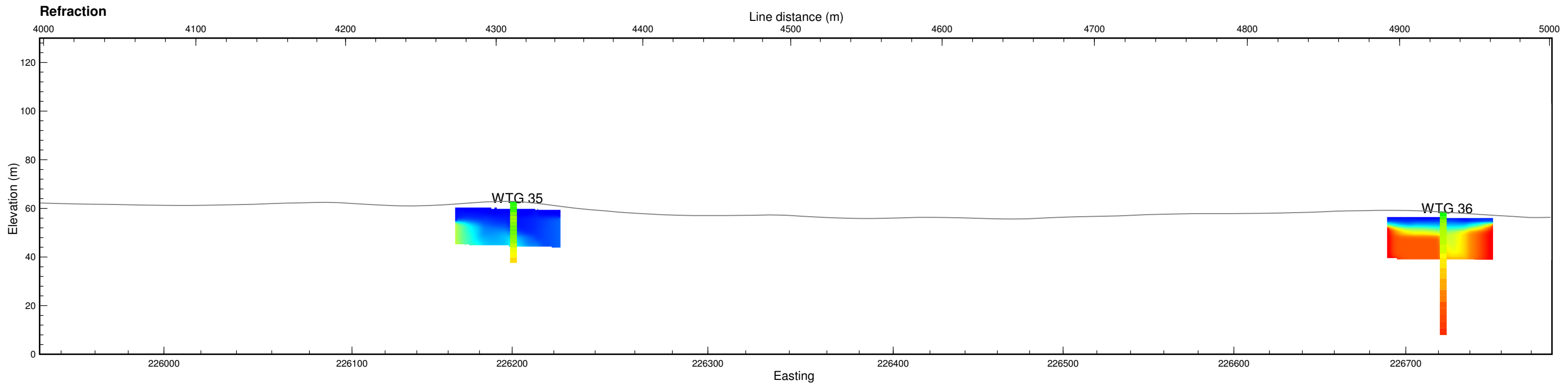
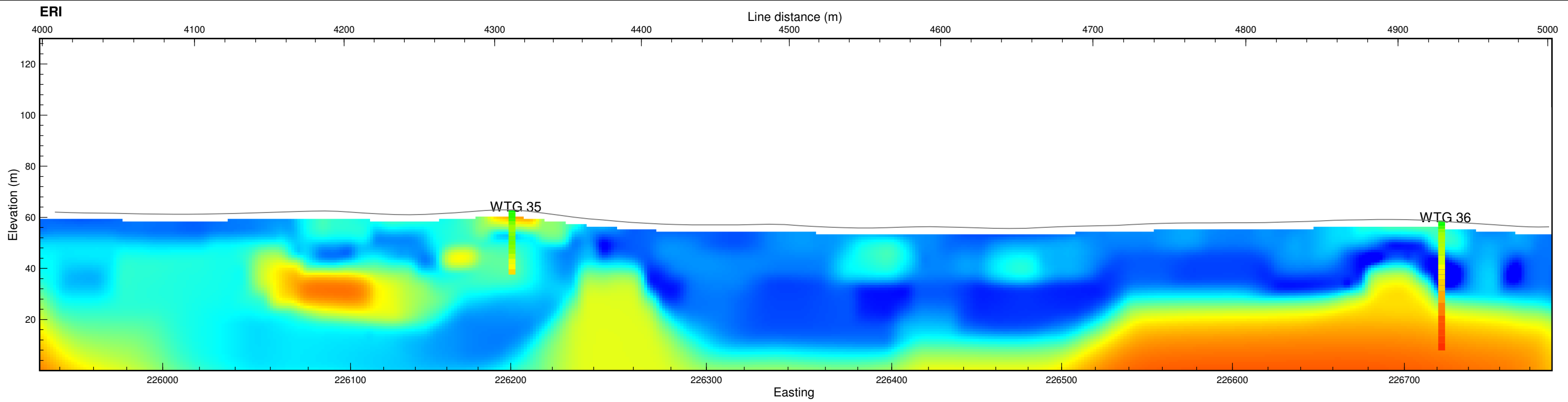




Notes:
 Plot 1: ERI pseudosection with MASW data overlay
 Plot 2: Refraction sections with MASW data overlay
 Data displayed in WGS84 zone S34
 Active line displayed in red on plan view

ESKOM
 SERE WIND ENERGY FACILITY
 ERI and Refraction with MASW overlay
 Row 2: 3000-4000m
 Prepared for BKS by E & EGS

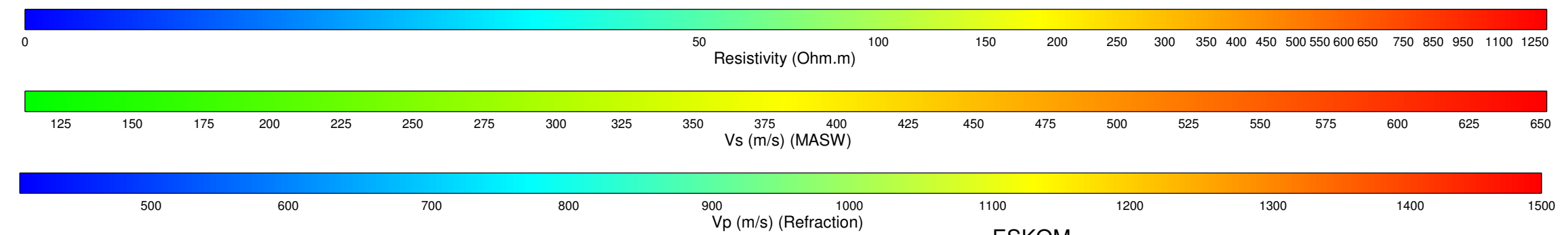
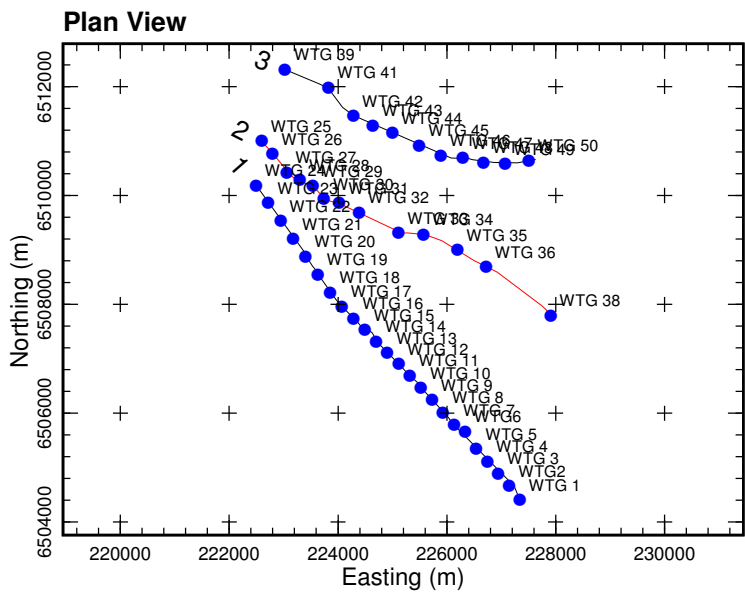
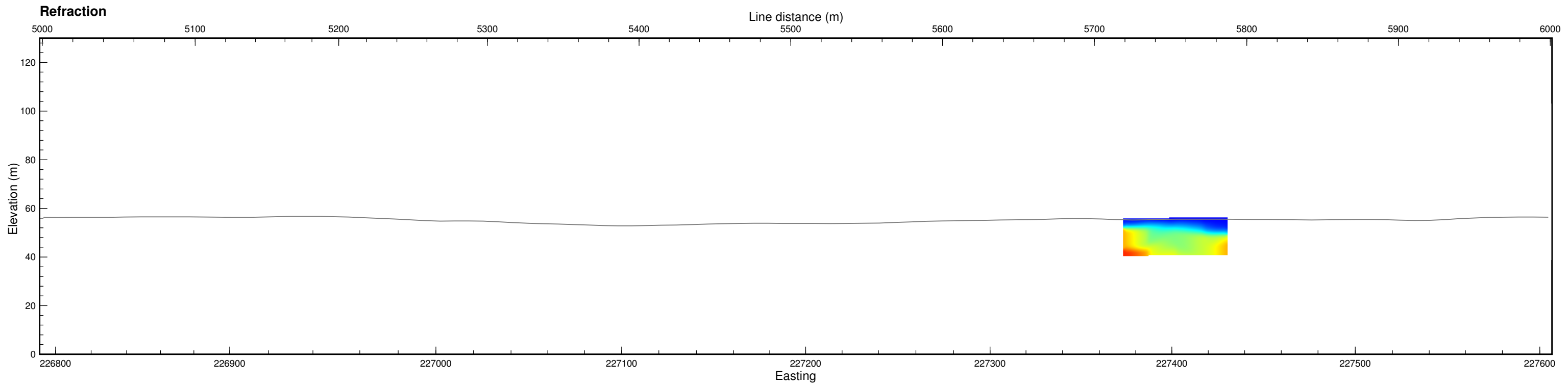
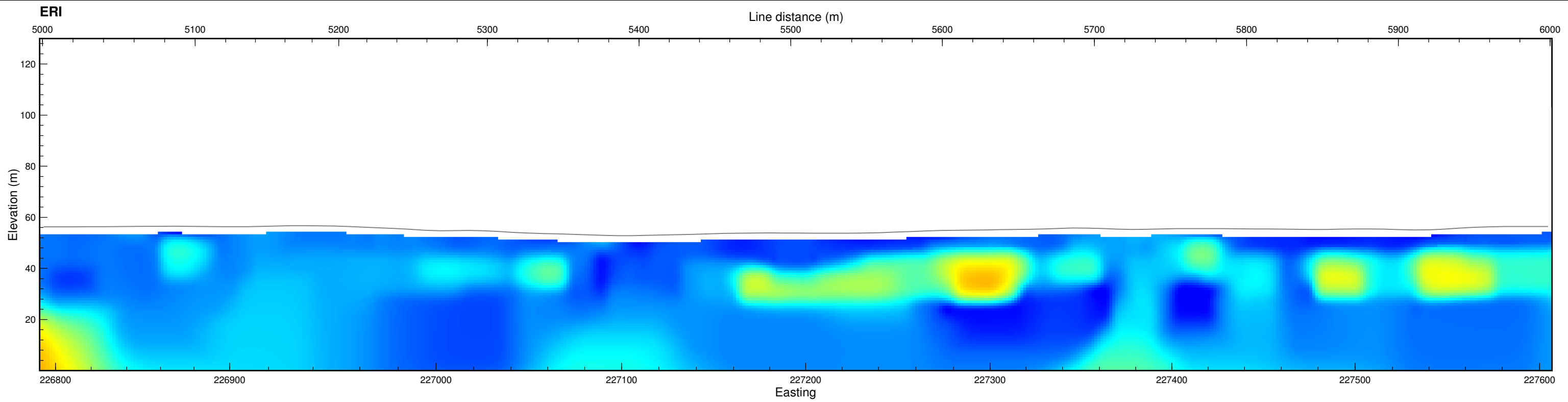




Notes:
 Plot 1: ERI pseudosection with MASW data overlain
 Plot 2: Refraction sections with MASW data overlain
 Data displayed in WGS84 zone S34
 Active line displayed in red on plan view

ESKOM
 SERE WIND ENERGY FACILITY
 ERI and Refraction with MASW overlain
 Row 2: 4000-5000m
 Prepared for BKS by E & EGS

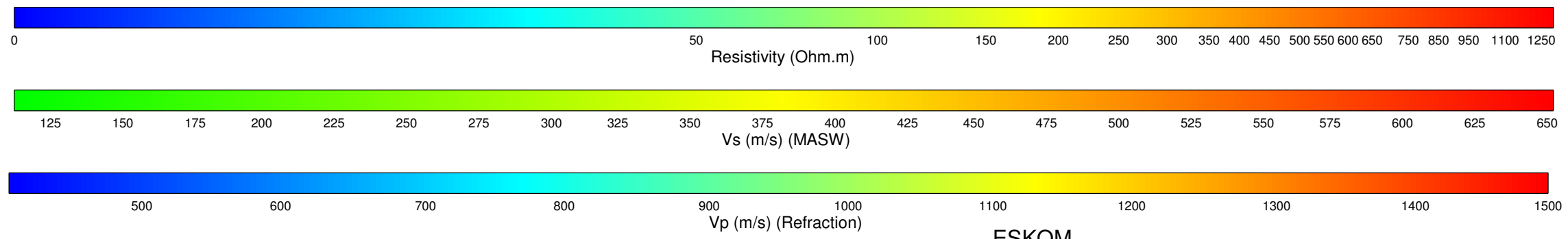
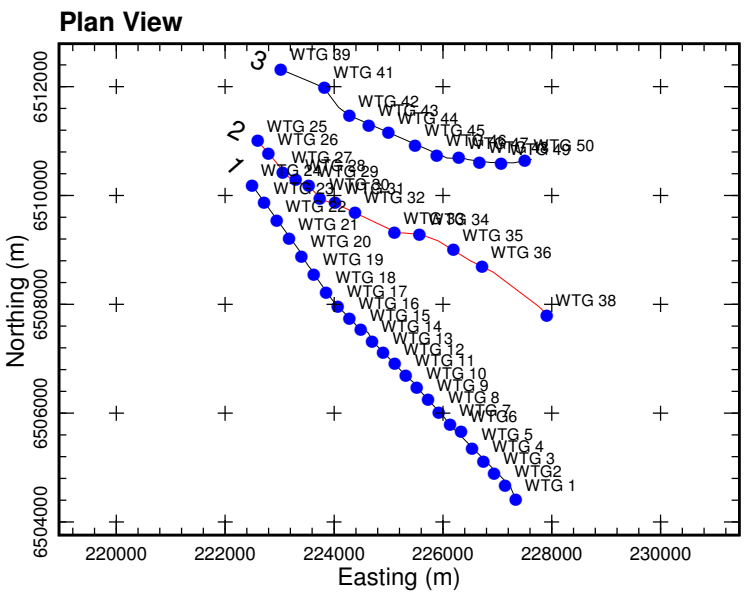
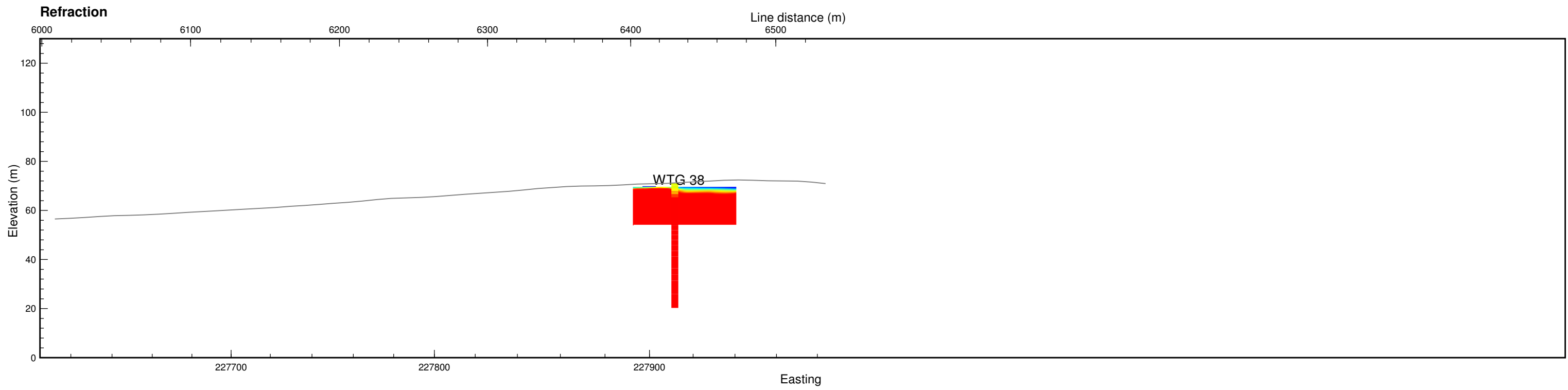
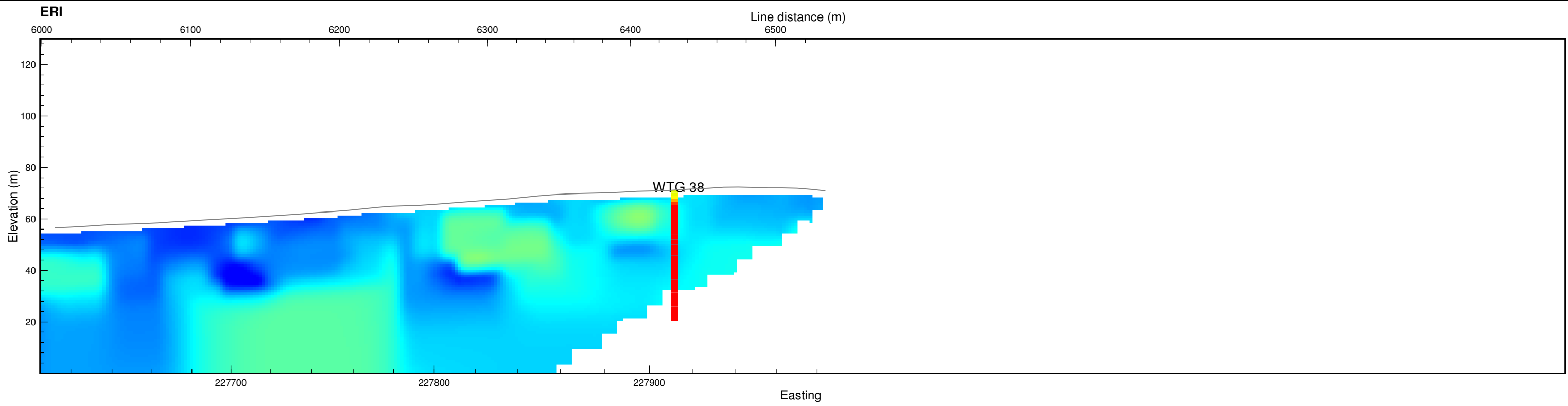




Notes:
 Plot 1: ERI pseudosection with MASW data overlay
 Plot 2: Refraction sections with MASW data overlay
 Data displayed in WGS84 zone S34
 Active line displayed in red on plan view

ESKOM
 SERE WIND ENERGY FACILITY
 ERI and Refraction with MASW overlay
 Row 2: 5000-6000m
 Prepared for BKS by E & EGS





Notes:
 Plot 1: ERI pseudosection with MASW data overlay
 Plot 2: Refraction sections with MASW data overlay
 Data displayed in WGS84 zone S34
 Active line displayed in red on plan view

ESKOM
 SERE WIND ENERGY FACILITY
 ERI and Refraction with MASW overlay
 Row 2: 6000-7000m
 Prepared for BKS by E & EGS

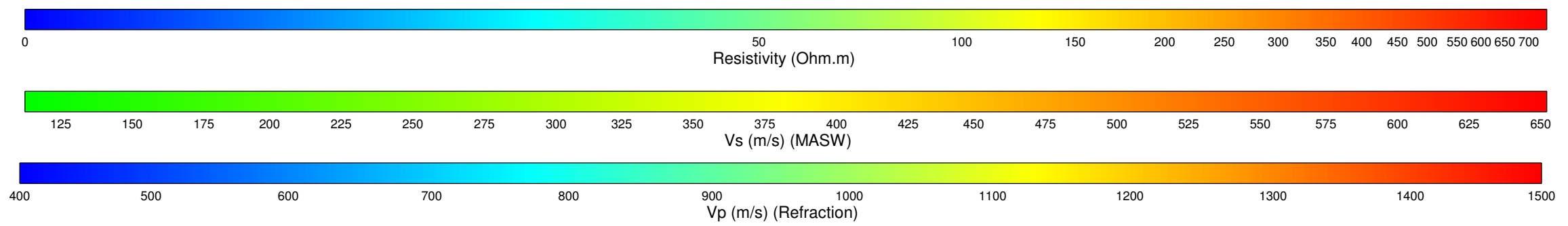
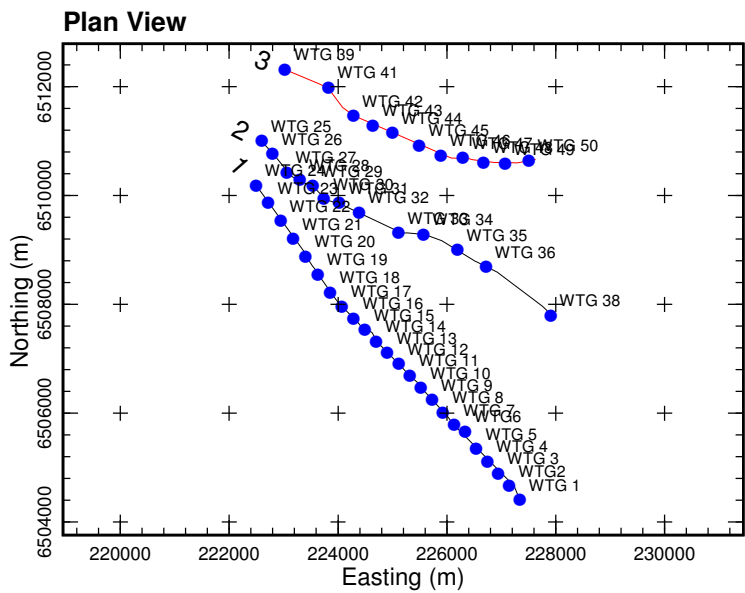
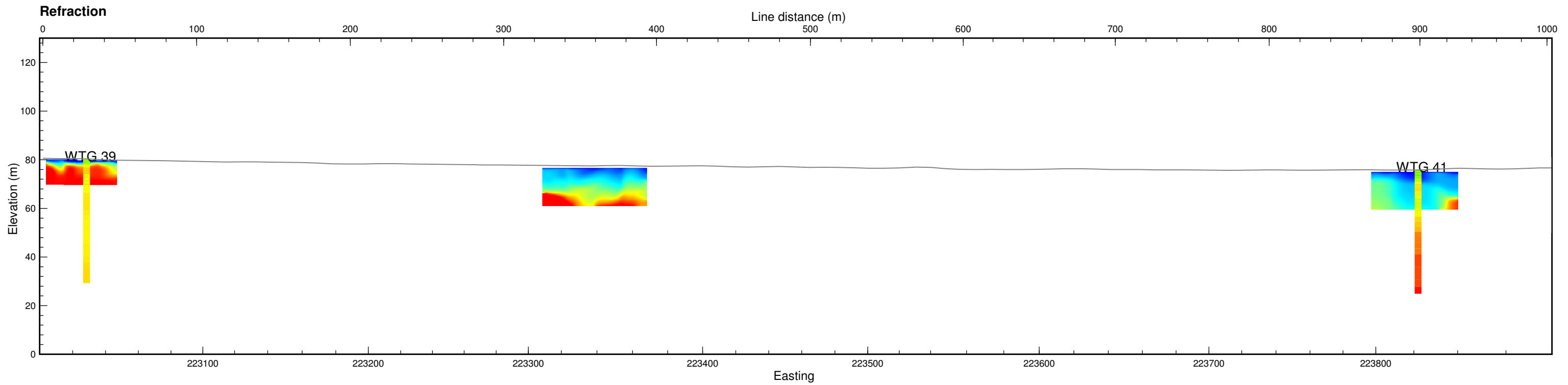
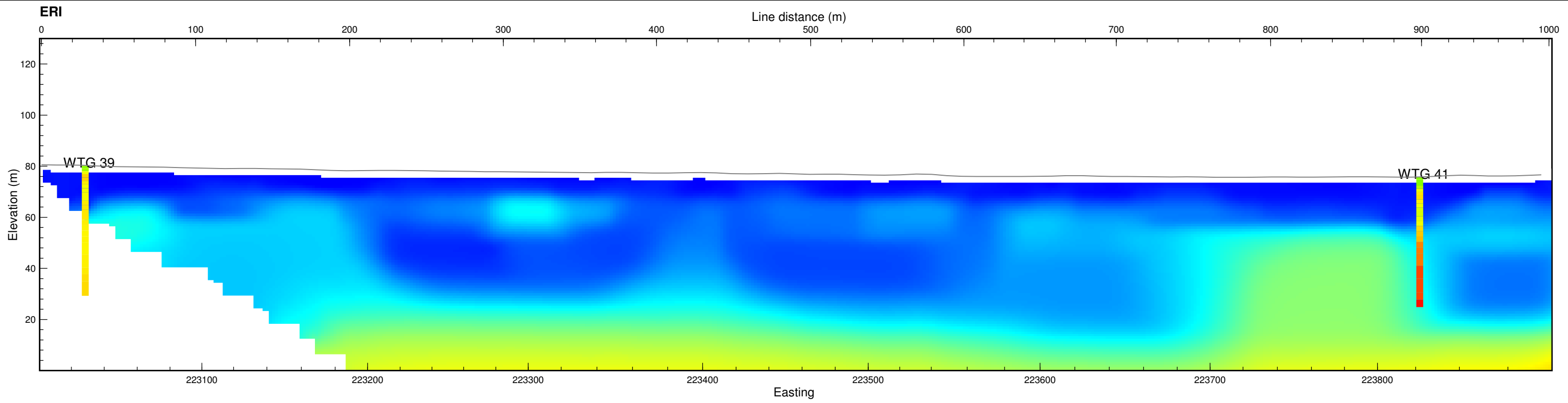


APPENDIX I:

SEISMIC REFRACTION AND ELECTRICAL RESISTIVITY

a (iii) ERI, Refraction with MASW Overlain

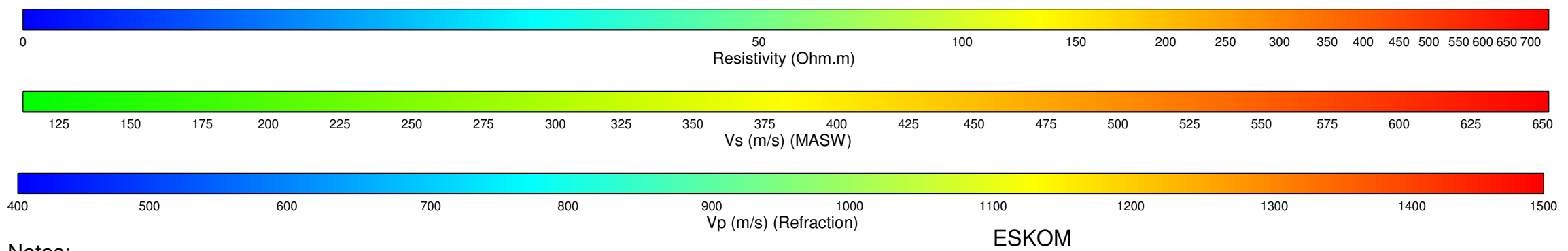
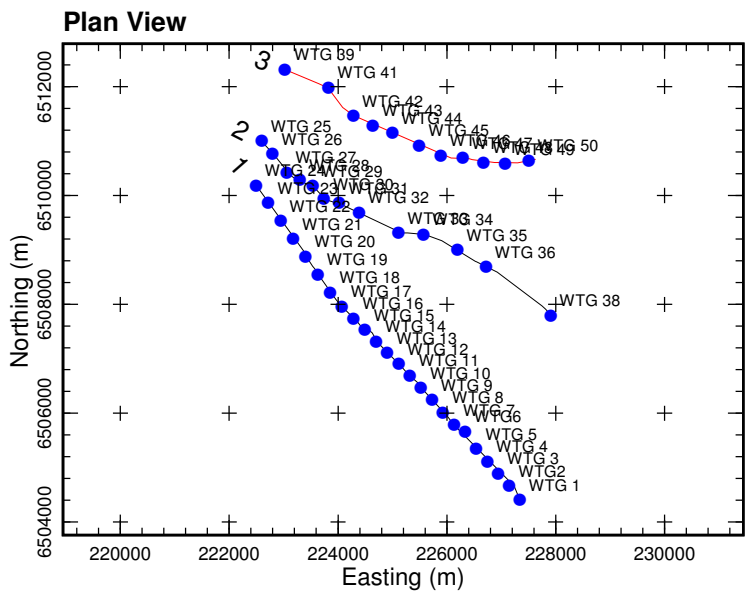
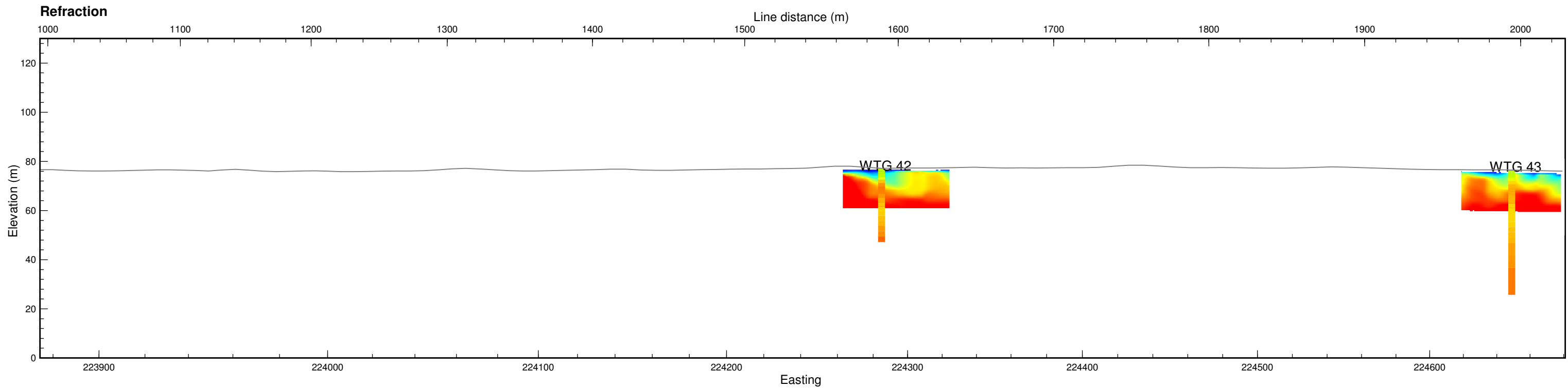
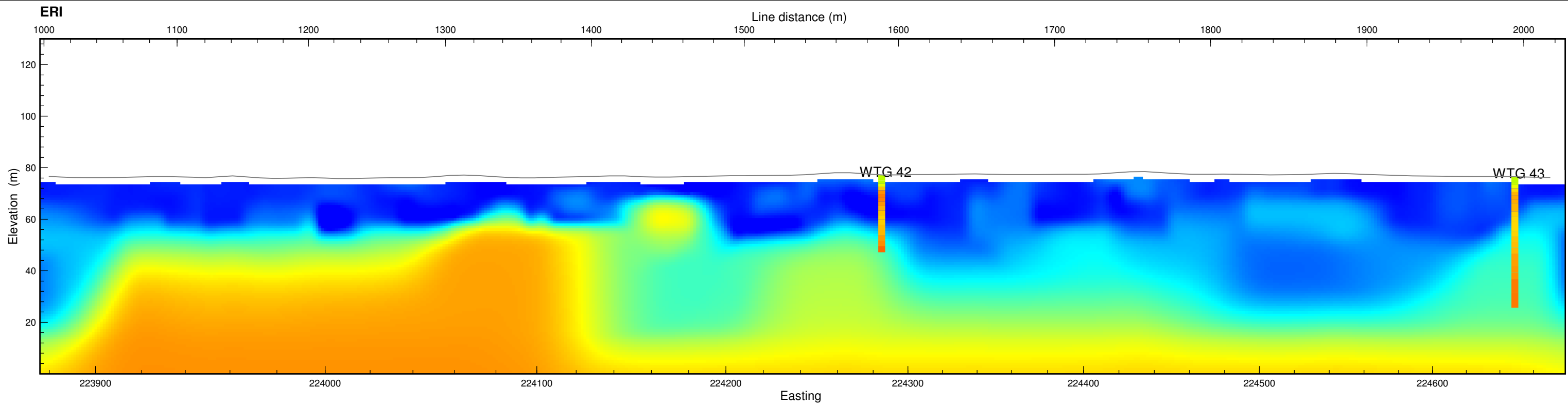
Line 3



Notes:
 Plot 1: ERI pseudosection with MASW data overlain
 Plot 2: Refraction sections with MASW data overlain
 Data displayed in WGS84 zone S34
 Active line displayed in red on plan view

ESKOM
 SERE WIND ENERGY FACILITY
 ERI and Refraction with MASW overlain
 Row 3: 0-1000m
 Prepared for BKS by E & EGS

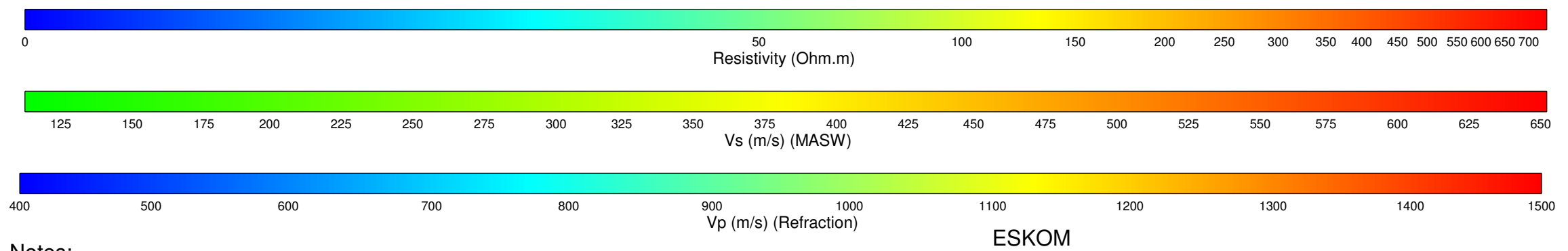
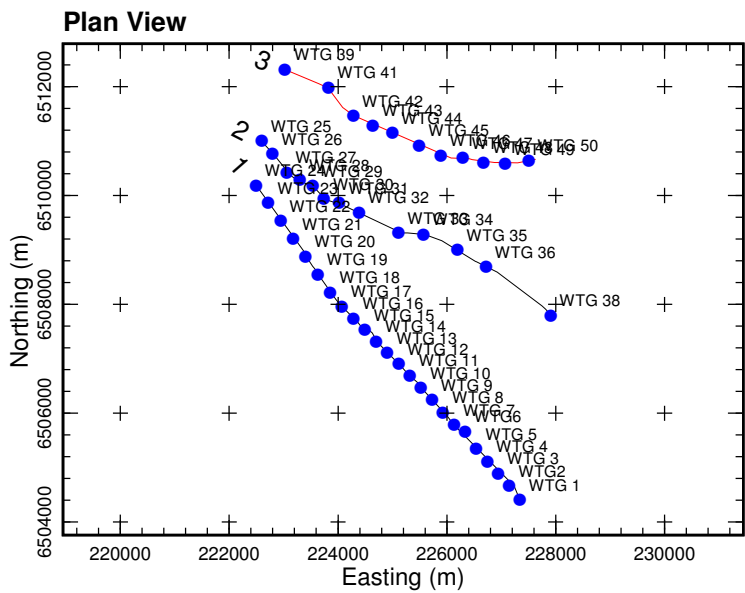
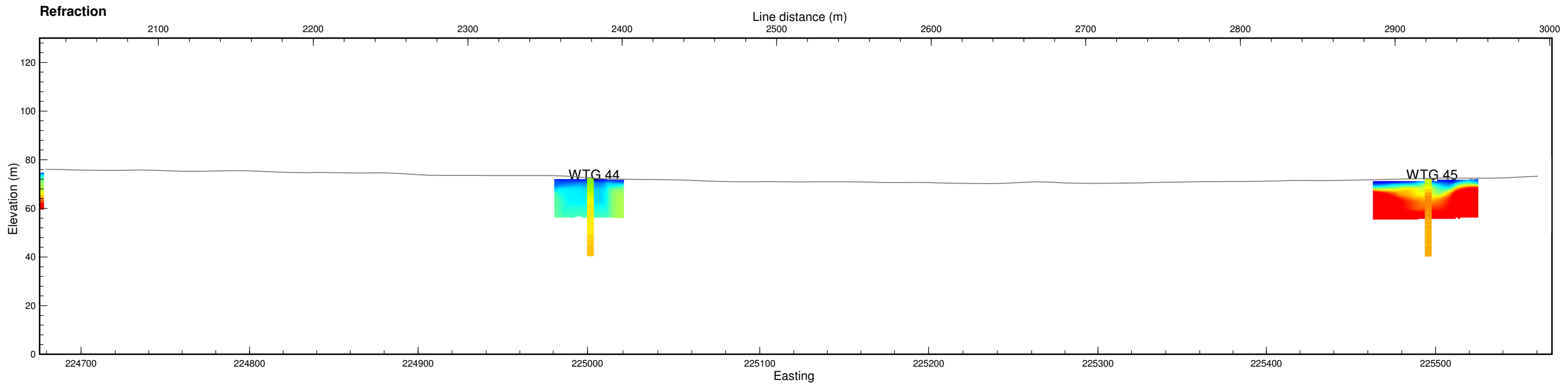
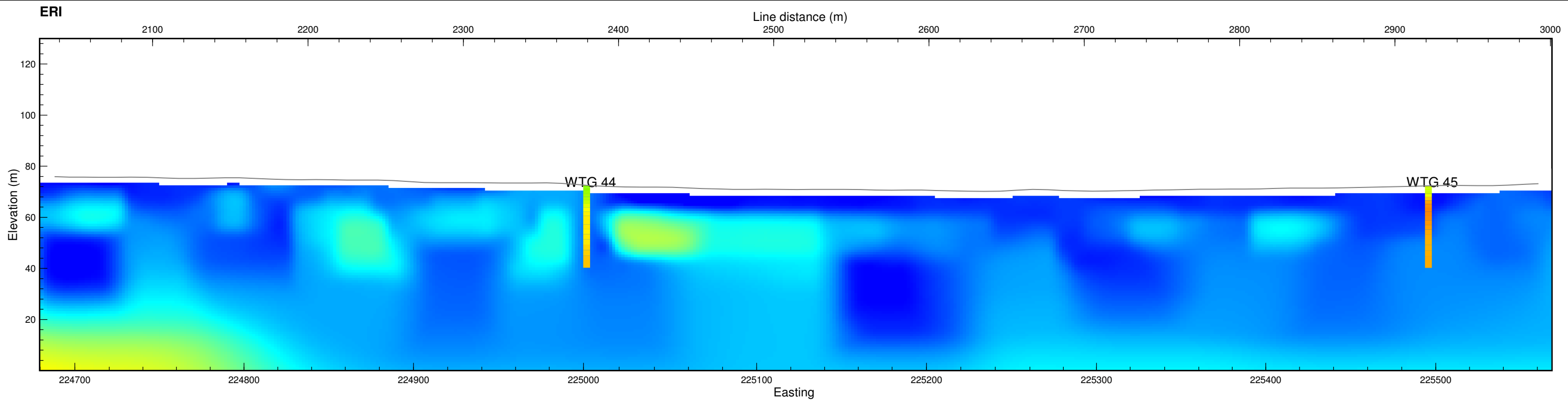




Notes:
 Plot 1: ERI pseudosection with MASW data overlain
 Plot 2: Refraction sections with MASW data overlain
 Data displayed in WGS84 zone S34
 Active line displayed in red on plan view

SERE WIND ENERGY FACILITY
 ERI and Refraction with MASW overlain
 Row 3: 1000-2000m
 Prepared for BKS by E & EGS

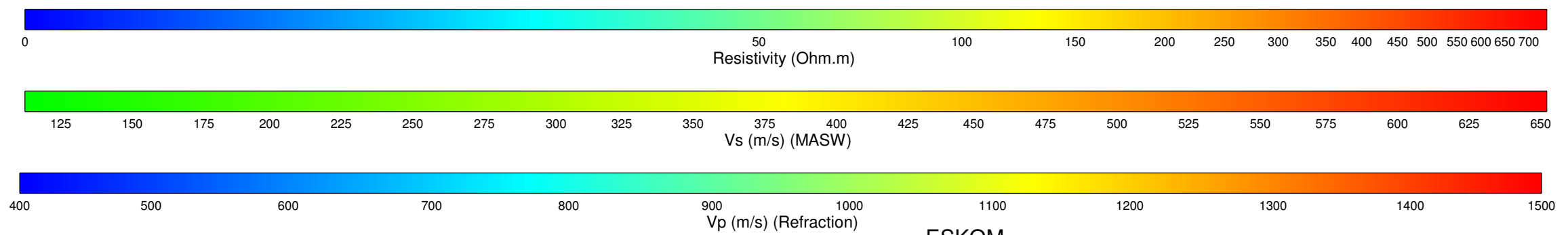
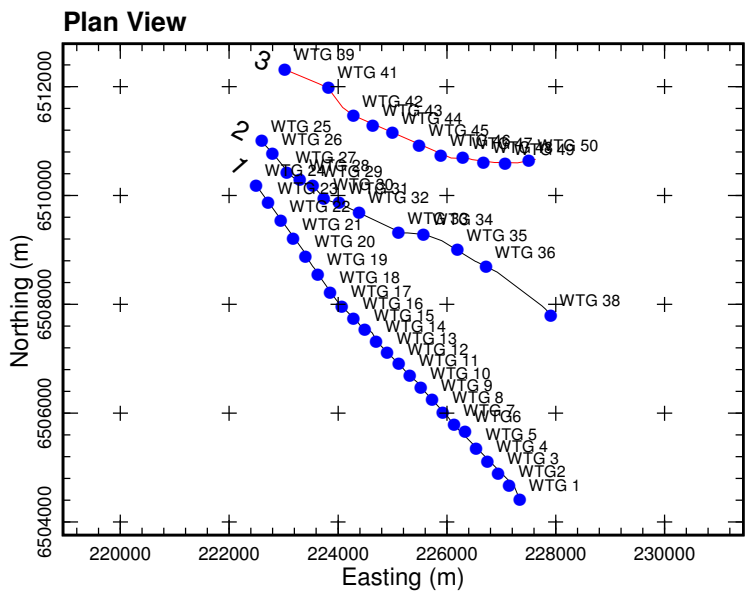
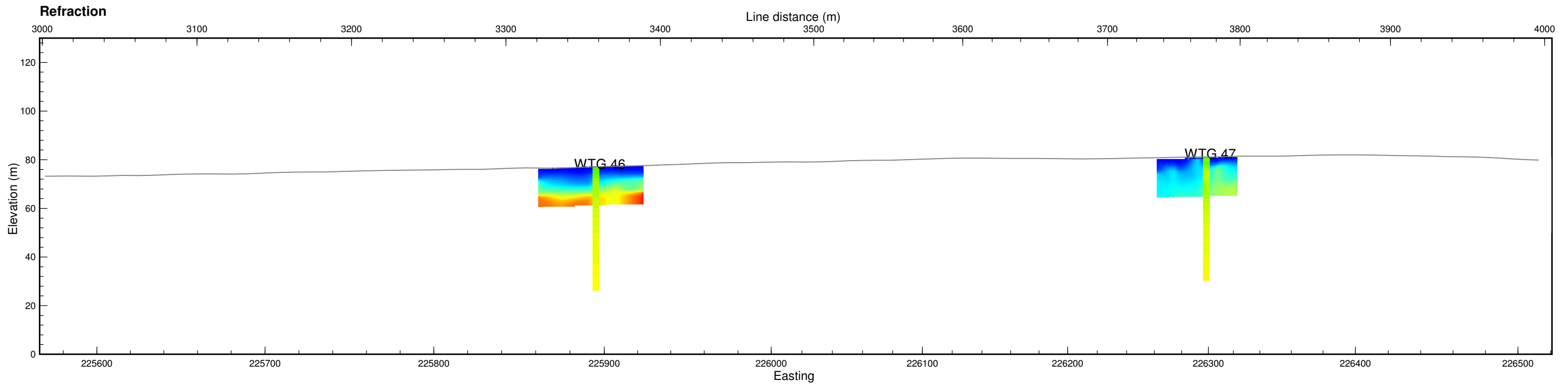
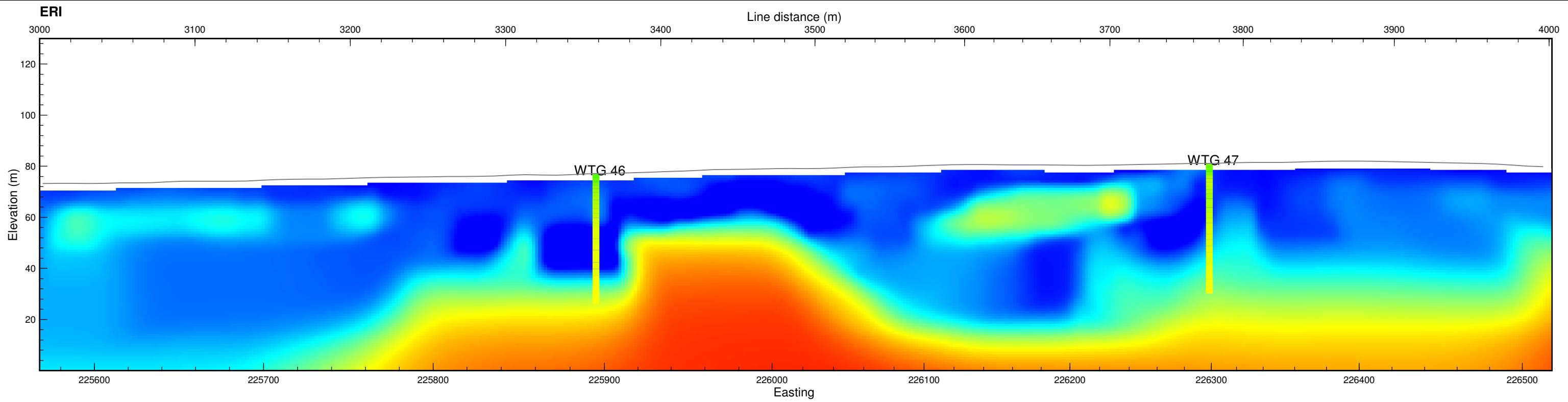




Notes:
 Plot 1: ERI pseudosection with MASW data overlain
 Plot 2: Refraction sections with MASW data overlain
 Data displayed in WGS84 zone S34
 Active line displayed in red on plan view

SERE WIND ENERGY FACILITY
 ERI and Refraction with MASW overlain
 Row 3: 2000-3000m
 Prepared for BKS by E & EGS

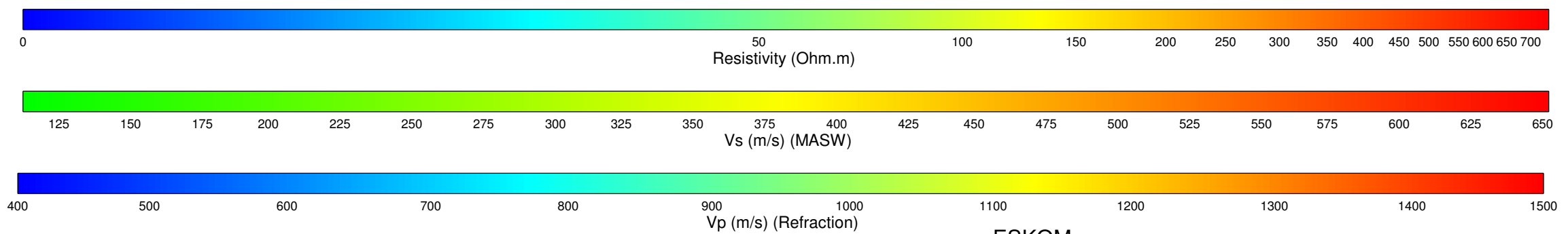
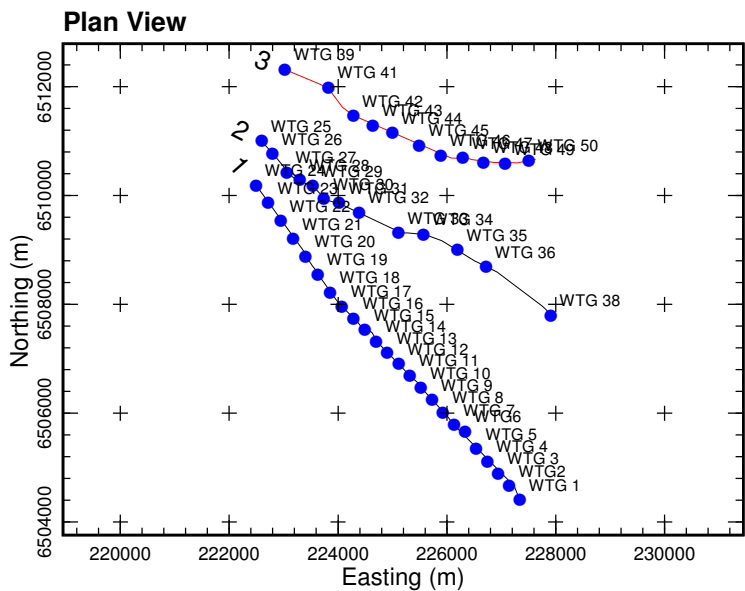
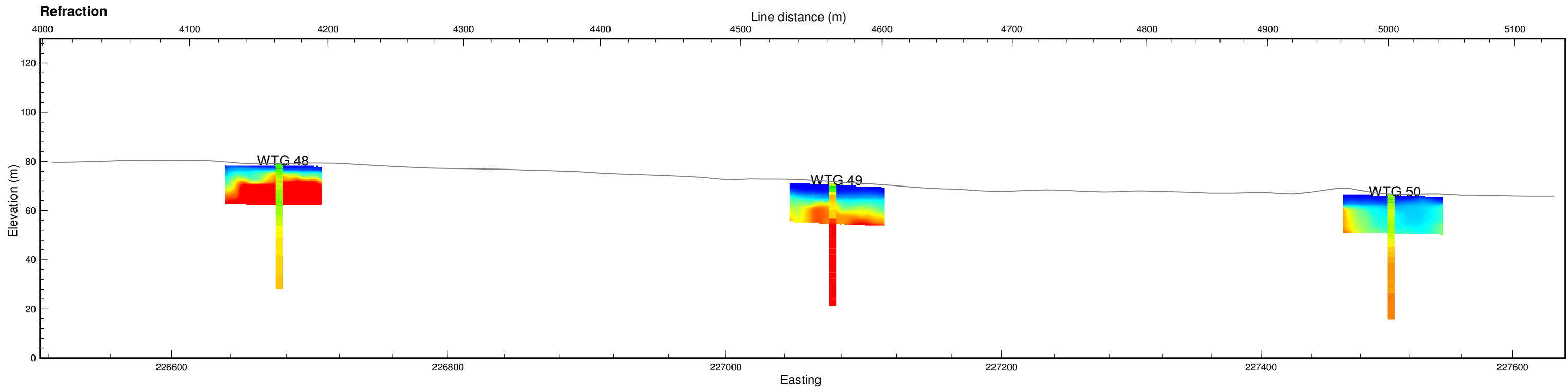
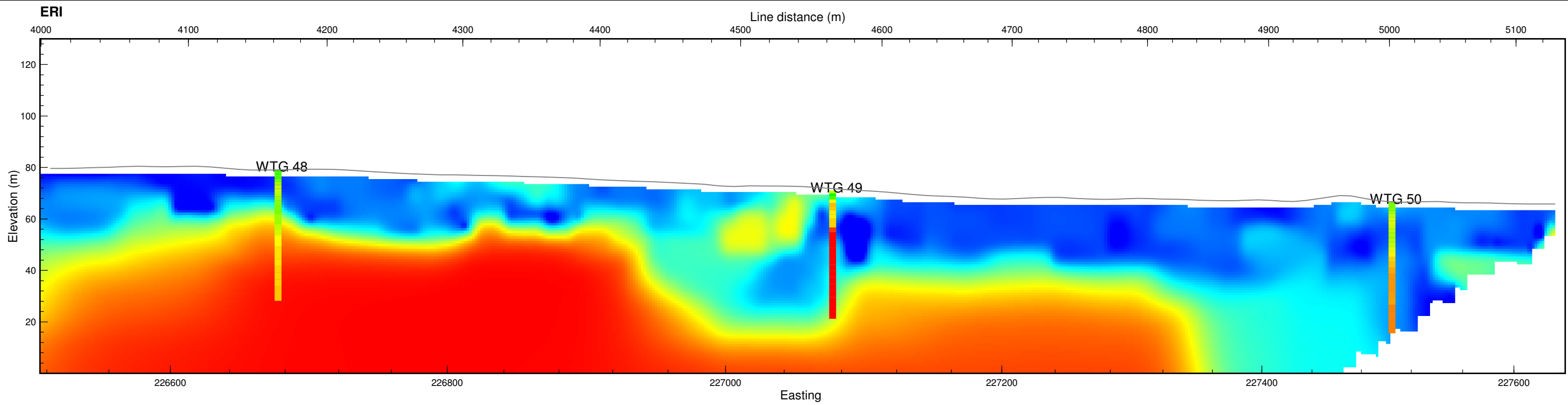




Notes:
 Plot 1: ERI pseudosection with MASW data overlain
 Plot 2: Refraction sections with MASW data overlain
 Data displayed in WGS84 zone S34
 Active line displayed in red on plan view

ESKOM
 SERE WIND ENERGY FACILITY
 ERI and Refraction with MASW overlain
 Row 3: 3000-4000m
 Prepared for BKS by E & EGS





Notes:
 Plot 1: ERI pseudosection with MASW data overlay
 Plot 2: Refraction sections with MASW data overlay
 Data displayed in WGS84 zone S34
 Active line displayed in red on plan view

ESKOM
 SERE WIND ENERGY FACILITY
 ERI and Refraction with MASW overlay
 Row 3: 4000-5000m
 Prepared for BKS by E & EGS

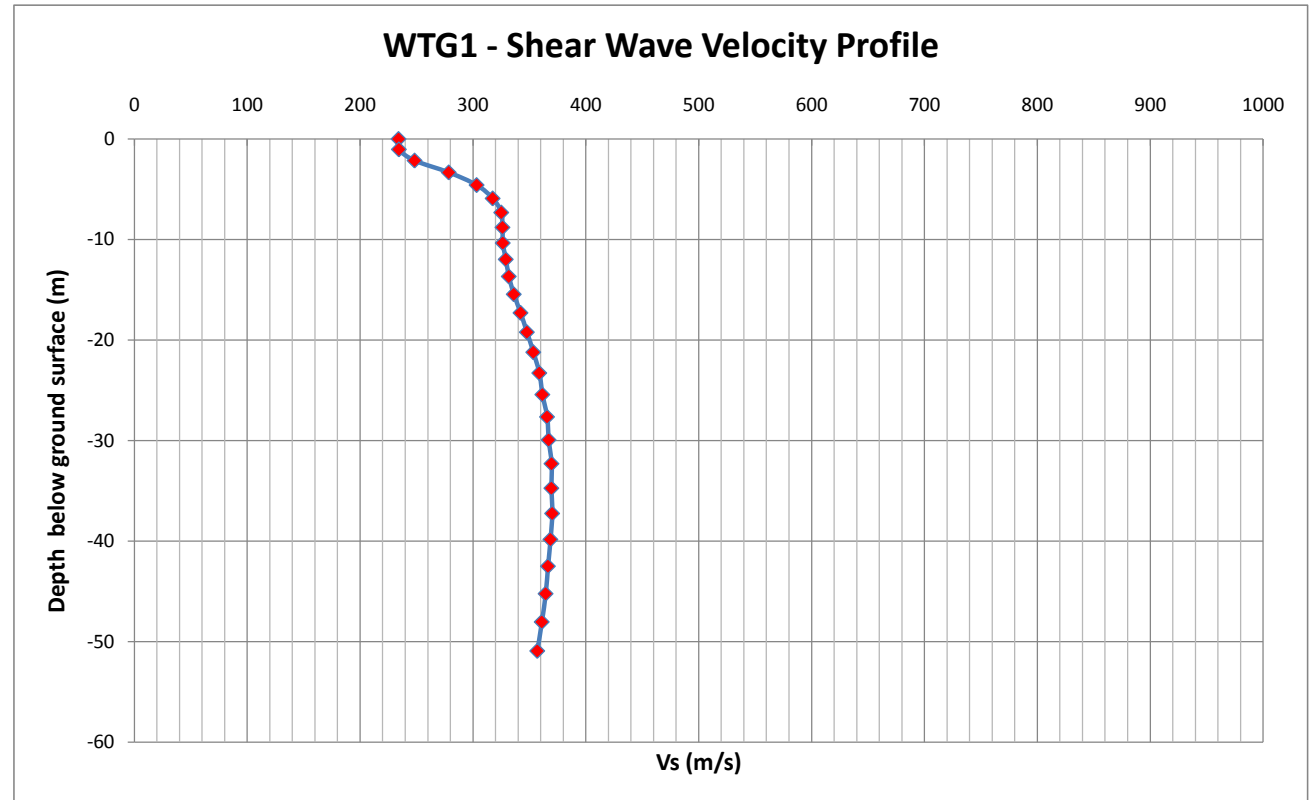


APPENDIX I:

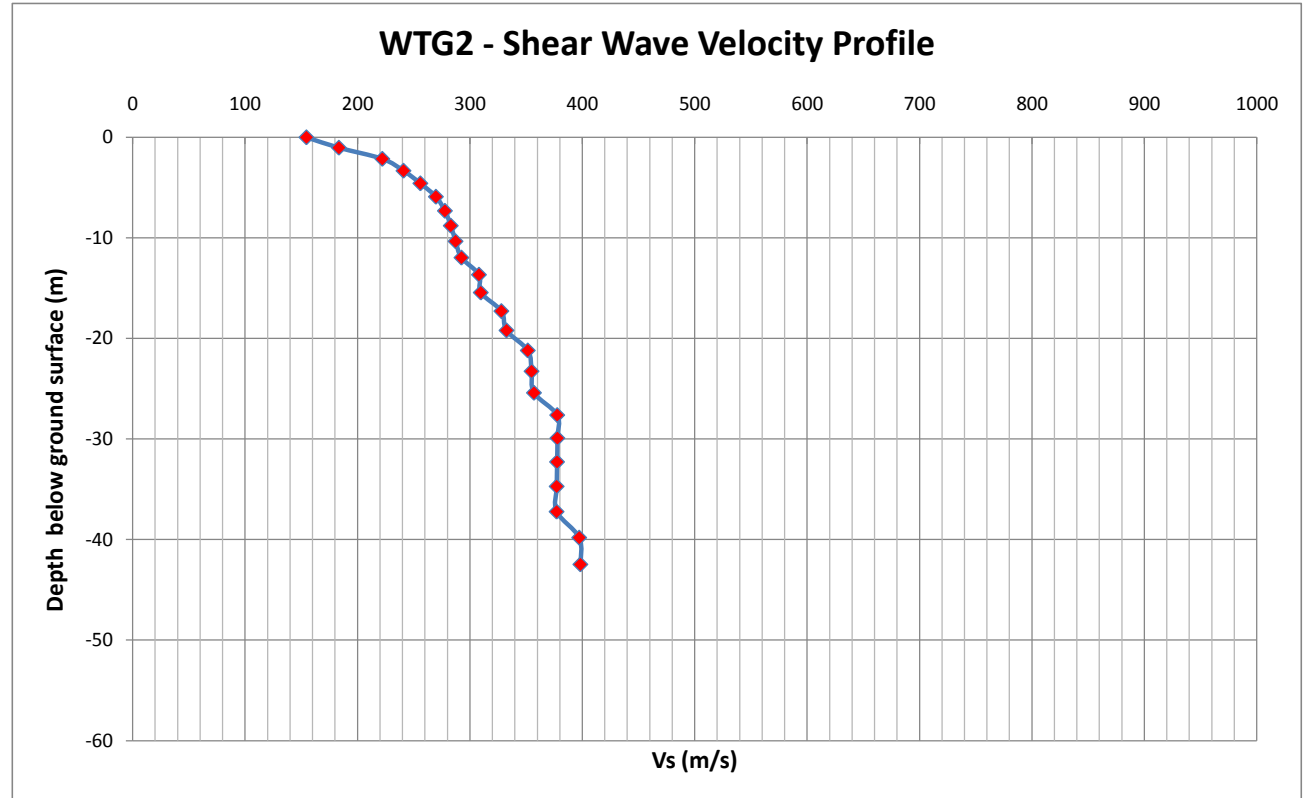
SEISMIC REFRACTION AND ELECTRICAL RESISTIVITY

a (iv) MASW Results

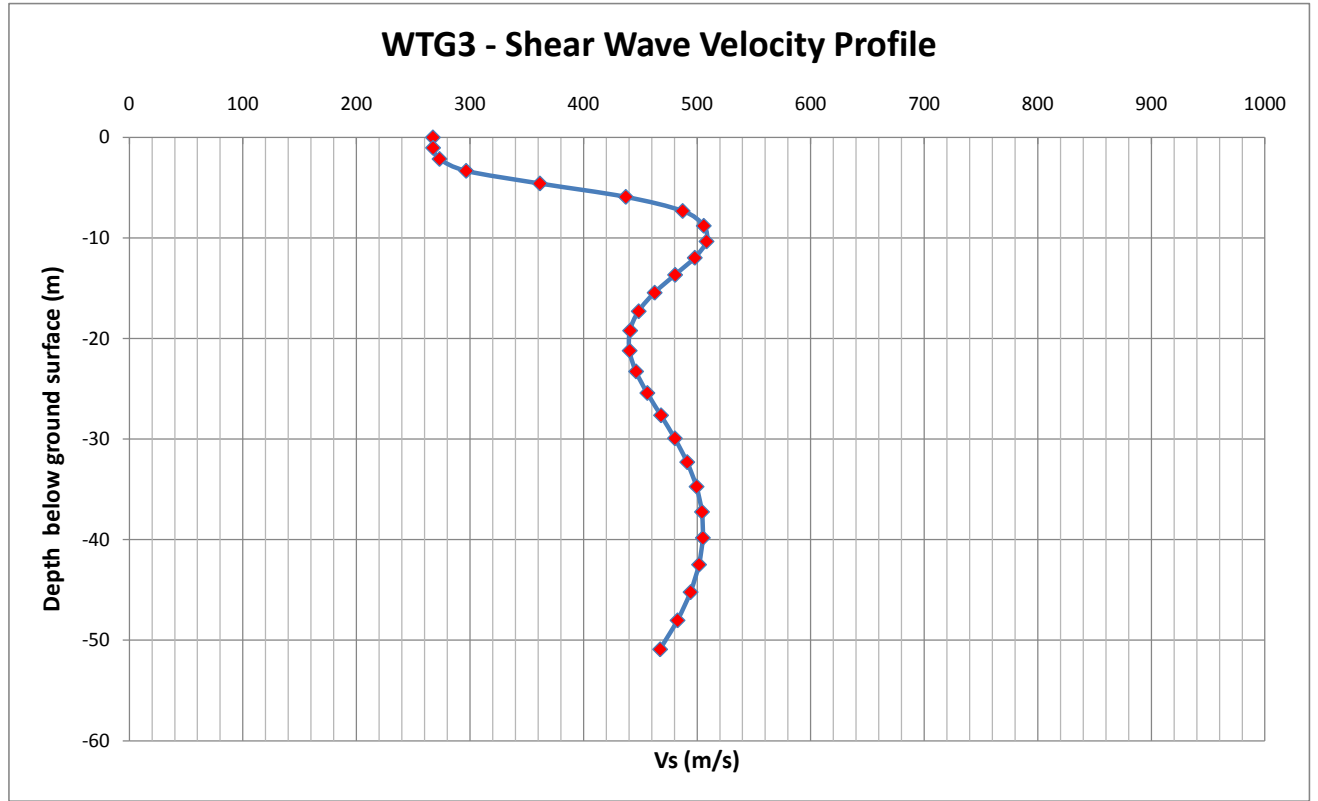
Depth(m)	Vs	Vp	Density	
0	0	234.0662	1578.253	1.812776
1.034483	-1.03448	234.3735	1578.958	1.812999
2.142857	-2.14286	248.2859	1591.063	1.816834
3.325123	-3.32512	278.5609	1614.719	1.824306
4.581281	-4.58128	303.2719	1631.417	1.829562
5.91133	-5.91133	317.4918	1641.827	1.832832
7.315271	-7.31527	325.1182	1651.326	1.83581
8.793104	-8.7931	326.196	1657.271	1.837672
10.34483	-10.3448	326.4464	1662.707	1.839373
11.97044	-11.9704	329.1146	1669.112	1.841375
13.66995	-13.67	331.7844	1673.132	1.842631
15.44335	-15.4434	336.1963	1676.938	1.843819
17.29064	-17.2906	342.1903	1681.022	1.845092
19.21182	-19.2118	347.8016	1683.863	1.845978
21.2069	-21.2069	353.5039	1686.545	1.846813
23.27586	-23.2759	358.8183	1688.963	1.847567
25.41872	-25.4187	361.5419	1688.963	1.847567
27.63547	-27.6355	365.6774	1691.21	1.848266
29.92611	-29.9261	367.0828	1691.21	1.848266
32.29064	-32.2906	369.6383	1693.316	1.848922
34.72906	-34.7291	369.5273	1693.316	1.848922
37.24138	-37.2414	370.2247	1695.036	1.849457
39.82759	-39.8276	368.6793	1695.036	1.849457
42.48769	-42.4877	366.475	1695.036	1.849457
45.22168	-45.2217	364.4122	1695.88	1.849719
48.02956	-48.0296	361.0044	1695.88	1.849719
50.91133	-50.9113	357.0197	1695.88	1.849719



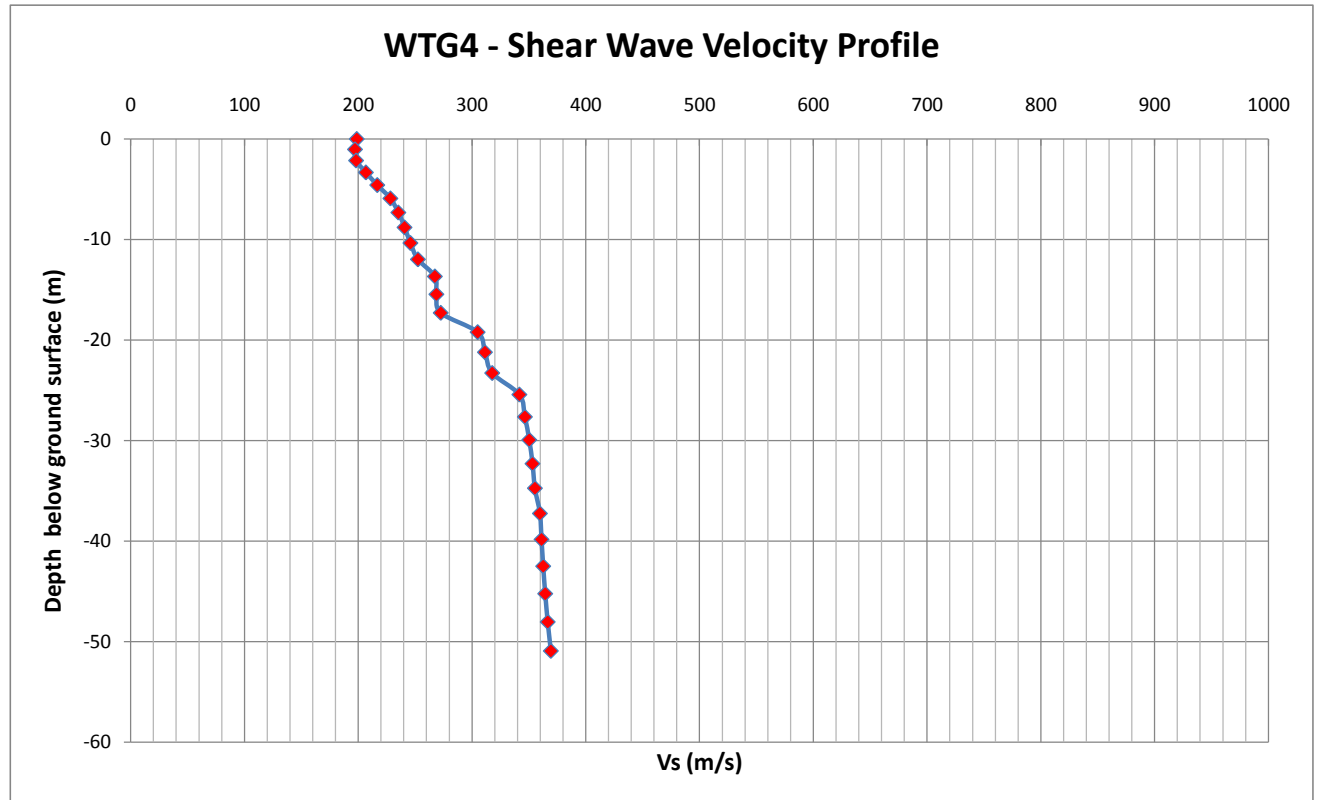
Depth(m)	Vs	Vp	Density	
0	0	154.6188	1496.199	1.786579
1.034483	-1.03448	183.4977	1510.98	1.791324
2.142857	-2.14286	222.1448	1542.588	1.801432
3.325123	-3.32512	240.9913	1565.709	1.808793
4.581281	-4.58128	256.0126	1582.108	1.813998
5.91133	-5.91133	269.8201	1594.751	1.818001
7.315271	-7.31527	277.8426	1603.433	1.820745
8.793104	-8.7931	283.0585	1612.811	1.823704
10.34483	-10.3448	287.3249	1622.885	1.826878
11.97044	-11.9704	292.5699	1632.959	1.830047
13.66995	-13.67	308.1378	1651.554	1.835882
15.44335	-15.4434	309.7629	1651.554	1.835882
17.29064	-17.2906	328.0746	1667.77	1.840956
19.21182	-19.2118	332.6651	1667.77	1.840956
21.2069	-21.2069	351.5829	1683.986	1.846016
23.27586	-23.2759	354.9396	1683.986	1.846016
25.41872	-25.4187	357.0845	1683.986	1.846016
27.63547	-27.6355	377.7596	1705.863	1.852821
29.92611	-29.9261	377.9186	1705.863	1.852821
32.29064	-32.2906	377.626	1705.863	1.852821
34.72906	-34.7291	377.2779	1705.863	1.852821
37.24138	-37.2414	377.2163	1705.863	1.852821
39.82759	-39.8276	397.3427	1727.735	1.8596
42.48769	-42.4877	398.3864	1727.735	1.8596



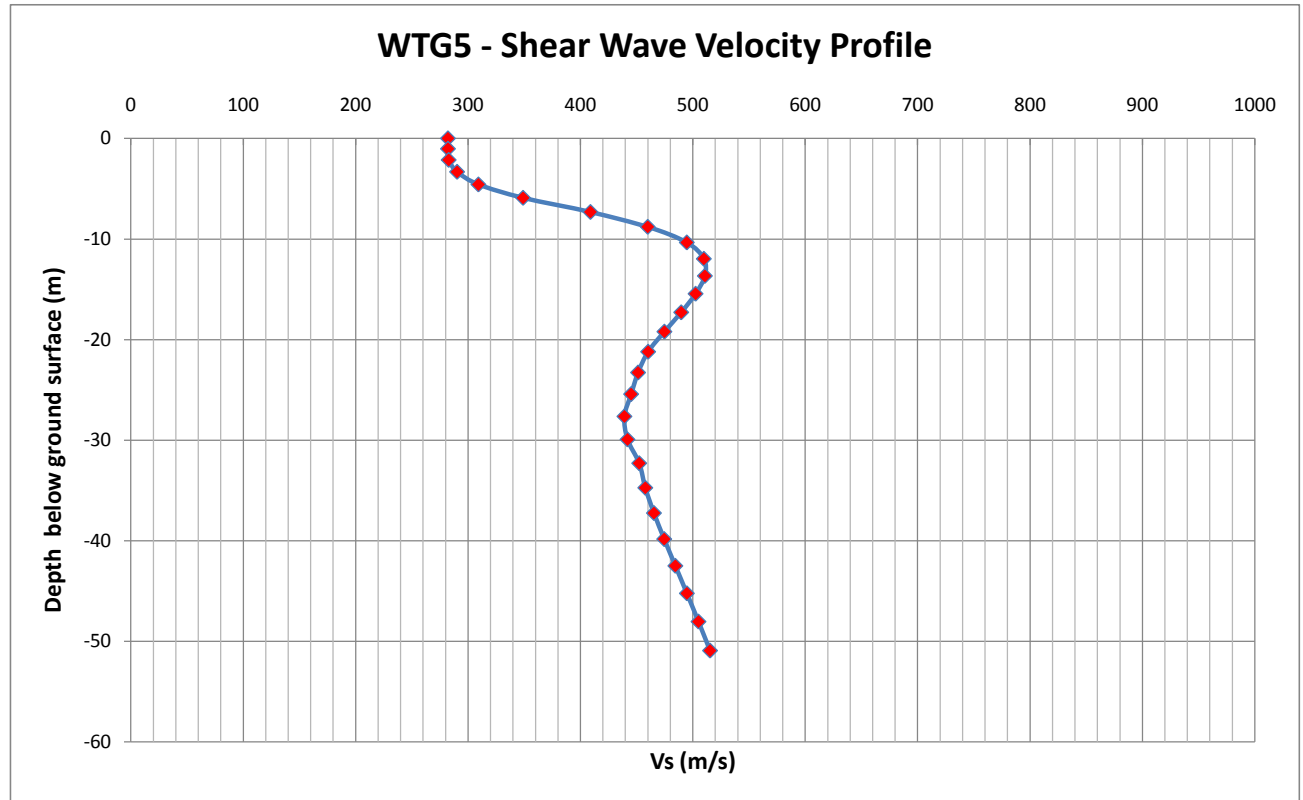
Depth(m)	Vs	Vp	Density	
0	0	267.2447	1691.406	1.848327
1.034483	-1.03448	267.3778	1691.406	1.848327
2.142857	-2.14286	273.1057	1691.406	1.848327
3.325123	-3.32512	296.5117	1693.912	1.849107
4.581281	-4.58128	361.4564	1725.69	1.858967
5.91133	-5.91133	437.0955	1764.806	1.871032
7.315271	-7.31527	487.1611	1783.739	1.876844
8.793104	-8.7931	505.7536	1783.739	1.876844
10.34483	-10.3448	508.193	1783.739	1.876844
11.97044	-11.9704	497.8414	1783.739	1.876844
13.66995	-13.67	480.534	1783.739	1.876844
15.44335	-15.4434	462.5206	1783.739	1.876844
17.29064	-17.2906	448.4607	1783.739	1.876844
19.21182	-19.2118	440.9575	1783.739	1.876844
21.2069	-21.2069	440.5133	1783.739	1.876844
23.27586	-23.2759	446.18	1783.739	1.876844
25.41872	-25.4187	456.0842	1783.739	1.876844
27.63547	-27.6355	468.1417	1783.739	1.876844
29.92611	-29.9261	480.3351	1783.739	1.876844
32.29064	-32.2906	491.1787	1783.739	1.876844
34.72906	-34.7291	499.4383	1783.739	1.876844
37.24138	-37.2414	504.1977	1783.739	1.876844
39.82759	-39.8276	504.9856	1783.739	1.876844
42.48769	-42.4877	501.6176	1783.739	1.876844
45.22168	-45.2217	494.139	1783.739	1.876844
48.02956	-48.0296	482.6639	1783.739	1.876844
50.91133	-50.9113	467.3332	1783.739	1.876844



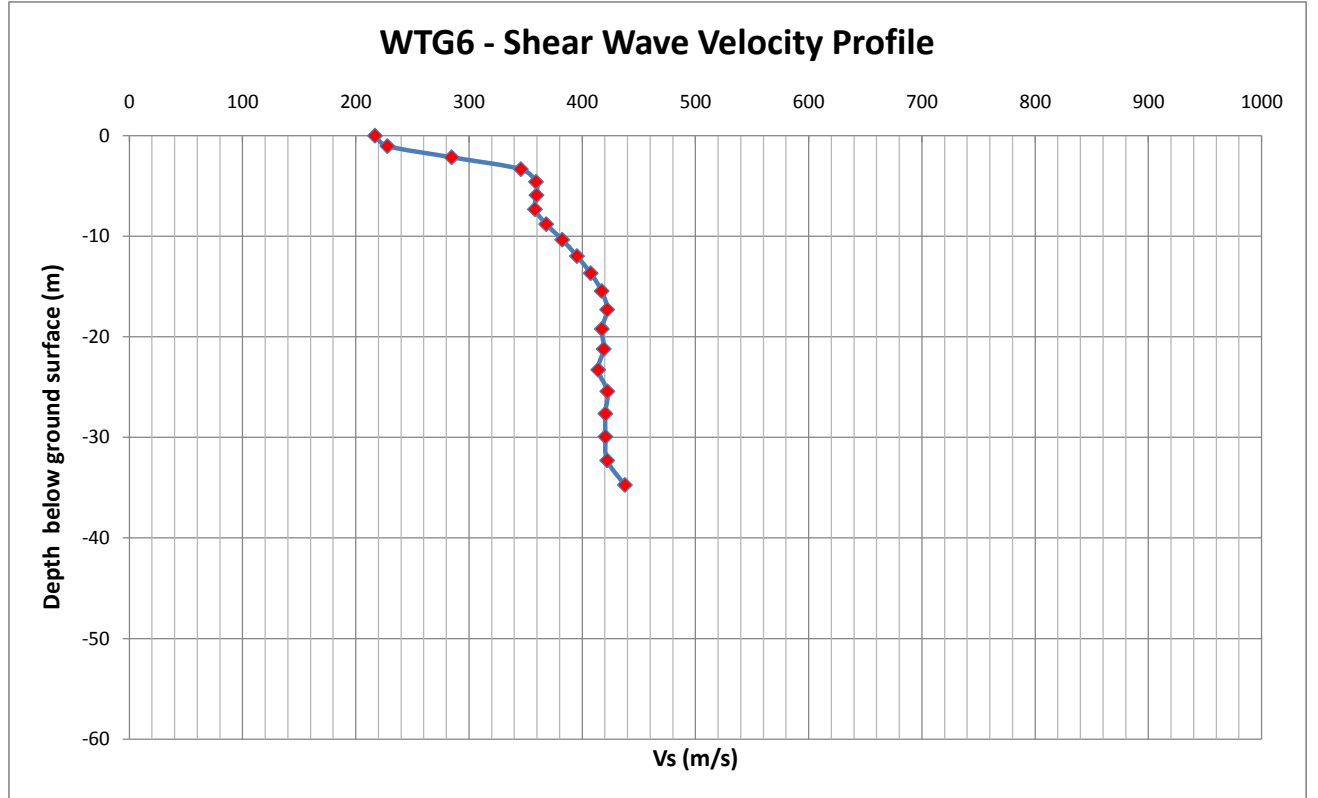
Depth(m)	Vs	Vp	Density	
0	0	198.7675	1521.809	1.794793
1.034483	-1.03448	197.2297	1521.588	1.794722
2.142857	-2.14286	198.1965	1525.869	1.796092
3.325123	-3.32512	206.7807	1536.15	1.799377
4.581281	-4.58128	216.7761	1545.188	1.802261
5.91133	-5.91133	228.3244	1556.014	1.80571
7.315271	-7.31527	235.3217	1564.092	1.80828
8.793104	-8.7931	240.7488	1573	1.811109
10.34483	-10.3448	245.9191	1582.858	1.814235
11.97044	-11.9704	252.5108	1593.604	1.817638
13.66995	-13.67	267.3908	1611.385	1.823254
15.44335	-15.4434	268.7531	1611.385	1.823254
17.29064	-17.2906	272.572	1611.385	1.823254
19.21182	-19.2118	304.9785	1641.135	1.832615
21.2069	-21.2069	311.387	1641.135	1.832615
23.27586	-23.2759	317.775	1641.135	1.832615
25.41872	-25.4187	341.6563	1661.26	1.838921
27.63547	-27.6355	346.4971	1661.26	1.838921
29.92611	-29.9261	350.3274	1661.26	1.838921
32.29064	-32.2906	353.1829	1661.26	1.838921
34.72906	-34.7291	355.2911	1661.26	1.838921
37.24138	-37.2414	359.6908	1664.342	1.839884
39.82759	-39.8276	361.0954	1664.342	1.839884
42.48769	-42.4877	362.5626	1664.342	1.839884
45.22168	-45.2217	364.3447	1664.342	1.839884
48.02956	-48.0296	366.5404	1664.342	1.839884
50.91133	-50.9113	369.2961	1664.342	1.839884



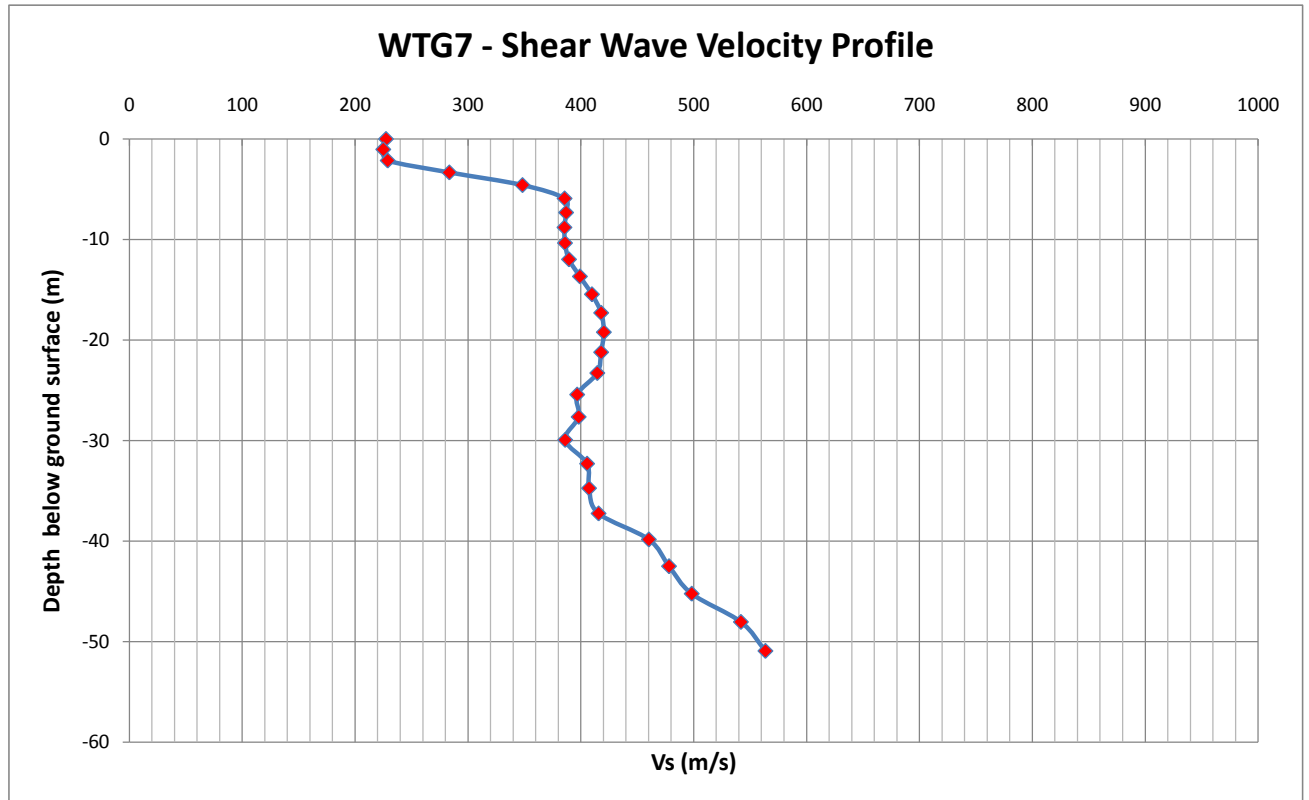
	Depth(m)	Vs	Vp	Density
	0	0	282.1906	1713.19
	1.034483	-1.03448	282.2143	1713.19
	2.142857	-2.14286	282.8639	1713.19
	3.325123	-3.32512	290.3245	1713.19
	4.581281	-4.58128	309.3012	1713.19
	5.91133	-5.91133	349.0228	1724.973
	7.315271	-7.31527	408.9499	1755.21
	8.793104	-8.7931	459.9023	1779.279
	10.34483	-10.3448	494.6654	1794.561
	11.97044	-11.9704	509.8427	1799.907
	13.66995	-13.67	510.7629	1801.263
	15.44335	-15.4434	502.4852	1802.243
	17.29064	-17.2906	489.7107	1804.718
	19.21182	-19.2118	474.763	1807.65
	21.2069	-21.2069	460.2821	1810.583
	23.27586	-23.2759	451.3227	1816.676
	25.41872	-25.4187	445.1497	1821.424
	27.63547	-27.6355	439.191	1821.424
	29.92611	-29.9261	441.9328	1826.171
	32.29064	-32.2906	452.3375	1835.091
	34.72906	-34.7291	457.7609	1835.091
	37.24138	-37.2414	465.4576	1835.091
	39.82759	-39.8276	474.5672	1835.091
	42.48769	-42.4877	484.504	1835.091
	45.22168	-45.2217	494.7474	1835.091
	48.02956	-48.0296	505.0799	1835.091
	50.91133	-50.9113	515.3644	1835.091



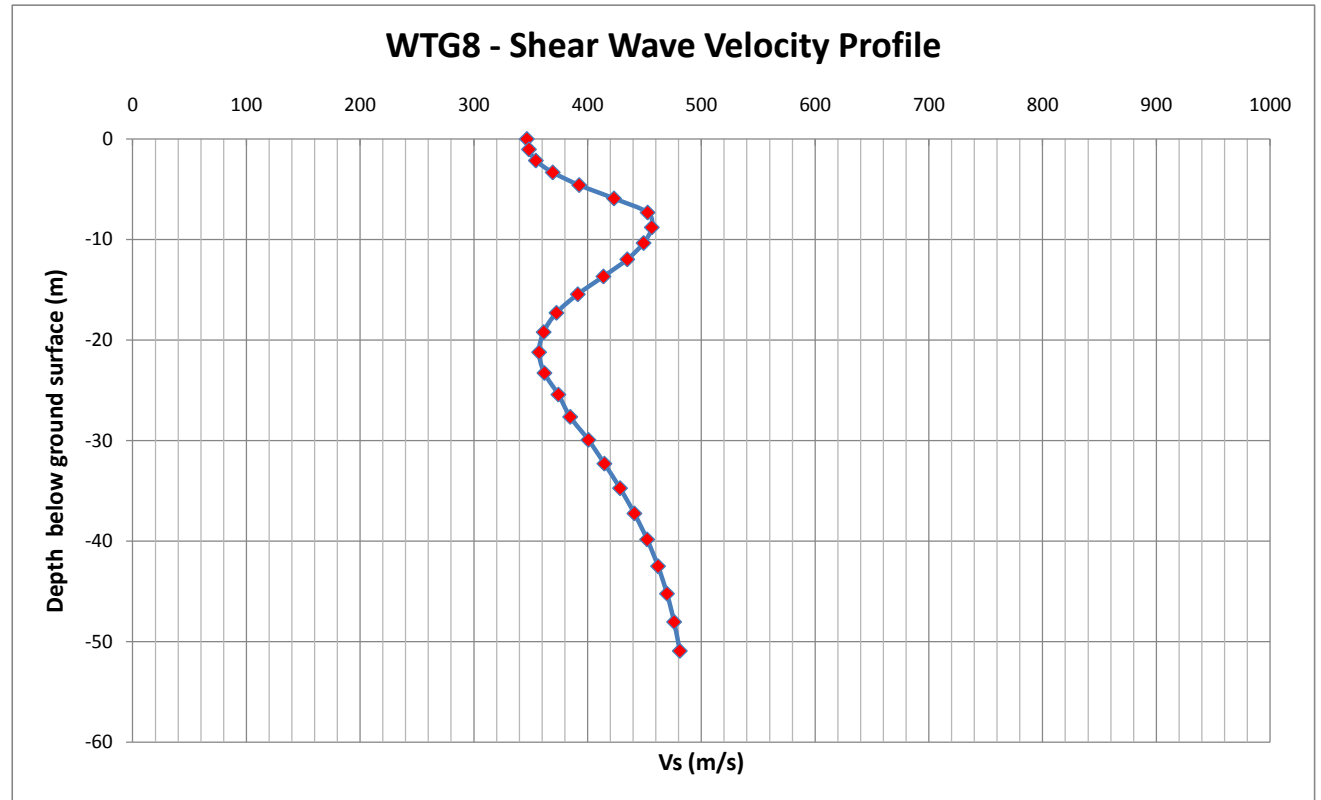
Depth(m)	Vs	Vp	Density	
0	0	216.8975	1609.78	1.822748
1.034483	-1.03448	227.8729	1609.78	1.822748
2.142857	-2.14286	284.5834	1628.798	1.828738
3.325123	-3.32512	345.7117	1662.712	1.839375
4.581281	-4.58128	359.0757	1676.643	1.843726
5.91133	-5.91133	359.5245	1694.939	1.849426
7.315271	-7.31527	358.1432	1707.492	1.853327
8.793104	-8.7931	368.105	1719.728	1.857121
10.34483	-10.3448	382.2384	1727.07	1.859394
11.97044	-11.9704	395.2492	1731.009	1.860613
13.66995	-13.67	407.3823	1737.296	1.862556
15.44335	-15.4434	417.0677	1746.053	1.865258
17.29064	-17.2906	421.9016	1753.947	1.867691
19.21182	-19.2118	417.206	1753.947	1.867691
21.2069	-21.2069	418.8838	1761.842	1.870121
23.27586	-23.2759	414.0225	1761.842	1.870121
25.41872	-25.4187	422.0921	1774.574	1.874033
27.63547	-27.6355	420.3645	1774.574	1.874033
29.92611	-29.9261	420.3706	1774.574	1.874033
32.29064	-32.2906	421.9507	1774.574	1.874033
34.72906	-34.7291	437.6001	1788.799	1.878394



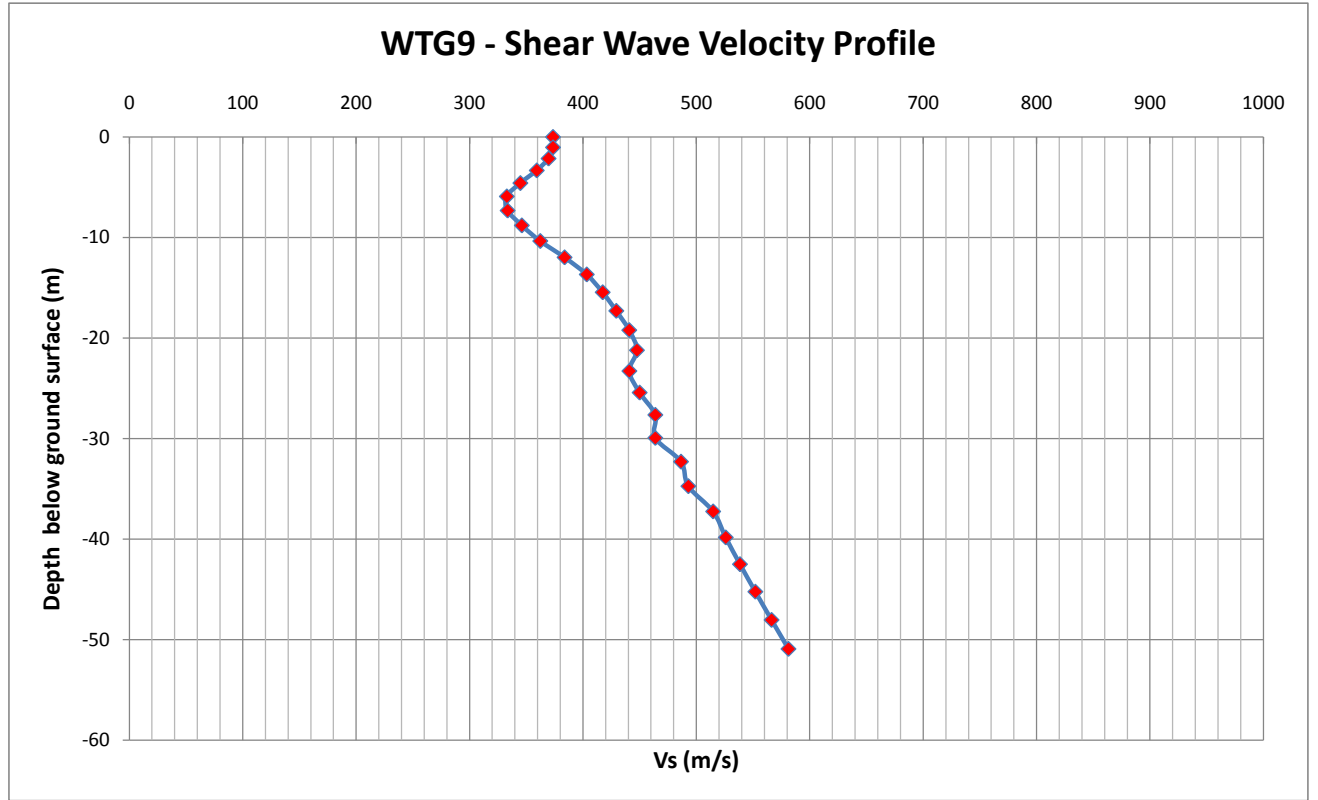
Depth(m)	Vs	Vp	Density	
0	0	227.266	1542.265	1.801329
1.034483	-1.03448	224.863	1539.598	1.800478
2.142857	-2.14286	228.779	1543.945	1.801865
3.325123	-3.32512	283.406	1604.581	1.821107
4.581281	-4.58128	348.194	1676.495	1.84368
5.91133	-5.91133	385.485	1717.888	1.856551
7.315271	-7.31527	386.815	1719.365	1.857009
8.793104	-8.7931	385.376	1717.767	1.856514
10.34483	-10.3448	385.865	1718.31	1.856682
11.97044	-11.9704	389.387	1722.22	1.857893
13.66995	-13.67	399.067	1732.964	1.861217
15.44335	-15.4434	409.728	1744.798	1.864871
17.29064	-17.2906	417.889	1753.857	1.867663
19.21182	-19.2118	420.272	1756.502	1.868478
21.2069	-21.2069	417.878	1753.845	1.867659
23.27586	-23.2759	414.46	1750.051	1.866491
25.41872	-25.4187	396.643	1730.274	1.860385
27.63547	-27.6355	397.969	1731.746	1.86084
29.92611	-29.9261	386.017	1718.479	1.856734
32.29064	-32.2906	405.439	1740.037	1.863402
34.72906	-34.7291	407.136	1741.921	1.863983
37.24138	-37.2414	415.614	1751.332	1.866885
39.82759	-39.8276	460.127	1800.741	1.882046
42.48769	-42.4877	477.992	1820.571	1.888095
45.22168	-45.2217	498.13	1842.924	1.89489
48.02956	-48.0296	541.699	1891.286	1.9095
50.91133	-50.9113	563.41	1915.385	1.916736



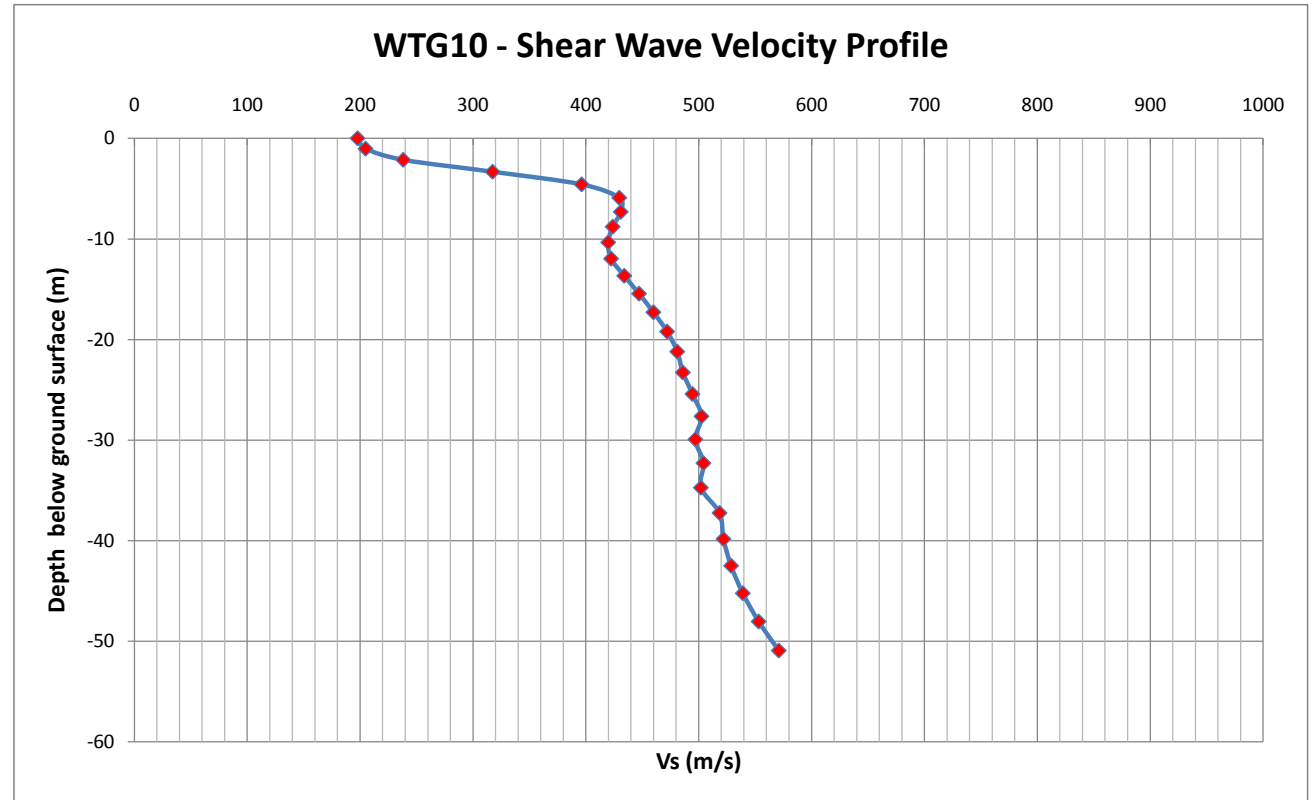
Depth(m)	Vs	Vp	Density	
0	0	346.4997	1747.635	1.865746
1.034483	-1.03448	348.3407	1747.635	1.865746
2.142857	-2.14286	354.4154	1747.635	1.865746
3.325123	-3.32512	369.2839	1747.635	1.865746
4.581281	-4.58128	392.4857	1747.846	1.865811
5.91133	-5.91133	423.0928	1753.193	1.867459
7.315271	-7.31527	452.6754	1762.188	1.870227
8.793104	-8.7931	456.3463	1752.833	1.867348
10.34483	-10.3448	449.1338	1745.674	1.865141
11.97044	-11.9704	434.7825	1744.026	1.864633
13.66995	-13.67	413.8458	1744.099	1.864655
15.44335	-15.4434	391.3058	1745.491	1.865085
17.29064	-17.2906	372.5437	1748.487	1.866009
19.21182	-19.2118	361.3203	1753.251	1.867477
21.2069	-21.2069	357.2823	1757.769	1.868868
23.27586	-23.2759	361.9794	1763.465	1.87062
25.41872	-25.4187	374.2487	1770.557	1.8728
27.63547	-27.6355	384.6335	1770.557	1.8728
29.92611	-29.9261	400.6305	1773.858	1.873813
32.29064	-32.2906	414.6965	1773.858	1.873813
34.72906	-34.7291	428.4531	1773.858	1.873813
37.24138	-37.2414	441.057	1773.858	1.873813
39.82759	-39.8276	452.249	1773.858	1.873813
42.48769	-42.4877	461.8311	1773.858	1.873813
45.22168	-45.2217	469.7197	1773.858	1.873813
48.02956	-48.0296	475.9836	1773.858	1.873813
50.91133	-50.9113	480.9697	1773.858	1.873813



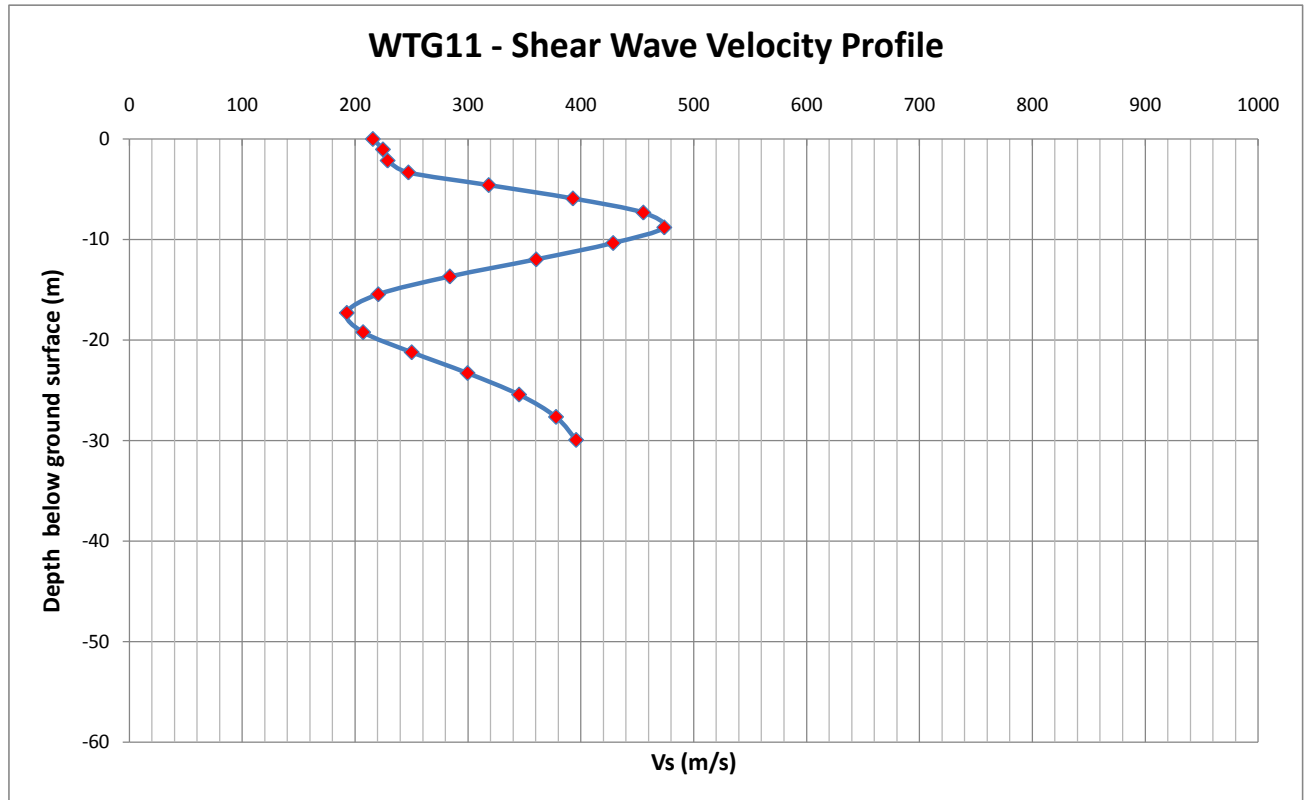
Depth(m)	Vs	Vp	Density	
0	0	373.6087	1700.063	1.851019
1.034483	-1.03448	373.6334	1700.063	1.851019
2.142857	-2.14286	369.6968	1700.063	1.851019
3.325123	-3.32512	359.2868	1700.063	1.851019
4.581281	-4.58128	344.8548	1700.063	1.851019
5.91133	-5.91133	332.9011	1701.507	1.851468
7.315271	-7.31527	333.6078	1710.328	1.854207
8.793104	-8.7931	346.1205	1723.797	1.858381
10.34483	-10.3448	362.399	1734.688	1.86175
11.97044	-11.9704	383.812	1748.074	1.865881
13.66995	-13.67	403.3654	1760.181	1.86961
15.44335	-15.4434	417.4129	1769.816	1.872572
17.29064	-17.2906	429.4146	1782.159	1.87636
19.21182	-19.2118	440.8384	1798.432	1.881341
21.2069	-21.2069	447.611	1812.446	1.885619
23.27586	-23.2759	440.9414	1812.446	1.885619
25.41872	-25.4187	449.9989	1828.709	1.890572
27.63547	-27.6355	463.816	1847.533	1.896287
29.92611	-29.9261	463.7947	1847.533	1.896287
32.29064	-32.2906	486.4548	1868.866	1.902742
34.72906	-34.7291	492.9532	1868.866	1.902742
37.24138	-37.2414	514.7973	1882.965	1.906995
39.82759	-39.8276	525.9151	1882.965	1.906995
42.48769	-42.4877	538.445	1882.965	1.906995
45.22168	-45.2217	552.0111	1882.965	1.906995
48.02956	-48.0296	566.2908	1882.965	1.906995
50.91133	-50.9113	581.1832	1882.965	1.906995



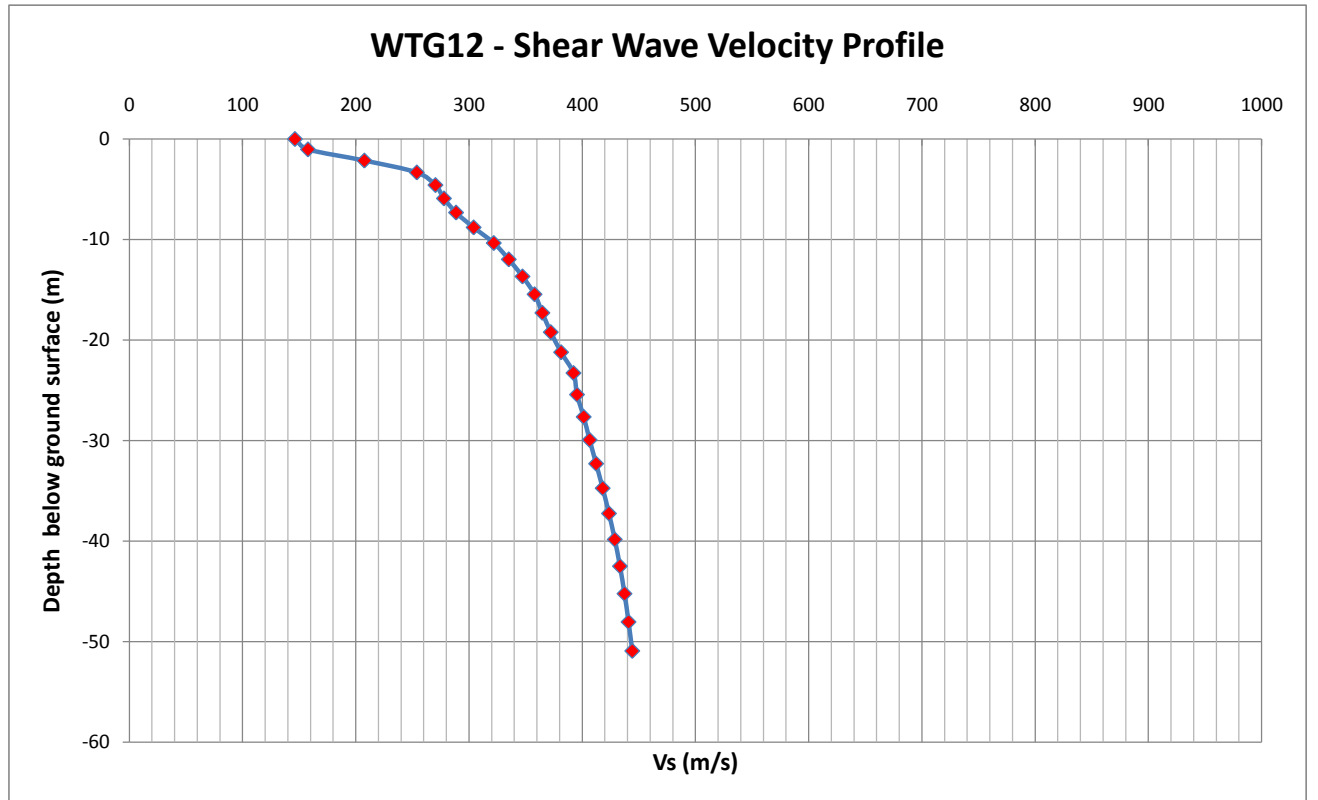
Depth(m)	Vs	Vp	Density	
0	0	197.7354	1624.023	1.827236
1.034483	-1.03448	204.8097	1624.023	1.827236
2.142857	-2.14286	238.1916	1624.023	1.827236
3.325123	-3.32512	317.343	1654.711	1.836871
4.581281	-4.58128	396.232	1704.647	1.852444
5.91133	-5.91133	429.5678	1733.559	1.861401
7.315271	-7.31527	430.8831	1747.578	1.865728
8.793104	-8.7931	423.7611	1759.005	1.869248
10.34483	-10.3448	419.8059	1769.938	1.87261
11.97044	-11.9704	422.3459	1779.863	1.875656
13.66995	-13.67	433.9759	1792.439	1.879508
15.44335	-15.4434	447.0983	1802.518	1.882589
17.29064	-17.2906	459.814	1811.404	1.885302
19.21182	-19.2118	471.9998	1821.465	1.888368
21.2069	-21.2069	480.9635	1830.855	1.891225
23.27586	-23.2759	485.9061	1838.767	1.893628
25.41872	-25.4187	494.435	1853.047	1.897958
27.63547	-27.6355	502.4295	1867.917	1.902455
29.92611	-29.9261	497.0293	1867.917	1.902455
32.29064	-32.2906	504.1752	1880.648	1.906297
34.72906	-34.7291	501.8768	1880.648	1.906297
37.24138	-37.2414	518.4465	1898.552	1.911685
39.82759	-39.8276	521.8843	1898.552	1.911685
42.48769	-42.4877	528.6691	1898.552	1.911685
45.22168	-45.2217	539.0459	1898.552	1.911685
48.02956	-48.0296	553.0707	1898.552	1.911685
50.91133	-50.9113	570.8687	1898.552	1.911685



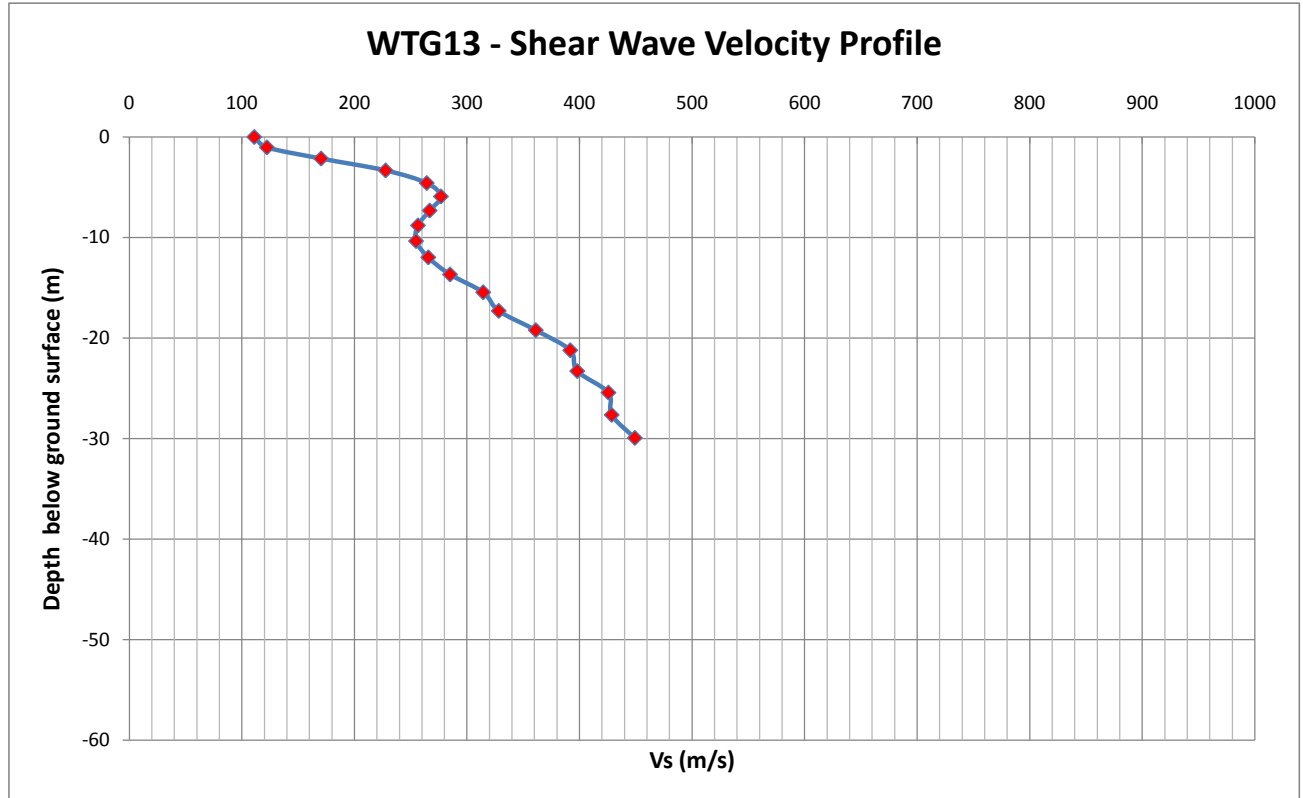
Depth(m)	Vs	Vp	Density	
0	0	215.639	1584.403	1.814725
1.034483	-1.03448	224.5642	1584.403	1.814725
2.142857	-2.14286	228.7132	1591.643	1.817017
3.325123	-3.32512	247.1401	1616.301	1.824804
4.581281	-4.58128	318.2566	1653.8	1.836586
5.91133	-5.91133	392.8459	1656.998	1.837587
7.315271	-7.31527	455.2537	1656.998	1.837587
8.793104	-8.7931	473.7954	1653.895	1.836615
10.34483	-10.3448	428.5222	1633.749	1.830295
11.97044	-11.9704	360.3212	1632.185	1.829803
13.66995	-13.67	283.8078	1636.479	1.831153
15.44335	-15.4434	220.4312	1639.544	1.832115
17.29064	-17.2906	192.5497	1643.354	1.833311
19.21182	-19.2118	207.0001	1650.492	1.835549
21.2069	-21.2069	250.0455	1656.998	1.837587
23.27586	-23.2759	299.5226	1656.998	1.837587
25.41872	-25.4187	345.1827	1656.998	1.837587
27.63547	-27.6355	377.9013	1656.998	1.837587
29.92611	-29.9261	395.6847	1656.998	1.837587



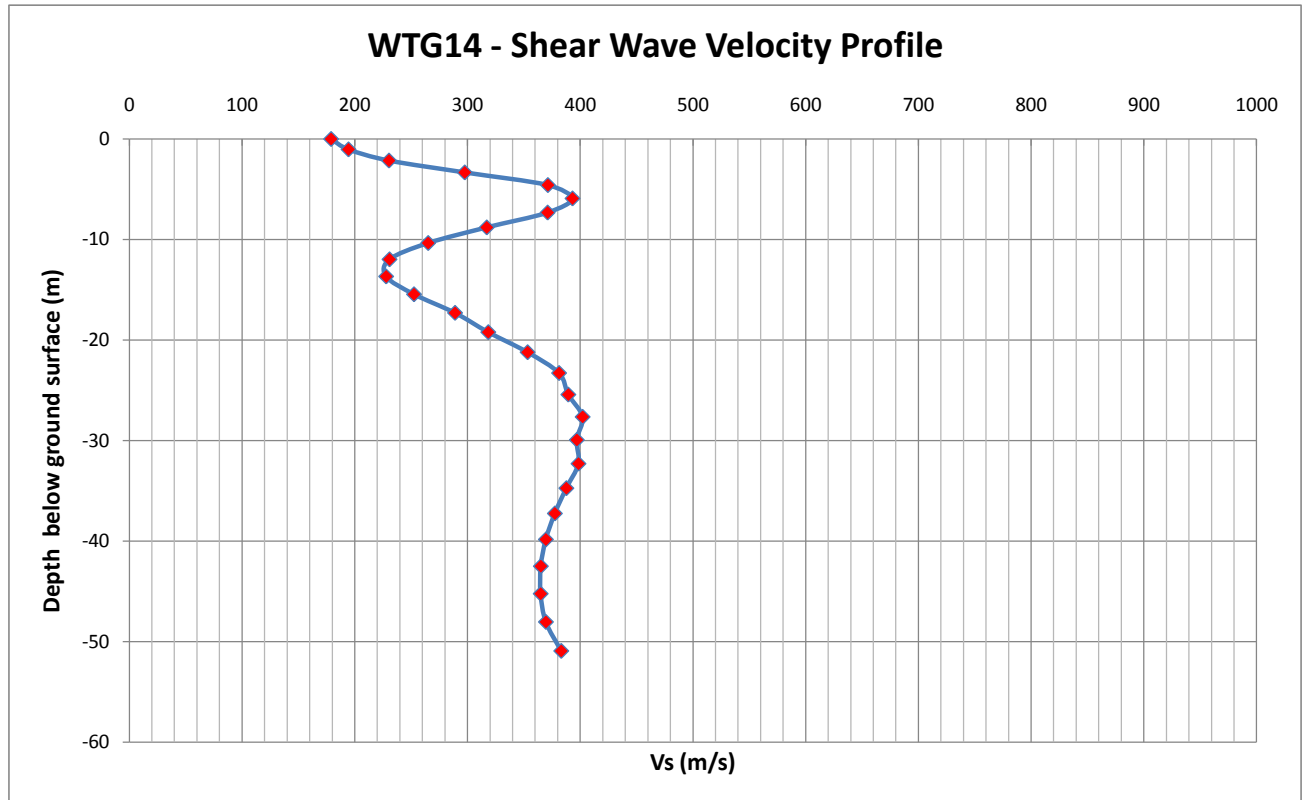
Depth(m)	Vs	Vp	Density	
0	0	146.169	1511.881	1.791613
1.034483	-1.03448	157.6743	1511.881	1.791613
2.142857	-2.14286	207.5418	1532.424	1.798187
3.325123	-3.32512	253.8488	1567.645	1.809409
4.581281	-4.58128	270.3221	1592.476	1.817281
5.91133	-5.91133	277.8358	1612.887	1.823728
7.315271	-7.31527	288.5592	1630.747	1.829352
8.793104	-8.7931	304.0868	1646.772	1.834383
10.34483	-10.3448	321.8835	1662.003	1.839153
11.97044	-11.9704	335.1404	1672.476	1.842426
13.66995	-13.67	347.2481	1683.59	1.845893
15.44335	-15.4434	357.921	1695.041	1.849458
17.29064	-17.2906	364.8273	1703.284	1.85202
19.21182	-19.2118	372.2732	1712.002	1.854727
21.2069	-21.2069	381.3693	1721.598	1.8577
23.27586	-23.2759	392.3132	1731.803	1.860858
25.41872	-25.4187	395.4375	1731.803	1.860858
27.63547	-27.6355	401.3473	1733.538	1.861394
29.92611	-29.9261	406.5829	1733.538	1.861394
32.29064	-32.2906	412.2957	1733.538	1.861394
34.72906	-34.7291	418.1058	1733.538	1.861394
37.24138	-37.2414	423.6755	1733.538	1.861394
39.82759	-39.8276	428.8032	1733.538	1.861394
42.48769	-42.4877	433.3828	1733.538	1.861394
45.22168	-45.2217	437.4106	1733.538	1.861394
48.02956	-48.0296	440.9677	1733.538	1.861394
50.91133	-50.9113	444.2663	1733.538	1.861394



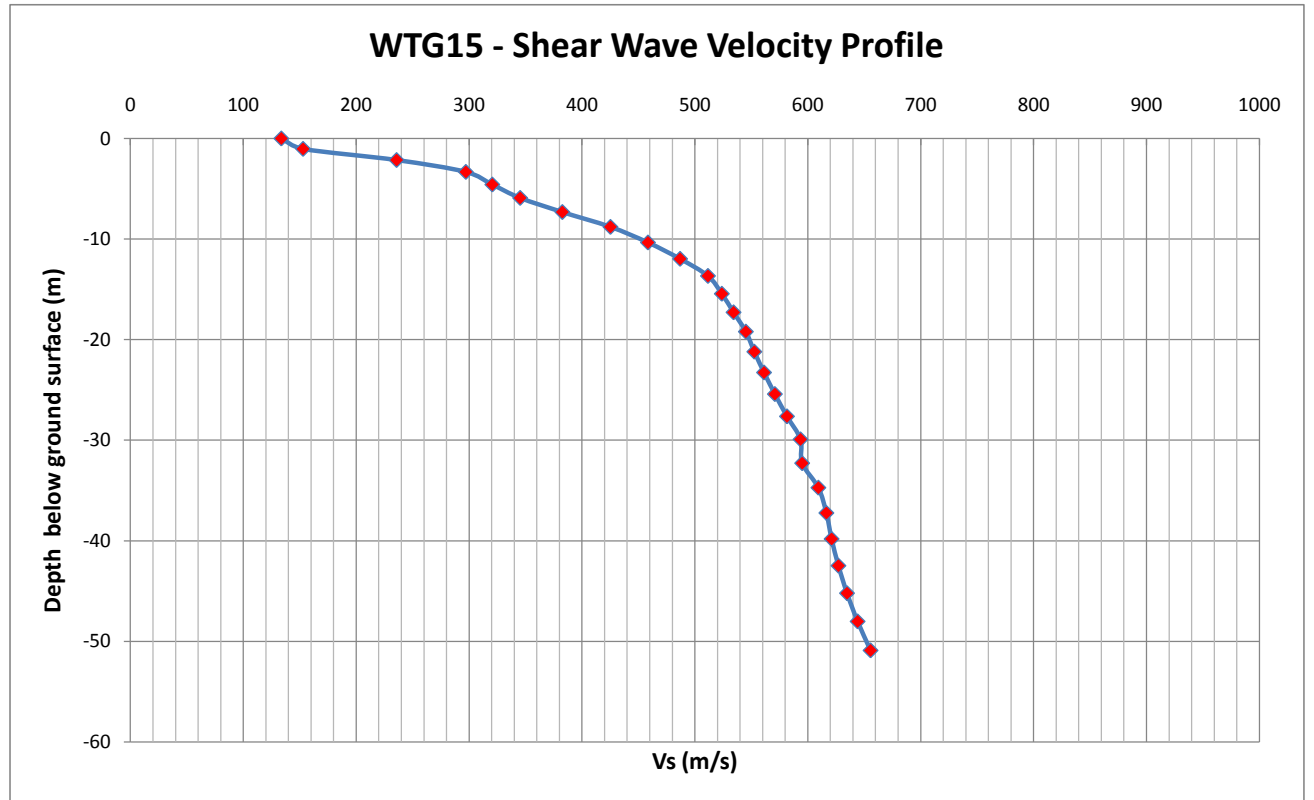
Depth(m)	Vs	Vp	Density	
0	0	111.0236	1466.316	1.776951
1.034483	-1.03448	122.2386	1466.316	1.776951
2.142857	-2.14286	170.3805	1493.569	1.785733
3.325123	-3.32512	227.7205	1536.99	1.799645
4.581281	-4.58128	264.2624	1564.319	1.808352
5.91133	-5.91133	276.8683	1578.375	1.812814
7.315271	-7.31527	266.8617	1583.104	1.814313
8.793104	-8.7931	256.4999	1596.356	1.818508
10.34483	-10.3448	254.7397	1615.846	1.824661
11.97044	-11.9704	265.6569	1637.393	1.83144
13.66995	-13.67	284.9641	1655.175	1.837016
15.44335	-15.4434	314.4252	1675.43	1.843348
17.29064	-17.2906	328.24	1675.43	1.843348
19.21182	-19.2118	361.1378	1698.137	1.850421
21.2069	-21.2069	391.7629	1721.831	1.857773
23.27586	-23.2759	397.9932	1721.831	1.857773
25.41872	-25.4187	425.7012	1748.228	1.865929
27.63547	-27.6355	428.589	1748.228	1.865929
29.92611	-29.9261	449.1715	1768.144	1.872058



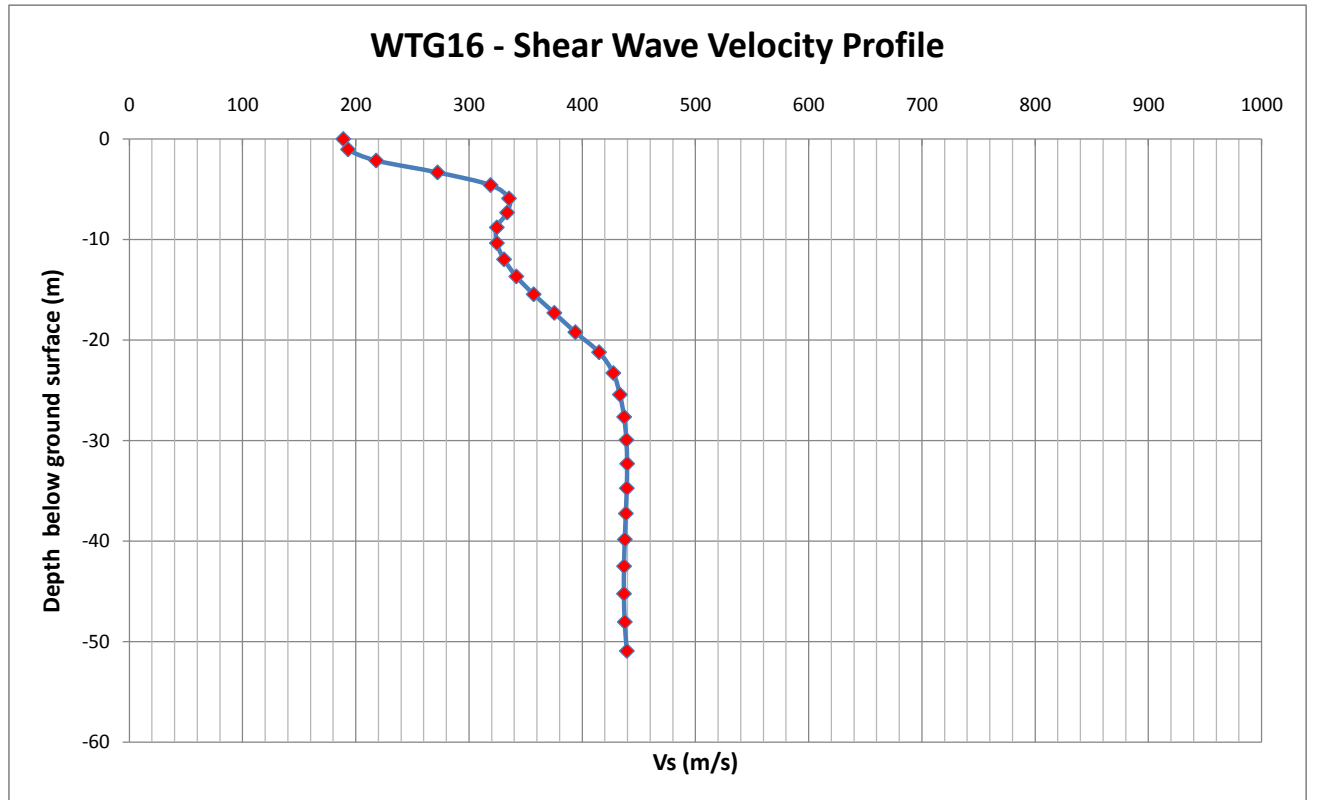
Depth(m)	Vs	Vp	Density
0	0	179.1314	1611.823
1.034483	-1.03448	194.554	1611.823
2.142857	-2.14286	230.44	1611.823
3.325123	-3.32512	297.5942	1623.061
4.581281	-4.58128	371.3059	1641.308
5.91133	-5.91133	393.1322	1631.911
7.315271	-7.31527	371.0635	1622.144
8.793104	-8.7931	317.1053	1615.406
10.34483	-10.3448	265.1889	1621.642
11.97044	-11.9704	230.9105	1628.945
13.66995	-13.67	227.929	1638.838
15.44335	-15.4434	252.6283	1650.987
17.29064	-17.2906	289.0077	1661.1
19.21182	-19.2118	318.4775	1661.1
21.2069	-21.2069	353.3292	1672.67
23.27586	-23.2759	381.2202	1685.362
25.41872	-25.4187	389.4441	1685.362
27.63547	-27.6355	402.1127	1698.573
29.92611	-29.9261	396.958	1698.573
32.29064	-32.2906	398.4294	1710.264
34.72906	-34.7291	387.6789	1710.264
37.24138	-37.2414	377.4917	1710.264
39.82759	-39.8276	369.5228	1710.264
42.48769	-42.4877	365.061	1710.264
45.22168	-45.2217	364.9307	1710.264
48.02956	-48.0296	369.5555	1710.264
50.91133	-50.9113	383.1393	1714.85



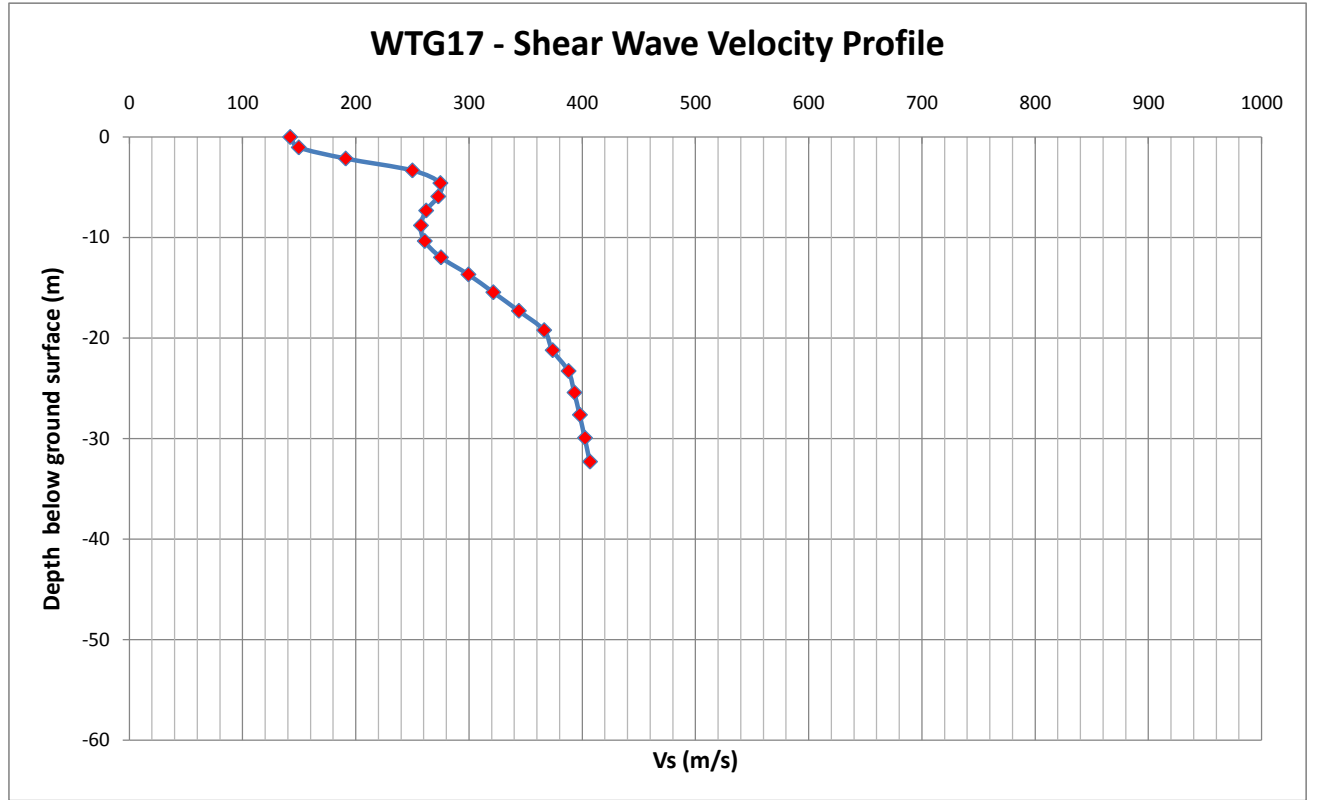
Depth(m)	Vs	Vp	Density	
0	0	133.5806	1529.234	1.797168
1.034483	-1.03448	152.8473	1529.234	1.797168
2.142857	-2.14286	235.6992	1556.905	1.805994
3.325123	-3.32512	297.0864	1612.009	1.823451
4.581281	-4.58128	320.5592	1659.785	1.838459
5.91133	-5.91133	345.2095	1703.611	1.852122
7.315271	-7.31527	382.6053	1743.546	1.864485
8.793104	-8.7931	425.2318	1779.01	1.875394
10.34483	-10.3448	458.4597	1803.34	1.882841
11.97044	-11.9704	486.9377	1826.586	1.889926
13.66995	-13.67	511.6411	1850.66	1.897235
15.44335	-15.4434	523.93	1864.694	1.901482
17.29064	-17.2906	534.3222	1878.643	1.905693
19.21182	-19.2118	545.2293	1893.813	1.91026
21.2069	-21.2069	552.7555	1904.925	1.913599
23.27586	-23.2759	561.3487	1916.506	1.917071
25.41872	-25.4187	570.9438	1928.331	1.92061
27.63547	-27.6355	581.6589	1940.458	1.924231
29.92611	-29.9261	593.6701	1953.084	1.927993
32.29064	-32.2906	595.1229	1953.084	1.927993
34.72906	-34.7291	609.4935	1966.378	1.931945
37.24138	-37.2414	616.5722	1970.442	1.933152
39.82759	-39.8276	621.2178	1970.442	1.933152
42.48769	-42.4877	627.2516	1970.442	1.933152
45.22168	-45.2217	634.867	1970.442	1.933152
48.02956	-48.0296	644.2656	1970.442	1.933152
50.91133	-50.9113	655.7414	1970.442	1.933152



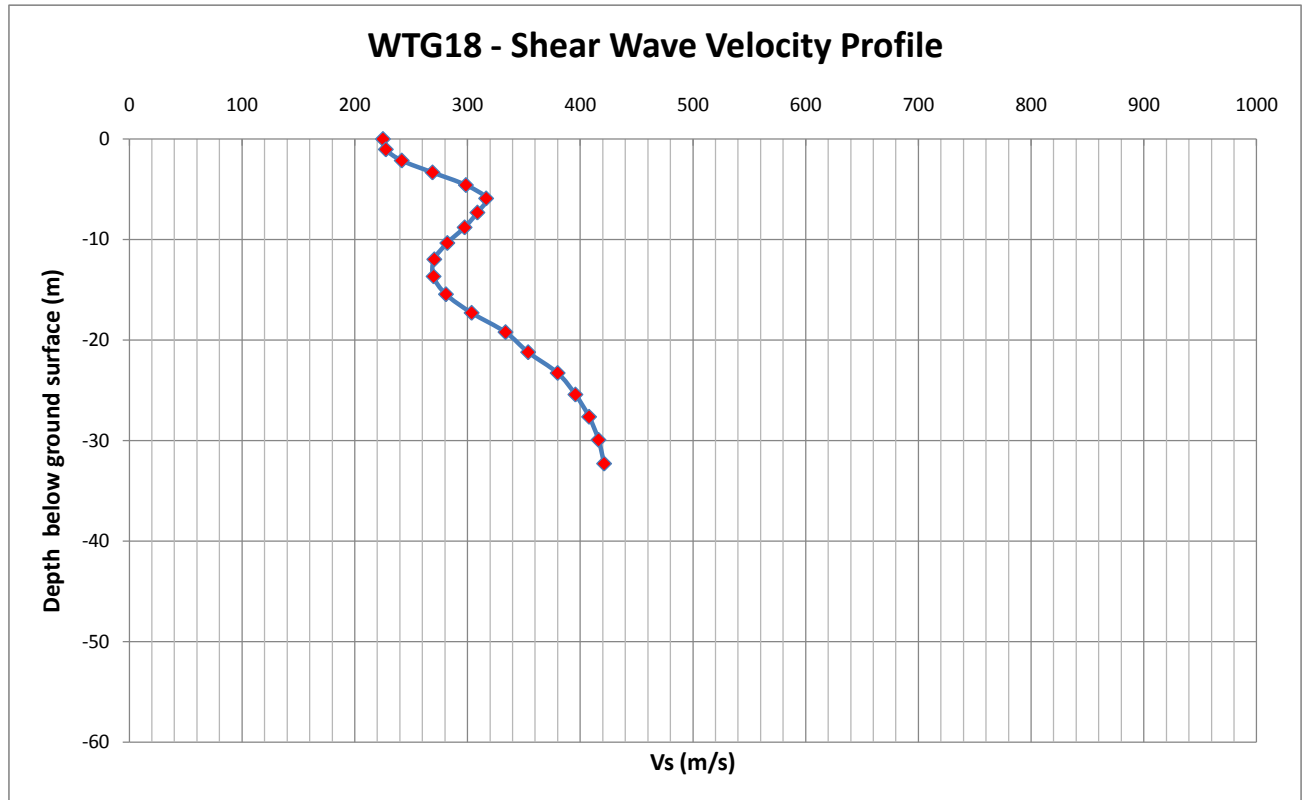
Depth(m)	Vs	Vp	Density	
0	0	188.8372	1577.764	1.812621
1.034483	-1.03448	193.0484	1577.764	1.812621
2.142857	-2.14286	217.8684	1581.289	1.813738
3.325123	-3.32512	272.0963	1604.144	1.820969
4.581281	-4.58128	318.9158	1629.93	1.829095
5.91133	-5.91133	335.231	1643.684	1.833415
7.315271	-7.31527	333.5415	1655.195	1.837023
8.793104	-8.7931	324.4675	1664.947	1.840074
10.34483	-10.3448	324.5305	1680.891	1.845051
11.97044	-11.9704	330.8613	1694.884	1.849409
13.66995	-13.67	341.69	1704.719	1.852466
15.44335	-15.4434	357.0271	1713.02	1.855042
17.29064	-17.2906	375.2512	1721.322	1.857615
19.21182	-19.2118	393.8345	1729.623	1.860184
21.2069	-21.2069	414.7878	1741.848	1.863961
23.27586	-23.2759	427.3652	1746.938	1.865531
25.41872	-25.4187	433.1971	1746.938	1.865531
27.63547	-27.6355	436.9573	1746.938	1.865531
29.92611	-29.9261	438.9347	1746.938	1.865531
32.29064	-32.2906	439.5912	1746.938	1.865531
34.72906	-34.7291	439.2964	1746.938	1.865531
37.24138	-37.2414	438.4792	1746.938	1.865531
39.82759	-39.8276	437.5529	1746.938	1.865531
42.48769	-42.4877	436.8745	1746.938	1.865531
45.22168	-45.2217	436.78	1746.938	1.865531
48.02956	-48.0296	437.5148	1746.938	1.865531
50.91133	-50.9113	439.3236	1746.938	1.865531



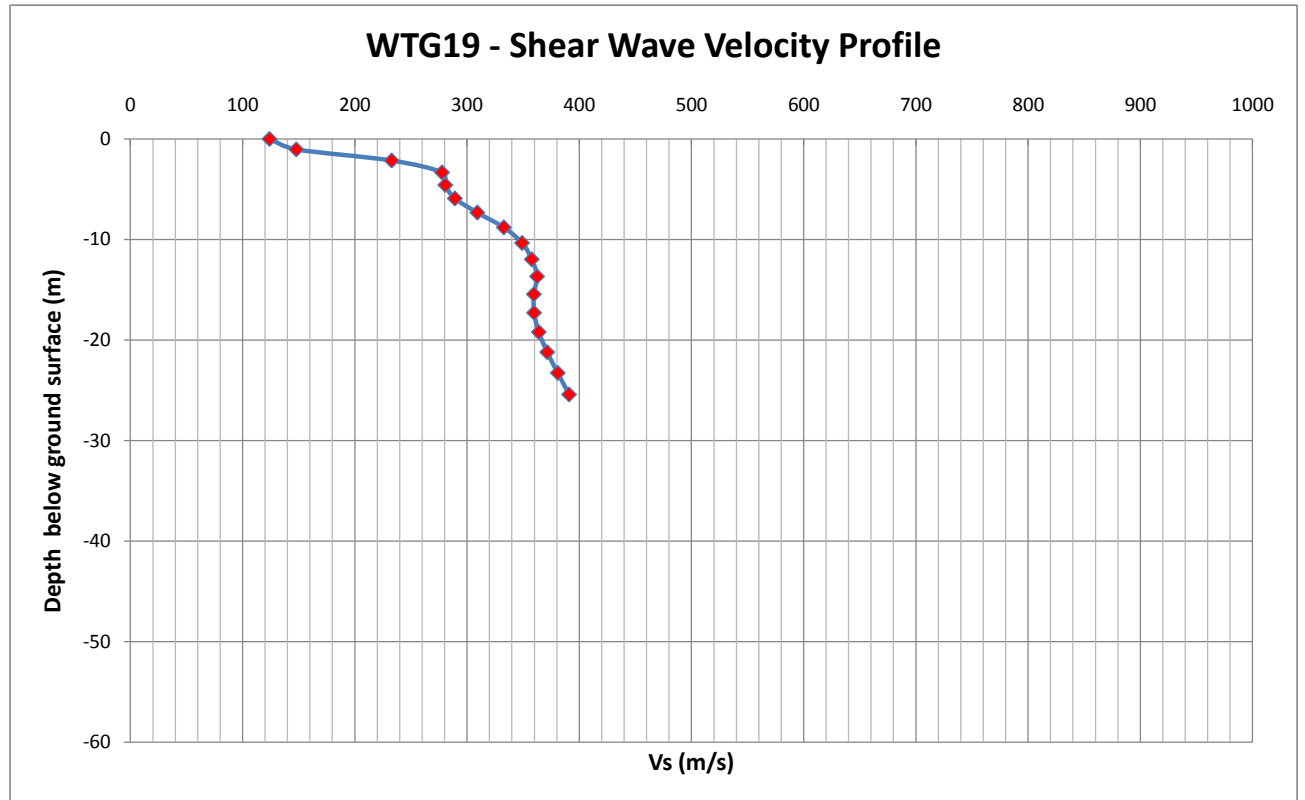
Depth(m)	Vs	Vp	Density	
0	0	142.0382	1503.125	1.788804
1.034483	-1.03448	149.6598	1503.125	1.788804
2.142857	-2.14286	191.0646	1519.486	1.794049
3.325123	-3.32512	249.9641	1556.166	1.805758
4.581281	-4.58128	274.6637	1574.31	1.811525
5.91133	-5.91133	272.799	1583.521	1.814446
7.315271	-7.31527	262.1092	1593.182	1.817504
8.793104	-8.7931	257.4921	1607.567	1.82205
10.34483	-10.3448	260.8784	1621.465	1.826431
11.97044	-11.9704	275.1754	1637.042	1.83133
13.66995	-13.67	299.4125	1656.282	1.837363
15.44335	-15.4434	321.3838	1669.722	1.841566
17.29064	-17.2906	343.9354	1683.521	1.845871
19.21182	-19.2118	366.2679	1698.318	1.850477
21.2069	-21.2069	373.7705	1698.318	1.850477
23.27586	-23.2759	387.8012	1707.057	1.853192
25.41872	-25.4187	393.0789	1707.057	1.853192
27.63547	-27.6355	397.8258	1707.057	1.853192
29.92611	-29.9261	402.3193	1707.057	1.853192
32.29064	-32.2906	406.7308	1707.057	1.853192



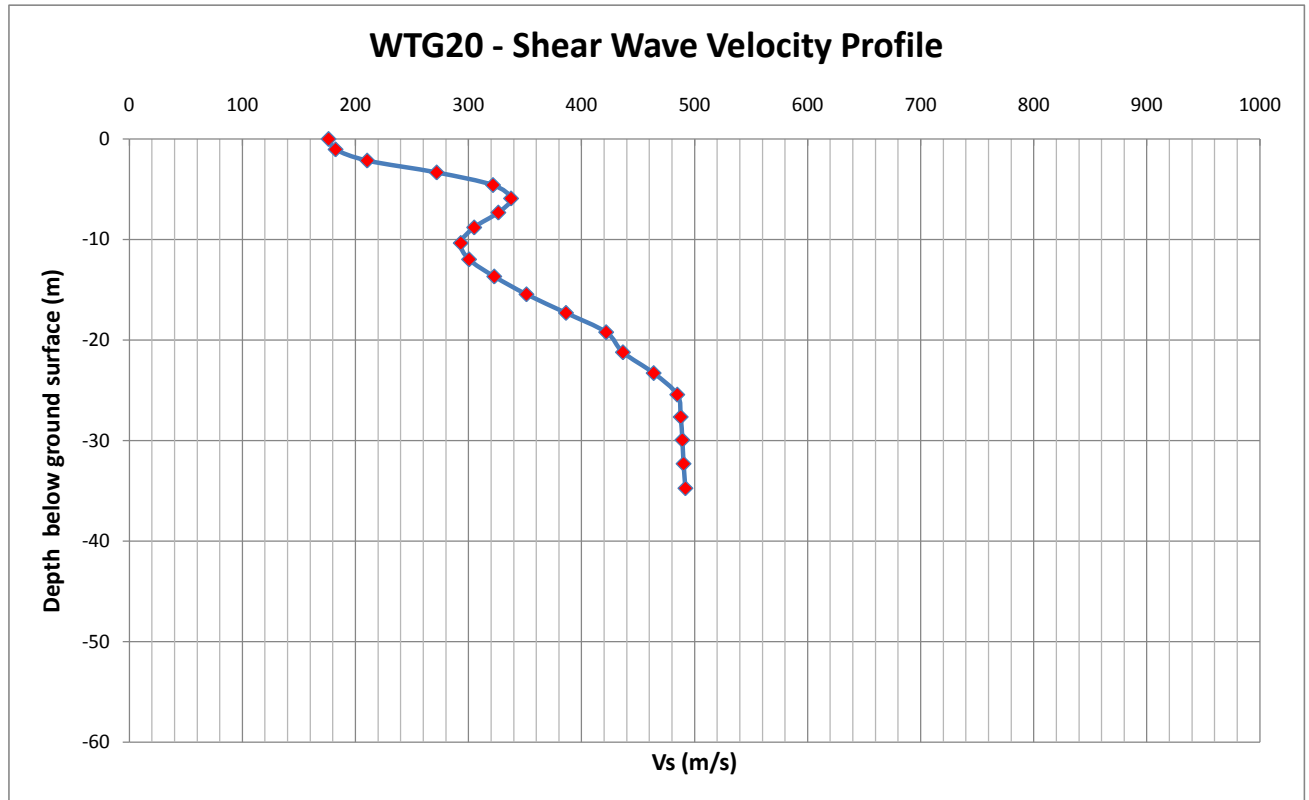
Depth(m)	Vs	Vp	Density
0	0	225.0786	1586.133
1.034483	-1.03448	227.6278	1586.133
2.142857	-2.14286	241.7408	1591.276
3.325123	-3.32512	269.0389	1601.877
4.581281	-4.58128	298.6549	1613.391
5.911133	-5.91133	316.6102	1621.071
7.315271	-7.31527	308.8656	1615.857
8.793104	-8.7931	297.52	1622.379
10.34483	-10.3448	282.1769	1631.81
11.97044	-11.9704	270.6316	1642.252
13.66995	-13.67	269.9791	1654.007
15.44335	-15.4434	280.9636	1665.043
17.29064	-17.2906	303.7217	1677.54
19.21182	-19.2118	333.8163	1691.186
21.2069	-21.2069	353.8812	1691.186
23.27586	-23.2759	380.0413	1699.264
25.41872	-25.4187	395.8099	1699.264
27.63547	-27.6355	407.946	1699.264
29.92611	-29.9261	416.304	1699.264
32.29064	-32.2906	421.263	1699.264



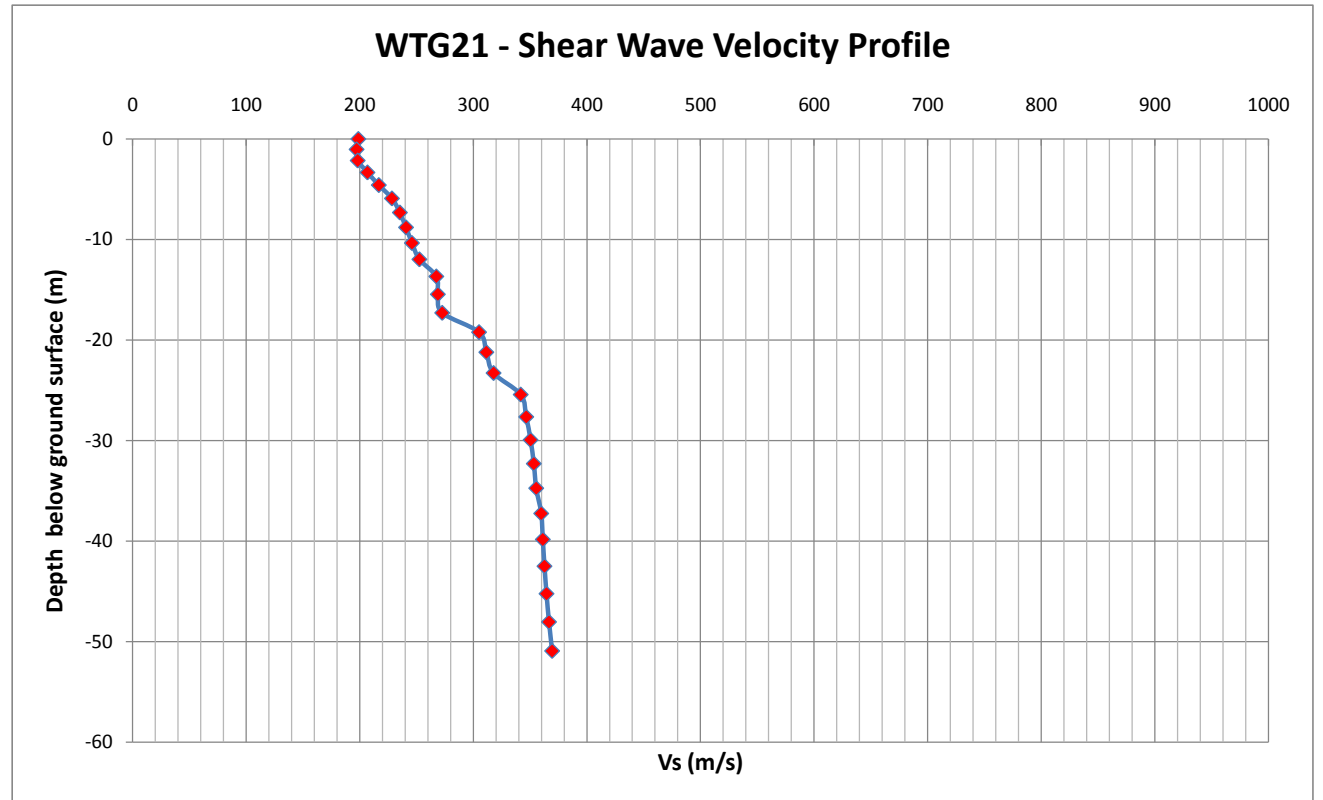
Depth(m)	Vs	Vp	Density
0	0	124.0543	1506.664
1.034483	-1.03448	147.9126	1507.616
2.142857	-2.14286	232.8036	1540.285
3.325123	-3.32512	277.6604	1583.893
4.581281	-4.58128	280.5731	1610.112
5.91133	-5.91133	289.1081	1630.823
7.315271	-7.31527	309.0982	1645.444
8.793104	-8.7931	332.6918	1658.491
10.34483	-10.3448	348.9351	1668.778
11.97044	-11.9704	357.567	1678.11
13.66995	-13.67	362.2977	1687.017
15.44335	-15.4434	359.4325	1687.017
17.29064	-17.2906	359.6669	1687.017
19.21182	-19.2118	363.8499	1687.017
21.2069	-21.2069	371.2872	1687.017
23.27586	-23.2759	380.7472	1687.017
25.41872	-25.4187	390.7841	1687.017



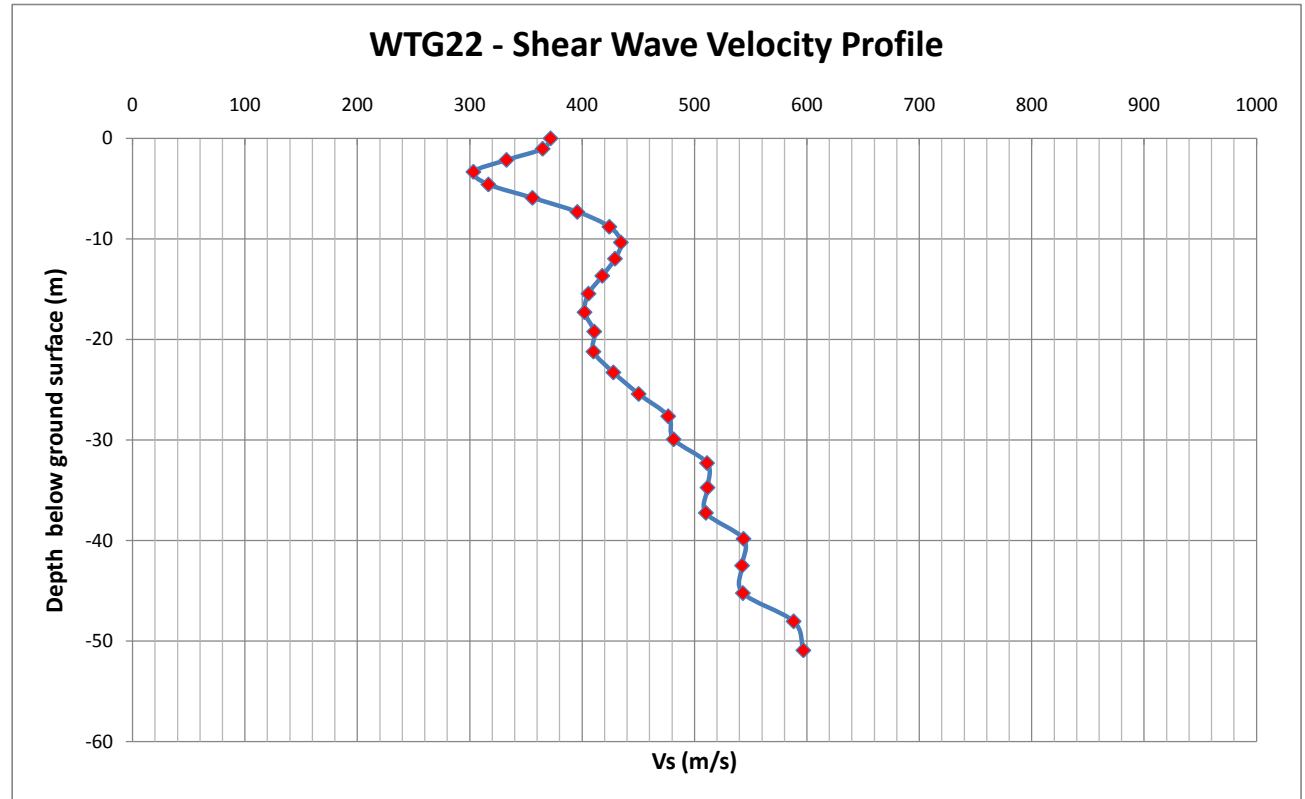
Depth(m)	Vs	Vp	Density	
0	0	176.2304	1569.151	1.809887
1.034483	-1.03448	182.4311	1569.151	1.809887
2.142857	-2.14286	210.3828	1572.465	1.810939
3.325123	-3.32512	271.8195	1598.184	1.819086
4.581281	-4.58128	321.6406	1621.769	1.826527
5.91133	-5.91133	337.6021	1633.932	1.830353
7.315271	-7.31527	326.351	1641.619	1.832767
8.793104	-8.7931	305.0094	1651.066	1.835729
10.34483	-10.3448	293.1464	1667.518	1.840877
11.97044	-11.9704	300.4791	1690.495	1.848043
13.66995	-13.67	322.7502	1712.794	1.854972
15.44335	-15.4434	351.2277	1729.299	1.860084
17.29064	-17.2906	386.1594	1747.223	1.865619
19.21182	-19.2118	421.6889	1766.24	1.871473
21.2069	-21.2069	436.5142	1766.24	1.871473
23.27586	-23.2759	463.6929	1785.145	1.877275
25.41872	-25.4187	484.5723	1801.691	1.882337
27.63547	-27.6355	487.5933	1801.691	1.882337
29.92611	-29.9261	489.068	1801.691	1.882337
32.29064	-32.2906	490.1244	1801.691	1.882337
34.72906	-34.7291	491.7548	1801.691	1.882337



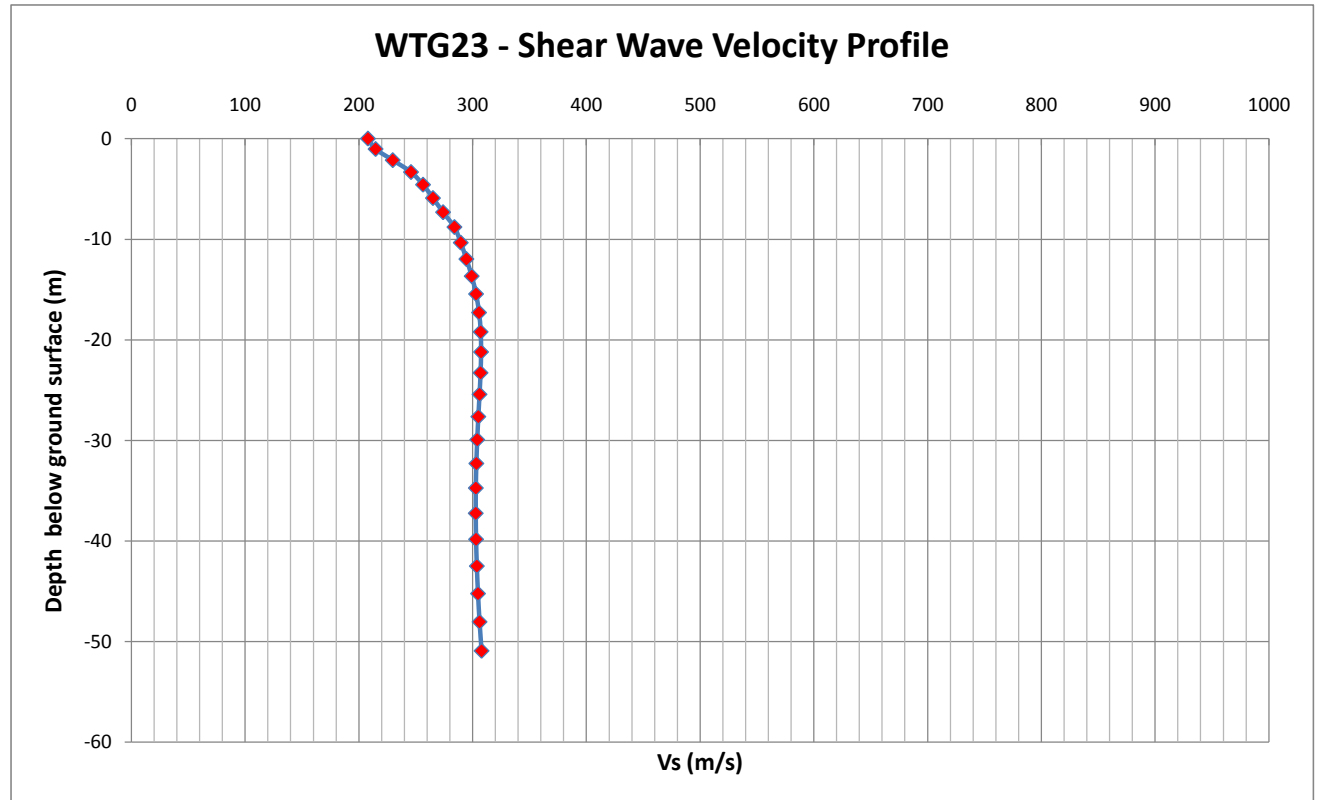
Depth(m)	Vs	Vp	Density	
0	0	198.7675	1521.809	1.794793
1.034483	-1.03448	197.2297	1521.588	1.794722
2.142857	-2.14286	198.1965	1525.869	1.796092
3.325123	-3.32512	206.7807	1536.15	1.799377
4.581281	-4.58128	216.7761	1545.188	1.802261
5.91133	-5.91133	228.3244	1556.014	1.80571
7.315271	-7.31527	235.3217	1564.092	1.80828
8.793104	-8.7931	240.7488	1573	1.811109
10.34483	-10.3448	245.9191	1582.858	1.814235
11.97044	-11.9704	252.5108	1593.604	1.817638
13.66995	-13.67	267.3908	1611.385	1.823254
15.44335	-15.4434	268.7531	1611.385	1.823254
17.29064	-17.2906	272.572	1611.385	1.823254
19.21182	-19.2118	304.9785	1641.135	1.832615
21.2069	-21.2069	311.387	1641.135	1.832615
23.27586	-23.2759	317.775	1641.135	1.832615
25.41872	-25.4187	341.6563	1661.26	1.838921
27.63547	-27.6355	346.4971	1661.26	1.838921
29.92611	-29.9261	350.3274	1661.26	1.838921
32.29064	-32.2906	353.1829	1661.26	1.838921
34.72906	-34.7291	355.2911	1661.26	1.838921
37.24138	-37.2414	359.6908	1664.342	1.839884
39.82759	-39.8276	361.0954	1664.342	1.839884
42.48769	-42.4877	362.5626	1664.342	1.839884
45.22168	-45.2217	364.3447	1664.342	1.839884
48.02956	-48.0296	366.5404	1664.342	1.839884
50.91133	-50.9113	369.2961	1664.342	1.839884



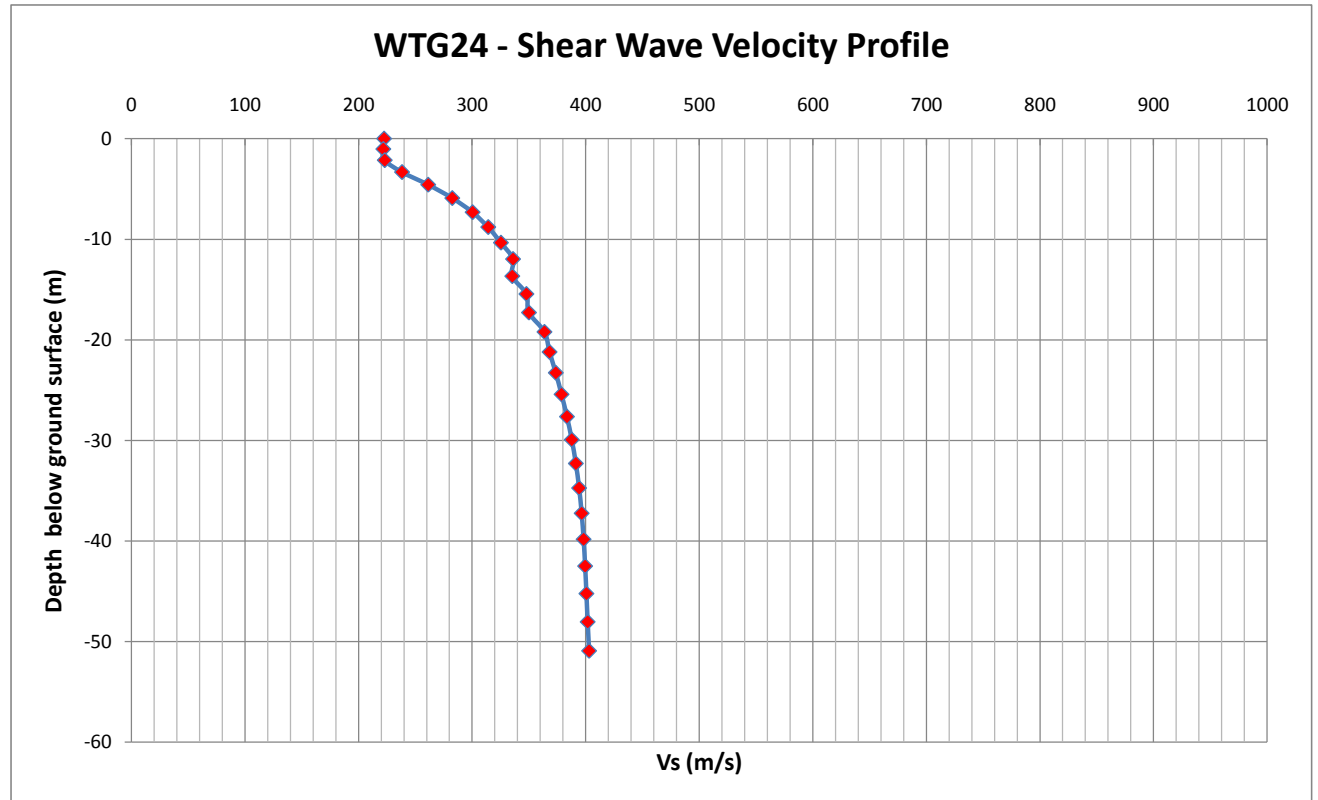
Depth(m)	Vs	Vp	Density	
0	0	371.9574	1680.683	1.844987
1.034483	-1.03448	364.9118	1680.683	1.844987
2.142857	-2.14286	332.7186	1681.36	1.845198
3.325123	-3.32512	303.3132	1684.076	1.846044
4.581281	-4.58128	316.6286	1702.186	1.851679
5.91133	-5.91133	355.8304	1720.455	1.857347
7.315271	-7.31527	395.7493	1732.431	1.861052
8.793104	-8.7931	424.2703	1743.224	1.864385
10.34483	-10.3448	434.4962	1752.533	1.867255
11.97044	-11.9704	429.2489	1760.672	1.869761
13.66995	-13.67	417.9539	1770.168	1.87268
15.44335	-15.4434	405.6655	1778.571	1.875259
17.29064	-17.2906	402.1887	1790.958	1.879055
19.21182	-19.2118	410.8022	1808.731	1.884486
21.2069	-21.2069	410.1129	1808.731	1.884486
23.27586	-23.2759	427.8259	1823.629	1.889026
25.41872	-25.4187	450.3462	1841.197	1.894366
27.63547	-27.6355	476.6093	1862.929	1.900948
29.92611	-29.9261	481.4694	1862.929	1.900948
32.29064	-32.2906	511.1564	1892.998	1.910015
34.72906	-34.7291	511.6133	1892.998	1.910015
37.24138	-37.2414	510.1623	1892.998	1.910015
39.82759	-39.8276	543.6354	1932.314	1.9218
42.48769	-42.4877	542.3533	1932.314	1.9218
45.22168	-45.2217	543.0841	1932.314	1.9218
48.02956	-48.0296	588.1935	1977.596	1.935273
50.91133	-50.9113	596.9031	1977.596	1.935273



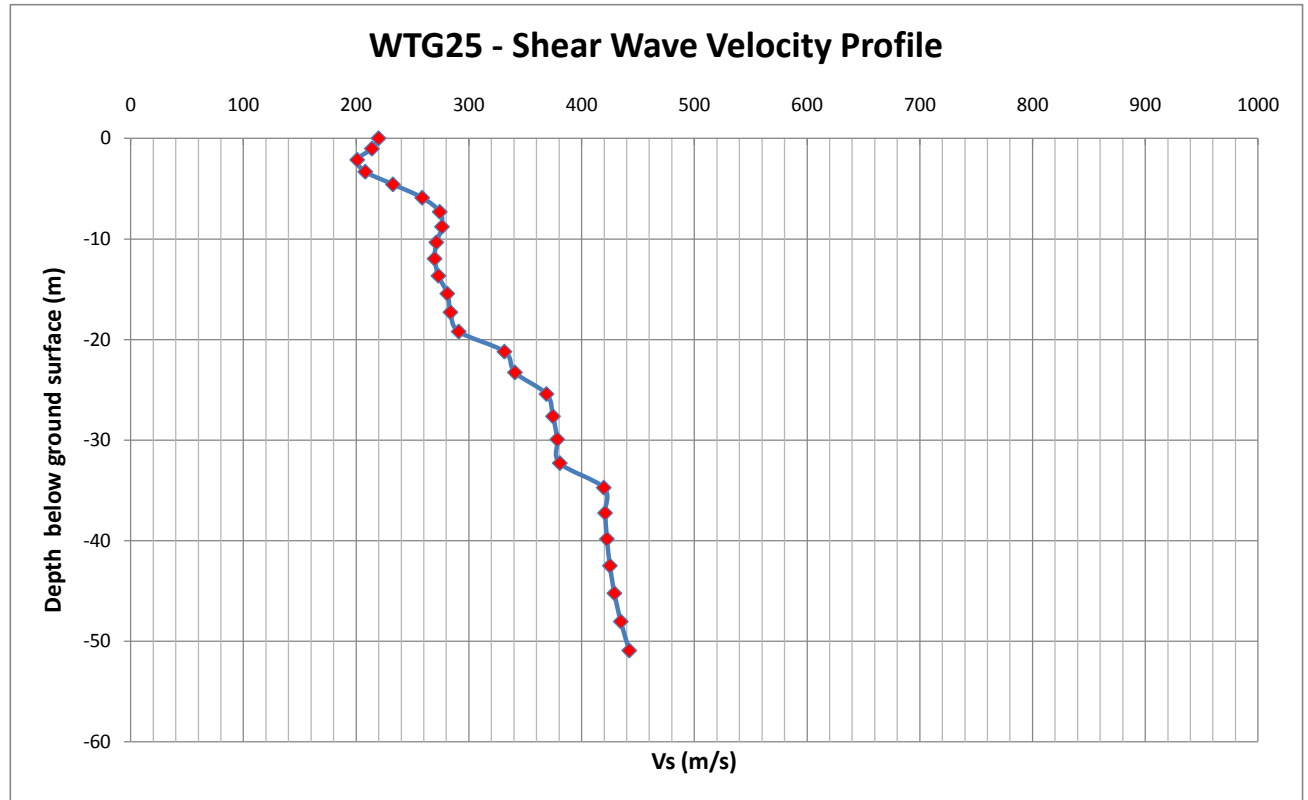
Depth(m)	Vs	Vp	Density
0	0	207.9799	1544.837
1.034483	-1.03448	214.6959	1549.086
2.142857	-2.14286	229.7847	1559.217
3.325123	-3.32512	245.8333	1574.037
4.581281	-4.58128	256.4198	1586.042
5.91133	-5.91133	265.1354	1595.992
7.315271	-7.31527	274.0366	1604.448
8.793104	-8.7931	284.0142	1612.157
10.34483	-10.3448	289.5927	1613.512
11.97044	-11.9704	294.516	1613.512
13.66995	-13.67	299.2033	1613.512
15.44335	-15.4434	303.0337	1613.512
17.29064	-17.2906	305.6752	1613.512
19.21182	-19.2118	307.078	1613.512
21.2069	-21.2069	307.4148	1613.512
23.27586	-23.2759	306.9865	1613.512
25.41872	-25.4187	306.093	1613.512
27.63547	-27.6355	305.0414	1613.512
29.92611	-29.9261	304.0649	1613.512
32.29064	-32.2906	303.2971	1613.512
34.72906	-34.7291	302.8463	1613.512
37.24138	-37.2414	302.7644	1613.512
39.82759	-39.8276	303.0557	1613.512
42.48769	-42.4877	303.7227	1613.512
45.22168	-45.2217	304.7405	1613.512
48.02956	-48.0296	306.1198	1613.512
50.91133	-50.9113	307.8708	1613.512



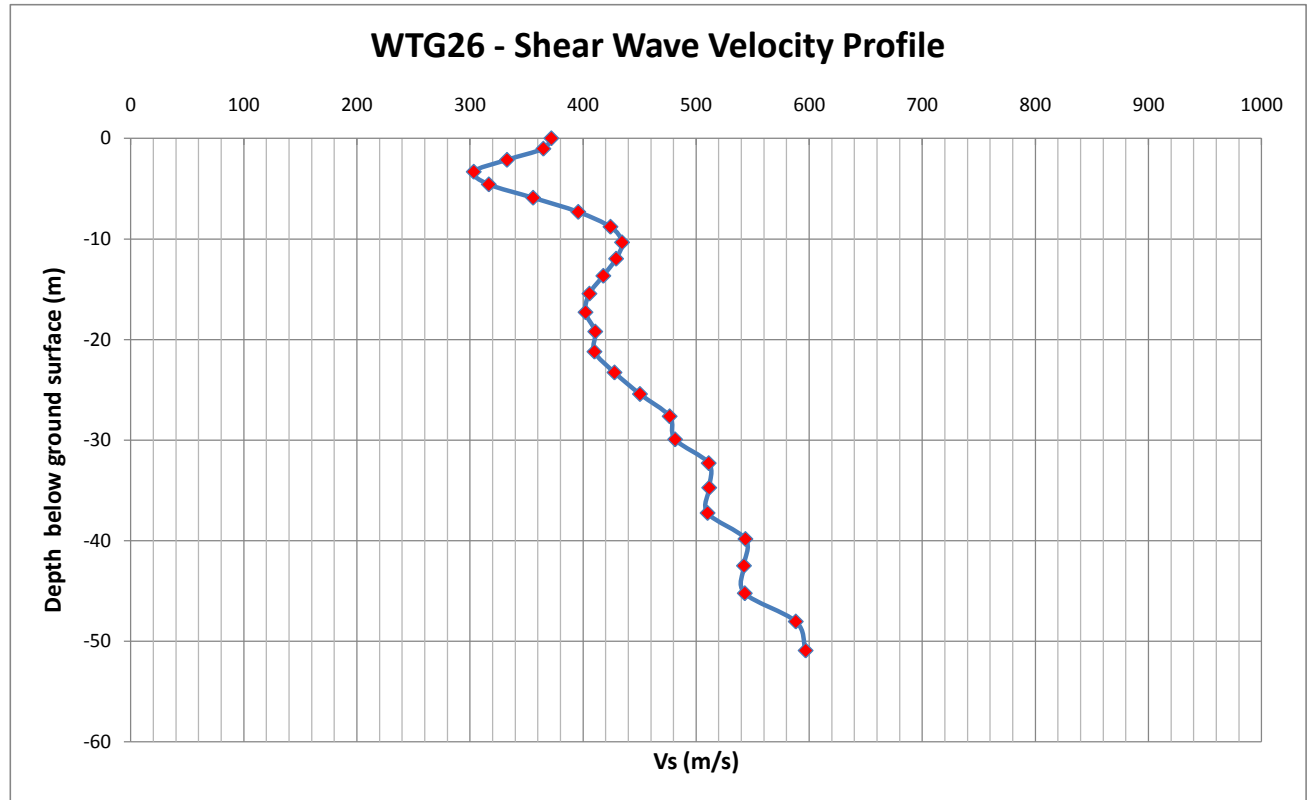
Depth(m)	Vs	Vp	Density	
0	0	222.4077	1549.079	1.803502
1.034483	-1.03448	221.7067	1551.231	1.804187
2.142857	-2.14286	222.9718	1560.151	1.807026
3.325123	-3.32512	238.1951	1579.947	1.813313
4.581281	-4.58128	261.2564	1601.023	1.819983
5.91133	-5.91133	282.4316	1617.417	1.825156
7.315271	-7.31527	300.3328	1632.34	1.829852
8.793104	-8.7931	314.1008	1646.146	1.834187
10.34483	-10.3448	325.2861	1659.446	1.838353
11.97044	-11.9704	335.9385	1672.747	1.84251
13.66995	-13.67	335.2749	1672.747	1.84251
15.44335	-15.4434	347.7055	1685.721	1.846557
17.29064	-17.2906	349.9566	1685.721	1.846557
19.21182	-19.2118	363.6104	1696.911	1.85004
21.2069	-21.2069	368.1097	1696.911	1.85004
23.27586	-23.2759	373.5858	1697.443	1.850205
25.41872	-25.4187	378.636	1697.443	1.850205
27.63547	-27.6355	383.4152	1697.443	1.850205
29.92611	-29.9261	387.6612	1697.443	1.850205
32.29064	-32.2906	391.2448	1697.443	1.850205
34.72906	-34.7291	394.1262	1697.443	1.850205
37.24138	-37.2414	396.3647	1697.443	1.850205
39.82759	-39.8276	398.0774	1697.443	1.850205
42.48769	-42.4877	399.4153	1697.443	1.850205
45.22168	-45.2217	400.5376	1697.443	1.850205
48.02956	-48.0296	401.6462	1697.443	1.850205
50.91133	-50.9113	402.9063	1697.443	1.850205



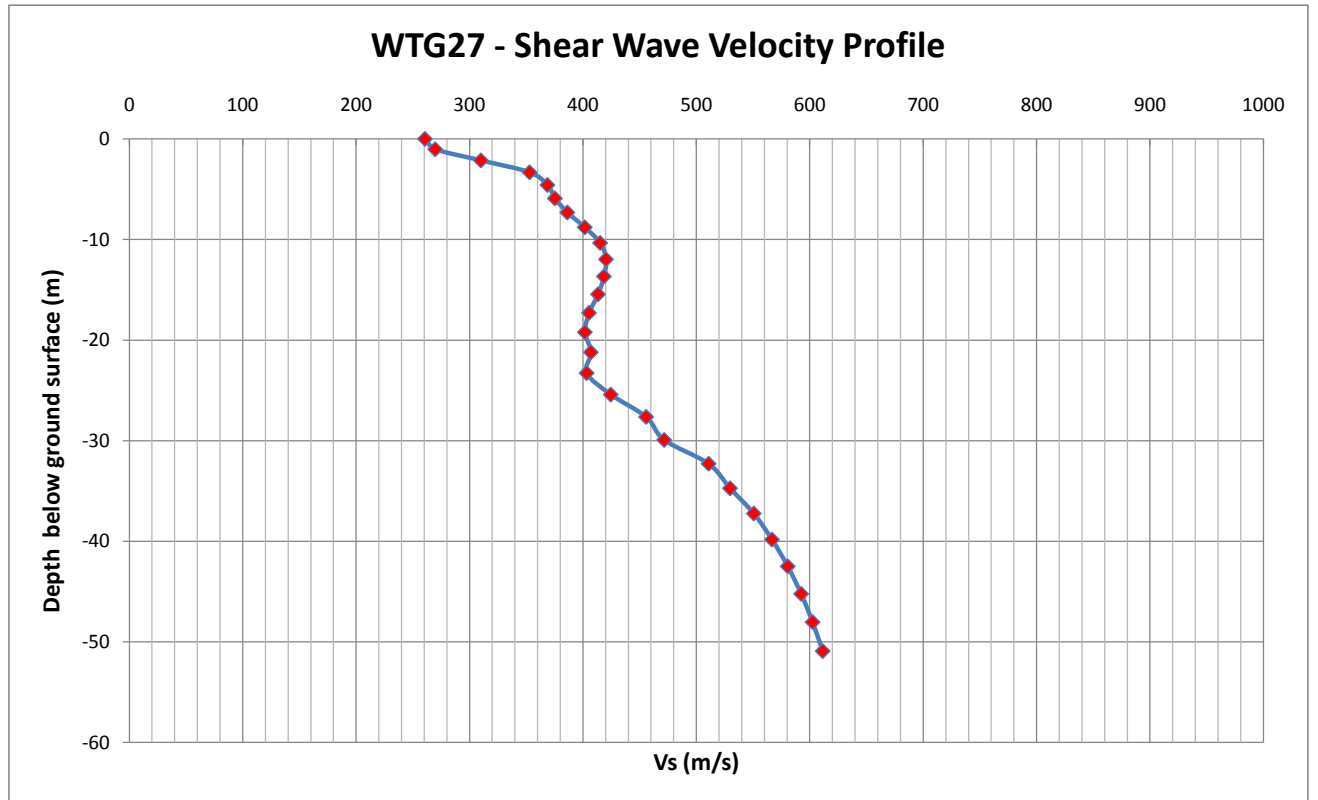
Depth(m)	Vs	Vp	Density	
0	0	219.8852	1533.929	1.798668
1.034483	-1.03448	213.9509	1534.41	1.798822
2.142857	-2.14286	200.9618	1538.581	1.800154
3.325123	-3.32512	208.0663	1552.461	1.804579
4.581281	-4.58128	232.6096	1567.248	1.809283
5.91133	-5.91133	258.6016	1579.374	1.813131
7.315271	-7.31527	274.1844	1589.159	1.816231
8.793104	-8.7931	276.1833	1596.663	1.818605
10.34483	-10.3448	271.1576	1604.834	1.821187
11.97044	-11.9704	269.6155	1618.234	1.825413
13.66995	-13.67	273.017	1632.773	1.829988
15.44335	-15.4434	280.9052	1645.264	1.83391
17.29064	-17.2906	283.6974	1645.264	1.83391
19.21182	-19.2118	291.0165	1645.264	1.83391
21.2069	-21.2069	331.5762	1679.752	1.844696
23.27586	-23.2759	340.9036	1679.752	1.844696
25.41872	-25.4187	368.9091	1702.173	1.851675
27.63547	-27.6355	374.6803	1702.173	1.851675
29.92611	-29.9261	378.4953	1702.173	1.851675
32.29064	-32.2906	380.7286	1702.173	1.851675
34.72906	-34.7291	419.7716	1744.095	1.864654
37.24138	-37.2414	420.9157	1744.095	1.864654
39.82759	-39.8276	422.5655	1744.095	1.864654
42.48769	-42.4877	425.191	1744.095	1.864654
45.22168	-45.2217	429.195	1744.095	1.864654
48.02956	-48.0296	434.861	1744.095	1.864654
50.91133	-50.9113	442.3918	1744.095	1.864654



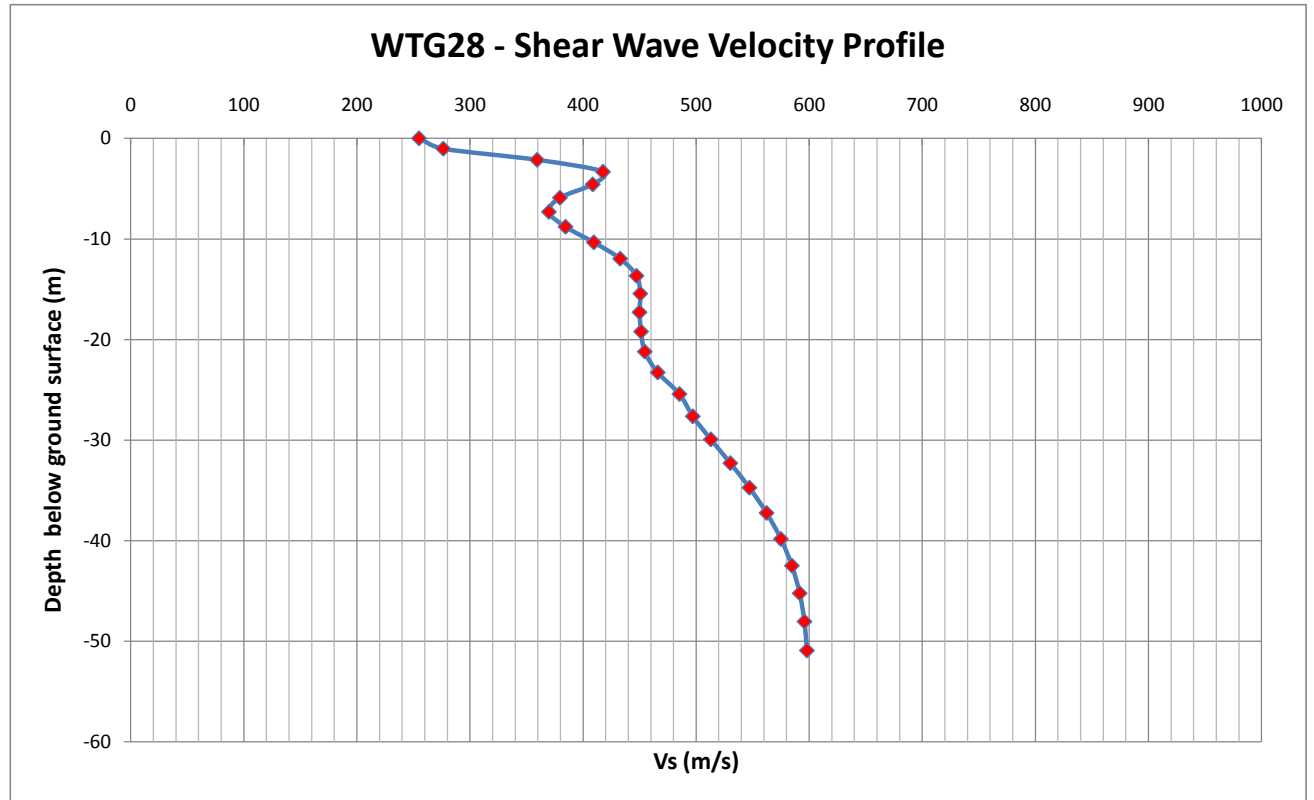
Depth(m)	Vs	Vp	Density	
0	0	371.9574	1680.683	1.844987
1.034483	-1.03448	364.9118	1680.683	1.844987
2.142857	-2.14286	332.7186	1681.36	1.845198
3.325123	-3.32512	303.3132	1684.076	1.846044
4.581281	-4.58128	316.6286	1702.186	1.851679
5.91133	-5.91133	355.8304	1720.455	1.857347
7.315271	-7.31527	395.7493	1732.431	1.861052
8.793104	-8.7931	424.2703	1743.224	1.864385
10.34483	-10.3448	434.4962	1752.533	1.867255
11.97044	-11.9704	429.2489	1760.672	1.869761
13.66995	-13.67	417.9539	1770.168	1.87268
15.44335	-15.4434	405.6655	1778.571	1.875259
17.29064	-17.2906	402.1887	1790.958	1.879055
19.21182	-19.2118	410.8022	1808.731	1.884486
21.2069	-21.2069	410.1129	1808.731	1.884486
23.27586	-23.2759	427.8259	1823.629	1.889026
25.41872	-25.4187	450.3462	1841.197	1.894366
27.63547	-27.6355	476.6093	1862.929	1.900948
29.92611	-29.9261	481.4694	1862.929	1.900948
32.29064	-32.2906	511.1564	1892.998	1.910015
34.72906	-34.7291	511.6133	1892.998	1.910015
37.24138	-37.2414	510.1623	1892.998	1.910015
39.82759	-39.8276	543.6354	1932.314	1.9218
42.48769	-42.4877	542.3533	1932.314	1.9218
45.22168	-45.2217	543.0841	1932.314	1.9218
48.02956	-48.0296	588.1935	1977.596	1.935273
50.91133	-50.9113	596.9031	1977.596	1.935273



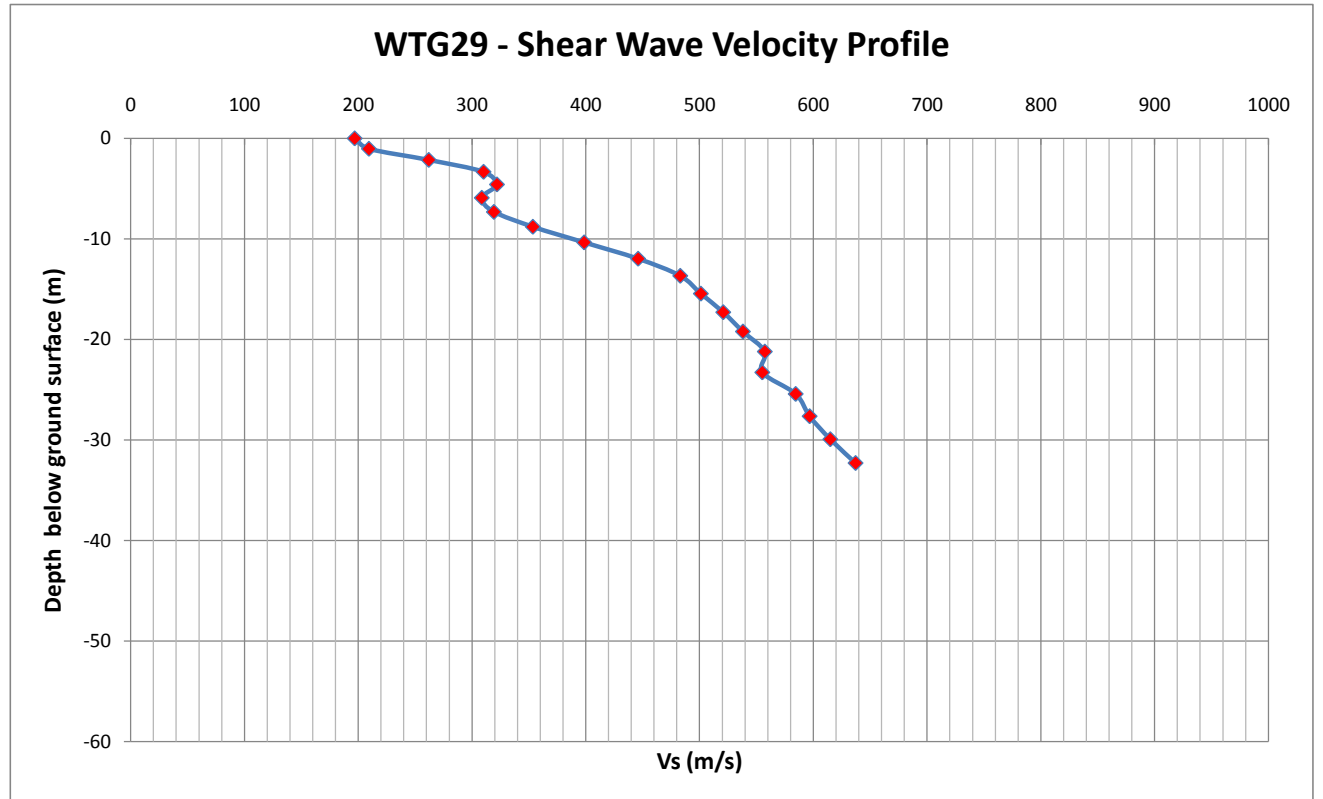
Depth(m)	Vs	Vp	Density	
0	0	260.7588	1635.481	1.830839
1.034483	-1.03448	269.8501	1636.628	1.8312
2.142857	-2.14286	310.1145	1654.663	1.836856
3.325123	-3.32512	353.0349	1685.251	1.84641
4.581281	-4.58128	368.7791	1704.507	1.8524
5.91133	-5.91133	375.2943	1718.859	1.856852
7.315271	-7.31527	386.3224	1730.947	1.860593
8.793104	-8.7931	401.7042	1740.153	1.863438
10.34483	-10.3448	415.2216	1746.864	1.865508
11.97044	-11.9704	420.3805	1751.032	1.866793
13.66995	-13.67	418.5513	1757.275	1.868716
15.44335	-15.4434	413.3815	1768.049	1.872029
17.29064	-17.2906	405.4454	1779.587	1.875571
19.21182	-19.2118	401.7375	1794.186	1.880042
21.2069	-21.2069	407.0775	1812.779	1.885721
23.27586	-23.2759	403.3338	1812.779	1.885721
25.41872	-25.4187	424.5805	1831.372	1.891382
27.63547	-27.6355	455.7909	1853.506	1.898097
29.92611	-29.9261	471.7127	1853.506	1.898097
32.29064	-32.2906	510.8796	1876.577	1.905069
34.72906	-34.7291	529.7577	1876.577	1.905069
37.24138	-37.2414	550.7092	1880.002	1.906102
39.82759	-39.8276	566.752	1880.002	1.906102
42.48769	-42.4877	580.6198	1880.002	1.906102
45.22168	-45.2217	592.4625	1880.002	1.906102
48.02956	-48.0296	602.5382	1880.002	1.906102
50.91133	-50.9113	611.4649	1880.002	1.906102



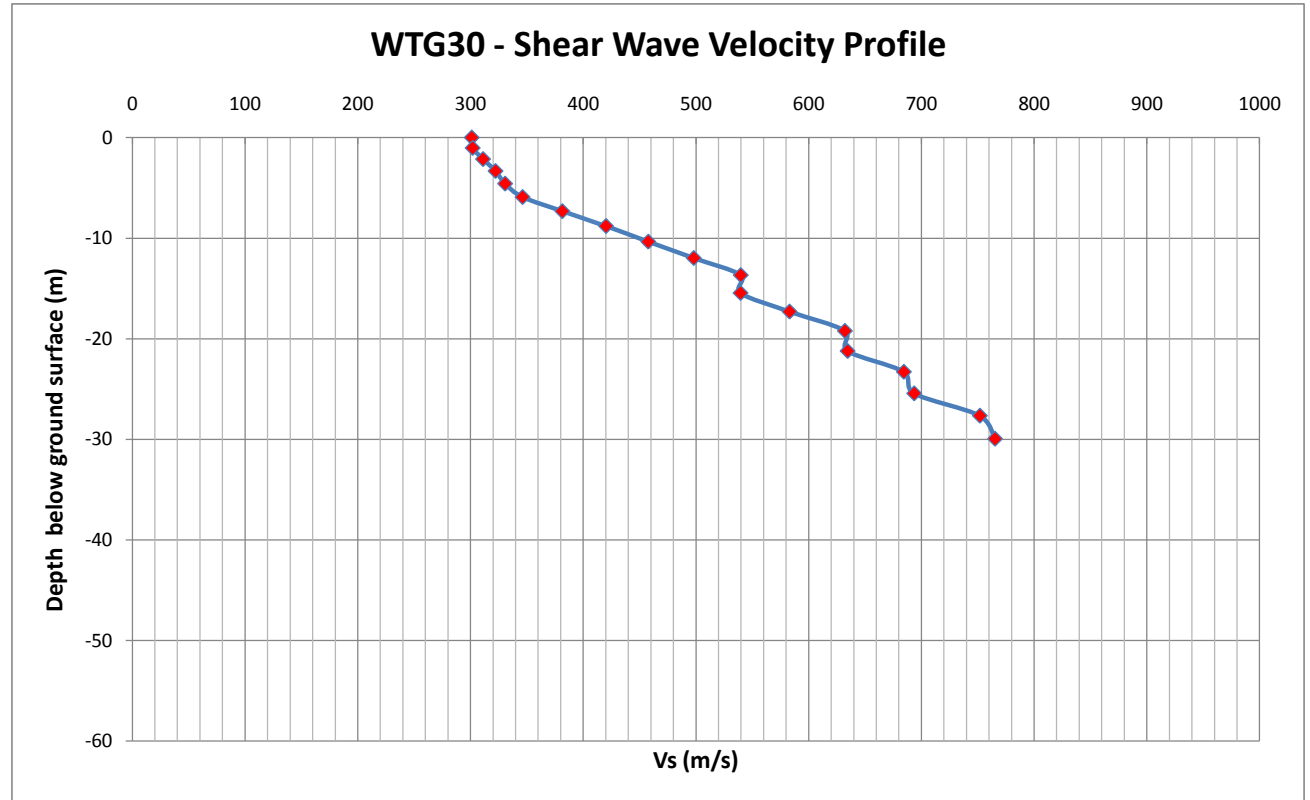
Depth(m)	Vs	Vp	Density	
0	0	254.9913	1672.931	1.842568
1.034483	-1.03448	276.4452	1672.931	1.842568
2.142857	-2.14286	359.4266	1691.918	1.848486
3.325123	-3.32512	417.6694	1713.805	1.855286
4.581281	-4.58128	408.6233	1722.017	1.85783
5.91133	-5.91133	379.6057	1732.541	1.861086
7.315271	-7.31527	369.898	1746.048	1.865257
8.793104	-8.7931	384.5556	1758.457	1.869079
10.34483	-10.3448	409.5728	1768.081	1.872039
11.97044	-11.9704	432.8773	1778.345	1.87519
13.66995	-13.67	447.3304	1790.137	1.878803
15.44335	-15.4434	450.6837	1801.373	1.882239
17.29064	-17.2906	449.9953	1814.586	1.886272
19.21182	-19.2118	451.3841	1830.295	1.891054
21.2069	-21.2069	454.6434	1842.976	1.894905
23.27586	-23.2759	466.1049	1856.918	1.89913
25.41872	-25.4187	485.2988	1871.554	1.903554
27.63547	-27.6355	497.0906	1871.554	1.903554
29.92611	-29.9261	513.0645	1871.895	1.903657
32.29064	-32.2906	530.3031	1871.895	1.903657
34.72906	-34.7291	547.1854	1871.895	1.903657
37.24138	-37.2414	562.3544	1871.895	1.903657
39.82759	-39.8276	575.0272	1871.895	1.903657
42.48769	-42.4877	584.7588	1871.895	1.903657
45.22168	-45.2217	591.5982	1871.895	1.903657
48.02956	-48.0296	595.838	1871.895	1.903657
50.91133	-50.9113	598.0135	1871.895	1.903657



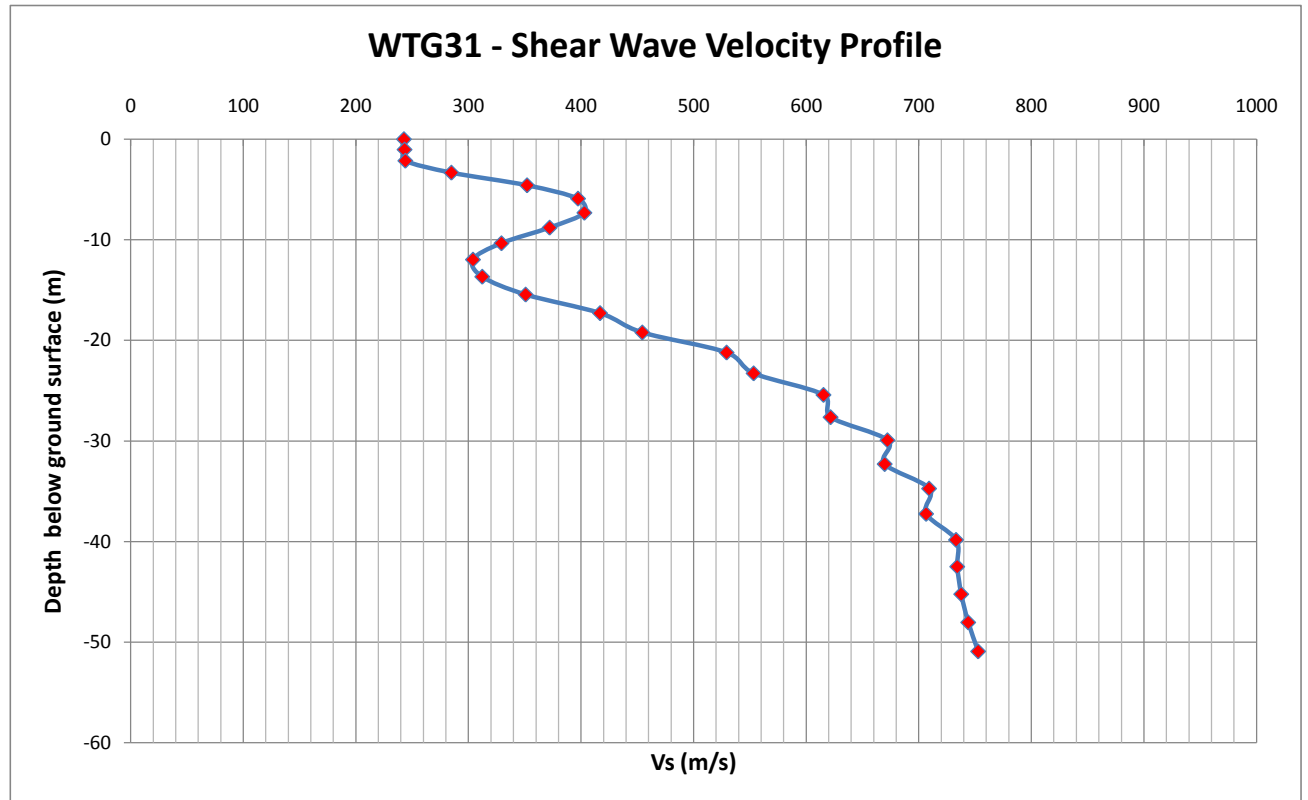
Depth(m)	Vs	Vp	Density	
0	0	196.7392	1573.586	1.811295
1.034483	-1.03448	209.2865	1574.219	1.811496
2.142857	-2.14286	261.9081	1593.683	1.817663
3.325123	-3.32512	310.0976	1624.778	1.827474
4.581281	-4.58128	321.8901	1652.92	1.83631
5.91133	-5.91133	308.5344	1671.234	1.842038
7.315271	-7.31527	319.1777	1704.183	1.8523
8.793104	-8.7931	353.4512	1738.384	1.862891
10.34483	-10.3448	398.5744	1768.493	1.872166
11.97044	-11.9704	446.0486	1800.48	1.881967
13.66995	-13.67	483.09	1830.227	1.891034
15.44335	-15.4434	501.2112	1850.569	1.897207
17.29064	-17.2906	520.9081	1881.083	1.906428
19.21182	-19.2118	538.2146	1911.597	1.9156
21.2069	-21.2069	557.4608	1941.609	1.924574
23.27586	-23.2759	555.2629	1941.609	1.924574
25.41872	-25.4187	584.6049	1968.432	1.932555
27.63547	-27.6355	596.884	1968.432	1.932555
29.92611	-29.9261	615.0708	1968.432	1.932555
32.29064	-32.2906	637.2774	1968.432	1.932555



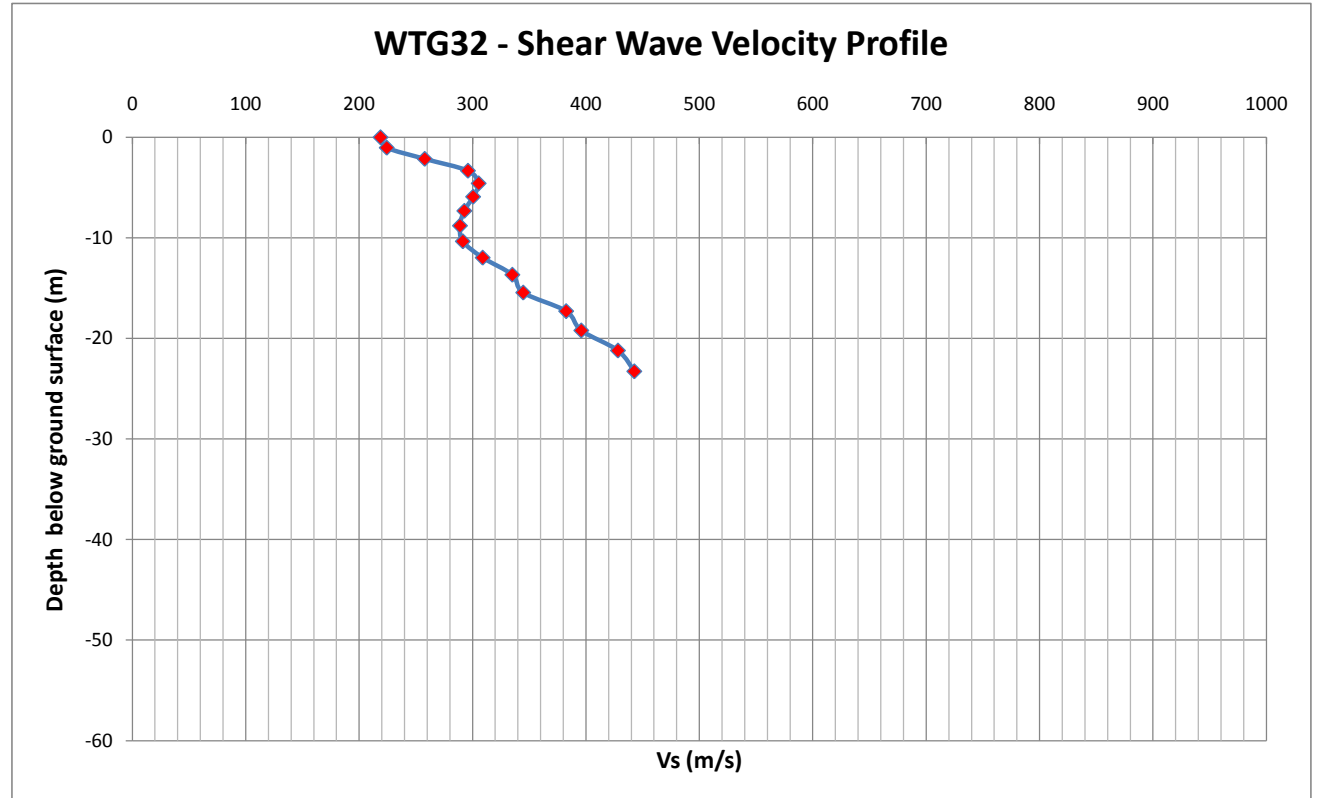
Depth(m)	Vs	Vp	Density	
0	0	301.0668	1649.722	1.835308
1.034483	-1.03448	301.8964	1649.722	1.835308
2.142857	-2.14286	311.102	1656.706	1.837495
3.325123	-3.32512	322.1733	1673.954	1.842887
4.581281	-4.58128	330.6653	1697.437	1.850203
5.91133	-5.91133	346.1731	1727.126	1.859411
7.315271	-7.31527	381.4246	1767.814	1.871957
8.793104	-8.7931	420.2056	1802.34	1.882535
10.34483	-10.3448	457.6652	1832.029	1.891581
11.97044	-11.9704	497.9829	1867.686	1.902386
13.66995	-13.67	539.6792	1910.035	1.915132
15.44335	-15.4434	539.4951	1910.035	1.915132
17.29064	-17.2906	582.9676	1959.88	1.930015
19.21182	-19.2118	632.048	2014.681	1.946228
21.2069	-21.2069	634.4723	2014.681	1.946228
23.27586	-23.2759	684.358	2063.558	1.960557
25.41872	-25.4187	693.521	2063.558	1.960557
27.63547	-27.6355	751.7721	2115.196	1.975561
29.92611	-29.9261	765.1935	2115.196	1.975561



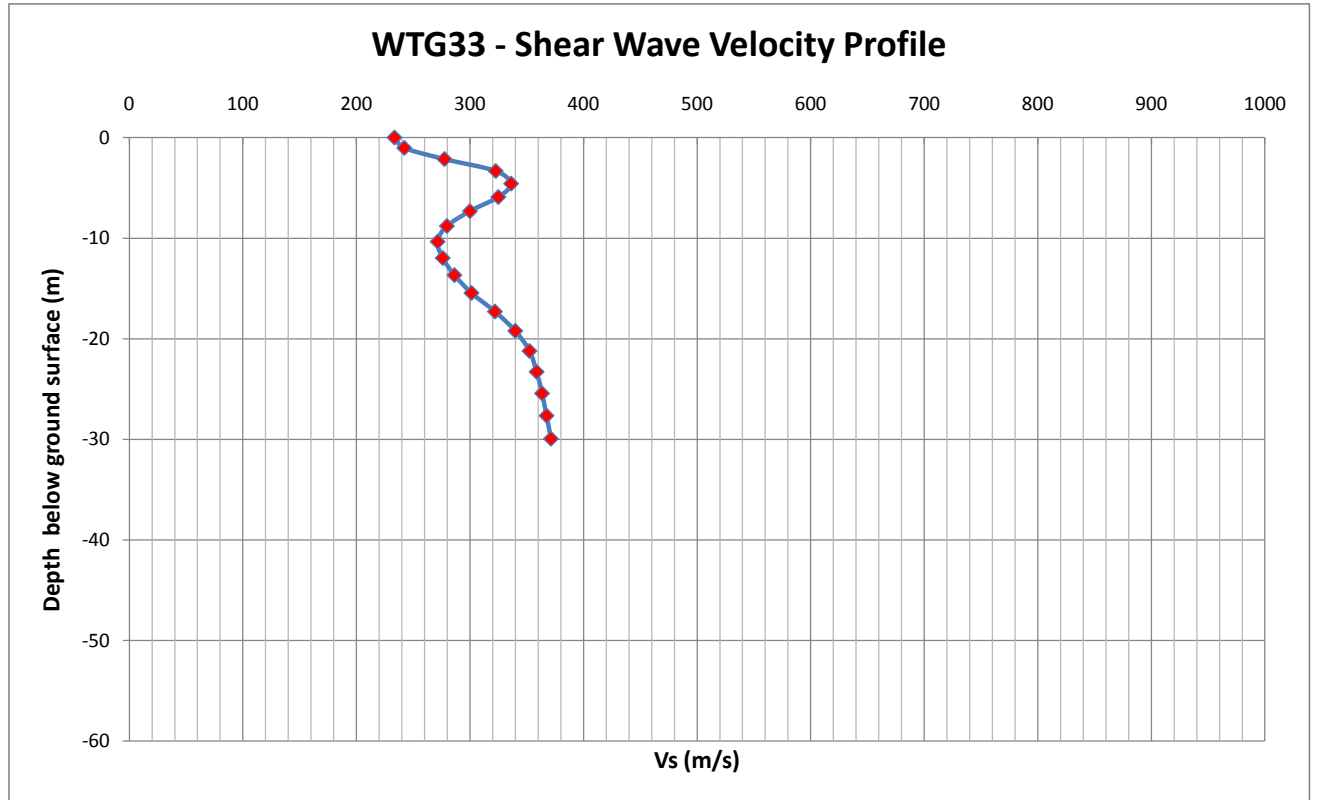
Depth(m)	Vs	Vp	Density
0	0	242.6398	
1.034483	-1.03448	243.1688	
2.142857	-2.14286	243.8636	
3.325123	-3.32512	284.7908	
4.581281	-4.58128	352.037	
5.91133	-5.91133	397.3224	
7.315271	-7.31527	402.9814	
8.793104	-8.7931	372.0758	
10.34483	-10.3448	329.2774	
11.97044	-11.9704	303.9664	
13.66995	-13.67	312.2209	
15.44335	-15.4434	350.7654	
17.29064	-17.2906	416.8813	
19.21182	-19.2118	454.4605	
21.2069	-21.2069	529.3356	
23.27586	-23.2759	553.362	
25.41872	-25.4187	615.4374	
27.63547	-27.6355	621.7315	
29.92611	-29.9261	672.2874	
32.29064	-32.2906	669.8245	
34.72906	-34.7291	709.2835	
37.24138	-37.2414	706.6219	
39.82759	-39.8276	733.2228	
42.48769	-42.4877	734.2882	
45.22168	-45.2217	737.8333	
48.02956	-48.0296	744.0524	
50.91133	-50.9113	752.8866	



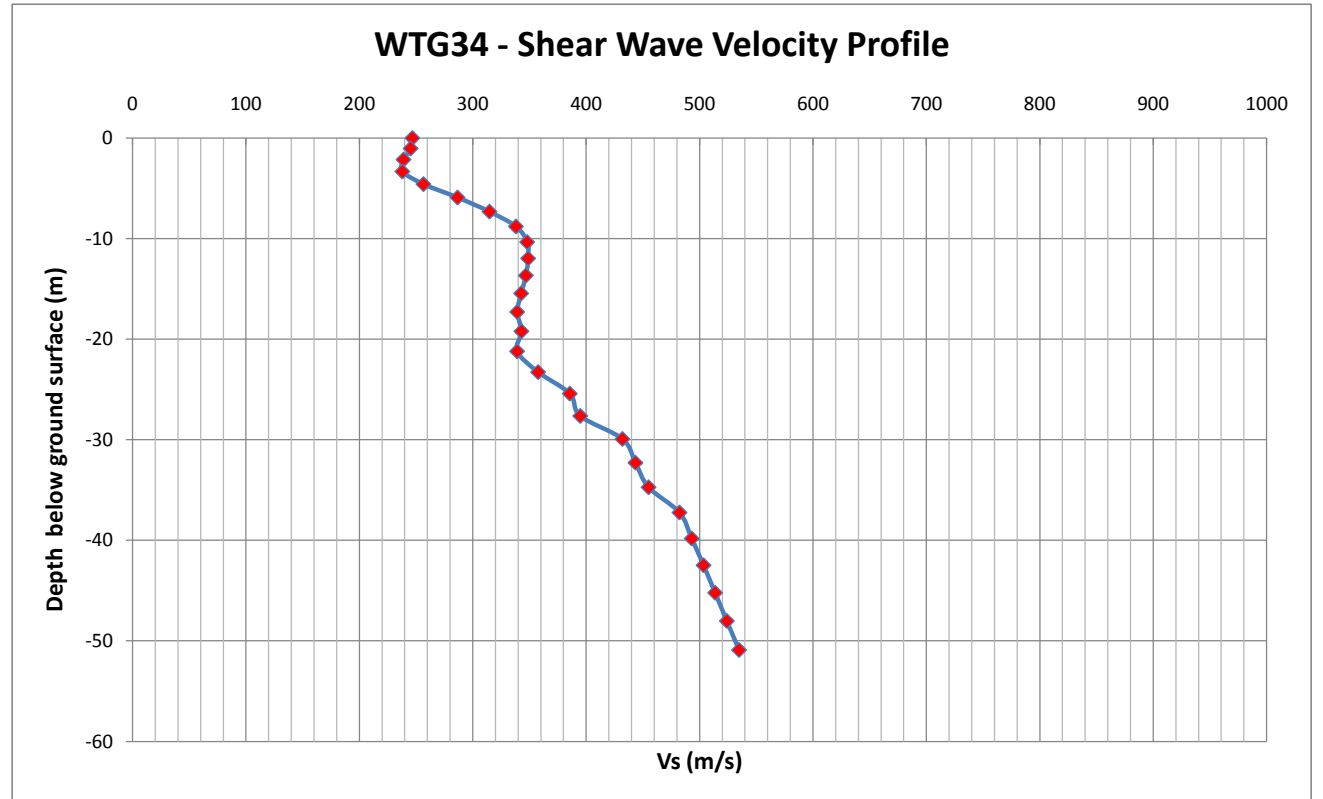
Depth(m)	Vs	Vp	Density	
0	0	218.8114	1580.275	1.813417
1.034483	-1.03448	224.2967	1580.275	1.813417
2.142857	-2.14286	257.7828	1592.781	1.817377
3.325123	-3.32512	295.9211	1611.445	1.823273
4.581281	-4.58128	305.3766	1617.742	1.825258
5.91133	-5.91133	300.466	1626.562	1.828035
7.315271	-7.31527	292.7219	1638.326	1.831733
8.793104	-8.7931	288.8771	1649.888	1.83536
10.34483	-10.3448	291.4052	1659.595	1.8384
11.97044	-11.9704	308.8928	1677.67	1.844047
13.66995	-13.67	335.0604	1699.734	1.850917
15.44335	-15.4434	344.6658	1699.734	1.850917
17.29064	-17.2906	382.5087	1728.632	1.859877
19.21182	-19.2118	395.8691	1728.632	1.859877
21.2069	-21.2069	428.1811	1748.773	1.866097
23.27586	-23.2759	442.6045	1748.773	1.866097



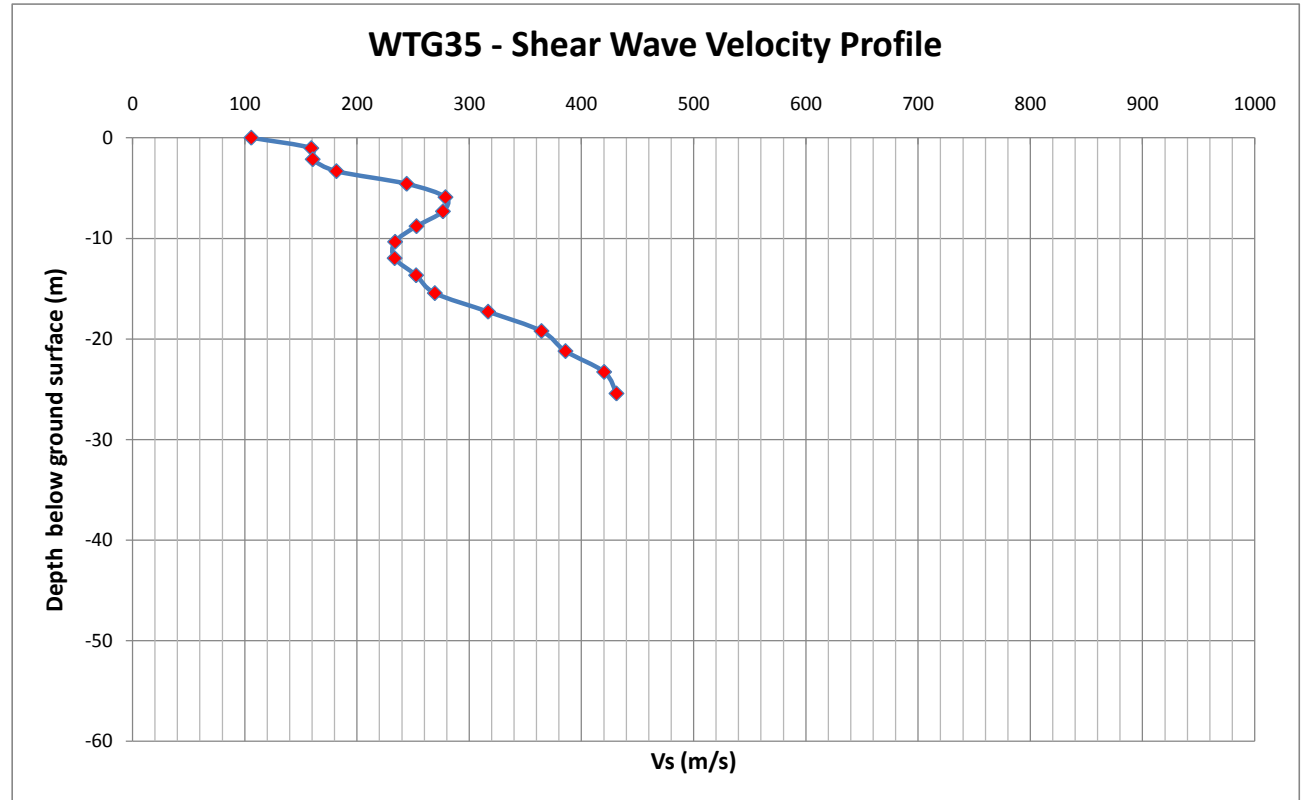
Depth(m)	Vs	Vp	Density	
0	0	233.4847	1617.851	1.825292
1.034483	-1.03448	242.1145	1617.851	1.825292
2.142857	-2.14286	277.4817	1622.242	1.826676
3.325123	-3.32512	322.6767	1631.396	1.829556
4.581281	-4.58128	336.233	1627.525	1.828338
5.91133	-5.91133	324.8899	1626.576	1.82804
7.315271	-7.31527	299.931	1627.734	1.828404
8.793104	-8.7931	279.6437	1633.052	1.830076
10.34483	-10.3448	271.4596	1640.11	1.832293
11.97044	-11.9704	276.0026	1647.976	1.834761
13.66995	-13.67	286.2639	1652.669	1.836231
15.44335	-15.4434	301.2853	1657.77	1.837829
17.29064	-17.2906	321.9411	1668.09	1.841056
19.21182	-19.2118	339.8386	1676.686	1.84374
21.2069	-21.2069	352.3872	1681.544	1.845255
23.27586	-23.2759	358.6173	1681.544	1.845255
25.41872	-25.4187	363.4338	1681.544	1.845255
27.63547	-27.6355	367.4189	1681.544	1.845255
29.92611	-29.9261	371.289	1681.544	1.845255



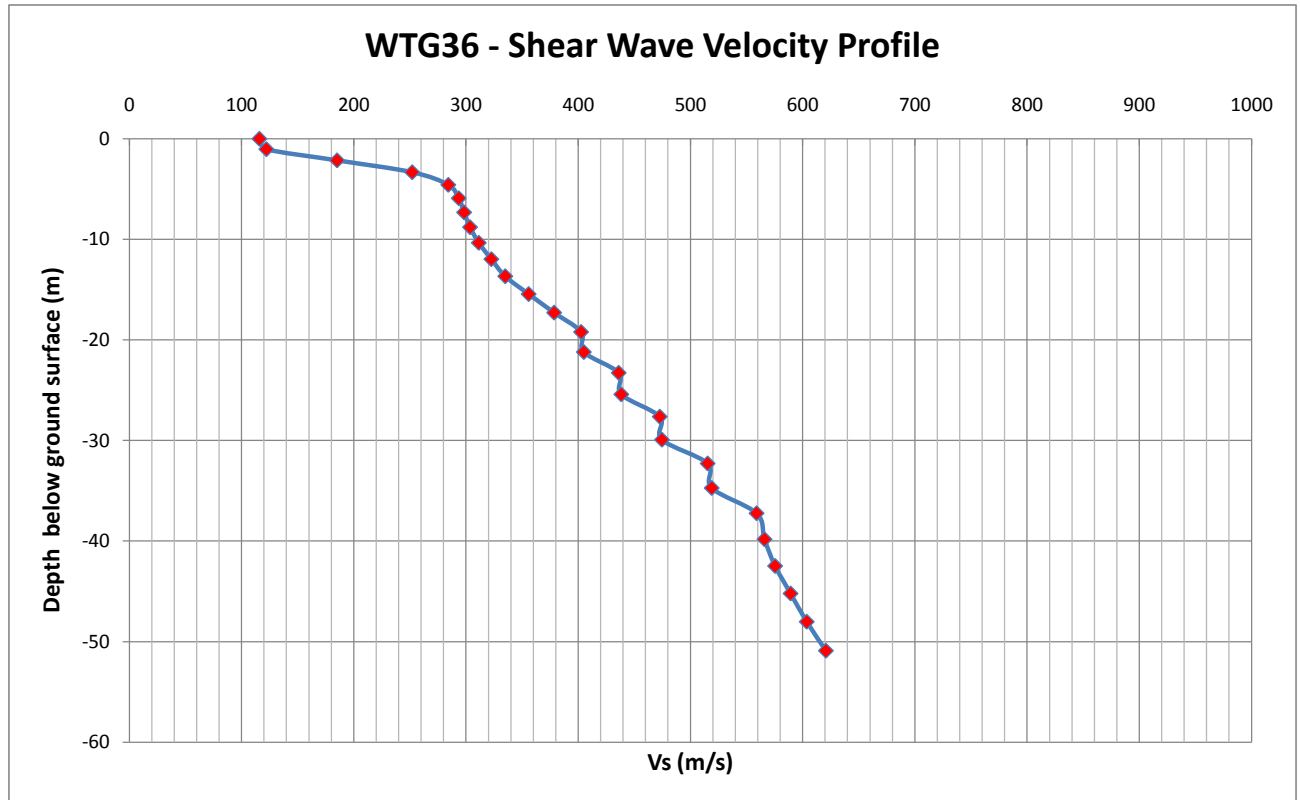
Depth(m)	Vs	Vp	Density	
0	0	246.8474	1584.712	1.814823
1.034483	-1.03448	245.2826	1584.712	1.814823
2.142857	-2.14286	239.0134	1584.712	1.814823
3.325123	-3.32512	238.0302	1590.755	1.816736
4.581281	-4.58128	256.5942	1609.531	1.822669
5.91133	-5.91133	286.6467	1630.256	1.829197
7.315271	-7.31527	314.8039	1644.525	1.833678
8.793104	-8.7931	338.0881	1657.724	1.837814
10.34483	-10.3448	347.9882	1665.705	1.840311
11.97044	-11.9704	348.8488	1673.877	1.842863
13.66995	-13.67	346.8588	1686.17	1.846697
15.44335	-15.4434	342.7342	1698.597	1.850564
17.29064	-17.2906	339.21	1709.837	1.854055
19.21182	-19.2118	342.9522	1724.348	1.858552
21.2069	-21.2069	339.1271	1724.348	1.858552
23.27586	-23.2759	357.6486	1742.899	1.864285
25.41872	-25.4187	385.5838	1766.927	1.871684
27.63547	-27.6355	394.7771	1766.927	1.871684
29.92611	-29.9261	431.9371	1796.122	1.880635
32.29064	-32.2906	443.4165	1796.122	1.880635
34.72906	-34.7291	454.9659	1796.122	1.880635
37.24138	-37.2414	482.2221	1813.938	1.886074
39.82759	-39.8276	492.9995	1813.938	1.886074
42.48769	-42.4877	503.4083	1813.938	1.886074
45.22168	-45.2217	513.6363	1813.938	1.886074
48.02956	-48.0296	523.9531	1813.938	1.886074
50.91133	-50.9113	534.709	1813.938	1.886074



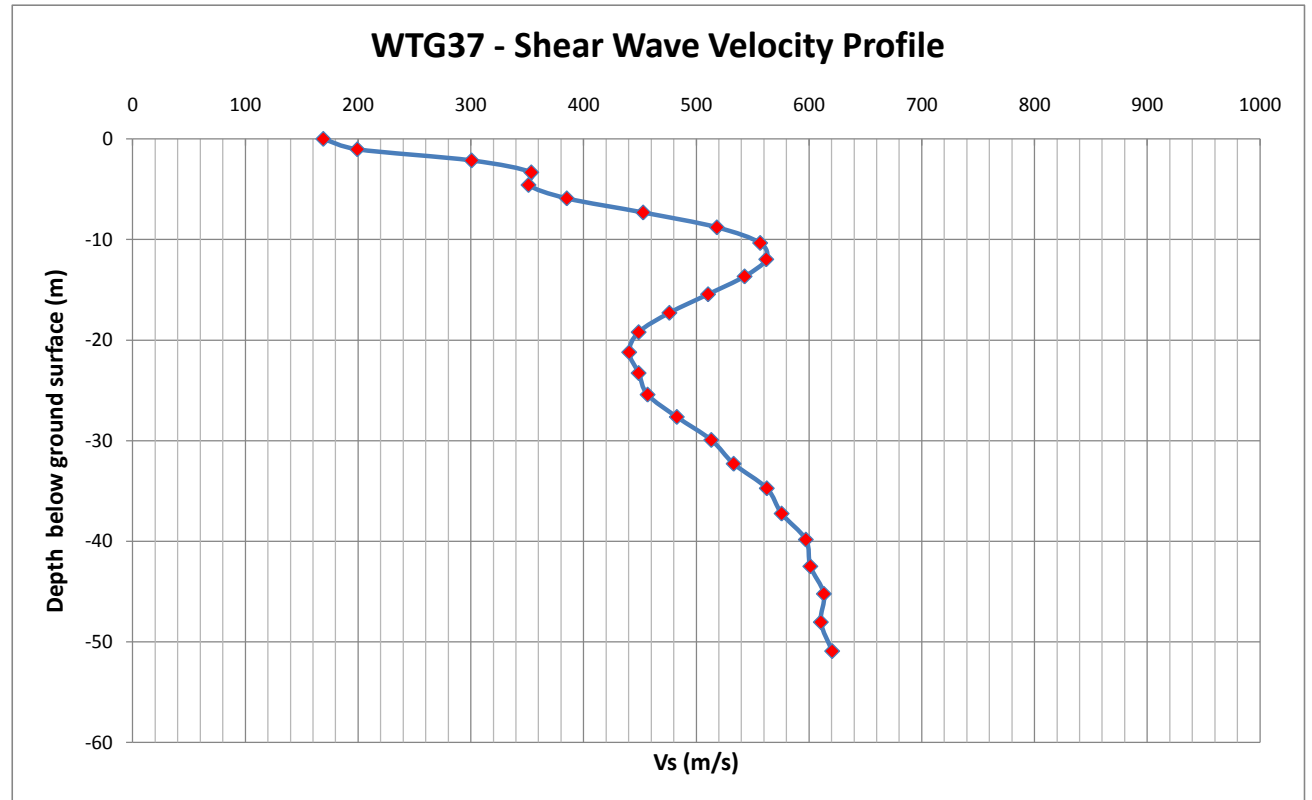
Depth(m)	Vs	Vp	Density	
0	0	105.7115	1442.703	1.769311
1.034483	-1.03448	159.2048	1459.518	1.774755
2.142857	-2.14286	160.45	1489.334	1.784371
3.325123	-3.32512	181.5895	1522.087	1.794882
4.581281	-4.58128	244.2273	1550.82	1.804056
5.91133	-5.91133	278.7979	1561.121	1.807335
7.315271	-7.31527	276.5501	1568.709	1.809747
8.793104	-8.7931	252.9745	1579.763	1.813254
10.34483	-10.3448	233.9043	1598.258	1.819109
11.97044	-11.9704	233.4871	1620.166	1.826022
13.66995	-13.67	252.6256	1640.648	1.832462
15.44335	-15.4434	269.3355	1640.648	1.832462
17.29064	-17.2906	316.8153	1666.046	1.840417
19.21182	-19.2118	364.3807	1691.167	1.848253
21.2069	-21.2069	385.7837	1691.167	1.848253
23.27586	-23.2759	420.2431	1711.582	1.854596
25.41872	-25.4187	431.2325	1711.582	1.854596



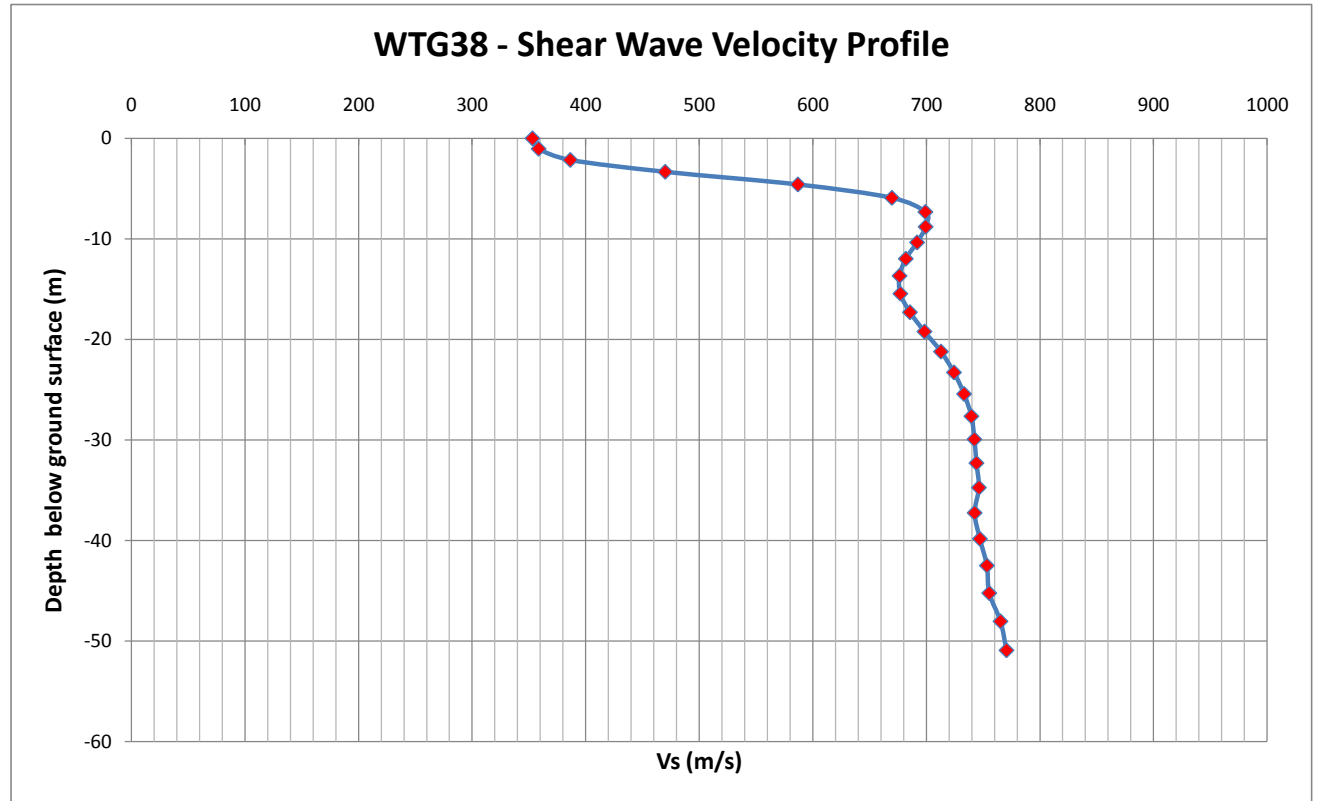
Depth(m)	Vs	Vp	Density	
0	0	116.0029	1471.223	1.778535
1.034483	-1.03448	122.2081	1473.452	1.779255
2.142857	-2.14286	185.1968	1500.38	1.787922
3.325123	-3.32512	252.1308	1553.769	1.804995
4.581281	-4.58128	284.3132	1592.471	1.817279
5.91133	-5.91133	293.6048	1614.18	1.824136
7.315271	-7.31527	298.3766	1630.311	1.829214
8.793104	-8.7931	303.652	1644.226	1.833585
10.34483	-10.3448	311.4699	1659.169	1.838266
11.97044	-11.9704	322.637	1676.542	1.843695
13.66995	-13.67	335.0335	1693.798	1.849072
15.44335	-15.4434	355.9062	1718.482	1.856735
17.29064	-17.2906	378.5997	1743.166	1.864368
19.21182	-19.2118	402.6282	1767.85	1.871968
21.2069	-21.2069	405.0787	1767.85	1.871968
23.27586	-23.2759	436.1181	1799.383	1.881631
25.41872	-25.4187	438.4385	1799.383	1.881631
27.63547	-27.6355	472.7065	1835.19	1.892542
29.92611	-29.9261	474.6612	1835.19	1.892542
32.29064	-32.2906	515.3736	1877.473	1.90534
34.72906	-34.7291	519.0196	1877.473	1.90534
37.24138	-37.2414	558.9698	1916.035	1.91693
39.82759	-39.8276	566.0156	1916.035	1.91693
42.48769	-42.4877	575.4691	1916.035	1.91693
45.22168	-45.2217	589.2946	1918.281	1.917603
48.02956	-48.0296	603.6512	1918.281	1.917603
50.91133	-50.9113	620.7484	1918.281	1.917603



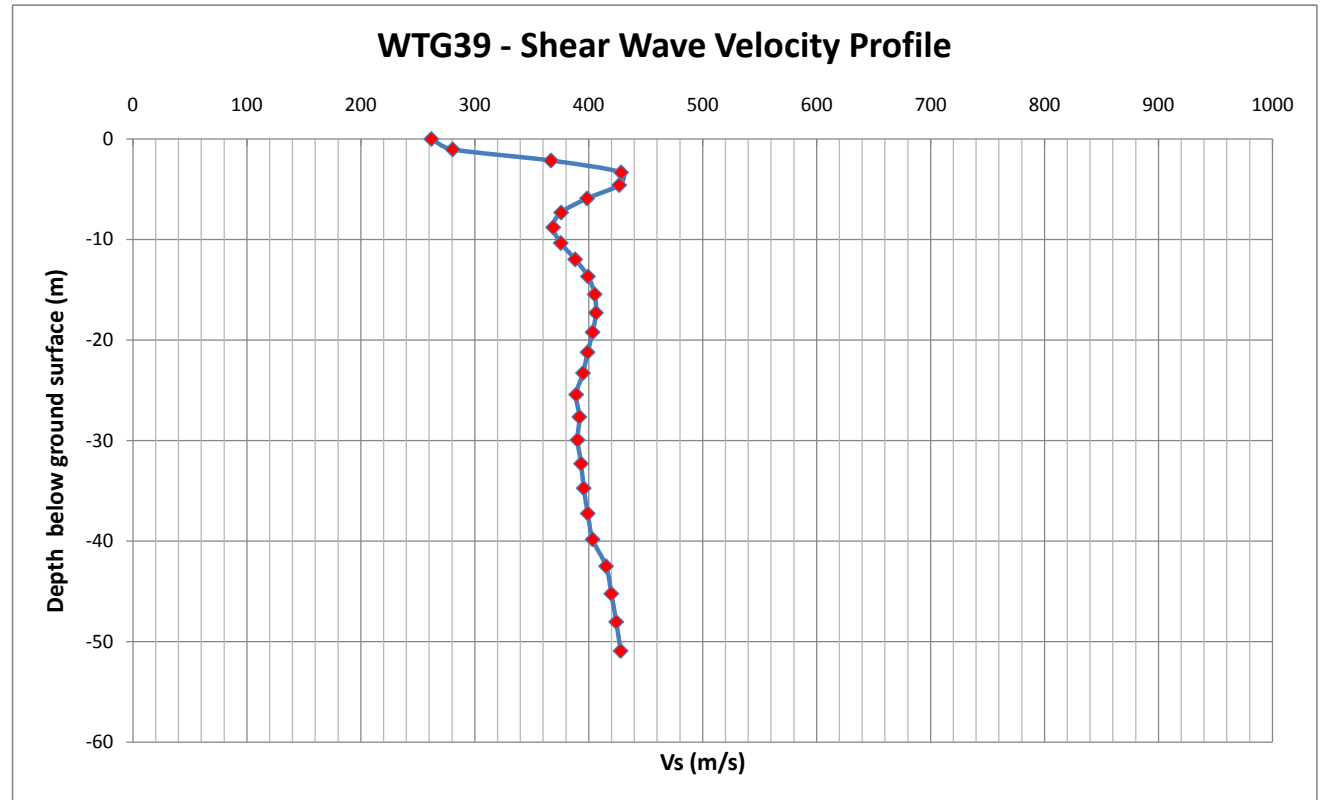
Depth(m)	Vs	Vp	Density	
0	0	169.2036	1583.224	1.814351
1.034483	-1.03448	199.3684	1583.683	1.814497
2.142857	-2.14286	300.7399	1615.303	1.82449
3.325123	-3.32512	353.6371	1677.023	1.843845
4.581281	-4.58128	351.1944	1722.303	1.857919
5.91133	-5.91133	385.1255	1769.86	1.872586
7.315271	-7.31527	452.8707	1801.106	1.882158
8.793104	-8.7931	518.2022	1813.76	1.88602
10.34483	-10.3448	556.6129	1816.398	1.886824
11.97044	-11.9704	561.9959	1817.056	1.887025
13.66995	-13.67	542.7828	1821.454	1.888365
15.44335	-15.4434	510.4064	1829.211	1.890725
17.29064	-17.2906	476.1125	1837.461	1.893231
19.21182	-19.2118	448.8434	1844.179	1.89527
21.2069	-21.2069	440.4686	1856.035	1.898863
23.27586	-23.2759	448.8318	1869.877	1.903047
25.41872	-25.4187	456.7873	1869.877	1.903047
27.63547	-27.6355	482.7047	1880.613	1.906286
29.92611	-29.9261	513.2671	1892.597	1.909895
32.29064	-32.2906	533.0951	1892.597	1.909895
34.72906	-34.7291	562.4822	1906.123	1.913958
37.24138	-37.2414	575.62	1906.123	1.913958
39.82759	-39.8276	597.1004	1920.688	1.918324
42.48769	-42.4877	601.0911	1920.688	1.918324
45.22168	-45.2217	613.095	1933.733	1.922224
48.02956	-48.0296	610.4188	1933.733	1.922224
50.91133	-50.9113	620.4368	1950.301	1.927165



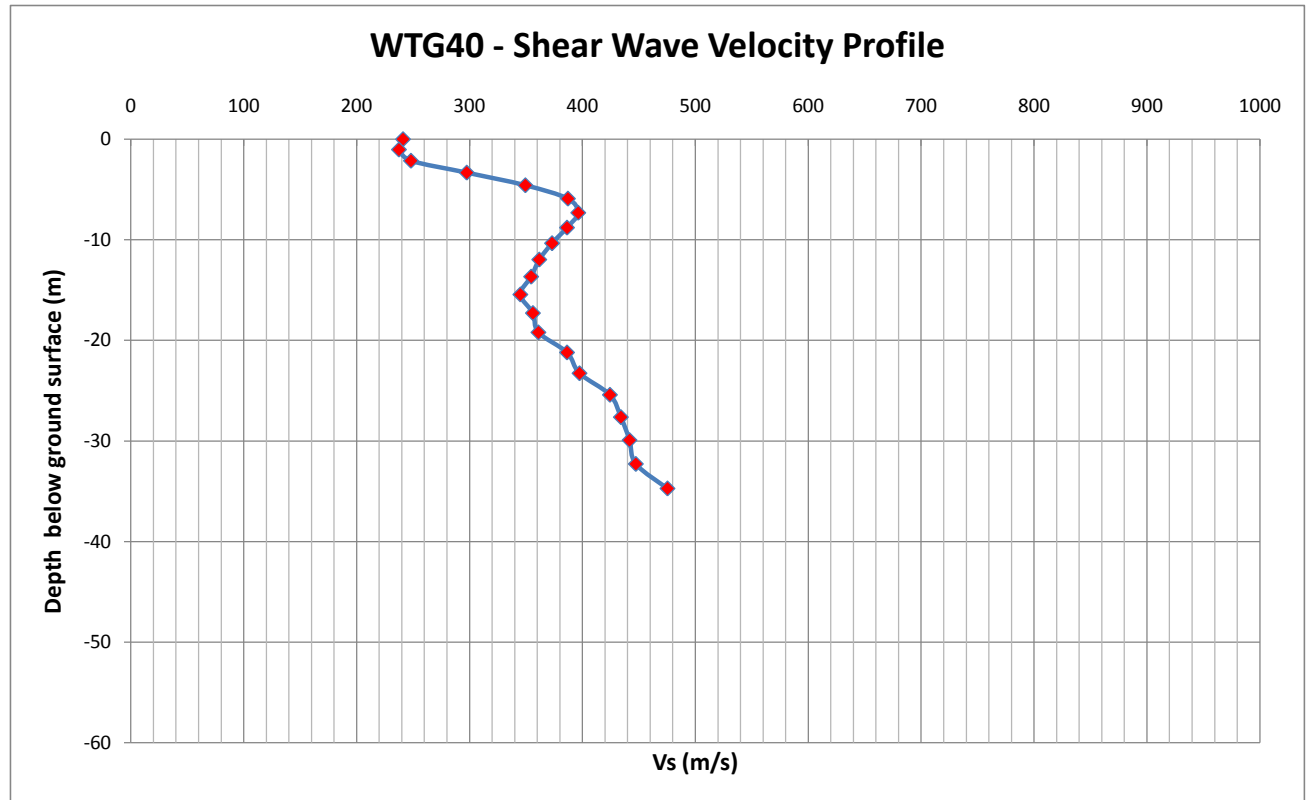
Depth(m)	Vs	Vp	Density	
0	0	353.0759	1831.27	1.891351
1.034483	-1.03448	358.4882	1831.27	1.891351
2.142857	-2.14286	386.374	1831.27	1.891351
3.325123	-3.32512	470.0062	1864.728	1.901492
4.581281	-4.58128	586.8844	1934.902	1.922573
5.91133	-5.91133	669.713	1988.62	1.938537
7.315271	-7.31527	699.1929	2009.856	1.944807
8.793104	-8.7931	699.4328	2021.074	1.94811
10.34483	-10.3448	691.8675	2034.936	1.952181
11.97044	-11.9704	681.9576	2046.527	1.955578
13.66995	-13.67	676.4299	2055.452	1.958189
15.44335	-15.4434	677.1746	2061.425	1.959934
17.29064	-17.2906	685.6089	2068.058	1.96187
19.21182	-19.2118	698.414	2075.408	1.964013
21.2069	-21.2069	712.9491	2083.999	1.966513
23.27586	-23.2759	724.3834	2091.283	1.96863
25.41872	-25.4187	733.2867	2098.968	1.970861
27.63547	-27.6355	739.7407	2107.418	1.97331
29.92611	-29.9261	742.3912	2114.06	1.975232
32.29064	-32.2906	744.1832	2121.405	1.977356
34.72906	-34.7291	746.3453	2128.976	1.979541
37.24138	-37.2414	742.6096	2128.976	1.979541
39.82759	-39.8276	747.2239	2136.278	1.981646
42.48769	-42.4877	753.3951	2143.113	1.983615
45.22168	-45.2217	755.4544	2143.113	1.983615
48.02956	-48.0296	765.3811	2149.812	1.985541
50.91133	-50.9113	770.6365	2149.812	1.985541



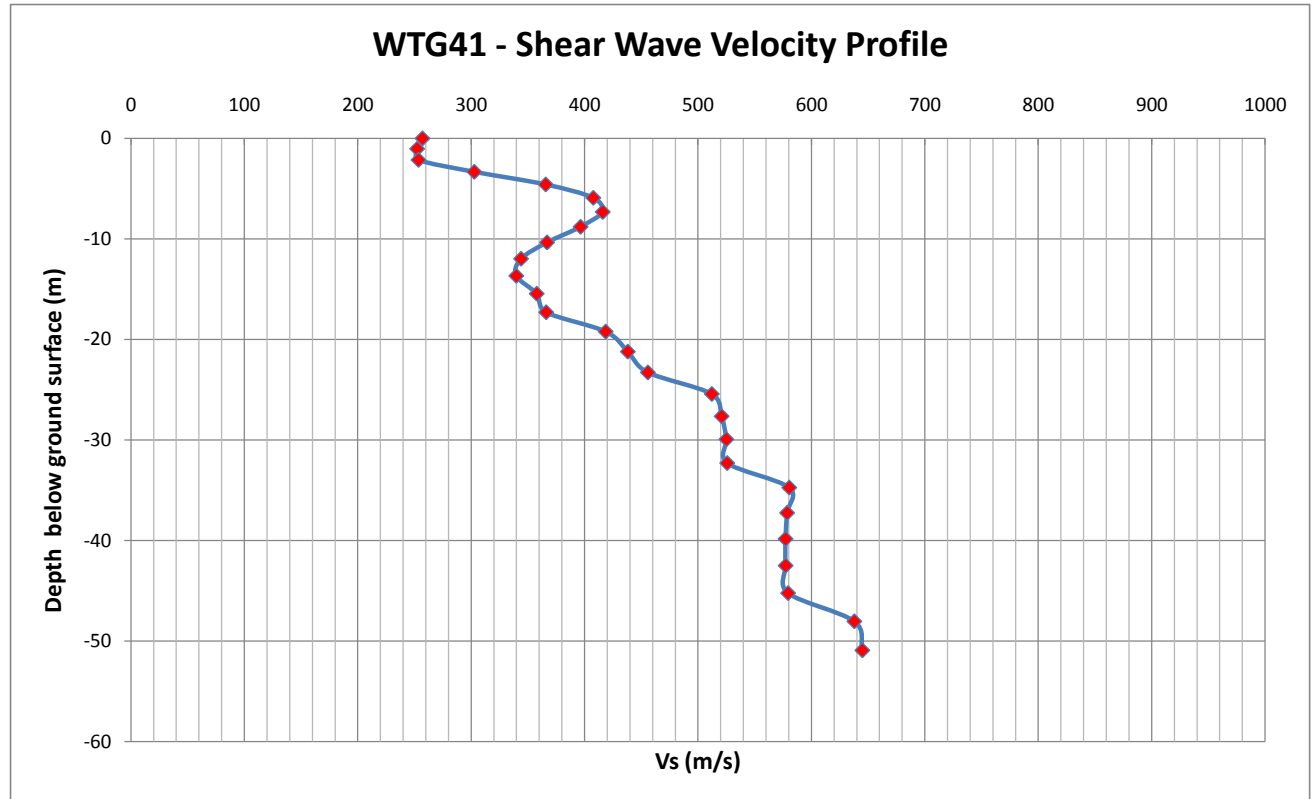
Depth(m)	Vs	Vp	Density	
0	0	261.7597	1682.665	1.845604
1.034483	-1.03448	280.4526	1682.665	1.845604
2.142857	-2.14286	366.8381	1704.659	1.852447
3.325123	-3.32512	428.4139	1720.398	1.857329
4.581281	-4.58128	426.7232	1722.884	1.858099
5.91133	-5.91133	398.5003	1726.05	1.859079
7.315271	-7.31527	375.7492	1728.544	1.85985
8.793104	-8.7931	368.7409	1728.215	1.859748
10.34483	-10.3448	375.4352	1728.321	1.859781
11.97044	-11.9704	388.0931	1729.954	1.860286
13.66995	-13.67	399.28	1732.172	1.860972
15.44335	-15.4434	405.1991	1734.049	1.861552
17.29064	-17.2906	406.324	1736.567	1.86233
19.21182	-19.2118	403.3326	1738.958	1.863069
21.2069	-21.2069	398.9464	1741.989	1.864004
23.27586	-23.2759	394.9546	1745.582	1.865113
25.41872	-25.4187	388.9686	1745.582	1.865113
27.63547	-27.6355	391.7233	1752.94	1.867381
29.92611	-29.9261	390.1742	1752.94	1.867381
32.29064	-32.2906	393.2492	1755.768	1.868252
34.72906	-34.7291	395.5886	1755.768	1.868252
37.24138	-37.2414	399.1125	1755.768	1.868252
39.82759	-39.8276	403.417	1755.768	1.868252
42.48769	-42.4877	415.1913	1763.727	1.870701
45.22168	-45.2217	419.7634	1763.727	1.870701
48.02956	-48.0296	424.0742	1763.727	1.870701
50.91133	-50.9113	427.9592	1763.727	1.870701



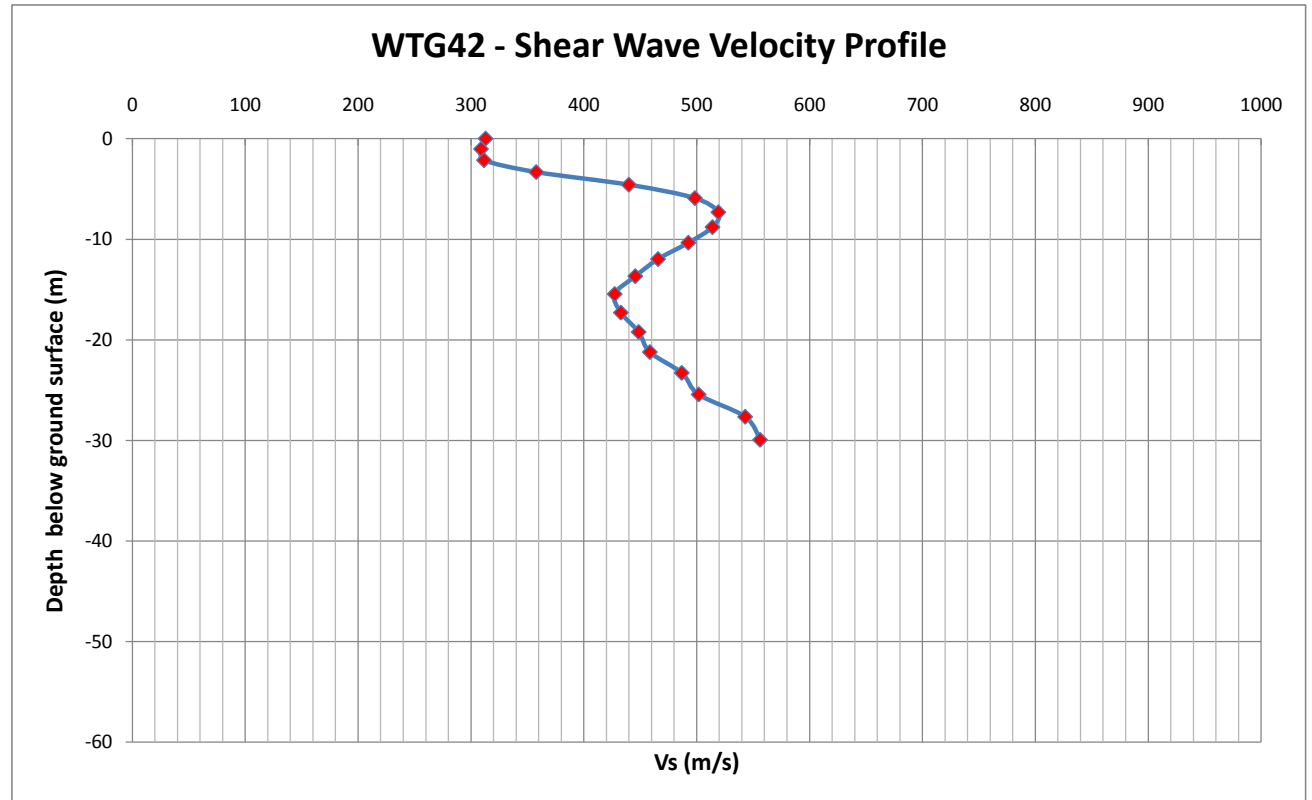
Depth(m)	Vs	Vp	Density	
0	0	241.0718	1590.697	1.816718
1.034483	-1.03448	237.4636	1590.697	1.816718
2.142857	-2.14286	248.0963	1606.053	1.821572
3.325123	-3.32512	297.5263	1645.414	1.833957
4.581281	-4.58128	349.496	1674.294	1.842993
5.91133	-5.91133	387.183	1692.884	1.848787
7.315271	-7.31527	396.3468	1696.108	1.84979
8.793104	-8.7931	386.3777	1695.066	1.849466
10.34483	-10.3448	373.1395	1700.985	1.851306
11.97044	-11.9704	361.7986	1711.276	1.854501
13.66995	-13.67	354.6088	1721.789	1.85776
15.44335	-15.4434	345.038	1721.789	1.85776
17.29064	-17.2906	356.1786	1735.968	1.862145
19.21182	-19.2118	361.0537	1735.968	1.862145
21.2069	-21.2069	386.3963	1753.849	1.867661
23.27586	-23.2759	397.4752	1753.849	1.867661
25.41872	-25.4187	424.4127	1771.465	1.873079
27.63547	-27.6355	434.1224	1771.465	1.873079
29.92611	-29.9261	441.7995	1771.465	1.873079
32.29064	-32.2906	447.3735	1771.465	1.873079
34.72906	-34.7291	475.4157	1798.646	1.881406



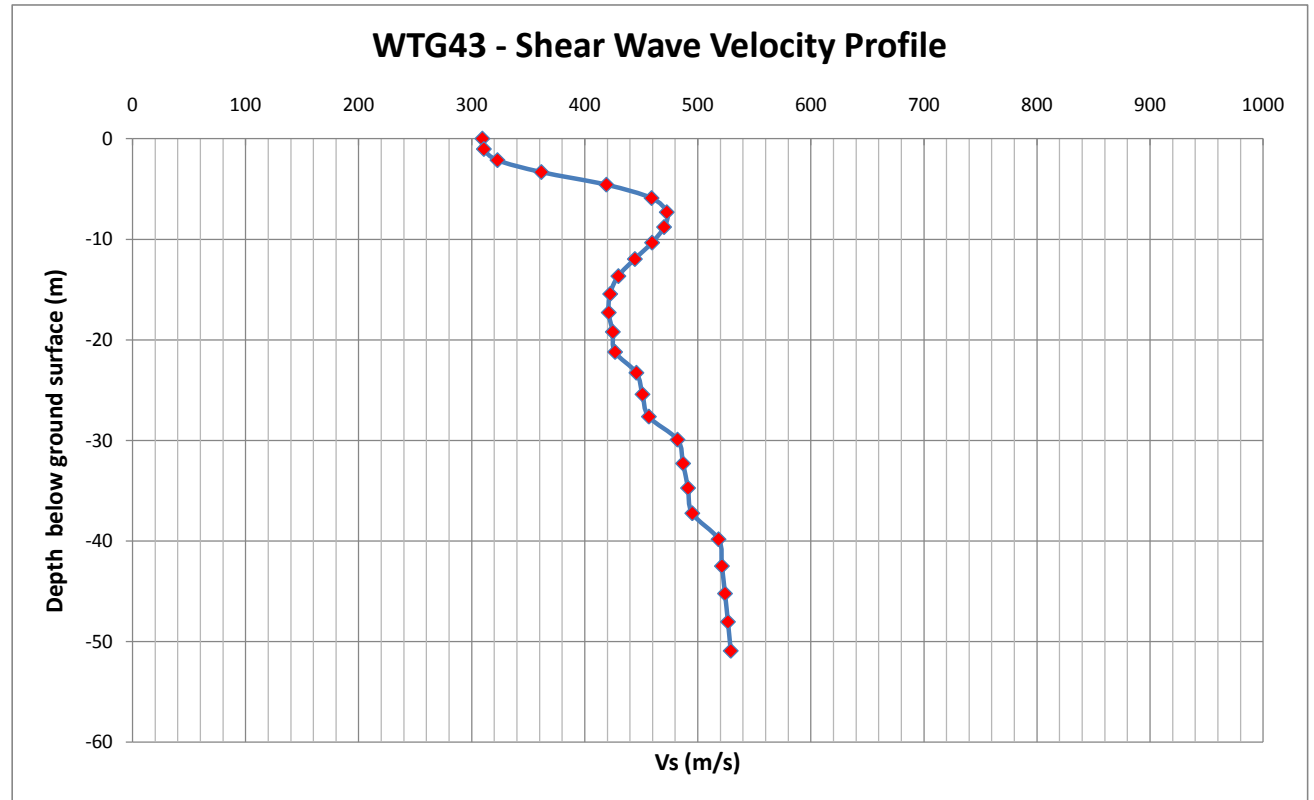
Depth(m)	Vs	Vp	Density	
0	0	256.996	1612.303	1.823544
1.034483	-1.03448	252.2946	1612.303	1.823544
2.142857	-2.14286	253.48	1621.643	1.826487
3.325123	-3.32512	302.6719	1657.364	1.837702
4.581281	-4.58128	365.6516	1686.052	1.84666
5.91133	-5.91133	407.6125	1700.409	1.851127
7.315271	-7.31527	415.9159	1705.542	1.852722
8.793104	-8.7931	396.4037	1707.566	1.85335
10.34483	-10.3448	366.8288	1713	1.855036
11.97044	-11.9704	343.9055	1724.153	1.858491
13.66995	-13.67	339.7201	1742.671	1.864215
15.44335	-15.4434	357.7063	1768.12	1.872051
17.29064	-17.2906	366.0544	1768.12	1.872051
19.21182	-19.2118	418.5039	1807.235	1.88403
21.2069	-21.2069	438.0325	1807.235	1.88403
23.27586	-23.2759	455.7319	1807.235	1.88403
25.41872	-25.4187	512.118	1854.934	1.898529
27.63547	-27.6355	520.7692	1854.934	1.898529
29.92611	-29.9261	524.9776	1854.934	1.898529
32.29064	-32.2906	525.6608	1854.934	1.898529
34.72906	-34.7291	580.3866	1917.256	1.917296
37.24138	-37.2414	578.472	1917.256	1.917296
39.82759	-39.8276	577.1285	1917.256	1.917296
42.48769	-42.4877	577.1922	1917.256	1.917296
45.22168	-45.2217	579.3672	1917.256	1.917296
48.02956	-48.0296	637.7906	1977.055	1.935113
50.91133	-50.9113	644.8395	1977.055	1.935113



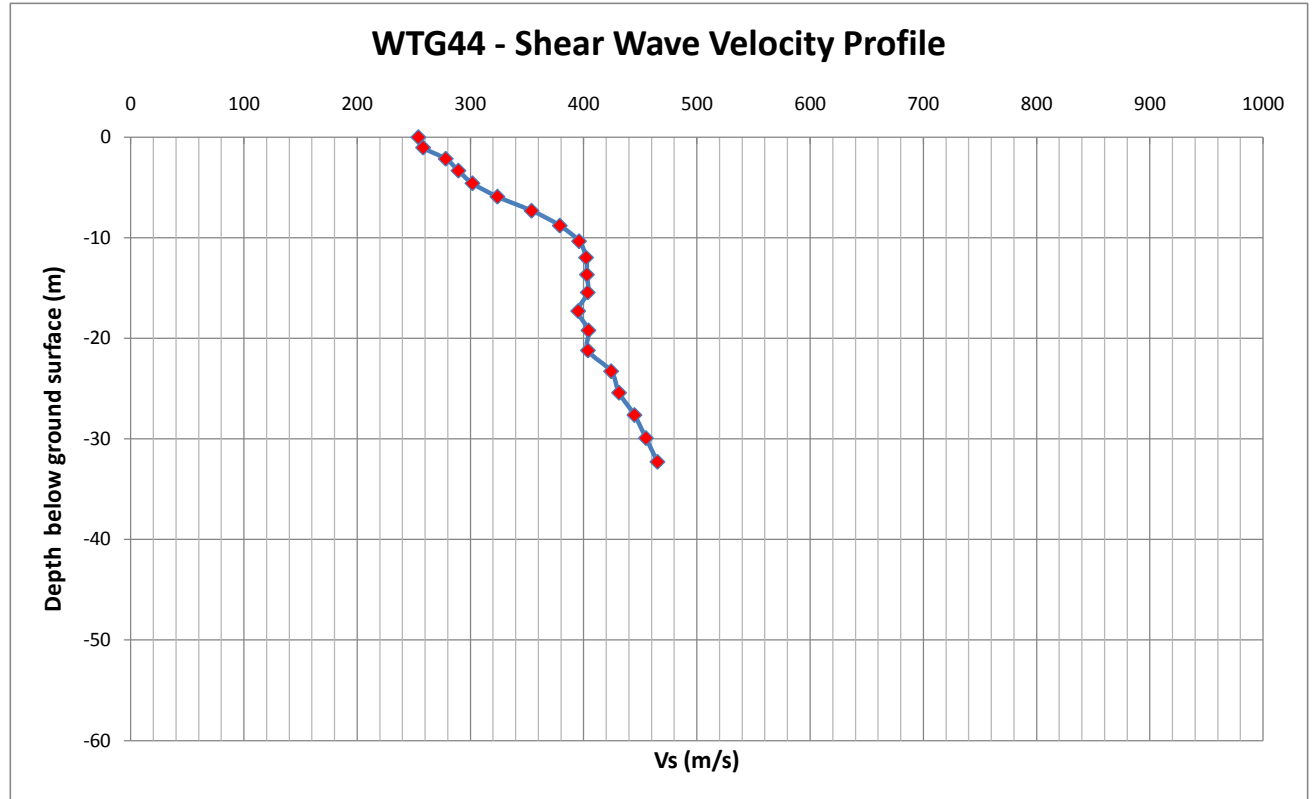
Depth(m)	Vs	Vp	Density	
0	0	313.0273	1694.669	1.849342
1.034483	-1.03448	308.9998	1694.669	1.849342
2.142857	-2.14286	311.6462	1701.757	1.851546
3.325123	-3.32512	357.8602	1733.374	1.861344
4.581281	-4.58128	439.9316	1779.697	1.875605
5.91133	-5.91133	498.4383	1800.949	1.88211
7.315271	-7.31527	519.2321	1803.414	1.882863
8.793104	-8.7931	514.0178	1805.669	1.883552
10.34483	-10.3448	492.6416	1810.409	1.884998
11.97044	-11.9704	465.7991	1816.1	1.886733
13.66995	-13.67	445.6229	1824.751	1.889368
15.44335	-15.4434	427.3921	1824.751	1.889368
17.29064	-17.2906	432.8753	1838.267	1.893476
19.21182	-19.2118	448.6327	1852.21	1.897704
21.2069	-21.2069	458.56	1852.21	1.897704
23.27586	-23.2759	486.7843	1868.296	1.90257
25.41872	-25.4187	501.7616	1868.296	1.90257
27.63547	-27.6355	542.976	1897.867	1.911479
29.92611	-29.9261	556.1981	1897.867	1.911479



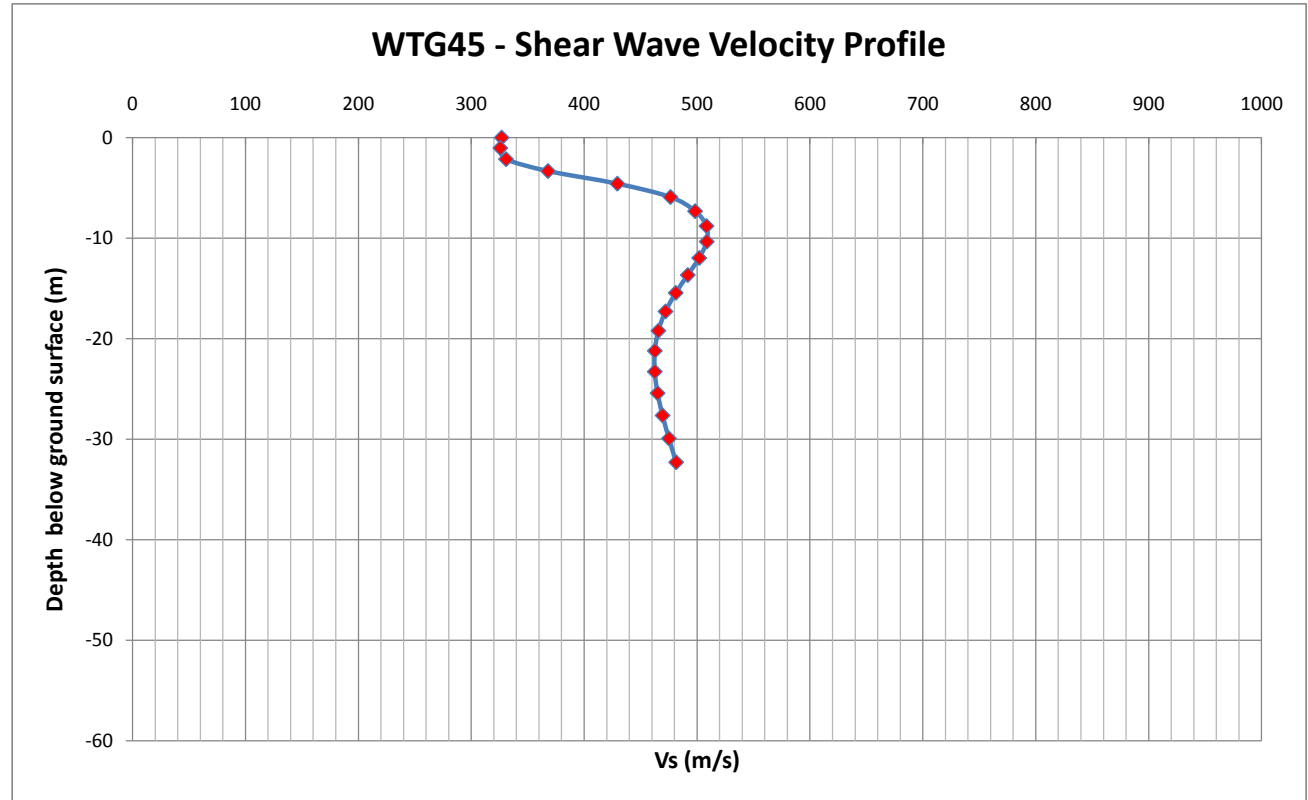
Depth(m)	Vs	Vp	Density	
0	0	309.315	1725.578	1.858933
1.034483	-1.03448	310.6326	1725.578	1.858933
2.142857	-2.14286	322.6805	1725.578	1.858933
3.325123	-3.32512	361.531	1736.245	1.862231
4.581281	-4.58128	419.1475	1760.408	1.86968
5.91133	-5.91133	459.1464	1773.997	1.873856
7.315271	-7.31527	472.6002	1776	1.874471
8.793104	-8.7931	470.2055	1778.327	1.875185
10.34483	-10.3448	459.6038	1783.317	1.876715
11.97044	-11.9704	444.3541	1787.06	1.877861
13.66995	-13.67	429.7353	1789.555	1.878625
15.44335	-15.4434	422.4853	1794.907	1.880263
17.29064	-17.2906	421.2227	1800.756	1.882051
19.21182	-19.2118	424.8388	1806.605	1.883837
21.2069	-21.2069	426.8377	1806.605	1.883837
23.27586	-23.2759	445.7106	1822.658	1.888731
25.41872	-25.4187	451.1226	1822.658	1.888731
27.63547	-27.6355	456.7556	1822.658	1.888731
29.92611	-29.9261	482.136	1844.824	1.895466
32.29064	-32.2906	487.0493	1844.824	1.895466
34.72906	-34.7291	491.4238	1844.824	1.895466
37.24138	-37.2414	495.2107	1844.824	1.895466
39.82759	-39.8276	518.4367	1866.899	1.902148
42.48769	-42.4877	521.4267	1866.899	1.902148
45.22168	-45.2217	524.168	1866.899	1.902148
48.02956	-48.0296	526.7573	1866.899	1.902148
50.91133	-50.9113	529.2425	1866.899	1.902148



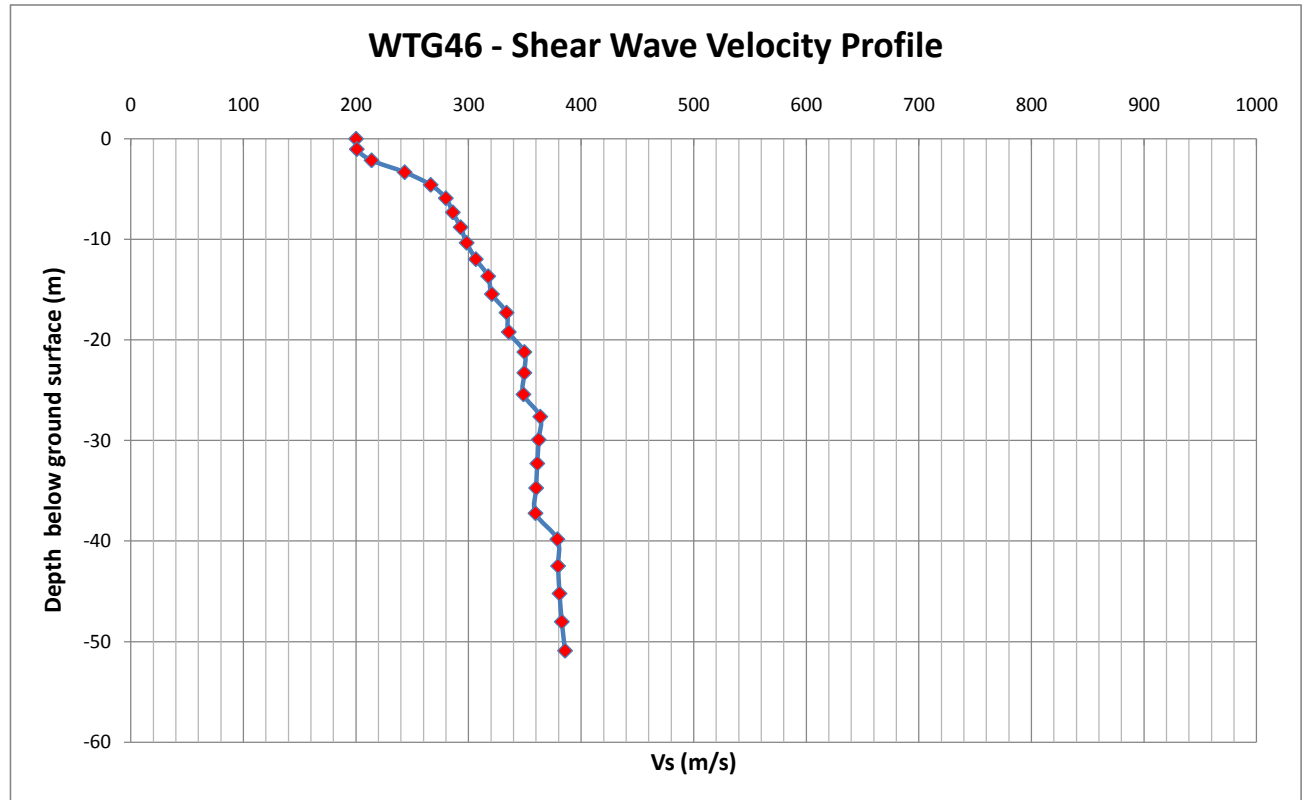
Depth(m)	Vs	Vp	Density	
0	0	254.0748	1599.686	1.819561
1.034483	-1.03448	258.2803	1599.686	1.819561
2.142857	-2.14286	278.2259	1614.964	1.824383
3.325123	-3.32512	289.4408	1632.454	1.829888
4.581281	-4.58128	301.8498	1655.286	1.837051
5.91133	-5.91133	323.8969	1678.095	1.84418
7.315271	-7.31527	354.0673	1698.555	1.850551
8.793104	-8.7931	378.9879	1711.5	1.854571
10.34483	-10.3448	395.9996	1722.313	1.857922
11.97044	-11.9704	402.2439	1730.296	1.860392
13.66995	-13.67	402.9812	1739.128	1.863121
15.44335	-15.4434	403.6876	1750.582	1.866655
17.29064	-17.2906	395.2429	1750.582	1.866655
19.21182	-19.2118	404.3254	1766.106	1.871432
21.2069	-21.2069	403.8573	1766.106	1.871432
23.27586	-23.2759	424.3596	1784.666	1.877128
25.41872	-25.4187	431.3852	1784.666	1.877128
27.63547	-27.6355	444.9482	1789.5	1.878608
29.92611	-29.9261	455.1116	1789.5	1.878608
32.29064	-32.2906	465.2702	1789.5	1.878608



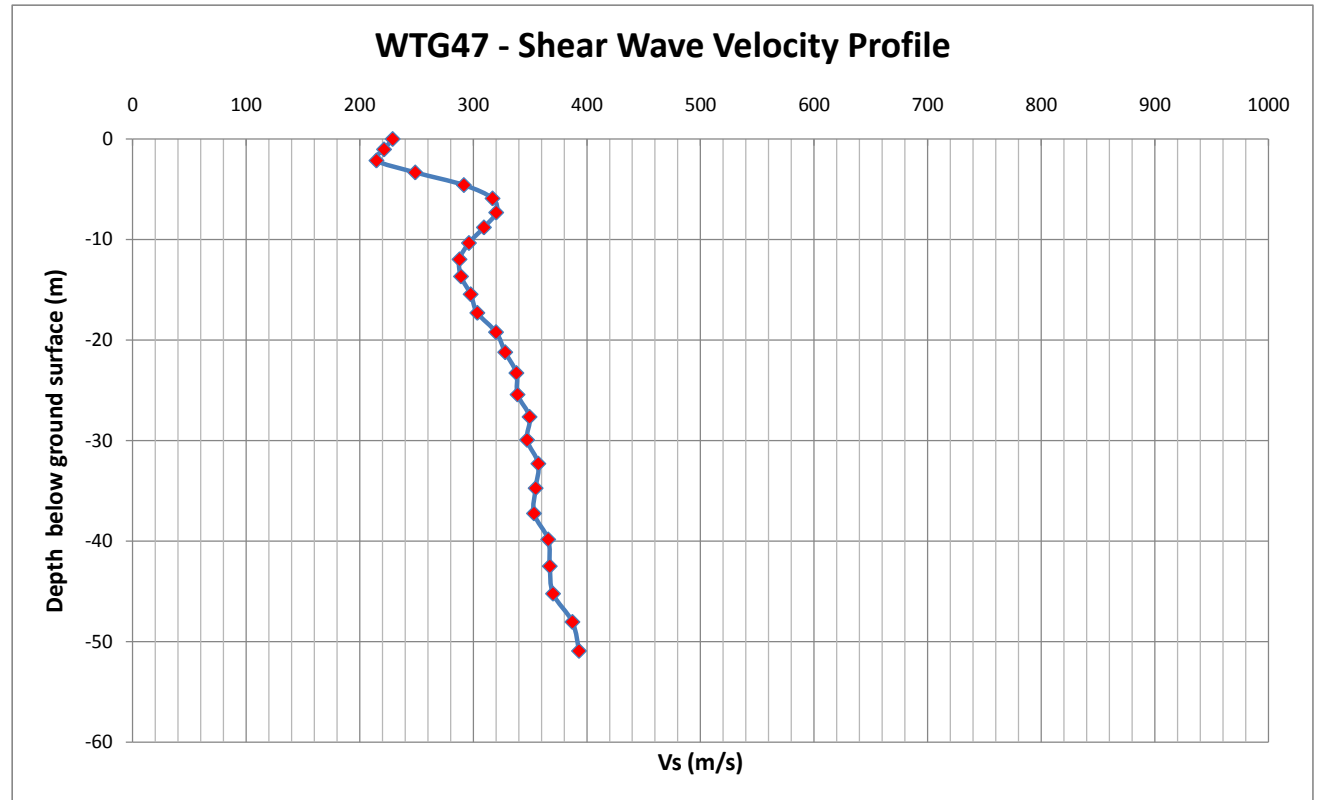
Depth(m)	Vs	Vp	Density
0	0	326.9392	1713.118
1.034483	-1.03448	325.7342	1713.118
2.142857	-2.14286	330.798	1716.504
3.325123	-3.32512	368.0029	1741.795
4.581281	-4.58128	429.423	1781.61
5.91133	-5.91133	476.5026	1803.678
7.315271	-7.31527	498.318	1805.027
8.793104	-8.7931	508.4048	1805.027
10.34483	-10.3448	508.6255	1805.027
11.97044	-11.9704	501.9835	1805.027
13.66995	-13.67	491.8442	1805.027
15.44335	-15.4434	481.1841	1805.027
17.29064	-17.2906	472.1053	1805.027
19.21182	-19.2118	465.7871	1805.027
21.2069	-21.2069	462.6506	1805.027
23.27586	-23.2759	462.5796	1805.027
25.41872	-25.4187	465.1028	1805.027
27.63547	-27.6355	469.5284	1805.027
29.92611	-29.9261	475.1861	1805.027
32.29064	-32.2906	481.5336	1805.027



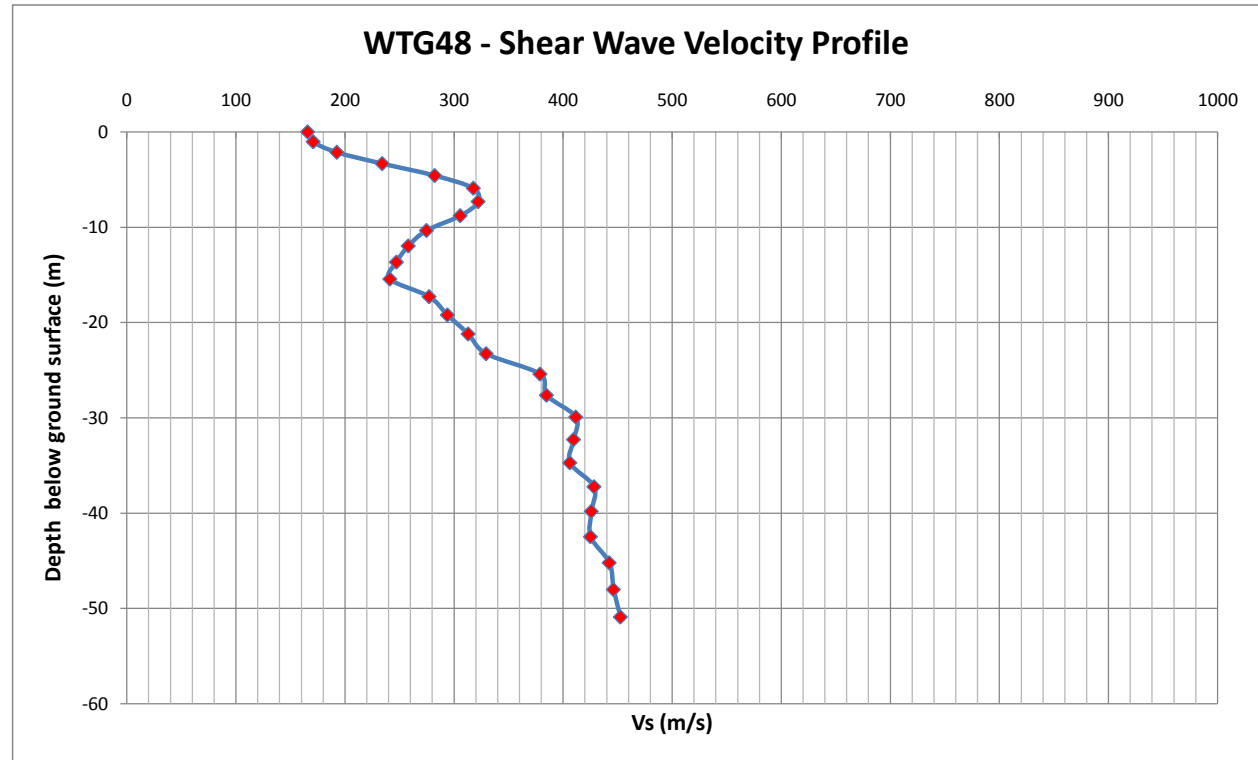
Depth(m)	Vs	Vp	Density	
0	0	200.0162	1539.036	1.800299
1.034483	-1.03448	200.6785	1539.715	1.800515
2.142857	-2.14286	213.774	1549.994	1.803793
3.325123	-3.32512	243.1914	1573.516	1.811273
4.581281	-4.58128	266.2957	1592.261	1.817213
5.91133	-5.91133	279.7499	1606.625	1.821752
7.315271	-7.31527	285.955	1617.388	1.825147
8.793104	-8.7931	292.8704	1629.344	1.82891
10.34483	-10.3448	298.225	1637.218	1.831385
11.97044	-11.9704	306.3934	1645.322	1.833928
13.66995	-13.67	317.4102	1654.614	1.83684
15.44335	-15.4434	320.672	1654.614	1.83684
17.29064	-17.2906	333.6998	1665.838	1.840352
19.21182	-19.2118	335.692	1665.838	1.840352
21.2069	-21.2069	349.5193	1680.182	1.84483
23.27586	-23.2759	349.4788	1680.182	1.84483
25.41872	-25.4187	348.7121	1680.182	1.84483
27.63547	-27.6355	363.6529	1698.103	1.85041
29.92611	-29.9261	362.2905	1698.103	1.85041
32.29064	-32.2906	360.9963	1698.103	1.85041
34.72906	-34.7291	359.9857	1698.103	1.85041
37.24138	-37.2414	359.4128	1698.103	1.85041
39.82759	-39.8276	378.8638	1719.682	1.857107
42.48769	-42.4877	379.4688	1719.682	1.857107
45.22168	-45.2217	380.7425	1719.682	1.857107
48.02956	-48.0296	382.7881	1719.682	1.857107
50.91133	-50.9113	385.6703	1719.682	1.857107



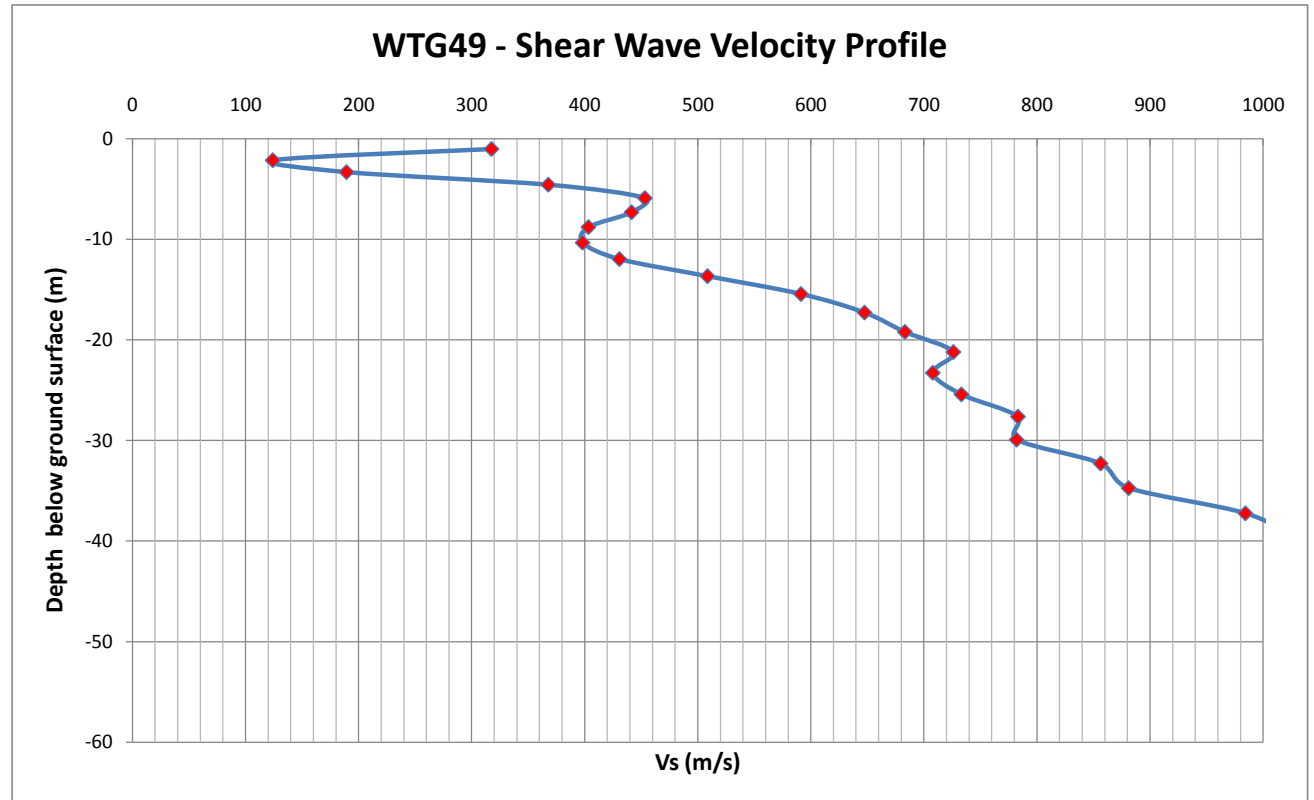
Depth(m)	Vs	Vp	Density
0	0	228.9618	1561.369
1.034483	-1.03448	221.3892	1561.369
2.142857	-2.14286	214.6898	1567.12
3.325123	-3.32512	248.8633	1592.391
4.581281	-4.58128	291.6554	1610.045
5.91133	-5.91133	316.8912	1618.439
7.315271	-7.31527	320.1208	1623.947
8.793104	-8.7931	309.31	1628.824
10.34483	-10.3448	296.1178	1633.797
11.97044	-11.9704	287.8291	1638.273
13.66995	-13.67	289.1196	1644.569
15.44335	-15.4434	297.6306	1651.52
17.29064	-17.2906	303.506	1651.52
19.21182	-19.2118	319.9556	1662.298
21.2069	-21.2069	328.0531	1665.15
23.27586	-23.2759	337.8941	1672.365
25.41872	-25.4187	338.9005	1672.365
27.63547	-27.6355	349.4896	1685.19
29.92611	-29.9261	347.3004	1685.19
32.29064	-32.2906	357.2071	1699.1
34.72906	-34.7291	354.8464	1699.1
37.24138	-37.2414	353.3987	1699.1
39.82759	-39.8276	365.9046	1713.093
42.48769	-42.4877	367.2701	1713.093
45.22168	-45.2217	370.1641	1713.093
48.02956	-48.0296	387.2094	1727.085
50.91133	-50.9113	393.026	1727.085



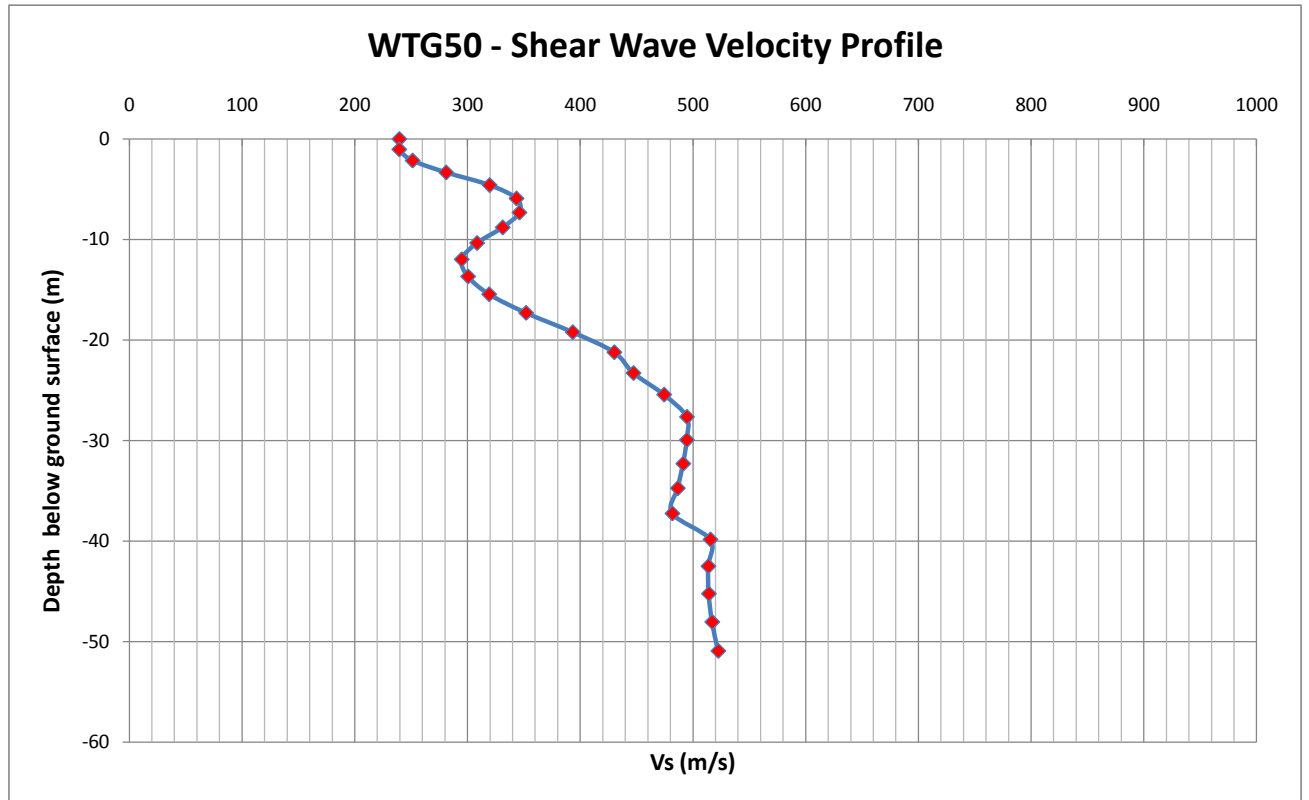
Depth(m)	Vs	Vp	Density
0	0	165.8121	1521.01
1.034483	-1.03448	170.9557	1521.01
2.142857	-2.14286	192.6337	1535.502
3.325123	-3.32512	234.2078	1566.652
4.581281	-4.58128	282.3206	1592.311
5.91133	-5.91133	317.7704	1603.47
7.315271	-7.31527	322.1572	1598.171
8.793104	-8.7931	305.7293	1596
10.34483	-10.3448	274.7919	1596
11.97044	-11.9704	258.0833	1613.888
13.66995	-13.67	247.2455	1626.256
15.44335	-15.4434	241.2459	1626.256
17.29064	-17.2906	277.2038	1656.27
19.21182	-19.2118	294.0197	1656.27
21.2069	-21.2069	313.0136	1656.27
23.27586	-23.2759	329.4865	1656.27
25.41872	-25.4187	378.8857	1698.653
27.63547	-27.6355	384.8213	1698.653
29.92611	-29.9261	411.6419	1727.175
32.29064	-32.2906	409.6639	1727.175
34.72906	-34.7291	406.2326	1727.175
37.24138	-37.2414	428.4172	1755.697
39.82759	-39.8276	425.9048	1755.697
42.48769	-42.4877	425.155	1755.697
45.22168	-45.2217	442.3334	1773.174
48.02956	-48.0296	446.2179	1773.174
50.91133	-50.9113	452.5931	1773.174



	Depth(m)	Vs	Vp	Density
	0	0		
1.034483	-1.03448	317.5773	1574.546	1.8116
2.142857	-2.14286	124.1276	1574.546	1.8116
3.325123	-3.32512	189.3261	1591.39	1.816937
4.581281	-4.58128	367.817	1635.546	1.83086
5.91133	-5.91133	453.2253	1685.069	1.846354
7.315271	-7.31527	441.4473	1731.005	1.860611
8.793104	-8.7931	403.293	1773.092	1.873578
10.34483	-10.3448	398.1641	1817.455	1.887146
11.97044	-11.9704	430.7076	1855.74	1.898773
13.66995	-13.67	508.626	1913.265	1.9161
15.44335	-15.4434	591.2603	1971.363	1.933425
17.29064	-17.2906	647.5088	2012.278	1.94552
19.21182	-19.2118	683.2133	2048.316	1.956102
21.2069	-21.2069	726.0342	2107.635	1.973373
23.27586	-23.2759	707.8902	2107.635	1.973373
25.41872	-25.4187	733.156	2156.533	1.987471
27.63547	-27.6355	783.1954	2226.608	2.007459
29.92611	-29.9261	781.9494	2226.608	2.007459
32.29064	-32.2906	856.3196	2296.012	2.027004
34.72906	-34.7291	881.1073	2296.012	2.027004
37.24138	-37.2414	984.3419	2369.76	2.047498
39.82759	-39.8276	1030.645	2369.76	2.047498
42.48769	-42.4877	1085.246	2369.76	2.047498
45.22168	-45.2217	1147.002	2369.76	2.047498
48.02956	-48.0296	1277.098	2438.972	2.066474
50.91133	-50.9113	1351.273	2438.972	2.066474



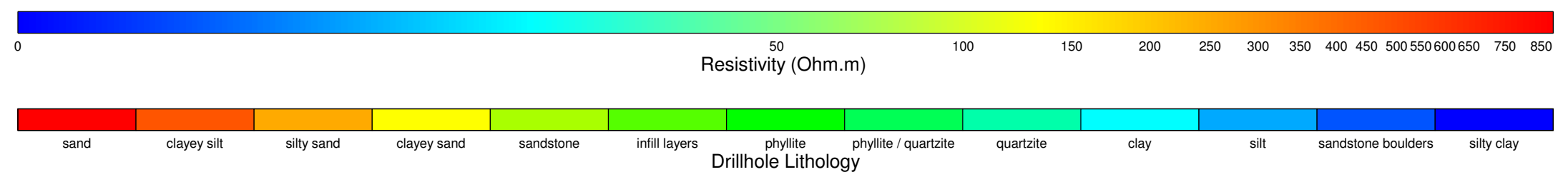
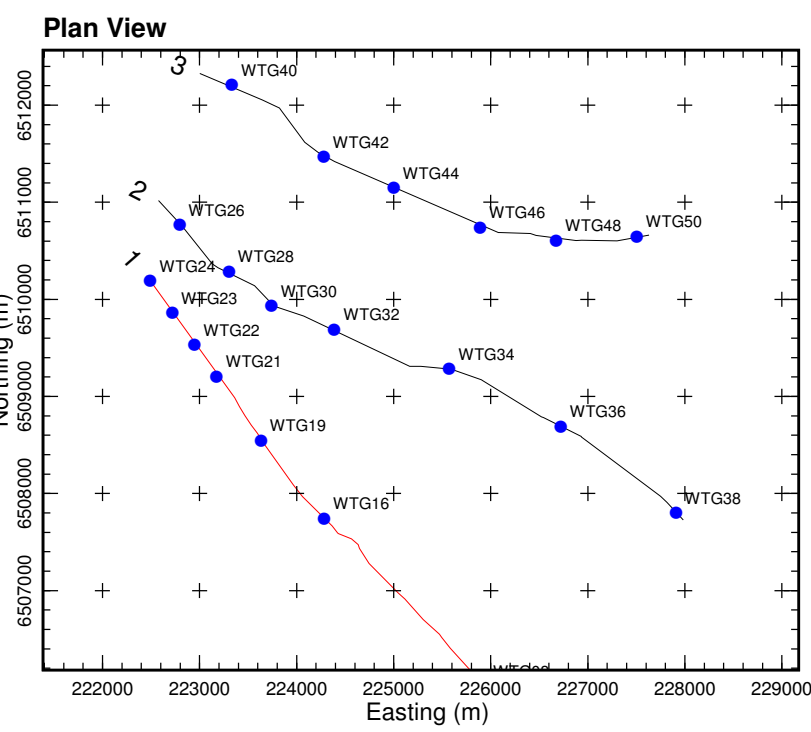
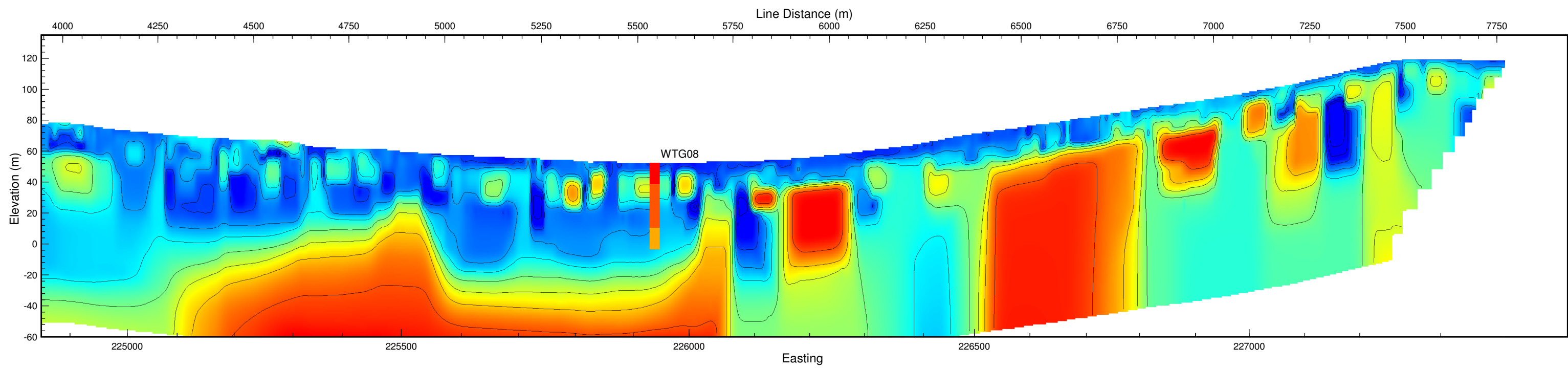
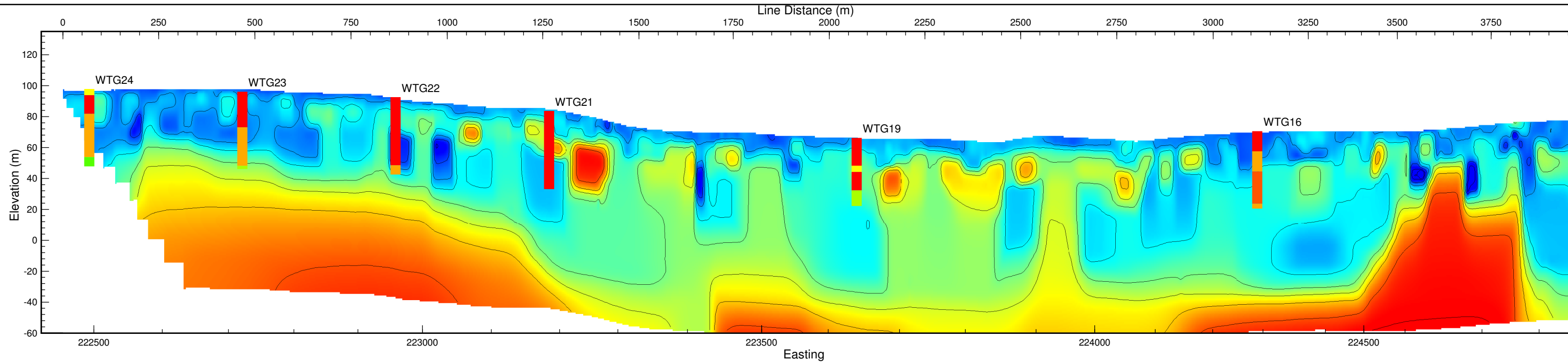
Depth(m)	Vs	Vp	Density	
0	0	239.6526	1590	1.816497
1.034483	-1.03448	239.5638	1590	1.816497
2.142857	-2.14286	251.4052	1603.103	1.82064
3.325123	-3.32512	281.1688	1622.98	1.826908
4.581281	-4.58128	319.6803	1640.735	1.832489
5.91133	-5.91133	343.479	1648.101	1.8348
7.315271	-7.31527	346.0928	1652.732	1.836251
8.793104	-8.7931	331.27	1659.889	1.838492
10.34483	-10.3448	308.557	1668.708	1.841249
11.97044	-11.9704	294.9186	1682.606	1.845586
13.66995	-13.67	300.5925	1702.231	1.851693
15.44335	-15.4434	319.2897	1718.095	1.856616
17.29064	-17.2906	351.9947	1735.766	1.862083
19.21182	-19.2118	393.3922	1757.171	1.868684
21.2069	-21.2069	430.2506	1774.276	1.873942
23.27586	-23.2759	447.219	1774.276	1.873942
25.41872	-25.4187	474.3991	1792.45	1.879511
27.63547	-27.6355	494.6176	1809.624	1.884759
29.92611	-29.9261	494.581	1809.624	1.884759
32.29064	-32.2906	491.355	1809.624	1.884759
34.72906	-34.7291	486.5423	1809.624	1.884759
37.24138	-37.2414	481.7499	1809.624	1.884759
39.82759	-39.8276	515.469	1851.085	1.897364
42.48769	-42.4877	513.6381	1851.085	1.897364
45.22168	-45.2217	514.0727	1851.085	1.897364
48.02956	-48.0296	517.0289	1851.085	1.897364
50.91133	-50.9113	522.427	1851.085	1.897364



APPENDIX I:

SEISMIC REFRACTION AND ELECTRICAL RESISTIVITY

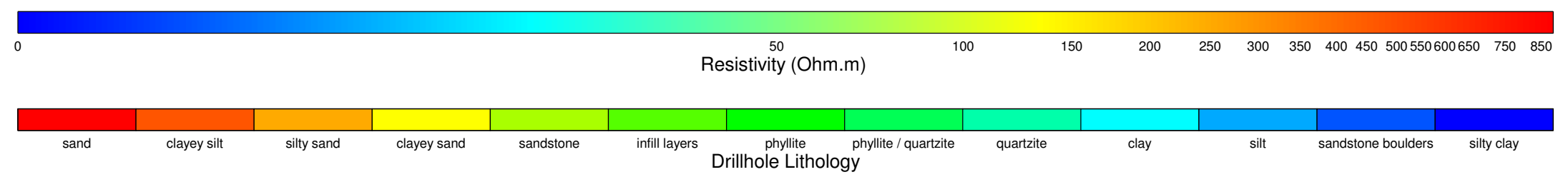
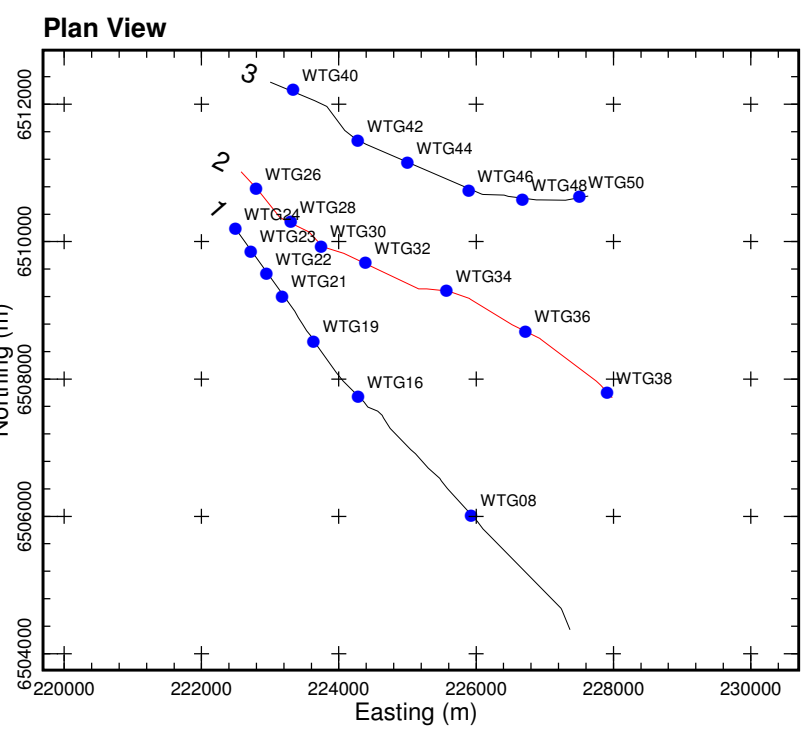
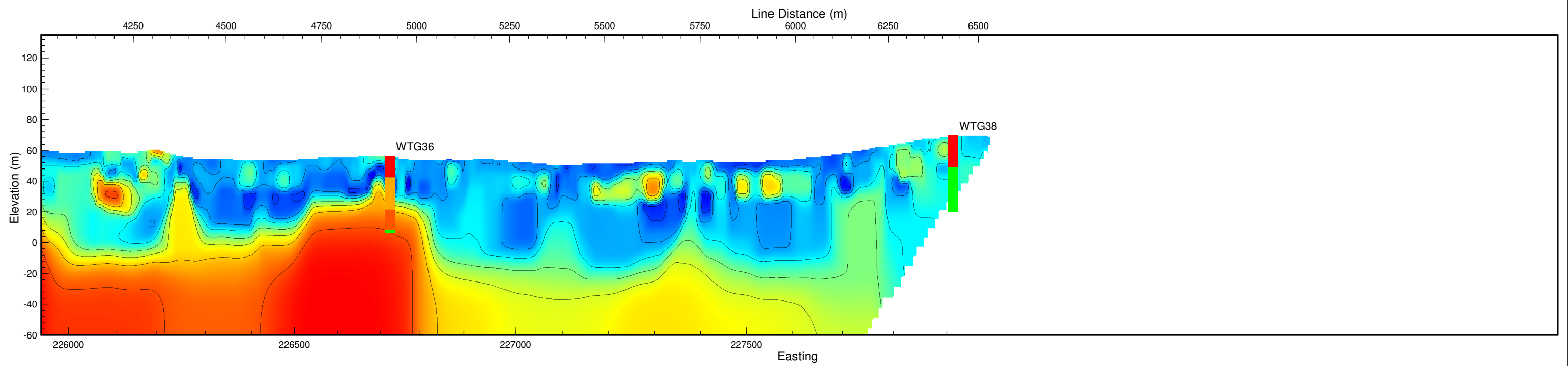
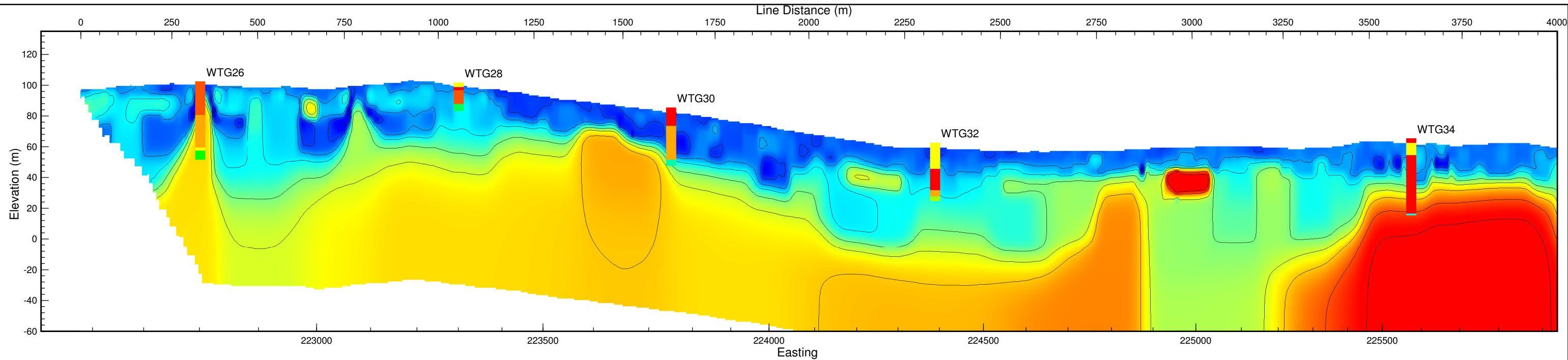
b (i) ERI with Boreholes Overlain



Notes:
 ERI pseudosection with MASW data overlain
 Vertical exaggeration 4:1
 Data displayed in WGS84 zone S34
 Active line displayed in red on plan view

ESKOM
 SERE WIND ENERGY FACILITY

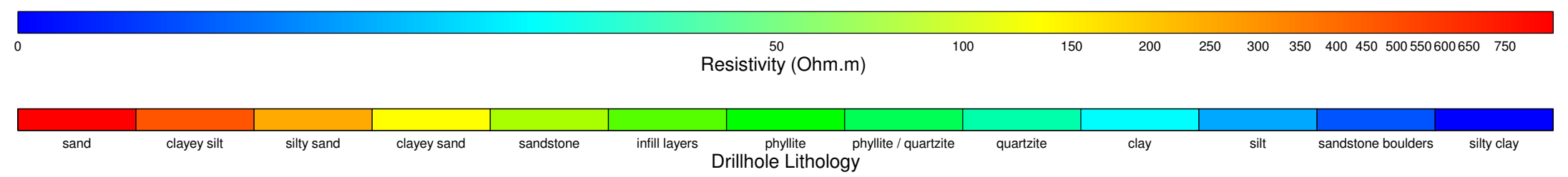
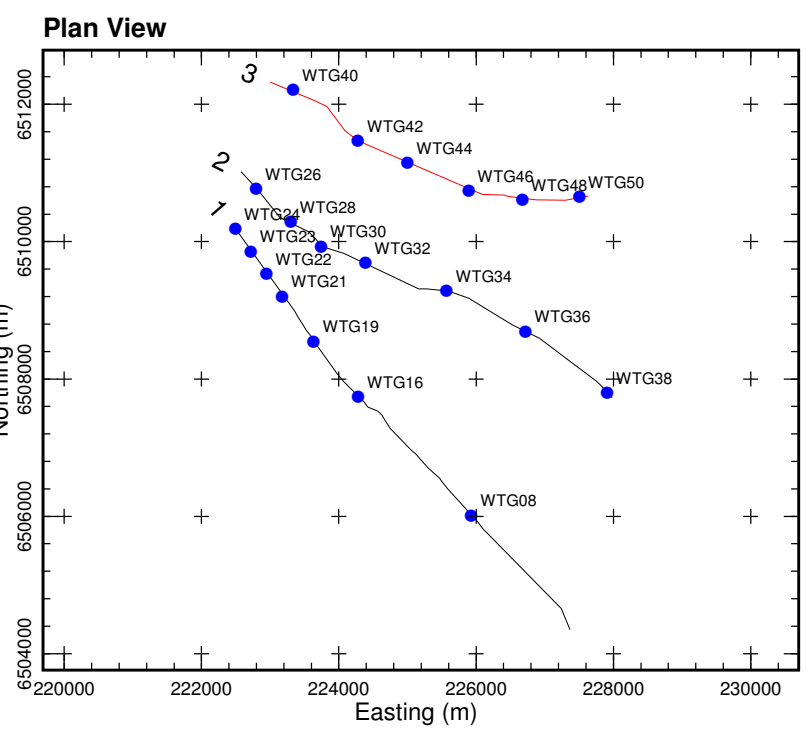
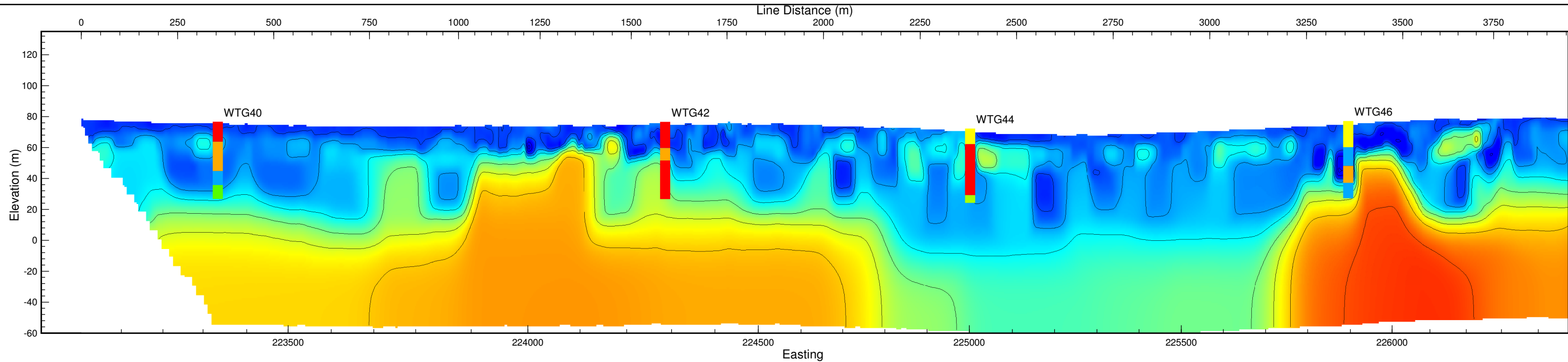
Figure 1: ERI line 1 with drillholes overlain



Notes:
 ERI pseudosection with MASW data overlain
 Vertical exaggeration 4:1
 Data displayed in WGS84 zone S34
 Active line displayed in red on plan view

ESKOM
 SERE WIND ENERGY FACILITY

Figure 2: ERI line 2 with drillholes overlain



Notes:
 ERI pseudosection with MASW data overlain
 Vertical exaggeration 4:1
 Data displayed in WGS84 zone S34
 Active line displayed in red on plan view

ESKOM
 SERE WIND ENERGY FACILITY

Figure 3: ERI line 3 with drillhole overlain

APPENDIX I:

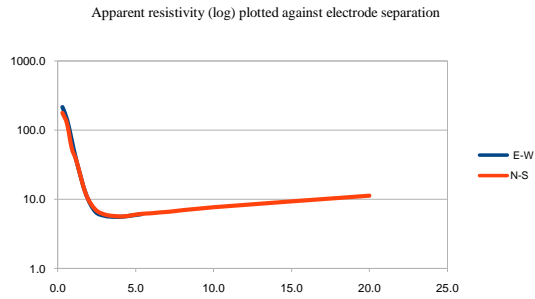
SEISMIC REFRACTION AND ELECTRICAL RESISTIVITY

b (ii) Resistivity Test Results

BH resistivity

1 E-W			
Spacing	Count	App. Resistivity	Resistance
0.3	38	215.4	114.25
0.6	52	141.0	37.40
0.9	32	71.4	12.62
1.2	33	36.1	4.79
1.8	31	12.1	1.07
2.4	29	6.7	0.44
3.0	26	5.8	0.31
3.6	23	5.6	0.25
4.2	20	5.6	0.21
4.8	17	5.8	0.19
5.4	12	6.1	0.18
6.0			
6.6			
7.2			
10.0			
20.0			

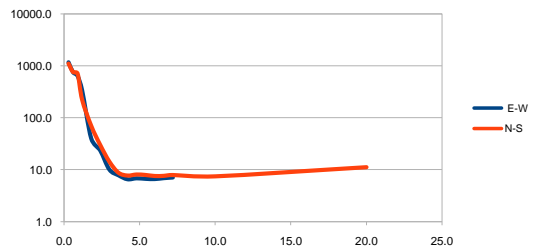
1 N-S			
Spacing	Count	App. Resistivity	Resistance
0.3	36	176.8	93.77
0.6	49	122.5	32.49
0.9	32	54.7	9.67
1.2	31	35.7	4.73
1.8	28	12.0	1.06
2.4	26	7.2	0.48
3.0	24	6.1	0.32
3.6	21	5.8	0.25
4.2	18	5.7	0.22
4.8	15	5.9	0.20
5.4	12	6.2	0.18
6.0	10	6.3	0.17
6.6	8	6.5	0.16
7.2	5	6.6	0.15
10.0		7.7	0.12
20.0		11.3	0.09



Spacing	Site 1 Apparent Resistivity	
	E-W	N-S
0.3	215.4	176.8
0.6	141.0	122.5
0.9	71.4	54.7
1.2	36.1	35.7
1.8	12.1	12.0
2.4	6.7	7.2
3.0	5.8	6.1
3.6	5.6	5.8
4.2	5.6	5.7
4.8	5.8	5.9
5.4	6.1	6.2
6		6.3
6.6		6.5
7.2		6.6
10		7.7
20		11.3

2 E-W			
Spacing	Count	App. Resistivity	Resistance
0.3	34	1172.7	622.05
0.6	48	754.3	200.05
0.9	30	640.6	113.26
1.2	29	338.3	44.86
1.8	25	40.2	3.55
2.4	20	23.4	1.55
3.0	22	10.1	0.53
3.6	20	7.8	0.35
4.2	17	6.5	0.25
4.8	14	6.8	0.23
5.4	11	6.7	0.20
6.0	10	6.6	0.18
6.6	8	6.9	0.17
7.2	4	7.1	0.16
10.0			
20.0			

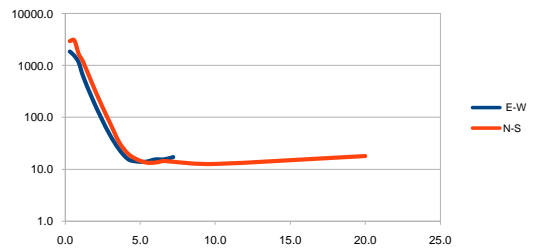
2 N-S			
Spacing	Count	App. Resistivity	Resistance
0.3	28	1095.8	581.27
0.6	44	749.9	198.88
0.9	30	703.9	124.45
1.2	31	221.5	29.38
1.8	28	69.5	6.14
2.4	26	29.6	1.96
3.0	24	14.2	0.76
3.6	21	8.7	0.38
4.2	18	7.7	0.29
4.8	15	8.0	0.27
5.4	12	7.9	0.23
6.0	10	7.5	0.20
6.6	7	7.6	0.18
7.2	4	7.9	0.17
10.0		7.4	0.12
20.0		11.1	0.09



Spacing	Site 2 Apparent Resistivity	
	E-W	N-S
0.3	1172.7	1095.8
0.6	754.3	749.9
0.9	640.6	703.9
1.2	338.3	221.5
1.8	40.2	69.5
2.4	23.4	29.6
3.0	10.1	14.2
3.6	7.8	8.7
4.2	6.5	7.7
4.8	6.8	8.0
5.4	6.7	7.9
6.0	6.6	7.5
6.6	6.9	7.6
7.2	7.1	7.9
10		7.4
20		11.1

3 E-W			
Spacing	Count	App. Resistivity	Resistance
0.3	37	1846.6	979.52
0.6	49	1538.0	407.92
0.9	32	1128.3	199.50
1.2	31	605.1	80.24
1.8	28	230.1	20.34
2.4	26	96.9	6.43
3.0	24	44.7	2.37
3.6	21	24.0	1.06
4.2	18	15.6	0.59
4.8	15	14.1	0.47
5.4	11	14.0	0.41
6.0	10	15.4	0.41
6.6	7	15.5	0.37
7.2	4	17.1	0.38
10.0			
20.0			

3 N-S			
Spacing	Count	App. Resistivity	Resistance
0.3	34	2928.8	1553.55
0.6	46	3037.9	805.72
0.9	32	1647.1	291.24
1.2	30	1153.0	152.91
1.8	28	440.8	38.97
2.4	26	176.8	11.72
3.0	24	75.7	4.01
3.6	21	32.8	1.45
4.2	18	19.7	0.75
4.8	15	15.3	0.51
5.4	12	13.4	0.39
6.0	10	13.4	0.36
6.6	8	14.4	0.35
7.2	4	13.9	0.31
10.0		12.6	0.20
20.0		17.9	0.14

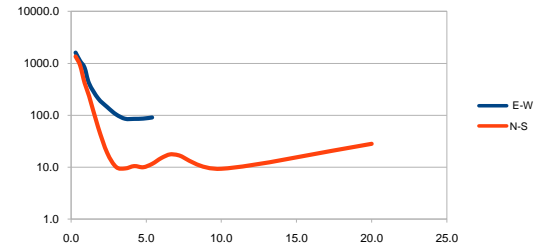


Spacing	Site 3 Apparent Resistivity	
	E-W	N-S
0.3	1846.6	2928.8
0.6	1538.0	3037.9
0.9	1128.3	1647.1
1.2	605.1	1153.0
1.8	230.1	440.8
2.4	96.9	176.8
3.0	44.7	75.7
3.6	24.0	32.8
4.2	15.6	19.7
4.8	14.1	15.3
5.4	14.0	13.4
6.0	15.4	13.4
6.6	15.5	14.4
7.2	17.1	13.9
10		12.6
20		17.9

BH resistivity

4 E-W			
Spacing	Count	App. Resistivity	Resistance
0.3	37	1611.2	854.65
0.6	54	1110.9	294.64
0.9	32	825.1	145.89
1.2	35	410.5	54.44
1.8	30	212.0	18.74
2.4	26	145.0	9.61
3.0	26	104.1	5.52
3.6	23	85.9	3.80
4.2	19	85.5	3.24
4.8	15	86.5	2.87
5.4	11	90.9	2.68
6.0			
6.6			
7.2			
10.0			
20.0			

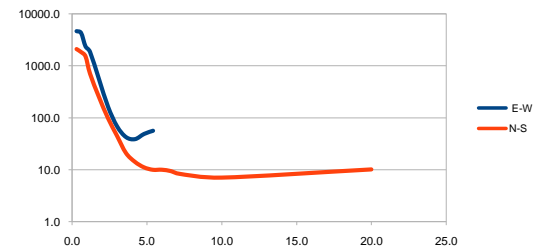
4 N-S			
Spacing	Count	App. Resistivity	Resistance
0.3	36	1362.7	722.82
0.6	49	919.4	243.86
0.9	32	420.7	74.38
1.2	31	234.9	31.15
1.8	28	59.0	5.22
2.4	26	19.1	1.26
3.0	22	10.2	0.54
3.6	19	9.5	0.42
4.2	16	10.6	0.40
4.8	14	10.1	0.33
5.4	9	11.7	0.34
6.0	6	15.1	0.40
6.6	4	17.8	0.43
7.2	2	16.9	0.37
10.0		9.4	0.15
20.0		28.4	0.23



4.0		
Spacing	E-W	N-S
0.3	1611.2	1362.7
0.6	1110.9	919.4
0.9	825.1	420.7
1.2	410.5	234.9
1.8	212.0	59.0
2.4	145.0	19.1
3.0	104.1	10.2
3.6	85.9	9.5
4.2	85.5	10.6
4.8	86.5	10.1
5.4	90.9	11.7
6.0		15.1
6.6		17.8
7.2		16.9
10		9.4
20		28.4

5 E-W			
Spacing	Count	App. Resistivity	Resistance
0.3	37	4647.3	2465.14
0.6	55	4305.5	1141.91
0.9	32	2357.5	416.84
1.2	35	1850.9	245.46
1.8	32	548.9	48.52
2.4	29	163.0	10.81
3.0	26	68.4	3.63
3.6	19	42.4	1.87
4.2	16	38.8	1.47
4.8	11	48.8	1.62
5.4	7	56.2	1.66
6.0			
6.6			
7.2			
10.0			
20.0			

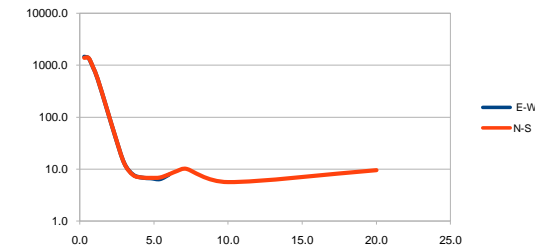
5 N-S			
Spacing	Count	App. Resistivity	Resistance
0.3	38	2100.2	1114.04
0.6	51	1841.4	488.39
0.9	32	1518.2	268.44
1.2	35	707.8	93.87
1.8	32	250.1	22.11
2.4	29	98.7	6.55
3.0	26	45.3	2.40
3.6	23	21.1	0.93
4.2	19	14.3	0.54
4.8	15	11.2	0.37
5.4	12	10.0	0.30
6.0	8	10.1	0.27
6.6	5	9.5	0.23
7.2	1	8.4	0.18
10.0		7.1	0.11
20.0		10.2	0.08



5.0		
Spacing	E-W	N-S
0.3	4647.3	2100.2
0.6	4305.5	1841.4
0.9	2357.5	1518.2
1.2	1850.9	707.8
1.8	548.9	250.1
2.4	163.0	98.7
3.0	68.4	45.3
3.6	42.4	21.1
4.2	38.8	14.3
4.8	48.8	11.2
5.4	56.2	10.0
6.0		10.1
6.6		9.5
7.2		8.4
10		7.1
20		10.2

6 E-W			
Spacing	Count	App. Resistivity	Resistance
0.3	30	1469.1	779.28
0.6	47	1371.0	363.62
0.9	32	908.1	160.57
1.2	31	551.9	73.19
1.8	28	153.1	13.54
2.4	26	41.8	2.77
3.0	22	13.0	0.69
3.6	20	7.8	0.35
4.2	18	6.9	0.26
4.8	14	6.7	0.22
5.4	11	6.4	0.19
6.0	6	7.8	0.21
6.6			
7.2			
10.0			
20.0			

6 N-S			
Spacing	Count	App. Resistivity	Resistance
0.3	33	1384.6	734.45
0.6	47	1371.0	363.62
0.9	32	908.1	160.57
1.2	31	551.9	73.19
1.8	28	153.1	13.54
2.4	26	41.8	2.77
3.0	23	12.8	0.68
3.6	21	7.6	0.34
4.2	18	6.9	0.26
4.8	15	6.8	0.22
5.4	12	6.9	0.20
6.0	9	7.9	0.21
6.6	7	9.3	0.22
7.2	5	10.1	0.22
10.0		5.6	0.09
20.0		9.5	0.08

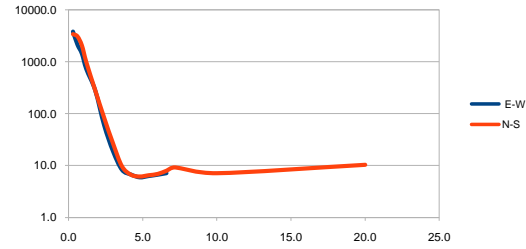


6.0		
Spacing	E-W	N-S
0.3	1469.1	1384.6
0.6	1371.0	1371.0
0.9	908.1	908.1
1.2	551.9	551.9
1.8	153.1	153.1
2.4	41.8	41.8
3.0	13.0	12.8
3.6	7.8	7.6
4.2	6.9	6.9
4.8	6.7	6.8
5.4	6.4	6.9
6.0	7.8	7.9
6.6		9.3
7.2		10.1
10		5.6
20		9.5

BH resistivity

7 E-W			
Spacing	Count	App. Resistivity	Resistance
0.3	34	3763.0	1996.08
0.6	48	2116.4	561.32
0.9	26	1416.4	250.44
1.2	28	713.0	94.55
1.8	28	277.6	24.54
2.4	26	59.6	3.95
3.0	22	18.8	1.00
3.6	20	8.3	0.37
4.2	18	6.7	0.25
4.8	15	5.9	0.20
5.4	12	6.3	0.19
6.0	10	6.7	0.18
6.6	8	7.1	0.17
7.2			
10.0			
20.0			

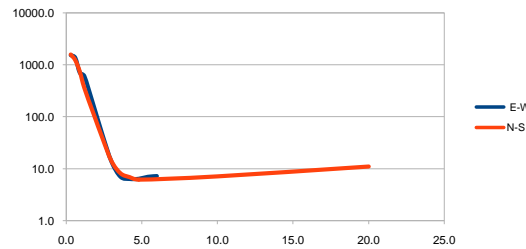
7 N-S			
Spacing	Count	App. Resistivity	Resistance
0.3	31	3375.9	1790.76
0.6	49	3057.0	810.79
0.9	32	2042.3	361.10
1.2	28	969.7	128.60
1.8	27	279.2	24.68
2.4	25	83.0	5.51
3.0	22	26.5	1.41
3.6	20	9.7	0.43
4.2	18	6.7	0.25
4.8	15	6.1	0.20
5.4	11	6.5	0.19
6.0	8	6.9	0.18
6.6	6	7.9	0.19
7.2	1	9.2	0.20
10.0		7.1	0.11
20.0		10.3	0.08



7.0		
Spacing	E-W	N-S
0.3	3763.0	3375.9
0.6	2116.4	3057.0
0.9	1416.4	2042.3
1.2	713.0	969.7
1.8	277.6	279.2
2.4	59.6	83.0
3.0	18.8	26.5
3.6	8.3	9.7
4.2	6.7	6.7
4.8	5.9	6.1
5.4	6.3	6.5
6.0	6.7	6.9
6.6	7.1	7.9
7.2		9.2
10		7.1
20		10.3

8 E-W			
Spacing	Count	App. Resistivity	Resistance
0.3	37	1542.4	818.17
0.6	49	1368.6	362.98
0.9	32	704.2	124.51
1.2	31	606.3	80.40
1.8	27	169.5	14.98
2.4	22	45.1	2.99
3.0	18	13.6	0.72
3.6	15	7.0	0.31
4.2	14	6.4	0.24
4.8	13	6.4	0.21
5.4	6	7.0	0.21
6.0	2	7.2	0.19
6.6			
7.2			
10.0			
20.0			

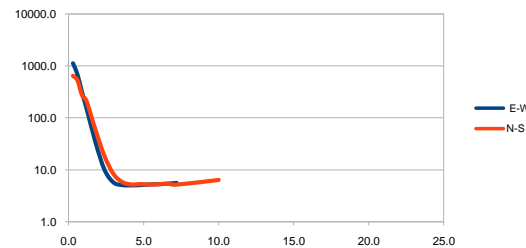
8 N-S			
Spacing	Count	App. Resistivity	Resistance
0.3	38	1586.9	841.76
0.6	51	1232.0	326.76
0.9	31	739.9	130.83
1.2	31	358.4	47.53
1.8	28	115.8	10.24
2.4	26	38.4	2.55
3.0	24	13.8	0.73
3.6	21	8.1	0.36
4.2	18	6.9	0.26
4.8	13	6.1	0.20
5.4			
6.0			
6.6			
7.2			
10.0		7.1	0.11
20.0		11.0	0.09



8.0		
Spacing	E-W	N-S
0.3	1542.4	1586.9
0.6	1368.6	1232.0
0.9	704.2	739.9
1.2	606.3	358.4
1.8	169.5	115.8
2.4	45.1	38.4
3.0	13.6	13.8
3.6	7.0	8.1
4.2	6.4	6.9
4.8	6.4	6.1
5.4	7.0	
6.0	7.2	
6.6		
7.2		
10		7.1
20		11.0

9 E-W			
Spacing	Count	App. Resistivity	Resistance
0.3	38	1121.8	595.05
0.6	51	681.5	180.74
0.9	32	311.0	54.99
1.2	31	152.7	20.24
1.8	28	33.5	2.96
2.4	25	9.9	0.66
3.0	22	5.7	0.30
3.6	20	5.0	0.22
4.2	17	5.0	0.19
4.8	15	5.1	0.17
5.4	12	5.2	0.15
6.0	10	5.3	0.14
6.6	8	5.4	0.13
7.2	5	5.6	0.12
10.0			
20.0			

9 N-S			
Spacing	Count	App. Resistivity	Resistance
0.3	34	643.8	341.48
0.6	47	526.0	139.52
0.9	30	273.3	48.32
1.2	31	210.7	27.95
1.8	28	58.7	5.19
2.4	26	18.4	1.22
3.0	23	8.3	0.44
3.6	20	5.8	0.26
4.2	16	5.2	0.20
4.8	14	5.3	0.18
5.4	12	5.2	0.15
6.0	9	5.3	0.14
6.6	7	5.4	0.13
7.2	5	5.2	0.11
10.0		6.4	0.10
20.0			

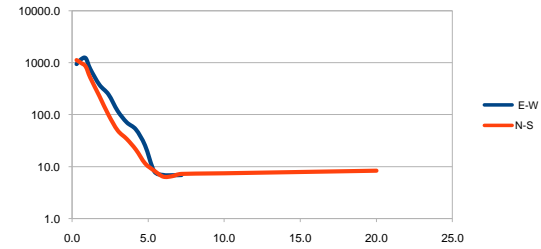


9.0		
Spacing	E-W	N-S
0.3	1121.8	643.8
0.6	681.5	526.0
0.9	311.0	273.3
1.2	152.7	210.7
1.8	33.5	58.7
2.4	9.9	18.4
3.0	5.7	8.3
3.6	5.0	5.8
4.2	5.0	5.2
4.8	5.1	5.3
5.4	5.2	5.2
6.0	5.3	5.3
6.6	5.4	5.4
7.2	5.6	5.2
10		6.4
20		

BH resistivity

10 E-W			
Spacing	Count	App. Resistivity	Resistance
0.3	23	939.8	498.50
0.6	45	1161.2	307.98
0.9	28	1222.6	216.17
1.2	25	760.1	100.79
1.8	24	376.9	33.32
2.4	23	244.8	16.23
3.0	21	118.0	6.26
3.6	17	70.9	3.14
4.2	14	51.8	1.96
4.8	9	25.6	0.85
5.4	10	8.2	0.24
6.0	10	6.9	0.18
6.6	8	6.8	0.16
7.2	5	6.9	0.15
10.0			
20.0			

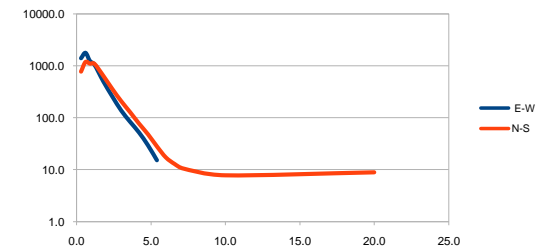
10 N-S			
Spacing	Count	App. Resistivity	Resistance
0.3	37	1123.7	596.06
0.6	51	988.1	262.08
0.9	31	845.0	149.41
1.2	30	515.2	68.33
1.8	26	227.9	20.15
2.4	23	98.5	6.53
3.0	23	49.5	2.63
3.6	21	33.8	1.49
4.2	18	21.1	0.80
4.8	15	11.5	0.38
5.4	12	8.3	0.24
6.0	9	6.4	0.17
6.6	8	6.5	0.16
7.2	1	7.2	0.16
10.0		7.4	0.12
20.0		8.3	0.07



10.0		
Spacing	E-W	N-S
0.3	939.8	1123.7
0.6	1161.2	988.1
0.9	1222.6	845.0
1.2	760.1	515.2
1.8	376.9	227.9
2.4	244.8	98.5
3.0	118.0	49.5
3.6	70.9	33.8
4.2	51.8	21.1
4.8	25.6	11.5
5.4	8.2	8.3
6.0	6.9	6.4
6.6	6.8	6.5
7.2	6.9	7.2
10		7.4
20		8.3

11 E-W			
Spacing	Count	App. Resistivity	Resistance
0.3	35	1395.6	740.30
0.6	53	1775.6	470.92
0.9	32	1230.2	217.52
1.2	35	1050.9	139.36
1.8	32	500.3	44.23
2.4	29	257.3	17.06
3.0	26	137.9	7.31
3.6	23	83.5	3.69
4.2	20	52.0	1.97
4.8	17	29.5	0.98
5.4	11	15.2	0.45
6.0			
6.6			
7.2			
10.0			
20.0			

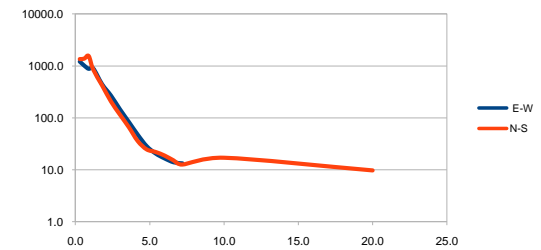
11 N-S			
Spacing	Count	App. Resistivity	Resistance
0.3	31	771.3	409.12
0.6	49	1181.7	313.41
0.9	32	1095.7	193.74
1.2	35	1090.7	144.64
1.8	32	638.9	56.49
2.4	29	357.5	23.71
3.0	26	208.0	11.03
3.6	23	127.7	5.64
4.2	20	76.9	2.91
4.8	16	47.9	1.59
5.4	13	28.1	0.83
6.0	11	17.2	0.46
6.6	8	12.8	0.31
7.2	5	10.5	0.23
10.0		7.8	0.12
20.0		8.9	0.07



11.0		
Spacing	E-W	N-S
0.3	1395.6	771.3
0.6	1775.6	1181.7
0.9	1230.2	1095.7
1.2	1050.9	1090.7
1.8	500.3	638.9
2.4	257.3	357.5
3.0	137.9	208.0
3.6	83.5	127.7
4.2	52.0	76.9
4.8	29.5	47.9
5.4	15.2	28.1
6.0		17.2
6.6		12.8
7.2		10.5
10		7.8
20		8.9

12 E-W			
Spacing	Count	App. Resistivity	Resistance
0.3	32	1214.7	644.31
0.6	46	1016.3	269.56
0.9	29	879.5	155.51
1.2	34	903.2	119.78
1.8	30	445.7	39.40
2.4	28	267.9	17.76
3.0	25	146.4	7.77
3.6	22	83.4	3.69
4.2	19	47.2	1.79
4.8	16	28.5	0.94
5.4	14	20.6	0.61
6.0	11	16.6	0.44
6.6	7	14.0	0.34
7.2	1	13.3	0.29
10.0			
20.0			

12 N-S			
Spacing	Count	App. Resistivity	Resistance
0.3	34	1345.1	713.53
0.6	46	1370.5	363.49
0.9	31	1542.4	272.72
1.2	31	851.6	112.94
1.8	28	420.1	37.14
2.4	26	205.9	13.65
3.0	24	115.1	6.11
3.6	21	66.0	2.92
4.2	18	35.6	1.35
4.8	15	24.6	0.82
5.4	12	22.0	0.65
6.0	7	18.8	0.50
6.6	8	15.2	0.37
7.2	5	12.6	0.28
10.0		17.0	0.27
20.0		9.7	0.08

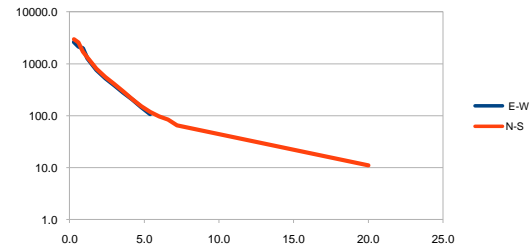


12.0		
Spacing	E-W	N-S
0.3	1214.7	1345.1
0.6	1016.3	1370.5
0.9	879.5	1542.4
1.2	903.2	851.6
1.8	445.7	420.1
2.4	267.9	205.9
3.0	146.4	115.1
3.6	83.4	66.0
4.2	47.2	35.6
4.8	28.5	24.6
5.4	20.6	22.0
6.0	16.6	18.8
6.6	14.0	15.2
7.2	13.3	12.6
10		17.0
20		9.7

BH resistivity

13 E-W			
Spacing	Count	App. Resistivity	Resistance
0.3	25	2608.3	1383.58
0.6	46	2138.2	567.11
0.9	32	1993.2	352.43
1.2	35	1271.9	168.67
1.8	32	759.4	67.14
2.4	29	526.2	34.89
3.0	26	383.3	20.33
3.6	23	277.8	12.28
4.2	20	204.7	7.75
4.8	17	145.4	4.82
5.4	12	106.4	3.13
6.0			
6.6			
7.2			
10.0			
20.0			

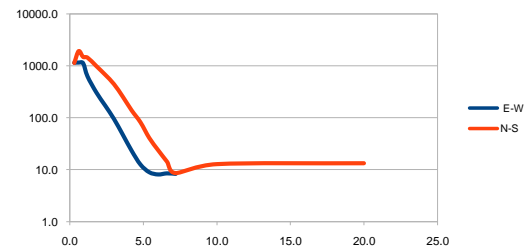
13 N-S			
Spacing	Count	App. Resistivity	Resistance
0.3	34	2970.8	1575.88
0.6	53	2572.6	682.33
0.9	32	1705.1	301.49
1.2	35	1319.7	175.01
1.8	32	803.7	71.05
2.4	29	553.3	36.68
3.0	26	405.5	21.51
3.6	23	293.9	12.99
4.2	20	208.4	7.90
4.8	17	153.6	5.09
5.4	14	117.6	3.47
6.0	11	96.9	2.57
6.6	8	83.6	2.02
7.2	4	65.4	1.45
10.0			
20.0		11.0	0.09



13.0		
Spacing	E-W	N-S
0.3	2608.3	2970.8
0.6	2138.2	2572.6
0.9	1993.2	1705.1
1.2	1271.9	1319.7
1.8	759.4	803.7
2.4	526.2	553.3
3.0	383.3	405.5
3.6	277.8	293.9
4.2	204.7	208.4
4.8	145.4	153.6
5.4	106.4	117.6
6		96.9
6.6		83.6
7.2		65.4
10		
20		11.0

14 E-W			
Spacing	Count	App. Resistivity	Resistance
0.3	36	1140.8	605.14
0.6	48	1148.6	304.65
0.9	30	1117.4	197.58
1.2	30	623.2	82.64
1.8	27	305.9	27.04
2.4	25	171.5	11.37
3.0	23	94.5	5.01
3.6	20	47.1	2.08
4.2	16	23.2	0.88
4.8	15	12.6	0.42
5.4	12	8.9	0.26
6.0	9	8.1	0.21
6.6	6	8.5	0.20
7.2	3	8.3	0.18
10.0			
20.0			

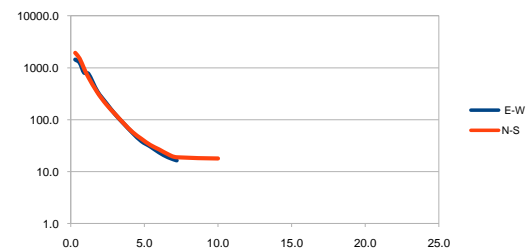
14 N-S			
Spacing	Count	App. Resistivity	Resistance
0.3	38	1126.5	597.54
0.6	50	1904.2	505.03
0.9	32	1472.7	260.40
1.2	31	1425.5	189.03
1.8	28	982.1	86.83
2.4	26	670.7	44.47
3.0	24	441.6	23.42
3.6	20	252.9	11.18
4.2	16	138.4	5.24
4.8	14	81.7	2.71
5.4	12	40.8	1.20
6.0	10	23.8	0.63
6.6	6	14.4	0.35
7.2	2	8.6	0.19
10.0		12.8	0.20
20.0		13.3	0.11



14.0		
Spacing	E-W	N-S
0.3	1140.8	1126.5
0.6	1148.6	1904.2
0.9	1117.4	1472.7
1.2	623.2	1425.5
1.8	305.9	982.1
2.4	171.5	670.7
3.0	94.5	441.6
3.6	47.1	252.9
4.2	23.2	138.4
4.8	12.6	81.7
5.4	8.9	40.8
6.0	8.1	23.8
6.6	8.5	14.4
7.2	8.3	8.6
10		12.8
20		13.3

15 E-W			
Spacing	Count	App. Resistivity	Resistance
0.3	38	1444.3	766.11
0.6	48	1257.5	333.52
0.9	31	808.7	142.99
1.2	31	763.6	101.26
1.8	28	353.7	31.27
2.4	26	210.6	13.96
3.0	24	128.6	6.82
3.6	21	84.1	3.72
4.2	18	55.8	2.11
4.8	15	38.6	1.28
5.4	12	30.6	0.90
6.0	10	23.5	0.62
6.6	8	19.0	0.46
7.2	5	16.5	0.36
10.0			
20.0			

15 N-S			
Spacing	Count	App. Resistivity	Resistance
0.3	29	1948.6	1033.62
0.6	46	1509.1	400.24
0.9	28	971.8	171.83
1.2	31	654.2	86.76
1.8	28	337.9	29.87
2.4	26	199.4	13.22
3.0	24	129.4	6.86
3.6	21	84.8	3.75
4.2	18	57.5	2.18
4.8	12	42.8	1.42
5.4	9	32.6	0.96
6.0	8	26.7	0.71
6.6	8	21.7	0.52
7.2	4	18.9	0.42
10.0		17.9	0.28
20.0			

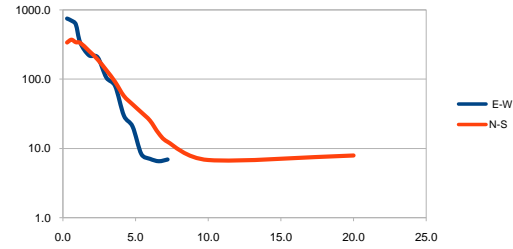


15.0		
Spacing	E-W	N-S
0.3	1444.3	1948.6
0.6	1257.5	1509.1
0.9	808.7	971.8
1.2	763.6	654.2
1.8	353.7	337.9
2.4	210.6	199.4
3.0	128.6	129.4
3.6	84.1	84.8
4.2	55.8	57.5
4.8	38.6	42.8
5.4	30.6	32.6
6.0	23.5	26.7
6.6	19.0	21.7
7.2	16.5	18.9
10		17.9
20		

BH resistivity

16 E-W			
Spacing	Count	App. Resistivity	Resistance
0.3	35	753.9	399.88
0.6	44	702.9	186.43
0.9	23	621.2	109.83
1.2	25	340.0	45.09
1.8	25	222.7	19.69
2.4	24	207.5	13.76
3.0	22	105.7	5.61
3.6	16	80.0	3.54
4.2	17	29.9	1.13
4.8	15	20.7	0.69
5.4	12	8.3	0.25
6.0	8	7.1	0.19
6.6	6	6.6	0.16
7.2	4	7.0	0.15
10.0			
20.0			

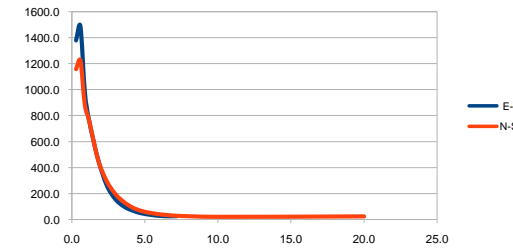
16 N-S			
Spacing	Count	App. Resistivity	Resistance
0.3	38	339.7	180.18
0.6	51	372.7	98.84
0.9	32	342.6	60.57
1.2	31	336.1	44.57
1.8	28	257.8	22.79
2.4	26	193.2	12.81
3.0	24	135.2	7.17
3.6	20	91.8	4.06
4.2	17	57.5	2.18
4.8	15	43.4	1.44
5.4	12	33.3	0.98
6.0	10	25.3	0.67
6.6	8	16.5	0.40
7.2	5	12.5	0.28
10.0		6.8	0.11
20.0		7.9	0.06



16.0		
Spacing	E-W	N-S
0.3	753.9	339.7
0.6	702.9	372.7
0.9	621.2	342.6
1.2	340.0	336.1
1.8	222.7	257.8
2.4	207.5	193.2
3.0	105.7	135.2
3.6	80.0	91.8
4.2	29.9	57.5
4.8	20.7	43.4
5.4	8.3	33.3
6.0	7.1	25.3
6.6	6.6	16.5
7.2	7.0	12.5
10		6.8
20		7.9

17 E-W			
Spacing	Count	App. Resistivity	Resistance
0.3	35	1379.7	731.85
0.6	54	1488.2	394.70
0.9	32	984.9	174.14
1.2	34	760.2	100.82
1.8	32	466.6	41.25
2.4	28	263.9	17.50
3.0	25	155.1	8.23
3.6	23	98.3	4.34
4.2	20	67.0	2.54
4.8	17	47.2	1.57
5.4	13	35.8	1.05
6.0	11	27.9	0.74
6.6	8	24.9	0.60
7.2	5	25.8	0.57
10.0			
20.0			

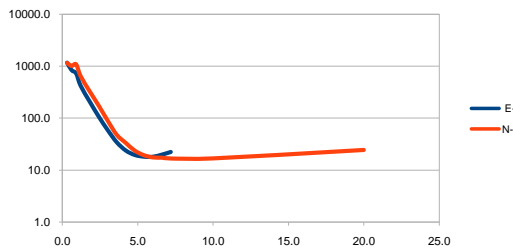
17 N-S			
Spacing	Count	App. Resistivity	Resistance
0.3	33	1158.7	614.65
0.6	55	1224.7	324.82
0.9	32	885.2	156.51
1.2	35	758.7	100.61
1.8	32	462.7	40.91
2.4	29	295.3	19.58
3.0	26	194.7	10.33
3.6	23	132.1	5.84
4.2	20	90.0	3.41
4.8	17	64.6	2.14
5.4	14	50.3	1.48
6.0	11	40.0	1.06
6.6	8	33.6	0.81
7.2	4	28.3	0.63
10.0		20.2	0.32
20.0		23.8	0.19



17.0		
Spacing	E-W	N-S
0.3	1379.7	1158.7
0.6	1488.2	1224.7
0.9	984.9	885.2
1.2	760.2	758.7
1.8	466.6	462.7
2.4	263.9	295.3
3.0	155.1	194.7
3.6	98.3	132.1
4.2	67.0	90.0
4.8	47.2	64.6
5.4	35.8	50.3
6.0	27.9	40.0
6.6	24.9	33.6
7.2	25.8	28.3
10		20.2
20		23.8

18 E-W			
Spacing	Count	App. Resistivity	Resistance
0.3	34	1177.2	624.42
0.6	53	845.6	224.27
0.9	32	732.8	129.57
1.2	35	424.1	56.25
1.8	32	211.0	18.65
2.4	29	108.7	7.21
3.0	26	59.4	3.15
3.6	23	34.7	1.53
4.2	20	24.0	0.91
4.8	17	19.7	0.65
5.4	14	18.3	0.54
6.0	11	18.2	0.48
6.6	8	19.9	0.48
7.2	5	22.5	0.50
10.0			
20.0			

18 N-S			
Spacing	Count	App. Resistivity	Resistance
0.3	28	1155.3	612.81
0.6	48	1011.4	268.24
0.9	32	1083.9	191.65
1.2	31	642.7	85.22
1.8	28	328.0	29.00
2.4	26	173.3	11.49
3.0	23	88.6	4.70
3.6	19	47.5	2.10
4.2	18	33.1	1.26
4.8	15	23.5	0.78
5.4	12	19.2	0.57
6.0	10	17.4	0.46
6.6	8	17.2	0.42
7.2	4	16.6	0.37
10.0		16.7	0.27
20.0		24.3	0.19

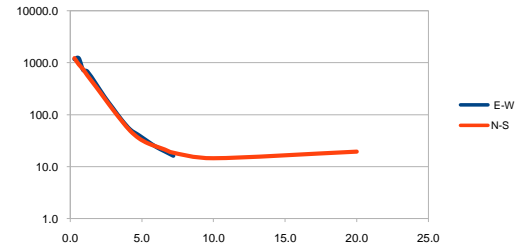


18.0		
Spacing	E-W	N-S
0.3	1177.2	1155.3
0.6	845.6	1011.4
0.9	732.8	1083.9
1.2	424.1	642.7
1.8	211.0	328.0
2.4	108.7	173.3
3.0	59.4	88.6
3.6	34.7	47.5
4.2	24.0	33.1
4.8	19.7	23.5
5.4	18.3	19.2
6.0	18.2	17.4
6.6	19.9	17.2
7.2	22.5	16.6
10		16.7
20		24.3

BH resistivity

19 E-W			
Spacing	Count	App. Resistivity	Resistance
0.3	38	1173.8	622.63
0.6	51	1225.9	325.13
0.9	32	732.7	129.54
1.2	31	680.4	90.22
1.8	28	394.8	34.91
2.4	26	221.9	14.72
3.0	24	132.5	7.03
3.6	20	79.5	3.52
4.2	18	51.7	1.96
4.8	14	40.3	1.34
5.4	12	30.9	0.91
6.0	10	24.1	0.64
6.6	8	19.8	0.48
7.2	5	16.3	0.36
10.0			
20.0			

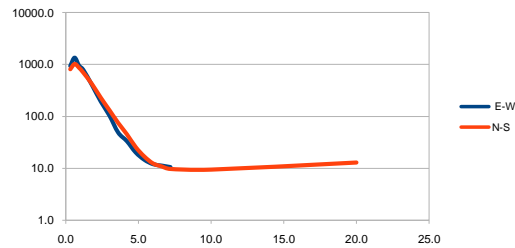
19 N-S			
Spacing	Count	App. Resistivity	Resistance
0.3	34	1226.0	650.32
0.6	49	929.8	246.61
0.9	32	748.4	132.32
1.2	31	570.5	75.66
1.8	28	346.2	30.61
2.4	26	206.3	13.68
3.0	24	123.4	6.54
3.6	21	75.9	3.36
4.2	18	48.5	1.84
4.8	15	35.0	1.16
5.4	12	28.3	0.83
6.0	10	24.5	0.65
6.6	8	21.3	0.51
7.2	5	18.5	0.41
10.0		14.5	0.23
20.0		19.4	0.15



19.0		
Spacing	E-W	N-S
0.3	1173.8	1226.0
0.6	1225.9	929.8
0.9	732.7	748.4
1.2	680.4	570.5
1.8	394.8	346.2
2.4	221.9	206.3
3.0	132.5	123.4
3.6	79.5	75.9
4.2	51.7	48.5
4.8	40.3	35.0
5.4	30.9	28.3
6.0	24.1	24.5
6.6	19.8	21.3
7.2	16.3	18.5
10		14.5
20		19.4

20 E-W			
Spacing	Count	App. Resistivity	Resistance
0.3	33	935.5	496.22
0.6	54	1350.3	358.13
0.9	32	950.8	168.11
1.2	35	784.8	104.07
1.8	32	397.7	35.16
2.4	29	193.6	12.84
3.0	26	103.3	5.48
3.6	21	48.7	2.15
4.2	20	33.2	1.26
4.8	17	20.2	0.67
5.4	14	14.6	0.43
6.0	11	12.0	0.32
6.6	7	11.2	0.27
7.2	4	10.5	0.23
10.0			
20.0			

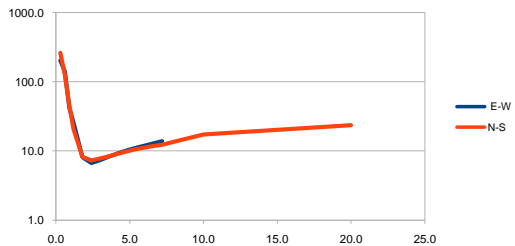
20 N-S			
Spacing	Count	App. Resistivity	Resistance
0.3	33	813.9	431.73
0.6	51	1028.2	272.70
0.9	32	870.6	153.93
1.2	31	699.6	92.78
1.8	28	418.7	37.02
2.4	26	230.1	15.25
3.0	24	132.1	7.01
3.6	21	75.2	3.32
4.2	18	45.4	1.72
4.8	15	25.9	0.86
5.4	12	17.0	0.50
6.0	10	12.5	0.33
6.6	8	10.9	0.26
7.2	5	9.8	0.22
10.0		9.5	0.15
20.0		13.0	0.10



20.0		
Spacing	E-W	N-S
0.3	935.5	813.9
0.6	1350.3	1028.2
0.9	950.8	870.6
1.2	784.8	699.6
1.8	397.7	418.7
2.4	193.6	230.1
3.0	103.3	132.1
3.6	48.7	75.2
4.2	33.2	45.4
4.8	20.2	25.9
5.4	14.6	17.0
6.0	12.0	12.5
6.6	11.2	10.9
7.2	10.5	9.8
10		9.5
20		13.0

21 E-W			
Spacing	Count	App. Resistivity	Resistance
0.3	35	202.6	107.49
0.6	53	140.7	37.33
0.9	32	42.3	7.49
1.2	35	25.7	3.41
1.8	32	8.1	0.72
2.4	29	6.7	0.45
3.0	26	7.4	0.39
3.6	23	8.3	0.37
4.2	20	9.2	0.35
4.8	17	10.2	0.34
5.4	14	11.1	0.33
6.0	11	12.0	0.32
6.6	8	12.8	0.31
7.2	5	13.7	0.30
10.0			
20.0			

21 N-S			
Spacing	Count	App. Resistivity	Resistance
0.3	37	262.0	138.97
0.6	55	124.7	33.08
0.9	29	45.4	8.03
1.2	35	20.6	2.74
1.8	32	8.2	0.72
2.4	29	7.3	0.48
3.0	26	7.8	0.41
3.6	23	8.4	0.37
4.2	20	9.1	0.34
4.8	17	9.9	0.33
5.4	14	10.6	0.31
6.0	11	11.1	0.29
6.6	8	11.7	0.28
7.2	5	12.2	0.27
10.0		17.3	0.28
20.0		23.6	0.19



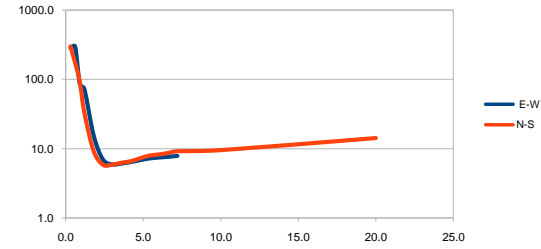
21.0		
Spacing	E-W	N-S
0.3	202.6	262.0
0.6	140.7	124.7
0.9	42.3	45.4
1.2	25.7	20.6
1.8	8.1	8.2
2.4	6.7	7.3
3.0	7.4	7.8
3.6	8.3	8.4
4.2	9.2	9.1
4.8	10.2	9.9
5.4	11.1	10.6
6.0	12.0	11.1
6.6	12.8	11.7
7.2	13.7	12.2
10		17.3
20		23.6

BH resistivity

22 E-W			
Spacing	Count	App. Resistivity	Resistance
0.3	37	281.8	149.50
0.6	53	298.6	79.20
0.9	32	85.9	15.18
1.2	34	72.2	9.57
1.8	31	15.4	1.36
2.4	29	7.0	0.46
3.0	26	5.9	0.31
3.6	23	6.1	0.27
4.2	20	6.4	0.24
4.8	17	6.8	0.23
5.4	14	7.2	0.21
6.0	11	7.5	0.20
6.6	8	7.6	0.18
7.2	5	7.9	0.17
10.0			
20.0			

22 N-S			
Spacing	Count	App. Resistivity	Resistance
0.3	37	301.4	159.87
0.6	51	173.8	46.08
0.9	31	92.5	16.36
1.2	31	32.7	4.34
1.8	28	9.1	0.81
2.4	26	5.8	0.39
3.0	24	5.9	0.31
3.6	20	6.2	0.28
4.2	18	6.6	0.25
4.8	15	7.3	0.24
5.4	12	7.9	0.23
6.0	10	8.2	0.22
6.6	8	8.6	0.21
7.2	5	9.2	0.20
10.0		9.5	0.15
20.0		14.2	0.11

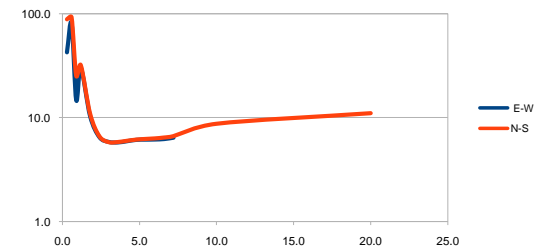
22.0		
Spacing	E-W	N-S
0.3	281.8	301.4
0.6	298.6	173.8
0.9	85.9	92.5
1.2	72.2	32.7
1.8	15.4	9.1
2.4	7.0	5.8
3.0	5.9	5.9
3.6	6.1	6.2
4.2	6.4	6.6
4.8	6.8	7.3
5.4	7.2	7.9
6.0	7.5	8.2
6.6	7.6	8.6
7.2	7.9	9.2
10		9.5
20		14.2



23 E-W			
Spacing	Count	App. Resistivity	Resistance
0.3	37	42.5	22.56
0.6	53	80.8	21.44
0.9	32	14.8	2.61
1.2	34	29.8	3.95
1.8	32	10.3	0.91
2.4	29	6.5	0.43
3.0	26	5.8	0.31
3.6	23	5.8	0.26
4.2	20	5.9	0.23
4.8	17	6.1	0.20
5.4	14	6.2	0.18
6.0	11	6.2	0.16
6.6	8	6.2	0.15
7.2	5	6.4	0.14
10.0			
20.0			

23 N-S			
Spacing	Count	App. Resistivity	Resistance
0.3	38	88.3	46.84
0.6	55	92.5	24.53
0.9	32	25.3	4.47
1.2	35	31.9	4.23
1.8	32	10.9	0.96
2.4	29	6.6	0.44
3.0	26	5.8	0.31
3.6	23	5.8	0.26
4.2	20	6.0	0.23
4.8	17	6.1	0.20
5.4	14	6.2	0.18
6.0	11	6.3	0.17
6.6	8	6.4	0.15
7.2	5	6.6	0.15
10.0		8.7	0.14
20.0		11.0	0.09

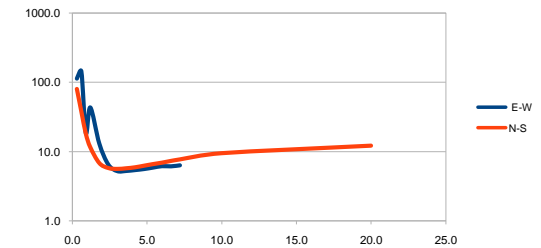
23.0		
Spacing	E-W	N-S
0.3	42.5	88.3
0.6	80.8	92.5
0.9	14.8	25.3
1.2	29.8	31.9
1.8	10.3	10.9
2.4	6.5	6.6
3.0	5.8	5.8
3.6	5.8	5.8
4.2	5.9	6.0
4.8	6.1	6.1
5.4	6.2	6.2
6.0	6.2	6.3
6.6	6.2	6.4
7.2	6.4	6.6
10		8.7
20		11.0



24 E-W			
Spacing	Count	App. Resistivity	Resistance
0.3	36	113.0	59.96
0.6	53	143.8	38.15
0.9	31	18.4	3.26
1.2	34	43.3	5.74
1.8	32	13.0	1.15
2.4	29	6.5	0.43
3.0	26	5.2	0.28
3.6	23	5.2	0.23
4.2	20	5.4	0.20
4.8	17	5.6	0.18
5.4	14	5.8	0.17
6.0	11	6.1	0.16
6.6	8	6.1	0.15
7.2	4	6.3	0.14
10.0			
20.0			

24 N-S			
Spacing	Count	App. Resistivity	Resistance
0.3	37	80.1	42.51
0.6	53	37.9	10.04
0.9	31	18.1	3.21
1.2	35	11.5	1.53
1.8	32	6.8	0.61
2.4	29	5.8	0.39
3.0	26	5.6	0.30
3.6	23	5.8	0.25
4.2	20	5.9	0.23
4.8	17	6.3	0.21
5.4	14	6.6	0.19
6.0	11	6.9	0.18
6.6	8	7.3	0.18
7.2	5	7.7	0.17
10.0		9.5	0.15
20.0		12.2	0.10

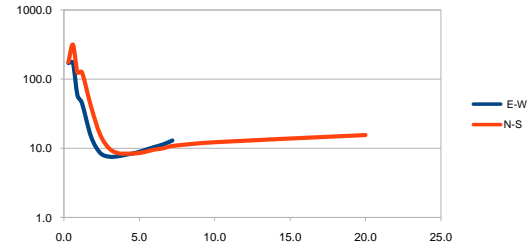
24.0		
Spacing	E-W	N-S
0.3	113.0	80.1
0.6	143.8	37.9
0.9	18.4	18.1
1.2	43.3	11.5
1.8	13.0	6.8
2.4	6.5	5.8
3.0	5.2	5.6
3.6	5.2	5.8
4.2	5.4	5.9
4.8	5.6	6.3
5.4	5.8	6.6
6.0	6.1	6.9
6.6	6.1	7.3
7.2	6.3	7.7
10		9.5
20		12.2



BH resistivity

25 E-W			
Spacing	Count	App. Resistivity	Resistance
0.3	35	170.6	90.49
0.6	55	172.3	45.71
0.9	32	58.5	10.34
1.2	35	45.2	5.99
1.8	32	14.9	1.31
2.4	29	8.7	0.58
3.0	26	7.6	0.40
3.6	23	7.7	0.34
4.2	20	8.2	0.31
4.8	17	8.7	0.29
5.4	14	9.5	0.28
6.0	11	10.5	0.28
6.6	8	11.5	0.28
7.2	5	13.0	0.29
10.0			
20.0			

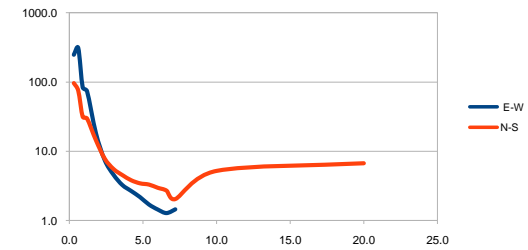
25 N-S			
Spacing	Count	App. Resistivity	Resistance
0.3	33	175.4	93.04
0.6	55	312.9	82.99
0.9	32	124.2	21.97
1.2	35	125.4	16.64
1.8	32	40.3	3.56
2.4	29	15.9	1.06
3.0	26	10.0	0.53
3.6	23	8.6	0.38
4.2	20	8.4	0.32
4.8	17	8.5	0.28
5.4	14	8.9	0.26
6.0	11	9.6	0.26
6.6	8	10.0	0.24
7.2	5	10.9	0.24
10.0		12.3	0.20
20.0		15.6	0.12



25.0		
Spacing	E-W	N-S
0.3	170.6	175.4
0.6	172.3	312.9
0.9	58.5	124.2
1.2	45.2	125.4
1.8	14.9	40.3
2.4	8.7	15.9
3.0	7.6	10.0
3.6	7.7	8.6
4.2	8.2	8.4
4.8	8.7	8.5
5.4	9.5	8.9
6.0	10.5	9.6
6.6	11.5	10.0
7.2	13.0	10.9
10		12.3
20		15.6

26 E-W			
Spacing	Count	App. Resistivity	Resistance
0.3	36	248.5	131.84
0.6	55	311.5	82.62
0.9	32	84.5	14.93
1.2	31	73.7	9.77
1.8	32	18.4	1.63
2.4	29	7.5	0.50
3.0	26	4.6	0.24
3.6	23	3.3	0.14
4.2	20	2.7	0.10
4.8	17	2.2	0.07
5.4	14	1.7	0.05
6.0	10	1.4	0.04
6.6	8	1.3	0.03
7.2	4	1.5	0.03
10.0			
20.0			

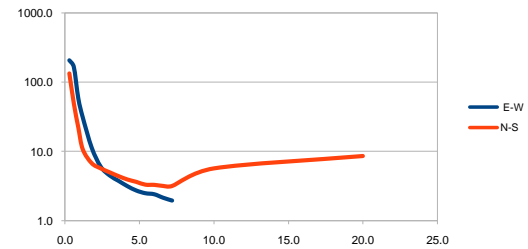
26 N-S			
Spacing	Count	App. Resistivity	Resistance
0.3	38	96.3	51.09
0.6	55	74.8	19.83
0.9	32	31.6	5.58
1.2	35	29.6	3.93
1.8	32	14.4	1.27
2.4	29	7.8	0.52
3.0	26	5.5	0.29
3.6	23	4.5	0.20
4.2	20	3.8	0.14
4.8	17	3.4	0.11
5.4	14	3.3	0.10
6.0	11	3.0	0.08
6.6	8	2.7	0.06
7.2	4	2.0	0.05
10.0		5.2	0.08
20.0		6.7	0.05



26.0		
Spacing	E-W	N-S
0.3	248.5	96.3
0.6	311.5	74.8
0.9	84.5	31.6
1.2	73.7	29.6
1.8	18.4	14.4
2.4	7.5	7.8
3.0	4.6	5.5
3.6	3.3	4.5
4.2	2.7	3.8
4.8	2.2	3.4
5.4	1.7	3.3
6.0	1.4	3.0
6.6	1.3	2.7
7.2	1.5	2.0
10		5.2
20		6.7

27 E-W			
Spacing	Count	App. Resistivity	Resistance
0.3	38	206.5	109.52
0.6	51	166.1	44.06
0.9	32	58.4	10.33
1.2	30	31.0	4.12
1.8	28	11.3	1.00
2.4	26	6.0	0.40
3.0	24	4.5	0.24
3.6	21	3.8	0.17
4.2	18	3.1	0.12
4.8	15	2.7	0.09
5.4	12	2.5	0.07
6.0	10	2.4	0.06
6.6	8	2.1	0.05
7.2	5	1.9	0.04
10.0			
20.0			

27 N-S			
Spacing	Count	App. Resistivity	Resistance
0.3	37	133.3	70.71
0.6	51	49.3	13.07
0.9	32	22.3	3.94
1.2	31	10.7	1.42
1.8	28	6.8	0.60
2.4	26	5.7	0.38
3.0	24	5.0	0.27
3.6	21	4.4	0.19
4.2	18	3.9	0.15
4.8	15	3.6	0.12
5.4	12	3.3	0.10
6.0	10	3.3	0.09
6.6	8	3.2	0.08
7.2	5	3.2	0.07
10.0		5.7	0.09
20.0		8.6	0.07

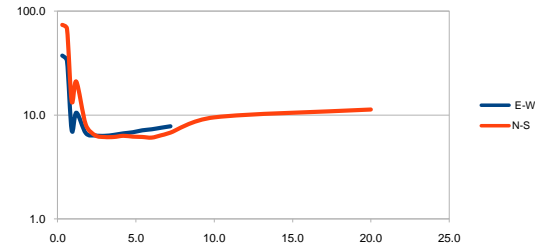


27.0		
Spacing	E-W	N-S
0.3	206.5	133.3
0.6	166.1	49.3
0.9	58.4	22.3
1.2	31.0	10.7
1.8	11.3	6.8
2.4	6.0	5.7
3.0	4.5	5.0
3.6	3.8	4.4
4.2	3.1	3.9
4.8	2.7	3.6
5.4	2.5	3.3
6.0	2.4	3.3
6.6	2.1	3.2
7.2	1.9	3.2
10		5.7
20		8.6

BH resistivity

28 E-W			
Spacing	Count	App. Resistivity	Resistance
0.3	36	37.4	19.85
0.6	52	33.3	8.84
0.9	32	7.1	1.26
1.2	35	10.5	1.40
1.8	32	6.7	0.59
2.4	29	6.3	0.42
3.0	26	6.3	0.33
3.6	23	6.4	0.28
4.2	20	6.7	0.25
4.8	17	6.8	0.23
5.4	14	7.1	0.21
6.0	11	7.3	0.19
6.6	8	7.5	0.18
7.2	5	7.8	0.17
10.0			
20.0			

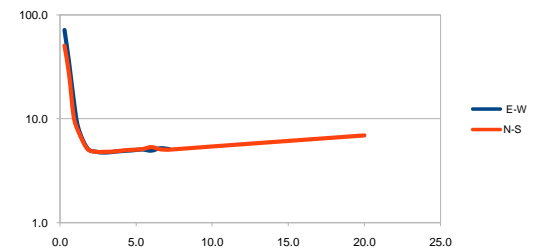
28 N-S			
Spacing	Count	App. Resistivity	Resistance
0.3	35	73.7	39.09
0.6	55	67.9	18.00
0.9	32	13.6	2.40
1.2	35	20.9	2.78
1.8	32	8.1	0.72
2.4	29	6.4	0.42
3.0	26	6.1	0.33
3.6	23	6.2	0.27
4.2	18	6.3	0.24
4.8	15	6.2	0.21
5.4	12	6.2	0.18
6.0	11	6.1	0.16
6.6	8	6.4	0.15
7.2	5	6.8	0.15
10.0		9.5	0.15
20.0		11.3	0.09



28 E-W		
Spacing	E-W	N-S
0.3	37.4	73.7
0.6	33.3	67.9
0.9	7.1	13.6
1.2	10.5	20.9
1.8	6.7	8.1
2.4	6.3	6.4
3.0	6.3	6.1
3.6	6.4	6.2
4.2	6.7	6.3
4.8	6.8	6.2
5.4	7.1	6.2
6.0	7.3	6.1
6.6	7.5	6.4
7.2	7.8	6.8
10		9.5
20		11.3

29 E-W			
Spacing	Count	App. Resistivity	Resistance
0.3	37	71.4	37.89
0.6	52	34.8	9.23
0.9	32	15.4	2.71
1.2	35	8.2	1.09
1.8	32	5.2	0.46
2.4	29	4.8	0.32
3.0	26	4.7	0.25
3.6	23	4.8	0.21
4.2	20	4.9	0.18
4.8	17	5.0	0.16
5.4	14	5.0	0.15
6.0	11	4.9	0.13
6.6	8	5.2	0.13
7.2	5	5.1	0.11
10.0			
20.0			

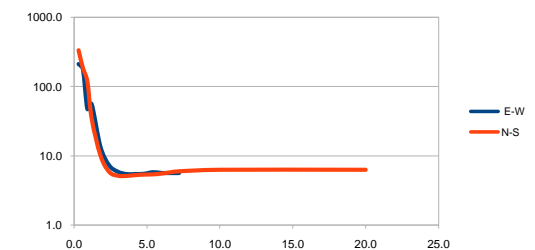
29 N-S			
Spacing	Count	App. Resistivity	Resistance
0.3	35	50.7	26.87
0.6	55	26.9	7.13
0.9	32	10.6	1.87
1.2	35	7.6	1.00
1.8	32	5.1	0.45
2.4	29	4.8	0.32
3.0	26	4.8	0.25
3.6	23	4.8	0.21
4.2	20	5.0	0.19
4.8	17	5.0	0.17
5.4	14	5.1	0.15
6.0	11	5.3	0.14
6.6	8	5.1	0.12
7.2	5	5.0	0.11
10.0		5.4	0.09
20.0		6.9	0.05



29.0		
Spacing	E-W	N-S
0.3	71.4	50.7
0.6	34.8	26.9
0.9	15.4	10.6
1.2	8.2	7.6
1.8	5.2	5.1
2.4	4.8	4.8
3.0	4.7	4.8
3.6	4.8	4.8
4.2	4.9	5.0
4.8	5.0	5.0
5.4	5.0	5.1
6.0	4.9	5.3
6.6	5.2	5.1
7.2	5.1	5.0
10		5.4
20		6.9

30 E-W			
Spacing	Count	App. Resistivity	Resistance
0.3	38	211.7	112.28
0.6	48	177.1	46.97
0.9	32	47.7	8.43
1.2	31	55.8	7.40
1.8	28	13.5	1.20
2.4	26	7.3	0.48
3.0	24	5.9	0.31
3.6	21	5.5	0.24
4.2	18	5.5	0.21
4.8	15	5.5	0.18
5.4	12	5.8	0.17
6.0	10	5.7	0.15
6.6	8	5.6	0.14
7.2	5	5.6	0.12
10.0			
20.0			

30 N-S			
Spacing	Count	App. Resistivity	Resistance
0.3	38	334.8	177.61
0.6	55	184.0	48.79
0.9	32	119.6	21.15
1.2	34	34.3	4.55
1.8	32	10.1	0.90
2.4	29	5.9	0.39
3.0	26	5.2	0.27
3.6	23	5.1	0.23
4.2	20	5.3	0.20
4.8	17	5.4	0.18
5.4	14	5.4	0.16
6.0	11	5.6	0.15
6.6	8	5.8	0.14
7.2	5	6.0	0.13
10.0		6.3	0.10
20.0		6.3	0.05

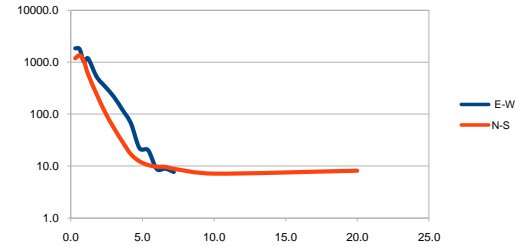


30.0		
Spacing	E-W	N-S
0.3	211.7	334.8
0.6	177.1	184.0
0.9	47.7	119.6
1.2	55.8	34.3
1.8	13.5	10.1
2.4	7.3	5.9
3.0	5.9	5.2
3.6	5.5	5.1
4.2	5.5	5.3
4.8	5.5	5.4
5.4	5.8	5.4
6.0	5.7	5.6
6.6	5.6	5.8
7.2	5.6	6.0
10		6.3
20		6.3

BH resistivity

31 E-W			
Spacing	Count	App. Resistivity	Resistance
0.3	27	1860.1	986.67
0.6	51	1807.5	479.39
0.9	32	1037.2	183.39
1.2	33	1189.2	157.71
1.8	30	528.0	46.68
2.4	28	339.7	22.53
3.0	25	217.8	11.56
3.6	22	122.4	5.41
4.2	18	66.7	2.53
4.8	15	22.2	0.74
5.4	12	20.4	0.60
6.0	10	8.9	0.24
6.6	8	9.0	0.22
7.2	5	7.7	0.17
10.0			
20.0			

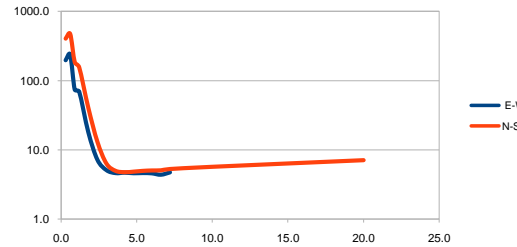
31 N-S			
Spacing	Count	App. Resistivity	Resistance
0.3	32	1194.7	633.71
0.6	53	1366.8	362.50
0.9	32	1067.9	188.83
1.2	33	588.7	78.06
1.8	32	241.4	21.34
2.4	29	107.1	7.10
3.0	26	54.4	2.89
3.6	23	29.5	1.30
4.2	20	16.9	0.64
4.8	17	12.4	0.41
5.4	14	10.5	0.31
6.0	11	9.8	0.26
6.6	8	9.7	0.23
7.2	5	8.9	0.20
10.0		7.2	0.11
20.0		8.2	0.07



31.0		
Spacing	E-W	N-S
0.3	1860.1	1194.7
0.6	1807.5	1366.8
0.9	1037.2	1067.9
1.2	1189.2	588.7
1.8	528.0	241.4
2.4	339.7	107.1
3.0	217.8	54.4
3.6	122.4	29.5
4.2	66.7	16.9
4.8	22.2	12.4
5.4	20.4	10.5
6.0	8.9	9.8
6.6	9.0	9.7
7.2	7.7	8.9
10		7.2
20		8.2

32 E-W			
Spacing	Count	App. Resistivity	Resistance
0.3	37	197.9	104.96
0.6	51	239.7	63.57
0.9	32	74.7	13.22
1.2	31	69.3	9.19
1.8	28	18.1	1.60
2.4	26	7.2	0.48
3.0	24	5.1	0.27
3.6	21	4.6	0.20
4.2	18	4.7	0.18
4.8	15	4.6	0.15
5.4	12	4.6	0.14
6.0	10	4.6	0.12
6.6	8	4.4	0.11
7.2	5	4.7	0.10
10.0			
20.0			

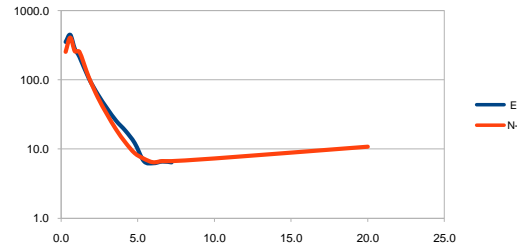
32 N-S			
Spacing	Count	App. Resistivity	Resistance
0.3	37	403.5	214.04
0.6	55	472.7	125.36
0.9	32	185.1	32.72
1.2	35	154.8	20.53
1.8	32	40.5	3.58
2.4	29	13.1	0.87
3.0	26	6.3	0.34
3.6	23	5.0	0.22
4.2	20	4.8	0.18
4.8	17	4.9	0.16
5.4	14	5.0	0.15
6.0	11	5.0	0.13
6.6	8	5.1	0.12
7.2	5	5.3	0.12
10.0		5.7	0.09
20.0		7.1	0.06



32.0		
Spacing	E-W	N-S
0.3	197.9	403.5
0.6	239.7	472.7
0.9	74.7	185.1
1.2	69.3	154.8
1.8	18.1	40.5
2.4	7.2	13.1
3.0	5.1	6.3
3.6	4.6	5.0
4.2	4.7	4.8
4.8	4.6	4.9
5.4	4.6	5.0
6.0	4.6	5.0
6.6	4.4	5.1
7.2	4.7	5.3
10		5.7
20		7.1

33 E-W			
Spacing	Count	App. Resistivity	Resistance
0.3	32	349.7	185.48
0.6	51	443.1	117.51
0.9	32	276.6	48.91
1.2	35	213.0	28.25
1.8	32	105.3	9.31
2.4	29	61.0	4.04
3.0	26	38.4	2.04
3.6	23	25.3	1.12
4.2	20	18.2	0.69
4.8	17	12.1	0.40
5.4	14	6.6	0.20
6.0	11	6.2	0.16
6.6	8	6.6	0.16
7.2	5	6.4	0.14
10.0			
20.0			

33 N-S			
Spacing	Count	App. Resistivity	Resistance
0.3	37	252.8	134.11
0.6	55	406.5	107.80
0.9	32	257.6	45.55
1.2	35	252.3	33.46
1.8	32	110.0	9.72
2.4	29	55.4	3.67
3.0	26	31.7	1.68
3.6	23	19.0	0.84
4.2	20	12.4	0.47
4.8	17	8.7	0.29
5.4	14	7.2	0.21
6.0	11	6.4	0.17
6.6	8	6.7	0.16
7.2	5	6.7	0.15
10.0		7.3	0.12
20.0		10.8	0.09

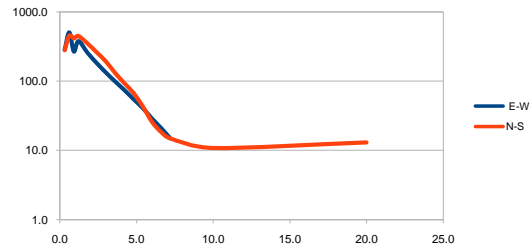


33.0		
Spacing	E-W	N-S
0.3	349.7	252.8
0.6	443.1	406.5
0.9	276.6	257.6
1.2	213.0	252.3
1.8	105.3	110.0
2.4	61.0	55.4
3.0	38.4	31.7
3.6	25.3	19.0
4.2	18.2	12.4
4.8	12.1	8.7
5.4	6.6	7.2
6.0	6.2	6.4
6.6	6.6	6.7
7.2	6.4	6.7
10		7.3
20		10.8

BH resistivity

34 E-W			
Spacing	Count	App. Resistivity	Resistance
0.3	37	282.7	149.94
0.6	51	505.8	134.15
0.9	32	267.6	47.32
1.2	31	378.0	50.13
1.8	28	255.5	22.59
2.4	26	181.8	12.05
3.0	24	132.6	7.03
3.6	21	98.7	4.36
4.2	18	74.4	2.82
4.8	15	54.9	1.82
5.4	12	40.9	1.21
6.0	10	28.9	0.77
6.6	8	21.0	0.51
7.2	5	14.9	0.33
10.0			
20.0			

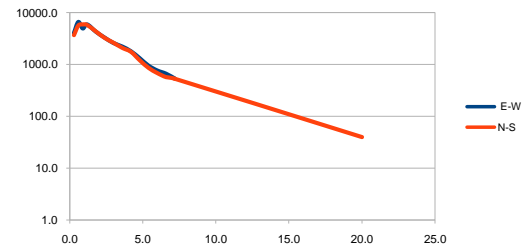
34 N-S			
Spacing	Count	App. Resistivity	Resistance
0.3	37	280.1	148.60
0.6	51	454.5	120.54
0.9	32	416.0	73.55
1.2	31	448.4	59.46
1.8	28	348.9	30.84
2.4	26	259.7	17.22
3.0	24	191.4	10.15
3.6	21	130.6	5.77
4.2	18	93.3	3.54
4.8	15	67.0	2.22
5.4	12	43.1	1.27
6.0	10	25.7	0.68
6.6	8	18.3	0.44
7.2	5	14.8	0.33
10.0		10.8	0.17
20.0		13.0	0.10



34.0		
Spacing	E-W	N-S
0.3	282.7	280.1
0.6	505.8	454.5
0.9	267.6	416.0
1.2	378.0	448.4
1.8	255.5	348.9
2.4	181.8	259.7
3.0	132.6	191.4
3.6	98.7	130.6
4.2	74.4	93.3
4.8	54.9	67.0
5.4	40.9	43.1
6.0	28.9	25.7
6.6	21.0	18.3
7.2	14.9	14.8
10		10.8
20		13.0

35 E-W			
Spacing	Count	App. Resistivity	Resistance
0.3	30	4031.3	2138.40
0.6	48	6571.7	1742.96
0.9	32	4922.3	870.34
1.2	31	5883.2	780.18
1.8	28	4273.1	377.77
2.4	26	3285.5	217.85
3.0	24	2590.7	137.42
3.6	21	2215.1	97.91
4.2	18	1795.5	68.03
4.8	15	1321.3	43.81
5.4	12	950.4	28.01
6.0	10	766.3	20.32
6.6	8	665.9	16.06
7.2	5	537.5	11.88
10.0			
20.0			

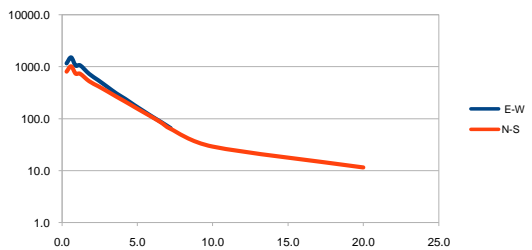
35 N-S			
Spacing	Count	App. Resistivity	Resistance
0.3	34	3670.4	1946.98
0.6	51	5634.1	1494.30
0.9	32	5906.9	1044.44
1.2	31	5782.3	766.80
1.8	28	4325.1	382.27
2.4	26	3247.3	215.32
3.0	24	2620.8	139.02
3.6	21	2089.2	92.35
4.2	18	1749.0	66.27
4.8	15	1200.7	39.81
5.4	12	857.7	25.28
6.0	10	680.5	18.05
6.6	7	568.3	13.70
7.2	5	527.9	11.67
10.0			
20.0		39.5	0.31



35.0		
Spacing	E-W	N-S
0.3	4031.3	3670.4
0.6	6571.7	5634.1
0.9	4922.3	5906.9
1.2	5883.2	5782.3
1.8	4273.1	4325.1
2.4	3285.5	3247.3
3.0	2590.7	2620.8
3.6	2215.1	2089.2
4.2	1795.5	1749.0
4.8	1321.3	1200.7
5.4	950.4	857.7
6.0	766.3	680.5
6.6	665.9	568.3
7.2	537.5	527.9
10		
20		39.5

36 E-W			
Spacing	Count	App. Resistivity	Resistance
0.3	32	1160.0	615.32
0.6	52	1513.2	401.33
0.9	32	1047.5	185.21
1.2	35	1062.6	140.91
1.8	32	725.8	64.17
2.4	29	548.8	36.39
3.0	26	409.7	21.73
3.6	23	306.3	13.54
4.2	20	238.7	9.04
4.8	17	181.4	6.01
5.4	14	139.8	4.12
6.0	11	108.1	2.87
6.6	8	84.7	2.04
7.2	5	65.6	1.45
10.0			
20.0			

36 N-S			
Spacing	Count	App. Resistivity	Resistance
0.3	35	805.8	427.44
0.6	53	1019.9	270.51
0.9	32	736.7	130.25
1.2	35	731.7	97.04
1.8	32	526.1	46.51
2.4	29	421.8	27.97
3.0	26	336.6	17.86
3.6	23	266.3	11.77
4.2	20	212.5	8.05
4.8	17	168.3	5.58
5.4	14	133.5	3.93
6.0	11	106.2	2.82
6.6	8	83.5	2.01
7.2	5	63.8	1.41
10.0		29.0	0.46
20.0		11.5	0.09

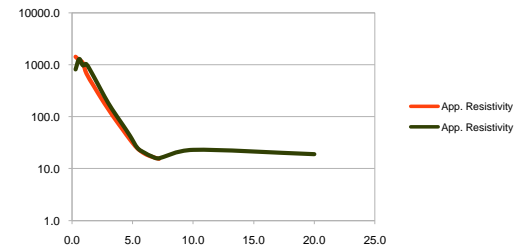


36.0		
Spacing	E-W	N-S
0.3	1160.0	805.8
0.6	1513.2	1019.9
0.9	1047.5	736.7
1.2	1062.6	731.7
1.8	725.8	526.1
2.4	548.8	421.8
3.0	409.7	336.6
3.6	306.3	266.3
4.2	238.7	212.5
4.8	181.4	168.3
5.4	139.8	133.5
6.0	108.1	106.2
6.6	84.7	83.5
7.2	65.6	63.8
10		29.0
20		11.5

BH resistivity

37 E-W			
Spacing	Count	App. Resistivity	Resistance
0.3	35	1428.8	757.92
0.6	55	1225.4	325.00
0.9	32	1090.4	192.80
1.2	35	676.5	89.71
1.8	32	390.1	34.49
2.4	29	229.6	15.23
3.0	26	139.6	7.41
3.6	23	87.3	3.86
4.2	20	56.1	2.12
4.8	17	36.0	1.19
5.4	14	24.5	0.72
6.0	11	19.4	0.51
6.6	8	16.8	0.41
7.2	5	15.3	0.34
10.0			
20.0			

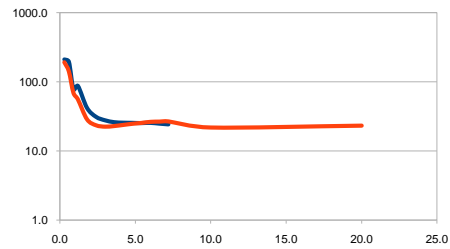
37 N-S			
Spacing	Count	App. Resistivity	Resistance
0.3	31	811.2	430.29
0.6	55	1286.9	341.32
0.9	32	969.0	171.33
1.2	35	1018.0	134.99
1.8	32	591.6	52.30
2.4	29	325.8	21.60
3.0	26	182.4	9.68
3.6	23	110.8	4.90
4.2	20	69.3	2.62
4.8	17	42.6	1.41
5.4	14	25.1	0.74
6.0	11	20.2	0.53
6.6	8	17.2	0.41
7.2	5	15.9	0.35
10.0		23.0	0.37
20.0		19.0	0.15



37.0		
Spacing	E-W	N-S
0.3	1428.8	811.2
0.6	1225.4	1286.9
0.9	1090.4	969.0
1.2	676.5	1018.0
1.8	390.1	591.6
2.4	229.6	325.8
3.0	139.6	182.4
3.6	87.3	110.8
4.2	56.1	69.3
4.8	36.0	42.6
5.4	24.5	25.1
6.0	19.4	20.2
6.6	16.8	17.2
7.2	15.3	15.9
10		
20		

38 E-W			
Spacing	Count	App. Resistivity	Resistance
0.3	34	209.6	111.18
0.6	50	193.8	51.39
0.9	32	77.9	13.77
1.2	31	87.0	11.54
1.8	28	42.1	3.72
2.4	26	31.3	2.07
3.0	24	27.8	1.48
3.6	21	26.2	1.16
4.2	18	25.7	0.98
4.8	15	25.6	0.85
5.4	12	25.4	0.75
6.0	10	25.6	0.68
6.6	8	25.0	0.60
7.2	5	24.3	0.54
10.0			
20.0			

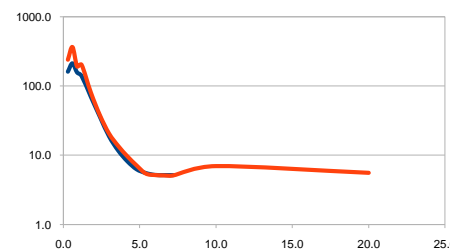
38 N-S			
Spacing	Count	App. Resistivity	Resistance
0.3	37	191.8	101.75
0.6	50	141.4	37.51
0.9	32	69.3	12.25
1.2	31	55.6	7.37
1.8	28	28.7	2.53
2.4	26	23.5	1.56
3.0	24	22.4	1.19
3.6	21	22.9	1.01
4.2	18	23.8	0.90
4.8	15	24.7	0.82
5.4	12	25.4	0.75
6.0	10	26.3	0.70
6.6	8	26.5	0.64
7.2	5	26.7	0.59
10.0		21.8	0.35
20.0		23.2	0.18



38.0		
Spacing	E-W	N-S
0.3	209.6	191.8
0.6	193.8	141.4
0.9	77.9	69.3
1.2	87.0	55.6
1.8	42.1	28.7
2.4	31.3	23.5
3.0	27.8	22.4
3.6	26.2	22.9
4.2	25.7	23.8
4.8	25.6	24.7
5.4	25.4	25.4
6.0	25.6	26.3
6.6	25.0	26.5
7.2	24.3	26.7
10		21.8
20		23.2

39 E-W			
Spacing	Count	App. Resistivity	Resistance
0.3	38	161.3	85.57
0.6	51	213.0	56.50
0.9	32	157.5	27.85
1.2	31	139.9	18.55
1.8	28	70.5	6.24
2.4	25	35.9	2.38
3.0	23	18.7	0.99
3.6	21	11.7	0.52
4.2	18	8.2	0.31
4.8	14	6.3	0.21
5.4	12	5.5	0.16
6.0	10	5.2	0.14
6.6	8	5.2	0.12
7.2	5	5.2	0.11
10.0			
20.0			

39 N-S			
Spacing	Count	App. Resistivity	Resistance
0.3	38	238.7	126.63
0.6	51	364.0	96.54
0.9	32	191.3	33.83
1.2	31	201.8	26.77
1.8	28	81.1	7.17
2.4	26	37.7	2.50
3.0	24	20.5	1.09
3.6	21	13.6	0.60
4.2	18	9.7	0.37
4.8	15	7.1	0.24
5.4	12	5.5	0.16
6.0	10	5.2	0.14
6.6	8	5.1	0.12
7.2	5	5.1	0.11
10.0		7.0	0.11
20.0		5.6	0.04

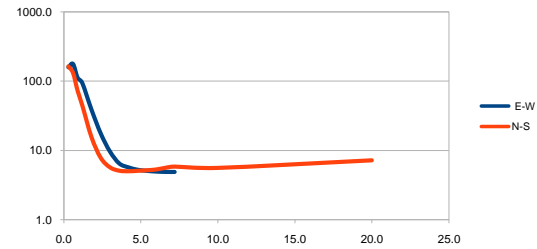


39.0		
Spacing	E-W	N-S
0.3	161.3	238.7
0.6	213.0	364.0
0.9	157.5	191.3
1.2	139.9	201.8
1.8	70.5	81.1
2.4	35.9	37.7
3.0	18.7	20.5
3.6	11.7	13.6
4.2	8.2	9.7
4.8	6.3	7.1
5.4	5.5	5.5
6.0	5.2	5.2
6.6	5.2	5.1
7.2	5.2	5.1
10		7.0
20		5.6

BH resistivity

40 E-W			
Spacing	Count	App. Resistivity	Resistance
0.3	38	158.4	84.02
0.6	51	177.1	46.98
0.9	32	111.6	19.73
1.2	31	94.1	12.48
1.8	28	38.7	3.42
2.4	25	17.5	1.16
3.0	23	9.6	0.51
3.6	21	6.5	0.29
4.2	18	5.7	0.22
4.8	14	5.2	0.17
5.4	12	5.1	0.15
6.0	10	4.9	0.13
6.6	8	4.9	0.12
7.2	5	4.9	0.11
10.0			
20.0			

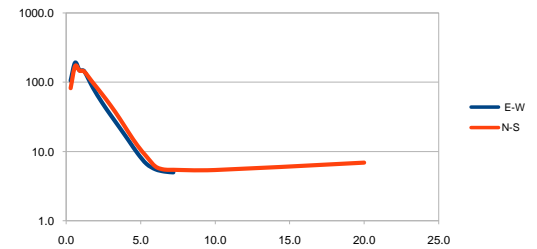
40 N-S			
Spacing	Count	App. Resistivity	Resistance
0.3	38	163.1	86.54
0.6	50	131.4	34.85
0.9	32	72.4	12.79
1.2	31	44.8	5.94
1.8	28	15.5	1.37
2.4	26	7.8	0.52
3.0	24	5.7	0.30
3.6	21	5.1	0.23
4.2	18	5.0	0.19
4.8	15	5.1	0.17
5.4	12	5.2	0.15
6.0	10	5.3	0.14
6.6	8	5.6	0.14
7.2	5	5.8	0.13
10.0		5.6	0.09
20.0		7.2	0.06



40.0		
Spacing	E-W	N-S
0.3	158.4	163.1
0.6	177.1	131.4
0.9	111.6	72.4
1.2	94.1	44.8
1.8	38.7	15.5
2.4	17.5	7.8
3.0	9.6	5.7
3.6	6.5	5.1
4.2	5.7	5.0
4.8	5.2	5.1
5.4	5.1	5.2
6.0	4.9	5.3
6.6	4.9	5.6
7.2	4.9	5.8
10		5.6
20		7.2

41 E-W			
Spacing	Count	App. Resistivity	Resistance
0.3	38	105.3	55.86
0.6	55	191.2	50.71
0.9	32	147.6	26.11
1.2	35	145.0	19.23
1.8	32	83.1	7.34
2.4	29	51.3	3.40
3.0	26	33.3	1.77
3.6	23	22.0	0.97
4.2	20	14.4	0.55
4.8	17	9.4	0.31
5.4	14	6.6	0.20
6.0	11	5.5	0.15
6.6	8	5.2	0.12
7.2	5	5.0	0.11
10.0			
20.0			

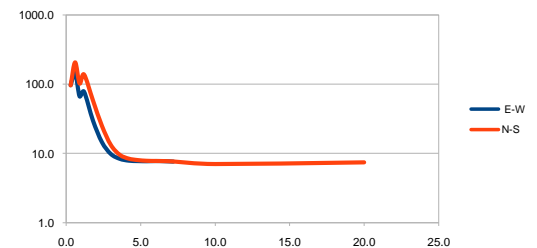
41 N-S			
Spacing	Count	App. Resistivity	Resistance
0.3	38	82.1	43.57
0.6	55	171.3	45.43
0.9	32	146.7	25.94
1.2	35	143.4	19.02
1.8	32	98.5	8.71
2.4	29	67.8	4.50
3.0	26	45.7	2.42
3.6	23	29.7	1.31
4.2	20	18.7	0.71
4.8	17	12.1	0.40
5.4	14	8.4	0.25
6.0	11	6.1	0.16
6.6	8	5.5	0.13
7.2	5	5.4	0.12
10.0		5.4	0.09
20.0		6.9	0.05



41.0		
Spacing	E-W	N-S
0.3	105.3	82.1
0.6	191.2	171.3
0.9	147.6	146.7
1.2	145.0	143.4
1.8	83.1	98.5
2.4	51.3	67.8
3.0	33.3	45.7
3.6	22.0	29.7
4.2	14.4	18.7
4.8	9.4	12.1
5.4	6.6	8.4
6.0	5.5	6.1
6.6	5.2	5.5
7.2	5.0	5.4
10		5.4
20		6.9

42 E-W			
Spacing	Count	App. Resistivity	Resistance
0.3	38	96.5	51.21
0.6	55	147.3	39.07
0.9	32	66.8	11.81
1.2	35	78.0	10.35
1.8	32	29.9	2.64
2.4	29	14.6	0.97
3.0	26	9.8	0.52
3.6	23	8.4	0.37
4.2	20	7.9	0.30
4.8	17	7.8	0.26
5.4	14	7.7	0.23
6.0	11	7.8	0.21
6.6	8	7.7	0.19
7.2	5	7.6	0.17
10.0			
20.0			

42 N-S			
Spacing	Count	App. Resistivity	Resistance
0.3	38	96.2	51.02
0.6	55	207.0	54.90
0.9	32	102.4	18.11
1.2	35	138.0	18.30
1.8	32	58.0	5.13
2.4	29	25.0	1.66
3.0	26	13.2	0.70
3.6	23	9.5	0.42
4.2	20	8.4	0.32
4.8	17	8.0	0.26
5.4	14	7.8	0.23
6.0	11	7.7	0.21
6.6	8	7.7	0.19
7.2	5	7.6	0.17
10.0		7.0	0.11
20.0		7.4	0.06

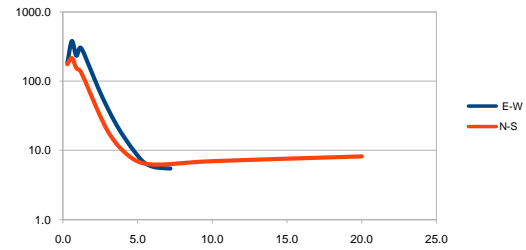


42.0		
Spacing	E-W	N-S
0.3	96.5	96.2
0.6	147.3	207.0
0.9	66.8	102.4
1.2	78.0	138.0
1.8	29.9	58.0
2.4	14.6	25.0
3.0	9.8	13.2
3.6	8.4	9.5
4.2	7.9	8.4
4.8	7.8	8.0
5.4	7.7	7.8
6.0	7.8	7.7
6.6	7.7	7.7
7.2	7.6	7.6
10		7.0
20		7.4

BH resistivity

43 E-W			
Spacing	Count	App. Resistivity	Resistance
0.3	36	181.2	96.10
0.6	55	378.1	100.28
0.9	31	232.2	41.06
1.2	35	302.0	40.05
1.8	32	157.0	13.88
2.4	29	76.6	5.08
3.0	26	40.6	2.15
3.6	23	23.2	1.02
4.2	20	14.5	0.55
4.8	17	9.6	0.32
5.4	14	6.8	0.20
6.0	11	5.8	0.16
6.6	8	5.6	0.13
7.2	5	5.5	0.12
10.0			
20.0			

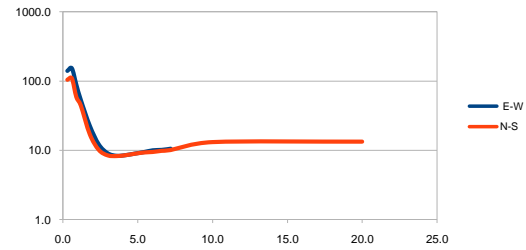
43 N-S			
Spacing	Count	App. Resistivity	Resistance
0.3	38	175.6	93.15
0.6	38	215.5	57.16
0.9	32	154.6	27.34
1.2	35	137.0	18.16
1.8	32	69.4	6.14
2.4	29	34.9	2.31
3.0	26	19.0	1.01
3.6	23	12.4	0.55
4.2	20	9.1	0.35
4.8	17	7.3	0.24
5.4	14	6.5	0.19
6.0	11	6.3	0.17
6.6	8	6.3	0.15
7.2	5	6.4	0.14
10.0		7.0	0.11
20.0		8.2	0.07



43.0		
Spacing	E-W	N-S
0.3	181.2	175.6
0.6	378.1	215.5
0.9	232.2	154.6
1.2	302.0	137.0
1.8	157.0	69.4
2.4	76.6	34.9
3.0	40.6	19.0
3.6	23.2	12.4
4.2	14.5	9.1
4.8	9.6	7.3
5.4	6.8	6.5
6.0	5.8	6.3
6.6	5.6	6.3
7.2	5.5	6.4
10		7.0
20		8.2

44 E-W			
Spacing	Count	App. Resistivity	Resistance
0.3	38	140.9	74.74
0.6	50	153.5	40.71
0.9	32	88.7	15.69
1.2	29	53.3	7.07
1.8	28	22.6	2.00
2.4	26	12.2	0.81
3.0	24	9.0	0.48
3.6	21	8.3	0.37
4.2	18	8.5	0.32
4.8	15	9.0	0.30
5.4	12	9.4	0.28
6.0	10	10.0	0.27
6.6	8	10.1	0.24
7.2	5	10.5	0.23
10.0			
20.0			

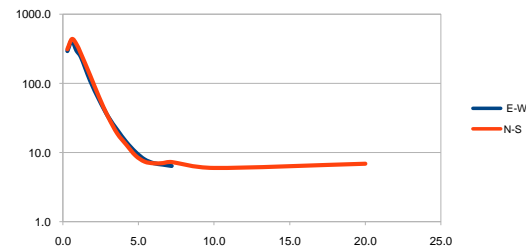
44 N-S			
Spacing	Count	App. Resistivity	Resistance
0.3	38	104.9	55.63
0.6	50	110.6	29.34
0.9	32	59.1	10.45
1.2	31	44.6	5.91
1.8	28	17.1	1.51
2.4	26	10.2	0.68
3.0	24	8.5	0.45
3.6	21	8.3	0.37
4.2	18	8.5	0.32
4.8	15	9.0	0.30
5.4	12	9.3	0.28
6.0	10	9.5	0.25
6.6	8	9.9	0.24
7.2	5	10.1	0.22
10.0		13.2	0.21
20.0		13.4	0.11



44.0		
Spacing	E-W	N-S
0.3	140.9	104.9
0.6	153.5	110.6
0.9	88.7	59.1
1.2	53.3	44.6
1.8	22.6	17.1
2.4	12.2	10.2
3.0	9.0	8.5
3.6	8.3	8.3
4.2	8.5	8.5
4.8	9.0	9.0
5.4	9.4	9.3
6.0	10.0	9.5
6.6	10.1	9.9
7.2	10.5	10.1
10		13.2
20		13.4

45 E-W			
Spacing	Count	App. Resistivity	Resistance
0.3	35	292.3	155.05
0.6	51	410.3	108.82
0.9	31	297.6	52.62
1.2	31	239.1	31.70
1.8	28	110.3	9.76
2.4	26	58.0	3.84
3.0	24	33.0	1.75
3.6	21	21.2	0.94
4.2	18	14.2	0.54
4.8	15	10.2	0.34
5.4	12	8.0	0.24
6.0	10	7.0	0.19
6.6	8	6.7	0.16
7.2	5	6.4	0.14
10.0			
20.0			

45 N-S			
Spacing	Count	App. Resistivity	Resistance
0.3	37	310.6	164.73
0.6	51	435.2	115.43
0.9	32	368.5	65.15
1.2	31	267.5	35.48
1.8	28	131.3	11.61
2.4	26	63.1	4.18
3.0	24	32.6	1.73
3.6	21	18.8	0.83
4.2	18	13.0	0.49
4.8	15	9.1	0.30
5.4	12	7.4	0.22
6.0	10	7.0	0.19
6.6	8	7.0	0.17
7.2	5	7.3	0.16
10.0		6.0	0.10
20.0		6.9	0.05



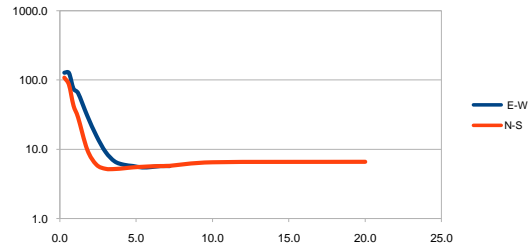
45.0		
Spacing	E-W	N-S
0.3	292.3	310.6
0.6	410.3	435.2
0.9	297.6	368.5
1.2	239.1	267.5
1.8	110.3	131.3
2.4	58.0	63.1
3.0	33.0	32.6
3.6	21.2	18.8
4.2	14.2	13.0
4.8	10.2	9.1
5.4	8.0	7.4
6.0	7.0	7.0
6.6	6.7	7.0
7.2	6.4	7.3
10		6.0
20		6.9

BH resistivity

46 E-W			
Spacing	Count	App. Resistivity	Resistance
0.3	36	128.1	67.96
0.6	49	127.2	33.74
0.9	32	75.0	13.26
1.2	30	64.9	8.61
1.8	28	30.6	2.71
2.4	26	15.7	1.04
3.0	24	9.2	0.49
3.6	21	6.7	0.30
4.2	18	6.0	0.23
4.8	15	5.7	0.19
5.4	12	5.5	0.16
6.0	10	5.6	0.15
6.6	8	5.7	0.14
7.2	5	5.7	0.13
10.0			
20.0			

46 N-S			
Spacing	Count	App. Resistivity	Resistance
0.3	37	107.9	57.23
0.6	51	85.7	22.72
0.9	32	42.6	7.53
1.2	31	28.8	3.81
1.8	28	9.9	0.87
2.4	26	6.0	0.40
3.0	24	5.2	0.28
3.6	21	5.2	0.23
4.2	18	5.3	0.20
4.8	15	5.5	0.18
5.4	12	5.6	0.16
6.0	10	5.7	0.15
6.6	8	5.7	0.14
7.2	5	5.8	0.13
10.0		6.5	0.10
20.0		6.6	0.05

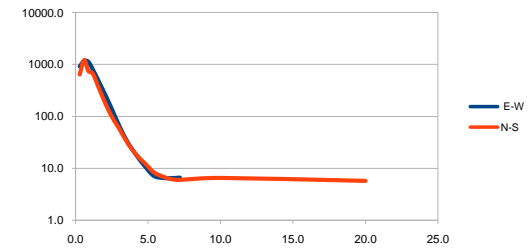
46.0		
Spacing	E-W	N-S
0.3	128.1	107.9
0.6	127.2	85.7
0.9	75.0	42.6
1.2	64.9	28.8
1.8	30.6	9.9
2.4	15.7	6.0
3.0	9.2	5.2
3.6	6.7	5.2
4.2	6.0	5.3
4.8	5.7	5.5
5.4	5.5	5.6
6.0	5.6	5.7
6.6	5.7	5.7
7.2	5.7	5.8
10		6.5
20		6.6



47 E-W			
Spacing	Count	App. Resistivity	Resistance
0.3	36	917.6	486.72
0.6	51	1172.7	311.04
0.9	32	1125.3	198.96
1.2	31	805.0	106.76
1.8	28	369.3	32.65
2.4	26	163.1	10.81
3.0	24	67.8	3.59
3.6	21	31.8	1.41
4.2	18	17.8	0.67
4.8	15	10.8	0.36
5.4	12	7.1	0.21
6.0	10	6.5	0.17
6.6	8	6.4	0.15
7.2	5	6.6	0.15
10.0			
20.0			

47 N-S			
Spacing	Count	App. Resistivity	Resistance
0.3	33	637.5	338.18
0.6	46	1205.9	319.83
0.9	29	739.2	130.71
1.2	29	662.6	87.87
1.8	23	263.8	23.32
2.4	20	112.1	7.43
3.0	19	58.9	3.13
3.6	18	30.6	1.35
4.2	13	18.2	0.69
4.8	12	12.3	0.41
5.4	10	8.4	0.25
6.0	10	6.9	0.18
6.6	8	6.2	0.15
7.2	5	6.0	0.13
10.0		6.5	0.10
20.0		5.7	0.05

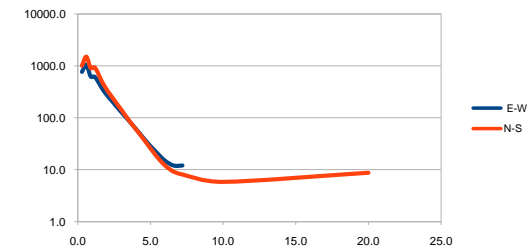
47.0		
Spacing	E-W	N-S
0.3	917.6	637.5
0.6	1172.7	1205.9
0.9	1125.3	739.2
1.2	805.0	662.6
1.8	369.3	263.8
2.4	163.1	112.1
3.0	67.8	58.9
3.6	31.8	30.6
4.2	17.8	18.2
4.8	10.8	12.3
5.4	7.1	8.4
6.0	6.5	6.9
6.6	6.4	6.2
7.2	6.6	6.0
10		6.5
20		5.7



48 E-W			
Spacing	Count	App. Resistivity	Resistance
0.3	31	765.8	406.20
0.6	49	1054.7	279.73
0.9	31	623.3	110.21
1.2	31	608.2	80.65
1.8	28	327.8	28.98
2.4	26	204.3	13.54
3.0	24	129.0	6.84
3.6	21	83.0	3.67
4.2	18	52.6	1.99
4.8	15	33.0	1.09
5.4	12	21.8	0.64
6.0	10	14.9	0.40
6.6	8	12.0	0.29
7.2	5	12.1	0.27
10.0			
20.0			

48 N-S			
Spacing	Count	App. Resistivity	Resistance
0.3	37	1012.9	537.27
0.6	51	1510.1	400.53
0.9	32	908.1	160.57
1.2	31	922.6	122.35
1.8	28	430.3	38.04
2.4	26	244.0	16.18
3.0	24	143.7	7.62
3.6	21	84.1	3.72
4.2	18	51.4	1.95
4.8	15	30.9	1.02
5.4	12	18.5	0.55
6.0	10	12.1	0.32
6.6	8	9.1	0.22
7.2	5	8.1	0.18
10.0		5.8	0.09
20.0		8.7	0.07

48.0		
Spacing	E-W	N-S
0.3	765.8	1012.9
0.6	1054.7	1510.1
0.9	623.3	908.1
1.2	608.2	922.6
1.8	327.8	430.3
2.4	204.3	244.0
3.0	129.0	143.7
3.6	83.0	84.1
4.2	52.6	51.4
4.8	33.0	30.9
5.4	21.8	18.5
6.0	14.9	12.1
6.6	12.0	9.1
7.2	12.1	8.1
10		5.8
20		8.7



BH resistivity

49 E-W

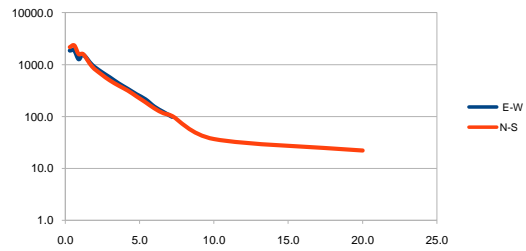
Spacing	Count	App. Resistivity	Resistance
0.3	30	1864.1	988.82
0.6	47	1875.6	497.47
0.9	31	1268.7	224.33
1.2	35	1557.3	206.51
1.8	32	994.6	87.93
2.4	29	735.6	48.78
3.0	26	569.0	30.18
3.6	23	433.5	19.16
4.2	20	342.7	12.99
4.8	17	268.0	8.89
5.4	14	214.4	6.32
6.0	11	155.0	4.11
6.6	8	122.8	2.96
7.2	5	98.4	2.17
10.0			
20.0			

49 N-S

Spacing	Count	App. Resistivity	Resistance
0.3	33	2160.0	1145.76
0.6	49	2333.7	618.94
0.9	32	1582.6	279.83
1.2	33	1583.9	210.04
1.8	31	912.9	80.71
2.4	29	656.7	43.54
3.0	26	493.3	26.17
3.6	23	391.6	17.31
4.2	20	315.6	11.96
4.8	17	243.3	8.07
5.4	14	187.4	5.52
6.0	11	143.1	3.79
6.6	7	115.7	2.79
7.2	4	101.8	2.25
10.0		36.9	0.59
20.0		22.2	0.18

49.0

Spacing	E-W	N-S
0.3	1864.1	2160.0
0.6	1875.6	2333.7
0.9	1268.7	1582.6
1.2	1557.3	1583.9
1.8	994.6	912.9
2.4	735.6	656.7
3.0	569.0	493.3
3.6	433.5	391.6
4.2	342.7	315.6
4.8	268.0	243.3
5.4	214.4	187.4
6.0	155.0	143.1
6.6	122.8	115.7
7.2	98.4	101.8
10		36.9
20		22.2



50 E-W

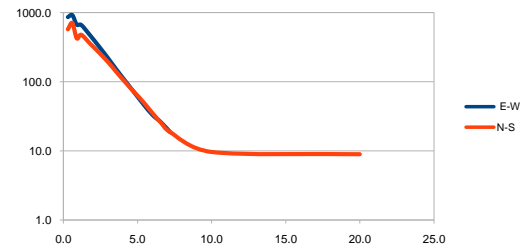
Spacing	Count	App. Resistivity	Resistance
0.3	38	853.6	452.81
0.6	38	911.2	241.67
0.9	32	662.0	117.04
1.2	35	657.6	87.20
1.8	32	464.9	41.11
2.4	29	321.2	21.29
3.0	26	218.9	11.61
3.6	23	146.6	6.48
4.2	20	100.1	3.79
4.8	17	68.6	2.28
5.4	14	47.0	1.38
6.0	11	33.2	0.88
6.6	8	25.7	0.62
7.2	5	18.6	0.41
10.0			
20.0			

50 N-S

Spacing	Count	App. Resistivity	Resistance
0.3	35	570.8	302.80
0.6	51	703.9	186.70
0.9	32	423.0	74.79
1.2	31	476.5	63.19
1.8	28	355.3	31.41
2.4	26	264.3	17.53
3.0	24	193.0	10.24
3.6	21	136.5	6.03
4.2	18	96.9	3.67
4.8	15	70.1	2.32
5.4	12	50.8	1.50
6.0	10	35.5	0.94
6.6	8	25.4	0.61
7.2	5	18.8	0.42
10.0		9.7	0.15
20.0		9.0	0.07

50.0

Spacing	E-W	N-S
0.3	853.6	570.8
0.6	911.2	703.9
0.9	662.0	423.0
1.2	657.6	476.5
1.8	464.9	355.3
2.4	321.2	264.3
3.0	218.9	193.0
3.6	146.6	136.5
4.2	100.1	96.9
4.8	68.6	70.1
5.4	47.0	50.8
6.0	33.2	35.5
6.6	25.7	25.4
7.2	18.6	18.8
10		9.7
20		9.0



APPENDIX J:
SEISMIC HAZARD AND DYNAMIC RESPONSE ASSESSMENT

APPENDIX J:

SEISMIC HAZARD AND DYNAMIC RESPONSE ASSESSMENT

Part 1: Probabilistic Seismic Hazard Analysis

Part 2: Dynamic Response of the Soil

APPENDIX J:

SEISMIC HAZARD AND DYNAMIC RESPONSE ASSESSMENT

Part 1: Probabilistic Seismic Hazard Analysis

**PART 1: PROBABILISTIC SEISMIC HAZARD ANALYSIS
FOR THE ESKOM SERE WIND FARM SITE, WESTERN CAPE**

By


V. Midzi, F. O. Strasser and B. Zulu






Report No. 2010 - 0235

CONFIDENTIAL

© Council for Geoscience

DOCUMENT APPROVAL SHEET

	COUNCIL FOR GEOSCIENCE (Seismology Unit)	REFERENCE: CGS REPORT.
		2010 - 0235
		REVISION 0
COPY No.	PROBABILISTIC SEISMIC HAZARD ANALYSIS FOR THE ESKOM SERE WIND FARM SITE, WESTERN CAPE	DATE OF RELEASE 19 November 2010

AUTHORS			
			
V. Midzi	F. O. Strasser	pp B Zulu	
ACCEPTED BY: 			AUTHORISED BY: 
M. R. G. Grobbelaar			G. Graham

REVISION	DESCRIPTION OF REVISION	DATE	MINOR REVISIONS APPROVAL

TABLE OF CONTENTS

List of Tables.....	iv
List of Figures.....	v
Definition of Terms & Abbreviations.....	vi
Executive Summary.....	x
1. Introduction.....	1
2. Seismotectonic Setting.....	2
3. Seismic Source Characterisation.....	8
4. Ground Motion Models.....	13
5. Probabilistic Seismic Hazard Assessment.....	19
6. Results.....	22
6.1 Deaggregation.....	25
7. Conclusions.....	29
References.....	31

List of Tables

Table 1. Recurrence parameters for area sources.....	11
Table 2. Recurrence parameters adopted for the ckbc fault source.....	12
Table 3. Horizontal component adjustments.....	15
Table 4. Magnitude adjustments required.....	15
Table 5. Summary of distance metrics used in selected GMPE's.....	16
Table 6. Style-of-faulting adjustments.....	17
Table 7. Adjustments for site conditions.....	18
Table 8. Weighting of GMPEs for all sources.....	20
Table 9. Weighting of crustal thickness values assigned for all source zones.....	21
Table 10. Mean and Median ground motions (GM) for 10% probability of exceedance in 50 years, expected at the wind farm site (PGA – Peak Ground Acceleration; SA – Spectral Acceleration).....	24
Table 11. Mean and median distances (D), magnitudes (M) and epsilon (ε) for the wind farm site for Sa(0.5), Sa(1.0), Sa(2.0) and Sa(3.0) at 10% probability of exceedance in 50 years.....	28

List of Figures

- Figure 1.** Basement geology of southern Africa showing the relation of the East African Rift system with respect to the mobile belts and continental cratons, Black triangle is proposed location of Wind farm site (Adapted from Fairhead & Stuart, 1982).....3
- Figure 2.** Spatial distribution of all earthquakes in the Council for Geoscience catalogue. Brown circle locations represent tectonic event whilst green square locations represent mining related seismicity. Events identified as explosions or likely explosions have been removed. Black triangle – Eskom Sere Wind farm Site.....5
- Figure 3.** Intraplate stress directions and regimes in the southern Africa region (Bird *et al.*, 2006). NF = Normal Faulting; NS = Normal-Oblique Faulting; SS= Strike-Slip Faulting; TS = Reverse-Oblique Faulting; TF = Reverse (Thrust) Faulting.....6
- Figure 4.** Locations of seismicity used in this investigation as obtained from the SANSN database. The circle of broken line marks a boundary of events in an area of radius 300km used in the calculation.....7
- Figure 5.** Seismic source model based on structural data and tectonic seismicity.....8
- Figure 6:** Mean (black line) and Median (red line) hazard curves at various preselected spectral parameters. AFE = Annual Frequency of Exceedance and SA = Spectral acceleration in g (9.8m/s^2).....22
- Figure 7.** Uniform Hazard Spectra at 1% damping for return period (RP) of 475 years expected at the Wind farm site. (Mean – Black line; Median – red line).....25
- Figure 8.** Deaggregation of the SERE Wind Farm site spectral acceleration at four different periods for 10% probability of exceedance in 50 years.....27
- Figure 9.** Hazard contribution by Epsilon at period, T = 0.5, 1.0, 2.0 and 3.0s.....28

Definition of Terms, Symbols and Abbreviations

Acceleration	The rate of change of particle velocity per unit time. Commonly expressed as a fraction or percentage of the acceleration due to gravity (g), where $g = 9.81 \text{ m/s}^2$.
Acceleration Response Spectra (ARS)	Spectral acceleration is the movement experienced by a structure during an earthquake.
Annual Frequency of Exceedance (AFE)	Rate at which a given level of ground motion is exceeded. This rate results from consideration of the seismicity model (location and frequency of earthquakes of a given size) and the ground motion model (distribution of ground motions expected at a given site conditional on a given earthquake scenario defined by the earthquake magnitude and distance from the site).
Attenuation	A decrease in seismic-signal amplitude as waves propagate from the seismic source. Attenuation is caused by geometric spreading of seismic-wave energy and by the absorption and scattering of seismic energy in different earth materials.
Attenuation relationship	See Ground-motion prediction equation
b -value (b)	A coefficient in the frequency-magnitude relation, $\log N(m) = a - bm$, obtained by Gutenberg and Richter (1941; 1949), where m is the earthquake magnitude and $N(m)$ is the number of earthquakes with magnitude greater than or equal to m . Estimated b -values for most seismic zones fall between 0.6 and 1.1.
Capable fault	A mapped fault that is deemed a possible site for a future earthquake with magnitude greater than some specified threshold.
Catalogue	A chronological listing of earthquakes. Early catalogues were purely descriptive, <i>i.e.</i> , they gave the date of each earthquake and some description of its effects. Modern catalogues are usually quantitative, <i>i.e.</i> , earthquakes are listed as a set of numerical parameters describing origin time, hypocenter location, magnitude, focal mechanism, moment tensor, etc.
CGS	Council for Geoscience
Damping ratio	The damping coefficient (the ratio of the viscous damping force to velocity) for a single-degree-of freedom oscillator expressed as a percentage of the critical damping coefficient (<i>i.e.</i> of the maximum value of the damping coefficient at which periodically attenuating oscillation is possible).
Design Earthquake	The postulated earthquake (commonly including a specification of the ground motion at a site) that is used for evaluating the earthquake resistance of a particular structure.
Earthquake	Ground shaking and radiated seismic energy caused most commonly by sudden slip on a fault, volcanic or magmatic activity, or other sudden stress changes in the Earth.
Elastic design spectrum (or spectra)	The specification of the required strength or capacity of the structure plotted as a function of the natural period or frequency of the structure and damping appropriate to earthquake response at the required level. Design spectra are often composed of straight line segments (Newmark and Hall, 1982) and/or simple curves, for example, as in most building codes, but they can also be constructed from statistics of response spectra of a suite of ground motions appropriate to the design earthquake(s). To be implemented, the requirements of a design spectrum are associated with allowable levels of stresses, ductilities, displacements or other measures of response.
Epicenter	The epicenter is the point on the earth's surface vertically above the hypocenter (or focus).
Epicentral distance (Δ)	Distance from the site to the epicenter of an earthquake.
Fault	A fracture or fracture zone in the Earth along which the two sides have been displaced relative to one another parallel to the fracture. The accumulated displacement may range from a fraction of a meter to many kilometres. The type of fault is

	specified according to the direction of this slip. Sudden movement along a fault produces earthquakes. Slow movement produces aseismic creep.
Focal depth (h)	Focal depth is the vertical distance between the hypocentre and epicentre.
Frequency	The number of cycles of a periodic motion (such as the ground shaking up and down or back and forth during an earthquake) per unit time; the reciprocal of period. Hertz (Hz), the unit of frequency, is equal to the number of cycles per second.
Ground motion	The movement of the Earth's surface from earthquakes or explosions. Ground motion is produced by waves that are generated by sudden slip on a fault or sudden pressure at the explosive source and travel through the earth and along its surface.
Ground motion parameter	Parameter characterizing the level of ground shaking at a given site. Commonly used ground-motion parameters include peak parameters (peak ground acceleration, PGA; peak ground velocity, PGV), spectral parameters (Fourier amplitude spectrum, FAS), energy-related parameters (Housner intensity, Arias intensity), duration and response ordinates (see Response spectrum).
Ground-motion prediction equation (attenuation relationship)	Equation relating an independent variable representing the level of ground shaking (generally, the logarithm of a ground-motion parameter) to a number of explanatory variables characterizing the physical processes associated with the generation and propagation of seismic waves. Explanatory variables commonly include magnitude, source-to-site distance and a parameter characterizing local site conditions. Modern equations also include additional parameters such as style-of-faulting, hanging-wall factor and depth-to-top-of-rupture. GMPEs are derived through regression on instrumentally recorded (empirical) data or data obtained from numerical simulations. A GMPE should include a measure of the variability associated with the prediction (see Sigma).
Hazard Curve	A plot of the expected frequency of exceedance over some specified time interval (generally a year) of various levels of a given ground-motion parameter.
Heterogeneity	A medium is heterogeneous when its physical properties change along the space coordinates. A critical parameter affecting seismic phenomena is the scale of heterogeneities as compared with the seismic wavelengths. For a relatively large wavelength, for example, an intrinsically isotropic medium with oriented heterogeneities may behave as a homogeneous anisotropic medium.
Hypocenter	The hypocenter is the point within the earth where an earthquake rupture starts. The epicenter is the point directly above it at the surface of the Earth. Also commonly termed the focus.
Hypocentral distance (r)	Distance from the site to the hypocenter of an earthquake.
Induced earthquake	An earthquake that results from changes in crustal stress and/or strength due to man-made sources (e.g., underground mining and filling of a reservoir), or natural sources (e.g., the fault slip of a major earthquake). As defined less rigorously, "induced" is used interchangeably with "triggered" and applies to any earthquake associated with a stress change, large or small.
Local Magnitude (M_L)	A magnitude scale introduced by Richter (1935) for earthquakes in southern California. M_L was originally defined as the logarithm of the maximum amplitude of seismic waves on a seismogram written by the Wood-Anderson seismograph (Anderson and Wood, 1925) at a distance of 100 km from the epicenter. In practice, measurements are reduced to the standard distance of 100 km by a calibrating function established empirically. Because Wood-Anderson seismographs have been out of use since the 1970s, M_L is now computed with a simulated Wood-Anderson records or by some more practical

	methods.
Magnitude	In seismology, a quantity intended to measure the size of earthquake and is independent of the place of observation. Richter magnitude or local magnitude (M_L) was originally defined in Richter (1935) as the logarithm of the maximum amplitude in micrometers of seismic waves in a seismogram written by a standard Wood-Anderson seismograph at a distance of 100 km from the epicenter. Empirical tables were constructed to reduce measurements to the standard distance of 100 km, and the zero of the scale was fixed arbitrarily to fit the smallest earthquake then recorded. The concept was extended later to construct magnitude scales based on other data, resulting in many types of magnitudes, such as body-wave magnitude (m_b), surface-wave magnitude (M_s), and moment magnitude (M_w). In some cases, magnitudes are estimated from seismic intensity data, tsunami data, or duration of coda waves. The word “magnitude” or the symbol M , without a subscript, is sometimes used when the specific type of magnitude is clear from the context, or is not really important.
Maximum Regional Earthquake Magnitude (M_{max})	Upper limit of magnitude for a given seismogenic zone or entire region. Also sometimes referred to as the maximum credible earthquake (MCE) in older texts.
Operating Basis Event (OBE)	Within the ICOLD guidelines, ground motion with a mean return period of the order of 145 years i.e. 50 % probability of exceedance in 100 years.
Oscillator	In earthquake engineering, an oscillator is an idealized damped mass-spring system used as a model of the response of a structure to earthquake ground motion. A seismograph is also an oscillator of this type
Peak Ground Acceleration (PGA)	The maximum acceleration amplitude measured (or expected) of an earthquake.
Probabilistic Seismic Hazard Analysis (PSHA)	Available information on earthquake sources in a given region is combined with theoretical and empirical relations among earthquake magnitude, distance from the source and local site conditions to evaluate the exceedance probability of a certain ground motion parameter, such as the peak acceleration, at a given site during a prescribed period.
Recurrence Interval	Time interval separating, on average, the reoccurrence of earthquakes of a given size (magnitude) at a given location or on a given seismic source.
Recurrence Parameters	Parameters characterising the distribution in time of earthquakes over a given geographic region or associated with a specific seismic source, as well as their relative sizes. Recurrence parameters generally include the activity rate, the
Response Spectral Ordinate	Maximum response of a single-degree-of-freedom oscillator (defined by its natural period and damping level) to a given ground-motion input (generally, an acceleration time-series).
Response spectrum	The response of the structure to a specified acceleration time series of a set of single-degree-of-freedom oscillators with chosen levels of viscous damping, plotted as a function of the undamped natural period or undamped natural frequency of the system. The response spectrum is used for the prediction of the earthquake response of buildings or other structures.
Return Period	Reciprocal of the annual frequency of exceedance of a ground motion. Not to be confused with recurrence interval, which characterises earthquakes, but not the resultant ground motion.
Seismic Hazard	Any physical phenomena associated with an earthquake (e.g., ground motion, ground failure, liquefaction, and tsunami) and their effects on land use, man-made structure and socio-economic systems that have the potential to produce a loss. It is also used without regard to a loss to indicate the probable level of ground shaking occurring at a given point within a certain period of time.
Seismic Wave	A general term for waves generated by earthquakes or explosions. There are many types of seismic waves. The principle ones are body waves, surface waves, and coda waves.

Seismic zone	An area of seismicity probably sharing a common cause.
Seismogenic	Capable of generating earthquakes.
Sigma	Aleatory ground-motion variability, taken equal to the standard deviation (scatter) associated with ground-motion prediction equations. Sigma has a strong influence on the shape of hazard curves derived in PSHA.
Strong ground motion	A ground motion having the potential to cause significant risk to a structure's architectural or structural components, or to its contents. One common practical designation of strong ground motion is a peak ground acceleration of 0.05g or larger.
Uniform Hazard Spectrum (UHS)	Spectrum constituted by the response ordinates corresponding to the same annual frequency of exceedance or return period

Executive Summary

Presented in this report are seismic hazard analysis results for a site located in the Western Cape, South Africa, in response to a request by BKS (Pty) Ltd. Wind turbines for the generation of electricity are to be constructed on the site. The wind farm site is located in the Namaqua – Natal Belt near the boundary with the Cape Fold belt. The stress regime in the area is strike – slip with an extensional stress component. Five area seismic sources with tectonic activity and one fault source were considered in the calculation. Since there are no ground-motion prediction equations (GMPEs) derived specifically for Southern Africa, equations have been selected from other regions on the basis of tectonic similarity with the region under investigation. Equations for Eastern North America, extensional regimes and Europe were selected and applied with weights of 0.5., 0.35 and 0.15 respectively. Such uncertainties in input parameters were addressed using a logic tree approach. A peak ground acceleration value of 0.047g was obtained at 1% critical damping and return period of 475 years. Mean and median uniform hazard spectra were also calculated and presented. Deaggregation helps to explain the typical size and distance of earthquakes making the largest contributions to the seismic hazard. Allocating the total hazard into contributions based on distance and magnitude helps to close the gap between the many earthquakes that go into hazard models and the scenario earthquakes required for engineering purposes. In this investigation, we performed deaggregation at the following periods, 0.5s, 1s, 2s, and 3s. Three of the deaggregations, $S_a(0.5)$, $S_a(2.0)$ & $S_a(3.0)$ have a simple unimodal distribution, whilst that of $S_a(1.0)$ has a hint of a bimodal distribution. Nearby sources (13 to 15km) at all spectral parameters are dominant with dominant magnitudes varying from 5.8 to 6.4.

1.0 Introduction

The work presented in this report is in response to an enquiry sent to Council for Geoscience (CGS) by Mr H. J. Tluczek of BKS (Pty) Ltd, requesting a seismic hazard investigation for a site located in the western Cape, South Africa, at coordinates (18.105°E, 31.518°S). Their client, ESKOM, intends to construct wind turbines at the site for generation of electricity. As requested by BKS (Pty) Ltd, the CGS provided ground motion parameters required for the seismic design of the wind farm. These included Peak Ground Acceleration (PGA) values, uniform hazard spectrum (UHS) for 10% probability of exceedance in 50 years (475 year return period, or 1: 475 annual frequency of exceedance) and deaggregation. No specific building code was provided to guide the work, but the CGS was informed by the client to assume guidelines for a normal multi-story building.

1.1 Scope of Work

The scope of work agreed between BKS (Pty) Ltd and the CGS, included the following elements:

- Review of local / regional geological and seismological information within 300km of the site;
- Preparation of a regional seismotectonic model on the basis of the earthquake catalogue defined above, as well as geological information regarding the tectonic structures of the area.
- Ground motion assessment in terms of PGA and UHS for a return period of 475 years.
- Deaggregation of spectral accelerations (Sa(0.5), Sa(1.0), Sa(2.0) and Sa(3.0)).

The seismic hazard assessment was performed based on a very simple geological model at the request of the client. This assessment considered the contributions of natural seismicity to the ground-shaking hazard, using a simplified seismotectonic model based on existing seismological data. The calculations were carried out within a probabilistic framework, and included consideration of

uncertainties associated with the inputs. These uncertainties were treated using a logic-tree methodology.

2.0 Seismotectonic setting

In seismic hazard analysis it is necessary to define a seismotectonic model for the region of interest. The model is derived through an analysis of structural, neotectonic and seismological data to establish links between seismicity and current deformation mechanisms with the ultimate goal being to individualize and delimit the different seismotectonic units (Terrier *et al.*, 2000). Seismotectonic units correspond to individual tectonic structures (*e.g.*, faults) or to geological and structural bodies of uniform seismicity. An ideal delineation of seismotectonic units requires a complete comprehension of the general geological setting and regional tectonics, including information regarding both historical and instrumental seismicity, as well as palaeoseismic and neotectonic features. However, information of this kind is often found to be incomplete, particularly in regions of low-to-moderate seismicity such as South Africa. As a result, uncertainties in the seismotectonic model were addressed.

2.1 Regional setting

Southern Africa is generally classified as a stable continental region (SCR, Johnston *et al.*, 1994), bounded to the northeast by the East African Rift system. The wind farm site is located in the Namaqua – Natal Belt near the boundary with the Cape Fold belt (Figure 1).

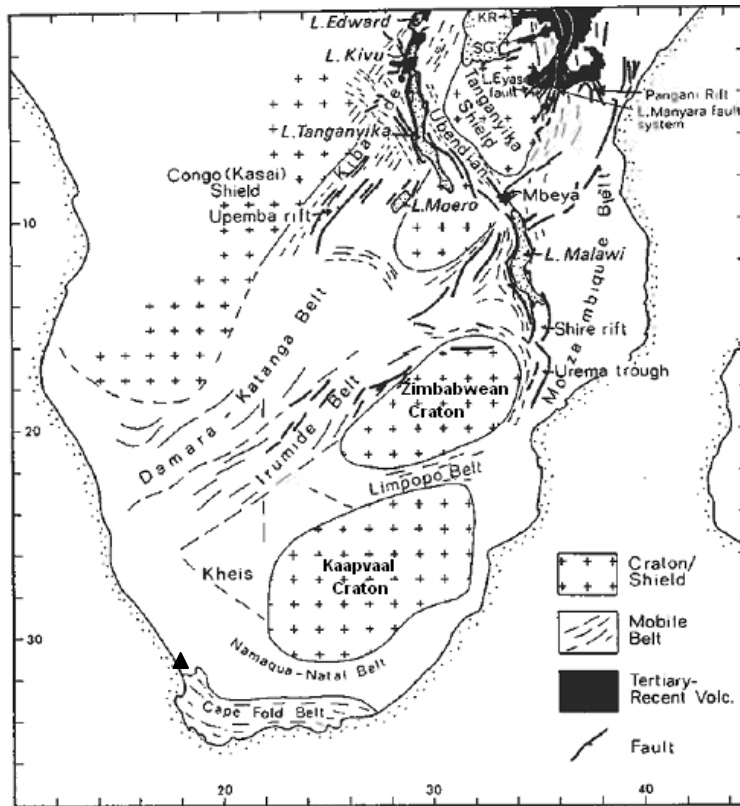


Figure 1: Basement geology of southern Africa showing the relation of the East African Rift system with respect to the mobile belts and continental cratons, Black triangle is proposed location of Wind farm site (Adapted from Fairhead & Stuart, 1982).

2.2 Types of seismicity

The seismic events encountered in the Southern Africa region (Figure 2) are generally classified into the following types (e.g., Gibowicz & Kijko, 1994):

- **Tectonic events:** these are earthquakes occurring naturally due to slip on capable faults; in stable continental regions, tectonic earthquakes can reach moderate-to-large (M 6 to 7) magnitudes, although the occurrence of such events is infrequent;

- **Mining-related events:** these are earthquakes occurring on tectonic faults, but which are thought to have been induced by stress changes created by mining activities. Such events can occasionally reach moderate magnitudes (M 4 to 5). However, ground motions from mining-related earthquakes attenuate much faster with distance than those from tectonic earthquakes. The wind farm site is located at a great distance (> 600km) from the nearest seismically active mining areas. Therefore, mining-related events were not considered in this hazard calculation.
- **Rockbursts and explosions:** these are events directly related to mining operations (e.g. blasts at Piketberg); such events are too small ($M < 3$) to generate ground motions that could affect engineered structures located outside the perimeter of the mine, and were therefore not considered here.

Criteria to distinguish between mining-related and natural seismicity generally concentrates on filtering out explosions. However, in the current study, the distinction is made based on the depth of the event:

- any event with a known depth less than 5km and located in known mining areas was classified as a mining-related event;
- any event with a known depth of at least 5 km or whose depth is unknown (as is the case for many historical tectonic events) was classified as tectonic.

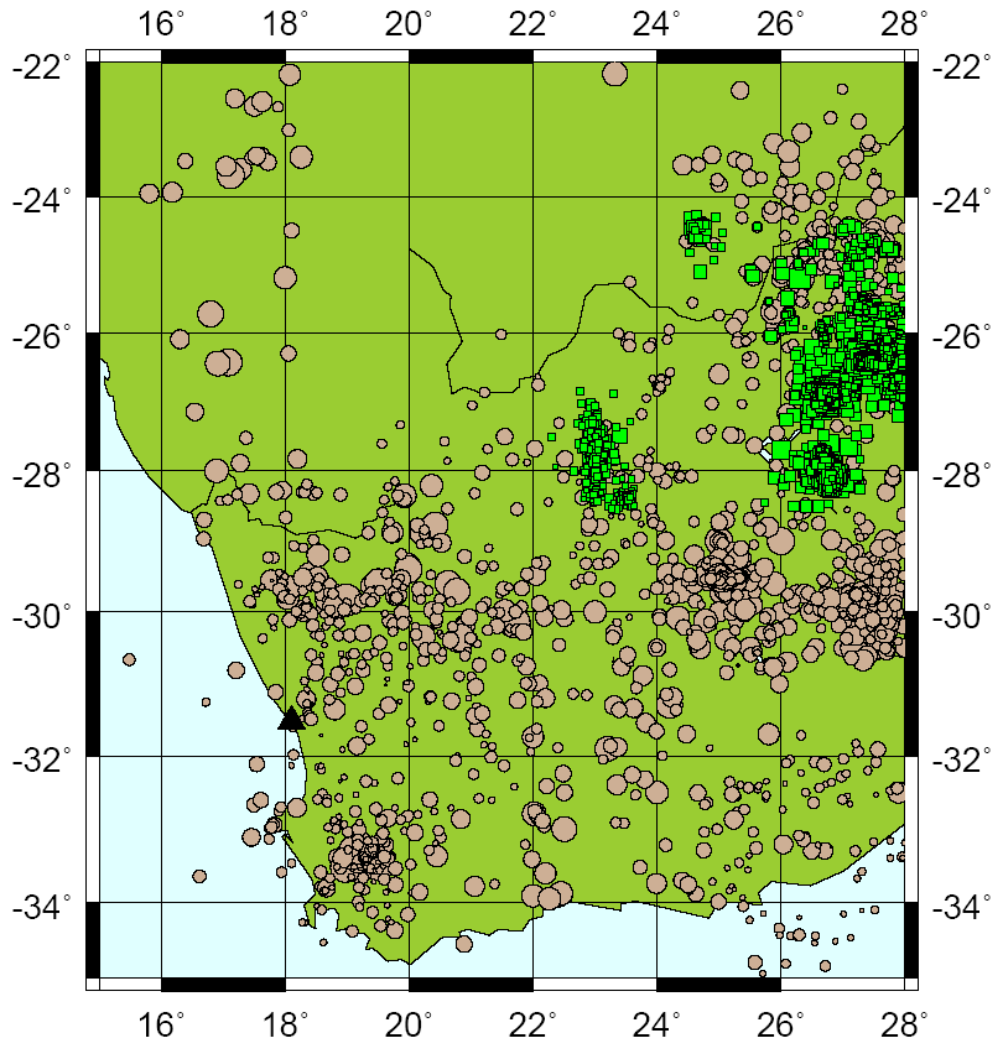


Figure 2. Spatial distribution of all earthquakes in the Council for Geoscience catalogue. Brown circle locations represent tectonic events whilst green square locations represent mining related seismicity. Events identified as explosions or likely explosions have been removed. Black triangle – Eskom Sere Wind farm Site.

2.3 Tectonic seismicity

Despite being a predominantly stable region, Southern Africa experiences a low level of seismicity. The regional stress field indicates an extensional tectonic regime, associated predominantly with normal faulting, as illustrated in Figure 3, but with a strike-slip stress regime in the South West corner of the country associated with strike-slip faulting.

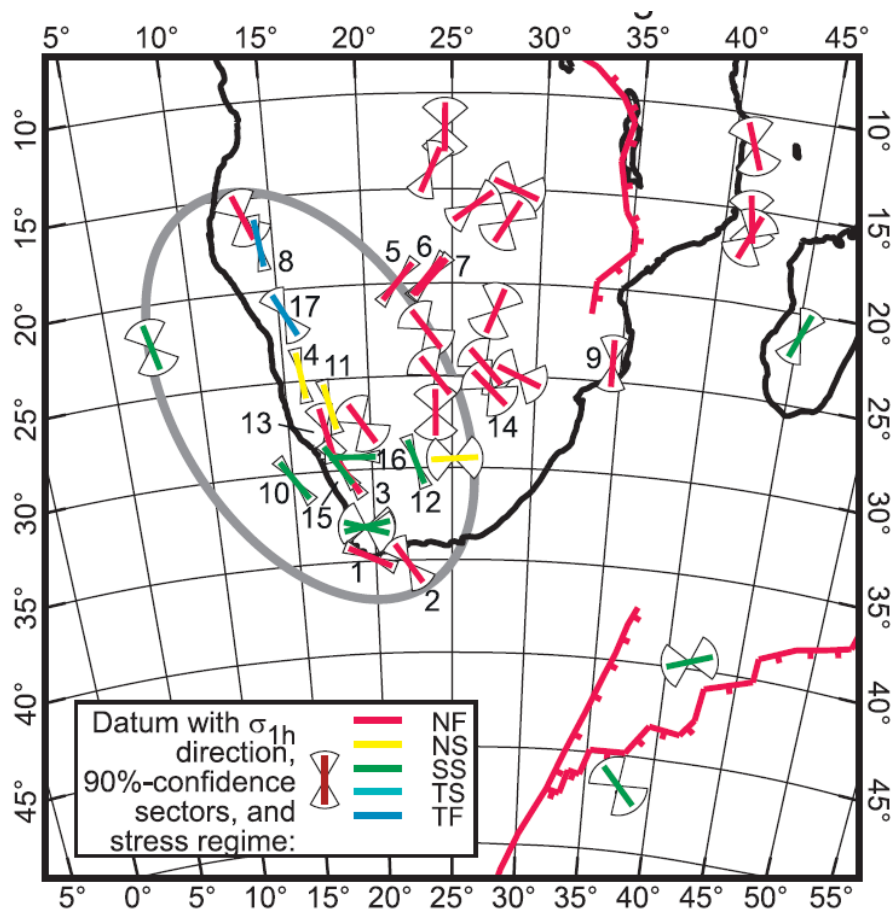


Figure 3. Intraplate stress directions and regimes in the southern Africa region (Bird *et al.*, 2006). NF = Normal Faulting; NS = Normal-Oblique Faulting; SS= Strike-Slip Faulting; TS = Reverse-Oblique Faulting; TF = Reverse (Thrust) Faulting

Seismicity in the south western part of South Africa is dominated by the cluster of events in the Ceres area (Figure 4), where the largest recorded earthquake in South Africa (M6.3, 29 September 1969) was located. Moderate seismicity is also observed to the north of the site in the Namaqua – Natal belt. Since seismic hazard analysis requires the derivation of rates of independent events, the catalogue was subjected to a declustering procedure in order to remove dependent events such as foreshocks, aftershocks and event clusters. The declustering was carried out using the technique described in Gardner & Knopoff (1974). The calculation of recurrence parameters is done using the declustered catalogue.

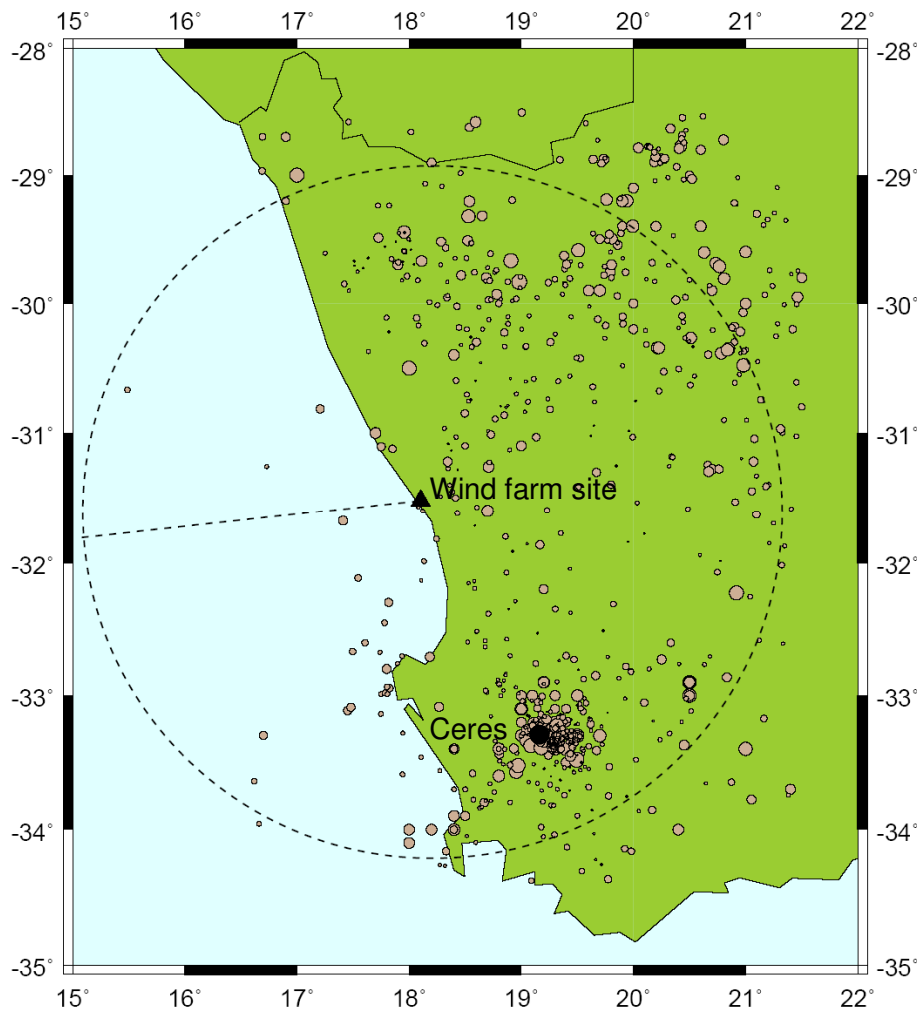


Figure 4. Locations of seismicity used in this investigation as obtained from the SANSN database. The circle of broken line marks a boundary of events in an area of radius 300km used in the calculation.

3.0 Seismic Source Characterisation

The seismic source model includes all seismic sources deemed capable of contributing to the ground-motion hazard at the site. In site seismic hazard studies dealing with tectonic seismicity, it is customary to include any source located within a radius of 300 km from the site. Additionally, any major fault structure identified in the immediate vicinity of the site that is considered to be potentially active, and can be clearly defined and characterised, is included as an individual source.

The seismic sources considered in the present study are shown in Figure 5. They include five area source zones (in which the distribution of seismicity is assumed to be spatially uniform, *i.e.* an earthquake of a given size is equally likely to occur at any point within the zone) and one fault zone. These sources are described individually below.

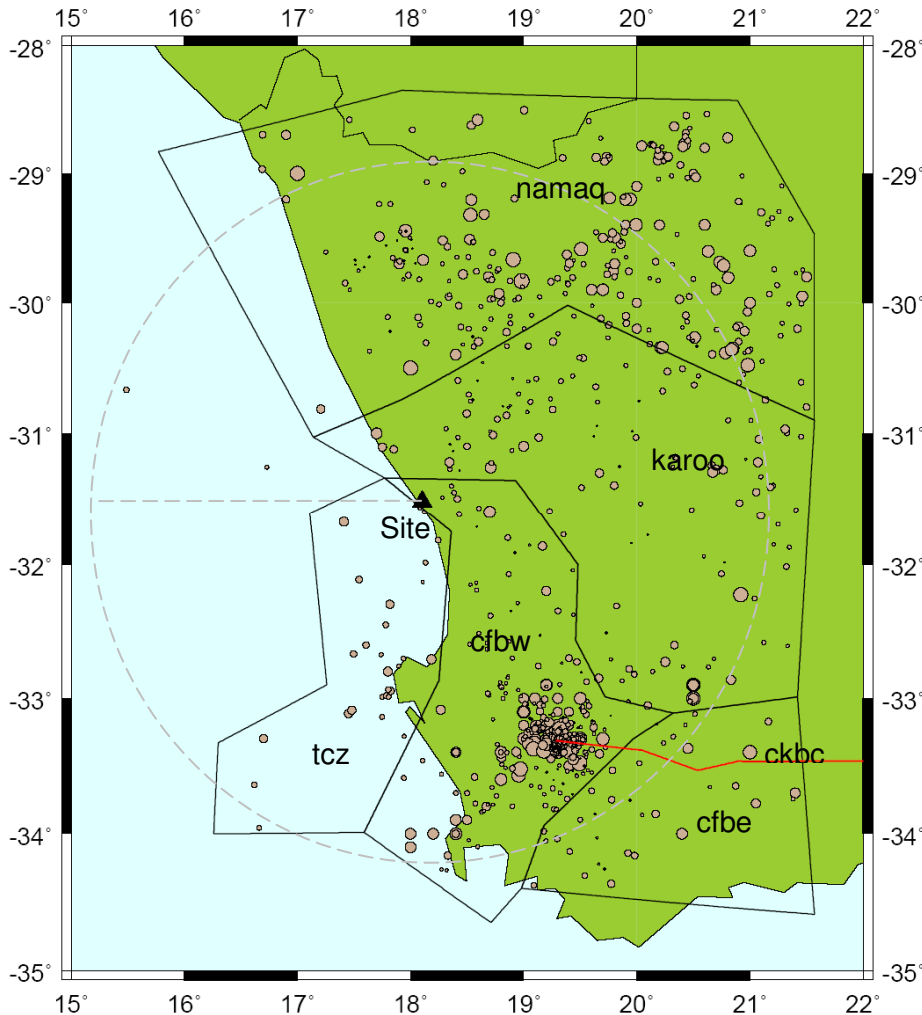


Figure 5. Seismic source model based on structural data and tectonic seismicity.

Cape Fold Belt West (cfbw)

This is a zone of concentrated activity including the Ceres cluster, located in the syntaxis region between east – west trending structures to the east and northerly trending structures in the western part of the Cape fold belt. The style of faulting in the zone is a mixture of strike – slip and normal faulting.

Cape Fold Belt East (cfbe)

The cfbe zone is modelled separate from cfbw by considering that there is a marked change in observed rates of seismicity between the syntaxis region and the east-west-trending structures in the eastern part of the fold belt. The observed style of faulting is predominantly normal faulting.

Namaqualand West (namaq)

The western part of the Namaqua-Natal belt is modelled as an area source zone hereafter referred to as the Namaqualand West (namaq) Zone. The boundaries of this zone are consistent with those defined by Hartnady & Partridge (1995). The observed seismicity, which is of normal faulting, is related to the presence of the Namaqua-Natal mobile belt. The stress regime (Johnston *et al.*, 1994) is extensional, NNE-SSW to ENE-WSW, based on focal mechanisms (Johnston *et al.*, 1994).

Karoo Low Zone (karoo)

The Karoo Low area correlates with positive gravity and magnetic anomalies and is a zone of relatively low seismicity. The northern boundary of the zone is modified from the southern boundary of Zones B and C of du Plessis (1996), whilst the southern boundary is on the limit of the Cape Fold Belt.

This region is also modeled as an area zone and referred to as the Karoo Low zone. Observed seismicity is of predominantly normal faulting.

Transitional Crust Zone (tcz)

This is a zone of crust considered to be transitional between the continental crust making up the zone cfbw and the extended oceanic crust to the west. The zone includes low seismicity of strike slip faulting.

Ceres – Kango – Bavianskooft – Coega Fault system (ckbc)

One of the seismic sources is modelled as a fault zone. The fault is located south east of the site and extends across almost the whole EW extension of the Cape Fold belt. Micro-seismicity of normal faulting has been associated with the fault as well as paleoseismological evidence of an early Holocene event of magnitude $M = 7.18 - 7.43$ (Goedhart, 2009)

3.1 Earthquake recurrence parameters

In order to assess the seismic hazard at the site, the seismic sources need to be characterised in terms of their earthquake recurrence, *i.e.* the relative frequency of occurrence of earthquakes with different sizes, as well as the maximum magnitude for each source.

The following recurrence parameters (Table 1) were determined for each source zone based on the earthquake catalogue. All five area sources were assumed to follow a Gutenberg-Richter distribution. The activity rate, $\lambda (M_L \geq 5.0)$ denotes the average number of earthquakes with a magnitude greater than or equal to 5.0 occurring each year. The b-value represents the slope of the Gutenberg-Richter relation, and controls the relative frequency of occurrence of earthquakes of different magnitudes. The

M_{max} values were deduced from the maximum observed magnitude values and are defined as the maximum possible earthquake magnitude for each source zone. In this investigation the parameters b value and M_{max} were determined using the maximum likelihood method.

Table 1. Recurrence parameters for area sources (In brackets are associated weights)

Seismic Source Zone	Maximum observed M_L	M_{max}	$\lambda(M_L \geq 5.0)$	b value
cfbw	6.3	6.75	0.0741	0.73
cfbe	5.2	5.61 (0.3)	0.0676	0.83
		7.20 (0.7)		
namaq	5.8	6.29	0.0708	0.86 (0.6)
			0.0831	1.03 (0.4)
karoo	5.6	5.90	0.0398	0.72
tcz	5.0	6.75	0.00263	0.95

For the ckbc fault source, two alternative recurrence models were used, the characteristic magnitude model of Youngs & Coppersmith (1985), and the maximum moment model. The first model was given a weight of 0.8, whilst the second one was given a weight of 0.2. For each model, two slip rates were assumed, 0.004 and 0.02 mm/year (Goedhart & Saunders, 2009). The M_{max} values were estimated from various fault properties (rupture area, subsurface rupture length, maximum displacement), which in turn depend on the crustal thickness and dip assumed. For the characteristic approach, three values of the recurrence rate (b -value) were considered (Table 2).

Table 2. Recurrence parameters adopted for the ckbc fault source

Crustal thickness (km)		Dip (degrees)		Slip rate (mm / year)		b value	
	Weight		Weight		Weight		Weight
10	0.3	45	0.4	0.004	0.6	0.85	0.185
12	0.4	60	0.4	0.02	0.4	0.95	0.630
15	0.3	70	0.2			1.05	0.185

4.0 Ground Motion Models

The ground-motion model predicts the distribution of ground-motions expected conditional on the occurrence of a given earthquake scenario (usually characterised in terms of magnitude, source-to-site distance and site conditions).

4.1 GMPE Selection

Ground motions from tectonic earthquakes

Since there are no ground-motion prediction equations (GMPEs) derived specifically for Southern Africa, equations were selected from other regions on the basis of tectonic similarity with the region under investigation.

- In view of its position relative to plate boundaries, relatively low level of earthquake activity, and the slow rates of crustal deformation, Southern Africa is generally considered a Stable Continental Region (SCR). Therefore, eastern North America (ENA) can be assumed to be analogous southern Africa. There are a number of ground-motion models for ENA. The selected SCR equation was presented by Atkinson & Boore (2006). It has the advantage of specifically including the average shear-wave velocity over the uppermost 30m, V_{S30} , as a predictive parameter.
- Unlike ENA, however, the current Southern African tectonic regime shows evidence of extensional tectonic stresses with normal faulting (Figure 3). Studies such as that by Johnston

et al. (1994) show that extensional tectonic stresses are uncommon within SCR, for which reason the equation of Pankow & Pechmann (2004), which is an update of the equation of Spudich *et al.* (1999) for extensional regimes, was also included.

- Finally, the geographic extension of the East African Rift to the south is poorly constrained and the mobile belt provinces of Southern Africa may in fact be somewhat more seismically active than typical SCRs, such as the central and eastern United States. Therefore, an equation from regions of active crustal seismicity was also included, although given a lower weight. The selected equation is that of Akkar & Bommer (2007) for Europe and the Middle East. It would have been equally acceptable to select one of the equations from the Next Generation of Attenuation (NGA) models, such as that of Boore & Atkinson (2008) for coastal California, which have been shown to predict ground motions that are closely comparable to those obtained from recent European equations (Stafford *et al.*, 2008). European equations, however, tend to include a larger proportion of data from normal-faulting events.

4.2 Parameter adjustments

It is important that equations used in seismic hazard calculations are consistent in terms of the variables considered. Therefore, where there are differences in terms of the definitions employed for the explanatory variables used in the parameterisation of the equation, or in the horizontal component definition used for the predicted variable, adjustment factors need to be applied (Bommer *et al.*, 2005).

Horizontal component definition

All ground motions calculated in the seismic hazard analysis are for the geometric mean of the two horizontal components of motion, which is the most commonly used horizontal component definition. The GMPEs considered here already use this component definition (Table 3).

Table 3. Horizontal component adjustments

Equation	Horizontal Component Definition	Adjustment
Atkinson & Boore (2006)	Geometric Mean	Not required
Pankow & Pechmann (2004)	Geometric Mean	Not required
Akkar & Bommer (2007)	Geometric Mean	Not required

Magnitude

The CGS catalogue of Southern African seismic events characterises event size in terms of local magnitude (M_L), whereas most of the GMPEs adopted for the hazard calculations use moment magnitude (M_w) (Table 4). In the absence of a locally derived magnitude conversion relationship, the assumption was made that for the range of magnitudes covered ($M_w \geq 5.0$), these two magnitude scales can be considered equivalent, *i.e.*, $M_L \cong M_w$. Although empirical relations between M_L and M_w generally show differences, there is theoretical support for the equivalence between these two magnitude scales (Deichmann, 2006).

Table 4. Magnitude adjustments required

Equation	Magnitude Scale	Adjustment
Atkinson & Boore (2006)	M_w	Not required ($M_L \sim M_w$)
Pankow & Pechmann (2004)	M_w	Not required ($M_L \sim M_w$)
Akkar & Bommer (2007)	M_w	Not required ($M_L \sim M_w$)

Distance

While the GMPE's considered use different distance metrics (Table 5), an explicit adjustment was not required since the hazard calculations use the appropriate distance metric in each case.

Table 5. Summary of distance metrics used in selected GMPE's

Equation	Distance Metric	Adjustment
Atkinson & Boore (2006)	Closest distance to fault rupture (R_{rup})	Not required
Pankow & Pechmann (2004)	Closest distance to surface projection of fault rupture (R_{jb})	Not required
Akkar & Bommer (2007)	Closest distance to surface projection of fault rupture (R_{jb})	Not required

Style-of-faulting

Although the GMPEs used in the hazard calculations were selected in order to be compatible with the tectonic setting of Southern Africa, the composition of the underlying dataset in terms of style-of-faulting is not always consistent with the predominantly normal faulting mechanisms of Southern African earthquakes. Therefore, adjustment factors to normal-faulting conditions were calculated based on the method of Bommer *et al.* (2003), as summarised in Table 6. For the Akkar & Bommer (2007) model, the style-of-faulting can be set explicitly and normal-faulting conditions are adopted.

Table 6. Style-of-faulting adjustments

Equation	Style-of-Faulting	Adjustment
Atkinson & Boore (2006)	Not included explicitly. Dataset is assumed to be 80% Reverse, 20% Strike-slip	$F_{N:EQ} = 0.8103$ for PGA $F_{N:EQ} = 0.8266$ at 0.2 s $F_{N:EQ} = 0.8615$ at 1.0 s
Pankow & Pechmann (2004)	Not included explicitly. Dataset is assumed to be 55% Strike-slip, 45% Normal	$F_{N:EQ} = 0.9722$ at all periods
Akkar & Bommer (2007)	3 categories (Normal, Strike-slip and Reverse)	Not required

Local site conditions

The ground-motion predictions for the site of interest need to take into consideration the local site conditions. According to communication from BKS (Pty) Ltd, the area in the vicinity of the wind farm site has bed rock with shear wave velocity of 750 – 800 m/s. Thus hazard calculations were done for engineering bed rock of $V_{S30} = 750\text{m/s}$.

The generic rock conditions and the default Atkinson & Boore (2006) definition are equivalent, hence no adjustment is necessary. For the Pankow & Pechmann (2004) and Akkar & Bommer (2007) equations, this condition can be assumed to be satisfied, since generic rock corresponds to a V_{S30} value around 800 m/s (Table 7).

Table 7. Adjustments for site conditions.

Equation	Site characterisation	Adjustment
Atkinson & Boore (2006)	Explicit V_{S30} term can be set to $V_{S30} = 750$ m/s	Not required
Pankow & Pechmann (2004)	2 categories (Rock and Soil)	Not required
Akkar & Bommer (2007)	3 categories (Rock, Stiff Soil and Soft Soil)	Not required

5.0 Probabilistic Seismic Hazard Analysis and Results

5.1 General Assumptions

The probabilistic seismic hazard calculations were carried out using the FRISK88M software developed by Risk Engineering, Inc, Boulder Colorado, USA. The following assumptions were made:

- All calculations were made for the return period of 475 years, where the return period (RP) is the reciprocal of the annual frequency of exceedance (AFE).
- The minimum magnitude adopted was $M_{\min} = 5.0$, which is consistent with the practice of excluding frequent, small events of little engineering significance.

5.2 Logic Tree

The logic-tree approach is used in seismic hazard analyses to incorporate epistemic uncertainty (uncertainty related to the lack of data or knowledge) by considering and ranking alternative options.

Ground-Motion Model

The selection of the appropriate ground-motion model is one of the major sources of uncertainty in seismic hazard analysis. Table 8 summarises the selected equations and the weights assigned to them in this study. The weights were assigned on the basis of the current state of knowledge.

- The sources within the mobile belt regions of South Africa could equally be a stable region or a region of more active, dominantly extensional tectonics. Consequently, the equation for ENA

was given a weight of 0.5. In broad terms, it is considered quite possible that the mobile belt provinces of South Africa are regions of active tectonic extension, so the equation of Pankow & Pechmann (2004) was given a weight of 0.35. Since it is somewhat less likely that these provinces are comparable to active crustal regions such as California and southern Europe, the Akkar and Bommer (2007) equation has a weighting of 0.15.

Table 8. Weighting of GMPEs for all sources

Atkinson & Boore (2006)	Pankow & Pechmann (2004)	Akkar & Bommer (2007)
0.50	0.35	0.15

Crustal Thickness

Crustal thickness is an estimate of the maximum thickness of the seismogenic crust. This assessment is made based on consideration of the focal depth distribution of instrumental earthquakes, tectonic models of the crust, and analogues to comparable tectonic environments (where accurate focal depth information is available). Given that we have limited information on earthquake focal depth in the region, three possible depth values were selected according to existing knowledge. These values were allocated weights as shown in Table 9.

Table 9. Weighting of crustal thickness values assigned for all source zones

Depth (km)	Weight
10	0.2
12	0.6
15	0.2

The logic tree was also implemented to address the various alternative recurrence parameters selected for the fault source (Table 2).

6.0 Results

The following results (Figure 6) represent the seismic hazard aggregated over all sources considered in the PSHA. The values (Table 10) include consideration of the site amplification through correction of the GMPE's used to represent a site with bed rock of average shear-wave velocity of $V_{S30} = 750$ m/s.

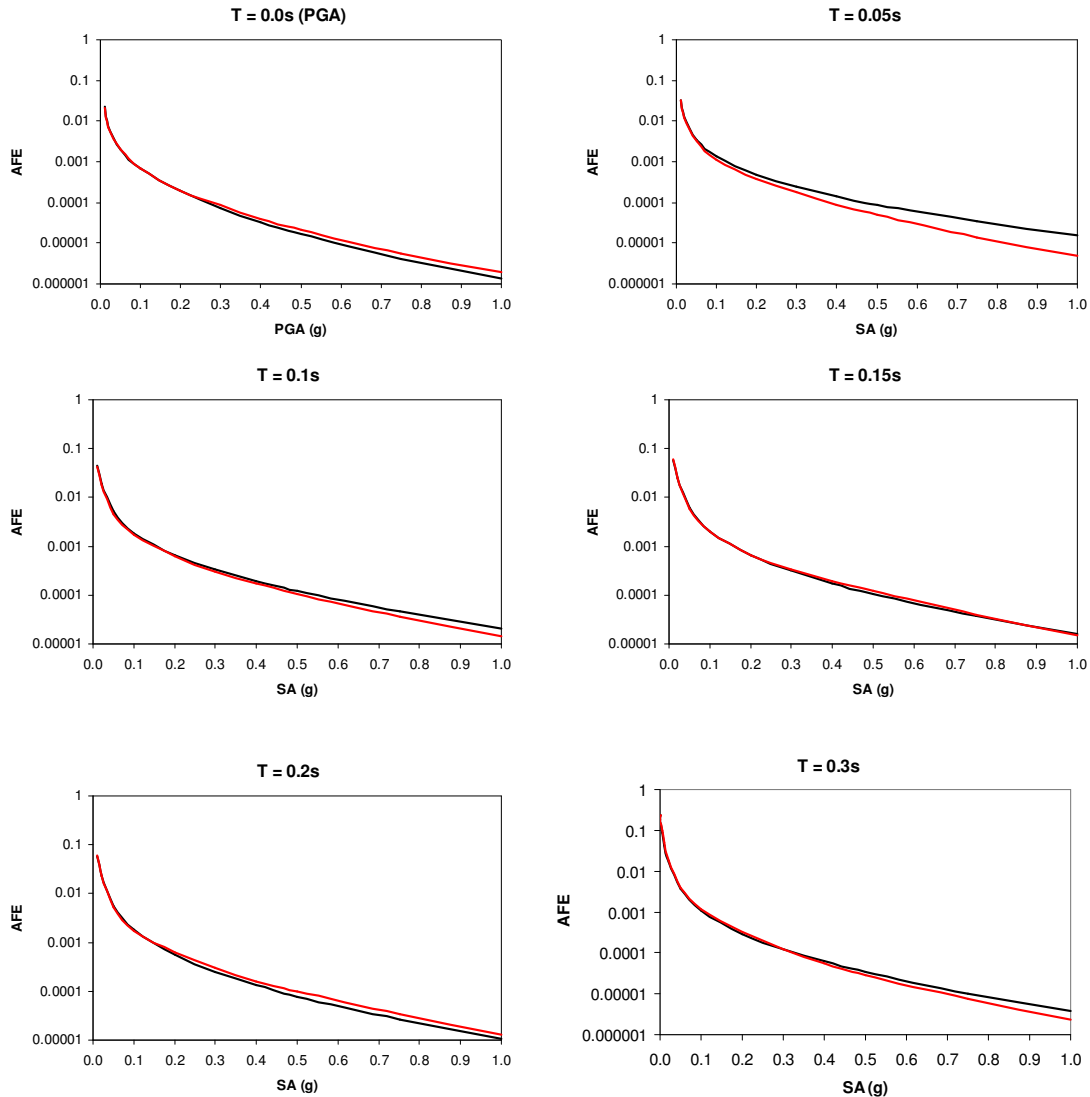


Figure 6. Mean (black line) and Median (red line) hazard curves at various preselected spectral parameters. AFE = Annual Frequency of Exceedance and SA = Spectral acceleration in g (9.8m/s^2)

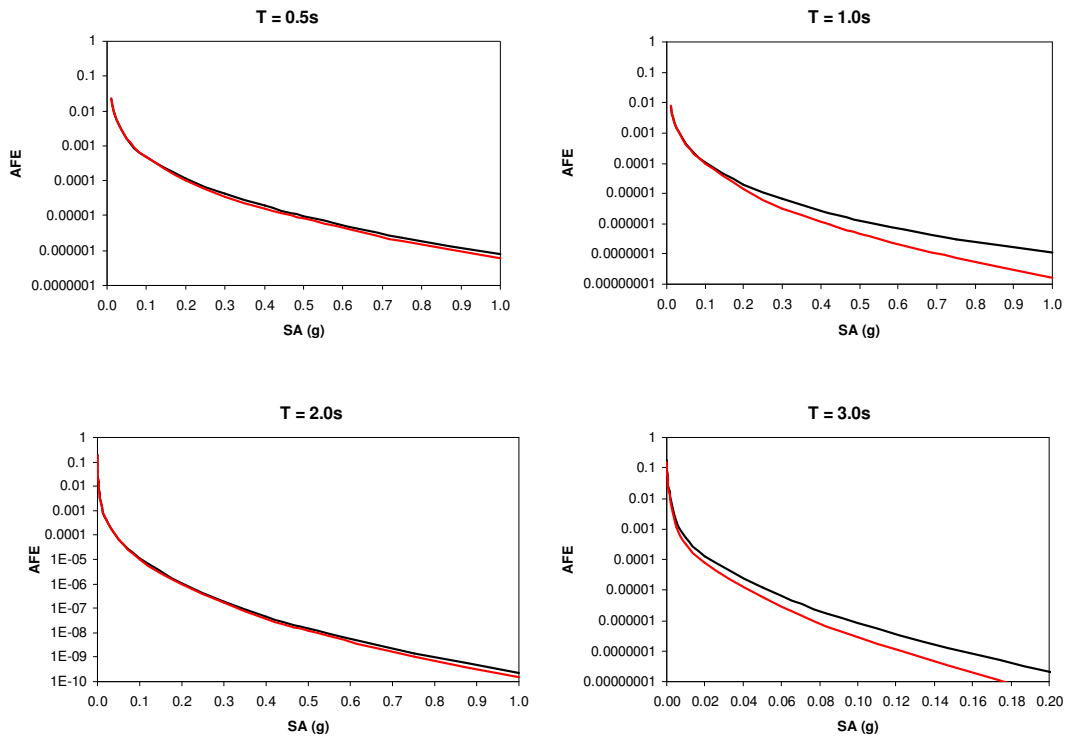


Figure 6. Mean (black line) and Median (red line) hazard curves at various preselected spectral parameters. AFE = Annual Frequency of Exceedance and SA = Spectral acceleration in g (9.8m/s^2)

As agreed to with the client, ground motion values were extracted from the data illustrated in Figure 6, for an annual frequency of exceedance (AFE) value of 1: 475 years (10% probability of exceedance in 50 years). The ground motion is given as spectral acceleration values in Table 10. Both mean and median results are presented for comparison. However, it is standard practice to use the mean values for less critical structures, especially where high annual frequencies of exceedance are considered.

Table 10. Mean and Median ground motions (GM) for annual frequencies of exceedance (AFE) of 1:475 expected at the wind farm site (PGA – Peak Ground Acceleration; SA – Spectral Acceleration)

Ground-Motion Parameter	Mean Expected GM Level (g)		Median Expected GM Level (g)	
	5% Damping	1% Damping	5% Damping	1% Damping
PGA (0.0s)	0.047	0.047	0.047	0.047
SA at 0.05s	0.0705	0.094	0.0655	0.087
SA at 0.10s	0.091	0.121	0.087	0.116
SA at 0.15s	0.0975	0.130	0.0945	0.126
SA at 0.20s	0.089	0.119	0.088	0.117
SA at 0.30s	0.0672	0.090	0.0705	0.094
SA at 0.50s	0.0435	0.058	0.0427	0.057
SA at 1.00s	0.022	0.029	0.021	0.028
SA at 2.00s	0.0081	0.011	0.0079	0.011
SA at 3.00s	0.0046	0.006	0.0038	0.005

Seismic hazard information is based on an inherent structural damping of 5%. Currently, discussion exists regarding the appropriate level of damping for use in modeling wind turbines for seismic loading. Factors such as operational state and direction of base excitation in comparison to wind direction will directly influence the effective damping (Prowell & Veers, 2009). However, in this simplified investigation, we are not modeling for all these factors. Thus 1% of critical damping, as suggested in IEC Annex C (IEC, 2005), was used. The 5% damped design response spectrum was adjusted to account for the assumed 1% damping in the turbine (Figure 7). Most published methods (Newmark and Hall, 1982; Naeim and Kircher, 2001; FEMA, 1998) for scaling a design response spectrum use a damping adjustment factor, B , to scale the 5% damped design response spectrum, R_5 , to the design response spectrum with the desired level of damping, R_x , following the relation:

$$R_x = \frac{R_{5\%}}{B} = \frac{R_{5\%}}{0.75} = R_{1\%}$$

Often B is considered to be a function of structural period. However, Naeim and Kircher (2001) suggest, based on an investigation of over 1,000 recorded acceleration time histories, that it is not necessary to vary the adjustment factor with the period. Adjustment factors for design response spectra to account for differences in damping are published from 2% to 20%. Since the IEC recommended damping level of 1% is outside of this range, the adjustment factor was extrapolated to 1% which resulted in a value of approximately 0.75 (Table 10).

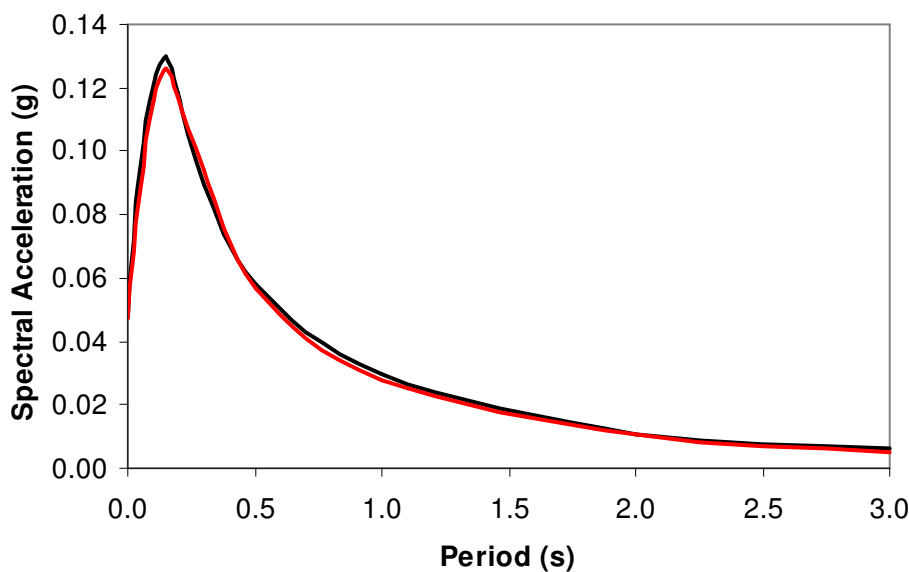


Figure 7: Uniform Hazard Spectra at 1% damping for return period (RP) of 475 years expected at the Wind farm site. (Mean – Black line; Median – red line)

6.1 Deaggregation

Deaggregation helps to explain the typical size and distance of earthquakes making the largest contributions to the seismic hazard. Allocating the total hazard into contributions based on distance and magnitude helps to close the gap between the many earthquakes that go into hazard models and the scenario earthquakes required for engineering purposes (Bazzurro & Cornell, 1999; Halchuk *et al.*, 2007). This leads to better choices for the characteristics of the design earthquake, as well as better choice of time histories. In this investigation, we performed deaggregation at the following periods,

0.5s, 1s, 2s, 3s using the MRE88 software, which is part of the FRISK88M software package. Performing deaggregations at more than one period helps to determine if one source dominates at all periods and also clarify the need for one, or more than one, design earthquake scenarios. In the processing we used 4 different sets of distance – magnitude bins to determine the best values to give accurate deaggregations. Presented here are results obtained using 10 km-wide distance and 0.2 unit-wide magnitude bins.

Our results also show the relative contributions to hazard from various levels of epsilon (ϵ). Epsilon is the normalised residual of the distribution of logarithmic ground-motion amplitudes, generally assumed to follow a normal distribution, and therefore represents a measure of the deviation from the median ground-motion value (Strasser *et al.*, 2008). Deaggregation with respect to epsilon therefore indicates whether the M-R- ϵ scenarios contributing most to the hazard are close to the expected ground-motion for M-R, i.e. $\epsilon=0$, and quantify the level of deviation when this is not the case.

The deaggregation plots showing contributions to hazard for the four spectral parameters are shown in Figure 8. The bar graphs give a visual impression of the contribution from each magnitude – distance bin. The contributions from various levels of epsilon are shown in Figure 9. In Table 11, are the mean / median distances and magnitudes selected for the site for spectral acceleration at 0.5, 1, 2 and 3 seconds at 10% probability of exceedance in 50 years.

Three of the deaggregations, Sa(0.5), Sa(2.0) & Sa(3.0) have a simple unimodal distribution. Only that of Sa(1.0) has a hint of a bimodal distribution. In all cases the influence on hazard of earthquakes of moderate size at close distances (Figure 8, Table 11) to the site are significant. The bimodal distribution in Sa(1.0) (Figure 8), implies a strong influence on hazard by a wider range of earthquake magnitudes. The mean and modal magnitude values are comparable; similar for the mean and modal distance values (about 13 - 15km). Nearby sources (13 to 15km) at all spectral parameters are

dominant with dominant magnitudes varying from 5.8 to 6.4. However, as expected, the larger magnitudes have more influence at longer periods. These results reflect the strong influence on hazard at the site of the Cape Fold Belt West (cfbw) seismic source in which the site is located.

Epsilon deaggregation (Figure 9) shows that the hazard is dominated by ground motions larger than the median, with period-dependent deviations: for 0.5s, most contributions are from ϵ values between 2 and 3, for 1.0s from ϵ values between 2.5 and 3.5, and for 2.0s and 3.0s, from ϵ values between 1.0 and 2.0.

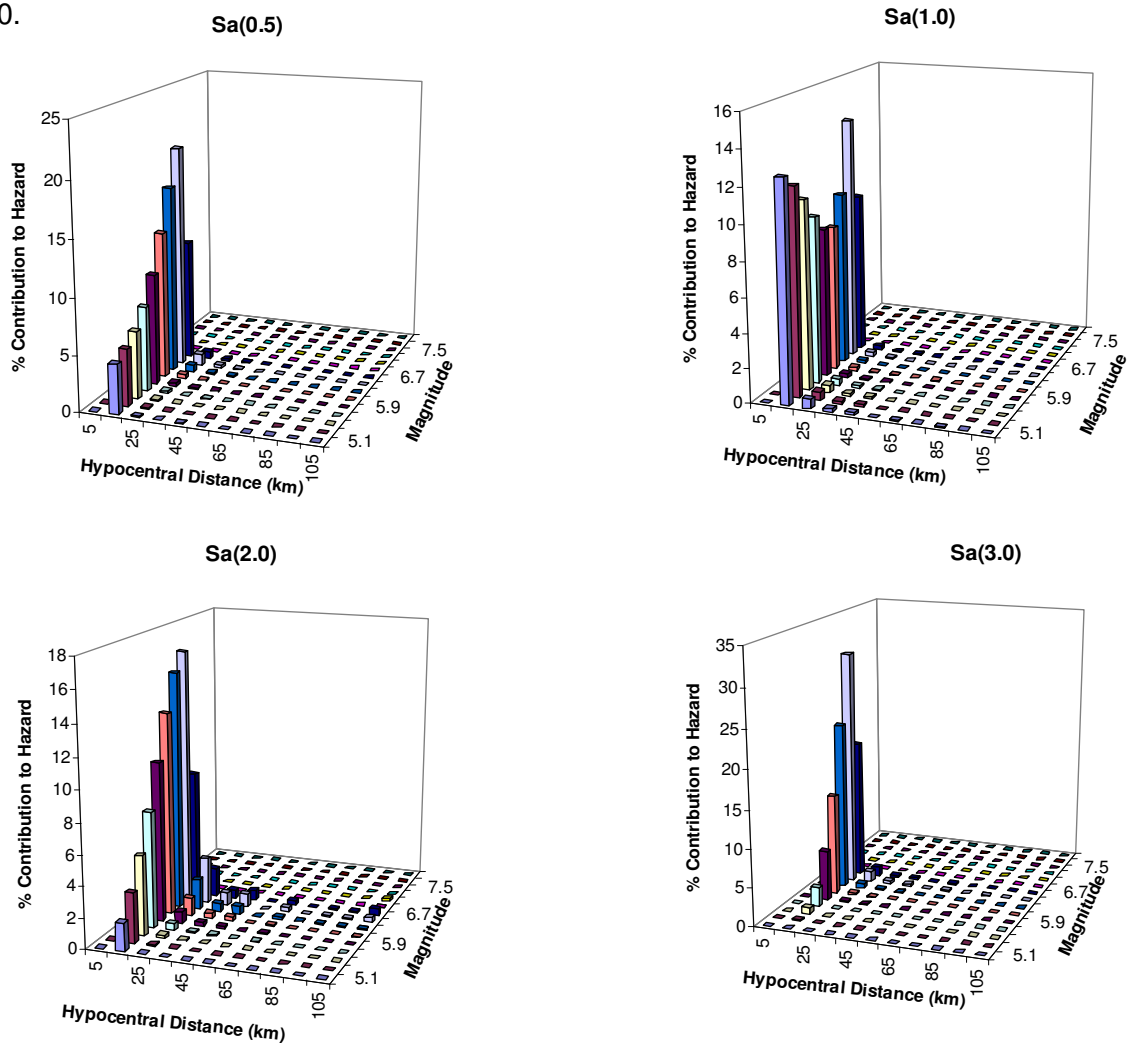


Figure 8. Deaggregation of the SERE Wind Farm site spectral acceleration at four different periods for 10% probability of exceedance in 50 years.

Table 11. Mean and median distances (**D**), magnitudes (**M**) and epsilon (**ε**) for the wind farm site for Sa(0.5), Sa(1.0), Sa(2.0) and Sa(3.0) at 10% probability of exceedance in 50 years.

Period (s)	Distance (km)		Magnitude		Epsilon	
	Mean	Median	Mean	Median	Mean	Median
0.5	15.9	13.8	6.1	6.25	2.28	2.3
1.0	15.9	13.75	5.8	5.85	2.93	2.9
2.0	20.6	13.75	6.1	6.25	1.64	1.5
3.0	16.3	13.75	6.3	6.45	1.70	1.7

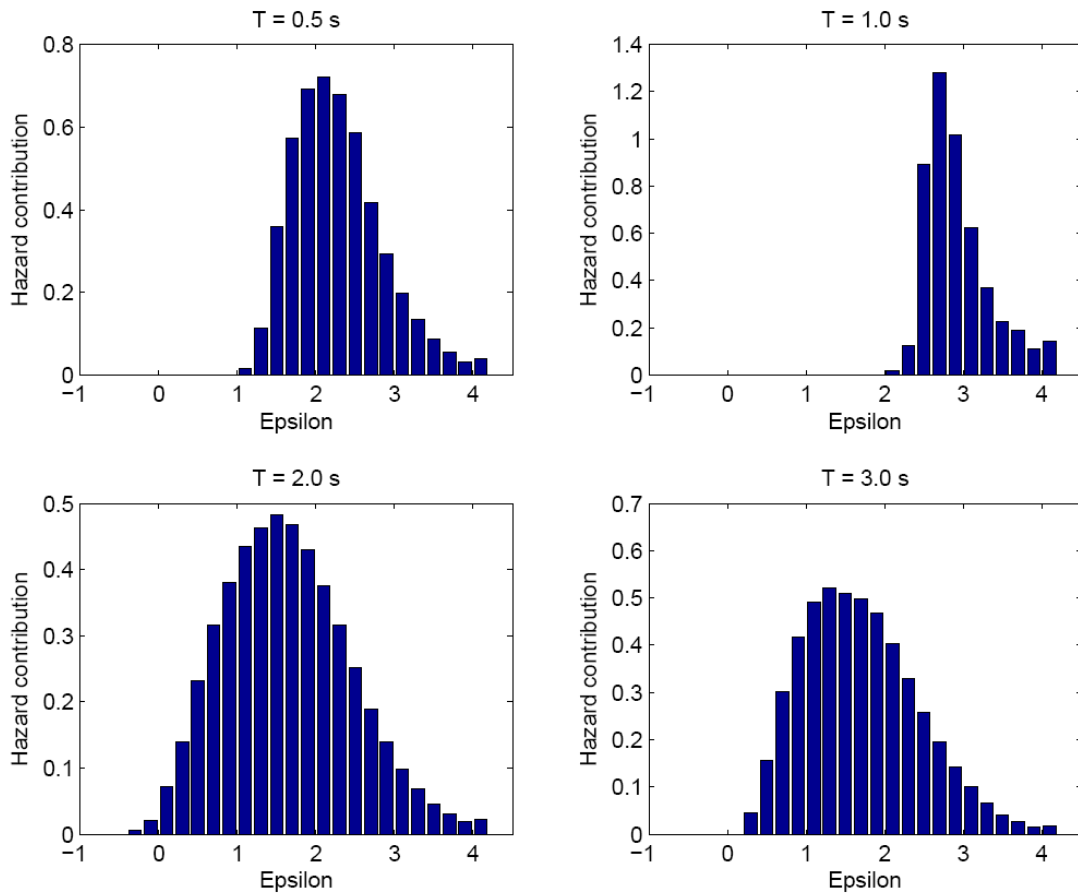


Figure 9. Hazard contribution by Epsilon at period, T = 0.5, 1.0, 2.0 and 3.0 s.

7.0 Conclusions

The following conclusions were reached for horizontal ground motion predicted for the Eskom SERE wind farm site:

- A site-specific probabilistic seismic hazard assessment determined site-specific ground-motion parameter values, corresponding to ground motion defined as that motion having a 10% probability of being exceeded over a lifetime of 50 years, (or annual frequency of exceedance (AFE) of 1:475 years). The hazard was determined for rock defined by a shear wave velocity of 750m/s as provided by BKS (Pty) Ltd.
- The peak ground acceleration value for a return period of 475 years was determined as, $PGA_{475} = 0.047g$. Spectral acceleration values were also obtained for selected response periods (Table 10) for 1% critical damping. These values were used to prepare mean and median uniform hazard spectra (Figure 6)
- Deaggregation showed that the hazard is dominated by nearby sources (13 – 15km) with moderate sized earthquakes (5.8 – 6.4). This corresponds to major contribution to the hazard by the Cape Fold Belt West source zone.
- These values were calculated by considering a source model that included local and regional seismic sources. At the request of the client, the assessment was based on a simplified geological model and existing information only.

- It should be noted that only those effects resulting directly from shaking of the ground are considered in this study. No consideration is given to hazard at the site due to surface faulting, and to secondary effects such as tsunamis, landslides or liquefaction.

References

- Akkar, S. and J.J. Bommer (2007). Prediction of elastic displacement response spectra at multiple damping levels in Europe and the Middle East. *Earthquake Engineering & Structural Dynamics*, **36**(10), 1275-1301.
- Atkinson, G.M. and D.M. Boore (2006). Earthquake ground-motion prediction equations for Eastern North America. *Bulletin of the Seismological Society of America*, **96**(6), 2181-2205.
- Bazzurro, P., and C. A. Cornell (1999). Disaggregation of seismic Hazard, *Bulletin of the Seismological Society of America*, **89**(2), 501 – 520.
- Bird, P., Z. Ben-Avraham, G. Schubert, M. Andreoli and G. Viola (2006). Patterns of stress and strain rate in southern Africa. *Journal of Geophysical Research*, **111**, Article B08402.
- Bommer, J., F. Scherbaum, H. Bungum, F. Cotton, F. Sabetta, and N. Abrahamson (2005). On the use of logic-trees for ground-motion prediction equations in seismic-hazard analysis. *Bulletin of the Seismological Society of America*, **95**(2), 377-389.
- Bommer, J.J., J. Douglas and F.O. Strasser (2003). Style-of-faulting in ground-motion prediction equations. *Bulletin of Earthquake Engineering*, **1**(2), 171-203.
- Boore, D.M. and G.M. Atkinson (2008). Ground-motion prediction equations for the average horizontal component of PGA, PGV, and 5% damped PSA at spectral periods between 0.01 s and 10.0 s. *Earthquake Spectra*, **24**(1), 99-138.
- Choi, Y. and J. Stewart (2005). Nonlinear site amplification as a function of 30m shear wave velocity. *Earthquake Spectra*, **21**(1), 1–30.
- Deichmann, N. (2006). Local magnitude, a moment revisited. *Bulletin of the Seismological Society of America*, **96**(4A), 1267-1277.
- du Plessis, A. (1996). Seismicity in South Africa and its Relationship to the Geology of the Region. *CGS Report No. 1996-0019*.
- Fairhead, J.D. and G.W. Stuart (1982). J.D. The seismicity of the East African rift system and comparison with other continental rifts, In: Palmason, G. (Editor), *Continental and Oceanic Rifts*, American Geophysical Union Geodynamic Series, **8**, 41–61.
- FEMA (1997) *NEHRP guidelines for the seismic rehabilitation of buildings*. FEMA-273, Federal Emergency Management Agency, Washington, DC, USA.
- Gardner, J.K. and L. Knopoff (1974). Is the sequence of earthquakes in Southern California, with aftershocks removed, Poissonian? *Bulletin of the Seismological Society of America*, **64**, 1363-1367.
- Gibowicz, S.J. and A. Kijko (1994). An Introduction to Mining Seismology. *International Geophysics Series*, **55**, Academic Press, New York, 355 pp.

- Goedhart, M.L. and I. Saunders (2009). Review of seismicity and fault reactivation in the south eastern Cape Fold Belt, South Africa, and proposals to improve the SANSN catalogue for use by non – seismologists, 2009 IASPEI conference, Cape Town, South Africa.
- Halchuk, S., J. Adams, and F. Anglin, (2007). Revised deaggregation of seismic hazard for selected Canadian cities, *Ninth Canadian Conference on Earthquake Engineering*, Ottawa, Ontario, Canada.
- Hartnady, C.J.H. and T.C. Partridge (1995). Neotectonic uplift in southern Africa: A brief review and geodynamic conjecture. *Proceedings of the Centennial Geocongress of the Geological Society of South Africa*, **1**, 456 – 459.
- IEC (2005). IEC 61400-1 Ed. 3: *Wind turbines - Part 1: Design requirements*. International Electrotechnical Commission, Geneva, Switzerland
- Johnston, A.C., K.J. Coppersmith, L.R. Kanter and C.A. Cornell (1994). The Earthquakes of Stable Continental Regions. Final Report submitted to Electric Power Research Institute (EPRI), TR-102261, Vols. 1 and 3.
- Naeim, F. and Kircher, C., (2001), On the Damping Adjustment Factors for Earthquake Response Spectra, *The Structural Design of Tall Buildings*, Vol. 10, 361-369, Wiley InterScience.
- Newmark, N. M., and W. J., Hall (1982). “Earthquake spectra and design,” *Engineering monographs on earthquake criteria, structural design, and strong motion records*, Earthquake Engineering Research Institute, University of California, Berkeley, Ca.
- Pankow, K.L. and J.C. Pechmann (2004). The SEA99 ground-motion predictive relations and new peak ground velocity relation. *Bulletin of the Seismological Society of America*, **94**(1), 341-348.
- Prowell, I. and P. Veers (2009). Assessment of Wind Turbine Seismic Risk: Existing Literature and Simple Study of Tower Moment Demand, SANDIA REPORT, SAND2009-1100.
- Spudich, P., W.B. Joyner, A.G. Lindh, D.M. Boore, B.M. Margaris and J.B. Fletcher (1999). SEA99: A revised ground motion prediction relation for use in extensional tectonic regimes. *Bulletin of the Seismological Society of America*, **89**(5), 1156-1170.
- Stafford, P.J., F.O. Strasser and J.J. Bommer (2008). An evaluation of the applicability of the NGA models to ground-motion prediction in the Euro-Mediterranean region. *Bulletin of Earthquake Engineering*, **6**(2), 149-177.
- Strasser, F.O., J.J. Bommer and N.A. Abrahamson (2008). Truncation of the log-normal distribution of ground-motion residuals, *Journal of Seismology* **12**(1), 79-105.
- Terrier, M., J.L. Blès, P. Godefroy, P. Dominique, M. Bour and C. Martin (2000). Zonation of Metropolitan France for the application of earthquake-resistant building regulations to critical facilities Part 1: Seismotectonic zonation. *Journal of Seismology*, **4**(3), 215-230.

Youngs, R.R. and K.J. Coppersmith (1985). Implications of fault slip rates and earthquake recurrence models to probabilistic seismic hazard estimates. *Bulletin of the Seismological Society of America*, **75**(4), 939-964.

APPENDIX J:

SEISMIC HAZARD AND DYNAMIC RESPONSE ASSESSMENT

Part 2 (a): Dynamic Response of the Soil - Report

Part 2: THE ESKOM Sere Wind Farm

Desktop Study:

Dynamic Response of the Soil to Strong Ground Motion

Date: 22 November 2010

CGS Report no: 2010-0240

Compiled by:

Artur Cichowicz
Seismology Unit
Council for Geoscience



Council for Geoscience



**COUNCIL FOR GEOSCIENCE
(Seismology Unit)**

REFERENCE:
CGS REPORT
2010-0240

REVISION 0

**THE Eskom Sere Wind Farm
Desktop Study:
Dynamic Response of the Soil to Strong
Ground Motion**

DATE OF RELEASE:
22 November 2010

COPY No.

AUTHOR

Dr A. Cichowicz

APPROVED BY:

Ms M. Grobbelaar

ACCEPTED BY:

Ms M. Singh

AUTHORISED BY:

Dr G. Graham

TABLE OF CONTENTS

Executive Summary	7
1 Terms of Reference	9
2 Introduction	10
3 Regulatory Framework for Wind Farms	11
4 One- dimension site response methodology	14
5 Processing field data to obtain shear wave velocity profiles	15
6 Modulus Reduction and Damping Function of Each Material Type.....	31
7 Selection and modification of the time history.....	33
8 Estimation of amplification factor (transfer function) at Sere Wind Farm sites	39
9 Surface Response Spectra	48
10 Amplification factor and surface response spectrum from the RRS analysis.....	55
11 Variability of the shear wave velocity profile	61
12 Conclusions.....	64
13 References.....	69

LIST OF FIGURES

Figure 1. Profile No. 1 (sand to depth). (Top Left) 12 shear velocity profilers and average shear velocity profile (red line); (Top Right) Model of the shear wave velocity profile (black line) and minimal and maximal range of velocity observations (red lines); (Bottom Left) Model of the shear wave velocity profile and average shear velocity profile plus/minus standard error (violet lines).	19
Figure 2. Profile No. 2 (shallow bedrock). (Top Left) 12 shear velocity profilers and average shear velocity profile (red line); (Top Right) Model of the shear wave velocity profile (black line) and minimal and maximal range of velocity observations (red lines); (Bottom Left) Model of the shear wave velocity profile and average shear velocity profile plus/minus standard error (violet lines).	20
Figure 3. Profile No.3 (sand underlain by silt / clay). (Top Left) 12 shear velocity profiles and average shear velocity profile (red line); (Top Right) Model of the shear wave velocity profile (black line) and minimal and maximal range of velocity observations (red lines); (Bottom Left) Model of the shear wave velocity profile and average shear velocity profile plus/minus standard error (violet lines).	21
Figure 4. Profile No. 4 (cemented material). (Top) Shear velocity profile; (Bottom) Model of the shear wave velocity profile.....	22
Figure 5. Profile 1 generalised geology and corresponding unit weight, shear modulus and shear wave velocity.....	27
Figure 6. Profile 2 generalised geology and corresponding unit weight, shear modulus and shear wave velocity.....	28
Figure 7. Profile 3 generalised geology and corresponding unit weight, shear modulus and shear wave velocity.....	29
Figure 8. Profile 4 generalised geology and corresponding unit weight, shear modulus and shear wave velocity.....	30
Figure 9. Generic stiffness reduction curves and hysteretic damping curves (EPRI, 1993) used in the present study.	32
Figure 10. Acceleration response spectra (1% Damping). Response spectra of scaled ground acceleration time history (blue colour): 1994 Northridge earthquake, Century City LACC North station and CON090 component. Target response spectrum (red colour): uniform hazard spectrum at 10% in 50 years hazard level.....	38

Figure 11. Acceleration response spectra (1% Damping). Response spectra of matched time history (blue colour): 1994 Northridge earthquake, Century City LACC North station, CON090 component. Target response spectrum (red colour): uniform hazard spectrum at 10% in 50 years hazard level. ... 38

Figure 12. Acceleration time histories. Scaled seed time history (red colour) for 1994 Northridge earthquake, Century City LACC North station, CON090 component and adjusted time history (blue colour) that matched the uniform hazard spectrum. 39

Figure 13. Profile No.1 (sand to depth). (Top) Transfer function for 12 time histories; (Bottom) average transfer function and average + std..... 42

Figure 14. Profile No. 2 (shallow bedrock). (Top) Transfer function for 12 time histories; (Bottom) average transfer function and average + std..... 43

Figure 15. Profile No. 3 (sand underlain by silt/clay). (Top) Transfer function for 12 time histories; (Bottom) average transfer function and average + std..... 44

Figure 16. Profile No. 4 (cemented material). (Top) Transfer function for 12 time histories; (Bottom) average transfer function and average + std..... 45

Figure 17. Two examples of response spectra for modified acceleration time history. The bedrock response spectrum (red line) has smaller values of acceleration that response spectrum observed on the surface (black line)..... 49

Figure 18. Two examples of surface response spectra for pair of horizontal components of acceleration time history. 50

Figure 19. Profile No. 1 (sand to depth). (Top) Surface response spectra for 12 horizontal components of modified acceleration time history; (Bottom) average surface response spectrum. 51

Figure 20. Profile No. 2 (shallow bedrock). (Top) Surface response spectra for 12 horizontal components of modified acceleration time history; (Bottom) average surface response spectrum. 52

Figure 21. Profile No. 3 (sand underlain by silt/clay). (Top) Surface response spectra for 12 horizontal components of modified acceleration time history; (Bottom) average surface response spectrum. 53

Figure 22. Profile No. 4 (cemented material). (Top) Surface response spectra for 12 horizontal components of modified acceleration time history; (Bottom) average surface response spectrum. 54

Figure 23. Profile No. 1 (sand to depth). (Top) Ratios of response spectra (RRS) for 12 acceleration time histories (green lines), average RRS (red line) and blue lines show the range from plus to minus

The Eskom Sere Wind Farm,
Dynamic Response of the Soil

one standard deviation of the average RRS; (Bottom) Surface response spectrum (blue line) and UHS (green line). 57

Figure 24. Profile No. 2 (shallow bedrock). (Top) Ratios of response spectra (RRS) for 12 acceleration time histories (gray lines), average RRS (red line) and blue lines show the range from plus to minus one standard deviation of the average RRS; (Bottom) Surface response spectrum (blue line) and UHS (green line). 58

Figure 25. Profile No. 3 (sand underlain by silt /clay). (Top) Ratios of response spectra (RRS) for 12 acceleration time histories (gray lines), average RRS (red line) and blue lines show the range from plus to minus one standard deviation of the average RRS; (Bottom) Surface response spectrum (blue line) and UHS (green line). 59

Figure 26. Profile No. 4 (cemented material). (Top) Ratios of response spectra (RRS) for 12 acceleration time histories (gray lines), average RRS (red line) and blue lines show the range from plus to minus one standard deviation of the average RRS; (Bottom) Surface response spectrum (blue line) and UHS (green line). 60

Figure 27. Amplification factor for randomized analysis of typical soil profile No. 2 62

LIST OF TABLES

Table 1. Typical soil profiles for the Sere Wind Farm.	16
Table 2. Physical properties for the various material types.....	16
Table 3. Profile No. 1 (sand to depth). List of parameters and their values used to estimate site effect.	23
Table 4. Profile No. 2 (shallow bedrock). List of parameters and their values used to estimate site effect.....	24
Table 5. Profile No. 3 (sand underlain by silt/clay). List of parameters and their values used to estimate site effect.....	25
Table 6. Profile No. 4 (cemented material). List of parameters and their values used to estimate site effect.....	26
Table 7. Earthquakes records used in ground response analyses	35
Table 8. Extended UHS (1% Damping).....	36
Table 9. Average amplification and standard deviation for profile No. 1 (sand to depth). Maximal amplification is 2.73 at period 0.31 sec	46
Table 10. Average amplification and standard deviation for profile No. 2 (shallow bedrock). Maximal amplification is 2.51 at period 0.25 sec	46
Table 11. Average amplification and standard deviation for profile No. 3 depth (sand underlain by silt/clay). Maximal amplification is 2.12 at period 0.29 sec.....	47
Table 12. Average amplification and standard deviation for profile No. 4 (cemented material). Maximal amplification is 2.64 at period 0.29 sec	47
Table 13. Amplification factor and standard deviation for randomized analysis of profile No.2 (shallow bedrock). Max amplification is 2.22 at period 0.29 sec.....	63

Executive Summary

An assessment of the dynamic response of the soil to strong ground motion at the planned Eskom Sere Wind Farm was undertaken. The assessment was carried out in accordance with the International Electrotechnical Commission, IEC, (2005) and Germanischer Lloyd, GL, (2010) guidance for the design and safety requirements of wind turbines. The objective of the site response analyses is to capture the effect of the soil layers on the ground motions recorded on the surface. The effect of site response is studied using the equivalent linear one-dimensional wave propagation analysis. One-dimensional site response analyses have been carried out to determine how various types of site profiles will potentially respond to earthquake ground motion.

As recommended by the GL (2010) guidance, six earthquakes were selected with two independent horizontal components each for modelling of dynamical soil response. Acceleration time histories, in order to be suitable for analysis, should have spectral characteristics compatible to the uniform hazard spectra (UHS). The amplitude of a recorded time history was therefore adjusted to match the UHS between 0.05 s and 4.5 s period. The modified acceleration records are used as input motion at the rock outcrop level for each of the soil types.

Four typical soil profiles within the Sere Wind Farm have been considered for this study. The depth to bedrock varies from 28 m to 150 m. At the site the shear modulus degradation curves and damping ratio curves are selected using generic data suitable to model pressure-dependent cohesionless soils, with gravel, sand, and low PI clays. Time history at the surface was obtained for each input ground motion. The effects of input motion uncertainty and uncertainty in soil properties are discussed throughout the report and quantified using standard deviation.

The amplification factor for four typical soil profiles was estimated using the transfer function method and the ratio of response spectra (RRS) method. The RRS approach forms the basis of the site response coefficients used in many building codes. Results of modelling indicate that the higher the depth of base rock level, the larger the value of amplification and higher the value of predominant period. The numerical values of the amplification factor and standard deviation for each period are presented. Both methods show dominant peaks for periods larger than 0.1 sec. The difference between both methods is observed only for periods lower than 0.1 sec.

Two methods were used to calculate surface response spectra, one from surface acceleration time history and the second from the average RRS. Using the surface ground motion for each typical soil profile, twelve response spectra and their corresponding averages were obtained for 1% damping. A smooth surface response spectrum was obtained from the product of the average RRS and the UHS. Both methods produce similar patterns in the response spectra at each of the four typical soil types observed. Soil amplifies ground motion in the period range from 0.1 to 0.5, almost twice the amount as compared to outcrop ground motion.

The implication of the soil amplification factor for the wind turbine structures is also discussed.

1 Terms of Reference

The Head of the Geotechnical Department, Mr. Ron Tluczek, at BKS (Pty) Ltd requested the Council for Geoscience (CGS) to undertake an investigation of the dynamic response of the soil to strong ground motion at the at the Eskom Sere Wind Farm.

The procedure for investigating the dynamic response of the soil to strong ground motion consists of the following steps:

- Typical soil profiles (soil models) are compiled to represent the range of ground conditions encountered at the site. Each profile is defined in terms of the soil material types encountered and the variation of shear wave velocity versus depth (see Section 5).
- Dynamical soil properties are assigned to the geological profile (see Section 6).
- Scaled time histories are then generated based on recorded ground motions at bedrock. Bedrock response spectra, representative of seismic hazard level at site are used to define appropriate earthquake strong-motion records for input as reference bedrock ground motions (see Section 7).
- Amplification factors are determined for each soil profile using two methods. One-dimensional site response analysis is carried out using the program Shake (see Sections 8, 10, and 11).
- Surface response spectra are obtained for a range of periods using two methods (see Section 9 and 10).

2 Introduction

Local site conditions play an important role in earthquake-resistant design and must be accounted for on a case-by-case basis. A significant part of damage observed in destructive earthquakes around the world is associated with seismic wave amplification due to local site effects. The local site conditions could be very different due to variations in thickness and properties of soil layers and could have significant effects on the characteristics of earthquake ground motions on the ground surface. The soil amplification factors are directly related to the shear-wave velocity profiles, modulus degradation and damping ratio of the soil. Site response analysis is therefore a fundamental part of assessing the seismic hazard.

There are theoretical reasons why ground surface motion should be influenced by local site conditions. At most sites the density and shear wave velocity of material near the surface are smaller than the rigid bedrock below. The conservation of elastic wave energy requires that the flow of energy (energy flux = density * shear velocity * particle velocity of ground²) from depth to the ground surface be constant. Therefore, since density and shear velocity decreases as waves approach the ground surface, the particle velocity of the ground must increase. The effect of scattering and material damping is neglected in the above descriptions.

Earthquake-resistant design of a new structure requires an analysis of its response to earthquake shaking. Ground motion can be specified in many different ways, i.e. peak ground acceleration, shapes of response spectra and time history.

3 Regulatory Framework for Wind Farms

Several standards for the design and safety requirements of wind turbines exist. The most significant is from the International Electrotechnical Commission (IEC, 2005), which is the leading organization that compiles international standards for electrical technologies. The IEC documents act as a basis for national standardization and also as a reference for international contracts. Part one IEC 61400-1, Wind turbines – Part 1: “Design requirements” (IEC, 2005) specifies minimum design requirements to assure the engineering integrity of wind turbines. Germanischer Lloyd (GL, 2010) is an internationally operating certification body for wind turbines. Certification of small, medium and large wind turbines is carried out on the basis of the GL’s Guideline for the Certification of Wind Turbines (GL, 2010). The GL’s guidelines for the earthquake requirements are very similar to those of IEC.

The IEC guidelines provide recommendations regarding the methods to use for the evaluation of the overall stability of the structure. The assessment of earthquake conditions is outlined in Clause 11.6 (Assessment of earthquake conditions) and Annex C (Assessment of earthquake loading).

IEC (2005) specifies the following:

- The ground acceleration shall be evaluated for a 475-year recurrence period.
- The seismic load evaluation may be carried out through frequency domain methods, in which case, the operational loads are added directly to the seismic load. The seismic load evaluation may be carried out through time-domain methods, in which case, sufficient simulations shall be undertaken that the operational load is representative of the time averaged values. For analysis carried out in the time-domain, a minimum number of six simulations must be performed per load case (GL, 2010).

According to (IEC, 2005) the procedure for assessment of earthquake loading includes the following steps which were followed in this investigation:

- evaluate or estimate the site and soil conditions required by the relevant local standard
- use the normalised design response spectrum and the seismic hazard-zoning factor to establish the acceleration at the first tower bending eigen-frequency assuming a damping of 1% of critical damping

The rest of the steps address issues that are relevant for the modelling of the dynamics of the structure, which is not covered by this report.

Wind turbines are not directly addressed in building code provisions, interpretations and implementations (South African National Standard, SANS, 10160-4:2008, Eurocode, EC, 2004). Building code procedures assume certain dynamic characteristics that are not always applicable to wind turbines. In some cases this can be shown to be both overly conservative and un-conservative with dependence on whether frequency or time domain methods are employed in the evaluation of seismic loading (Ntambakwa and Rogers , 2009, Prowell and Veers, 2009). It is recognized that the dynamic behaviour of wind turbines is distinct of other building structures (Prowell *et al.* 2008).

IEC Guidelines suggest the use of a damping ratio of 1%, however, assumed levels of damping embedded in the design response spectrum of building codes are typically 5%. (e.g. SANS 10160-4, 2008).

The potential for local ground conditions to significantly effect ground motion characteristics has been recognised for some time. Local ground response refers to the influence of shallow geological materials on a nearly vertical propagating wave. A local site effect analysis should be conducted to evaluate the response of local soil conditions that is caused by the motion of the bedrock immediately beneath it. There are three methods to account for soil influence on ground motion:

1. Seismic design is often performed using procedures outlined in building codes. In most international seismic codes for building design, site effects on seismic actions are included by specifying several site categories. The selection of appropriate response spectra according to soil categories is the simplest way to account for site effects in engineering projects. Site factors and site classifications are included in building codes such as SANS (2008) and EC (2004). Although these codes do consider site effects, they do so by lumping groups of similar soil profiles together, so that their provisions apply to a broad range of soil conditions within which the local conditions of a particular site are expected to fall. The site classifications used in earthquake regulations have been based on the use of the V_{s30} parameter. However, many seismologists and engineers have expressed some reluctance in using it since this single parameter does not capture the physics of the site amplification. The single V_{s30} parameter can only be considered as a proxy to such parameters.

2. Attenuation relationships that include soil corrections. Empirical methods use the seismic records from the local site, where the amplification and frequency content could be determined directly. Strong ground motion attenuation relationships that include the influence of local site conditions are used to calculate site amplification or de-amplification. The soil correction is performed using the shear wave velocity correction term in the attenuation relations.

3. Site effects are ideally modelled using the full soil profile. If the geotechnical characteristics of a site are known then, the site effects should be estimated using numerical analysis. The one dimension response is the main method used in practice. For one dimensional response analysis the soil and bedrock surface are assumed to be extending horizontally. The method uses the linear or nonlinear geotechnical parameters of the soil to estimate the ground response for a specific input motion. The theoretical methods require detailed analysis of the geotechnical information relating to the subsurface of the region.

If geotechnical data is not available for the particular site, method 1 or 2 should be used but in this investigation method 3 is used.

4 One- dimension site response methodology

The results of the seismic hazard assessment, shear wave velocity profiles and lithology data from the site are used to perform a site response analysis. The most widely used analytical method is the multiple reflection models for the propagation of S-waves in a one-dimensional column. Site effect is modelled by Shake (Idriss and Sun, 1992), the one-dimensional site response program. The Shake software calculates the seismic site response based on the solution of vertical propagation of shear waves through a one-dimensional column of soil in the frequency domain. The S-waves propagates from bedrock outcrop through a column of visco-elastic layers. It is based on the continuous solution to the wave equation adapted for use with transient motions. Nonlinearity of the shear modulus and damping is accounted for by the use of equivalent linear soil properties using an iterative procedure to obtain values of modulus and damping, which are compatible with the effective strains in each layer. The non-linear behaviour of soils is well known and can be determined very well in the laboratory. Shear strength reduces with increasing shear strain, while damping increases with increasing shear strain. Those relationships can be tested and plotted in curves, called shear modulus reduction curves and damping curves, respectively.

The Shake program needs specific geotechnical inputs. These parameters could be obtained using direct, in situ, measurements, from drilling and subsequent laboratory measurement or from known relations. The minimum input parameters are as follows:

- soil type
- thickness of the layers
- unit weight of the material

- shear modulus value of the material or shear wave velocity.
- dynamic soil properties (degradation curves)
- earthquake acceleration time history

The input time series could be assigned to the rock or other sub layers that the soil profile have. The output acceleration is computed at the specified sub-layer.

5 Processing field data to obtain shear wave velocity profiles

At the proposed location of the Sere Wind Farm shear wave velocity models were created for four typical soil profiles at the site.

Six typical soil profiles were provided by BKS. Site grouping was performed using borehole, geotechnical and geophysical information. In the second step Mr Ron Tluczek combined data into four typical soil profiles (see Table 1.) and provided physical parameters for material properties (see Table 2.). Material properties required for the site response analysis included unit weight, shear wave velocity, modulus reduction curve, and the damping curve for the soil layers as well as the bedrock half space. Unit weight and shear wave velocity are estimated using available borehole data and the surface wave survey.

Table 1. Typical soil profiles for the Sere Wind Farm.

Nr	Profile Type	Profile characteristic	WTG Site Number
1	Sand to depth	0-102 m with silty sand between 30-47 m assume bedrock at 150 m	1,2,4,14,18,21,33,35, 48
2	Shallow Bedrock	0-22 m sand 22-28m clayey silt > 28 m bedrock	19,26, 28,29,30,31,32, 36,38,41,49,50
3	Sand underlain by silt/clay	0-26 m sand > 26 m clay/ silt Assume bedrock at 100m	6,10,12,16,20,22,23,24 25,27,34,37,39,40,43,44, 46,47
4	Cemented Material	0-24 m sand 24-25 m cobbles and boulders 25-31 m silty sand 31- 34 m cemented material > 34 m silty sand Assume bedrock at 100m	20

Table 2. Physical properties for the various material types

Material Types	Shear Velocity m/s	Plasticity Index %	In-Situ Dry Density kN/m ³	In-Situ Moisture Content %
Sand	350 – 400	Nil	1500	13
Silty Sand	400 – 500	4 – 6	1800	14
Clayey Silt	400 - 600	4 – 10	1800	20
Bedrock	750 – 800	Nil	2000	0
Clay / Silt	400 – 600	10 – 20	1800	30 – 40

The Eskom Sere Wind Farm,
Dynamic Response of the Soil

Cobbles and Boulders	400 - 600	Nil	1850	15
Cemented Material	400 - 600	Nil	1850	15

The last column of Table 1 shows that the typical soil profiles 1, 2 and 3 resulted from combining data from several WTG sites. The shear wave velocity profiles that belong to one type of soil have different values of velocities (see Figure 1, 2 and 3 top left). The average velocity profile is also shown in Figures 1, 2 and 3 (red lines). The shear-wave velocity of engineering bedrock was set at 750-800 m/s.

The shear wave velocity model for soil profile No. 1 (sand to depth) is formed using the average shear velocity measurements up to a depth of 50 m obtained from the shear wave survey. The average shear wave velocity for silty sand was extracted (Table 2) for depths 50 to 102m as indicated by the borehole information in Table 1. Resistivity profiles indicate that silty sand could extend to depths below 102m. Using all the above information, the depth to rock-like material was assumed to be 150 m. Thereafter the bedrock shear wave velocity value was assumed.

The shear wave velocity model for typical soil profile No. 2 (shallow bedrock) is based on an average shear velocity to the depth of 28 m obtained from the shear wave survey and below that depth bedrock is assumed (see Table 1 and 2).

The shear wave velocity model for typical soil profile No. 3 (sand underlain by silt and clay) is constructed using average shear velocity data to the depth of 50 m obtained from the shear wave survey and borehole information to the depth of 100 m (see Table 1 and 2).

The shear wave velocity model for typical soil profile No. 4 (cemented material) is constructed using shear velocity data to the depth of 50 m obtained from the shear wave survey and borehole information to the depth of 100 m (see Table 1 and 2). Note that variability caused

by velocity is not included in the analysis because only one shear wave velocity profile and one borehole are available for this soil profile.

It is desirable to measure shear wave velocities in all soil layers. However, for the sites with deep soil, shear wave velocities may be estimated based on data available for similar soils. Figures 1, 2, 3 and 4 show available shear wave measurements for each soil profile type and assumed velocity models developed up to depth of bedrock. Tables 3, 4, 5 and 6 show values of shear velocity profiles used in the Shake analysis in the next section. These tables display an average velocity, standard deviation and a minimum and maximum value at each depth. The second column, Type, refers to the Electric Power Research Institute, EPRI, modulus reduction and damping curves (see Section 6). The variability of velocities will be used to estimate the uncertainty in the site effect. Figures 5, 6, 7 and 8 show soil type, density, shear modulus and shear velocity profiles for all soil types used in the analysis.

The Eskom Sere Wind Farm,
Dynamic Response of the Soil

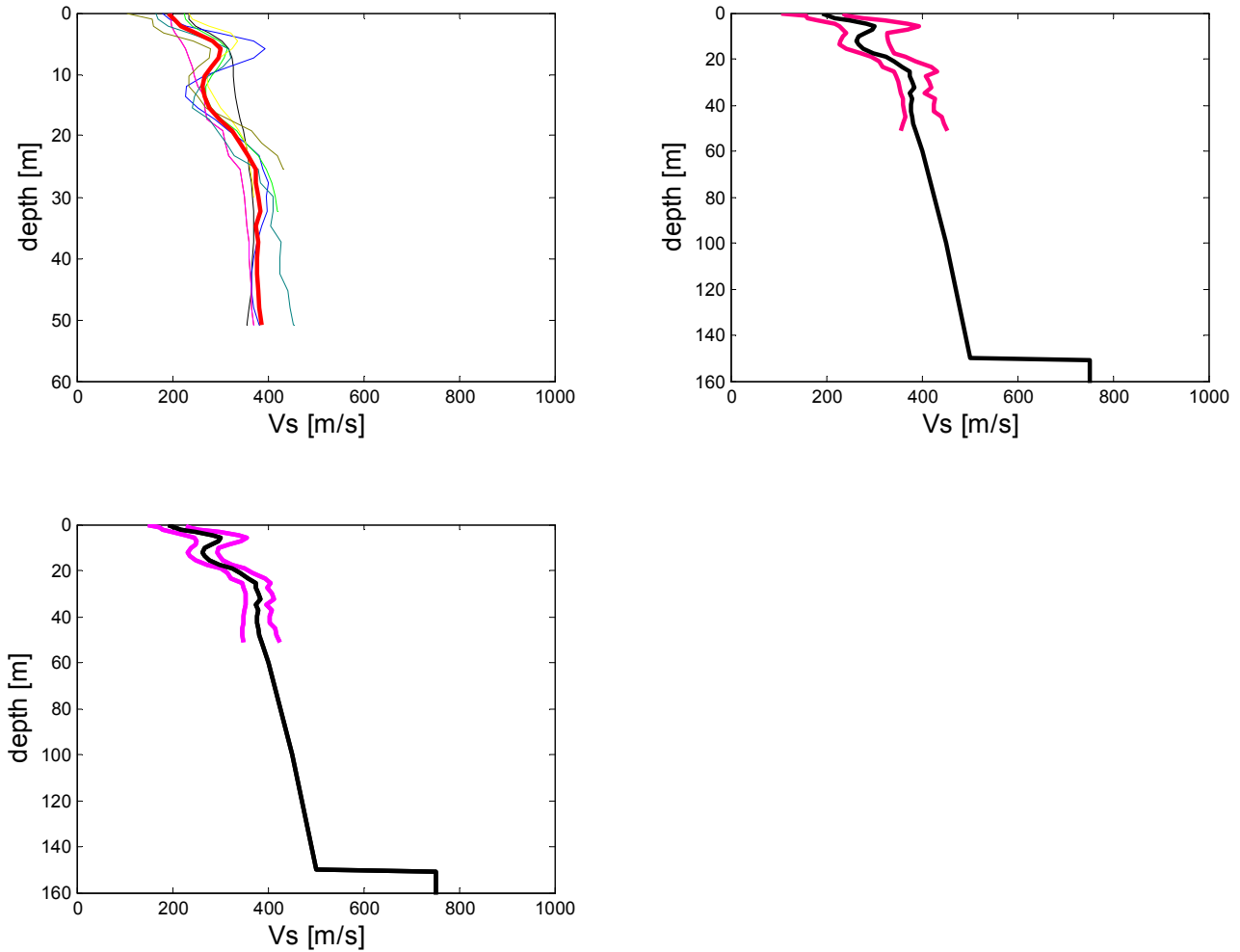


Figure 1. Profile No. 1 (sand to depth). (Top Left) 12 shear velocity profilers and average shear velocity profile (red line); (Top Right) Model of the shear wave velocity profile (black line) and minimal and maximal range of velocity observations (red lines); (Bottom Left) Model of the shear wave velocity profile and average shear velocity profile plus/minus standard error (violet lines).

The Eskom Sere Wind Farm,
Dynamic Response of the Soil

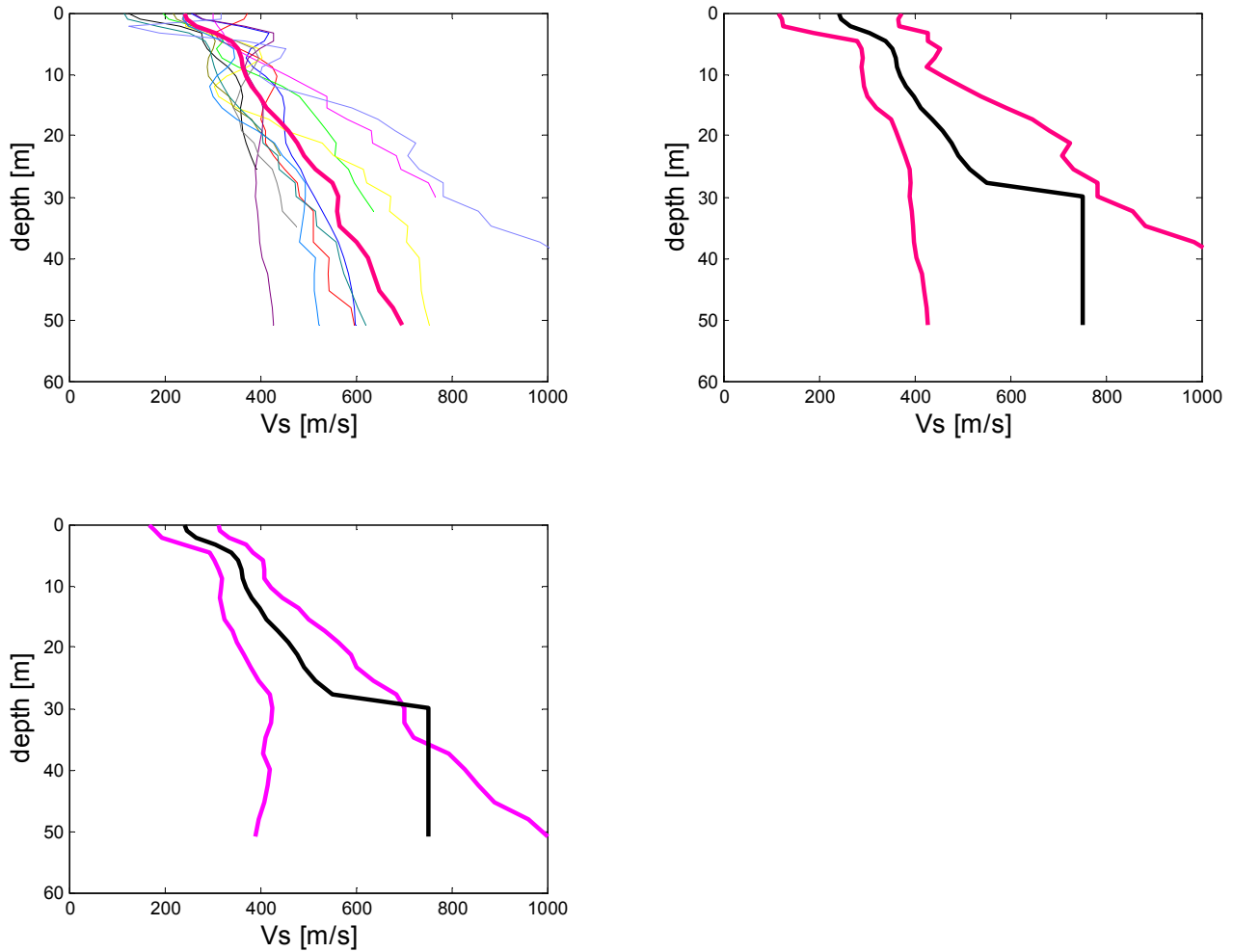


Figure 2. Profile No. 2 (shallow bedrock). (Top Left) 12 shear velocity profiles and average shear velocity profile (red line); (Top Right) Model of the shear wave velocity profile (black line) and minimal and maximal range of velocity observations (red lines); (Bottom Left) Model of the shear wave velocity profile and average shear velocity profile plus/minus standard error (violet lines).

The Eskom Sere Wind Farm,
Dynamic Response of the Soil

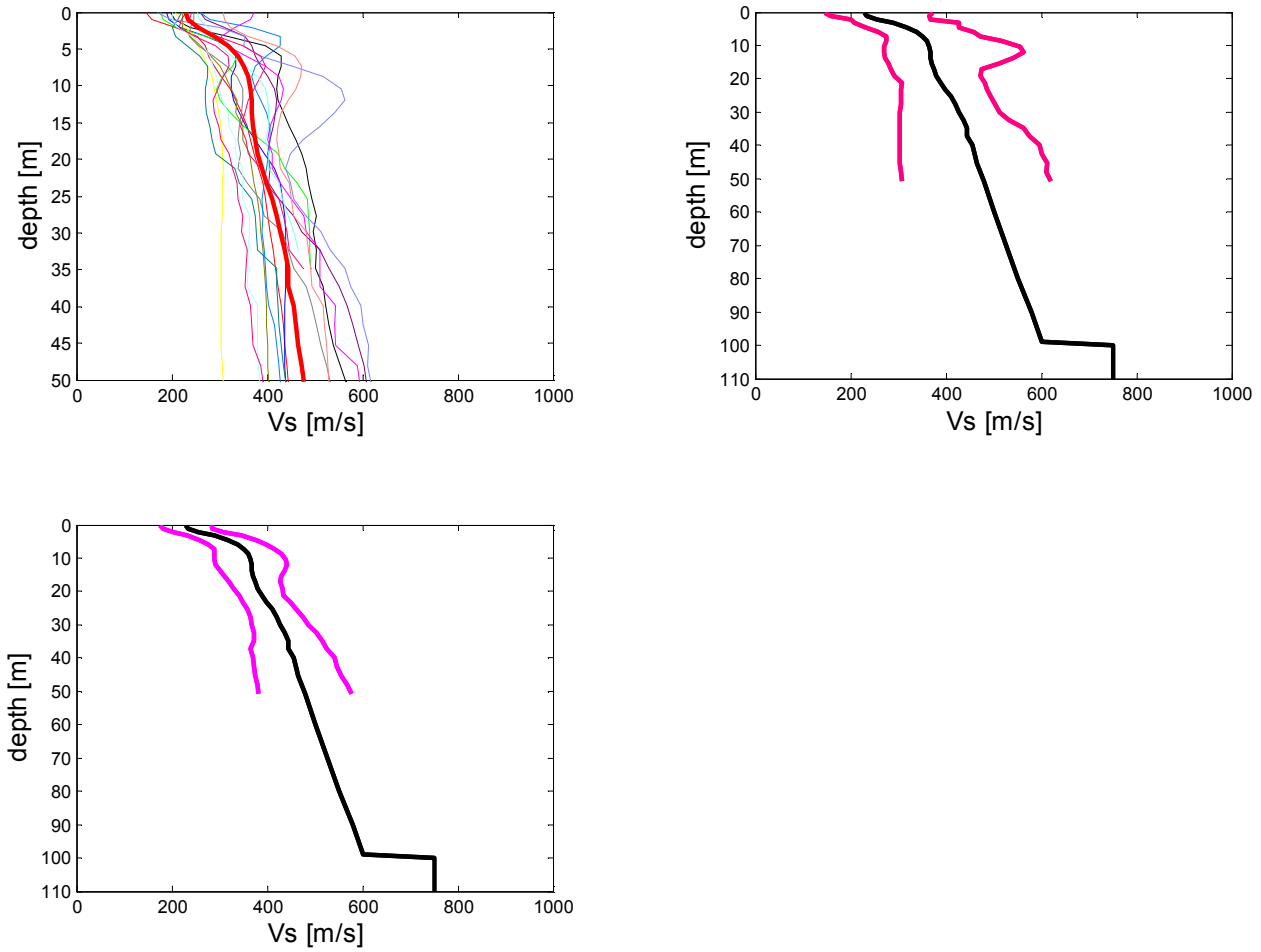


Figure 3. Profile No.3 (sand underlain by silt / clay). (Top Left) 12 shear velocity profiles and average shear velocity profile (red line); (Top Right) Model of the shear wave velocity profile (black line) and minimal and maximal range of velocity observations (red lines); (Bottom Left) Model of the shear wave velocity profile and average shear velocity profile plus/minus standard error (violet lines).

The Eskom Sere Wind Farm,
Dynamic Response of the Soil

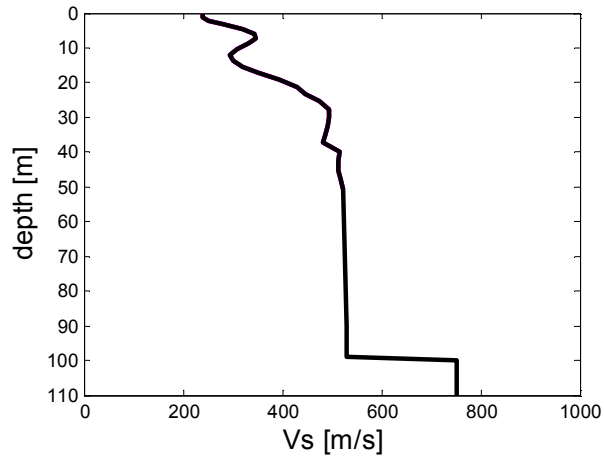
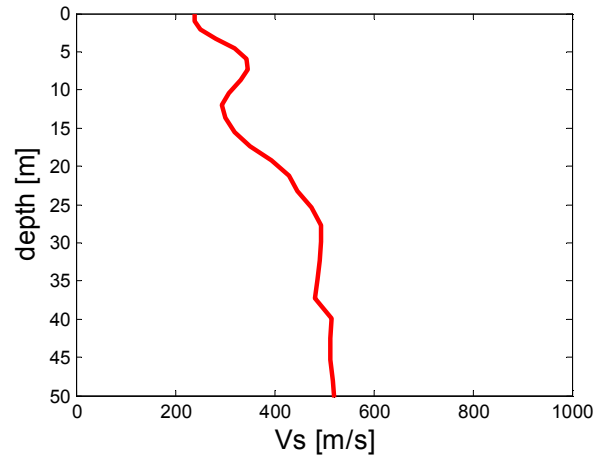


Figure 4. Profile No. 4 (cemented material). (Top) Shear velocity profile; (Bottom) Model of the shear wave velocity profile.

The Eskom Sere Wind Farm,
Dynamic Response of the Soil

Table 3. Profile No. 1 (sand to depth). List of parameters and their values used to estimate site effect.

No	Type	Δh [m]	h [m]	V_s [m/s]	std [m/s]	V_{s-min} [m/s]	V_{s-max} [m/s]
1	1	1.0	0.0	192.6	43.0	105.7	234.1
2	1	1.1	1.0	202.9	29.8	159.2	242.1
3	1	1.2	2.1	218.4	37.6	160.5	277.5
4	1	1.3	3.3	249.7	49.8	181.6	322.7
5	1	1.3	4.6	283.7	55.5	216.8	371.3
6	2	1.4	5.9	300.7	54.7	228.3	393.1
7	2	1.5	7.3	296.8	46.4	235.3	371.1
8	2	1.6	8.8	282.6	34.3	240.7	326.2
9	2	1.6	10.3	268.2	28.8	233.9	326.4
10	2	1.7	12.0	262.9	31.0	230.9	329.1
11	2	1.8	13.7	268.8	30.9	227.9	331.8
12	3	1.8	15.4	277.4	29.7	241.2	336.2
13	3	1.9	17.3	299.5	25.9	272.6	342.2
14	3	2.0	19.2	326.0	24.4	294.0	364.4
15	3	2.1	21.2	341.8	27.1	311.4	385.8
16	3	2.1	23.3	358.0	35.8	317.8	420.2
17	3	2.2	25.4	375.5	30.1	341.7	431.2
18	3	2.3	27.6	374.4	24.8	346.5	407.9
19	3	2.4	29.9	380.6	27.7	350.3	416.3
20	3	2.4	32.3	384.2	29.5	353.2	421.3
21	3	2.5	34.7	374.8	22.0	355.3	406.2
22	4	2.6	37.2	379.1	28.6	359.7	428.4
23	4	2.7	39.8	377.3	27.5	361.1	425.9
24	4	2.7	42.5	376.4	27.3	362.6	425.2
25	4	2.8	45.2	380.1	34.8	364.3	442.3
26	4	2.9	48.0	382.0	36.0	361.0	446.2
27	4	12.0	60.0	400.0			
28	4	15.0	75.0	450.0			
29	4	25.0	100.0	450.0			
30	5	50.0	149.5	500.0			
31	6		150.0	750.0			

The Eskom Sere Wind Farm,
Dynamic Response of the Soil

Table 4. Profile No. 2 (shallow bedrock). List of parameters and their values used to estimate site effect.

No	Type	Δh [m]	h [m]	V_s [m/s]	std [m/s]	V_{s-min} [m/s]	V_{s-max} [m/s]
1	1	1.0	0.0	240.5	73.2	116.0	372.0
2	1	1.1	1.0	247.1	68.3	122.2	364.9
3	1	1.2	2.1	264.6	70.2	124.1	366.8
4	1	1.3	3.3	305.0	64.9	189.3	428.4
5	1	1.3	4.6	338.7	45.1	280.6	426.7
6	2	1.4	5.9	354.4	50.8	289.1	453.2
7	2	1.5	7.3	360.8	47.3	292.7	441.4
8	2	1.6	8.8	364.1	43.5	288.9	424.3
9	2	1.6	10.3	369.7	52.7	291.4	457.7
10	2	1.7	12.0	381.2	66.3	294.9	498.0
11	2	1.8	13.7	399.6	79.9	300.6	539.7
12	3	1.8	15.4	414.1	88.0	319.3	591.3
13	3	1.9	17.3	438.0	96.1	352.0	647.5
14	3	2.0	19.2	457.5	105.3	361.1	683.2
15	3	2.1	21.2	477.7	111.3	371.3	726.0
16	3	2.1	23.3	491.2	110.6	380.7	707.9
17	3	2.2	25.4	516.3	121.0	389.0	733.2
18	3	2.3	27.6	552.0	132.5	391.7	783.2
19	6		29.9	750.0			

The Eskom Sere Wind Farm,
Dynamic Response of the Soil

Table 5. Profile No. 3 (sand underlain by silt/clay). List of parameters and their values used to estimate site effect.

No	Type	Δh [m]	h [m]	V_s [m/s]	std [m/s]	V_{s-min} [m/s]	V_{s-max} [m/s]
1	1	1.0	0.0	229.6	54.4	146.2	372.0
2	1	1.1	1.0	233.9	51.0	157.7	364.9
3	1	1.2	2.1	256.2	51.8	201.0	366.8
4	1	1.3	3.3	289.7	57.6	208.1	428.4
5	1	1.3	4.6	318.0	59.6	232.6	426.7
6	1	1.4	5.9	338.5	60.2	258.6	459.1
7	2	1.5	7.3	351.9	62.8	274.0	472.6
8	2	1.6	8.8	360.0	69.9	276.2	518.2
9	2	1.6	10.3	364.6	75.6	271.2	556.6
10	2	1.7	12.0	367.1	74.3	269.6	562.0
11	2	1.8	13.7	369.0	67.7	273.0	542.8
12	3	1.8	15.4	371.3	59.4	280.9	510.4
13	3	1.9	17.3	374.4	53.1	283.7	476.1
14	3	2.0	19.2	380.9	50.3	291.0	472.0
15	3	2.1	21.2	388.9	46.6	307.4	481.0
16	3	2.1	23.3	398.7	49.5	307.0	485.9
17	3	2.2	25.4	409.5	51.9	306.1	494.4
18	3	2.3	27.6	420.1	55.2	305.0	502.4
19	3	2.4	29.9	428.2	59.5	304.1	513.3
20	3	2.4	32.3	437.1	65.6	303.3	533.1
21	3	2.5	34.7	444.0	71.2	302.8	562.5
22	4	2.6	37.2	444.7	80.0	302.8	575.6
23	4	2.7	39.8	455.6	85.6	303.1	597.1
24	4	2.7	42.5	459.9	87.4	303.7	601.1
25	4	2.8	45.2	464.6	90.5	304.7	613.1
26	4	2.9	48.0	472.9	94.2	306.1	610.4
27	4	12.0	60.0	500.0			
28	4	20.0	80.0	550.0			
29	4	10.0	90.0	580.0			
30	5	9.0	99.0	600.0			
31	6		100.0	750.0			

The Eskom Sere Wind Farm,
Dynamic Response of the Soil

Table 6. Profile No. 4 (cemented material). List of parameters and their values used to estimate site effect.

No	Type	Δh [m]	h [m]	V_s [m/s]
1	1	1.0	0.0	239.7
2	1	1.1	1.0	239.6
3	1	1.2	2.1	251.4
4	1	1.3	3.3	281.2
5	1	1.3	4.6	319.7
6	2	1.4	5.9	343.5
7	2	1.5	7.3	346.1
8	2	1.6	8.8	331.3
9	2	1.6	10.3	308.6
10	2	1.7	12.0	294.9
11	2	1.8	13.7	300.6
12	3	1.8	15.4	319.3
13	3	1.9	17.3	352.0
14	3	2.0	19.2	393.4
15	3	2.1	21.2	430.3
16	3	2.1	23.3	447.2
17	3	2.2	25.4	474.4
18	3	2.3	27.6	494.6
19	3	2.4	29.9	494.6
20	3	2.4	32.3	491.4
21	3	2.5	34.7	486.5
22	4	2.6	37.2	481.7
23	4	2.7	39.8	515.5
24	4	2.7	42.5	513.6
25	4	2.8	45.2	514.1
26	4	2.9	48.0	517.0
27	4	12.0	60.0	530.0
28	4	10.0	70.0	530.0
29	4	15.0	85.0	540.0
30	4	14.0	99.0	540.0
31	6			750.0

The Eskom Sere Wind Farm,
Dynamic Response of the Soil

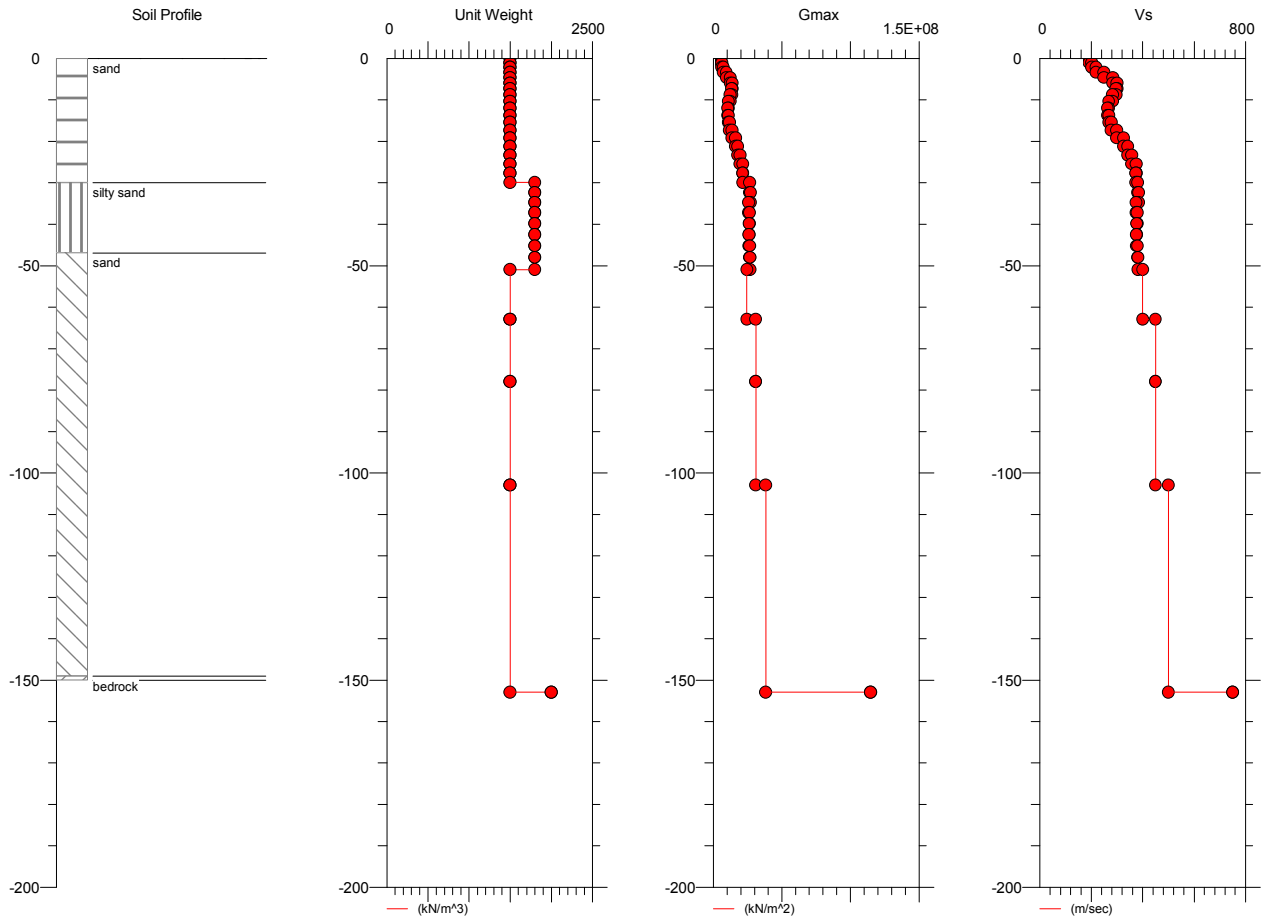


Figure 5. Profile 1 generalised geology and corresponding unit weight, shear modulus and shear wave velocity.

The Eskom Sere Wind Farm, Dynamic Response of the Soil

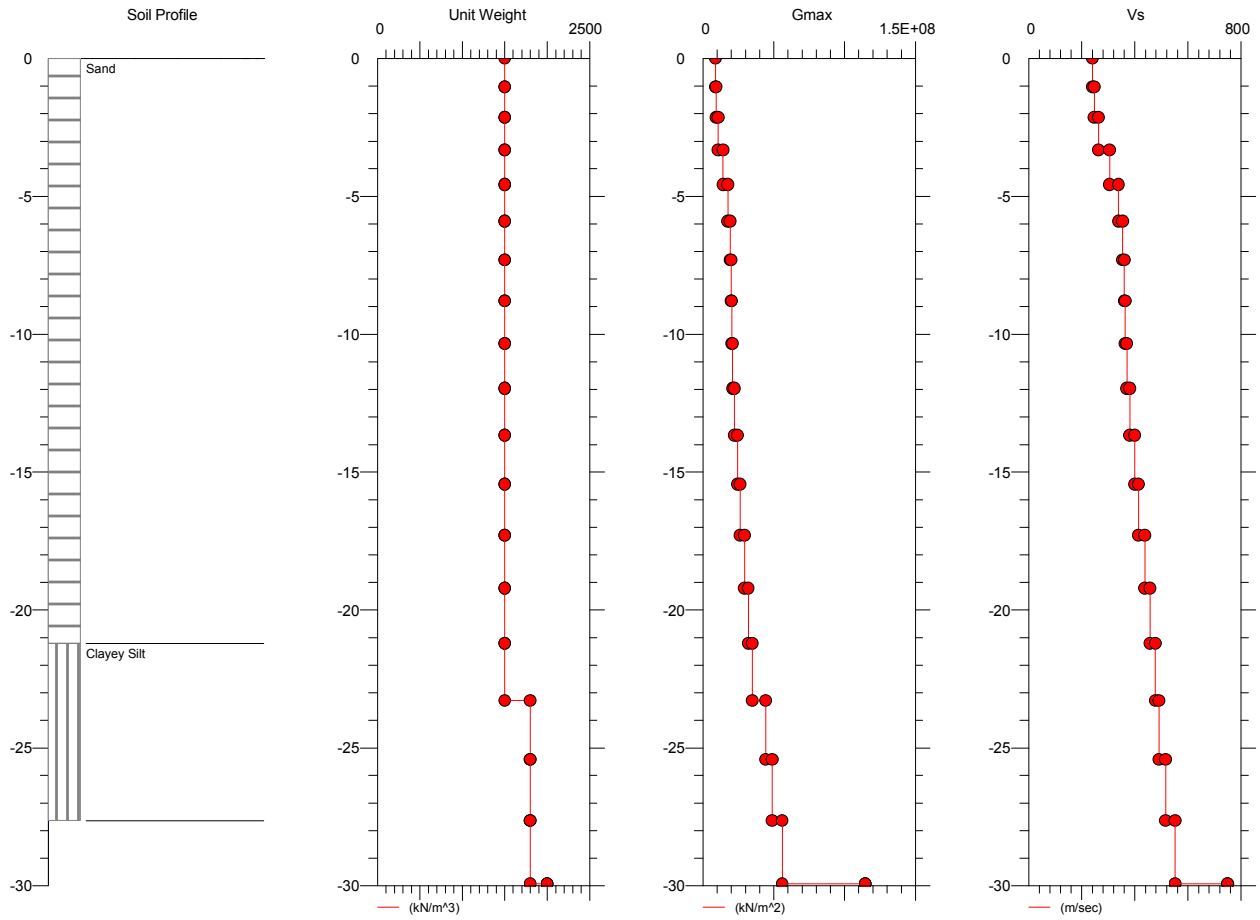


Figure 6. Profile 2 generalised geology and corresponding unit weight, shear modulus and shear wave velocity.

The Eskom Sere Wind Farm, Dynamic Response of the Soil

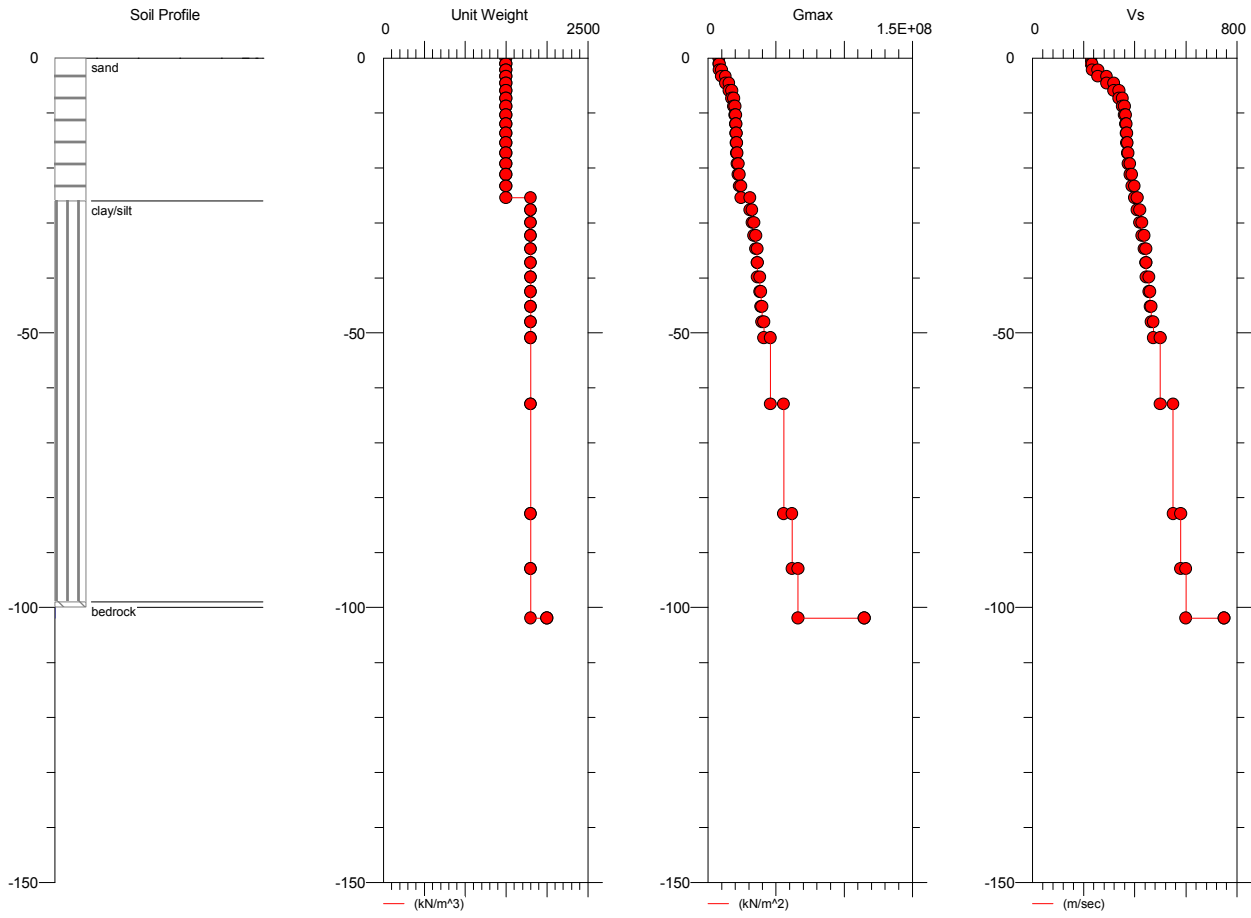


Figure 7. Profile 3 generalised geology and corresponding unit weight, shear modulus and shear wave velocity.

The Eskom Sere Wind Farm,
Dynamic Response of the Soil

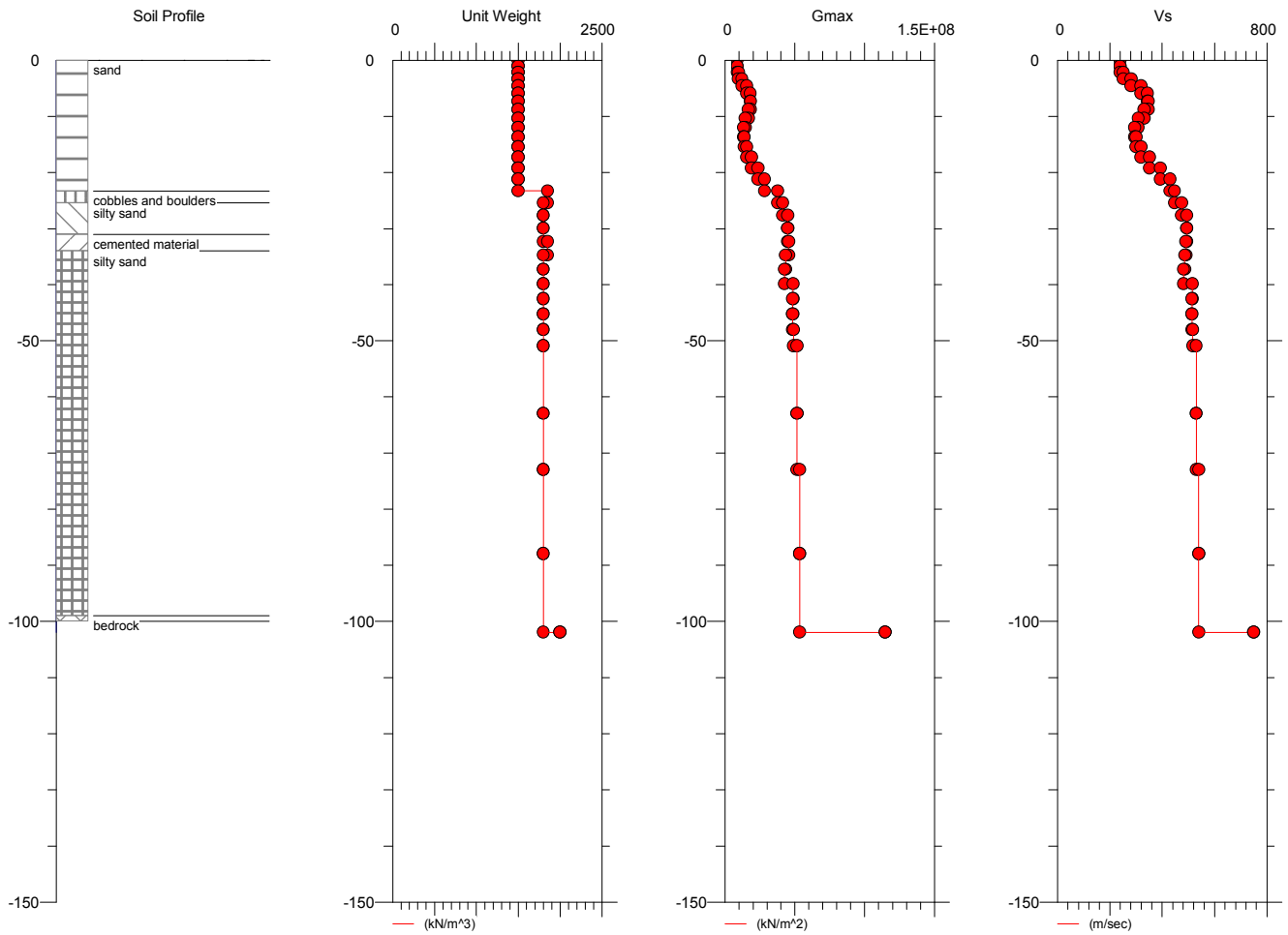


Figure 8. Profile 4 generalised geology and corresponding unit weight, shear modulus and shear wave velocity.

6 Modulus Reduction and Damping Function of Each Material Type

Material properties required for the site response analysis include a modulus reduction curve and damping curve for the soil layers as well as for the bedrock. The non-linear behaviour of soils is well known and can be determined in a laboratory environment. Shear strength reduces with increasing shear strain, while damping increases with increasing shear strain. Those relationships can be plotted on curves, called shear modulus reduction curves and damping curves, respectively. In the case of local shear modulus reduction curves and damping curves being unavailable, well established published stiffness reduction curves (generic curves) should be used.

At the Sere Wind Farm site the shear modulus degradation curves and damping ratio curves were selected using generic data. Typically, modulus reduction curves and damping curves are selected on the basis of published relationships for similar soils (e.g., Seed and Idriss, 1970; Seed et al., 1986; Sun et al., 1988; Vucetic and Dobry, 1991; Electric Power Research Institute, EPRI, 1993; Kramer, 1996). EPRI (1993) develops a set of dynamic curves to represent six different ranges of depths, down to a depth of 305 m. The generic curves developed by EPRI (1993) are most suitable to model pressure-dependent cohesionless soils, with gravels, sands, and low PI clays and were, therefore, used to model soil at the Sere Wind Farm site. Table 2 shows physical parameters of the soil material at the Sere Wind Farm.

It should be noted that some generic average curves have been proposed for different types of materials such as sand or clay, but the actual behaviour of a given soil at a given site may differ from these averages.

The Eskom Sere Wind Farm,
Dynamic Response of the Soil

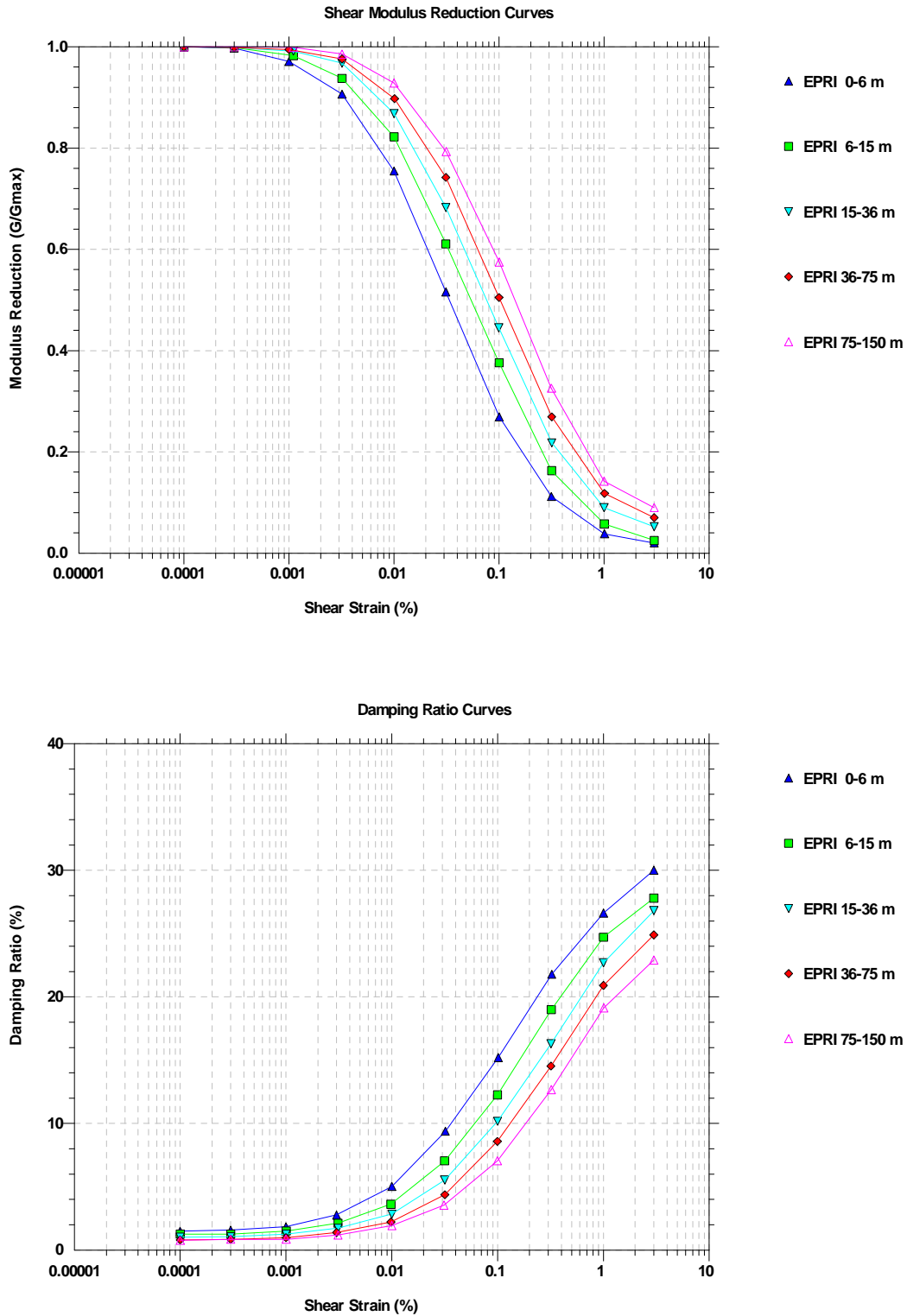


Figure 9. Generic stiffness reduction curves and hysteretic damping curves (EPRI, 1993) used in the present study.

7 Selection and modification of the time history

The inherent variability of real earthquake motions means that it will often be necessary to run large numbers of dynamic analyses in order to obtain stable estimates of the structure's response. The required number of dynamic analyses can be significantly reduced, if the real records are first matched to the target response spectrum by eliminating the largest differences between the target response spectrum and the response spectrum of individual accelerograms. The matching method retains most of the characteristics of real earthquake records. In this way the number of time-consuming structural analyses is reduced.

The seismic hazard analysis described in Part 1 of this investigation (Midzi *et al.*, 2010) provides a target response spectrum (uniform hazard spectra, UHS) for ground conditions corresponding to bedrock with a shear wave velocity of 750 - 800 m/s. These hazard values must be adjusted for ground conditions at the top of the soil column.

The probabilistic seismic hazard analysis, PSHA, is able to quantify and account for the random uncertainties associated with estimation of the seismicity and the attenuation characteristics of the sites. However, the physical image of an earthquake in terms of magnitude and distance is lost in the PSHA analysis. For physical interpretation of the results from PSHA it is desirable to have a characteristic earthquake which is compatible with the results of the PSHA method. This can be achieved through the de-aggregation of the probabilistic seismic hazard. The de-aggregation reveals the earthquake-distance combinations that make the largest contribution to the total hazard. The de-aggregation for Sere Wind Farm site for the peak ground acceleration, PGA, indicates that most of the hazard comes from a magnitude 6.4 earthquake at a distance of 13 -15 km.

The earthquake input signal at the bedrock should ideally be available from a recent earthquake that happened at a nearby site. This requires the availability of a network of accelerometers. In most cases, unfortunately, there is no such network in operation. As an

alternative input a signal could be chosen from the vast database that is already on the Internet. The selecting of strong ground motion records requires consideration of the controlling earthquake magnitude, distance and site conditions. The strong dependency of the spectral shape on magnitude can be observed and, consequently, the magnitude values of the real record need to be close to the target magnitude, while the distance value can have a larger range of values. Bommer and Acevedo (2004) show that distance has little influence on spectral shape and recommend a narrow search window in terms of magnitude but allow broad limits in terms of distance.

Details of the original earthquake recorded are given in Table 7. Table 7 shows the strong ground motions that were obtained from an online strong ground motion database, Pacific Earthquake Engineering Research, PEER, (2010). The PEER strong ground motion database contains 1557 records from 143 earthquakes. As recommended by the GL (2010) guidance, six earthquakes were selected with two independent horizontal components each. A suite of 12 acceleration time histories (pairs of two horizontal components for 6 earthquakes) were selected for use in site response analysis. It may not always be possible to find a good match between the site parameters and the existing strong motion records, and it may be necessary to use a record that does not match the site parameter criteria and scale it to fit those parameters. The suite of ground motion has magnitudes ranging between 6.5 and 6.7 and site to source distance ranging between 10.3 and 29.6 km.

The Eskom Sere Wind Farm,
Dynamic Response of the Soil

Table 7. Earthquakes records used in ground response analyses

RECORD NUMBER	COMPONENT	EARTHQUAKE	STATION	MAGNITUDE Ms	CLOSEST DISTANCE [km]	HYPOCENTRAL DISTANCE [km]
s1	CCN090	NORTHRIDGE, USA 01/17/94 12:31	CENTURY CITY LACC NORTH, 090	6.7	25.7	18.3
s2	CCN360	NORTHRIDGE, USA 01/17/94 12:31	CENTURY CITY LACC NORTH, 360	6.7	25.7	18.3
s3	H-Z08000	COALINGA ,USA 05/02/83 23:42,	PARKFIELD - FAULT ZONE 8, 000	6.5	29.6	-
s4	H-Z08090	COALINGA, USA 05/02/83 23:42	PARKFIELD - FAULT ZONE 8, 090	6.5	29.6	-
s5	A-TMZ000	FRIULI, ITALY 05/06/76 20:00	TOLMEZZO, 000	6.5	15.8	20.8
s6	A-TMZ270	FRIULI, ITALY 05/06/76 20:00,	TOLMEZZO, 270	6.5	15.8	20.8
s7	COR-L	CORINTH, GREECE 02/24/81,00:00	CORINTH, LONGITUDINAL	6.6	10.3	21
s8	COR-T	CORINTH, GREECE 02/24/81, 00:00	CORINTH, TRANSVERSE	6.6	10.3	21
s9	H-CPE147	IMPERIAL VALLEY, USA 10/15/79 23:16,	CERRO PRIETO, 147	6.5	15.2	24.8
s10	H-CPE237	IMPERIAL VALLEY, USA 10/15/79 23:16,	CERRO PRIETO, 237	6.5	15.2	24.8
s11	LO4111	SAN FERNANDO, USA 02/09/71 14:00,	LAKE HUGHES #4, 111	6.6	25	24.2
s12	LO4201	SAN FERNANDO, USA 02/09/71 14:00,	LAKE HUGHES #4, 201	6.6	25	24.2

The Eskom Sere Wind Farm,
Dynamic Response of the Soil

The site specific UHS is developed for the period range of 0.05 sec to 3.0 sec. The natural period of the structure is 3 sec. Guidance given in seismic design codes on how to select appropriate real records is usually focused on compatibility with the response spectrum and seismogram parameters. The average spectrum of the scaled records should always be larger than 90% of the target spectrum in the periods between 0.2 T and 2.0 T, where T is the fundamental period of the structure (EC, 2004). The US standards (American Society of Civil Engineers, ASCE, 2007) recommend that the average spectrum of the scaled records should be equal to 1.3 times the target spectrum in the periods between 0.2 T and 1.5 T. Since the natural period T of the structure is 3 sec, the periods recommended by EC are between 0.6 sec and 6 sec and those recommended by ASCE standard are between 0.6 sec and 4.5 sec.

The UHS can be extended to 4.5 sec period by assuming that spectral acceleration is inversely proportional to period (Council on Tall Buildings and Urban Habitat, CTBUH, Seismic Working Group 2008). Table 8 shows the extended UHS.

Table 8. Extended UHS (1% Damping)

Period [sec]	Respond Spectra [g]
0.0	0.047
0.05	0.087
0.10	0.116
0.15	0.126
0.20	0.117
0.3	0.094
0.5	0.057
1.0	0.028
2.0	0.011
3.0	0.005
4.5	0.003

Figure 10 shows an example of the response spectra of the selected acceleration time history and the UHS. The rest of the data from Table 7 are presented in Appendix 1. Acceleration time histories suitable for further analysis should have spectral characteristics compatible to the UHS at the site. The UHS is defined as the target spectrum. Therefore the amplitude of a recorded time history should be modified in a way that the response spectrum matches the target spectrum. The target spectrum has to be matched for periods close to the natural period of the structure.

Various methods have been developed to modify a reference time history so that its response spectrum is compatible with a specified target spectrum. A time domain method preserves the general non-stationary characteristic of the reference time series. A commonly used method adjusts the time history in the time domain by adding wavelets to the reference time history and also preserves the non-stationary characteristics of the original ground motion (Hancock *et al.*, 2006).

Six sets of two orthogonal, modified earthquake acceleration records are used in this analysis. The ground motion acceleration is adjusted so it matches the target spectrum between 0.05 s and 4.5 s period. The maximum spectral misfit is less than 5% after wavelet adjustment (see Figure 11). Figure 12 shows an example of the scaled observed data and synthetic input motions adjusted to the target spectrum. The rest of the results are presented in Appendix 1 and waveforms are on the attached CD.

The Eskom Sere Wind Farm,
Dynamic Response of the Soil

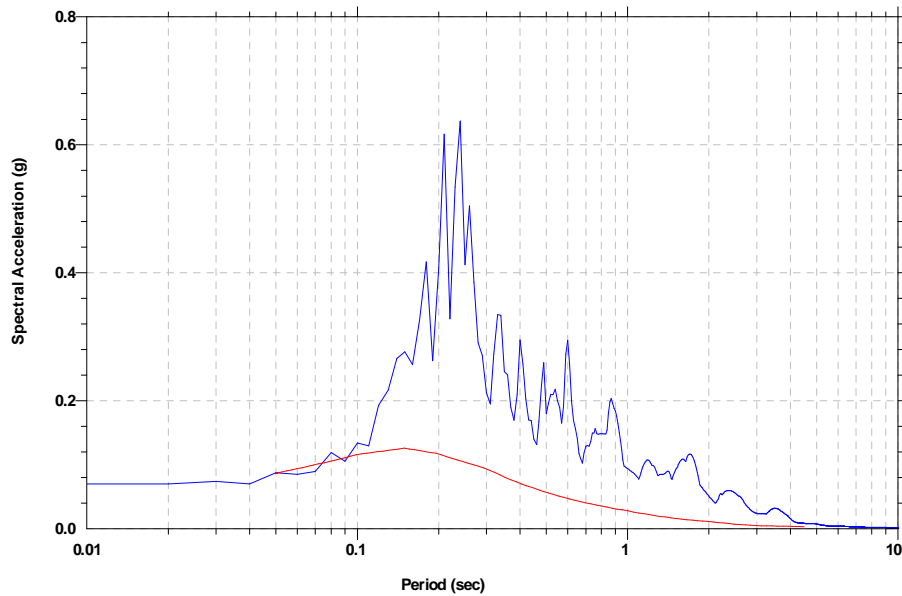


Figure 10. Acceleration response spectra (1% Damping). Response spectra of scaled ground acceleration time history (blue colour): 1994 Northridge earthquake, Century City LACC North station and CON090 component. Target response spectrum (red colour): uniform hazard spectrum at 10% in 50 years hazard level.

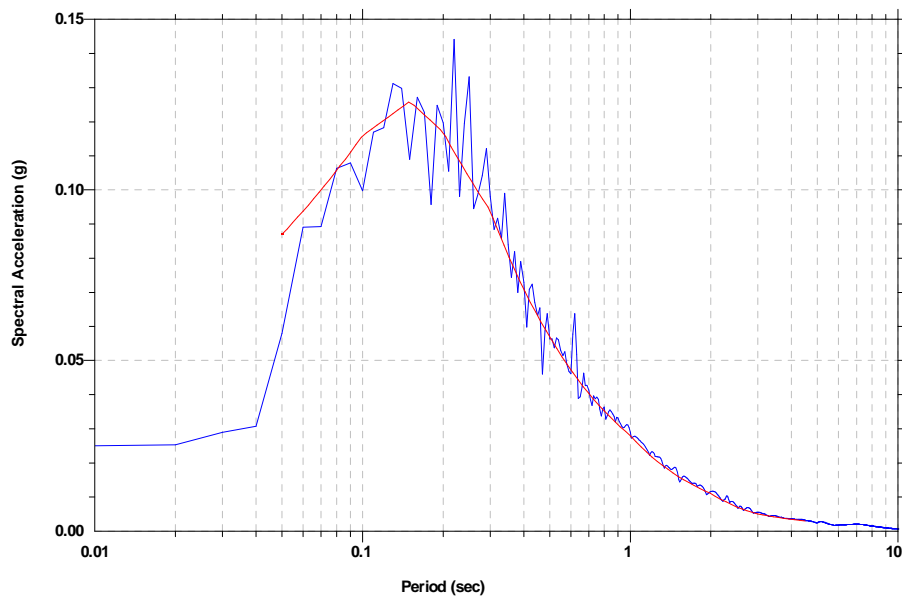


Figure 11. Acceleration response spectra (1% Damping). Response spectra of matched time history (blue colour): 1994 Northridge earthquake, Century City LACC North station, CON090 component. Target response spectrum (red colour): uniform hazard spectrum at 10% in 50 years hazard level.

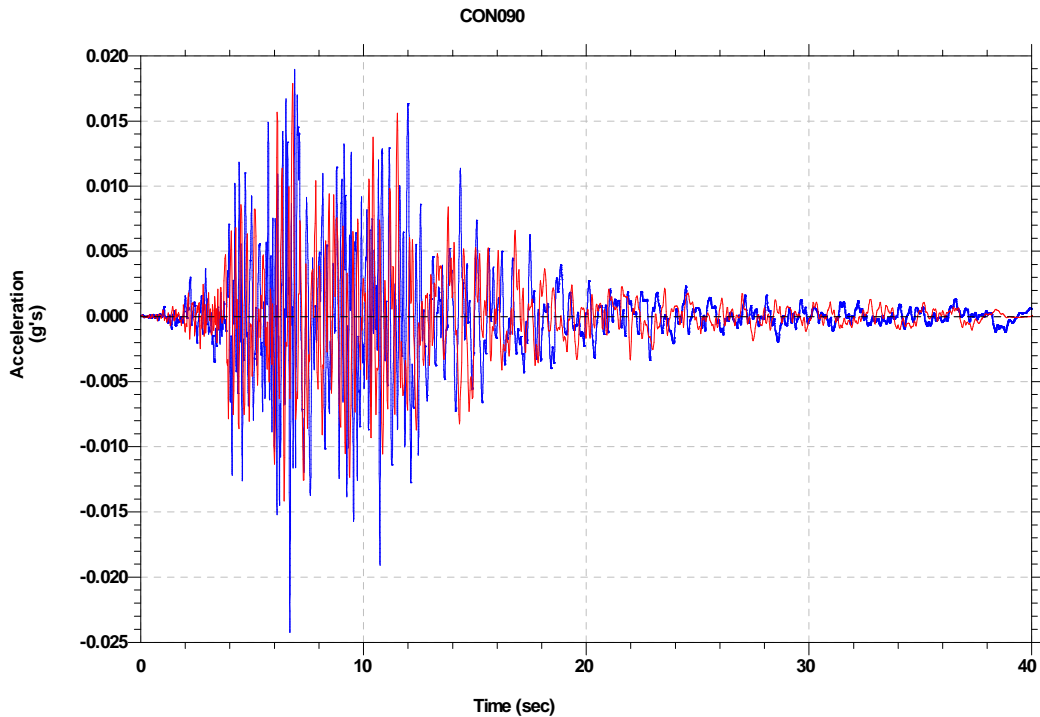


Figure 12. Acceleration time histories. Scaled seed time history (red colour) for 1994 Northridge earthquake, Century City LACC North station, CON090 component and adjusted time history (blue colour) that matched the uniform hazard spectrum.

8 Estimation of amplification factor (transfer function) at Sere Wind Farm sites

The transfer function is defined as the ratio of the Fourier amplitude spectrum of surface motions to the Fourier amplitude spectrum of the corresponding motions on a rock outcrop. Site response transfer function is the amplification factor for the specified frequency range. To carry out the Shake analysis a 1D geologic model of the soil column was created for each soil type (see Figures 5, 6, 7 and 8). The modified acceleration time histories were used as input motions at the outcropping ground (at the bottom of soil column) for each of the four typical soil profiles. The ground motion at the surface is the output of modelling.

It is expected that the turbine foundation will be at a depth of about 3 m, therefore, the amplification factor is defined between the bedrock layer and a layer at a depth of 3 meters (i.e. top 3 meters of soil is removed from analysis).

The variability of input ground motion and its effect on the amplification factor was included in the analysis. In order to incorporate these uncertainties, a series of one-dimension site response analyses were undertaken for a wide range of input acceleration time histories. The transfer function was calculated for each type of soil column using twelve time histories selected to characterize an earthquake. These results were then used to determine ground motion amplitude and period-dependent factors for each of the site classes.

The top of Figures 13, 14, 15 and 16 show the amplification factor for 12 input ground motions for profiles 1-4, respectively. The bottom of Figures 13, 14, 15 and 16 show the mean and mean plus one standard deviation of the site response analysis for the twelve input acceleration time histories. Tables 9, 10, 11 and 12 display numerical values of amplification factors for different periods as well as standard deviation error.

The maximum amplifications are observed at low periods. These periods for each site are listed below:

- Profile No. 1 (bedrock depth 150 m) maximal amplification 2.77 at 0.31 sec
- Profile No. 2 (bedrock depth 28 m) maximal amplification 2.51 at 0.25 sec
- Profile No. 3 (bedrock depth 100 m) maximal amplification 2.12 at 0.29 sec
- Profile No. 4 (bedrock depth 100 m) maximal amplification 2.64 at 0.29 sec

The maximum amplifications are much lower than the natural frequency of the turbine. It means that the fundamental mode of the turbine will be not affected by maximal amplification of soil resonance.

According to EC and US standards the lowest period that should be considered is 0.6 sec. Figures 13, 14, 15 and 16 and Tables 9, 10, 11 and 12 show maximum amplification in periods relevant to the turbine. These amplifications for each site are listed below:

- Profile No. 1 (from 0.6 sec 3 sec) maximal amplification 1.7 at 1.0 sec
- Profile No. 2 (from 0.6 sec 3 sec) maximal amplification 1.2 at 0.6 sec
- Profile No. 3 (from 0.6 sec 3 sec) maximal amplification 1.9 at 0.7 sec
- Profile No. 4 (from 0.6 sec 3 sec) maximal amplification 1.8 at 0.7 sec

The most outstanding feature of the amplification factor is the amplitude peak in the range 1.2 to 1.9 for period range 0.6 to 1.0 sec.

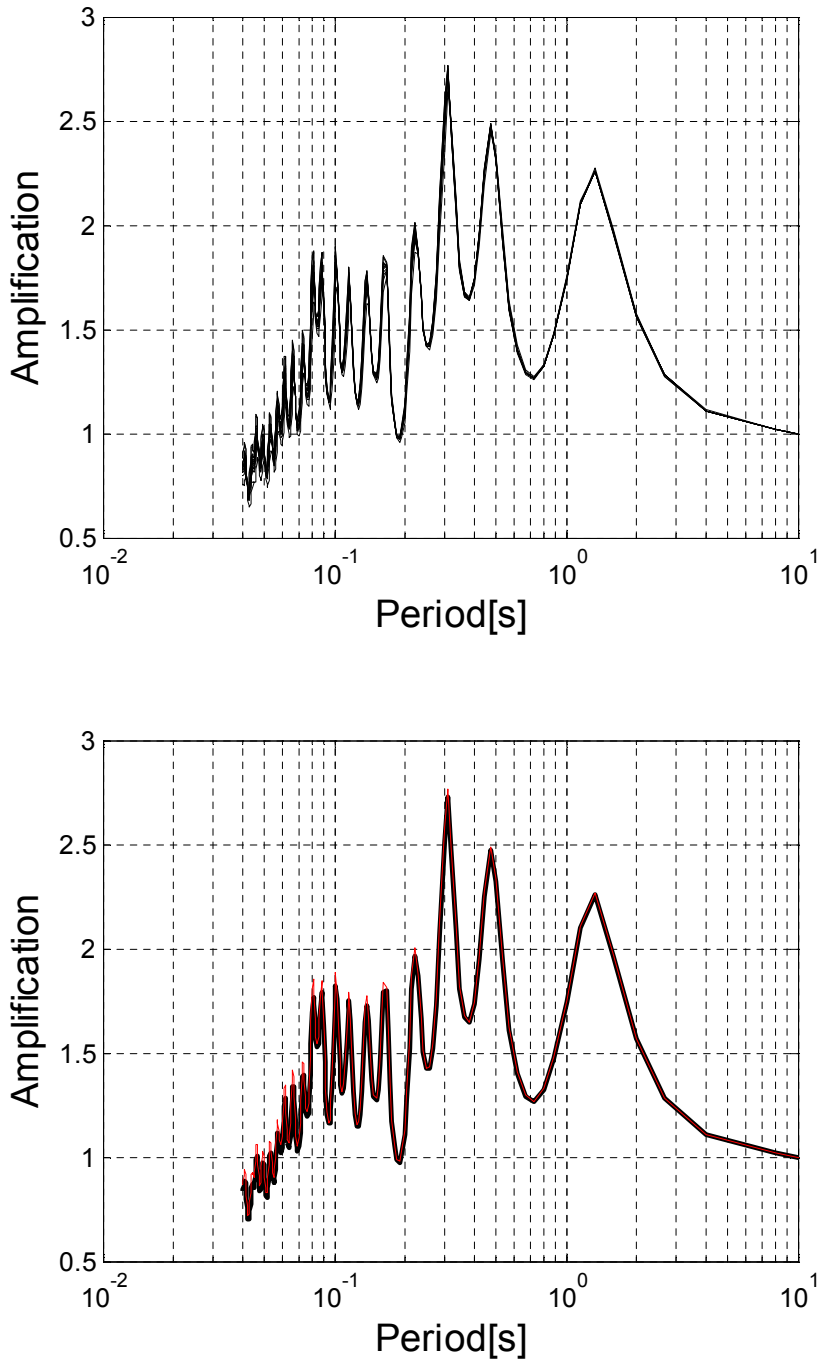


Figure 13. Profile No.1 (sand to depth). (Top) Transfer function for 12 time histories; (Bottom) average transfer function and average + std.

The Eskom Sere Wind Farm,
Dynamic Response of the Soil

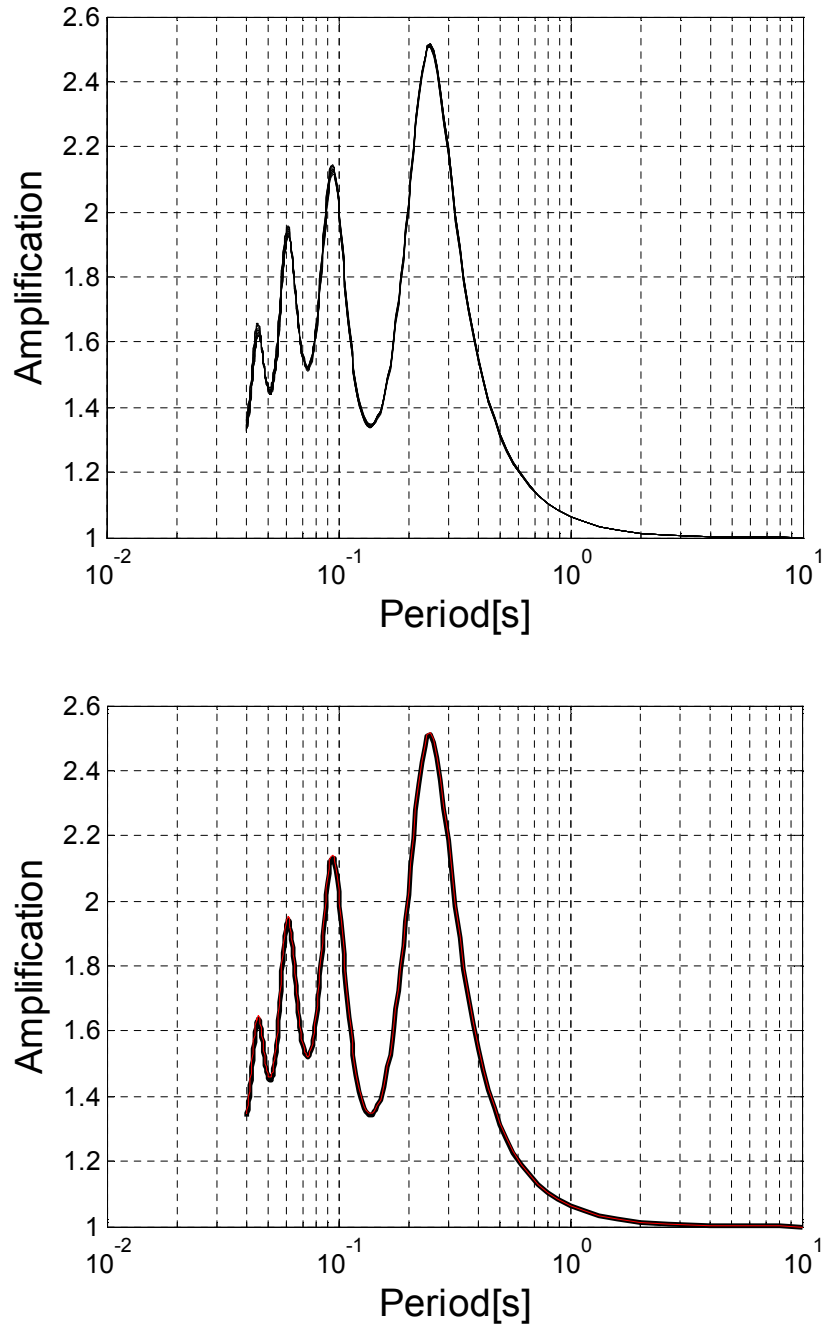


Figure 14. Profile No. 2 (shallow bedrock). (Top) Transfer function for 12 time histories; (Bottom) average transfer function and average + std.

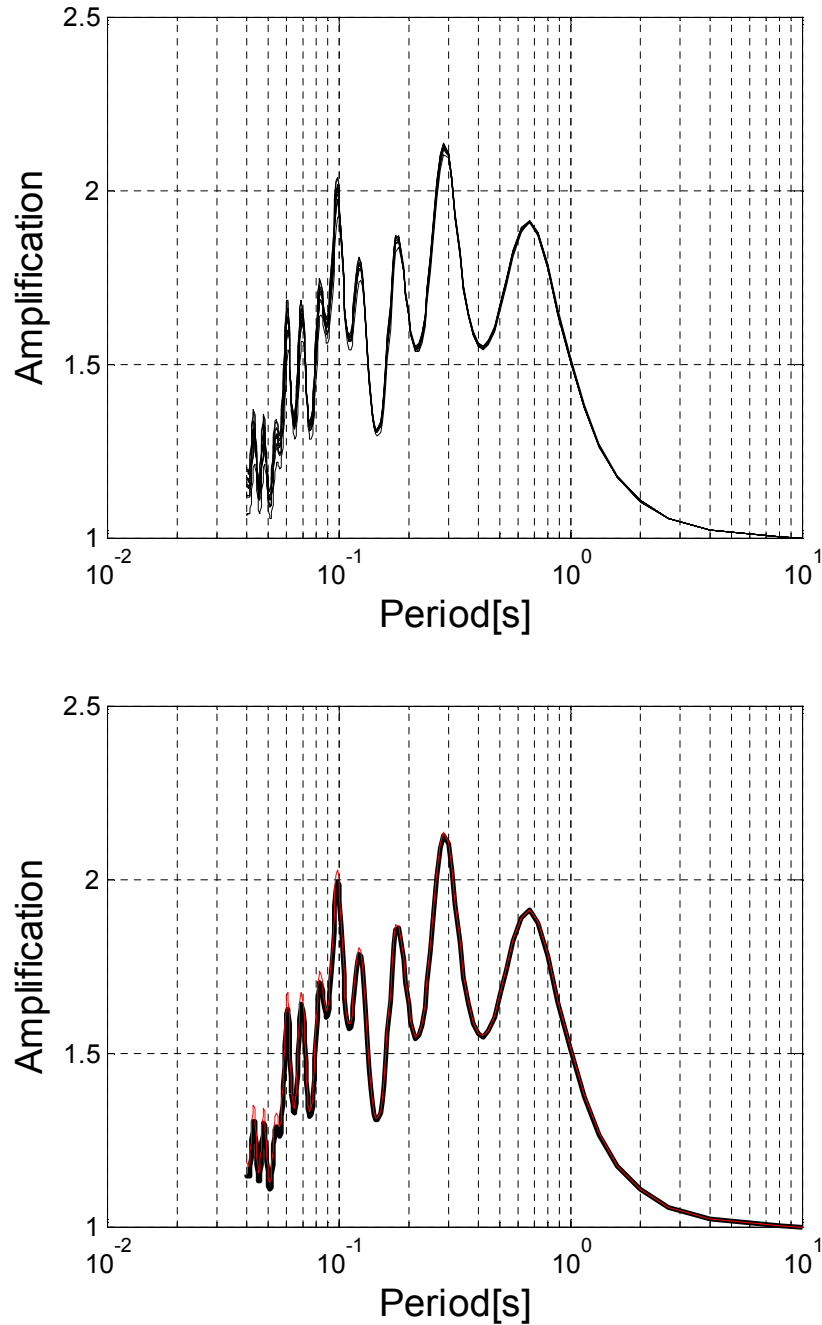


Figure 15. Profile No. 3 (sand underlain by silt/clay). (Top) Transfer function for 12 time histories; (Bottom) average transfer function and average + std.

The Eskom Sere Wind Farm,
Dynamic Response of the Soil

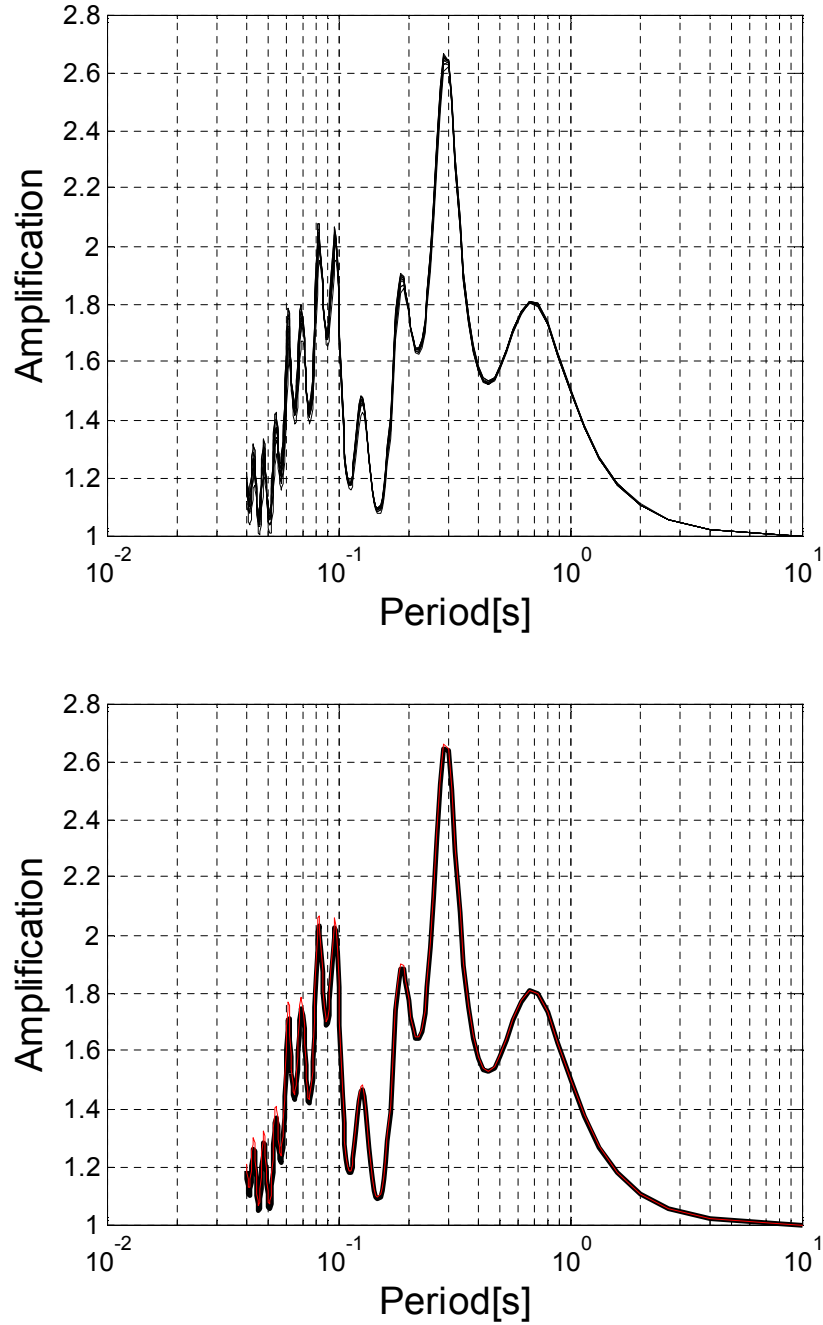


Figure 16. Profile No. 4 (cemented material). (Top) Transfer function for 12 time histories; (Bottom) average transfer function and average + std.

The Eskom Sere Wind Farm,
Dynamic Response of the Soil

Table 9. Average amplification and standard deviation for profile No. 1 (sand to depth). Maximal amplification is 2.73 at period 0.31 sec

No	Period [sec]	Amp	std
1	0.05	0.89	0.013
2	0.06	1.15	0.078
3	0.06	1.15	0.078
4	0.07	1.04	0.032
5	0.08	1.69	0.111
6	0.09	1.61	0.019
7	0.10	1.71	0.090
8	0.20	1.11	0.025
9	0.30	2.63	0.061
10	0.40	1.74	0.009
11	0.50	2.32	0.013
12	0.60	1.46	0.010
13	0.70	1.27	0.004
14	0.80	1.32	0.002
15	0.90	1.50	0.004
16	1.00	1.74	0.005
17	2.00	1.56	0.004
18	3.00	1.21	0.002
19	4.00	1.11	0.001
20	5.00	1.06	0.000
21	6.00	1.04	0.000
22	7.00	1.03	0.000
23	8.00	1.02	0.000
24	9.00	1.02	0.000
25	10.00	1.00	0.000

Table 10. Average amplification and standard deviation for profile No. 2 (shallow bedrock). Maximal amplification is 2.51 at period 0.25 sec

No	Period [sec]	Amp	std
1	0.05	1.45	0.006
2	0.06	1.93	0.014
3	0.06	1.93	0.014
4	0.07	1.56	0.005
5	0.08	1.64	0.012
6	0.09	2.06	0.017
7	0.10	2.03	0.008
8	0.20	2.02	0.009
9	0.30	2.15	0.010
10	0.40	1.55	0.005
11	0.50	1.31	0.003
12	0.60	1.20	0.002
13	0.70	1.14	0.001
14	0.80	1.11	0.001
15	0.90	1.08	0.001
16	1.00	1.06	0.001
17	2.00	1.01	0.000
18	3.00	1.00	0.000
19	4.00	1.00	0.000
20	5.00	1.00	0.000
21	6.00	1.00	0.000
22	7.00	1.00	0.000
23	8.00	1.00	0.000
24	9.00	1.00	0.000
25	10.00	1.00	0.000

The Eskom Sere Wind Farm,
Dynamic Response of the Soil

Table 11. Average amplification and standard deviation for profile No. 3 depth (sand underlain by silt/clay). Maximal amplification is 2.12 at period 0.29 sec

No	Period [sec]	Amp	std
1	0.05	1.12	0.017
2	0.06	1.63	0.047
3	0.06	1.63	0.047
4	0.07	1.63	0.026
5	0.08	1.54	0.039
6	0.09	1.61	0.023
7	0.10	1.98	0.023
8	0.20	1.64	0.004
9	0.30	2.08	0.004
10	0.40	1.55	0.003
11	0.50	1.66	0.005
12	0.60	1.87	0.004
13	0.70	1.90	0.002
14	0.80	1.78	0.004
15	0.90	1.63	0.004
16	1.00	1.51	0.004
17	2.00	1.11	0.001
18	3.00	1.04	0.000
19	4.00	1.02	0.000
20	5.00	1.01	0.000
21	6.00	1.01	0.000
22	7.00	1.00	0.000
23	8.00	1.00	0.000
24	9.00	1.00	0.000
25	10.00	1.00	0.000

Table 12. Average amplification and standard deviation for profile No. 4 (cemented material). Maximal amplification is 2.64 at period 0.29 sec

No	Period [sec]	Amp	std
1	0.05	1.06	0.015
2	0.06	1.65	0.076
3	0.06	1.65	0.076
4	0.07	1.73	0.024
5	0.08	1.85	0.059
6	0.09	1.70	0.018
7	0.10	1.82	0.015
8	0.20	1.78	0.004
9	0.30	2.60	0.006
10	0.40	1.57	0.006
11	0.50	1.58	0.004
12	0.60	1.75	0.003
13	0.70	1.81	0.003
14	0.80	1.73	0.004
15	0.90	1.61	0.004
16	1.00	1.50	0.004
17	2.00	1.11	0.001
18	3.00	1.04	0.000
19	4.00	1.02	0.000
20	5.00	1.01	0.000
21	6.00	1.01	0.000
22	7.00	1.00	0.000
23	8.00	1.00	0.000
24	9.00	1.00	0.000
25	10.00	1.00	0.000

9 Surface Response Spectra

The response spectra describe the maximum response of a single degree of freedom (SDOF) system to a particular input motion as a function of the natural period and damping ratio of the SDOF system (Kramer 1996). A response spectrum is the collection of the responses of SDOF oscillators with different natural periods subjected to the shaking from a given earthquake. The SDOF oscillator may be regarded as the simplest model of a building that is separated from the basement. Traditionally, response spectra have been used to characterize input ground motions. Such characterizations allow different input motions to be distinguished on the basis of how they affect structural response. Spectra are developed for specific percentages of critical damping.

A ground response analysis is performed to predict the motion at the surface of the soil profile. The effect of site response is studied using the equivalent linear one-dimensional wave propagation analysis implemented in the program Shake. Figure 17 shows two examples of response spectra for a modified acceleration time history. The bedrock response spectrum (red line) has smaller values of acceleration than the response spectrum observed on the surface (black line). The figure illustrates that soil amplifies seismic signal in a broad range of periods. The overall increase in the amplitude of surface response spectra in comparison to bedrock response spectra is observed from 1.0 sec towards lower periods.

The variability of input ground motion has an effect on the estimation of surface response spectra. Figure 18 shows two examples of surface response spectra for a pair of the horizontal components of the modified acceleration time history.

Figures 19, 20, 21 and 22 show surface acceleration response spectra obtained for 1% damping for soil profiles 1-4, respectively. The tops of the figures show the effect of the variability of input ground motion. Twelve response spectra are plotted on top of each other

The Eskom Sere Wind Farm,
Dynamic Response of the Soil

for each typical soil profile. The bottom of Figures 19, 20, 21 and 22 display the average response spectra obtained from 12 acceleration time histories. The highest peak responses at all typical soil profiles are observed at a period of 0.3 sec.

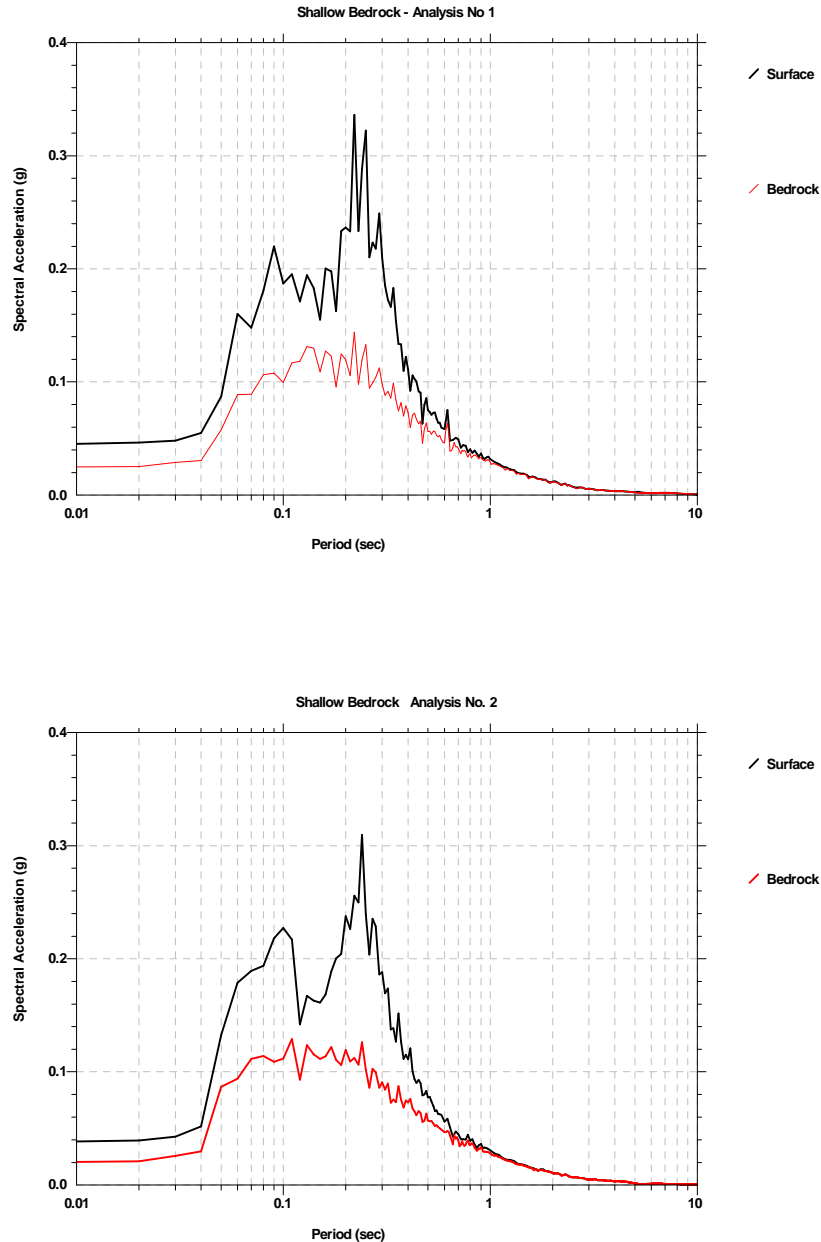


Figure 17. Two examples of response spectra for modified acceleration time history. The bedrock response spectrum (red line) has smaller values of acceleration that response spectrum observed on the surface (black line)

The Eskom Sere Wind Farm,
Dynamic Response of the Soil

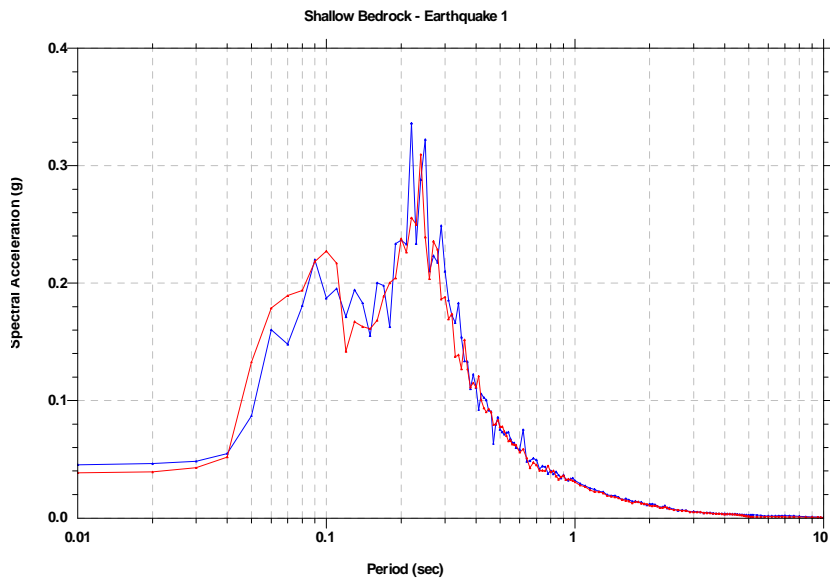
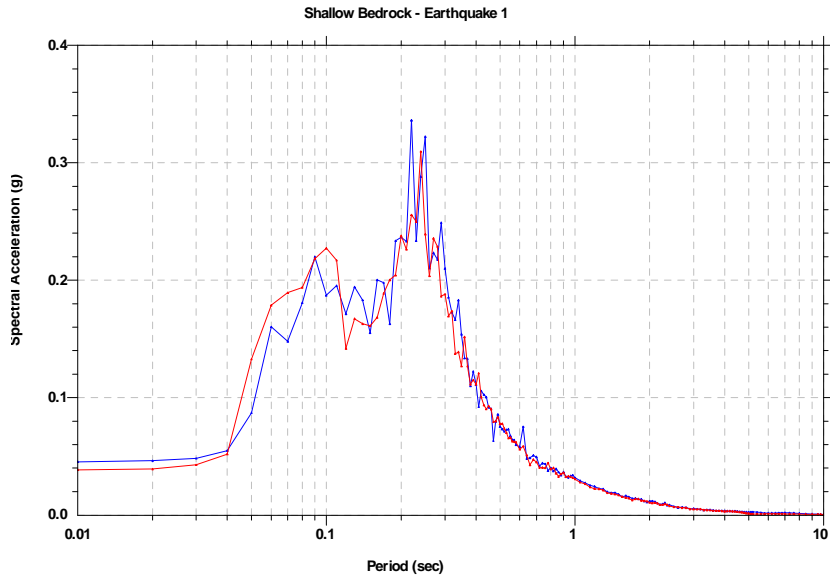


Figure 18. Two examples of surface response spectra for pair of horizontal components of acceleration time history.

The Eskom Sere Wind Farm,
Dynamic Response of the Soil

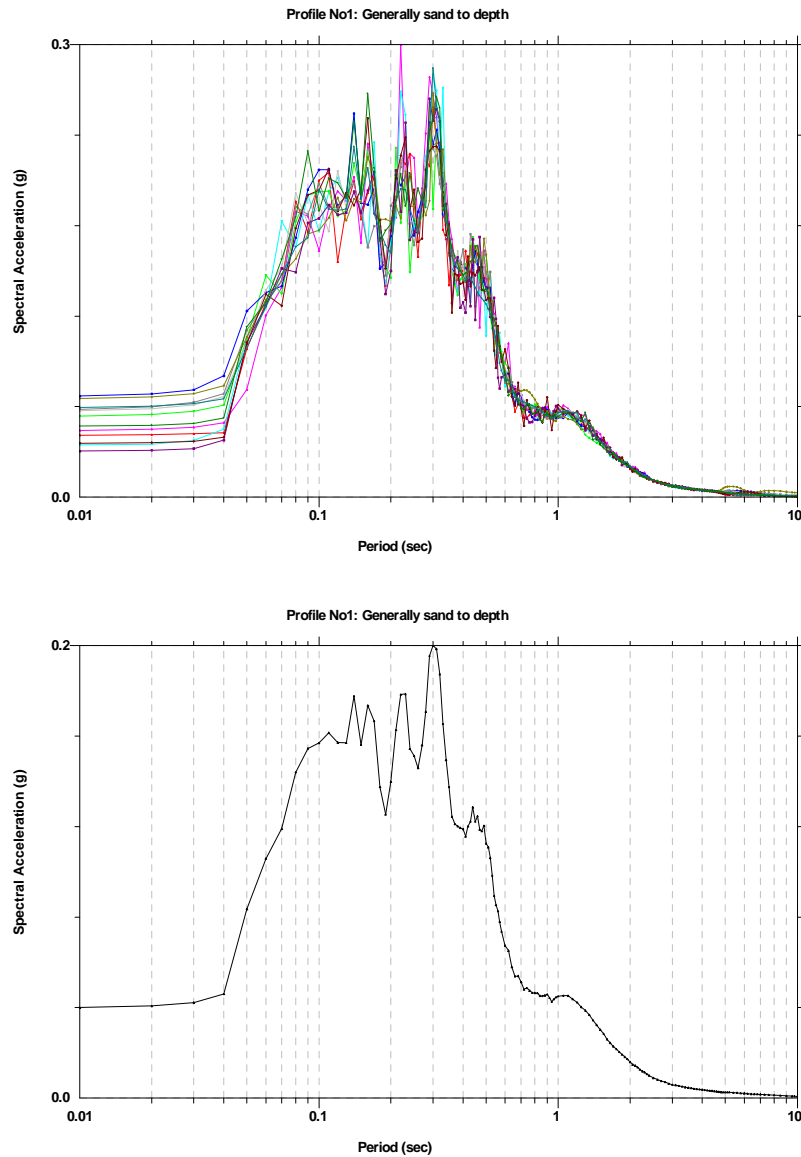


Figure 19. Profile No. 1 (sand to depth). (Top) Surface response spectra for 12 horizontal components of modified acceleration time history; (Bottom) average surface response spectrum.

The Eskom Sere Wind Farm,
Dynamic Response of the Soil

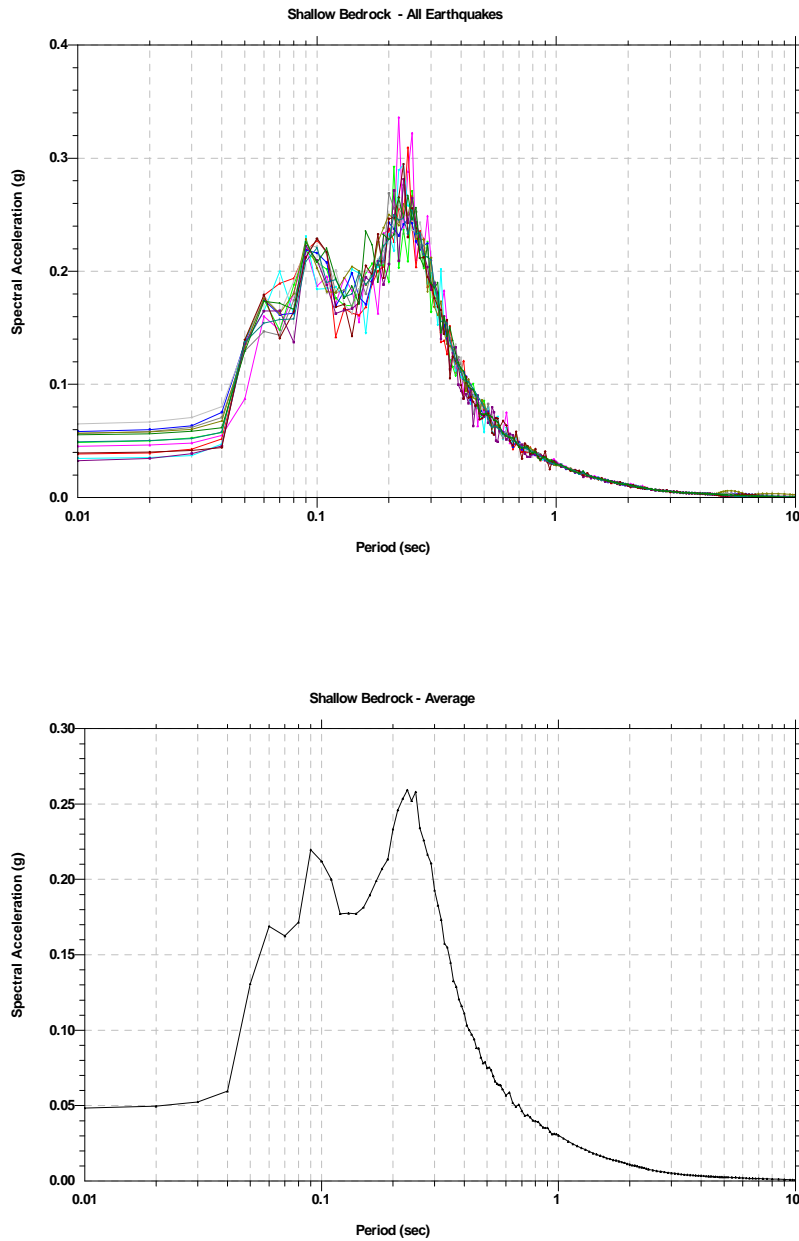


Figure 20. Profile No. 2 (shallow bedrock). (Top) Surface response spectra for 12 horizontal components of modified acceleration time history; (Bottom) average surface response spectrum.

The Eskom Sere Wind Farm,
Dynamic Response of the Soil

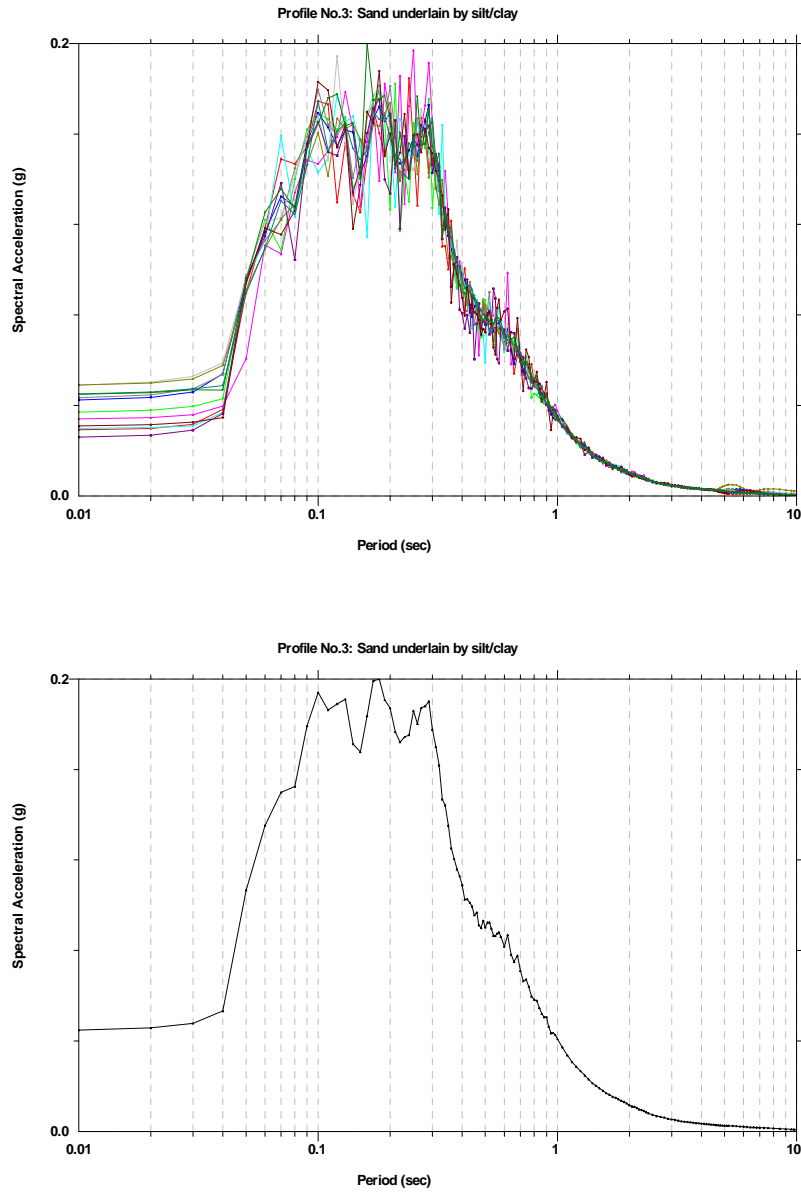


Figure 21. Profile No. 3 (sand underlain by silt/clay). (Top) Surface response spectra for 12 horizontal components of modified acceleration time history; (Bottom) average surface response spectrum.

The Eskom Sere Wind Farm,
Dynamic Response of the Soil

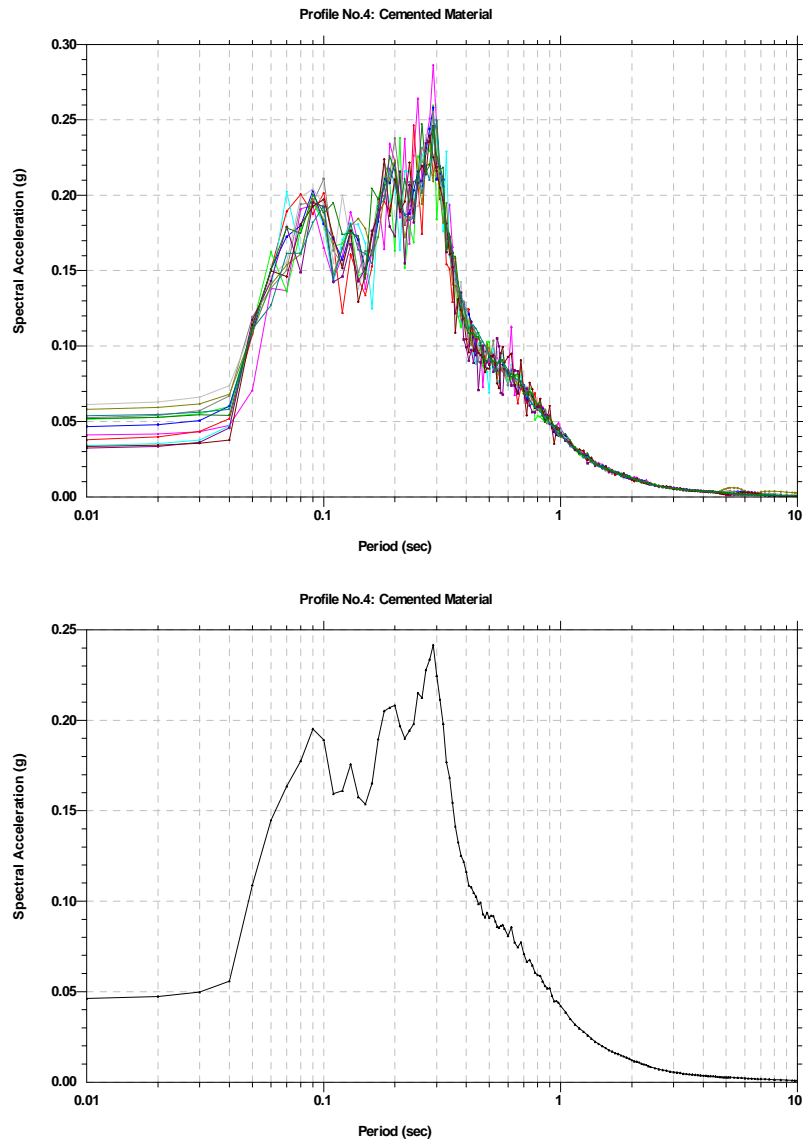


Figure 22. Profile No. 4 (cemented material). (Top) Surface response spectra for 12 horizontal components of modified acceleration time history; (Bottom) average surface response spectrum.

10 Amplification factor and surface response spectrum from the RRS analysis

The amplification of seismic waves propagated up through a soil column is a function of the dynamic response characteristics of the soil profile and the characteristics of the outcrop rock motions. One way to quantify the influence of site conditions on motions experienced at the surface of a profile is by the Ratio of Response Spectra (RRS) method. The RRS is defined as the ratio of response spectra at the surface over the response spectra of outcrop input motion. The RRS is calculated for several surface-outcrop motion pairs, and then the mean values are obtained. The result of the analysis can be used to obtain a soil response spectrum by multiplying the mean curve of the resultant RRS curves by a rock response spectrum or its smooth analogue by the UHS. The RRS approach forms the basis of the site response coefficients used in many building codes. The values of site response coefficients are based on quantifying the influence of site conditions on ground motions by RRS. The RRS is described by the mean values and their corresponding standard deviations.

The RRS for four typical soil profiles and the 12 input motions are shown in Figures 23, 24, 25 and 26. The general shape of the RRS, average RRS and the range from plus to minus one standard deviation of the average RRS are presented for all of the input motions. The estimates of site response (quantified by RRS) are affected by the choice of input motion. The approach taken in this study is to generate a suite of input motions that would represent a "reasonable" estimate of an outcrop rock input motion for events of the characteristic magnitude, and at the same time would incorporate a reasonable measure of variability.

Figures 23, 24, 25 and 26 (bottom) show surface response spectra obtained from the product of the average RRS and UHS. The soil column amplifies ground motion almost twice in a period range from 0.1 to 0.5 sec in comparison to outcrop ground motion. The same patterns are observed in the response spectra at each of the four typical soil types.

A comparison between the transfer function method and the RRS method may be seen in Figures 13 and 23 have similar amplification features for periods larger than 0.1 sec. The same conclusion is observed by an analysis of a pair of Figures 14 - 24, 15 - 25 and 16 – 26. The difference between the transfer function and the RRS methods is observed only for periods lower than 0.1 sec.

The Eskom Sere Wind Farm,
Dynamic Response of the Soil

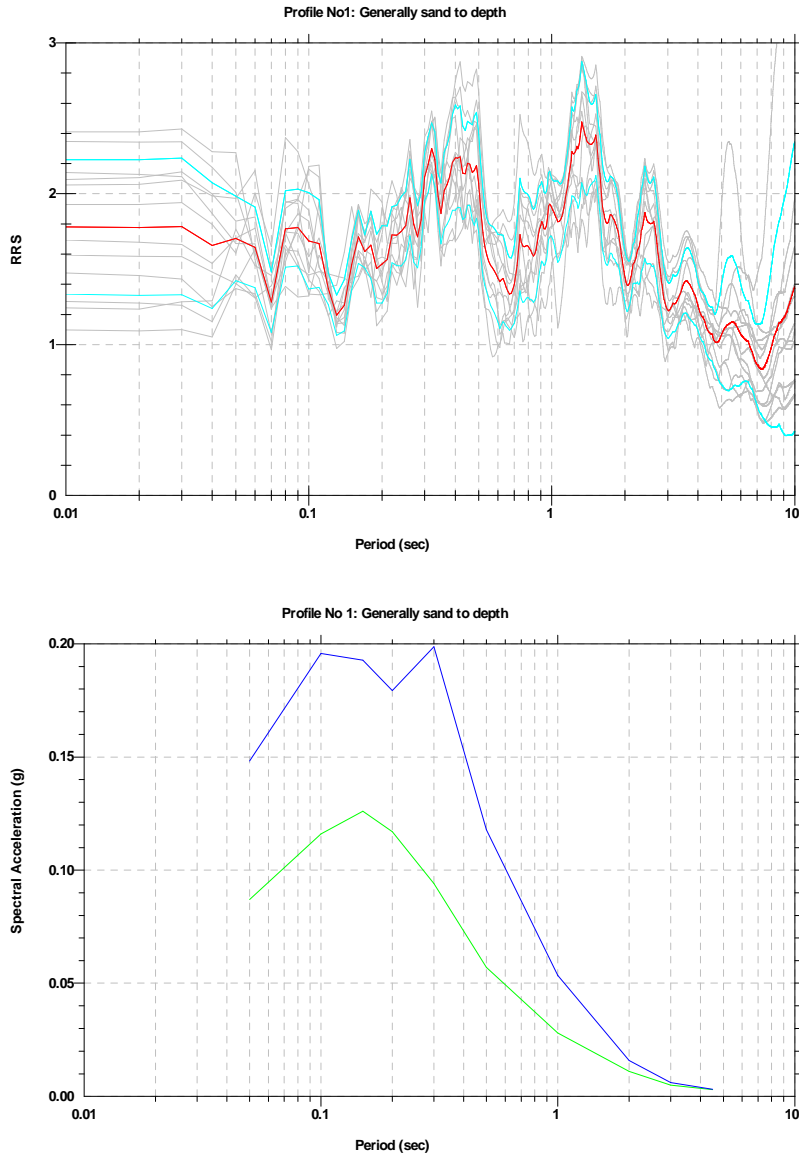


Figure 23. Profile No. 1 (sand to depth). (Top) Ratios of response spectra (RRS) for 12 acceleration time histories (green lines), average RRS (red line) and blue lines show the range from plus to minus one standard deviation of the average RRS; (Bottom) Surface response spectrum (blue line) and UHS (green line).

The Eskom Sere Wind Farm,
Dynamic Response of the Soil

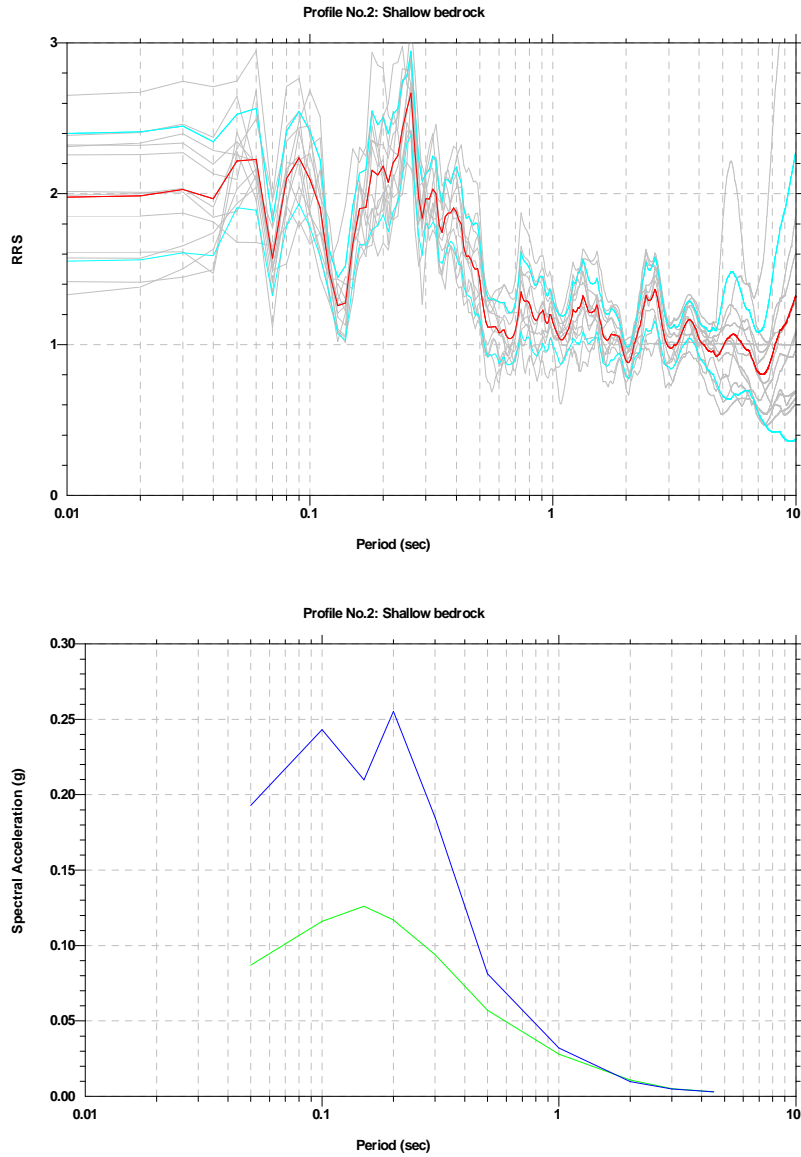


Figure 24. Profile No. 2 (shallow bedrock). (Top) Ratios of response spectra (RRS) for 12 acceleration time histories (gray lines), average RRS (red line) and blue lines show the range from plus to minus one standard deviation of the average RRS; (Bottom) Surface response spectrum (blue line) and UHS (green line).

The Eskom Sere Wind Farm,
Dynamic Response of the Soil

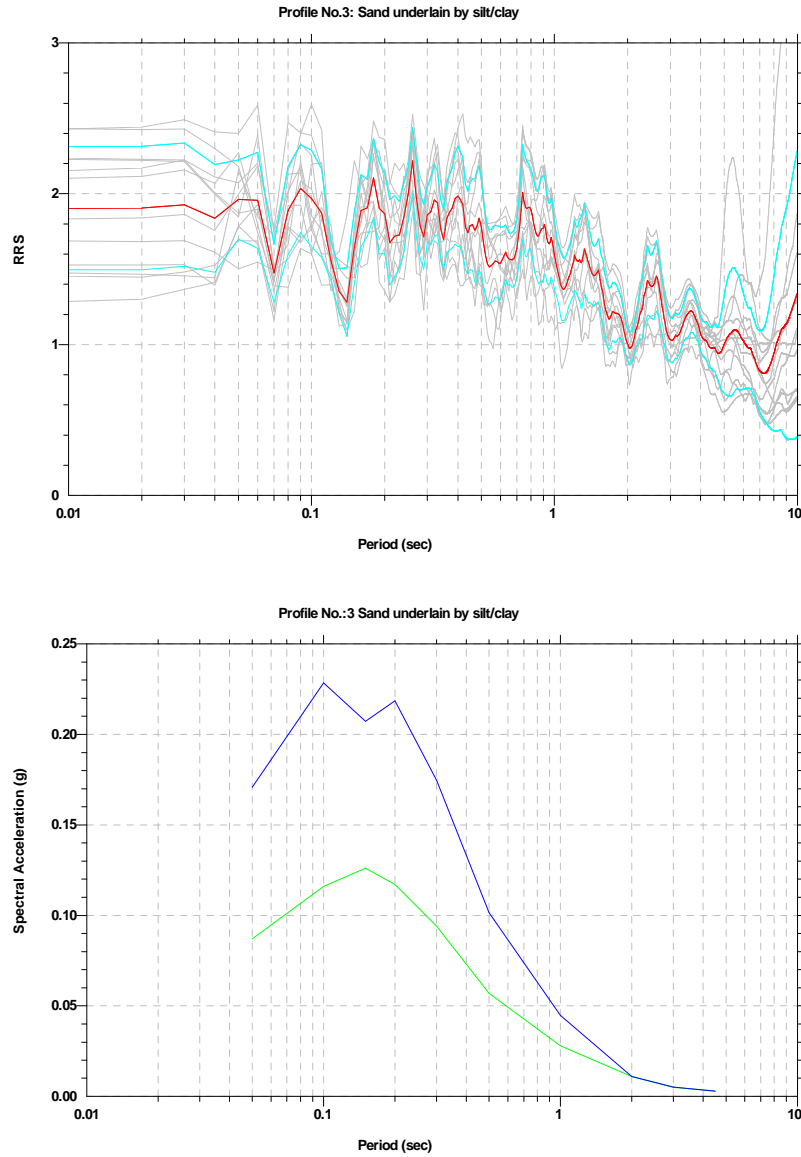


Figure 25. Profile No. 3 (sand underlain by silt /clay). (Top) Ratios of response spectra (RRS) for 12 acceleration time histories (gray lines), average RRS (red line) and blue lines show the range from plus to minus one standard deviation of the average RRS; (Bottom) Surface response spectrum (blue line) and UHS (green line).

The Eskom Sere Wind Farm,
Dynamic Response of the Soil

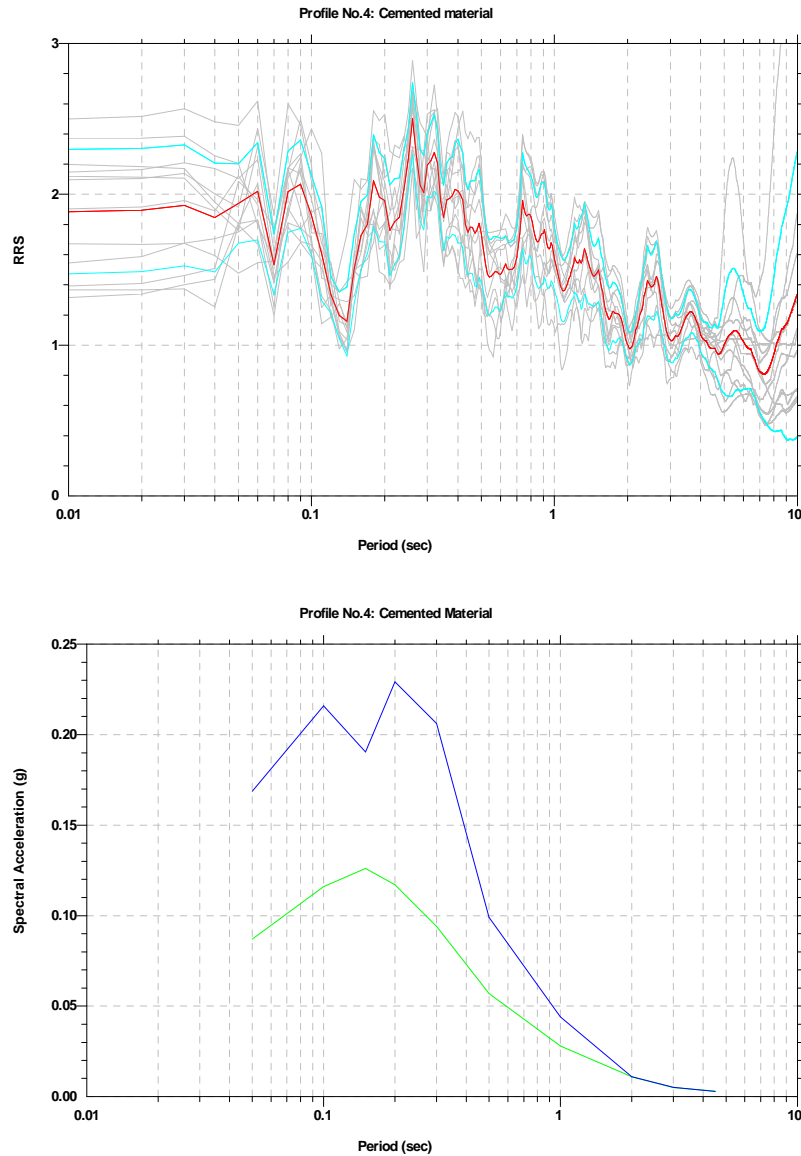


Figure 26. Profile No. 4 (cemented material). (Top) Ratios of response spectra (RRS) for 12 acceleration time histories (gray lines), average RRS (red line) and blue lines show the range from plus to minus one standard deviation of the average RRS; (Bottom) Surface response spectrum (blue line) and UHS (green line).

11 Variability of the shear wave velocity profile

The effect of variability of input ground motion is incorporated in the analysis throughout all the steps of data processing. However, as is often the case in geotechnical analysis, the input parameters of both soil properties and input ground motions are subject to variability. It is expected that shear wave profiles that belong to one typical soil profile should have small variations of velocity as it can be seen on Figure 1. However, the typical soil profile No. 2 (Figure 2) shows significant shear wave profile variability. The sensitivity analysis was performed to investigate the effects of the variability of shear wave velocity on the amplification factor at soil profile No.2. This was done by randomizing the shear velocity profiles. Those profiles were created by using the random generated shear wave velocity from intervals between the lower and upper bounds of the shear velocity. In this method the number of soil columns generated depends on the number of samples selected from shear velocity intervals and number of acceleration time history sets used.

The result of the sensitivity analysis is shown on Figure 27. Figure 27 should be investigated in comparison with Figure 14, which shows the amplification factor for an average velocity profile. Both analyses reveal dominant soil amplification around 0.3 sec. However, the amplitudes of amplifications are different. The average profile (Figure 14) has an average amplification factor of 2.5 and the randomized analysed profile (Figure 27) has an average amplification factor of 2.2. The standard deviation in analysis with the average velocity profile is very small in comparison with the randomized analysis (see Table 10 and Table 13).

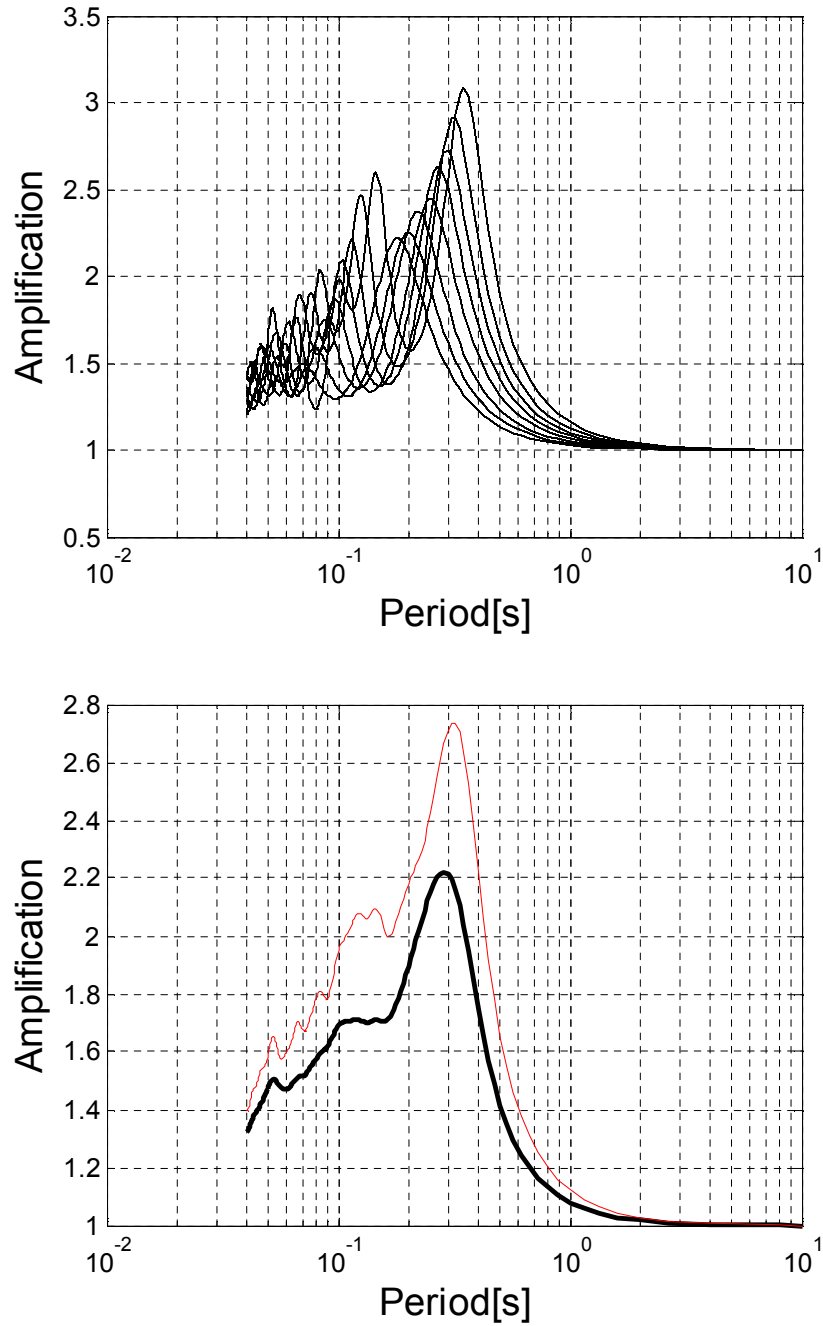


Figure 27. Amplification factor for randomized analysis of typical soil profile No. 2

The Eskom Sere Wind Farm,
Dynamic Response of the Soil

Table 13. Amplification factor and standard deviation for randomized analysis of profile No.2 (shallow bedrock). Max amplification is 2.22 at period 0.29 sec

No	Period [sec]	Amp	std
1	0.05	1.48	0.119
2	0.06	1.47	0.129
3	0.06	1.47	0.129
4	0.07	1.52	0.160
5	0.08	1.58	0.207
6	0.09	1.62	0.164
7	0.10	1.69	0.258
8	0.20	1.89	0.285
9	0.30	2.21	0.508
10	0.40	1.75	0.474
11	0.50	1.41	0.243
12	0.60	1.26	0.144
13	0.70	1.18	0.096
14	0.80	1.13	0.070
15	0.90	1.10	0.053
16	1.00	1.08	0.042
17	2.00	1.02	0.010
18	3.00	1.01	0.005
19	4.00	1.00	0.003
20	5.00	1.00	0.002
21	6.00	1.00	0.001
22	7.00	1.00	0.001
23	8.00	1.00	0.001
24	9.00	1.00	0.000
25	10.00	1.00	0.000

12 Conclusions

This report presents the analysis of a dynamic response of the soil to a strong ground motion for the planned Eskom Sere Wind Farm site. An assessment of the dynamic response of the soil to strong ground motion was carried out in accordance with the IEC (2005) and GL (2010) standards for the design and safety requirements of wind turbines.

The ground-motion predictions for the site of interest need to take into consideration the local site conditions. Design of ground motions must be compatible with the soil conditions at the design site. The effect of site response is studied using the equivalent linear one-dimensional wave propagation analysis. The site classification, based on average soil's shear wave velocity in the upper 30 meters, may not be a good indicator of site response to deep soil.

The effect of input motion uncertainty and uncertainties in soil properties are discussed throughout the report and quantified using the standard deviation.

Model of soil columns

Geotechnical models of typical soil profiles were provided by Mr Ron Tluczek from BKS using borehole, laboratory and geophysical information. Four soil profile types within Sere Wind farm with depth to bedrock varying from 28 m to 150 m have been considered for this study. The first 50 m of the shear velocity profile model is based on an average velocity observed during a surface wave survey. Below a depth of 50 m the velocity model was constructed using material properties obtained from rotary cored boreholes and percussion boreholes. In the case of a typical soil profile No.1 (sand to depth), the shear velocity model below a depth of 100 m was assumed using some indication from the resistivity investigation. At the Sere Wind Farm site the shear modulus degradation curves and damping ratio curves were selected using generic data suitable for deep soil conditions. The generic curves developed

by EPRI (1993) are most suitable to model pressure-dependent cohesionless soils, soils with gravels, sands, and low PI clays, and are therefore used to model soil at this site.

Acceleration time histories

The seismic hazard analysis described in Part 1 of this investigation, provides uniform hazard spectra (UHS) at bedrock level ($V_s=750\text{m/s}$) and information that most of the hazard comes from a magnitude 6.4 earthquake at a distance of 13 -15 km. The UHS was available for the period range of 0.05 sec to 3.0 sec. Since the natural period of the structure is 3 sec, the UHS was extended to 4.5 sec period to comply with EC and US standards. The above information is required for the selection process of the appropriate ground motion records required for modelling of the dynamical soil response. As recommended by the GL (2010) guidance, six earthquakes were selected with two independent horizontal components each. The amplitude of the recorded time history was adjusted, so it could match the UHS between 0.05 sec and 4.5 sec period. The modified acceleration records were used as input motion at the outcrop level for each of the site types.

Amplification factor using transfer function method

In general, it can be said that the higher the depth of base rock level, the larger the value of amplification and higher the value of predominant period. These periods and amplification factors for each site are listed below:

- Profile No. 1 (bedrock depth 150 m) maximal amplification 2.77 at 0.31 sec
- Profile No. 2 (bedrock depth 28 m) maximal amplification 2.51 at 0.25 sec
- Profile No. 3 (bedrock depth 100 m) maximal amplification 2.12 at 0.29 sec
- Profile No. 4 (bedrock depth 100 m) maximal amplification 2.64 at 0.29 sec

The shape of the amplification factor function is presented in Figure 13 (soil profile No.1), Figure 14 (soil profile No. 2), Figures 15 (soil profile No. 3) and Figures 16 (soil profile No. 4). The numerical values of amplification factor functions and standard deviations for each period

are presented in Table 9 (soil profile No.1), Table 10 (soil profile No. 2), Table 11 (soil profile No. 3) and Table 12 (soil profile No. 4).

Amplification factor with the RRS method

The amplification factor caused by the soil column could be quantified by the Ratios of Response Spectra (RRS). The RRS approach forms the basis of the site response coefficients used in many building codes and it is recommended by regulators. The RRS was calculated for the 12 surface-outcrop motion pairs, and then the mean values were obtained (see Figures 23, 24, 25 and 26 (top figures)). The estimates of site response quantified by the RRS method were affected by the choice of input motion. Amplification factor was obtained as well using the transfer function. Both methods demonstrated that the dominant peaks for the periods larger than 0.1 sec were similar (see Figure pairs 13-23, 14 - 24, 15 - 25 and 16 – 26). The difference between both methods is observed only for periods lower than 0.1 sec and is not important for analysing the structure with a natural period of 3 sec.

Surface Response Spectra

Two methods were used to calculate the surface response spectra: one from surface acceleration time history and the second from the average RRS. Using surface ground motion for each typical soil profile, twelve response spectra and their averages were obtained for 1% damping (see Figures 19, 20, 21, and 22). A smooth surface response spectrum was obtained from the product of the average RRS and the UHS (see Figures 23, 24, 25 and 26 and numerical values in the table below)

The Eskom Sere Wind Farm,
Dynamic Response of the Soil

Period [sec]	UHS - outcrop response spectrum [g]	Response Spectrum for Typical Soil Profiles [g]			
		No 1	No. 2	No. 3	No. 4
0.05	0.087	0.148	0.193	0.171	0.169
0.1	0.116	0.195	0.243	0.228	0.216
0.15	0.126	0.193	0.210	0.207	0.190
0.2	0.117	0.179	0.255	0.219	0.229
0.3	0.094	0.199	0.185	0.175	0.206
0.5	0.057	0.118	0.081	0.101	0.099
1.0	0.028	0.053	0.032	0.045	0.044
2.0	0.011	0.015	0.010	0.011	0.011
3.0	0.005	0.006	0.005	0.005	0.005
4.5	0.003	0.003	0.003	0.003	0.003

Similar patterns of response spectra at each of the four typical soil types were observed. Soil amplifies ground motion in a period range from 0.1 to 0.5, almost twice of that of the outcrop ground motion.

Structure (turbine) related implication

According to the building regulation codes, a band of periods from 0.6 to 6 sec (EC, 2004) or from 0.6 to 4.5 sec (ASCE, 2007) should be analyzed for the structure with the natural period of 3 sec. Soil columns do not amplify response spectra between 2.0 sec to 4.5 sec, therefore, the fundamental mode of the turbine will not be affected by soil conditions. However, response spectra in the period range 0.6 sec – 2.0 sec are gradually affected by the soil

column and at a period of 0.6 sec the amplification factor in comparison to outcrop motion is almost 2. This indicates that the higher mode of the turbine could be affected by soil conditions. Recent research indicates that dynamical analysis of the turbine should include vibration caused by higher modes.

Attachment with acceleration time histories

Modified acceleration time histories at the outcrop level and surface level for each type of soil column are attached as separate files.

13 References

ASCE, 2007, American Society of Civil Engineers, ASCE/SEI 41-06. ,Seismic rehabilitation of existing buildings, American Society of Civil Engineers, Reston, Va.

Bommer, J. J. and Acevedo, A. B. 2004, The use of real earthquake accelrograms as input to dynamic analysis, Journal of Earthquake Engineering 8, p43-91.

CTBUH, 2008, Recommendation for the seismic design of high-rise buildings, Council on Tall Buildings and Urban Habitat, CTBUH –Publication.

EC, 2004, Eurocode, EC, Design of structures for earthquake resistance, BSEN 1998-5:2004

EPRI, 1993, Electric Power Research Institute, Guidelines for determining design basis ground motions, Report EPRI TR-102293. Palo Alto, California.

GL, 2010, Germanischer Lloyd, GL, Guideline for the certification of wind turbines”, Edition 2010. Hamburg, Germany.

Hancock, J., Watson-Lamprey, J., Abrahamson, N., Bommer, J., Markatis, A., McCoy, E., and Mendis,R., 2006, An Improved method of matching response spectra of recorded earthquake ground motions using wavelets, Journal of Earthquake Engineering, Vol. 10, pp. 67-89

Idriss,I.M. and Sun,J.I., 1992, User’s Manual for SHAKE91, Center for Geotechnical Modeling, Department of Civil and Environmental Engineering, University of California, Davis, California, USA.

IEC, 2005, International Electrotechnical Commission, IEC, Wind Turbines – Part 1: Design Requirements 3-rd Editions. IEC 61400-1:2005-08, IEC, Geneva, Switzerland.

Kramer, S. L.,1996, Geotechnical earthquake engineering, Prentice-Hall, Upper Saddle River, New Jersey, ISBN 0-13-374943-6.

Midzi, V., Strasser F.O., and Zulu,B., 2010, Part 1: Probabilistic seismic hazard analysis for the ESKOM Sere Wind Farm Site, Western Cape, Report No. 2010-0235

Ntambakwa, E., and Rofers, M., 2009, Seismic forces for wind turbine foundations, wind turbine structures, dynamics, loads and control, American Wind Energy Association(AWEA) Wind-power Conference.

PEER, 2010, Database, <http://peer.berkeley.edu/nga/index.html>, Pacific Earthquake Engineering Research, University of California, Berkeley.

Prowell, I., Veletzos, M. Elgamal, E., 2008, Full scale testing for investigation of wind turbine seismic response,unpublished,<http://www.scribd.com/doc/33472910/Full-Scale-Testing-for-Investigation-of-Wind-Turbine-Seismic-Response>

Prowell,I., and Veers,P., 2009, Assessment of wind turbine seismic risk: existing literature and simple study of tower moment demand, Sandia National Laboratories, SAND2009-1100.

SANS, 2008, South African National Standard, Basis of structural design and actions for buildings and industrial structures, Part4: Seismic actions and general requirements for buildings. SANS 10160-4:2008 (Edition1).

Seed, H.B., Wong, R.T., Idriss, I.M., and Tokimatsu,K., 1986, "Moduli and Damping Factors for Dynamic Analyses of Cohesionless Soils," Journal of Geotechnical Engineering, ASCE, Vol. 112, No. 11: 1016-1032.

Seed, H.B., and Idriss,I.M., 1970, Soil Moduli and damping factors for dynamic response analyses, Report EERC 70-10. Berkeley: University of California, Earthquake Engineering Research Center.

Sun, J. I., Golesorkhi,R., and Seed H.B., 1988, Dynamic moduli and damping ratios for cohesive soils, Report UBC/EERC-88/15. Berkeley: University of California, Earthquake Engineering Research Center.

Vucetic, M. and Dobry, R., 1991, Effect of soil plasticity on cyclic response, Journal of Geotechnical Engineering, 117(1): 89-107.

APPENDIX J:

SEISMIC HAZARD AND DYNAMIC RESPONSE ASSESSMENT

Part 2 (b): Dynamic Response of the Soil – Appendix

“Dynamic Response of the Soil to Strong Ground Motion”

Appendix: Dynamic Response of the Soil to Strong Ground Motion

Table 1. Earthquakes records used in ground response analyses

RECORD NUMBER	COMPONENT	EARTHQUAKE	STATION	MAGNITUDE Ms	CLOSEST DISTANCE [km]	HYPOCENTRAL DISTANCE [km]
s1	CCN090	NORTHRIDGE,USA 01/17/94 12:31	CENTURY CITY LACC NORTH, 090	6.7	25.7	18.3
s2	CCN360	NORTHRIDGE,USA 01/17/94 12:31	CENTURY CITY LACC NORTH, 360	6.7	25.7	18.3
s3	H-Z08000	COALINGA ,USA 05/02/83 23:42,	PARKFIELD - FAULT ZONE 8, 000	6.5	29.6	-
s4	H-Z08090	COALINGA,USA 05/02/83 23:42	PARKFIELD - FAULT ZONE 8, 090	6.5	29.6	-
s5	A-TMZ000	FRIULI, ITALY 05/06/76 20:00	TOLMEZZO, 000	6.5	15.8	20.8
s6	A-TMZ270	FRIULI, ITALY 05/06/76 20:00,	TOLMEZZO, 270	6.5	15.8	20.8
s7	COR-L	CORINTH, GREECE 02/24/81,00:00	CORINTH, LONGITUDINAL	6.6	10.3	21
s8	COR-T	CORINTH, GREECE 02/24/81, 00:00	CORINTH, TRANSVERSE	6.6	10.3	21
s9	H-CPE147	IMPERIAL VALLEY,USA 10/15/79 23:16,	CERRO PRIETO, 147	6.5	15.2	24.8
s10	H-CPE237	IMPERIAL VALLEY,USA 10/15/79 23:16,	CERRO PRIETO, 237	6.5	15.2	24.8
s11	LO4111	SAN FERNANDO,USA 02/09/71 14:00,	LAKE HUGHES #4, 111	6.6	25	24.2
s12	LO4201	SAN FERNANDO,USA 02/09/71 14:00,	LAKE HUGHES #4, 201	6.6	25	24.2

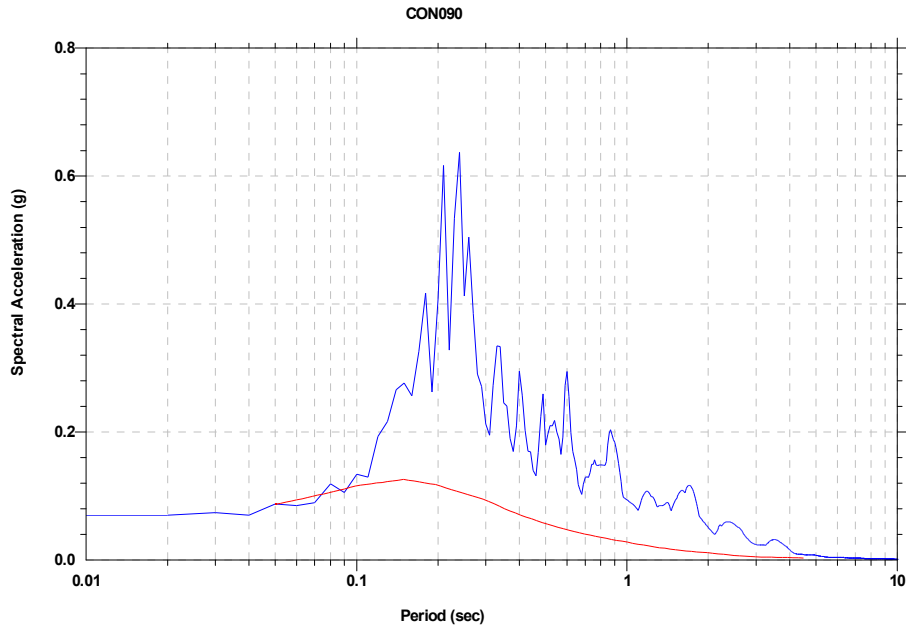


Figure.1 Acceleration response spectra (1% Damping in g's). Response spectra of scaled ground acceleration time history (blue colour): 1994 Northridge earthquake, Century City LACC North station and CON090 component. Target response spectrum (red colour): uniform hazard spectrum at 10% in 50 years hazard level

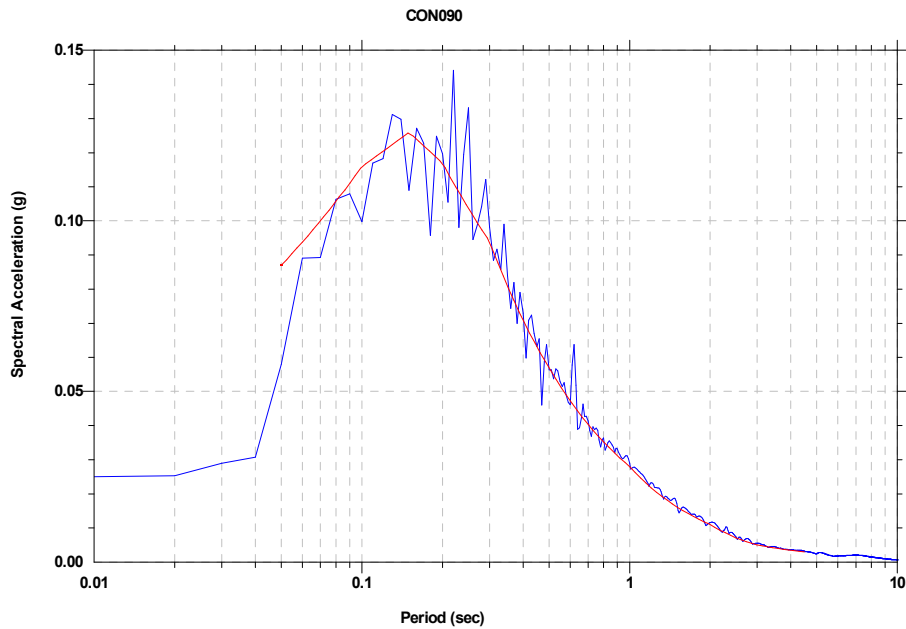


Figure. 2 Acceleration response spectra (1% Damping in g's). Response spectra of matched time history (blue colour): 1994 Northridge earthquake, Century City LACC North station, CON090 component. Target response spectrum (red colour): uniform hazard spectrum at 10% in 50 years hazard level.

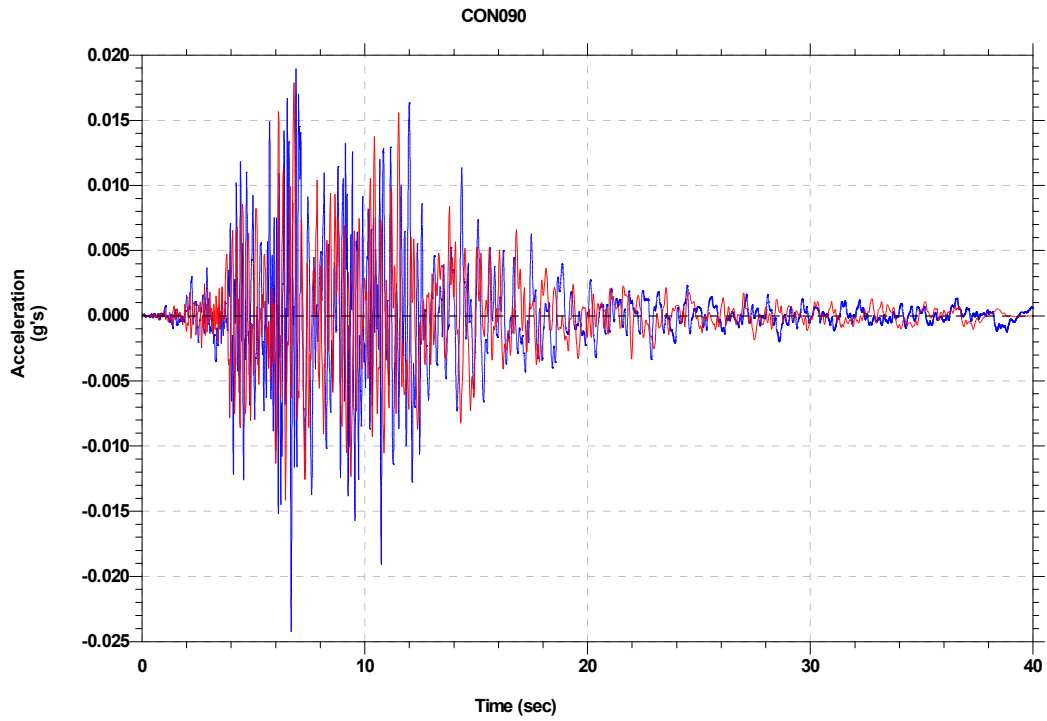


Figure.3 Acceleration time histories. Scaled seed time history (red colour) for 1994 Northridge earthquake, Century City LACC North station, CON090 component and adjusted time history (blue colour) that matched the uniform hazard spectrum.

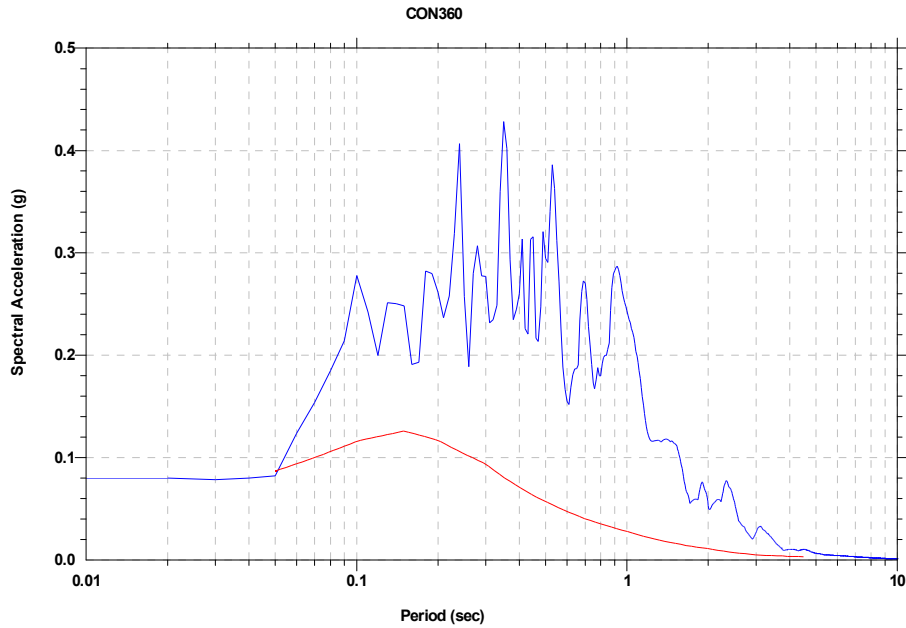


Figure.4 Acceleration response spectra (1% Damping in g's). Response spectra of scaled ground acceleration time history (blue colour): 1994 Northridge earthquake, Century City LACC North station and CON360 component. Target response spectrum (red colour): uniform hazard spectrum at 10% in 50 years hazard level

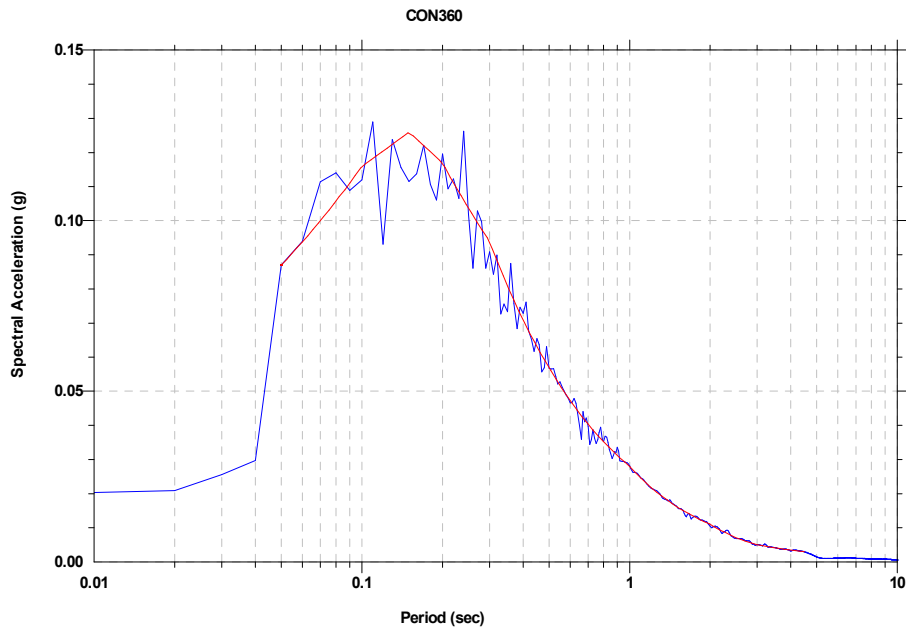


Figure. 5 Acceleration response spectra (1% Damping in g's). Response spectra of matched time history (blue colour): 1994 Northridge earthquake, Century City LACC North station, CON360 component. Target response spectrum (red colour): uniform hazard spectrum at 10% in 50 years hazard level.

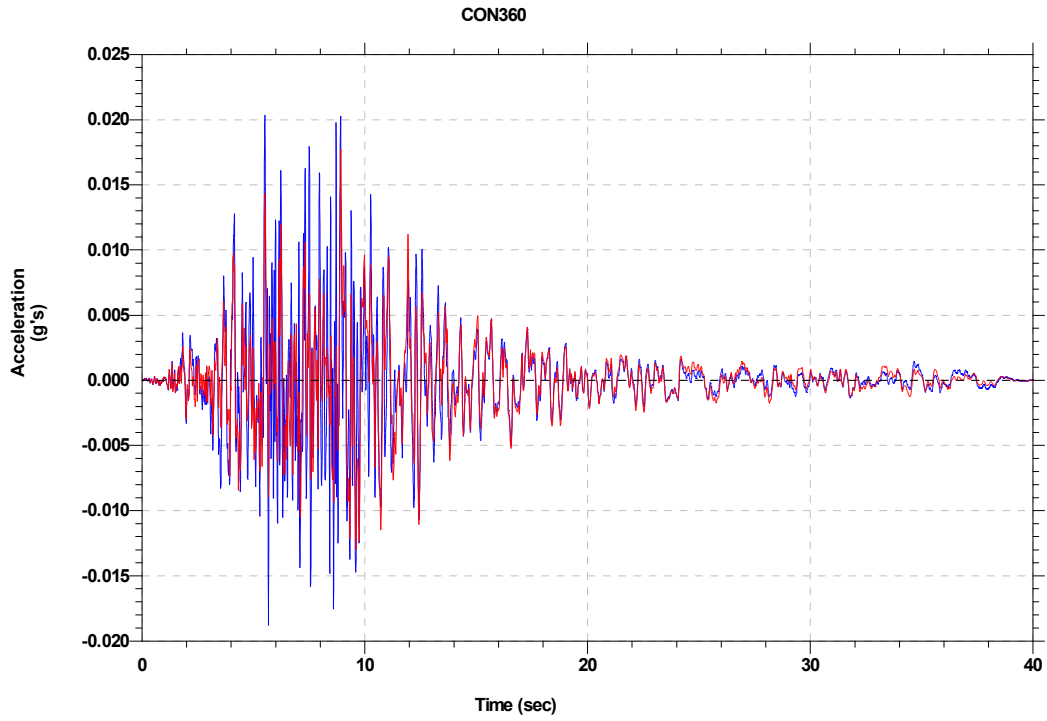


Figure.6 Acceleration time histories. Scaled seed time history (red colour) for 1994 Northridge earthquake, Century City LACC North station, CON360 component and adjusted time history (blue colour) that matched the uniform hazard spectrum.

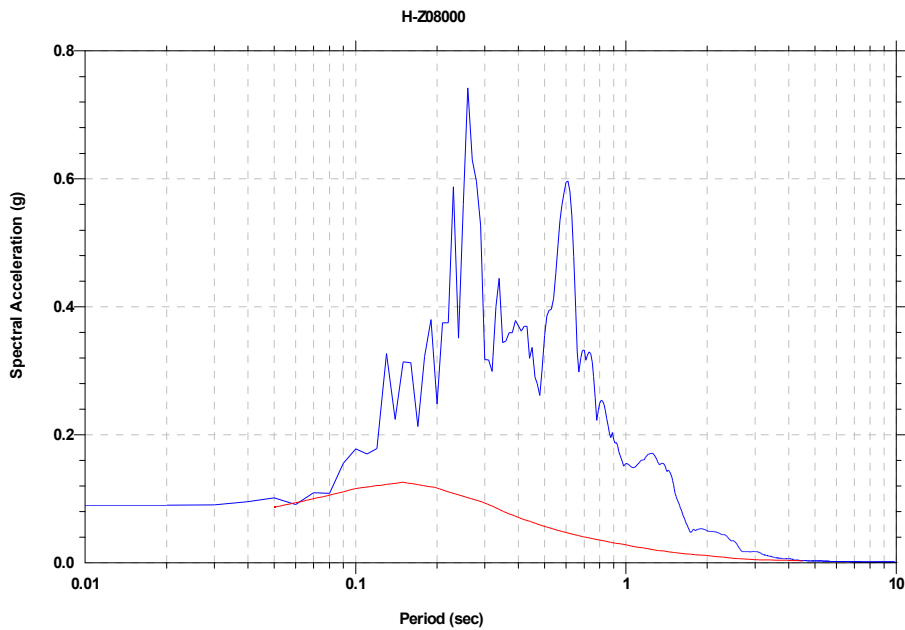


Figure.7 Acceleration response spectra (1% Damping in g's). Response spectra of scaled ground acceleration time history (blue colour): 1983 Coaling earthquake, Parkfield Fault Zone 8 station and H-Z08000 component. Target response spectrum (red colour): uniform hazard spectrum at 10% in 50 years hazard level

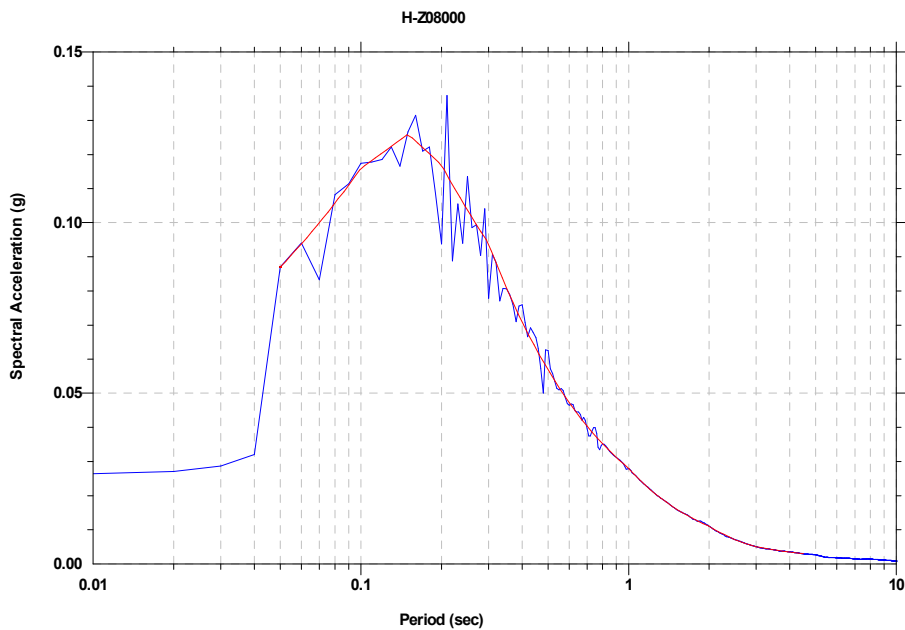


Figure. 8 Acceleration response spectra (1% Damping in g's). Response spectra of matched time history (blue colour): 1983 Coaling earthquake, Parkfield Fault Zone 8 station and H-Z08000 component. Target response spectrum (red colour): uniform hazard spectrum at 10% in 50 years hazard level.

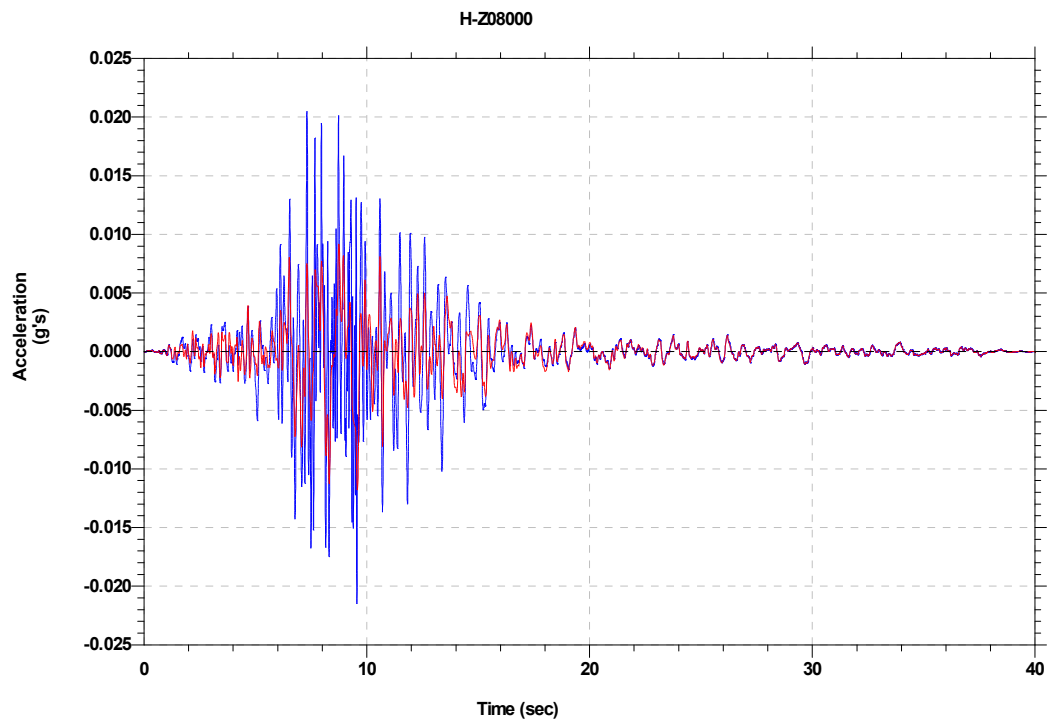


Figure.9 Acceleration time histories. Scaled seed time history (red colour) for 1983 Coaling earthquake, Parkfield Fault Zone 8 station and H-Z08000 component and adjusted time history (blue colour) that matched the uniform hazard spectrum.

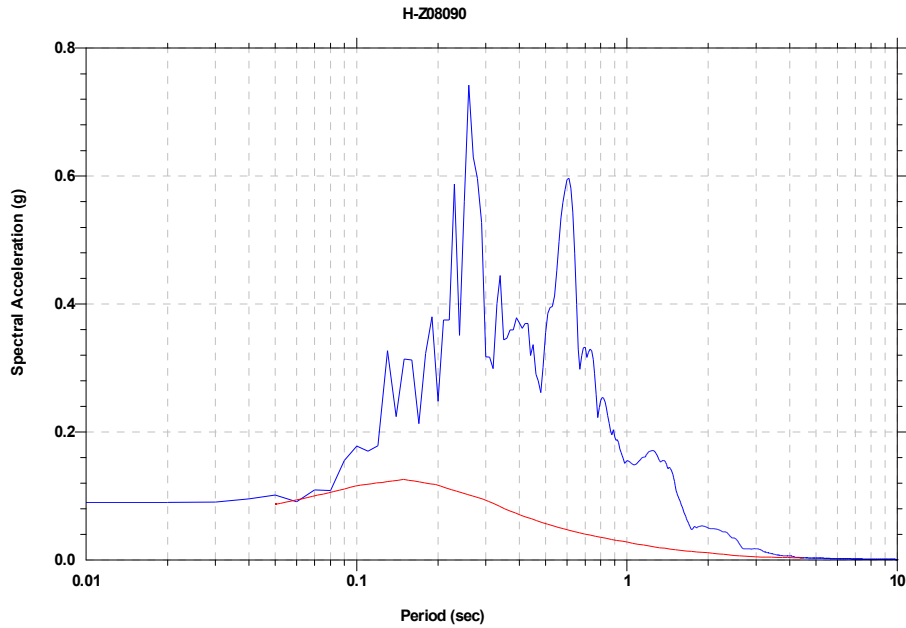


Figure.10 Acceleration response spectra (1% Damping in g's). Response spectra of scaled ground acceleration time history (blue colour): 1983 Coaling earthquake, Parkfield Fault Zone 8 station and H-Z08090 component. Target response spectrum (red colour): uniform hazard spectrum at 10% in 50 years hazard level

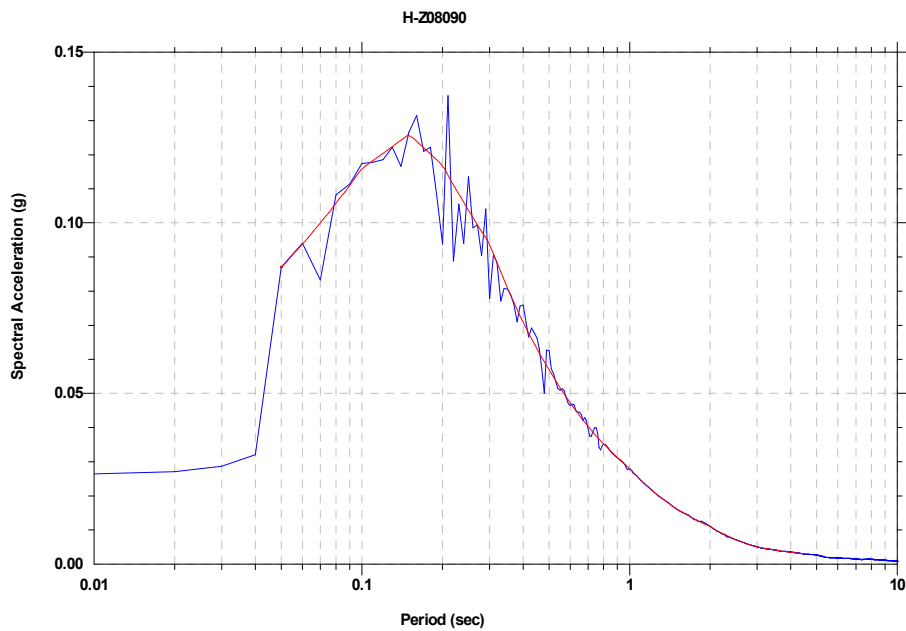


Figure. 11 Acceleration response spectra (1% Damping in g's). Response spectra of matched time history (blue colour): 1983 Coaling earthquake, Parkfield Fault Zone 8 station and H-Z08090 component. Target response spectrum (red colour): uniform hazard spectrum at 10% in 50 years hazard level.

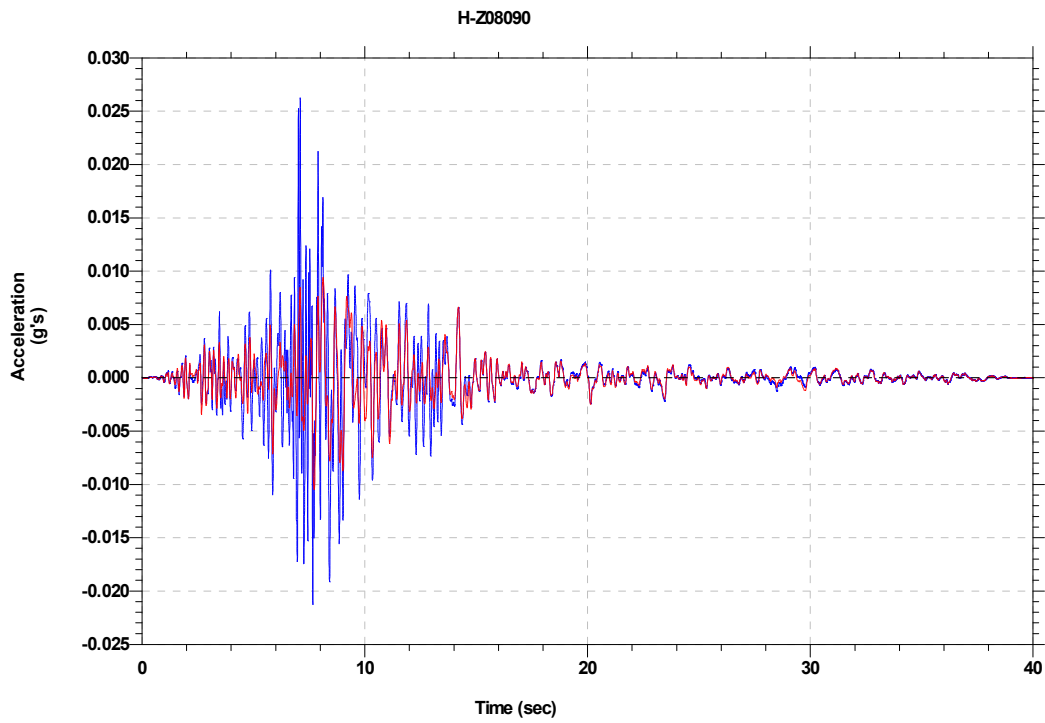


Figure.12 Acceleration time histories. Scaled seed time history (red colour) for 1983 Coaling earthquake, Parkfield Fault Zone 8 station and H-Z08090 component and adjusted time history (blue colour) that matched the uniform hazard spectrum.

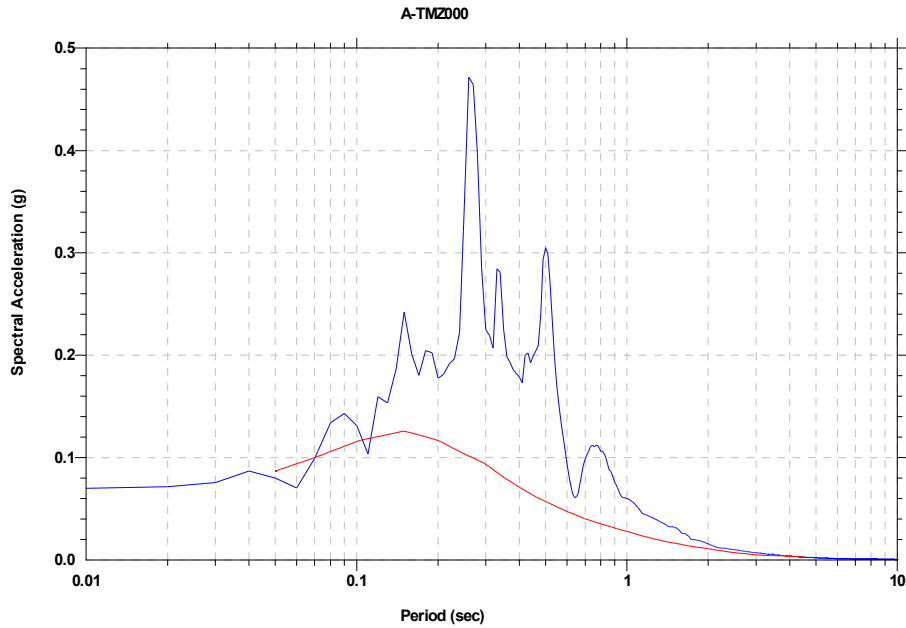


Figure.13 Acceleration response spectra (1% Damping in g's). Response spectra of scaled ground acceleration time history (blue colour):1974 Friuli, Italy earthquake, Tolmezzo station and A-TMZ000 component. Target response spectrum (red colour): uniform hazard spectrum at 10% in 50 years hazard level

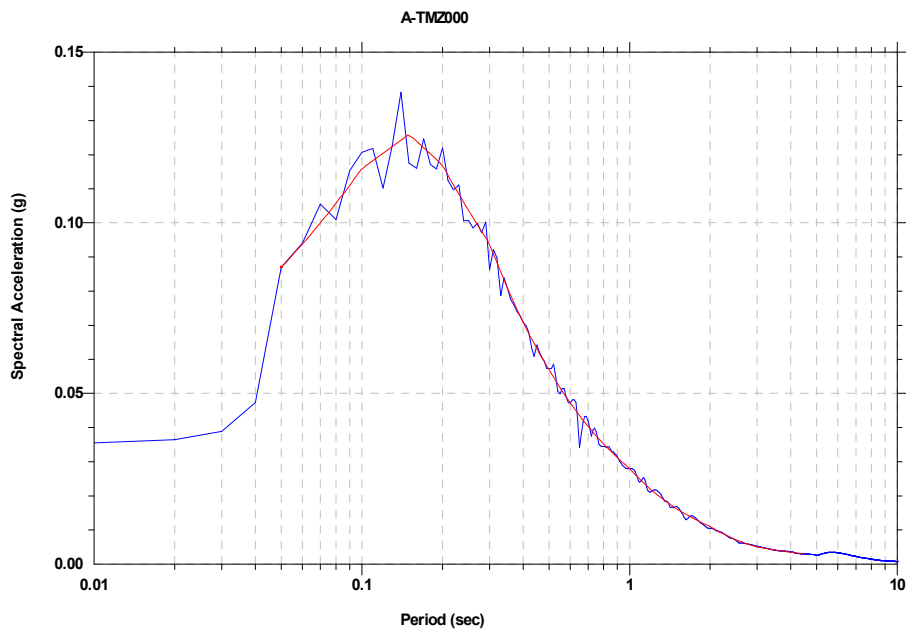


Figure. 14 Acceleration response spectra (1% Damping in g's). Response spectra of matched time history (blue colour): 1974 Friuli, Italy earthquake, Tolmezzo station and A-TMZ000 component. Target response spectrum (red colour): uniform hazard spectrum at 10% in 50 years hazard level.

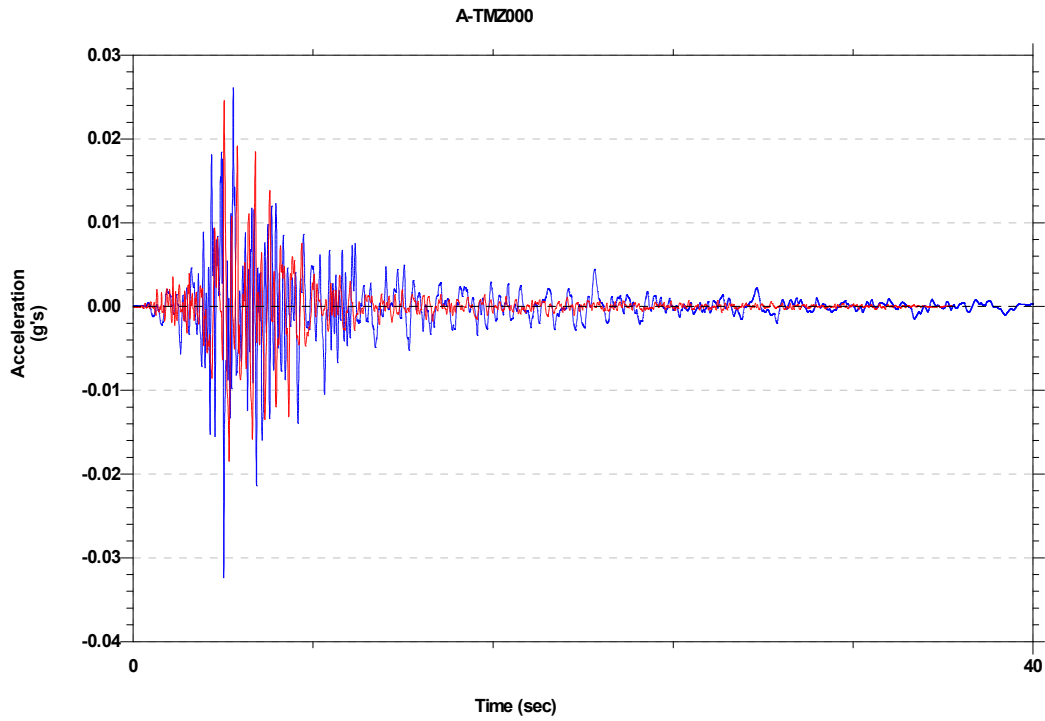


Figure.15 Acceleration time histories. Scaled seed time history (red colour) for 1974 Friuli, Italy earthquake, Tolmezzo station and A-TMZ000 component and adjusted time history (blue colour) that matched the uniform hazard spectrum.

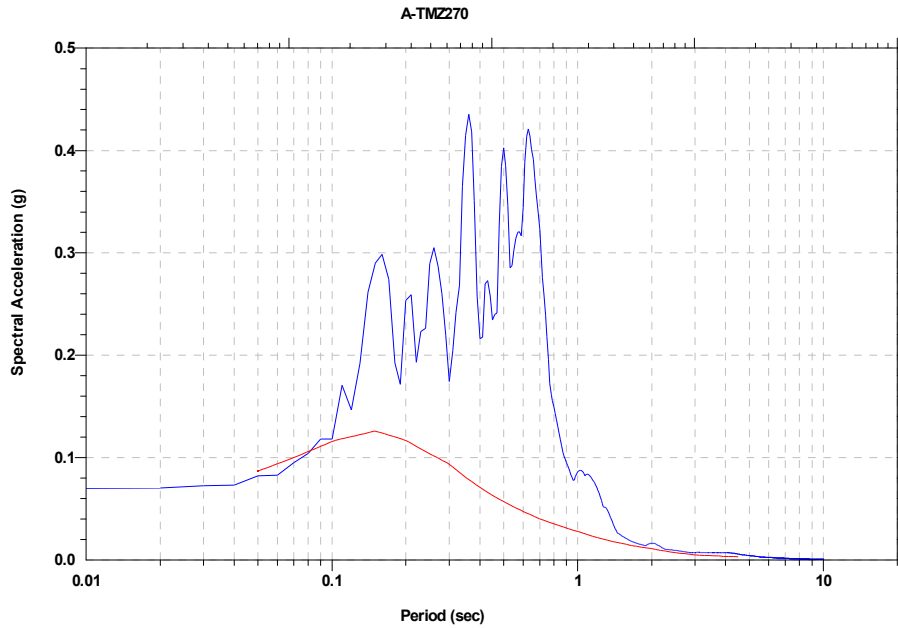


Figure.16 Acceleration response spectra (1% Damping in g's). Response spectra of scaled ground acceleration time history (blue colour): 1974 Friuli, Italy earthquake, Tolmezzo station and A-TMZ270 component. Target response spectrum (red colour): uniform hazard spectrum at 10% in 50 years hazard level

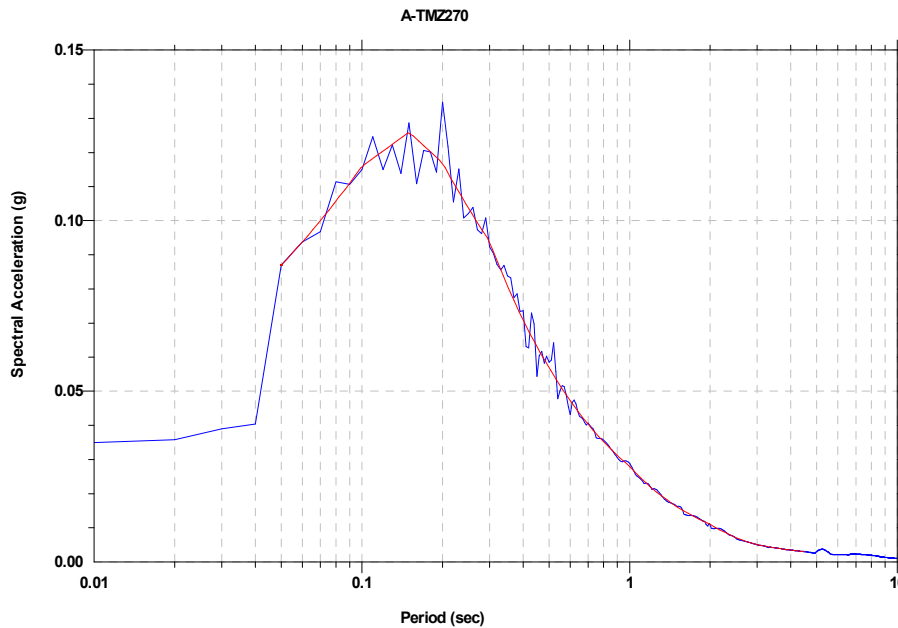


Figure. 17 Acceleration response spectra (1% Damping in g's). Response spectra of matched time history (blue colour): 1974 Friuli, Italy earthquake, Tolmezzo station and A-TMZ270 component. Target response spectrum (red colour): uniform hazard spectrum at 10% in 50 years hazard level.

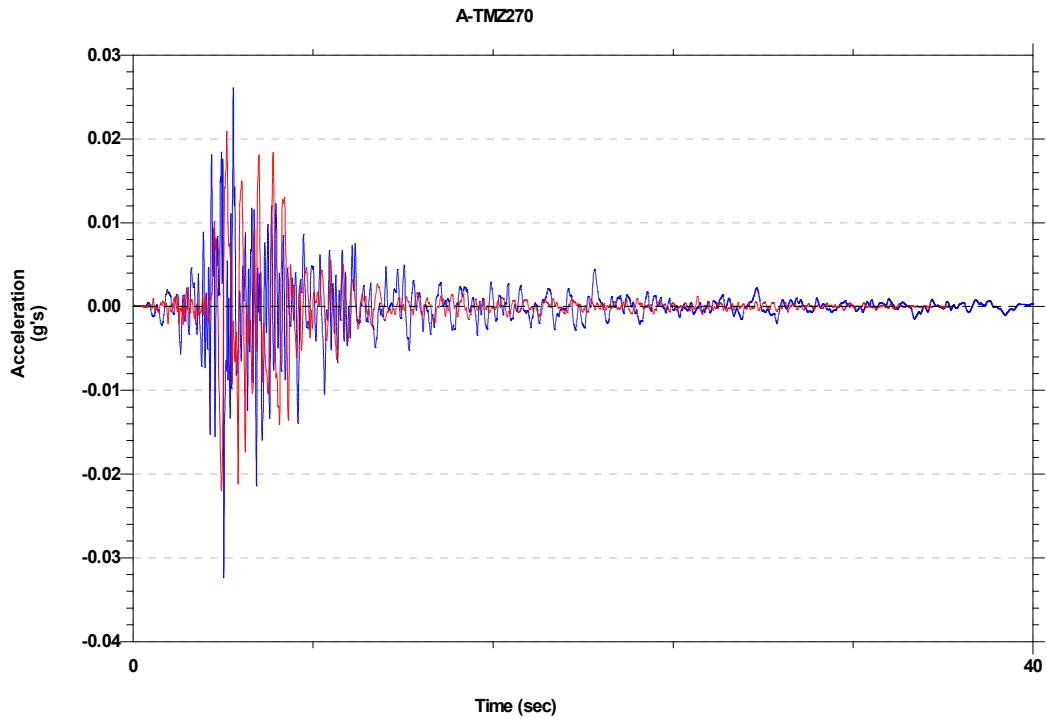


Figure.18 Acceleration time histories. Scaled seed time history (red colour) for 1974 Friuli, Italy earthquake, Tolmezzo station and A-TMZ270 component and adjusted time history (blue colour) that matched the uniform hazard spectrum.

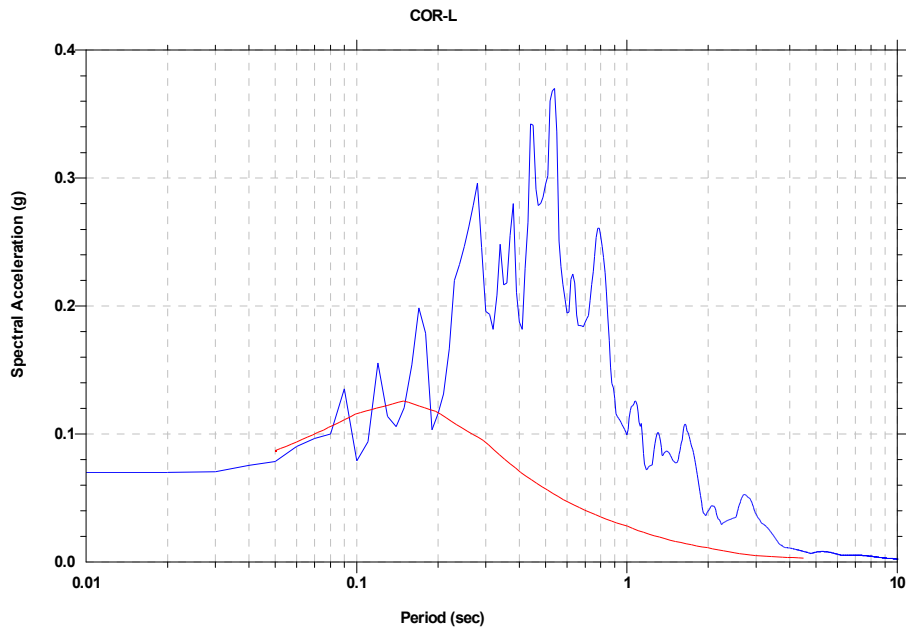


Figure.19 Acceleration response spectra (1% Damping in g's). Response spectra of scaled ground acceleration time history (blue colour):1981 Corinth, Greece earthquake, Corinth station and longitudinal component. Target response spectrum (red colour): uniform hazard spectrum at 10% in 50 years hazard level

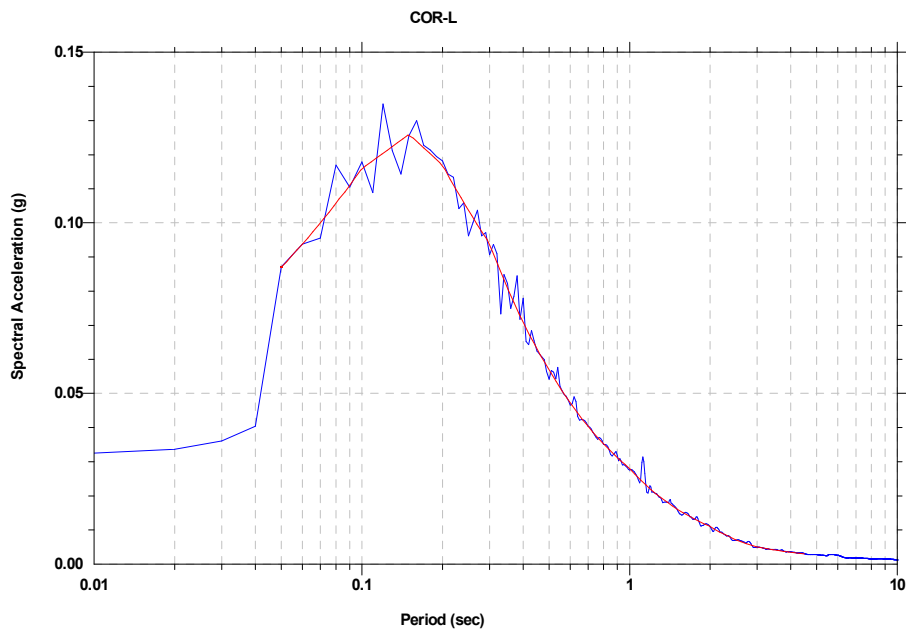


Figure. 20 Acceleration response spectra (1% Damping in g's). Response spectra of matched time history (blue colour): 1981 Corinth, Greece earthquake, Corinth station and longitudinal component. Target response spectrum (red colour): uniform hazard spectrum at 10% in 50 years hazard level.

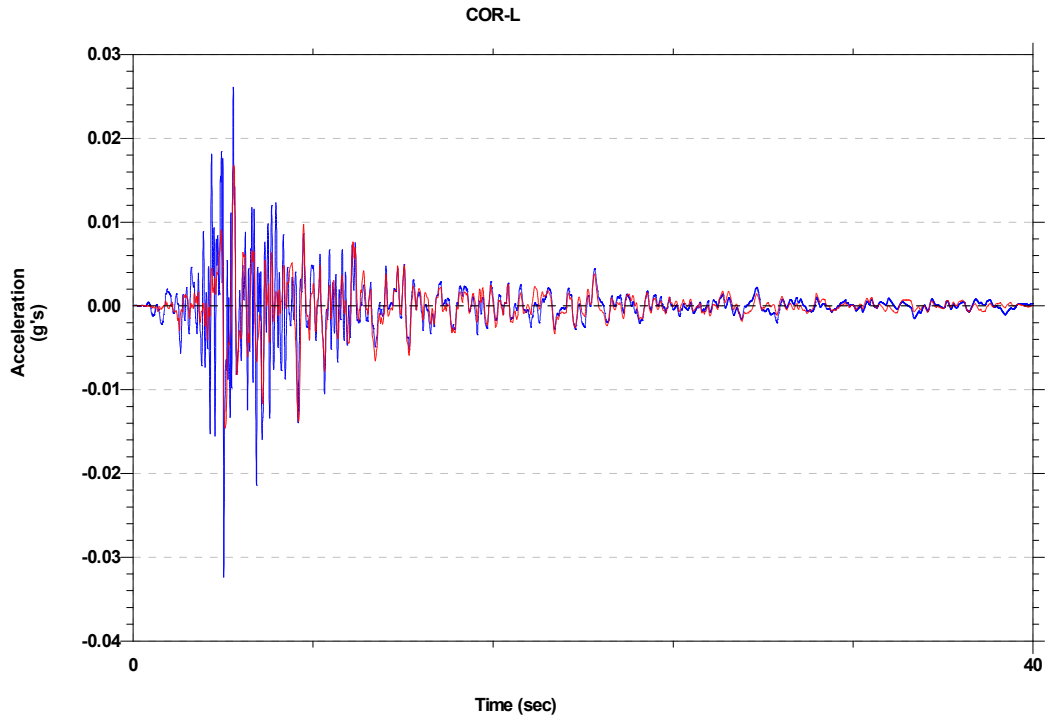


Figure.21 Acceleration time histories. Scaled seed time history (red colour) for 1981 Corinth, Greece earthquake, Corinth station and longitudinal component and adjusted time history (blue colour) that matched the uniform hazard spectrum.

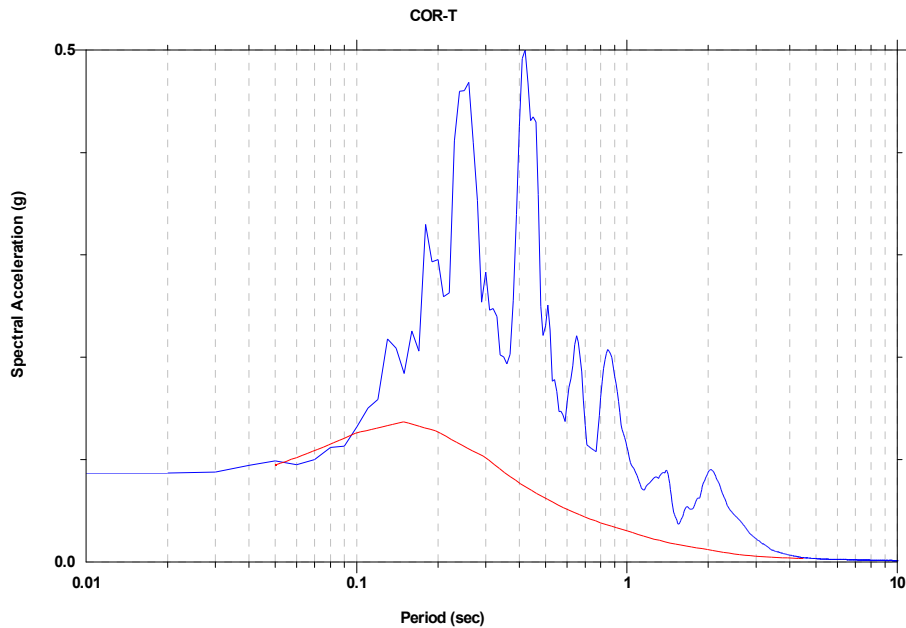


Figure.22 Acceleration response spectra (1% Damping in g's). Response spectra of scaled ground acceleration time history (blue colour):1981 Corinth Greece earthquake, Corinth station and transverse component. Target response spectrum (red colour): uniform hazard spectrum at 10% in 50 years hazard level

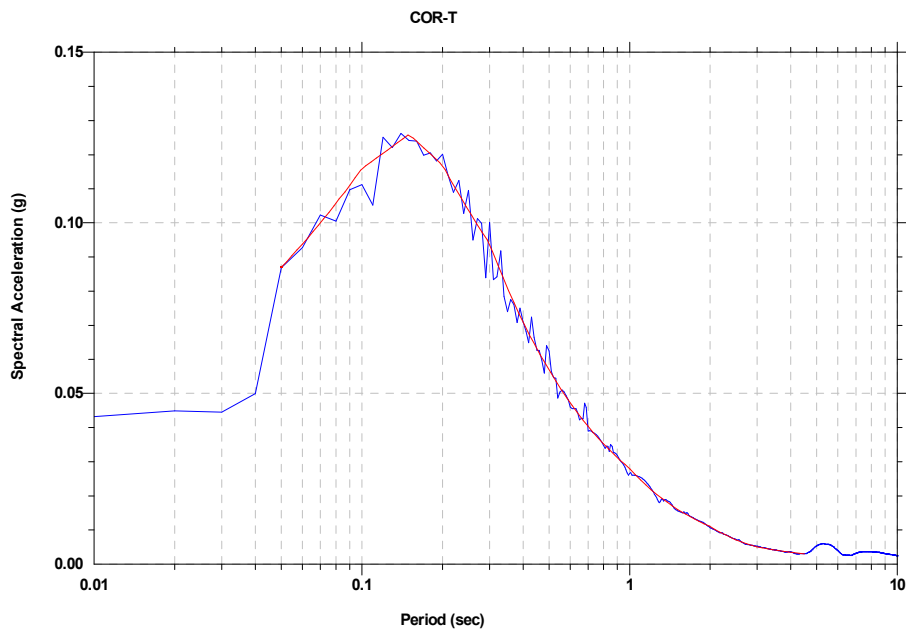


Figure. 23 Acceleration response spectra (1% Damping in g's). Response spectra of matched time history (blue colour): 1981 Corinth, Greece earthquake, Corinth station and transverse component. Target response spectrum (red colour): uniform hazard spectrum at 10% in 50 years hazard level.

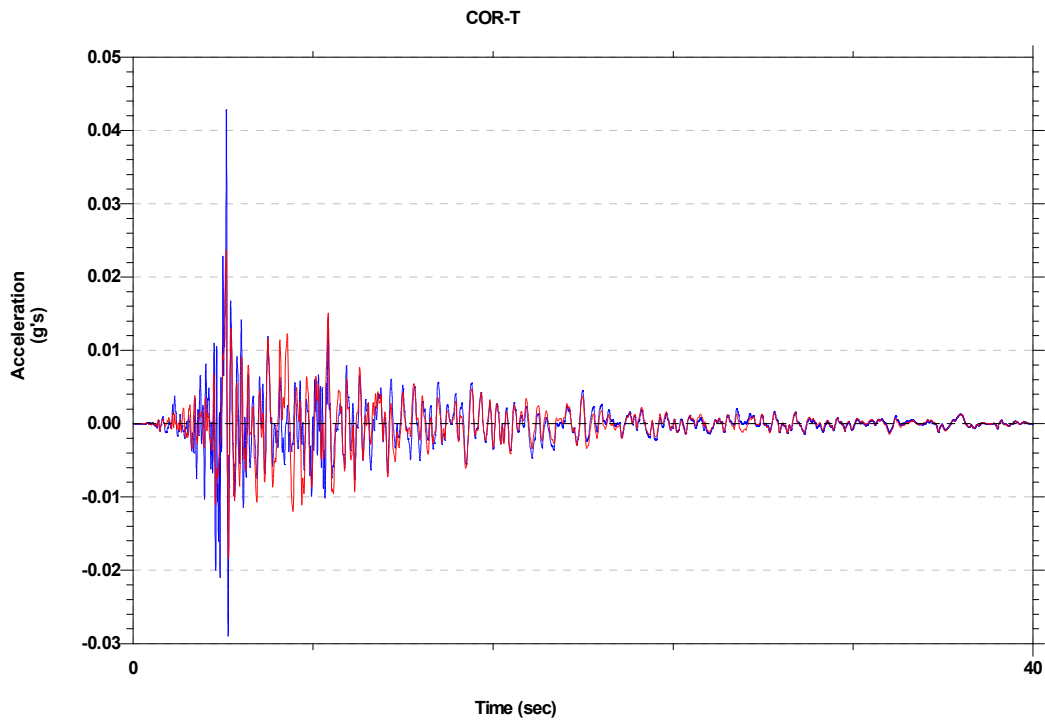


Figure.24 Acceleration time histories. Scaled seed time history (red colour) for 1981 Corinth, Greece earthquake, Corinth station and transverse component and adjusted time history (blue colour) that matched the uniform hazard spectrum.

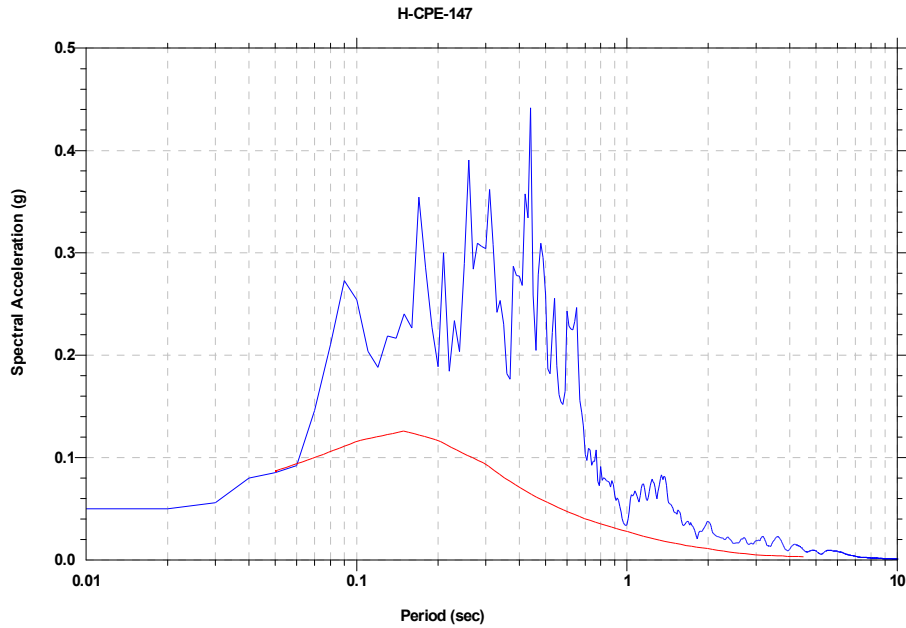


Figure.25 Acceleration response spectra (1% Damping in g's). Response spectra of scaled ground acceleration time history (blue colour):1981 Imperial Valley earthquake, Cerro Prieto station and H-CPE147 component. Target response spectrum (red colour): uniform hazard spectrum at 10% in 50 years hazard level

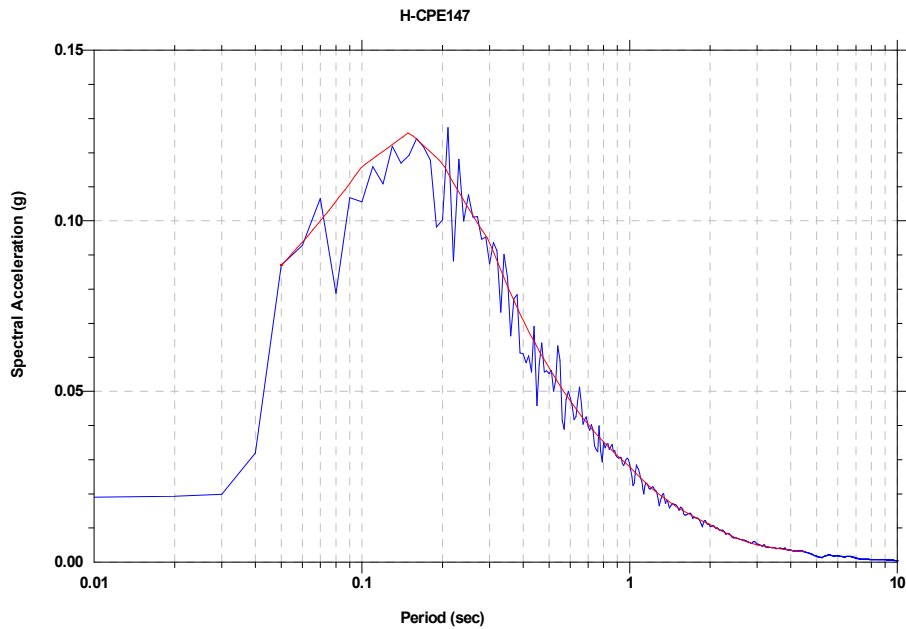


Figure. 26 Acceleration response spectra (1% Damping in g's). Response spectra of matched time history (blue colour): 1981 Imperial Valley earthquake, Cerro Prieto station and H-CPE147 component. Target response spectrum (red colour): uniform hazard spectrum at 10% in 50 years hazard level.

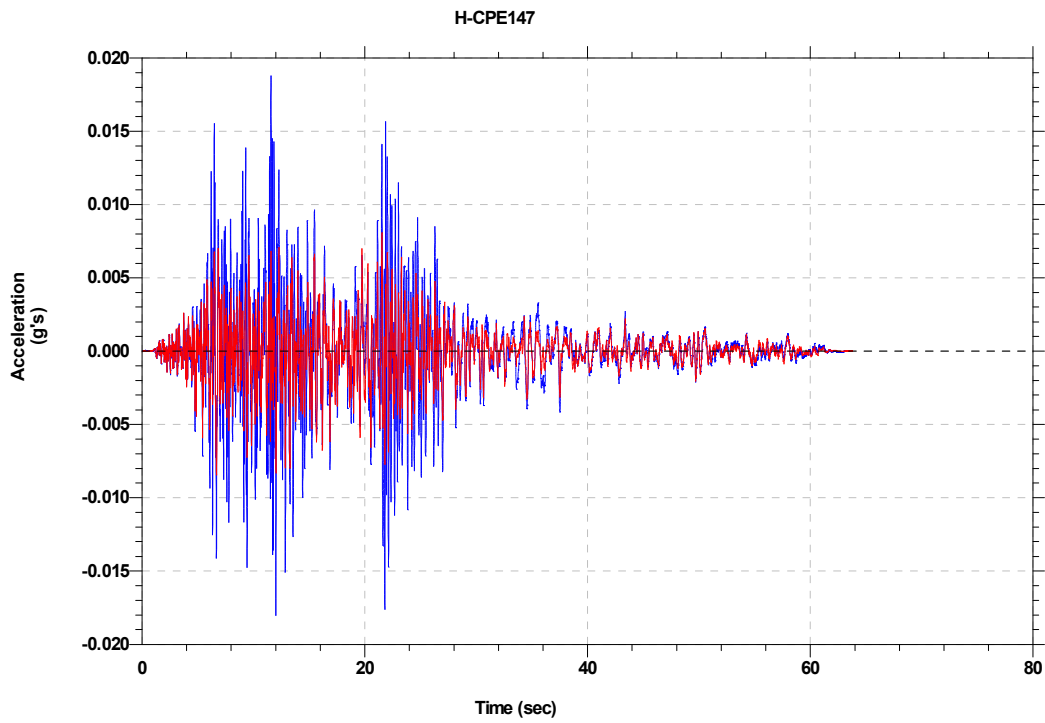


Figure.27 Acceleration time histories. Scaled seed time history (red colour) for 1981 Imperial Valley earthquake, Cerro Prieto station, H-CPE147 component and adjusted time history (blue colour) that matched the uniform hazard spectrum.

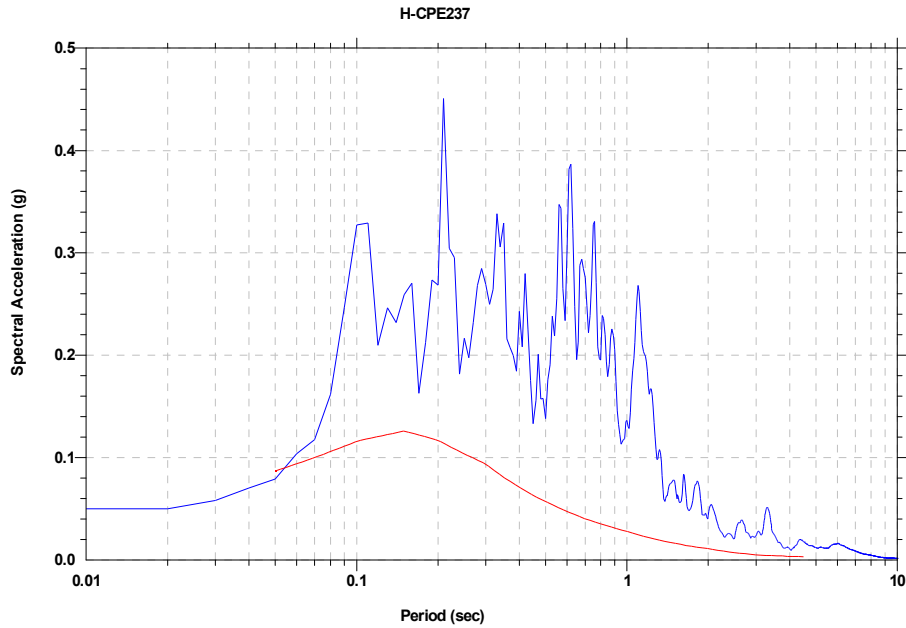


Figure.28 Acceleration response spectra (1% Damping in g's). Response spectra of scaled ground acceleration time history (blue colour):1981 Imperial Valley earthquake, Cerro Prieto station and H-CPE237 component. Target response spectrum (red colour): uniform hazard spectrum at 10% in 50 years hazard level

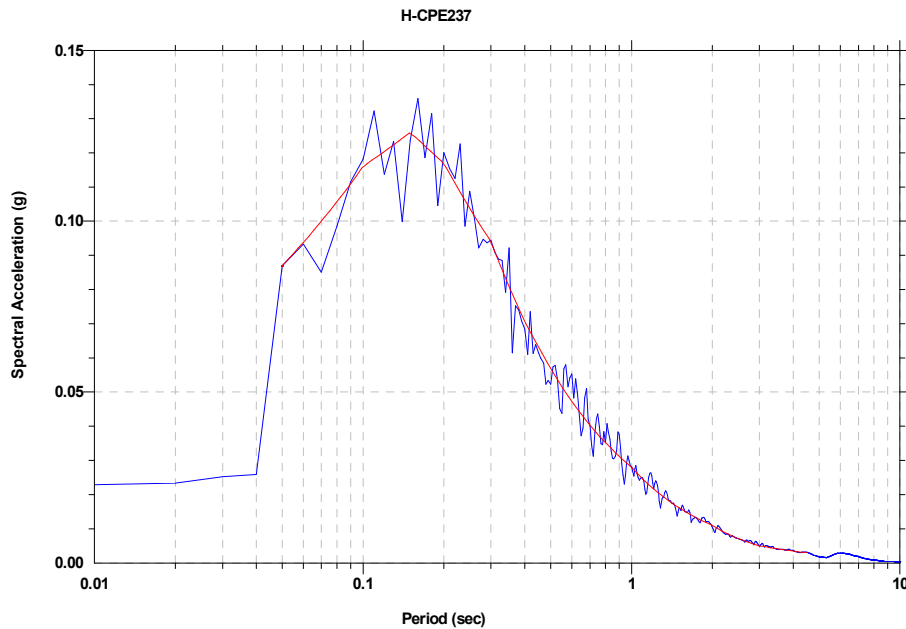


Figure. 29 Acceleration response spectra (1% Damping in g's). Response spectra of matched time history (blue colour): 1981 Imperial Valley earthquake, Cerro Prieto station and H-CPE237 component. Target response spectrum (red colour): uniform hazard spectrum at 10% in 50 years hazard level.

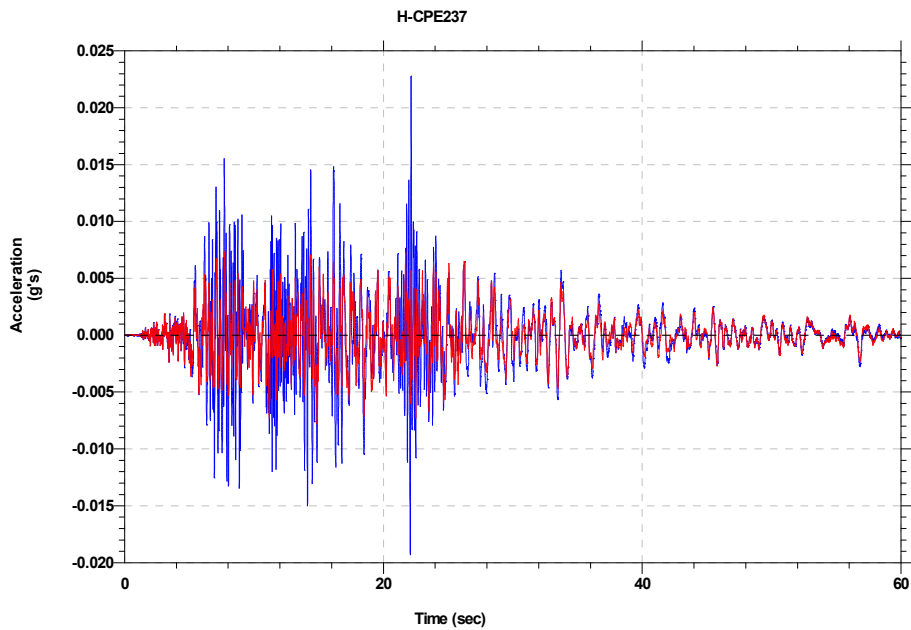


Figure.30 Acceleration time histories. Scaled seed time history (red colour) for 1981 Imperial Valley earthquake, Cerro Prieto station, H-CPE237 component and adjusted time history (blue colour) that matched the uniform hazard spectrum.

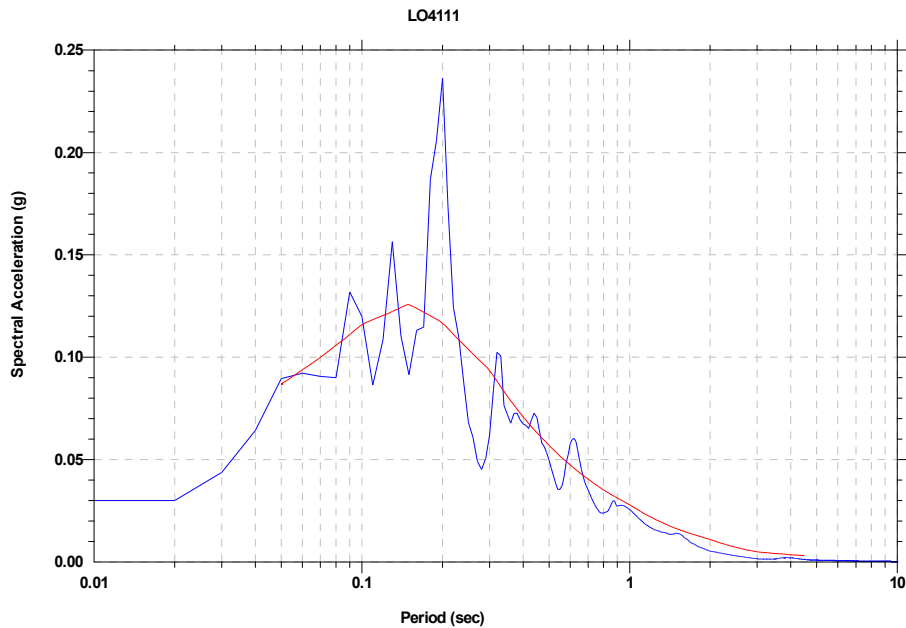


Figure.31 Acceleration response spectra (1% Damping in g's). Response spectra of scaled ground acceleration time history (blue colour): 1971 San Fernando earthquake, Lake Hughes station and LO4111 component. Target response spectrum (red colour): uniform hazard spectrum at 10% in 50 years hazard level

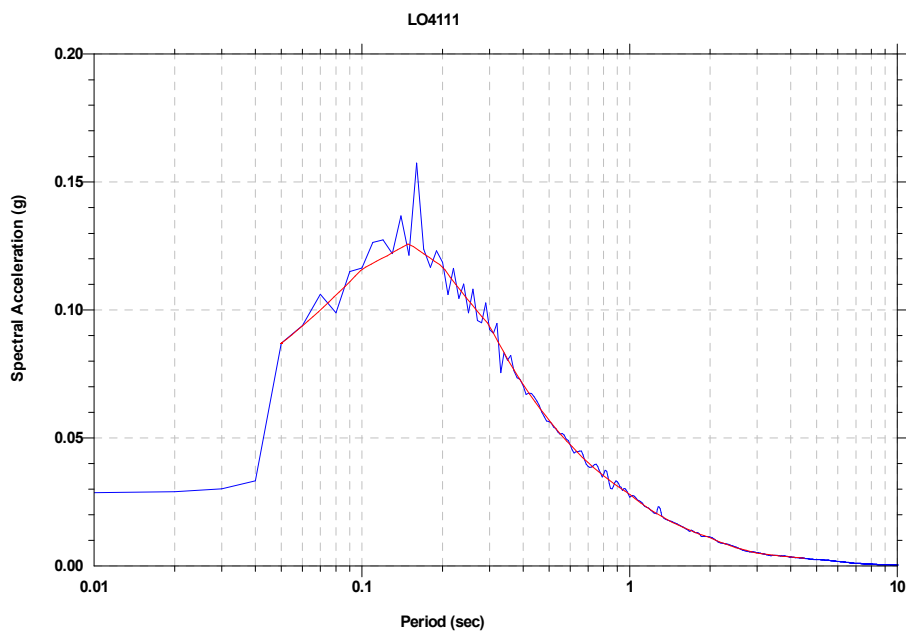


Figure. 32 Acceleration response spectra (1% Damping in g's). Response spectra of matched time history (blue colour): 1971 San Fernando earthquake, Lake Hughes station and LO4111 component. Target response spectrum (red colour): uniform hazard spectrum at 10% in 50 years hazard level.

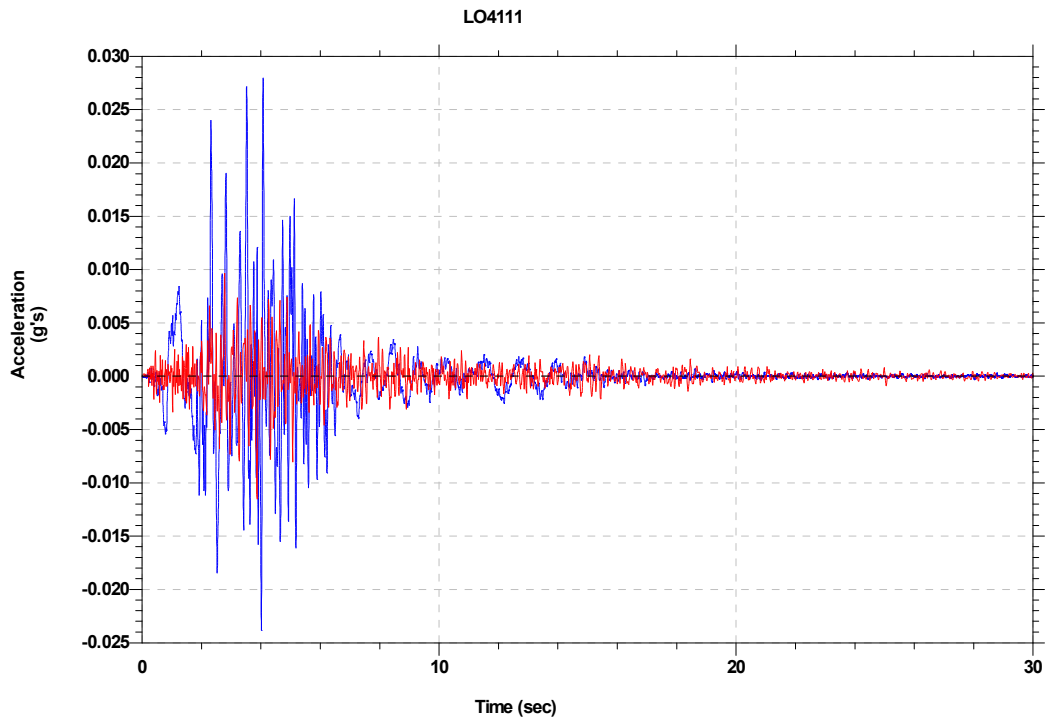


Figure.33 Acceleration time histories. Scaled seed time history (red colour) for 1971 San Fernando earthquake, Lake Hughes station and LO4111 component and adjusted time history (blue colour) that matched the uniform hazard spectrum.

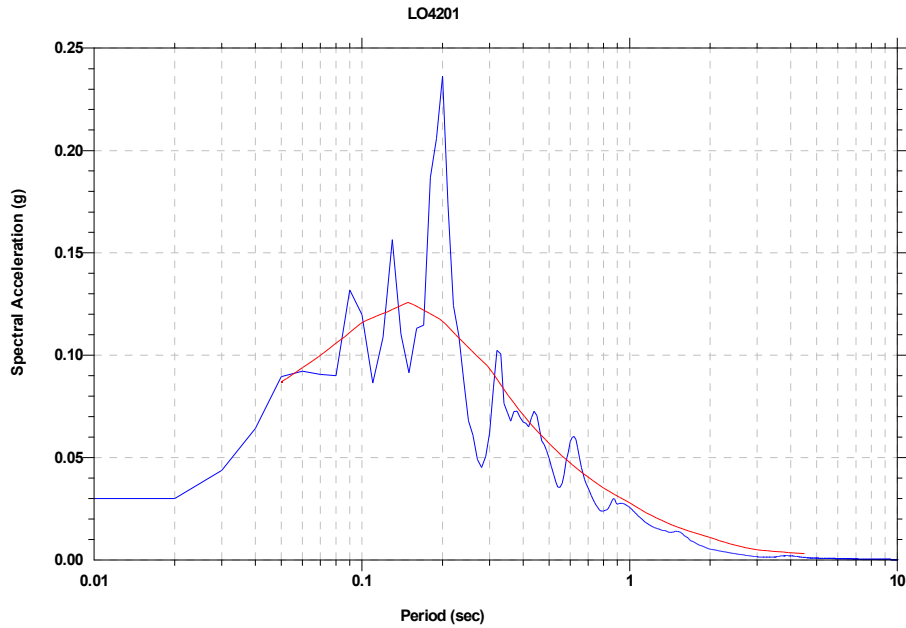


Figure.34 Acceleration response spectra (1% Damping in g's). Response spectra of scaled ground acceleration time history (blue colour):1971 San Fernando earthquake, Lake Hughes station and LO4201 component. Target response spectrum (red colour): uniform hazard spectrum at 10% in 50 years hazard level.

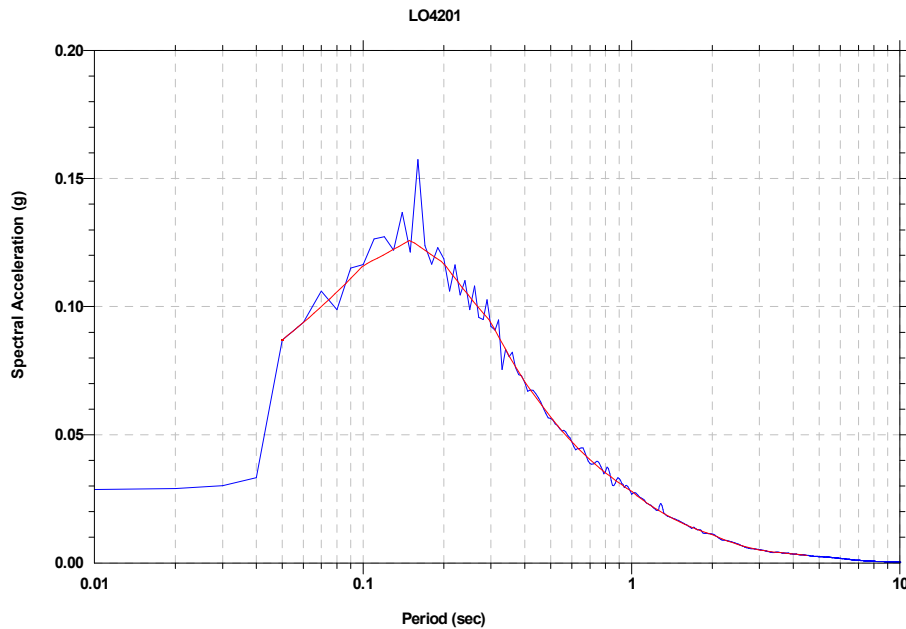


Figure. 35 Acceleration response spectra (1% Damping in g's). Response spectra of matched time history (blue colour): 1971 San Fernando earthquake, Lake Hughes station and LO4201 component. Target response spectrum (red colour): uniform hazard spectrum at 10% in 50 years hazard level.

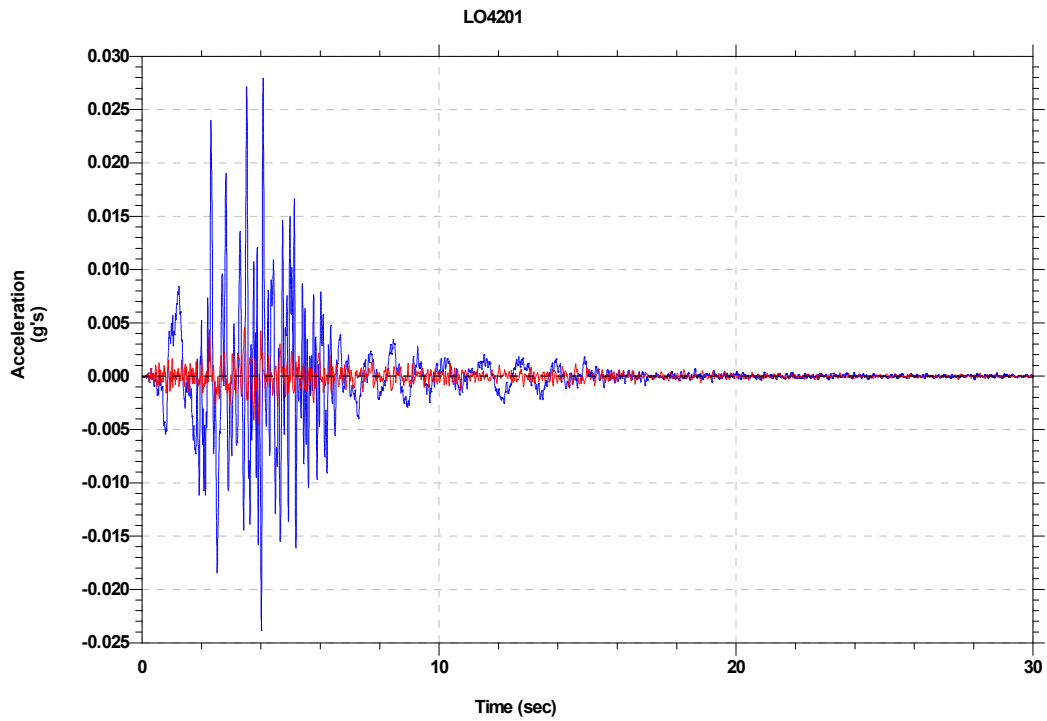


Figure.36 Acceleration time histories. Scaled seed time history (red colour) for 1971 San Fernando earthquake, Lake Hughes station and LO4201 component and adjusted time history (blue colour) that matched the uniform hazard spectrum.

**APPENDIX K:
LABORATORY RESULTS**

APPENDIX K:

LABORATORY RESULTS

- a) Collapse Potential**
- b) Foundation Indicator**
- c) Shear Box Results**

APPENDIX K:

LABORATORY RESULTS

a) Collapse Potential

GEOSCIENCE LABORATORIES

CONSOLIDATION TEST

SUMMARY OF READINGS

PROJECT : Soillab

INITIAL DIAL READING = 1.083 mm
 RING DIAMETER = 76.25 mm
 H1 = 18.85 mm
 H_s = 10.6 mm

PROJECT NO : L100865
 SAMPLE NO : 16483
 POSITION: TWTG 4 *gill wash*
 2.8m

OEDOMETER NO : 8
 BEAM RATIO : 11

BEAM LOAD (kg)	COMMENTS	PRESSURE (Kpa)	DIAL READING (mm)	UNCORRECTED DEFLECTION (mm)	MACHINE CORRECTION (mm)	CORRECTED DEFLECTION (mm)	HEIGHT CHANGE (mm)	VOID RATIO
0.0		0.00	1.083	1.083	0.000	0	18.850	0.7783
0.1		2.36	1.073	0.010	0.001	0.009	18.841	0.7775
1.0		23.63	1.022	0.061	0.020	0.041	18.809	0.7744
2.0		47.26	0.994	0.089	0.029	0.060	18.790	0.7726
4.0		94.53	0.961	0.122	0.042	0.080	18.770	0.7708
8.0		189.05	0.849	0.234	0.059	0.175	18.675	0.7618
8.0	SAT	189.05	0.844	0.239	0.059	0.180	18.670	0.7613
16.0		378.10	0.714	0.369	0.080	0.289	18.561	0.7510

COLLAPSE POTENTIAL: 0.03%

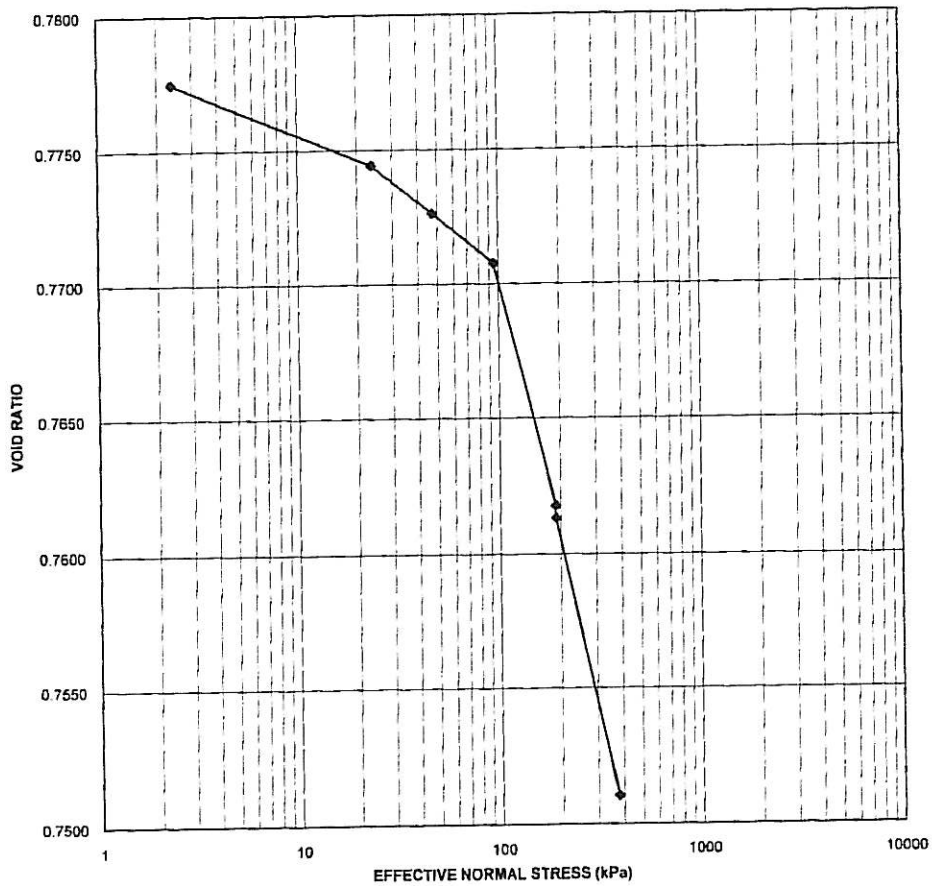
GEOSCIENCE LABORATORIES

CONSOLIDATION TEST

PROJECT : Soillab

PROJECT NO : L100865
SAMPLE NO : 16463

SAMPLE DESCRIPTION	: yellow brown silty coarse sand (cemented)	SPECIFIC DENSITY (EST)	= 2.65
STATE OF SAMPLE	: undisturbed	FINAL SATURATION	= 0.85
DRY DENSITY	= 1490 Kg/m ³	FINAL MOISTURE CONTENT	= 23.66 %
INITIAL SATURATION	= 0.54	FINAL VOID RATIO	= 0.7510
INITIAL MOISTURE CONTENT	= 15.75 %		
INITIAL VOID RATIO	= 0.7783		



GEOSCIENCE LABORATORIES

CONSOLIDATION TEST

SUMMARY OF READINGS

PROJECT : Soilab
 INITIAL DIAL READING = 1.068 mm
 RING DIAMETER = 75.9 mm
 H1 = 19.1 mm
 H_s = 11.65 mm

PROJECT NO : L100865
 SAMPLE NO : 10157
 POSITION: TWTG 4 (checked)
 2.5 m
 OEDOMETER NO : 1
 BEAM RATIO : 11

BEAM LOAD	COMMENTS	PRESSURE	DIAL READING	UNCORRECTED DEFLECTION	MACHINE CORRECTION	CORRECTED DEFLECTION	HEIGHT CHANGE	VOID RATIO
(kg)		(Kpa)	(mm)	(mm)	(mm)	(mm)	(mm)	
0.0		0.00	1.068	1.068	0.000	0	19.100	0.6395
0.1		2.38	1.054	0.014	0.001	0.013	19.087	0.6384
1.0		23.85	0.988	0.080	0.013	0.067	19.033	0.6337
2.0		47.70	0.952	0.116	0.022	0.094	19.006	0.6314
4.0		95.40	0.876	0.192	0.032	0.160	18.940	0.6258
8.0		190.80	0.796	0.272	0.045	0.227	18.873	0.6200
8.0	SAT	190.80	0.776	0.292	0.045	0.247	18.853	0.6183
16.0		381.60	0.634	0.434	0.064	0.370	18.730	0.6077

COLLAPSE POTENTIAL: 0.10%

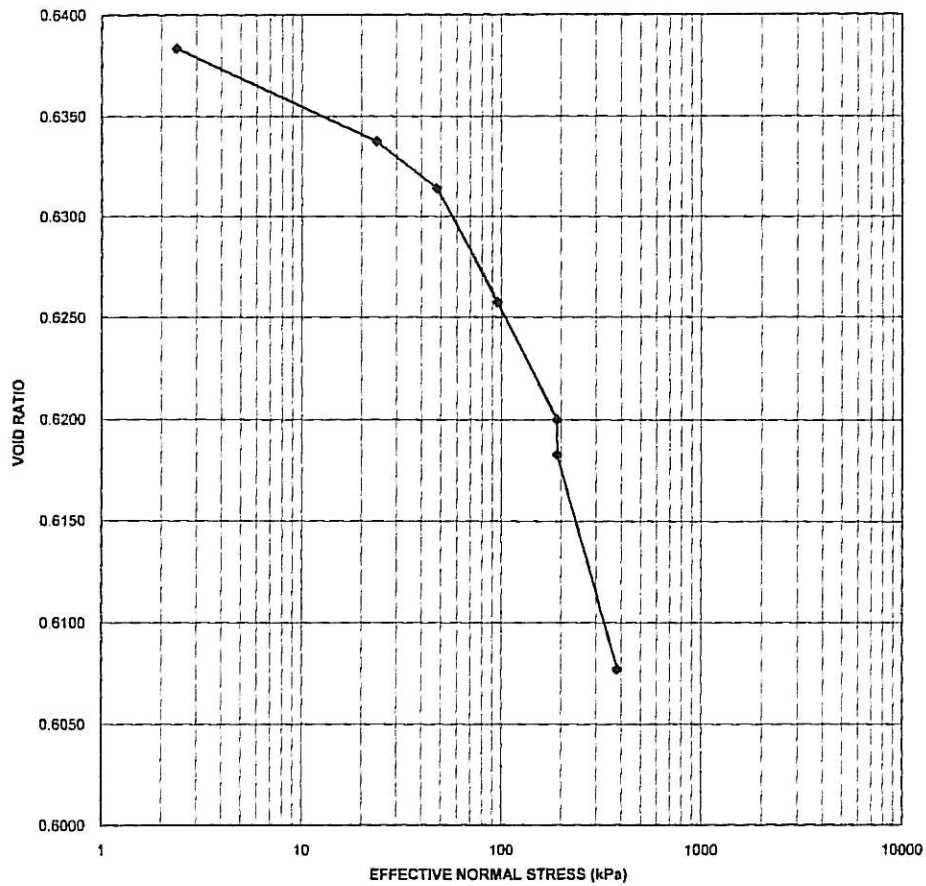
GEOSCIENCE LABORATORIES

CONSOLIDATION TEST

PROJECT : Soillab

PROJECT NO : L100865
SAMPLE NO : 16467

SAMPLE DESCRIPTION	:	yellow orange silty coarse sand (cemented)		
STATE OF SAMPLE	:	undisturbed		
DRY DENSITY	=	1616 Kg/m ³	SPECIFIC DENSITY (EST)	= 2.65
INITIAL SATURATION	=	0.33	FINAL SATURATION	= 0.67
INITIAL MOISTURE CONTENT	=	8.08 %	FINAL MOISTURE CONTENT	= 14.66 %
INITIAL VOID RATIO	=	0.6395	FINAL VOID RATIO	= 0.6077



GEOSCIENCE LABORATORIES

CONSOLIDATION TEST

SUMMARY OF READINGS

PROJECT : Soilab
INITIAL DIAL READING = 1.049 mm
RING DIAMETER = 75 mm
H1 = 18.7 mm
H_s = 12.59 mm

PROJECT NO : L100865
SAMPLE NO : 16464
POSITION : T WTG 16 *Still was*
2.4m

OEDOMETER NO : 3
BEAM RATIO : 11

BEAM LOAD	COMMENTS	PRESSURE	DIAL READING	UNCORRECTED DEFLECTION	MACHINE CORRECTION	CORRECTED DEFLECTION	HEIGHT CHANGE	VOID RATIO
(kg)		(Kpa)	(mm)	(mm)	(mm)	(mm)	(mm)	
0.0		0.00	1.049	1.049	0.000	0	18.700	0.4853
0.1		2.44	1.028	0.021	0.002	0.019	18.681	0.4838
1.0		24.43	0.928	0.121	0.015	0.106	18.594	0.4769
2.0		48.85	0.865	0.184	0.022	0.162	18.538	0.4724
4.0		97.70	0.816	0.233	0.032	0.201	18.499	0.4693
8.0		195.41	0.715	0.334	0.045	0.289	18.411	0.4624
8.0	SAT	195.41	0.439	0.610	0.045	0.565	18.135	0.4404
16.0		390.81	0.265	0.784	0.064	0.720	17.980	0.4281

COLLAPSE POTENTIAL: 1.48%

GEOSCIENCE LABORATORIES

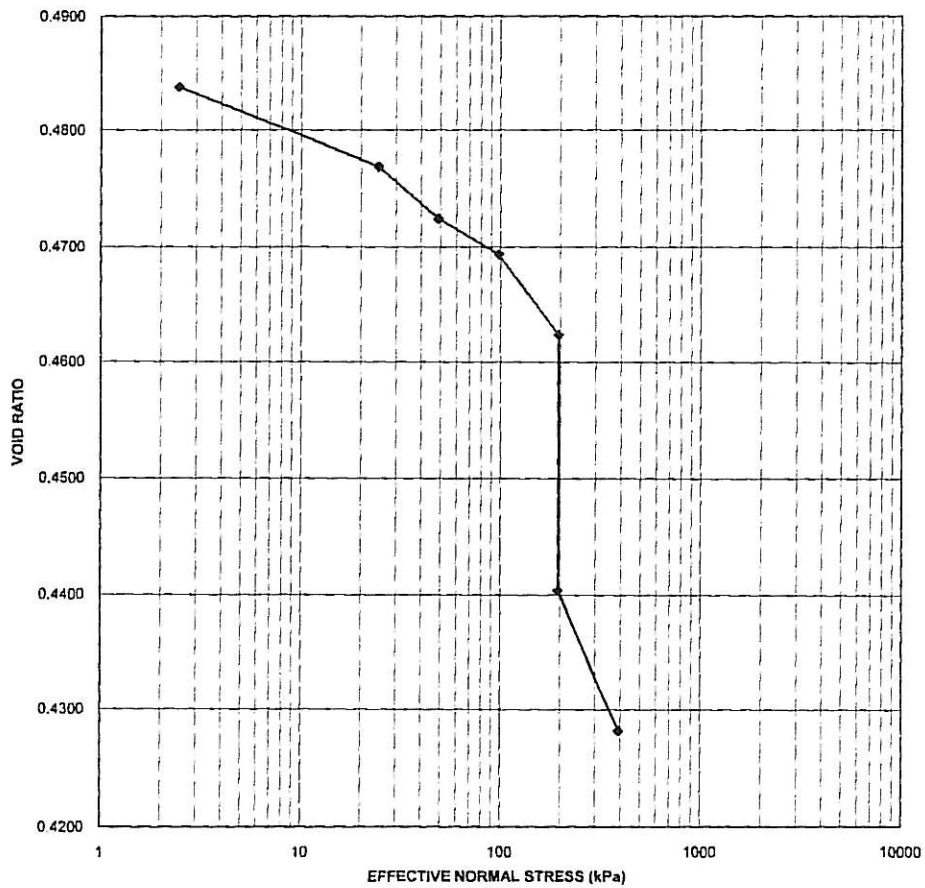
CONSOLIDATION TEST

PROJECT : Soilab

PROJECT NO : L100865
SAMPLE NO : 16464

SAMPLE DESCRIPTION : yellow orange silty sand
STATE OF SAMPLE : undisturbed
DRY DENSITY = 1784 Kg/m³
INITIAL SATURATION = 0.47
INITIAL MOISTURE CONTENT = 8.55 %
INITIAL VOID RATIO = 0.4853

SPECIFIC DENSITY (EST) = 2.65
FINAL SATURATION = 0.90
FINAL MOISTURE CONTENT = 14.56 %
FINAL VOID RATIO = 0.4281



GEOSCIENCE LABORATORIES

CONSOLIDATION TEST

SUMMARY OF READINGS

PROJECT : Soillab
 INITIAL DIAL READING = 1.153 mm
 RING DIAMETER = 76.2 mm
 H1 = 19.1 mm
 Hs = 13.28 mm

PROJECT NO : L100865
 SAMPLE NO : 16465
 POSITION : T WTG 16 *Shihwadi*
 3.1-3.5m

OEDOMETER NO : 4
 BEAM RATIO : 11

BEAM LOAD	COMMENTS	PRESSURE	DIAL READING	UNCORRECTED DEFLECTION	MACHINE CORRECTION	CORRECTED DEFLECTION	HEIGHT CHANGE	VOID RATIO
(kg)		(Kpa)	(mm)	(mm)	(mm)	(mm)	(mm)	
0.0		0.00	1.153	1.153	0.000	0	19.100	0.4383
0.1		2.37	1.128	0.025	0.001	0.024	19.076	0.4364
1.0		23.66	1.017	0.136	0.021	0.115	18.985	0.4296
2.0		47.33	0.957	0.196	0.031	0.165	18.935	0.4258
4.0		94.65	0.839	0.314	0.044	0.270	18.830	0.4179
8.0		189.30	0.699	0.454	0.060	0.394	18.706	0.4086
8.0	SAT	189.30	0.691	0.462	0.060	0.402	18.698	0.4080
16.0		378.60	0.520	0.633	0.082	0.551	18.549	0.3968

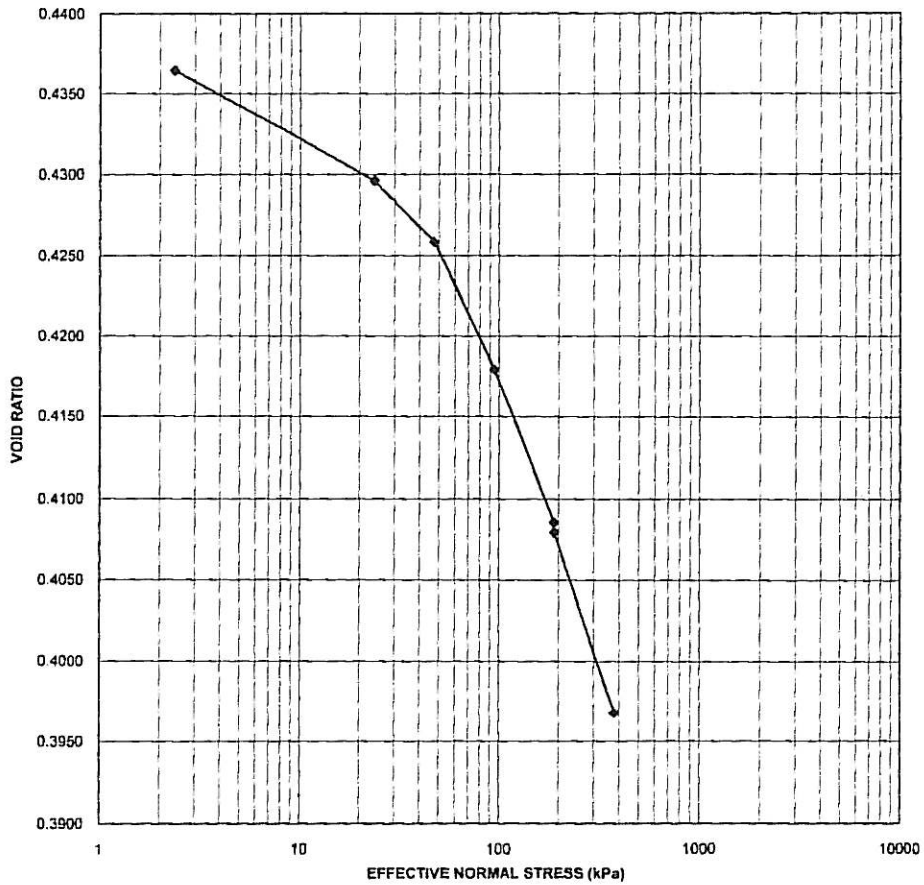
COLLAPSE POTENTIAL: 0.04%

GEOSCIENCE LABORATORIES
CONSOLIDATION TEST

PROJECT : Soillab

PROJECT NO : L100865
SAMPLE NO : 16465

SAMPLE DESCRIPTION	:	yellow orange silty sand		
STATE OF SAMPLE	:	undisturbed		
DRY DENSITY	=	1842 Kg/m ³	SPECIFIC DENSITY (EST)	= 2.65
INITIAL SATURATION	=	0.5	FINAL SATURATION	= 0.84
INITIAL MOISTURE CONTENT	=	8.21 %	FINAL MOISTURE CONTENT	= 12.64 %
INITIAL VOID RATIO	=	0.4383	FINAL VOID RATIO	= 0.3968



GEOSCIENCE LABORATORIES

CONSOLIDATION TEST

SUMMARY OF READINGS

PROJECT : Soilab

PROJECT NO : L100865

SAMPLE NO : 164AR

POSITION: WTG 16 Gillman
4.85-5.03

INITIAL DIAL READING = 1.092 mm

RING DIAMETER = 50.05 mm

H1 = 20.55 mm

Hs = 13.52 mm

OEDOMETER NO : 8

BEAM RATIO : 11

BEAM LOAD (kg)	COMMENTS	PRESSURE (Kpa)	DIAL READING (mm)	UNCORRECTED DEFLECTION (mm)	MACHINE CORRECTION (mm)	CORRECTED DEFLECTION (mm)	HEIGHT CHANGE (mm)	VOID RATIO
0.0		0.00	1.092	1.092	0.000	0	20.550	0.5200
0.05		2.74	1.085	0.007	0.001	0.006	20.544	0.5195
0.55		30.17	1.033	0.059	0.012	0.047	20.503	0.5165
1.05		57.59	0.999	0.093	0.020	0.073	20.477	0.5146
2.05		112.44	0.953	0.139	0.029	0.110	20.440	0.5118
3.55		194.71	0.895	0.197	0.042	0.155	20.395	0.5085
3.55	SAT	194.71	0.890	0.202	0.042	0.160	20.390	0.5081
6.55		359.26	0.816	0.276	0.055	0.221	20.329	0.5036

COLLAPSE POTENTIAL: 0.03%

GEOSCIENCE LABORATORIES

CONSOLIDATION TEST

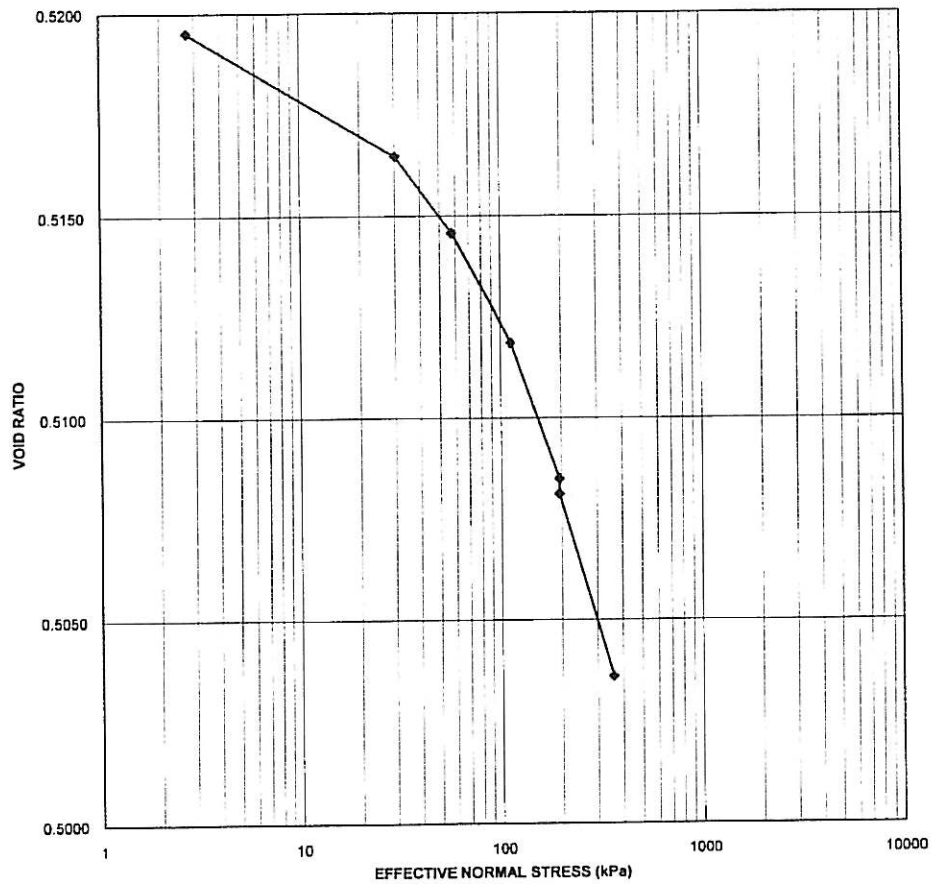
PROJECT : Soillab

PROJECT NO : L100865

SAMPLE NO : 16468

SAMPLE DESCRIPTION : lt orange brown sand
STATE OF SAMPLE : undisturbed
DRY DENSITY = 1743 Kg/m³
INITIAL SATURATION = 0.78
INITIAL MOISTURE CONTENT = 15.24 %
INITIAL VOID RATIO = 0.52

SPECIFIC DENSITY (EST) = 2.65
FINAL SATURATION = 0.73
FINAL MOISTURE CONTENT = 13.82 %
FINAL VOID RATIO = 0.5036



GEOSCIENCE LABORATORIES

CONSOLIDATION TEST

SUMMARY OF READINGS

PROJECT : Soillab
 INITIAL DIAL READING = 1.062 mm
 RING DIAMETER = 50.05 mm
 H₁ = 20.5 mm
 H_s = 12.09 mm

PROJECT NO : L100865
 SAMPLE NO : 16469
 POSITION: WTG 21
 4.98-5.29
 OEDOMETER NO : 7
 BEAM RATIO : 11

BEAM LOAD (kg)	COMMENTS	PRESSURE (Kpa)	DIAL READING (mm)	UNCORRECTED DEFLECTION (mm)	MACHINE CORRECTION (mm)	CORRECTED DEFLECTION (mm)	HEIGHT CHANGE (mm)	VOID RATIO
0.0		0.00	1.062	1.062	0.000	0	20.500	0.6956
0.05		2.74	1.051	0.011	0.003	0.008	20.492	0.6950
0.55		30.17	0.982	0.080	0.030	0.050	20.450	0.6915
1.05		57.59	0.935	0.127	0.038	0.089	20.411	0.6883
2.05		112.44	0.861	0.201	0.052	0.149	20.351	0.6833
3.55		194.71	0.750	0.312	0.071	0.241	20.259	0.6757
3.55	SAT	194.71	0.710	0.352	0.071	0.281	20.219	0.6724
6.55		359.26	0.563	0.499	0.088	0.411	20.089	0.6616

COLLAPSE POTENTIAL: 0.19%

GEOSCIENCE LABORATORIES

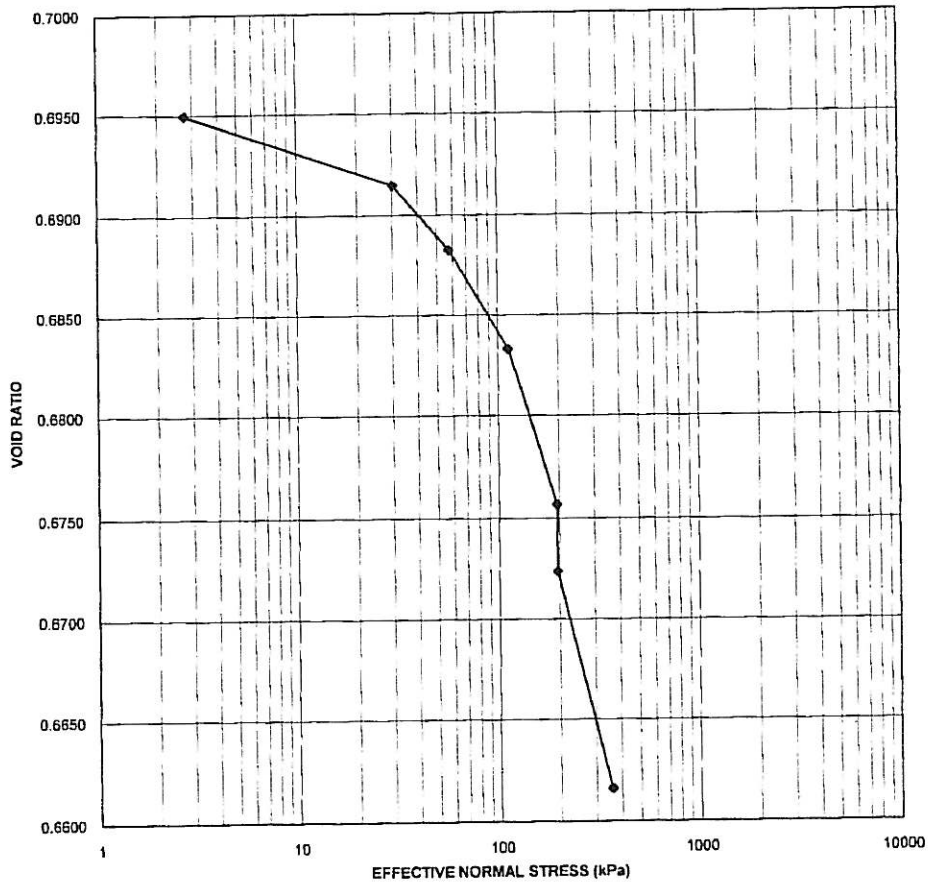
CONSOLIDATION TEST

PROJECT : Soilab

PROJECT NO : L100865
SAMPLE NO : 16469

SAMPLE DESCRIPTION : lt yellow brown sand
STATE OF SAMPLE : undisturbed
DRY DENSITY = 1563 Kg/m³
INITIAL SATURATION = 0.55
INITIAL MOISTURE CONTENT = 14.54 %
INITIAL VOID RATIO = 0.6956

SPECIFIC DENSITY (EST) = 2.65
FINAL SATURATION = 0.84
FINAL MOISTURE CONTENT = 20.97 %
FINAL VOID RATIO = 0.6616



GEOSCIENCE LABORATORIES

CONSOLIDATION TEST

SUMMARY OF READINGS

PROJECT : Soillab
INITIAL DIAL READING = 1.086 mm
RING DIAMETER = 50.05 mm
H₁ = 20.4 mm
H_s = 12.42 mm

PROJECT NO : L100865
SAMPLE NO : 16470
POSITION: WTG 23
4.50-4.85
OEDOMETER NO : 6
BEAM RATIO : 11

BEAM LOAD (kg)	COMMENTS	PRESSURE (Kpa)	DIAL READING (mm)	UNCORRECTED DEFLECTION (mm)	MACHINE CORRECTION (mm)	CORRECTED DEFLECTION (mm)	HEIGHT CHANGE (mm)	VOID RATIO
0.0		0.00	1.086	1.086	0.000	0	20.400	0.6425
0.05		2.74	1.074	0.012	0.001	0.011	20.389	0.6416
0.55		30.17	1.006	0.080	0.007	0.073	20.327	0.6366
1.05		57.59	0.952	0.134	0.012	0.122	20.278	0.6327
2.05		112.44	0.872	0.214	0.021	0.193	20.207	0.6270
3.55		194.71	0.754	0.332	0.035	0.297	20.103	0.6186
3.55	SAT	194.71	0.742	0.344	0.035	0.309	20.091	0.6176
6.55		359.26	0.600	0.486	0.048	0.438	19.962	0.6072

COLLAPSE POTENTIAL: 0.06%

GEOSCIENCE LABORATORIES

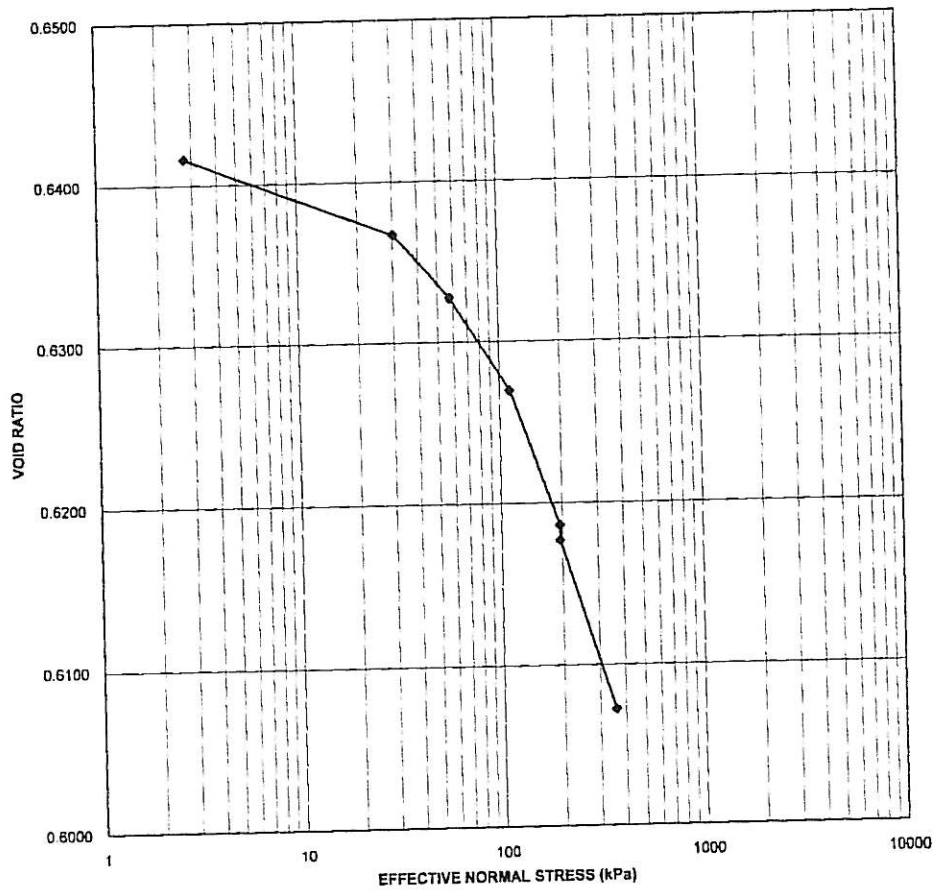
CONSOLIDATION TEST

PROJECT : Soilab

PROJECT NO : L100865
SAMPLE NO : 16470

SAMPLE DESCRIPTION : orange brown sand
STATE OF SAMPLE : undisturbed
DRY DENSITY = 1613 Kg/m³
INITIAL SATURATION = 0.85
INITIAL MOISTURE CONTENT = 20.73 %
INITIAL VOID RATIO = 0.6425

SPECIFIC DENSITY (EST) = 2.65
FINAL SATURATION = 0.95
FINAL MOISTURE CONTENT = 21.7 %
FINAL VOID RATIO = 0.6072



GEOSCIENCE LABORATORIES

CONSOLIDATION TEST

SUMMARY OF READINGS

PROJECT : Soilab

PROJECT NO : L100865
 SAMPLE NO : 16471
 POSITION: WTG 26
 5.02-5.27

INITIAL DIAL READING = 1.096 mm
 RING DIAMETER = 50.05 mm
 H1 = 20.6 mm
 H_s = 7.94 mm

OEDOMETER NO : 1
 BEAM RATIO : 11

BEAM LOAD	COMMENTS	PRESSURE	DIAL READING	UNCORRECTED DEFLECTION	MACHINE CORRECTION	CORRECTED DEFLECTION	HEIGHT CHANGE	VOID RATIO
(kg)		(Kpa)	(mm)	(mm)	(mm)	(mm)	(mm)	
0.0		0.00	1.096	1.096	0.000	0	20.600	1.5945
0.05		2.74	1.090	0.006	0.001	0.005	20.595	1.5938
0.55		30.17	1.046	0.050	0.008	0.042	20.558	1.5892
1.05		57.59	1.000	0.096	0.013	0.083	20.517	1.5840
2.05		112.44	0.952	0.144	0.022	0.122	20.478	1.5791
3.55		194.71	0.890	0.206	0.032	0.174	20.426	1.5725
3.55	SAT	194.71	0.886	0.210	0.032	0.178	20.422	1.5720
6.55		359.26	0.788	0.308	0.042	0.266	20.334	1.5610

COLLAPSE POTENTIAL: 0.02%

GEOSCIENCE LABORATORIES

CONSOLIDATION TEST

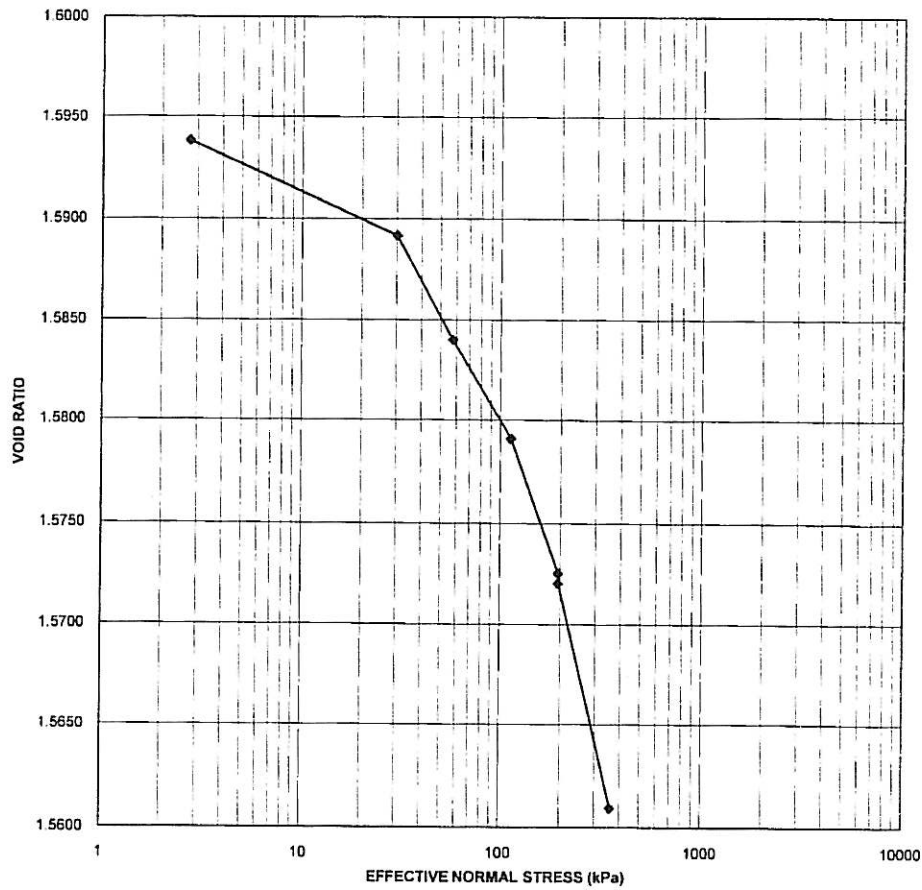
PROJECT : Soillab

PROJECT NO : L100865

SAMPLE NO : 16471

SAMPLE DESCRIPTION : grey clay
STATE OF SAMPLE : undisturbed
DRY DENSITY = 1021 Kg/m³
INITIAL SATURATION = 0.79
INITIAL MOISTURE CONTENT = 47.81 %
INITIAL VOID RATIO = 1.5945

SPECIFIC DENSITY (EST) = 2.65
FINAL SATURATION = 0.80
FINAL MOISTURE CONTENT = 57.28 %
FINAL VOID RATIO = 1.5610



GEOSCIENCE LABORATORIES

CONSOLIDATION TEST

SUMMARY OF READINGS

PROJECT : Soillab

PROJECT NO : L100865
 SAMPLE NO : 16472
 POSITION: WTG 28
 6.34-6.53

INITIAL DIAL READING = 6.066 mm
 RING DIAMETER = 50.05 mm
 H1 = 20.6 mm
 H_s = 13.35 mm

OEDOMETER NO : 1
 BEAM RATIO : 11

BEAM LOAD (kg)	COMMENTS	PRESSURE (Kpa)	DIAL READING (mm)	UNCORRECTED DEFLECTION (mm)	MACHINE CORRECTION (mm)	CORRECTED DEFLECTION (mm)	HEIGHT CHANGE (mm)	VOID RATIO
0.0		0.00	6.066	6.066	0.000	0	20.600	0.5431
0.05		2.74	6.048	0.018	0.001	0.017	20.583	0.5418
0.55		30.17	5.750	0.316	0.008	0.308	20.292	0.5200
1.05		57.59	5.520	0.546	0.013	0.533	20.067	0.5031
2.05		112.44	5.264	0.802	0.022	0.780	19.820	0.4846
3.55		194.71	5.028	1.040	0.032	1.008	19.592	0.4676
3.55	SAT	194.71	5.022	1.044	0.032	1.012	19.588	0.4673
6.55		359.26	4.738	1.328	0.042	1.286	19.314	0.4467

COLLAPSE POTENTIAL: 0.02%

GEOSCIENCE LABORATORIES

CONSOLIDATION TEST

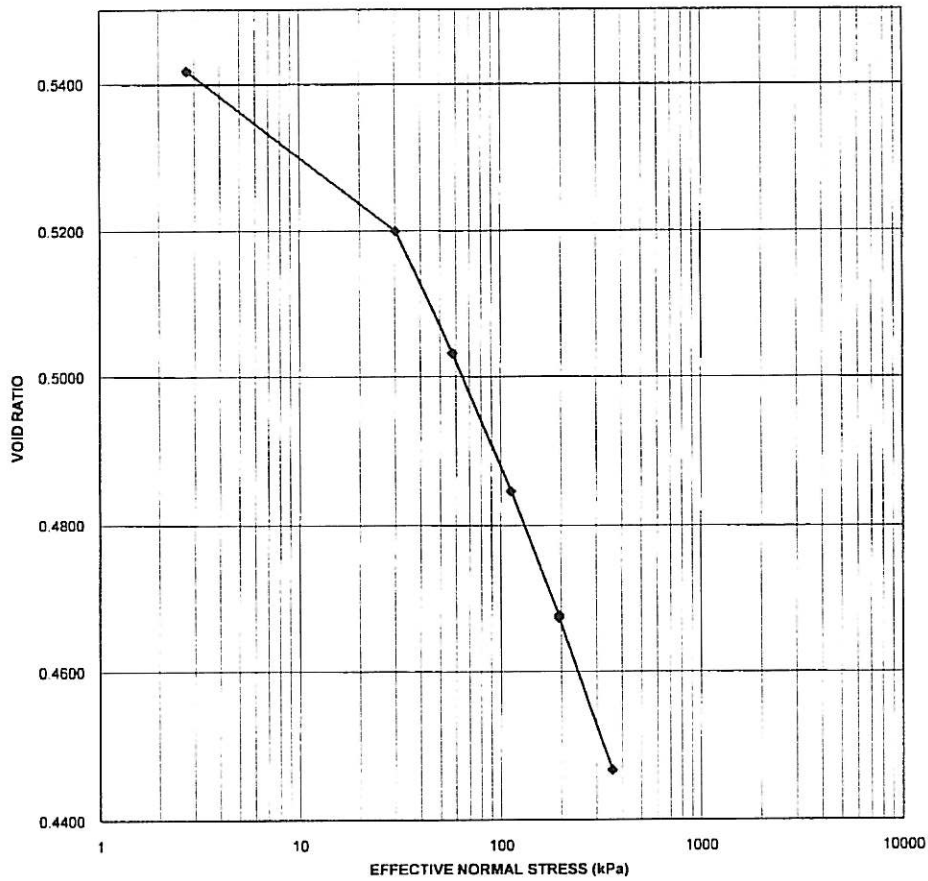
PROJECT : Soillab

PROJECT NO : L100865

SAMPLE NO : 16472

SAMPLE DESCRIPTION : white silt
STATE OF SAMPLE : undisturbed
DRY DENSITY = 1717 Kg/m³
INITIAL SATURATION = 0.76
INITIAL MOISTURE CONTENT = 15.58 %
INITIAL VOID RATIO = 0.5431

SPECIFIC DENSITY (EST) = 2.65
FINAL SATURATION = 1.17
FINAL MOISTURE CONTENT = 19.7 %
FINAL VOID RATIO = 0.4467



GEOSCIENCE LABORATORIES

CONSOLIDATION TEST

SUMMARY OF READINGS

PROJECT : Soilab
 INITIAL DIAL READING = 1.194 mm
 RING DIAMETER = 76.4 mm
 H1 = 19.2 mm
 H_s = 12.16 mm

PROJECT NO : L100865
 SAMPLE NO : 16466
 POSITION: T WTG 34
 2.0-2.3m *SHILLWAN*
 OEDOMETER NO : 2
 BEAM RATIO : 11

BEAM LOAD	COMMENTS	PRESSURE	DIAL READING	UNCORRECTED DEFLECTION	MACHINE CORRECTION	CORRECTED DEFLECTION	HEIGHT CHANGE	VOID RATIO
(kg)		(Kpa)	(mm)	(mm)	(mm)	(mm)	(mm)	
0.0		0.00	1.194	1.194	0.000	0	19.200	0.5789
0.1		2.35	1.106	0.088	0.001	0.087	19.113	0.5718
1.0		23.54	0.712	0.482	0.012	0.470	18.730	0.5403
2.0		47.08	0.630	0.564	0.018	0.546	18.654	0.5340
4.0		94.16	0.500	0.694	0.027	0.667	18.533	0.5241
8.0		188.31	0.364	0.830	0.041	0.789	18.411	0.5141
8.0	SAT	188.31	0.304	0.890	0.041	0.849	18.351	0.5091
16.0		376.62	0.136	1.058	0.061	0.997	18.203	0.4970

COLLAPSE POTENTIAL: 0.63%

GEOSCIENCE LABORATORIES

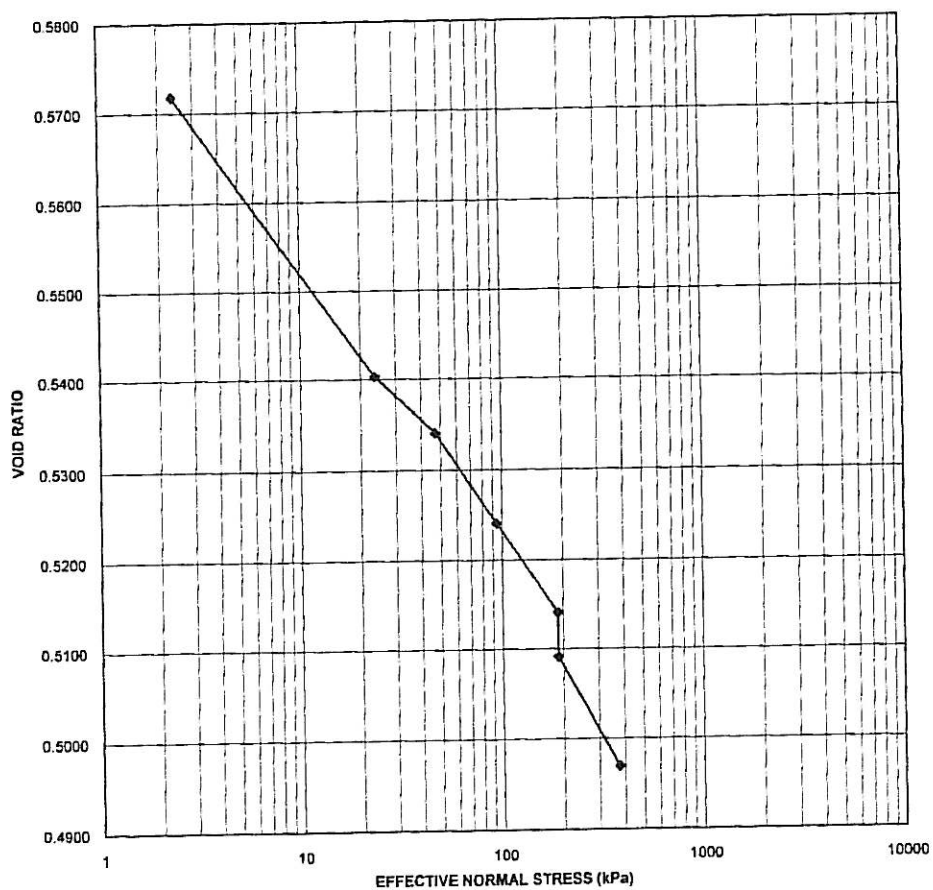
CONSOLIDATION TEST

PROJECT : Soilfab

PROJECT NO : L100865
SAMPLE NO : 16466

SAMPLE DESCRIPTION : red orange silty sand
STATE OF SAMPLE : undisturbed
DRY DENSITY = 1679 Kg/m³
INITIAL SATURATION = 0.2
INITIAL MOISTURE CONTENT = 4.3 %
INITIAL VOID RATIO = 0.5789

SPECIFIC DENSITY (EST) = 2.65
FINAL SATURATION = 0.78
FINAL MOISTURE CONTENT = 14.65 %
FINAL VOID RATIO = 0.4970



GEOSCIENCE LABORATORIES
 CONSOLIDATION TEST

SUMMARY OF READINGS

PROJECT : Soillab

INITIAL DIAL READING = 1.144 mm
 RING DIAMETER = 76.05 mm
 H1 = 18.9 mm
 Hs = 11.74 mm

PROJECT NO : L100865
 SAMPLE NO : 16460
 POSITION: T WTG 46

OEDOMETER NO : 6
 BEAM RATIO : 11

1.5m *[Signature]*

BEAM LOAD (kg)	COMMENTS	PRESSURE (Kpa)	DIAL READING (mm)	UNCORRECTED DEFLECTION (mm)	MACHINE CORRECTION (mm)	CORRECTED DEFLECTION (mm)	HEIGHT CHANGE (mm)	VOID RATIO
0.0		0.00	1.144	1.144	0.000	0	18.900	0.6099
0.1		2.38	1.130	0.014	0.002	0.012	18.888	0.6089
1.0		23.76	1.044	0.100	0.012	0.088	18.812	0.6024
2.0		47.51	1.000	0.144	0.021	0.123	18.777	0.5994
4.0		95.02	0.870	0.274	0.035	0.239	18.661	0.5895
8.0		190.05	0.772	0.372	0.052	0.320	18.580	0.5826
8.0	SAT	190.05	0.676	0.468	0.052	0.416	18.484	0.5744
16.0		380.10	0.524	0.620	0.070	0.550	18.350	0.5630

COLLAPSE POTENTIAL: 0.51%

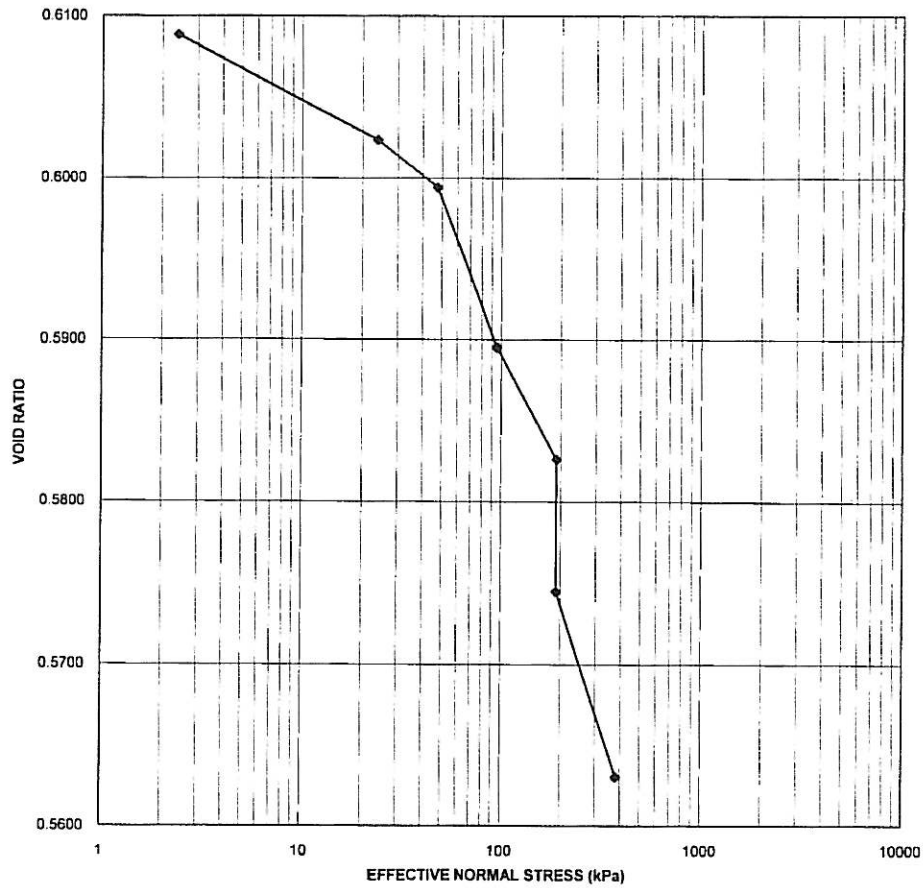
GEOSCIENCE LABORATORIES

CONSOLIDATION TEST

PROJECT : Soilab

PROJECT NO : L100865
SAMPLE NO : 16460

SAMPLE DESCRIPTION	:	yellow olive silty coarse sand (cemented)		
STATE OF SAMPLE	:	undisturbed		
DRY DENSITY	=	1647 Kg/m ³	SPECIFIC DENSITY (EST)	= 2.65
INITIAL SATURATION	=	0.57	FINAL SATURATION	= 0.92
INITIAL MOISTURE CONTENT	=	13.06 %	FINAL MOISTURE CONTENT	= 19.61 %
INITIAL VOID RATIO	=	0.6099	FINAL VOID RATIO	= 0.5630



APPENDIX K:

LABORATORY RESULTS

b) Foundation Indicator

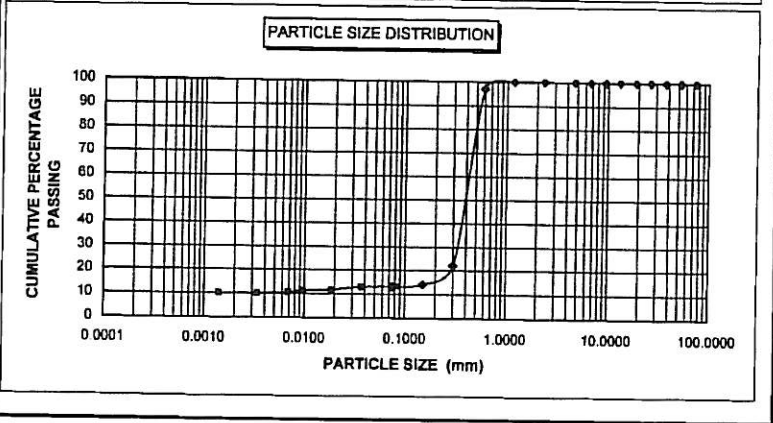
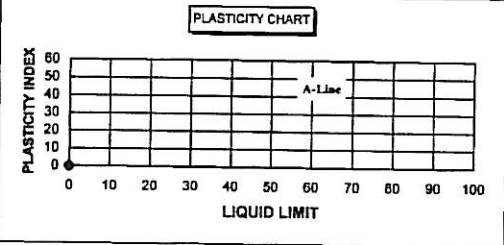
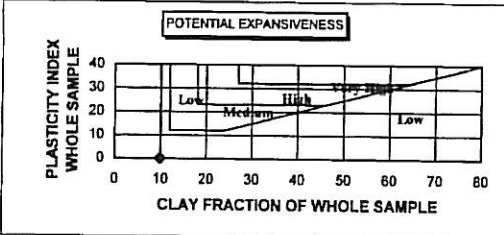
SOILLAB (PTY) LTD.
 Reg No. 2008/003519/07
 WESTERN CAPE

PARTICLE SIZE ANALYSIS

Test Method: ASTM D422

PROJECT : ESKOM SERE WINDFARM SK9904
 CLIENT : BKS
 DATE : 08.09.2010

SAMPLE / HOLE No.	TWGT16	LIQUID LIMIT : 0	% CLAY : 10.0
DEPTH (m)	1.5-5.0	PLASTICITY INDEX : NP	% SILT : 3
POSITION		LINEAR SHRINKAGE : 0	% SAND : 87
DESCRIPTION OF MATERIAL	YL BR CLAYEY SAND	MOISTURE CONTEN : 8.3	% GRAVEL : 0
SCREEN ANALYSIS (% PASSING)	75.0	100	
	53.0	100	
	37.5	100	
	26.5	100	
	19.0	100	
	13.2	100	
	9.5	100	
	6.7	100	
	4.75	100	
	2.36	100	
	1.18	100	
MECHANICAL ANALYSIS	0.600	97	
	0.300	22	
	0.150	14	
	0.075	13	
	0.080	13.2	
	0.037	12.8	
	0.019	11.6	
	0.010	11.2	
	0.007	10.4	
	0.003	10.0	
0.001	10.0		
0.000	0.0		
0.000	0.0		



[Signature]
 GENERAL MANAGER - SOILLAB

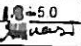
R 0.20

SOILLAB (PTY)LTD
 Reg No 2006/003519/07
 WESTERN CAPE

PARTICLE SIZE ANALYSIS

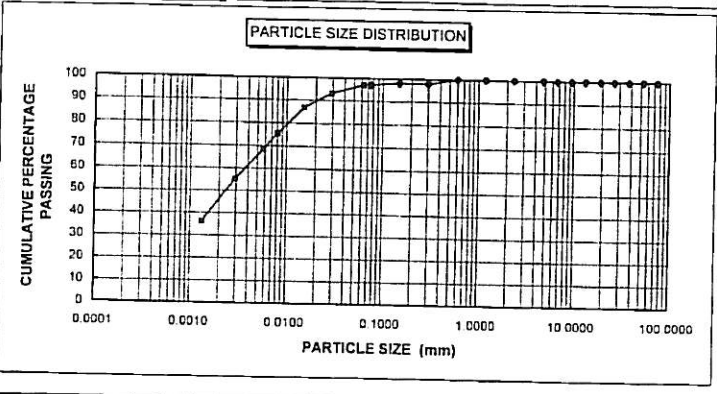
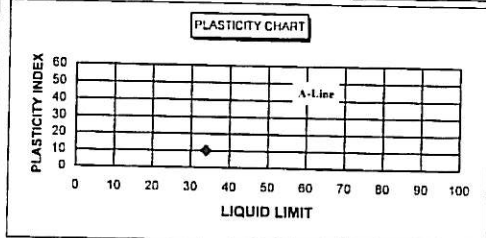
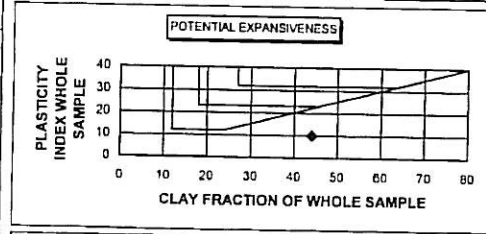
Test Method: ASTM D422


PROJECT : ESKOM SERE WINDFARM SK9963
 CLIENT : BKS
 DATE : 01.09.2010

SAMPLE /HOLE No : TWTG26
 DEPTH (m) : 5.0
 POSITION : 
 DESCRIPTION OF MATERIAL : L/GREY CLAY
 LIQUID LIMIT : 34 % CLAY : 44.2
 PLASTICITY INDEX : 10 % SILT : 53
 LINEAR SHRINKAGE : 5 % SAND : 3
 MOISTURE CONTEN : 31.4 % GRAVEL : 0

SCREEN ANALYSIS (% PASSING)	100
75.0	100
53.0	100
37.5	100
26.5	100
19.0	100
13.2	100
9.5	100
6.7	100
4.75	100
2.36	100
1.18	100
0.600	100
0.300	98
0.150	98
0.075	97

MECHANICAL ANALYSIS	97.0
0.063	97.0
0.029	93.2
0.015	86.7
0.008	75.5
0.006	68.4
0.003	55.2
0.001	36.3
0.000	0.0
0.000	0.0




 GENERAL MANAGER - SOILLAB

R 020

SOILLAB (PTY)LTD
 Reg No. 2008/003519/07
 WESTERN CAPE

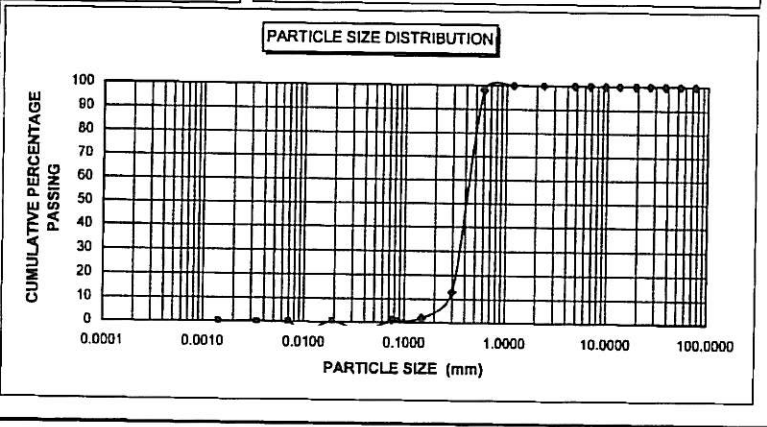
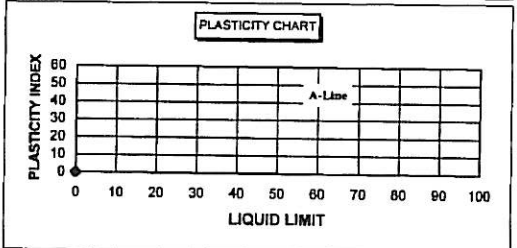
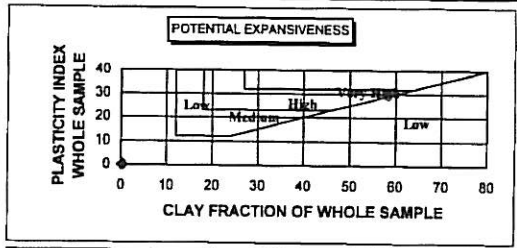
PARTICLE SIZE ANALYSIS

Test Method: ASTM D422

PROJECT	: ESKOM SERE WINDFARM	SK9904
CLIENT	: BKS	
DATE	: 08.09.2010	

SAMPLE / HOLE No.	TWTG34	LIQUID LIMIT	: 0	% CLAY	: 0.3
DEPTH (m)	2.2-2.4	PLASTICITY INDEX	: NP	% SILT	: -2
POSITION		LINEAR SHRINKAGE	: 0	% SAND	: 102
DESCRIPTION OF MATERIAL	YELLOW ORANGE SAND	MOISTURE CONTEN	: 0.7	% GRAVEL	: 0

SCREEN ANALYSIS (% PASSING)	75.0	100
	53.0	100
	37.5	100
	26.5	100
	19.0	100
	13.2	100
	9.5	100
	6.7	100
	4.75	100
	2.36	100
	1.18	100
	0.600	98
0.300	13	
0.150	2	
0.075	1	
MECHANICAL ANALYSIS	0.083	1.1
	0.038	-4.0
	0.019	0.6
	0.010	-4.5
	0.007	0.3
	0.003	0.3
	0.001	0.3
	0.000	0.0
0.000	0.0	



[Signature]
 GENERAL MANAGER - SOILLAB

R 0.20

SOILLAB (PTY)LTD
 Reg. No. 2008/003519/07
 WESTERN CAPE

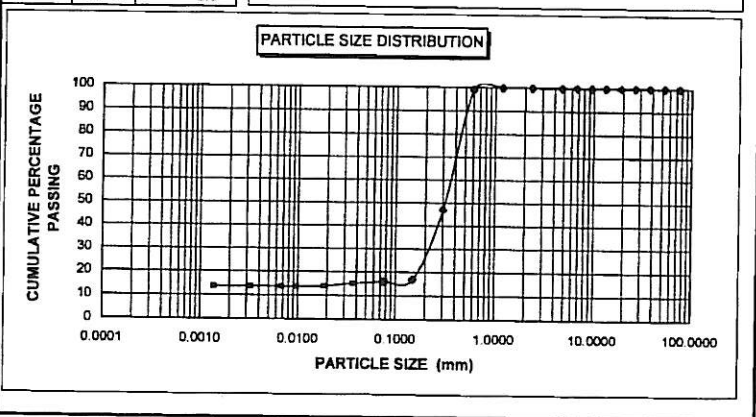
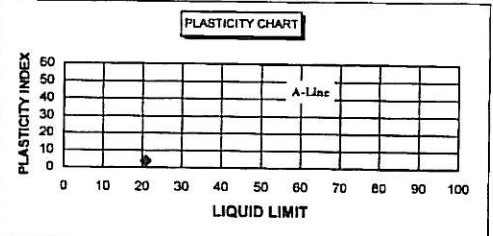
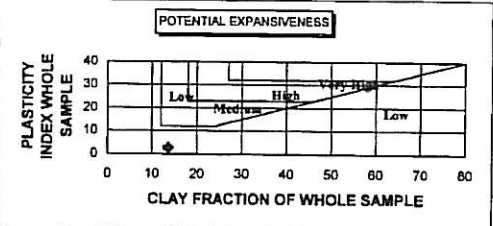
PARTICLE SIZE ANALYSIS

Test Method: ASTM D422

PROJECT : ESKOM SERE WINDFARM SK9904
 CLIENT : BKS
 DATE : 08.09.2010

SAMPLE / HOLE No : TWTG34
 DEPTH (m) : 2.4-4.5
 POSITION :
 DESCRIPTION OF MATERIAL : RD BROWN CLAYEY SAND
 LIQUID LIMIT : 21 % CLAY : 13.7
 PLASTICITY INDEX : 4 % SILT : 2
 LINEAR SHRINKAGE : 2 % SAND : 84
 MOISTURE CONTEN : 6.5 % GRAVEL : 0

SCREEN ANALYSIS (% PASSING)		
75.0		100
53.0		100
37.5		100
26.5		100
19.0		100
13.2		100
9.5		100
6.7		100
4.75		100
2.36		100
1.18		100
0.600		99
0.300		47
0.150		17
0.075		16
MECHANICAL ANALYSIS		
0.079		16.1
0.036		15.3
0.018		14.0
0.010		13.7
0.007		13.7
0.003		13.7
0.001		13.7
0.000		0.0
0.000		0.0



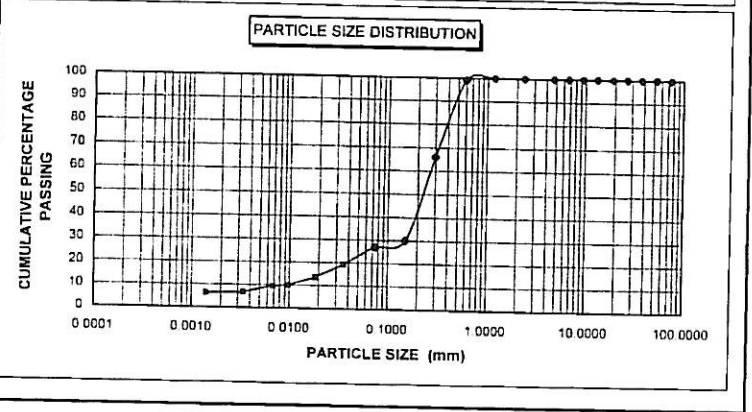
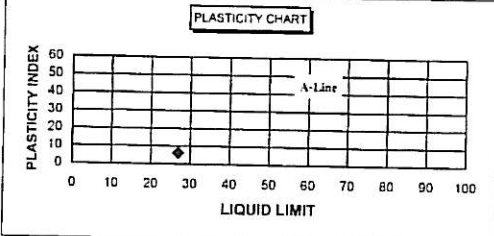
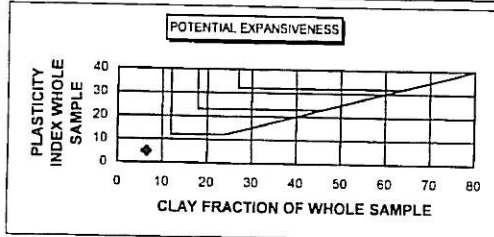
[Signature]
 GENERAL MANAGER, SOILLAB

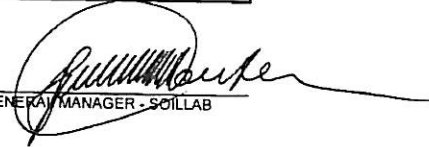
R 0.20

SOILLAB (PTY)LTD Reg No 2008/003519/07 WESTERN CAPE	PARTICLE SIZE ANALYSIS Test Method: ASTM D422	
	PROJECT : ESKOM SERE WINDFARM CLIENT : BKS DATE : 01.09.2010	SK9963

SAMPLE / HOLE No.	TWTG41	LIQUID LIMIT : 27	% CLAY : 6.5
DEPTH (m)	0.9-1.6	PLASTICITY INDEX : 6	% SILT : 18
POSITION	g1111111111	LINEAR SHRINKAGE : 3	% SAND : 76
DESCRIPTION OF MATERIAL	Silty Sand	MOISTURE CONTEN : 11.4	% GRAVEL : 0

SCREEN ANALYSIS (% PASSING)	DEPTH (m)	MECHANICAL ANALYSIS
75.0	100	0.073
53.0	100	0.035
37.5	100	0.018
26.5	100	0.010
19.0	100	0.007
13.2	100	0.003
9.5	100	0.001
6.7	100	0.000
4.75	100	0.000
2.36	100	0.000
1.18	100	0.000
0.600	99	0.000
0.300	66	0.000
0.150	30	0.000
0.075	27	0.000



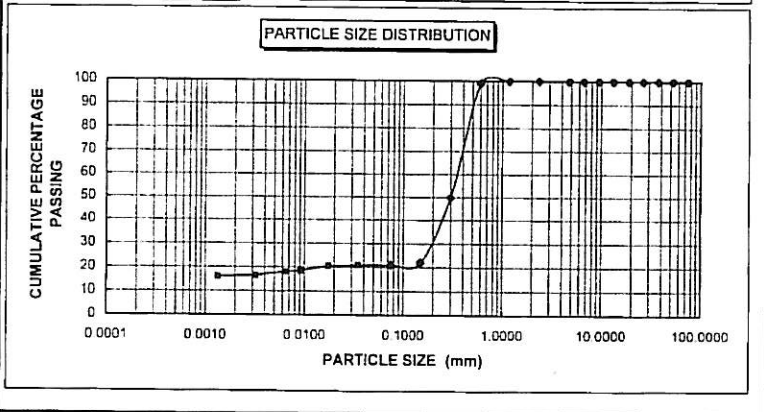

 GENERAL MANAGER - SOILLAB

R 0 20

SOILLAB (PTY)LTD Reg No 2008/003519/07 WESTERN CAPE	PARTICLE SIZE ANALYSIS Test Method: ASTM D422
------------------------------------------------------------------	---------------------------------------------------------

PROJECT :	ESKOM SERE WINDFARM	SK9963
CLIENT :	BKS	
DATE :	01.09.2010	

SAMPLE / HOLE No	TWTG41	LIQUID LIMIT : 0	% CLAY : 16.2
DEPTH (m)	1.6-5.0	PLASTICITY INDEX : N.P	% SILT : 5
POSITION		LINEAR SHRINKAGE : 0	% SAND : 79
DESCRIPTION OF MATERIAL	% CLAYEY SAND	MOISTURE CONTEN : 8	% GRAVEL : 0
SCREEN ANALYSIS (% PASSING)	75.0		
	53.0		
	37.5		
	26.5		
	19.0		
	13.2		
	9.5		
	6.7		
	4.75		
	2.36		
	1.18		
	0.600		
	0.300		
	0.150		
MECHANICAL ANALYSIS	0.075		
	21.0		
	20.9		
	20.6		
	18.5		
	18.0		
	16.4		
	16.1		
	0.0		
	0.0		
	0.0		



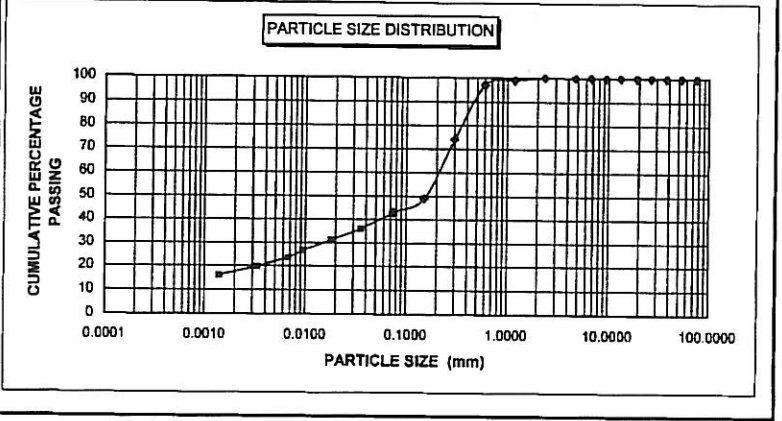
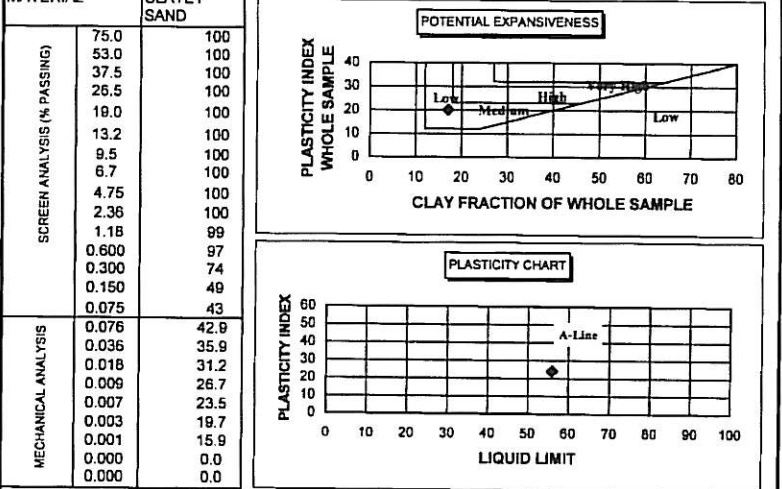
GENERAL MANAGER - SOILLAB

R 0.20

SOILLAB (PTY)LTD. Reg. No. 2008/003519/07 WESTERN CAPE	PARTICLE SIZE ANALYSIS Test Method: ASTM D422
---------------------------------------------------------------------	---------------------------------------------------------

PROJECT	: ESKOM SERE WINDFARM	SK9904
CLIENT	: BKS	
DATE	: 08.09.2010	

SAMPLE / HOLE No.	TWTG46	LIQUID LIMIT : 56	% CLAY : 17.1
DEPTH (m)	0.9-2.0	PLASTICITY INDEX : 24	% SILT : 23
POSITION		LINEAR SHRINKAGE : 12	% SAND : 59
DESCRIPTION OF MATERIAL	YELLOW BR CLAYEY SAND	MOISTURE CONTEN : 14.7	% GRAVEL : 0



GENERAL MANAGER - SOILLAB

R 0.20

SOILLAB (PTY)LTD
 Reg No. 2008/003516/07
 WESTERN CAPE

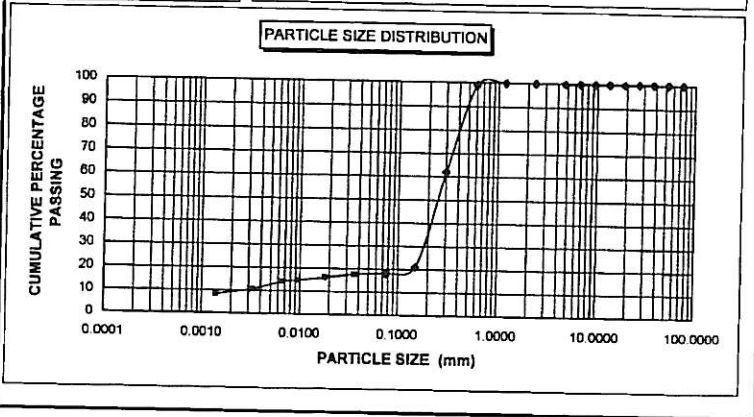
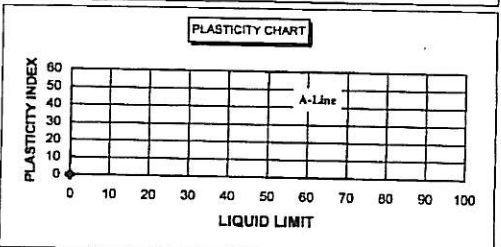
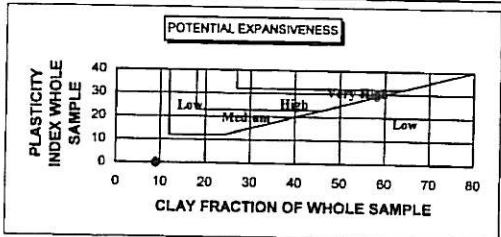
PARTICLE SIZE ANALYSIS

Test Method: ASTM D422

PROJECT : ESKOM SERE WINDFARM SK9904
 CLIENT : BKS
 DATE : 08.09.2010

SAMPLE / HOLE No. : TWG48
 DEPTH (m) : 2.0-5.0
 POSITION :
 DESCRIPTION OF MATERIAL : YELLOW BR CLAYEY SAND
 LIQUID LIMIT : 0 % CLAY : 9.1
 PLASTICITY INDEX : NP % SILT : 9
 LINEAR SHRINKAGE : 0 % SAND : 82
 MOISTURE CONTEN : 8.9 % GRAVEL : 0

SCREEN ANALYSIS (% PASSING)	75.0	100
	53.0	100
	37.5	100
	26.5	100
	19.0	100
	13.2	100
	9.5	100
	6.7	100
	4.75	100
	2.36	100
	1.18	100
	0.600	99
	0.300	62
	0.150	21
	0.075	18
MECHANICAL ANALYSIS	0.078	18.1
	0.036	17.7
	0.018	16.1
	0.009	14.8
	0.007	14.1
	0.003	10.6
	0.001	8.4
	0.000	0.0
	0.000	0.0



[Signature]
 GENERAL MANAGER - SOILLAB

R 0 20

APPENDIX K:

LABORATORY RESULTS

c (i) Shear Box Results – Undisturbed Dry

GEO SCIENCE

LABORATORIES (PTY) LTD

BRADFORD CLOSE, AIRPORT INDUSTRIAL, P.O. BOX 288 PAROW 7499
TELEPHONE: (021) 934 1114 FAX: (021) 934 8161

CLIENT: Soillab
P.O Box 585
Kraaifontein
7569

PROJECT: Soillab

JOB NO: L100865

DIRECT SHEAR TEST

Sample Number	16461	Test type	Consolidated drained
Sample Type	undisturbed	Sample Position	TWTG 4 @ 2.8m
Description	ff yellow brown silty coarse sand- highly cemented		

Handwritten signature

Length (mm)	60.00	Specific Gravity (est)	2.650
Breadth (mm)	60.00	Displacement mm/min	0.0480

RESULTS AT START OF TEST

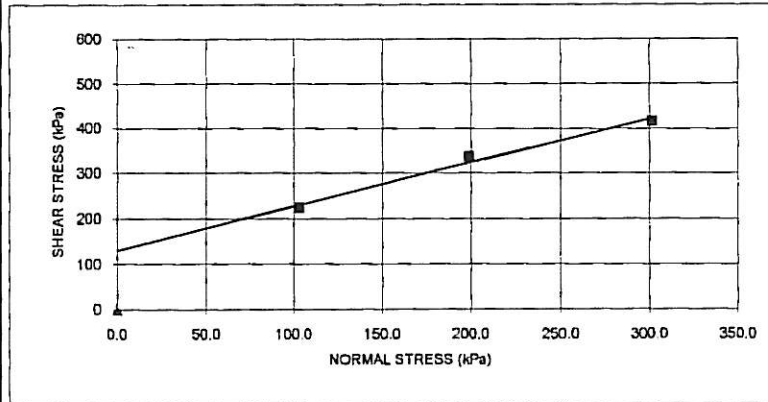
Void Ratio	0.81	0.79	0.83
Moisture Content %	12.40	12.40	12.40
Dry Density	1465	1477	1447

RESULTS AT END OF TEST

Void Ratio	0.73	0.78	0.73
Moisture Content %	24.33	25.16	27.34

PEAK SHEAR STRENGTH

Shear Stress kPa	223.89	337.22	417.22
Normal Stress kPa	102.79	198.72	301.51



	C kPa	Degrees
Peak	131.0	44.1

Apparent angle of internal shearing resistance given by regression (°)	44.1
Apparent cohesion given by regression (kPa)	131.0

GEO SCIENCE

LABORATORIES (PTY) LTD

BRADFORD CLOSE, AIRPORT INDUSTRIAL, P.O. BOX 268 PAROW 7499
 TELEPHONE: (021) 934 1114 FAX: (021) 934 9181

CLIENT: Soilab
 P.O Box 585
 Kraaifontein
 7569

PROJECT: Soilab

JOB NO: L100865

DIRECT SHEAR TEST

Sample Number	16467	Test type	Consolidated drained
Sample Type	undisturbed	Sample Position	TWTG 4 @ 2.8m
Description	yellow orange silty coarse sand- highly cemented		

Length (mm)	60.00	Specific Gravity (est)	2.650
Breadth (mm)	60.00	Displacement mm/min	0.0480

RESULTS AT START OF TEST

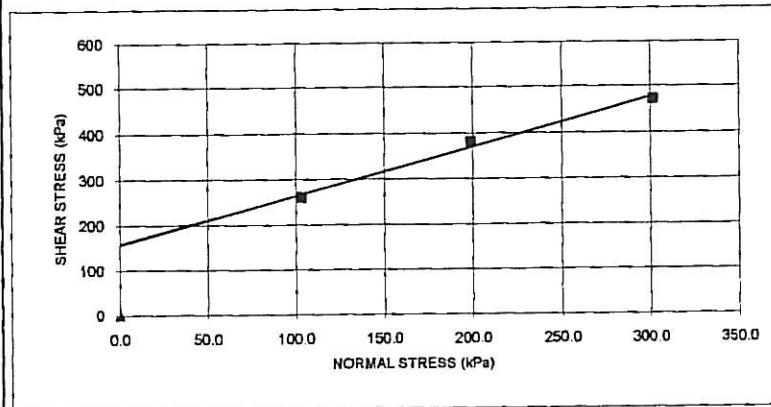
Void Ratio	0.70	0.71	0.73
Moisture Content %	7.10	7.10	7.10
Dry Density	1555	1550	1534

RESULTS AT END OF TEST

Void Ratio	0.70	0.62	0.73
Moisture Content %	23.85	20.76	23.95

PEAK SHEAR STRENGTH

Shear Stress kPa	260.56	381.94	472.22
Normal Stress kPa	102.79	198.72	301.51



	C kPa	Degrees
Peak	157.9	46.7

Apparent angle of internal shearing resistance given by regression (°)	46.7
Apparent cohesion given by regression (kPa)	157.9

GEO SCIENCE

LABORATORIES (PTY) LTD

BRADFORD CLOSE, AIRPORT INDUSTRIAL, P.O. BOX 288 PAROW 7459
TELEPHONE: (021) 934 1114 FAX: (021) 934 8161

CLIENT: Soillab
P.O Box 585
Kraaifontein
7569

PROJECT: Soillab

JOB NO: L100865

DIRECT SHEAR TEST

Sample Number	16464	Test type	Consolidated drained
Sample Type	undisturbed	Sample Position	WTG 16 @ 2.4m
Description	yellow orange silty sand		

Soillab

Length (mm)	60.00	Specific Gravity (est)	2.650
Breadth (mm)	60.00	Displacement mm/min	0.0480

RESULTS AT START OF TEST

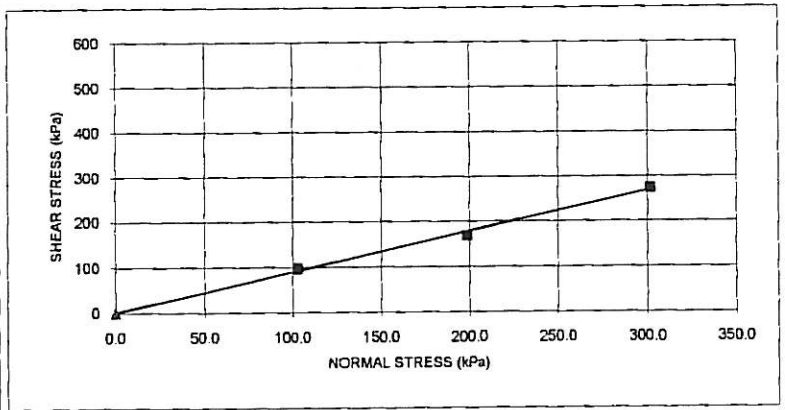
Void Ratio	0.53	0.51	0.51
Moisture Content %	7.30	7.30	7.30
Dry Density	1728	1759	1760

RESULTS AT END OF TEST

Void Ratio	0.53	0.51	0.50
Moisture Content %	15.64	15.96	16.84

PEAK SHEAR STRENGTH

Shear Stress kPa	97.78	168.61	274.72
Normal Stress kPa	102.79	198.72	301.51



	C kPa	Degrees
Peak	1.1	41.7

Apparent angle of internal shearing resistance given by regression (°)	41.7
Apparent cohesion given by regression (kPa)	1.1

GEO SCIENCE

LABORATORIES (PTY) LTD

BRADFORD CLOSE, AIRPORT INDUSTRIAL, P.O. BOX 266 PAROW 7499
TELEPHONE: (021) 934 1114 FAX: (021) 934 8161

CLIENT: Soilab
P.O Box 585
Kraaifontein
7569

PROJECT: Soilab

JOB NO: L100865

DIRECT SHEAR TEST

Sample Number	16465	Test type	Consolidated drained
Sample Type	undisturbed	Sample Position	TWTG 16 @ 3.1-3.5m
Description	yellow orange silty sand		

Length (mm)	60.00	Specific Gravity (est)	2.650
Breadth (mm)	60.00	Displacement mm/min	0.0480

RESULTS AT START OF TEST

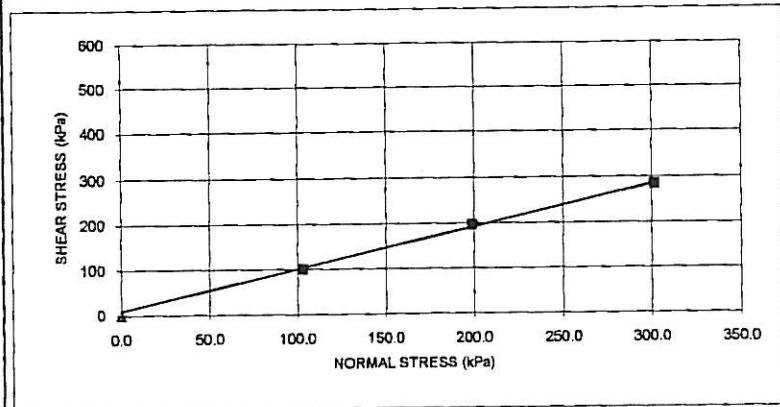
Void Ratio	0.47	0.44	0.46
Moisture Content %	7.30	7.30	7.30
Dry Density	1800	1839	1812

RESULTS AT END OF TEST

Void Ratio	0.47	0.42	0.45
Moisture Content %	15.75	15.58	15.65

PEAK SHEAR STRENGTH

Shear Stress kPa	101.67	196.94	284.72
Normal Stress kPa	102.79	198.72	301.51



	C kPa	Degrees
Peak	9.4	42.6

Apparent angle of internal shearing resistance given by regression (°)	42.6
Apparent cohesion given by regression (kPa)	9.4

GEO SCIENCE

LABORATORIES (PTY) LTD

BRADFORD CLOSE, AIRPORT INDUSTRIAL, P.O. BOX 286 PAROW 7499
TELEPHONE: (021) 934 1114 FAX: (021) 934 8161

CLIENT: Soillab
P.O Box 585
Kraaifontein
7569

PROJECT: Soillab

JOB NO: L100865

DIRECT SHEAR TEST

Sample Number	16466	Test type	Consolidated drained
Sample Type	undisturbed	Sample Position	T WTG 34 @ 2.0-2.3m <i>SHI</i> <i>near</i>
Description	red orange silty sand		

Length (mm)	60.00	Specific Gravity (est)	2.650
Breadth (mm)	60.00	Displacement mm/min	0.0480

RESULTS AT START OF TEST

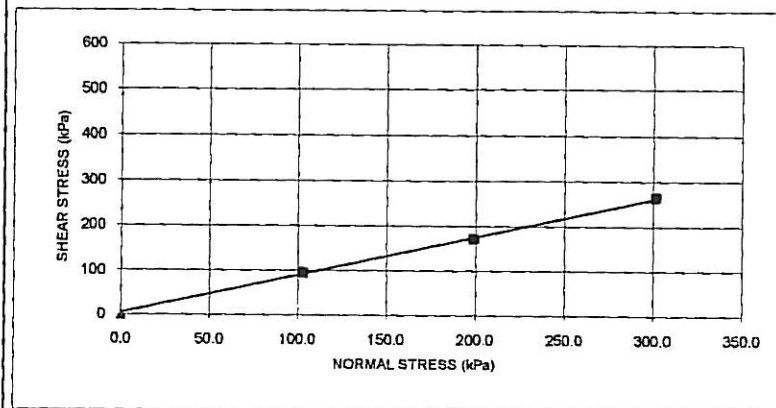
Void Ratio	0.63	0.66	0.66
Moisture Content %	3.40	3.40	3.40
Dry Density	1626	1593	1597

RESULTS AT END OF TEST

Void Ratio	0.63	0.63	0.66
Moisture Content %	18.26	18.17	19.77

PEAK SHEAR STRENGTH

Shear Stress kPa	95.00	171.39	264.72
Normal Stress kPa	102.79	198.72	301.51



	C kPa	Degrees
Peak	5.2	40.5

Apparent angle of internal shearing resistance given by regression (°)	40.5
Apparent cohesion given by regression (kPa)	5.2

APPENDIX K:

LABORATORY RESULTS

c (ii) Shear Box Results – Remoulded Saturated

GEO SCIENCE

LABORATORIES (PTY) LTD

CLIENT: Soillab
P.O Box 585
Kraaifontein
7569

PROJECT: Soillab

JOB NO: L100865

DIRECT SHEAR TEST

Sample Number	16465	Test type	Consolidated drained
Sample Type	<2mm remoulded	Sample Position	WTG 16 @ 3.1-3.5m
Description	yellow orange silty sand <i>yellow orange silty sand</i>		

Length (mm)	60.00	Specific Gravity (est)	2.650
Breadth (mm)	60.00	Displacement mm/min	0.0480

RESULTS AT START OF TEST

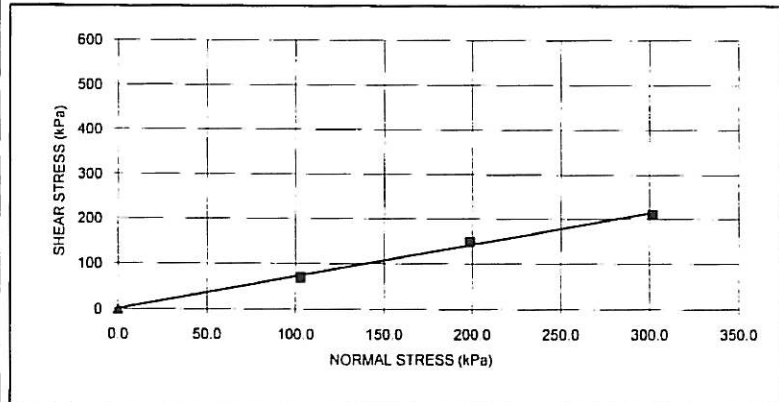
Void Ratio	1.21	1.20	1.20
Moisture Content %	5.90	5.90	5.60
Dry Density	1200	1206	1204

RESULTS AT END OF TEST

Void Ratio	1.20	1.05	1.18
Moisture Content %	20.61	20.47	19.31

PEAK SHEAR STRENGTH

Shear Stress kPa	70.00	149.72	211.11
Normal Stress kPa	102.79	198.72	301.51



	C kPa	Degrees
Peak	1.1	35.3

Apparent angle of internal shearing resistance given by regression (°)	35.3
Apparent cohesion given by regression (kPa)	1.1

GEOSCIENCE

LABORATORIES (PTY) LTD

CLIENT: Soillab
P.O Box 585
Kraaifontein
7569

PROJECT: Soillab

JOB NO: L100865

DIRECT SHEAR TEST

Sample Number	16466	Test type	Consolidated drained
Sample Type	<2mm remoulded	Sample Position	T WTG 34 @ z.0 -2.3m
Description	red orange silty sand <i>SMW</i>		

Length (mm)	60.00	Specific Gravity (est)	2.650
Breadth (mm)	60.00	Displacement mm/min	0.0480

RESULTS AT START OF TEST

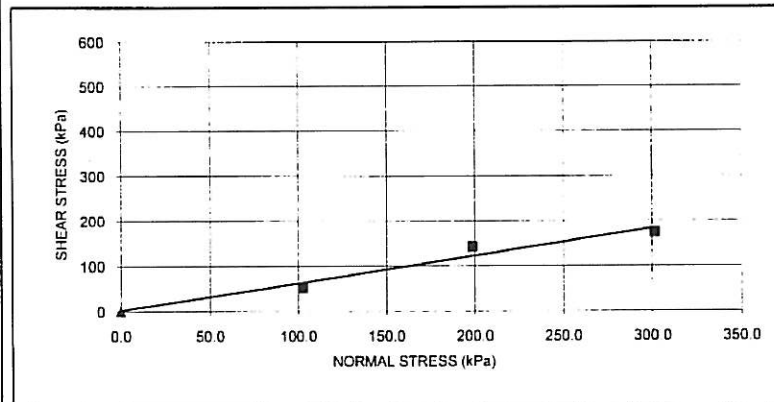
Void Ratio	0.97	0.97	0.98
Moisture Content %	3.50	3.50	3.50
Dry Density	1342	1345	1336

RESULTS AT END OF TEST

Void Ratio	0.93	0.90	0.80
Moisture Content %	21.11	20.82	21.29

PEAK SHEAR STRENGTH

Shear Stress kPa	53.06	143.06	173.61
Normal Stress kPa	102.79	198.72	301.51



	C kPa	Degrees
Peak	2.0	31.1

Apparent angle of internal shearing resistance given by regression (°)	31.1
Apparent cohesion given by regression (kPa)	2.0

GEO SCIENCE

LABORATORIES (PTY) LTD

CLIENT: Soillab
P.O Box 585
Kraaifontein
7569

PROJECT: Soillab

JOB NO: L100865

DIRECT SHEAR TEST

Sample Number	16460	Test type	Consolidated drained
Sample Type	<2mm remoulded	Sample Position	T WTG 46 @ 1.5m
Description	yellow olive silty sand		

Length (mm)	60.00	Specific Gravity (est)	2.650
Breadth (mm)	60.00	Displacement mm/min	0.0480

RESULTS AT START OF TEST

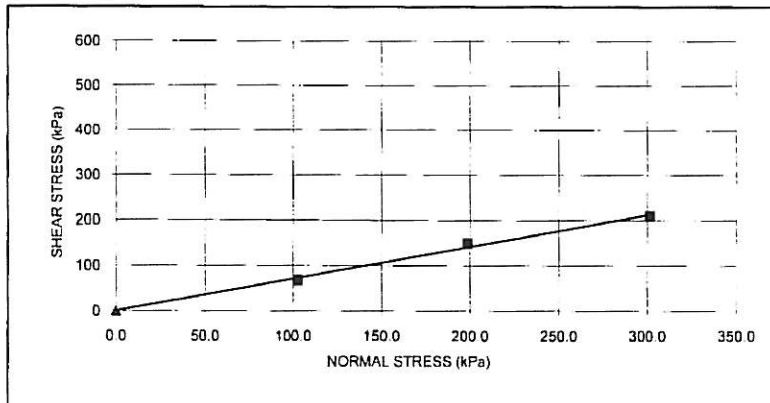
Void Ratio	0.99	0.97	0.98
Moisture Content %	8.60	8.60	8.60
Dry Density	1334	1334	1338

RESULTS AT END OF TEST

Void Ratio	0.96	0.88	0.96
Moisture Content %	37.01	32.18	25.97

PEAK SHEAR STRENGTH

Shear Stress kPa	68.33	149.72	208.89
Normal Stress kPa	102.79	198.72	301.51



	C kPa	Degrees
Peak	0.5	35.2

Apparent angle of internal shearing resistance given by regression (°)	35.2
Apparent cohesion given by regression (kPa)	0.5